ACS SYMPOSIUM SERIES 809

CO_2 Conversion and Utilization

EDITED BY

Chunshan Song, Anne M. Gaffney,
and Kaoru Fujimoto

Downloaded by 217.66.152.143 on September 14, 2012 | http://pubs.acs.org
Publication Date: January 24, 2002 | doi: 10.1021/bk-2002-0809.fw001

CO_2 Conversion and Utilization

American Chemical Society
Library
1155 16th St., N.W.
Washington, D.C. 20036

In CO2 Conversion and Utilization; Song, C., et al.;
ACS Symposium Series; American Chemical Society: Washington, DC, 2002.

Downloaded by 217.66.152.143 on September 14, 2012 | http://pubs.acs.org
Publication Date: January 24, 2002 | doi: 10.1021/bk-2002-0809.fw001

American Chemical Society
Library
1155 16th St., N.W.
Washington, D.C. 20036

ACS SYMPOSIUM SERIES **809**

CO_2 Conversion and Utilization

Chunshan Song, Editor
Pennsylvania State University

Anne F. Gaffney, Editor
Rohm and Haas Company

Kaoru Fujimoto, Editor
The University of Kitakyushu
(Formerly University of Tokyo)

American Chemical Society, Washington, DC

Downloaded by 217.66.152.143 on September 14, 2012 | http://pubs.acs.org
Publication Date: January 24, 2002 | doi: 10.1021/bk-2002-0809.fw001

Library of Congress Cataloging-in-Publication Data

COO conversion and utilization / Chunshan Song, Anne F. Gaffney, Kaoru Fujimoto, editors.

p. cm.—(ACS symposium series ; 809)

Includes bibliographical references and index.

ISBN 0–8412–3747–6

1. Carbon dioxide—Congresses. 2. Carbon dioxide—Environmental aspects—Congresses.

I. Song, Chunshan. II. Gaffney, Anne F., 1954- III. Fujimoto, Kaoru, 1941. IV. American Chemical Society. Division of Petroleum Chemistry. V. American Chemical Society. Meeting (219th : 2000 : San Francisco, Calif.) VI. Series.

QD181.C1 C52 2001
546′6812—dc21
2001053943

The paper used in this publication meets the minimum requirements of American National Standard for Information Sciences—Permanence of Paper for Printed Library Materials, ANSI Z39.48–1984.

Copyright © 2002 American Chemical Society

Distributed by Oxford University Press

All Rights Reserved. Reprographic copying beyond that permitted by Sections 107 or 108 of the U.S. Copyright Act is allowed for internal use only, provided that a per-chapter fee of $20.50 plus $0.75 per page is paid to the Copyright Clearance Center, Inc., 222 Rosewood Drive, Danvers, MA 01923, USA. Republication or reproduction for sale of pages in this book is permitted only under license from ACS. Direct these and other permission requests to ACS Copyright Office, Publications Division, 1155 16th St., N.W., Washington, DC 20036.

The citation of trade names and/or names of manufacturers in this publication is not to be construed as an endorsement or as approval by ACS of the commercial products or services referenced herein; nor should the mere reference herein to any drawing, specification, chemical process, or other data be regarded as a license or as a conveyance of any right or permission to the holder, reader, or any other person or corporation, to manufacture, reproduce, use, or sell any patented invention or copyrighted work that may in any way be related thereto. Registered names, trademarks, etc., used in this publication, even without specific [illegible] by law.

QD 181 .C1C52 2002 c. 1

PRINTED IN THE UNITED S[illegible]

Downloaded by 217.66.152.143 on September 14, 2012 | http://pubs.acs.org
Publication Date: January 24, 2002 | doi: 10.1021/bk-2002-0809.fw001

Downloaded by 217.66.152.143 on September 14, 2012 | http://pubs.acs.org
Publication Date: January 24, 2002 | doi: 10.1021/bk-2002-0809.fw001

Foreword

The ACS Symposium Series was first published in 1974 to provide a mechanism for publishing symposia quickly in book form. The purpose of the series is to publish timely, comprehensive books developed from ACS sponsored symposia based on current scientific research. Occasionally, books are developed from symposia sponsored by other organizations when the topic is of keen interest to the chemistry audience.

Before agreeing to publish a book, the proposed table of contents is reviewed for appropriate and comprehensive coverage and for interest to the audience. Some papers may be excluded to better focus the book; others may be added to provide comprehensiveness. When appropriate, overview or introductory chapters are added. Drafts of chapters are peer-reviewed prior to final acceptance or rejection, and manuscripts are prepared in camera-ready format.

As a rule, only original research papers and original review papers are included in the volumes. Verbatim reproductions of previously published papers are not accepted.

ACS Books Department

Downloaded by 217.66.152.143 on September 14, 2012 | http://pubs.acs.org
Publication Date: January 24, 2002 | doi: 10.1021/bk-2002-0809.pr001

Preface

Conversion and utilization of carbon dioxide, CO_2, is an important area of research for effective resource utilization and for sustainable development. CO_2 is also a greenhouse gas whose concentration in the atmosphere has increased considerably in the last century. Consequently, CO_2 utilization should be considered as an integral part of carbon dioxide management, because chemical conversion can not only add value to CO_2 disposal, but also have environmental benefits. To foster the research and development in this area, we organized a symposium on CO_2 Conversion and Utilization as a part of the 219th American Chemical Society (ACS) National Meeting, March 26–31, 2000, in San Francisco, California. This symposium was sponsored by the ACS Division of Petroleum Chemistry, Inc. This book was developed based on this ACS symposium.

This book contains 25 peer-reviewed chapters that cover various aspects of CO_2 conversion and utilization. Most of the chapters were developed from ACS papers presented at the above-mentioned symposium, and several chapters were invited contributions from leaders in the related research areas. The technical contents can be grouped into the following topics: (1) general overview, (2) synthesis of organic chemicals, (3) CO_2 reduction over heterogeneous catalysts, (4) synthesis gas production from CO_2 reforming, (5) effects of pressure and reactor type on CO_2 reforming, (6) photocatalytic and electrochemical reduction, and (7) use of supercritical CO_2 fluid.

The individual chapters are contributed by active research groups from university, national laboratories, and industrial research organizations worldwide. The invited review chapters by leading experts cover the state of the arts in a wide variety of specific research topics, including CO_2 mitigation and fuel production by Meyer Steinberg; organic chemicals synthesis using CO_2 as a building block by Michele Aresta; multifunctional catalysts for effective conversion of CO_2 to valuable compounds by Tomoyuki Inui; CO_2 emission reductions at the source by new catalytic technology by Leo Manzer; photocatalytic reduction of CO_2 with H_2O by Hiromi Yamashita and Masakazu Anpo; and use of supercritical-CO_2 as a medium in catalytic reaction processes by Bala Subramaniam and Daryle H. Busch. An introductory overview, which discusses the basic problems, scope, challenges, and opportunities of CO_2 conversion and utilization, is provided by Chunshan Song.

All the contributions including the invited reviews were sent to two or three referees, and only the manuscripts that passed through the peer review process were incorporated in this book. As a result, some of the contributed manuscripts were not accepted, and most manuscripts were accepted after some revisions.

We thank all the authors of the ACS book chapters, especially those who contributed to both the ACS book and the ACS symposium. We are very grateful to the authors of invited reviews, which substantially enhanced the breadth and depth of the scientific contents of this book. We express our sincere appreciation to all the peer reviewers whose time and efforts in evaluating the manuscripts have enhanced the quality of most chapters in the book, to the ACS Division of Petroleum Chemistry, Inc. for sponsoring this symposium, to the Department of Energy and Geo-Environmental Engineering of the Pennsylvania State University for the general support of this book project with respect to numerous mailings and communications, and to ACS Books Department for the skillful assistance of Kelly Dennis and Stacy VanDerWall in the acquisition process and of Margaret Brown in the editing and production process.

Chunshan Song
Department of Energy & Geo-Environmental Engineering
The Pennsylvania State University
206 Hosler Building
University Park, PA 16802–5000

Anne M. Gaffney
Rohm and Haas Company
727 Norristown Rd.
Spring House, PA 19477–0904

Kaoru Fujimoto
(Formerly University of Tokyo)
Department of Chemical Process and Environments
Faculty of International Engineering
The University of Kitakyushu
Wakamatsu-ku, Kitakyushu City,
Fukuoka 808–0135, Japan

Downloaded by 217.66.152.143 on September 14, 2012 | http://pubs.acs.org
Publication Date: January 24, 2002 | doi: 10.1021/bk-2002-0809.pr001

Chapter 1

CO_2 Conversion and Utilization: An Overview

Chunshan Song

Clean Fuels and Catalysis Program, The Energy Institute, and Department of Energy & Geo-Environmental Engineering, The Pennsylvania State University, 209 Academic Projects Building, University Park, PA 16802

Downloaded by 217.66.152.143 on September 14, 2012 | http://pubs.acs.org
Publication Date: January 24, 2002 | doi: 10.1021/bk-2002-0809.ch001

This article provides an introductory overview for defining the scope, potential and limitations of carbon dioxide (CO_2) conversion and utilization. There are various sources of CO_2 emissions, which are dominated by combustion of liquid, solid, and gaseous fuels. The amount of CO_2 consumption for organic chemicals is relatively small compared to CO_2 emitted from fossil fuel combustion. However, CO_2 conversion and utilization should be an integral part of carbon management. Proper use of CO_2 for chemical processing can add value to the CO_2 disposal by making industrially useful carbon-based products. Studies on CO_2 conversion into carbon-based chemicals and materials are important for sustainable development. CO_2 conversion and utilization could also be positioned as a step for CO_2 recycling and resource conservation.

Carbon dioxide, CO_2, is a colorless and odorless gas. The molecule is linear with a double bond between the carbon and oxygen atoms (O=C=O). CO_2 occurs in nature and serves as source of carbon for photosynthesis of plants and crops. It is present in atmosphere with a volumetric concentration of 0.037 % (368 parts per million by volume) as of December 1999 (1). Combustion of most carbon-containing substances produces CO_2. Energy utilization in modern societies today is based on combustion of carbonaceous fuels, which are

In CO2 Conversion and Utilization; Song, C., et al.;
ACS Symposium Series; American Chemical Society: Washington, DC, 2002.

dominated by the three fossil fuels-coal, petroleum, and natural gas. Complete oxidation or combustion of any carbon-based organic matter produces CO_2, but until recently, CO_2 gas was generally thought to be harmless. In fact, CO_2 plays an important role in the Earth's carbon cycle, and is a necessary ingredient in the life cycle of animals and plants (2, 3). However, CO_2 is also a greenhouse gas (GHG), and the concentration of CO_2 in the atmosphere has increased significantly (1, 4, 5). There are increasing concerns for global warming and thus heightened interest worldwide for reducing the emissions of greenhouse gases, particularly CO_2 (4, 5).

This article is a general overview on CO_2 emissions, CO_2 conversion and utilization. The purposes of this overview are to define the scope, limitations, and potential of CO_2 conversion and utilization, and to discuss the challenges and opportunities, because CO_2 conversion and utilization should be an integral part of carbon management. Specific topical reviews are available on synthesis of organic chemicals by Aresta (6, 7), on chemical conversion of CO_2 over heterogeneous catalysts by Inui et al. (8, 9), Arakawa (10) and Park et al. (11), on synthesis gas production from CO_2 reforming of methane by Rostrup-Nielsen et al. (12, 13), Wang et al. (14) and Bradford and Vannice (15), on reactions in supercritical CO_2 as a reaction medium by Leitner (16) and Subramaniam and Busch (17), on polymer synthesis and processing using supercritical CO_2 by Cooper (18), on thermodynamics of chemical reactions by Xu and Moulijn (19), and on various chemical reactions involving CO_2 in the books by Paul and Pradier (4) and by Halmann and Steinberg (5).

Downloaded by 217.66.152.143 on September 14, 2012 | http://pubs.acs.org
Publication Date: January 24, 2002 | doi: 10.1021/bk-2002-0809.ch001

Sources of CO_2 Emissions

The sources of CO_2 emissions include stationary, mobile, and natural sources, as listed in Table 1. The anthropogenic emissions include those from energy utilization in stationary and mobile sources, but exclude natural sources.

Table 2 shows the worldwide CO_2 emissions from the consumption of fossil fuels during 1980-1997 in million metric tons of carbon equivalent (MMTCE) (20, 21). Most countries in the world are consuming fossil fuels in stationary and/or mobile devices and thus contribute to CO_2 emissions.

Table 3 shows the U.S. emissions of CO_2 from different sectors including residential, commercial, industrial and transportation sectors (22, 23). It is clear from Table 3 that every sector is contributing for CO_2 emissions, even the residential homes are responsible because the electricity used in this sector is derived largely by fossil fuel-based electric power plants. During 1980-1997, CO_2 emissions from U.S. industrial sector decreased somewhat (from 484.6 to 482.9 MMTCE), but those from transportation sector increased significantly, from 378.1 to 473.1 MMTCE.

Within the industrial sector, there are two principal routes of CO_2 formation, manufacturing of industrial products where CO_2 is a byproduct from the process (such as the processes for production of cement, limestone, hydrogen, and ethylene oxide), and from energy supply (either as process heat or as electricity) by combustion of fossil fuels which produces CO_2.

Downloaded by 217.66.152.143 on September 14, 2012 | http://pubs.acs.org
Publication Date: January 24, 2002 | doi: 10.1021/bk-2002-0809.ch001

Table 1. Sources of Carbon Dioxide (CO_2) Emissions

Stationary Sources	Mobile Sources	Natural Sources
Fossil Fuel-based Electric Power Plants	Cars, and Sports Utility Vehicles	Humans
Independent Power Producers	Trucks and Buses	Animals
Manufacturing Plants in Industry[a]	Aircrafts	Plant & Animal Decay
Commercial & Residential Buildings	Trains & Ships	Land Emission/Leakage
Flares of Gas at Fields	Construction Vehicles	Volcano
Military & Government Facilities	Military Vehicles & Devices	Earthquake

a) Major concentrated CO_2 sources include plants for manufacturing cement, limestone, hydrogen, ammonia, and soda ash as well as fermentation processes and chemical oxidation processes.

Downloaded by 217.66.152.143 on September 14, 2012 | http://pubs.acs.org
Publication Date: January 24, 2002 | doi: 10.1021/bk-2002-0809.ch001

Table 2. World CO_2 Emissions from the Consumption of Fossil Fuels during 1980-1997 (in Million Metric Tons of Carbon Equivalent)

World Regions	**1980**	**1990**	**1997**
North America	1484.2	1561.4	1725.8
Central and South America	173.0	187.4	242.5
Western Europe	1022.1	1011.2	990.2
Eastern Europe & Former U.S.S.R.	1111.4	1297.9	851.8
Middle East	137.2	200.8	264.0
Africa	145.7	198.4	236.4
Far East and Oceania	977.2	1429.9	1921.1
World Total	**5050.8**	**5886.9**	**6231.7**
Selected Countries			
United States	1290.8	1352.1	1488.5
Former U.S.S.R.	807.3	1035.7	N/A
Russia	N/A	N/A	421.8
China	393.0	620.4	821.8
Japan	260.4	273.6	296.7
Germany	N/A	N/A	234.4
Germany, East	82.6	78.4	N/A
Germany, West	207.7	188.8	N/A
United Kingdom	167.7	167.4	156.9
Canada	125.2	127.8	143.4
France	135.4	103.1	101.7
Poland	115.2	90.8	95.2
Italy	102.4	113.3	115.8
Former Czechoslovakia	88.5	79.7	N/A
India	82.2	155.7	237.3
Mexico	68.1	81.2	93.7
South Africa	64.2	80.5	98.9
Spain	59.0	62.0	67.8
Australia	54.3	74.4	88.8
Netherlands	53.3	59.9	64.4
Brazil	51.8	57.7	77.3
Romania	46.8	49.5	31.3
Belgium	37.4	34.2	36.8
Korea, South	35.0	60.6	116.3
Venezuela	25.0	29.8	37.3
Sweden	24.1	14.8	15.1
Indonesia	23.2	40.0	67.1
Turkey	18.0	35.0	44.6
Austria	16.5	16.1	16.8
Switzerland	13.1	12.1	12.6

Sources: DOE, EIA, 1998, 1999; N/A: not available, or not applicable.

Table 4 shows the U.S. CO_2 emissions from electricity-generating units that include both electric utilities and non-utilities (independent power producers) (22, 23). There are far more coal-fired units in the electric utilities, while natural gas-fired units are more popular among the independent producers. Overall, CO_2 emissions from utilities and non-utilities contribute 523.4 and 134.4 MMTCE, respectively. Coal-fired units produced most CO_2 (496.6 MMTCE), followed by gas-fired units (89.3 MMTCE) and petroleum-based units (22.4 MMTCE).

In addition to CO_2, there are several other greenhouse gases (GHGs). Table 5 shows the U.S. emissions of greenhouse gases during 1990-1997, based on a report published in 2000 by the Energy Information Administration of U.S. Department of Energy (24). Methane, nitrous oxides and fluorinated compounds have much stronger greenhouse gas effects than CO_2. However, their amounts are much smaller. The emissions of all the GHGs are shown on the same basis using the same unit of million metric tons of carbon equivalent (MMTCE) based on global warming potential (24). The 1997 GHG emissions in the U.S. reached 1816 MMTCE, including contributions by CO_2 (1505 MMTCE), CH_4 (165 MMTCE), NOx (103 MMTCE) and other greenhouse gases totaling 38 MMTCE. It is clear from these data that CO_2 is by far the most dominant GHG.

Downloaded by 217.66.152.143 on September 14, 2012 | http://pubs.acs.org
Publication Date: January 24, 2002 | doi: 10.1021/bk-2002-0809.ch001

Control of CO_2 Emissions

Figure 1 shows the key issues related to greenhouse gas control and utilization. The basic issues of GHG control involve energy economics, policy regulations, environmental protection and global climate change. Control of CO_2 emissions is among most important areas of GHG control. The anthropogenic emissions of GHGs are due mainly to the fossil energy utilization. The economic development in the U.S. has benefited greatly from relatively cheap energy sources. The idea for regulation of CO_2 emissions by ratifying Kyoto Protocol has not been popular in the U.S., although emissions of pollutants (SOx, NOx, CO, HC, particulate matters, etc.) are being regulated strictly in the U.S. On the other hand, carbon tax has already been implemented for CO_2 emissions in some countries in Western Europe.

There are five broadly defined technical options for control of CO_2 emissions: energy choices, energy efficiency, CO_2 capture, CO_2 sequestration, and CO_2 utilization. These options are briefly discussed below.

Energy choice is the basic consideration for selecting the primary energy input for new installations of energy systems or for switching between different forms of energy for existing energy systems. One can reduce the CO_2 emission per million BTU by selecting the less CO_2-intensive form of energy, for example, natural gas versus coal. An empirical rule of thumb is the atomic hydrogen-to-carbon ratio; the higher the H/C ratio, the lower the amount of CO_2 per million BTU. The H/C ratio decreases in the order of natural gas (about 3-4), petroleum (about 1.8-2.0), and coal (about 0.8-1.2). Fuel decarbonization before combustion is an option that is being studied as one way to mitigate CO_2 emissions to atmosphere (5), which is also related to the above discussion with respect to fuel H/C ratio changes.

Table 3. U.S. CO_2 Emissions from Different Sectors (Million Metric Tons of Carbon Equivalent)

CO_2 Emissions Sources	1980	1990	1997
CO_2 from Residential Sector	248.4	253.1	286.5
CO_2 from Commercial Sector	178.3	206.8	237.2
CO_2 from Industrial Sector	484.6	454.1	482.9
CO_2 from Transportation Sector	378.1	432.1	473.1
CO_2 from End-Use Total	1289.4	1346.1	1479.6
CO_2 from Electric Utilities*	418.4	476.9	523.4

Sources: DOE, EIA, 1998, 1999

*Electric Utility emissions are distributed across end-use sectors.

Table 4. U.S. CO_2 Emission from Electricity-Generating Units (Million Metric Tons of Carbon Equivalent)

CO_2 Emissions Sources	1990	1995	1997
Coal-Fired Units at Electric Utilities	409.9	434.3	471.3
Petroleum-Fired Units at Electric Utilities	25.3	13.0	15.0
Gas-Fired Units at Electric Utilities	39.2	44.5	36.0
Other Units at Electric Utilities	1.2	0.8	1.0
Emissions at Electric Utilities, Sub-total	475.5	492.7	523.4
Coal-Fired Units at Nonutilities	17.8	24.6	25.3
Petroleum-Fired Units at Nonutilities	4.3	7.3	7.4
Gas-Fired Units at Nonutilities	39.2	57.6	53.2
Other Units at Nonutilities	37.4	45.9	48.4
Emissions at Nonutilities, Sub-total	98.7	135.5	134.4
CO_2 from Coal-Fired Units, Total	427.7	458.9	496.6
CO_2 from Petroleum-Fired Units, Total	29.6	20.3	22.4
CO_2 from Gas-Fired Units, Total	78.4	102.1	89.3
CO_2 from Other Units, Total	38.5	46.8	49.4
Total CO_2 Emissions from Generators	574.2	628.1	657.7

Sources: DOE, EIA, 1998, 1999

Downloaded by 217.66.152.143 on September 14, 2012 | http://pubs.acs.org
Publication Date: January 24, 2002 | doi: 10.1021/bk-2002-0809.ch001

Downloaded by 217.66.152.143 on September 14, 2012 | http://pubs.acs.org
Publication Date: January 24, 2002 | doi: 10.1021/bk-2002-0809.ch001

Table 5. U.S. Emissions of Greenhouse Gases during 1990-1999 Based on Global Warming Potential[a] (Million Metric Tons of Carbon Equivalent)

Gas	1990	1995	1997	1999-P
Carbon Dioxide	1,351	1,435	1,505	1,527
Methane	182	179	172	165
Nitrous Oxide	99	106	104	103
HFCs, PFCs, and SF6	24	29	35	38
Total	1,655	1,748	1,816	1,833

a) Source: EIA Report, US DOE, EIA/DOE-0573(99), October 31, 2000

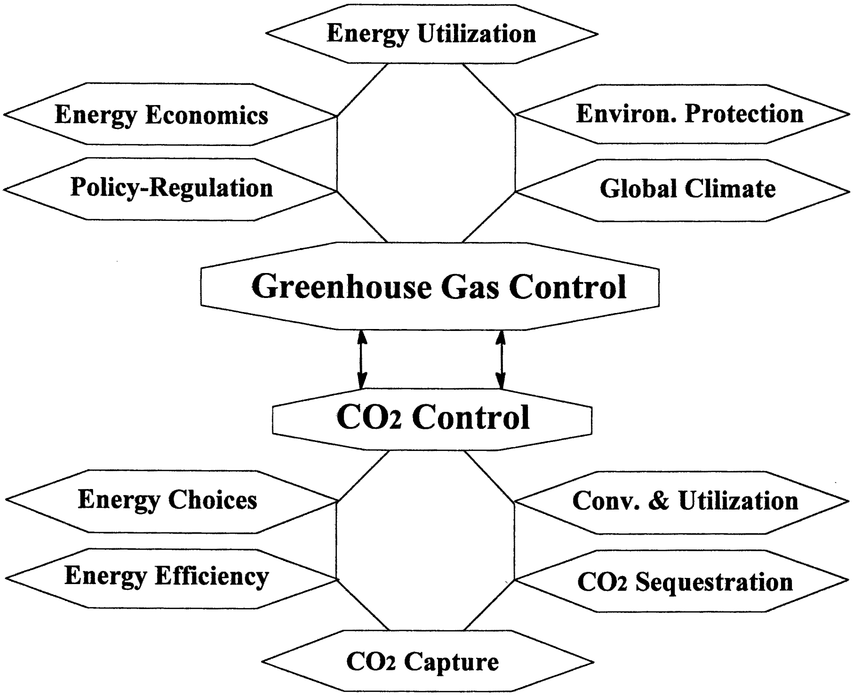
Energy Utilization
Energy Economics
Environ. Protection
Policy-Regulation
Global Climate
Greenhouse Gas Control
CO_2 Control
Energy Choices
Conv. & Utilization
Energy Efficiency
CO_2 Sequestration
CO_2 Capture

Figure 1. Key issues for control of greenhouse gas and related technical areas for CO_2 control.

An alternative is to use more renewable energy. Common renewable energy forms include hydropower, solar energy, wind energy, and biomass. Biomass and animal wastes are opportunity fuels whose use is also encouraged where available. They are not completely CO_2-neutral, because the collection and transportation of biomass consume energy and fuels. The issues of major concerns on biomass include the regional and seasonal availability as well as energy density and energy demand-supply balance. Combination of biomass with fossil energy in certain ways including conversion is also being explored (25). Solar energy could also be used in selected endothermic chemical processes to reduce the need for using heat from combustion of fossil fuels which also produces CO_2. The issues of concerns for renewable energy in general are energy density, availability, energy efficiency, and capital cost.

Development for improved energy efficiency is an important area that has a major impact on CO_2 reduction. Existing energy utilization systems in the fossil fuel-based electricity generators in the U.S. have an average efficiency of about 35% (26). In other words, about 65% of the useful energy input to the electric power units is wasted as conversion loss. The efficiencies for the automobiles are even lower, less than 20% (27). While significant improvements of energy efficiencies have been achieved in the past decades in power generation technologies and in transportation vehicles, there is a thermodynamic limit for the heat engines by Carnot cycle, which basically dictates the operation. Development and implementation of new energy utilization systems such as IGCC for coal-based power plants, GTCC for natural gas-based power plants, and fuel cell-based hybrid motors for transportation, could increase the energy efficiencies significantly, by 30% or more. The same principle can be applied to chemical industry, where more efficient process or more selective catalyst can make a process such as oxidation reaction more selective such that CO_2 formation is minimized at the source, thus improving the process efficiency, conserving hydrocarbon resource, and reducing CO_2 formation at the source (28).

Downloaded by 217.66.152.143 on September 14, 2012 | http://pubs.acs.org
Publication Date: January 24, 2002 | doi: 10.1021/bk-2002-0809.ch001

CO_2 Capture and Sequestration

CO_2 capture involves chemical or physical separation of CO_2 from gas mixtures. Common methods include absorption using an agent such as monoethanol amine, physical adsorption using solid adsorbent, cryogenic separation at low temperatures, and membrane separation (see below). CO_2 sequestration refers to long-term storage of CO_2 in various reservoir locations with large capacity, such as geologic formations, ocean, aquifers, and forest (29-31).

The industrial separation of CO_2 from flue gas of power plants is currently carried out by using absorption process with monoethanol amine as the liquid absorbent (32, 33). It is usually carried out using gas mixtures that contain CO_2 in relatively high concentrations. Large-scale separations in industry are currently based on chemical absorption of CO_2 from concentrated gas mixtures such as flue gases from power plants, from hydrogen plants or from ammonia plants. The Fluor Daniel ECONAMINE FG CO_2 recovery process that was developed by Dow Chemical is one of the widely used commercial processes (34). The process uses an amine solution, in which a proprietary additive is present, to remove CO_2 economically from low-pressure, oxygen-containing streams such as flue gas. Some recent large-scale designs for CO_2 recovery from flue gas are proposed for use in CO_2-enhanced oil recovery (35). It is known that for the conventional liquid scrubber, the sterically hindered amine requires considerably less energy for regeneration than conventional monoethanolamine (36). A team of researchers at Argonne National Laboratory has conducted a study to identify and evaluate the advantages and deficiencies of several technologies for capturing CO_2 from the flue gas of utility boilers, including chemical solvent, cryogenic, membrane, physical absorption, and physical adsorption methods (37).

Downloaded by 217.66.152.143 on September 14, 2012 | http://pubs.acs.org
Publication Date: January 24, 2002 | doi: 10.1021/bk-2002-0809.ch001

Physical adsorption can be used for separation of gas mixtures. Activated carbons and carbon molecular sieves are readily available commercially, and many studies have been conducted on CO_2 adsorption using such materials. A well-planned and carefully conducted study by Yang and coworkers at SUNY-Buffalo has demonstrated that PSA by using carbon molecular sieve could generate pure CO_2 at low recovery, but generally the kinetic selectivity of CO_2/N_2 is not high enough (38). Separation of CO_2 from air is usually not economical, but there are special applications for such separation in spacecraft using solid sorbent.

CO_2 capture and sequestration (storage) are active areas of study worldwide, and recent reviews are available on the state of the art (29, 31, 33), on the options for CO_2 removal from fossil-fueled power plants (39, 40), on U.S. DOE perspectives (41, 42), on the international perspectives (43), and on the membrane technologies for gas separation in general (44). As indicated in most reviews, technologies for capturing CO_2 are available but are still relatively energy-intensive and thus relatively expensive. Further research, particularly novel approaches, are necessary for lowering the cost of CO_2 utilization. An alternative approach has been proposed to use CO_2 along with H_2O and O_2 in flue gas for tri-reforming of natural gas without CO_2 pre-separation (45).

CO_2 Conversion and Utilization

CO_2 conversion refers to its transformation to chemically different forms that contain the carbon of CO_2 or that makes use of active "oxygen atom" from CO_2. CO_2 utilization includes the uses of CO_2 in both physical processes such as extraction and chemical processes such as chemical synthesis. The objectives of research and development efforts on CO_2 conversion and utilization can include one or more of the following specific goals depending on the applications: (1) to make use of CO_2 for environmentally-benign physical or chemical processing based on the unique physical or chemical properties of CO_2; (2) to produce useful chemicals and materials using CO_2 as a reactant or feedstock; (3) to replace a hazardous substance or a less-effective substance in existing processes with CO_2 as an alternate medium or solvent or co-reactant or a combination of them; (4) to use CO_2 for recovering energy or for growing biomass while reducing its emissions to the atmosphere by sequestration; (5) to recycle CO_2 as carbon source for chemicals and fuels; (6) to convert CO_2 under geologic-formation conditions into "new fossil" energies.

Table 6 shows the properties of carbon dioxide (2, 3, 46-48). CO_2 may be used as a gas, liquid, and solid. At atmospheric pressure, CO_2 is about 1.5 times as heavy as air (2, 3). CO_2 may be liquefied by compressing to 2 MPa and cooling to –18 °C, or by compressing to higher pressure of 5.78 MPa at 21 °C. If liquid CO_2 is cooled further to -56.6 °C, the pressure drops to 0.518 MPa, solid CO_2 is formed which co-exists with liquid and gaseous CO_2. This is known as the triple point. The solid CO_2 can sublimate directly into gas (without going through the liquid phase) upon absorbing heat, and thus it is called dry ice. CO_2 can not exist as liquid below the triple point. If the pressure on dry ice is reduced to atmospheric pressure, the temperature of dry ice drops to -78.5 °C. CO_2 can not be liquefied above 31 °C, the critical temperature. It exists as supercritical fluid when the temperature and pressure are above 31 °C (Tc) and 7.38 MPa (Pc), respectively.

Currently, CO_2 is used as refrigerant for food preservation, beverage carbonation agent, inert medium (such as fire extinguisher), pressurizing agent, supercritical solvent, chemical reactant (urea, etc.), neutralizing agent, and as gas for greenhouses (2, 3, 46, 49). Solid CO_2 (dry ice) has a greater refrigeration effect than water ice. Dry ice is also usually much colder than water ice, and the dry ice sublimates to a gas as it absorbs heat. It should be noted that the use of CO_2 for refrigeration does not contribute to reduction of CO_2 emissions.

Thermodynamics of CO_2 Conversion. Figure 2 illustrates the thermodynamics of CO_2 conversion, where Gibbs free energy of CO_2 and related substances are shown along with CO_2. The data for plotting Figure 2 were taken mainly from two comprehensive chemical handbooks (47, 48). CO_2 is a highly stable molecule. Consequently a substantial input of energy, effective reaction conditions, and often active catalysts, are necessary for chemical conversion of CO_2. In other words, many reactions for CO_2 conversion involve positive change in enthalpy, ΔH, and thus they are endothermic. However, it should be pointed out that the chemical reactions are driven by the difference in Gibbs free energy between the products and reactants at certain conditions, as shown by the equation below.

$$\Delta G = \Delta H - T\,\Delta S$$

There appears to be some perceptions by many people that CO_2 conversion would be so endothermic that its conversion would not be feasible. It is true that endothermic reactions consume energy. However, endothermic reactions can be feasible and indeed useful. There are many chemical manufacturing plants that are operated based on endothermic reactions in the chemical industry, and these include pyrolysis (thermal cracking) of

Downloaded by 217.66.152.143 on September 14, 2012 | http://pubs.acs.org
Publication Date: January 24, 2002 | doi: 10.1021/bk-2002-0809.ch001

Downloaded by 217.66.152.143 on September 14, 2012 | http://pubs.acs.org
Publication Date: January 24, 2002 | doi: 10.1021/bk-2002-0809.ch001

Table 6. Physical and Chemical Properties of Carbon Dioxide

Property	Value and Unit
Sublimation point at 1 atm (101.3 kPa)	- 78.5 °C
Triple point at 5.1 atm (518 kPa)	- 56.5 °C
Critical temperature (T_c)	31.04 °C
Critical pressure (P_c)	72.85 atm (7383 kPa)
Critical density (ρ_c)	0.468 g/cm^3 or 468 g/L
Gas density at 0 °C and 1 atm (101.3 kPa)	1.976 g/L
Liquid density at 0 °C and 1 atm (101.3 kPa) 25 °C and 1 atm CO_2 (101.3 kPa)	 928 g/L 0.712 vol/vol
Solid density	1560 g/L
Specific volume at 1 atm and 21 °C	0.546 m^3/kg
Latent heat of vaporization At the triple point (- 78.5 °C) At 0 °C	 353.4 J/g 231.3 J/g
Viscosity at 25 °C and 1 atm CO_2 (101.3 kPa)	0.015 cP (mPas)
Solubility in water at 0 °C and 1 atm (101.3 kPa) 25 °C and 1 atm (101.3 kPa)	0.3346 g CO_2/100 g-H_2O or 1.713 mL CO_2/mL-H_2O at 0 °C 0.1449 g CO_2/100 g-H_2O or 0.759 mL CO_2/mL-H_2O at 25 °C
Heat of formation at 25 °C	- 393.5 kJ/mol
Entropy of formation at 25 °C	213.6 J/K•mol
Gibbs free energy of formation at 25 °C	- 394.3 kJ/mol

Downloaded by 217.66.152.143 on September 14, 2012 | http://pubs.acs.org
Publication Date: January 24, 2002 | doi: 10.1021/bk-2002-0809.ch001

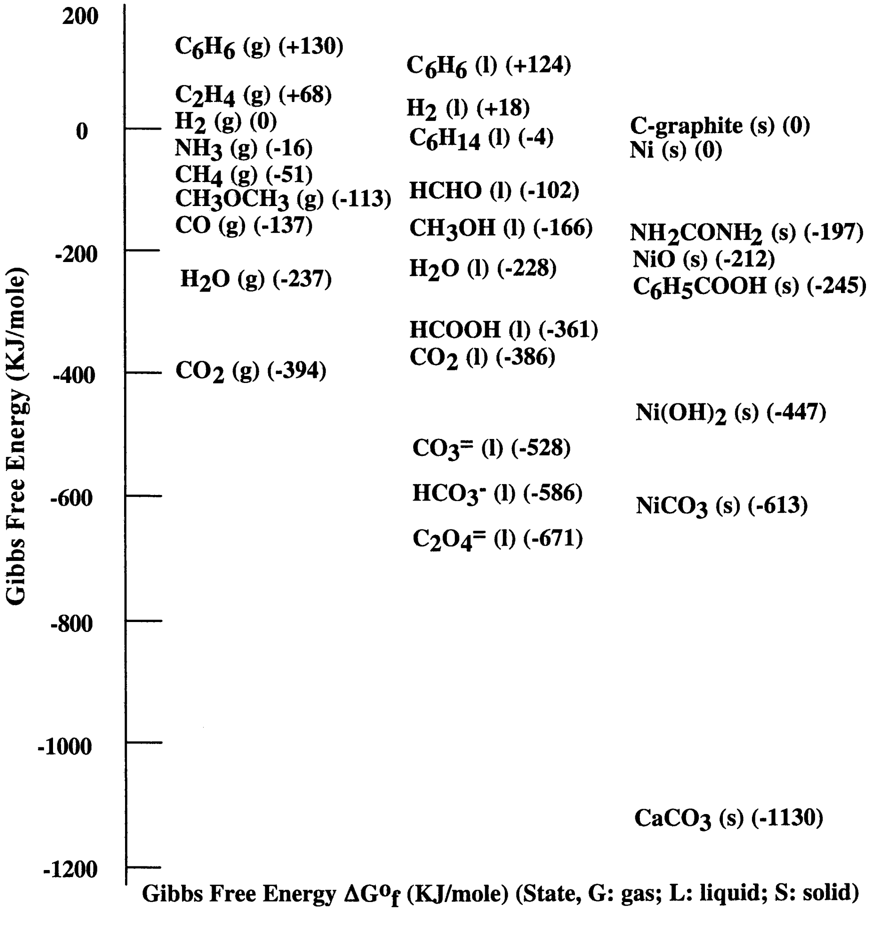

Figure 2. Gibbs free energy of formation for CO_2 and related molecules.

hydrocarbons for manufacture of ethylene and propylene, dehydrogenation reaction for manufacture of petrochemicals such as styrene from ethylbenzene, and steam reforming of hydrocarbons for producing synthesis gas and hydrogen. A simple comparison between steam reforming of methane and CO_2 reforming of methane can illustrate this point. Both reactions are endothermic that require over 200 kJ of energy input per mole of CH_4, but CO_2 reforming requires about 20% more energy input compared to steam reforming. The two reactions give synthesis gas products with different H_2/CO molar ratios; both are useful for certain applications.

A careful analysis of the thermodynamic data in Figure 2 would reveal that it is more energy-demanding if one were to use only CO_2 as a single reactant, but it becomes easier thermodynamically if CO_2 is used as a co-reactant with another substance that has higher Gibbs free energy, such as CH_4, carbon (graphite) and H_2. This trend can also be seen by the change in the reaction heat for reactions with CO_2 as the single reactant [e.g., $CO_2 = CO + 1/2\ O_2$; $\Delta H° = +293$ kJ/mole CO_2] and with CO_2 as a co-reactant [e.g., $CO_2 + H_2 = CO\ (g) + H_2O\ (g)$; $\Delta H° = +51$ kJ/mole CO_2].

Current Status and Potential Market of CO_2 Utilization. Table 7 shows the 1999 U.S. annual production of CO_2, CO_2-based and CO_2-related chemicals, as well as synthetic organic chemicals and materials (50), in which some 1999 data were derived by estimation based on 1994 data (51). Currently, the U.S. production of liquid and solid CO_2 amounts to 5.36 million tonnes per year (Table 7), which is mainly consumed in the food and beverage industries (refrigerant, coolant, and carbonated drinks). In addition, there are about 10 million tones of CO_2 consumed in making 4.95 million tones of urea fertilizers and 8.47 million tones of urea for chemicals synthesis (Table 7).

The author did an analysis by calculation to set the potential upper limit of hypothetical CO_2 demand for making organic chemicals and materials. Table 7 also shows the potential upper limit of CO_2 demand estimated by the author for chemicals and materials. The methodology of estimation used here is based on that used by Steinberg (5) with modification by considering carbon equivalence in this work. Steinberg used the production data for the plastics in the U.S. in 1980 (5). The present estimation for the carbon-based synthetic materials is based on the U.S. production of plastics, fibers, and rubbers in the 1999 (50). If we assume that the potential upper limit of chemical market demand is that for making all the carbon-based synthetic materials plus several CO_2-related major chemicals and materials using CO_2, then the upper limit of potential CO_2 demand for synthetic organic chemicals and polymer materials could increase to 44.41 million metric tons of carbon equivalent (Table 7). This calculated numbers all correspond to a stoichiometric reaction system where all the carbon in CO_2 is converted to the chemicals (urea, methanol, etc.) and synthetic polymer materials (plastics, fibers, rubbers). This is, of course, a hypothetical scenario, but it does provide an useful measure in terms of order of magnitude.

Downloaded by 217.66.152.143 on September 14, 2012 | http://pubs.acs.org
Publication Date: January 24, 2002 | doi: 10.1021/bk-2002-0809.ch001

Table 7. U.S. Production of Synthetic Plastics and Related Chemicals in 1999 and Estimated Potential Upper Limit of CO_2 Demand for Chemicals and Materials

Chemicals & Materials	Production in Common Units[a]	Metric Tons (Tonnes)
Synthetic Plastics:	80,727 millions of lb	36,650,058
Synthetic Fibers	10,219 millions lb	4,639,426
Synthetic Rubbers	2,414 thousands of metric tons	2,414,000
	1. Polymers Subtotal (1999) =	37,584,996 as C 43,703,484 as Comp
Ammonia (reference for urea) (1999)[a]	14,972 thousands of tons	13,579,604
Urea for fertilizer (1999)[a,b]	5,453 thousands of tons	4,945,871
Urea for chemicals (1999)[a,b]	18,660 millions of lb[b]	8,471,640
Urea for chemicals (1994)[c]	15.90 billions of lb (7,952 thousands of tons)	7,218,600
	2. Urea-equivalent CO_2(1999)=	2,686,185 as C 9,839,508 as CO_2
Methanol for chemicals (1994)[c]	12.18 billions of lb	5,529,720
	3. MeOH-Equivalent CO_2(1999)[f]	2,428,590 as C 8,895,937 as CO_2
CO_2 – Liquid+Solid (1994)[c,d]	11.80 billions of lb (5,899 thousands of tons)	5,357,200
	4. Liquid+Solid CO_2 (1999)[e]	1,711,143 as C 6,267,924 as CO_2
Ultimate U.S. CO_2 demand for chemicals & materials	Total US Potential (1+2+3+4) =	44.4 MMT[g] as C 162.8 MMT as CO_2
Ultimate world CO_2 demand for chemicals & materials	Estimated for World Potential	177.6 MMT as C 651.3 MMT as CO_2

a) Source: ACS. Facts & Figures for the Chemical Industry. C&EN, June 26, 2000, 48-89; b) A significant fraction of the urea is used for making thermosetting plastics that are included in synthetic plastics (2,691 millions of lb urea-based thermosetting resins were produced in 1999); c) Source: ACS. Facts & Figures for the Chemical Industry. C&EN, June 24, 1996, 38-79; d) Liquid and solid CO_2 only; e) 1999 production of liquid+CO2 was estimated (as 1.17 times 1994 production); f) 1999 production of methanol was estimated (as 1.17 times 1994 production); g) MMT: Million metric ton.

Downloaded by 217.66.152.143 on September 14, 2012 | http://pubs.acs.org
Publication Date: January 24, 2002 | doi: 10.1021/bk-2002-0809.ch001

The upper limit of potential market demand worldwide for CO_2 in making organic chemicals and materials is estimated to be 178 million metric tons of carbon equivalent. The detailed statistical data of chemicals production in 1999 are not available for all the countries in the world, but the author did a simplified estimation based on the U.S. chemical production. U.S. chemical industry is the largest in the world, and the plants in the U.S. provide 24% of the world's total chemical production (52). Consequently, the upper limit of potential market demand for CO_2 in the world is estimated by the author to be 4 times that for the U.S.

Table 8 shows the U.S. production of liquid fuels in 1999 (26). The amount of liquid fuels consumed in the U.S. has reached 13.60 million barrel per day, in which 12.75 million barrels per day liquid fuels were used for transportation fuels. By simple calculation of carbon equivalence, it becomes apparent that the liquid fuels correspond to a very large amount of carbon that is on the same order of magnitude with the CO_2 emitted from fossil fuel-based electric power plants in the U.S., as can be seen from Table 8. The total production of liquid fuels in the world is estimated to be about 4 times of the U.S. annual production, based on the fact that U.S. petroleum consumption is about 25% of the world total consumption (26).

Table 9 shows the order of magnitude estimates by the author for CO_2 utilization, based on the data shown in Tables 7 and 8. For comparison, Table 10 shows the order of magnitude estimates published in a recent review by Herzog for the worldwide capacity of various options for CO_2 sequestration (31). The worldwide capacity for utilization of CO_2 for making chemicals and materials is less than 1 Giga tonnes of carbon per year, which is relatively small compared to the several other options such as ocean sequestration. However, it should be noted that the amount of CO_2 that can be utilized for making chemicals and materials can be potentially large enough for expanding commercial-scale applications worldwide.

Challenges and Strategies for CO_2 Conversion and Utilization

Figure 3 is an outline of possible chemical processes that may be used for CO_2 conversion and utilization. There are non-catalytic chemical processes, processes using heterogeneous or homogeneous catalysis, photo-chemical and photo-catalytic reduction, bio-chemical and enzymatic conversion, electro-chemical and electro-catalytic conversion, as well as solar-thermal/catalytic processes. Most of the processes are subjects of research in the laboratory, and few processes have reached large-scale production. A number of reviews have been published concerning various chemical reactions and processes for chemical conversion of CO_2 (4-19, 43, 53, 54).

There exist some chemical processes for CO_2 conversion in chemical industry, for which synthesis of urea from ammonia and CO_2 [$CO_2 + 2\ NH_3 = H_2N\text{-}CO\text{-}NH_2 + H_2O$] and the production of salicylic acid from phenol and CO_2 [$C_6H_5\text{-}OH + CO_2 = C_6H_5(OH)COOH$] are representative examples. Urea is used for making various polymer materials and also for producing fertilizers. As

Downloaded by 217.66.152.143 on September 14, 2012 | http://pubs.acs.org
Publication Date: January 24, 2002 | doi: 10.1021/bk-2002-0809.ch001

Downloaded by 217.66.152.143 on September 14, 2012 | http://pubs.acs.org
Publication Date: January 24, 2002 | doi: 10.1021/bk-2002-0809.ch001

Table 8. U.S. Production of Liquid Fuels in 1999

U.S. Fuels	1999 Daily Production[a]	1999 Annual Production	Total Annual Production[b]	C-Equivalent of Annual Prod[c]
	Million barrels per day	Million barrels per Year	Million Metric Tons (Tonnes)	Million Metric Tons (Tonnes)
Gasoline	8.38	3058.7	354.8	301.6
Distillate Fuels (Diesel, etc)	3.55	1295.8	171.0	145.4
Jet Fuel	1.67	609.6	77.4	65.8
	Total = 13.60 [12.75 in transportation]		U.S. total =	512.8
			World liquid fuel[d] =	2051.2
			1997 US Electric Utilities Annual CO_2 Emissions	523.4 as C

a) Source: EIA, AER, US DOE, 2000.

b) 1 barrel of oil (US) = 42 US gallons = 0.15899 cubic meters (m^3) = 158.99 liters. Assume average density values of the fuels at ambient temperatures as follows: 0.73 g/mL for gasoline; 0.80 g/mL for jet fuel; 0.83 g/mL for distillate fuels (diesel fuel and heating oils).

c) Assume the average carbon content in the liquid fuels is 85 wt%.

d) Estimated based on the fact that U.S. petroleum consumption is about 25% of the world's total consumption.

Downloaded by 217.66.152.143 on September 14, 2012 | http://pubs.acs.org
Publication Date: January 24, 2002 | doi: 10.1021/bk-2002-0809.ch001

Table 9. Order of Magnitude Estimates for the Worldwide Capacity of CO_2 Utilization

Option of CO_2 Utilization	Worldwide Capacity
	(Order of Magnitude in Giga Ton Carbon)
Non-chemical Utilization	0.01 – 0.1 GtC per year
Chemicals & Materials[a]	0.1 – 1 GtC per year
Synthetic Liquid Fuels[a]	1 – 10 GtC per year

a) Estimated by C. Song based on the U.S. and the world production of chemicals and materials as well as liquid fuels in 1999.

Table 10. Order of Magnitude Estimates for the Worldwide Capacity of Various Sinks[a]

Sequestration Option	Worldwide Capacity
	(Order of Magnitude in Giga Ton Carbon)
Ocean	1000s GtC
Deep saline Formations	100s – 1000s GtC
Depleted Oil and Gas Reservoirs	100s GtC
Coal Seams	10s – 100s GtC
Terrestrial	10s GtC
Utilization (Chemical Conversion)	< 1 GtC per year

a) Source. H. J. Herzog. Using Carbon Capture and Sequestration technologies to Address Climate Change Concerns. Am. Chem. Soc. Div. Fuel Chem. Prepr., 2001, 46(1), 53-55.

Downloaded by 217.66.152.143 on September 14, 2012 | http://pubs.acs.org
Publication Date: January 24, 2002 | doi: 10.1021/bk-2002-0809.ch001

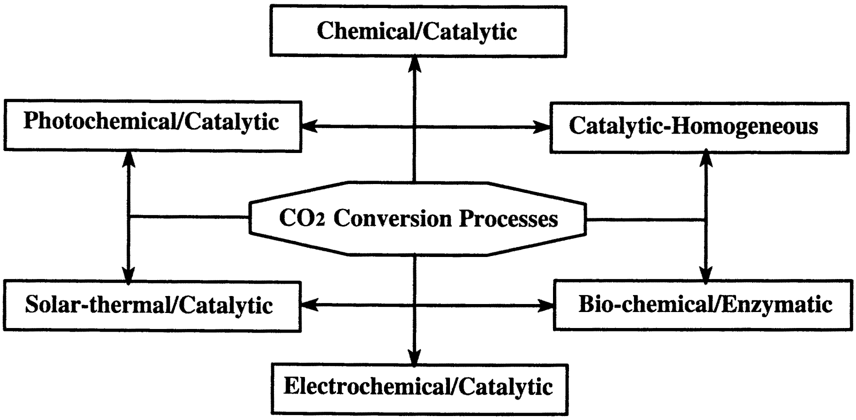
Chemical/Catalytic
Photochemical/Catalytic
Catalytic-Homogeneous
CO2 Conversion Processes
Solar-thermal/Catalytic
Bio-chemical/Enzymatic
Electrochemical/Catalytic

Figure 3. Chemical processes for CO_2 conversion and utilization.

an example of the usefulness of salicylic acid, acetyl salicylic acid is used for making Aspirin, a common medicine.

Urea Synthesis

$$CO_2 + NH_3 = H_2N\text{-}CO\text{-}NH_2 + H_2O$$

Salicylic Acid Synthesis

$$C_6H_5\text{-}OH + CO_2 = C_6H_4(OH)COOH$$

Barriers for CO_2 Conversion and Utilization. There are significant barriers for promoting or enhancing utilization of CO_2 in chemical processes. Such barriers and possible strategies to overcome them are briefly outlined below.

- **1) Costs of CO_2 capture, separation, purification, and transportation to user site.**

One of the strategies would be to identify and use concentrated CO_2-containing gas mixtures at or near the sites of chemical conversion and utilization. From the separation side, better separation methods and improved engineering of separation process can lower this barrier.

However, if it is beneficial and practically applicable, a new processing scheme for using CO_2 in gas mixture without pre-separation of CO_2 would be desired. A proposed new approach is to make industrially useful synthesis gas with desired H_2/CO ratios by using CO_2 along with H_2O and O_2 in flue gas for tri-reforming of natural gas without CO_2 pre-separation (45).

- **2) Energy requirements of CO_2 chemical conversion (plus source & cost of H_2 if involved).**

The corresponding strategies are to use CO_2 as a co-reactant along with one or more compounds that have higher Gibbs free energies, and to identify and use an effective catalyst that can give higher conversion at lower temperatures. CO_2 reduction by hydrogenation has been studied and reported by many research groups. For such processes, H_2 will need to be made from processes that do not co-produce CO_2. It should be noted that H_2 is currently produced by reforming of hydrocarbons which is an energy-intensive process and accompanied by CO_2 formation both from the conversion process and from the combustion of the fuels which is used to provide the process heat (54).

- **3) Market size limitations, and lack of investment-incentives for CO_2-based chemicals.**

The estimated or perceived market sizes for CO_2 conversion vary for different applications. If all carbon-based synthetic chemicals and materials can be made using CO_2, then the current annual production of such chemicals and materials could provide an estimated upper limit of market demands for CO_2 for chemicals and materials.

Downloaded by 217.66.152.143 on September 14, 2012 | http://pubs.acs.org
Publication Date: January 24, 2002 | doi: 10.1021/bk-2002-0809.ch001

- **4) Lack of socio-economical and political driving forces that facilitate enhanced CO_2 utilization.**

There are several ways for an industrialized society to encourage more utilization of CO_2. If an environment-conscious society wants to promote CO_2 utilization, various incentives could be given to manufacturers that produce useful chemicals and materials using CO_2, or make use of CO_2 for environmentally-benign processing (such as replacement of phosgene). If the consumers and buyers in the industrialized societies recognize the need to such a level as to support CO_2 utilization, price differential could be instituted for CO_2 utilization which may be characterized as "carbon pricing for greenness".

Downloaded by 217.66.152.143 on September 14, 2012 | http://pubs.acs.org
Publication Date: January 24, 2002 | doi: 10.1021/bk-2002-0809.ch001

Strategy for Research on CO_2 Utilization. The strategic directions for research and development on CO_2 utilization may include but are not limited to the following considerations along with some specific examples. Figure 4 illustrates the utilization of CO_2 with and without chemical conversion processing.

- **1) To produce useful chemicals and materials using CO_2 as a co-reactant or co-feed.**

Many processes could be designed for using CO_2, but the chemicals and materials that have large market demands are relatively limited. An existing industrial process is urea synthesis, which has already found industrial application as fertilizer and as monomer for thermosetting polymers. Expanding applications of urea-based polymers can create more demand on CO_2 and NH_3 for urea synthesis. For the development of new processes, one of preferred approaches is to explore alternate processes for using CO_2 as a co-reactant in making chemicals that have relatively large market or potentially large demand in the near future.

Production of synthesis gas would fit in this category. Synthesis gas with desired H_2/CO ratios can be used for synthesizing chemicals such as methanol and acetic acid by oxo synthesis, olefinic chemicals and ultra-clean hydrocarbon fuels by Fischer-Tropsch synthesis, and also for electricity generation by using either the GTCC (gas turbine combined cycle) or high-temperature fuel cells such as molten carbonate fuel cells or solid-oxide fuel cells. Using CO_2 and methane by dry reforming alone or in combination with steam reforming, and the synthesis of methanol and synthesis of hydrocarbon chemicals using CO_2-rich synthesis gas would fit in this category. Because of the problem of carbon formation and the limited applications of the synthesis gas with low H_2/CO ratios (around 1) from CO_2 reforming, the combined reforming that involves both CO_2 reforming and steam reforming may be preferred for large-scale applications (13, 45, 55).

Downloaded by 217.66.152.143 on September 14, 2012 | http://pubs.acs.org
Publication Date: January 24, 2002 | doi: 10.1021/bk-2002-0809.ch001

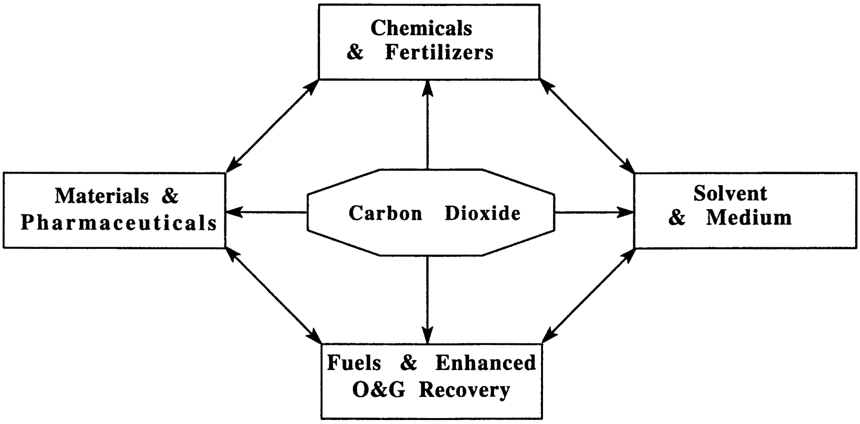
Chemicals & Fertilizers
Materials & Pharmaceuticals
Carbon Dioxide
Solvent & Medium
Fuels & Enhanced O&G Recovery

Figure 4. Utilization of CO_2 with and without chemical conversion processing.

Downloaded by 217.66.152.143 on September 14, 2012 | http://pubs.acs.org
Publication Date: January 24, 2002 | doi: 10.1021/bk-2002-0809.ch001

- **2) To make use of CO_2 based on the unique physical or chemical properties of CO_2 such as supercritical extraction using SC-CO_2 as a solvent.**

Environment-friendly and energy-efficient processes can be designed by using CO_2 for separation and chemical reaction and materials synthesis. For example, supercritical CO_2 can be used as either a solvent for separation or as a medium for chemical reaction, or as both a solvent and a reactant. Use of supercritical CO_2 (SC-CO_2) allows contaminant-free supercritical extraction of various substances ranging from beverage materials (such as coffee bean), foods (such as potato chips), and organic and inorganic functional materials, to herbs and pharmaceuticals and soils.

Some chemical reactions can benefit from using CO_2 as a mild oxidant, or as a selective source of "oxygen" atoms. For example, the use of CO_2 has been found to be beneficial for selective dehydrogenation of ethylbenzene to form styrene, and for dehydrogenation of lower alkanes such as ethane, propane and butane to form ethylene, propylene, and butene, respectively. Some recent studies have been reviewed by Park et al. on heterogeneous catalytic conversion using CO_2 as an oxidant (11).

- **3) To replace a hazardous or less-effective substance in existing processes with CO_2 as an alternate medium or solvent or co-reactant or a combination of them.**

Some of the existing industrial chemical processes use hazardous substances as reactant or reaction medium which could be replaced by CO_2 or supercritical CO_2. One area in this category is replacement of phosgene by CO_2, which has been discussed by Aresta for various chemical processes (56). Shown below is a comparison of different chemical processes for making dimethyl carbonate, an industrially useful chemical. U.S. phosgene use was estimated to be about 1.2 million tonnes per year (56, 57). In terms of environmental benefits, the new CO_2-based route is superior to the existing industrial processes that are based on either phosgene or CO, as both chemicals are toxic.

Conventional Route (By SNPE, 1970s):

$$COCl_2 + 2\ CH_3OH = CH_3OCOOCH_3 + 2\ HCl$$

$$CO + Cl_2 = COCl_2 \text{ (Phosgene)}$$

EniChem DMC Process (By EniChem – 12000 tons/Yr)

$$CO + 1/2\ O_2 + 2\ CH_3OH = CH_3OCOOCH_3 + H_2O$$

Ube DMC Process (By Ube Chemical – 3000 tons/Yr)

$$CO + 2\ RONO = ROC(O)OR + 2\ NO$$

New CO_2-Based Route

$$CO_2 + 2\ CH_3OH = CH_3OCOOCH_3 + H_2O$$

More recent studies by Dibenedetto and Aresta (58) have shown that direct oxidative carboxylation can be achieved using an olefin and CO_2 under an oxidative condition, which can produce the cyclic carbonate chemicals that are currently synthesized in industry by using phosgene.

- **4) To use CO_2 for energy recovery while reducing its emissions to the atmosphere by sequestration.**

CO_2 in flue gas from power plants may be used for enhanced recovery of oil and natural gas, and for enhanced coal bed methane recovery. For enhanced oil recovery, the requirement for CO_2 purity is minimum, and thus the cost of gas processing (prior to use) is lower.

Another approach in this direction is the so-called ocean fertilization which make use of CO_2 in specific locations in the ocean and sun light to grow biomass (59).

- **5) To recycle CO_2 as C-source for chemicals and fuels.**

Recycling of CO_2 as carbon source for chemicals and fuels should be considered for applications where CO_2 can be used that have desired environmental benefits. Although permanent storage seems preferred for carbon sequestration, CO_2 recycling would also make sense if such an option can indeed lead to less consumption of carbon-based fossil resources without producing more CO_2 from the whole integrated system.

The amount of liquid fuel consumed in the U.S. has reached 13.60 million barrel per day, which correspond to a very large amount of carbon that is estimated to be on the same order of magnitude with the CO_2 emitted from fossil fuel-based electric power plants. The proposed approaches include hydrogenation of CO_2 with H_2 to methanol (60, 61), and conversion of CO_2 in flue gas by tri-reforming to synthesis gas ($CO + H_2$) with desired H_2/CO ratios for chemicals and fuels synthesis (45).

- **6) To convert CO_2 under geologic-formation conditions into "new fossil" energies.**

Existing fossil fuels are believed to have originated from bio-chemical and geo-chemical transformations of organic substances that were initially present on the surface of the earth over the course of millions of years, which may be viewed as a detour in the carbon cycle. For example, numerous studies have shown that coal was formed from bio-chemical degradation and geo-chemical maturation of higher plant materials that were formed initially on the surface of the earth via photosynthesis from CO_2 and H_2O. A new way of thinking has led to approaches of converting CO_2 directly in geologic formations during its long-term storage. This is still a new topic for which only a few reports are available (62-64).

Downloaded by 217.66.152.143 on September 14, 2012 | http://pubs.acs.org
Publication Date: January 24, 2002 | doi: 10.1021/bk-2002-0809.ch001

Conclusions

CO_2 conversion and utilization is an important part of CO_2 management strategy, although the amount of CO_2 that can be converted to chemicals and materials is relatively small compared to the amount of anthropogenic CO_2 emitted from fossil fuel combustion. CO_2 is a carbon source and an unique substance, and CO_2 utilization represents an important aspect of greenhouse gas control and sustainable development.

Proper and enhanced uses of CO_2 can have not only environmental benefits, but also add value to the CO_2 disposal by making industrially useful carbon-based chemical products. There exist barriers and challenges for promoting CO_2 utilization, which include but are not limited to the following: 1) Costs of CO_2 capture, separation, purification, and transportation to user site; 2) Energy requirements of CO_2 chemical conversion (plus source & cost of H_2 if involved); 3) Market size limitations, and lack of investment-incentives for CO_2-based chemicals; and 4) Lack of socio-economical and political driving forces that facilitate enhanced CO_2 utilization.

The following strategic considerations may be helpful for future directions: 1) To produce useful chemicals and materials using CO_2 as a co-reactant or co-feed; 2) To make use of CO_2 based on the unique physical or chemical properties of CO_2 such as supercritical extraction using SC-CO_2 as a solvent; 3) To replace a hazardous or less-effective substance in existing processes with CO_2 as an alternate medium or solvent or co-reactant or a combination of them; 4) To use CO_2 for energy recovery while reducing its emissions to the atmosphere by sequestration (storage); 5) To recycle CO_2 as C-source for chemicals and fuels; and 6) To convert CO_2 under geologic-formation conditions into "new fossil" energies.

Acknowledgments

The author gratefully acknowledge the helpful discussions with Prof. Michele Aresta of University of Bari, Italy, Prof. Tomoyuki Inui of Air Water Inc. (formerly at Kyoto University), Japan, Dr. John Armor of Air Products and Chemicals Inc., Mr. Howard Herzog of Massachusetts Institute of Technology, Dr. David Beecy, Dr. Robert Kane, Dr. Curt White, Dr. Robert Warzinski and Dr. Donald Kraftsman of U.S. Department of Energy, Dr. Meyer Steinberg of Brookhaven National Laboratory, Prof. Alan Scaroni and Prof. Harold Schobert of Pennsylvania State University, Mr. Wei Pan and Dr. Srinivas Srimat of Pennsylvania State University. The research on tri-reforming by the author received financial support by UCR Innovative Concepts Program of U.S. Department of Energy (DE-FG26-00NT40829).

Downloaded by 217.66.152.143 on September 14, 2012 | http://pubs.acs.org
Publication Date: January 24, 2002 | doi: 10.1021/bk-2002-0809.ch001

References

1. Keeling, C. D.; Whorf, T. P. Atmospheric CO_2 Records from Sites in the SIO Air Sampling Network. In Trends: A Compendium of Data on Global Change. Carbon Dioxide Information Analysis Center, Oak Ridge National Laboratory, U. S. Department of Energy, Oak Ridge, TN, U.S.A., August 2000.
2. Lindsey, J. S. Carbon Dioxide. McGraw-Hill Encyclopedia of Chemistry, McGraw-Hill, Second Edition, New York, 1993, pp. 157-159.
3. Pierantozzi, R. Carbon Dioxide. Kirk-Othmer Encyclopedia of Chemical Technology. Fourth Edition. Vol. 5, John Wiley and Sons,. New York, 1993, pp. 35-53.
4. Paul, J.; Pradier, C.-M. (Eds.). Carbon Dioxide Chemistry: Environmental Issues. Royal Society of Chemistry, Cambridge, UK, 1994, 405 pp.
5. Halmann, M. M.; Steinberg, M. Greenhouse Gas Carbon Dioxide Mitigation: Science and Technology. Lewis Publishers, Boca Raton, FL, 1999, 568 pp.
6. Aresta M. Perspectives of Carbon Dioxide Utilisation in the Synthesis of Chemicals. Coupling Chemistry with Biotechnology. Stud. Surf. Sci. Catal., 1998, 114, 65-76.
7. Aresta, M. Key Issues in Carbon Dioxide Utilisation as a Building Block for Molecular Organic Compounds in the Chemical Industry. In *CO_2 Conversion and Utilization*. Song, C.; Eds.; Gaffney, A. M.; Fujimoto, K. American Chemical Society, Washington DC, 2001, in press.
8. Inui, T.; Anpo, M.; Izui, K.; Yanagida, S.; Yamaguchi, T. (Eds.). Advances in Chemical Conversions for Mitigating Carbon Dioxide (Studies in Surface Science and Catalysis, Vol. 114), Elsevier, Amsterdam, 1998, 691 pp.
9. Inui, T. Effective Conversion of CO_2 to Valuable Compounds by Using Multi-functional Catalysts. In *CO_2 Conversion and Utilization*. Song, C.; Gaffney, A. M.; Fujimoto, K.; Eds.; American Chemical Society, Washington DC, 2001, in press.
10. Arakawa H. Research and Development on New Synthetic Routes for Basic Chemicals by Catalytic Hydrogenation of CO_2. Stud. Surf. Sci. Catal., 1998, 114, 19-30.
11. Park, S.-E.; Yoo, J. S.; Chang, J.-S.; lee, K.Y.; Park, M. S. Heterogeneous Catalytic Activation of Carbon Dioxide as an Oxidant. Am. Chem. Soc. Div. Fuel Chem. Prepr., 2001, 46(1), 115-118.
12. Rostrup-Nielsen, J.R. Aspects of CO_2-Reforming Of Methane. Stud. Surf. Sci. Catal., 1994, 81, 25-41.

Downloaded by 217.66.152.143 on September 14, 2012 | http://pubs.acs.org
Publication Date: January 24, 2002 | doi: 10.1021/bk-2002-0809.ch001

13. Rostrup-Nielsen, J.R.; Hansen, B. J.H.; Aparicio, L.M. Reforming of Hydrocarbons into Synthesis Gas on Supported Metal Catalysts. Sekiyu Gakkaishi, 1997, 40 (5), 366-377.
14. Wang, S.B.; Lu G.Q.M.; Millar, G.J. Carbon dioxide reforming of methane to produce synthesis gas over metal-supported catalysts: State of the art. Energy & Fuels, 1996, 10 (4), 896-904.
15. Bradford, M.C.J.; Vannice, M. A. CO_2 reforming of CH_4. Catal. Rev.-Sci. Eng., 1999, 41 (1), 1-42.
16. Leitner, W. Reactions in Supercritical Carbon Dioxide ($scCO_2$). Top. Curr. Chem. 1999, 206, 107-132.
17. Subramaniam, B.; Busch, D.H. Use of Dense-Phase Carbon Dioxide in Catalysis. In *CO_2 Conversion and Utilization*. Song, C.; Eds.; Gaffney, A. M.; Fujimoto, K. American Chemical Society, Washington DC, 2001, in press.
18. Cooper, A. I. Polymer Synthesis and Processing Using Supercritical Carbon Dioxide. J. Mater. Chem. 2000, 10 (2), 207-234.
19. Xu, X.D.; Moulijn, J.A. Mitigation of CO2 by Chemical Conversion: Plausible Chemical Reactions and Promising Products. Energy & Fuels, 1996, 10 (2), 305-325.
20. EIA/IEO. International Energy Outlook (IEO), Energy Information Administration, U.S. Department of Energy, DOE/EIA-0484(97), July 1998.
21. EIA/IEO. International Energy Outlook (IEO), Energy Information Administration, U.S. Department of Energy, 1999.
22. EIA/AER. Annual Energy Review (AER) 1997, Energy Information Administration, U.S. Department of Energy, Report No. DOE/EIA-0384(97), July 1998.
23. EIA/AER. Annual Energy Review (AER) 1998, Energy Information Administration, U.S. Department of Energy, 1999.
24. EIA/GHG. Emission of Greenhouse Gases in the United States 1999. Report No. EIA/DOE-0573(99), Energy Information Administration, US Department of Energy, October 31, 2000.
25. Lee, K.-W. Clean Fuels from Biomass. Am. Chem. Soc. Div. Fuel Chem. Prepr., 2001, 46(1), 61-64.
26. EIA/AER. Annual Energy Review (AER) 1999, Energy Information Administration, US Department of Energy, September 2000.
27. DOE/EPA. Fuel Economy. Internet Resource Developed by U.S. Department of Energy and U.S. Environmental Protection Agency, http://www.fueleconomy.gov/feg/atv.shtml. Viewed May 20, 2001.
28. Manzer, L. E. CO_2 Emission Reductions: An Opportunity for New Catalytic Technology. In *CO_2 Conversion and Utilization*. Song, C.; Gaffney, A. M.; Fujimoto, K.; Eds.; American Chemical Society, Washington DC, 2001, in press.

Downloaded by 217.66.152.143 on September 14, 2012 | http://pubs.acs.org
Publication Date: January 24, 2002 | doi: 10.1021/bk-2002-0809.ch001

29. DOE/OS-FE. Carbon Sequestration. State of the Science. Office of Science and Office of Fossil Energy, U.S. Department of Energy, February 1999.
30. Herzog, H.J.; Drake, E.M. Carbon Dioxide Recovery and Disposal from Large Energy Systems. Ann. Rev. Energ. Env., 1996, 21, 145-166.
31. Herzog, H. J. Using Carbon Capture and Sequestration Technologies to Address Climate Change Concerns. Am. Chem. Soc. Div. Fuel Chem. Prepr., 2001, 46(1), 53-55.
32. Chakma A. CO_2 Capture Processes - Opportunities for improved energy efficiencies. Energy Conversion and Management, 1997, 38, S51-S56.
33. Smith, I. M. CO_2 Reduction – Prospects for Coal. IEA Report No. CCC/26, IEA Coal Research, London, U.K., 1999, 84 pp.
34. Sander, M.T.; Mariz, C.L. The Fluor Daniel ECONAMINE FG Proces - Past Experience and Present-Day Focus. Energy Conversion and Management, 1992, 33 (5-8), 341-348.
35. Mariz C. L. Carbon Dioxide Recovery: Large Scale Design Trends. J. Canadian Petroleum Technology, 1998, 37 (7), 42-47.
36. Mimura, T.; Shimojyo, S.; Suda, T.; Iijima, M.; Mitsuoka, S. Development of Energy-Saving Absorbents for the Recovery of Carbon-Dioxide from Boiler Flue-Gas. Kagaku Kogaku Ronbun, 1995, 21 (3), 478-485.
37. Wolsky, A. M.; Daniels, E. J.; Jody, B. J. CO_2 Capture from the Flue-Gas of Conventional Fossil-Fuel-Fired Power-Plants. Environ Prog. 1994, 13 (3), 214-219.
38. Kikkinides, E. S.; Yang, R. T.; Cho, S. H. Concentration and Recovery of CO_2 from Flue-Gas by Pressure Swing Adsorption. Ind. Eng. Chem. Res., 1993, 32 (11), 2714-2720.
39. Gottlicher G, Pruschek R. Comparison of CO_2 Removal Systems for Fossil-Fueled Power Plant Processes. Energy Conversion and Management, 1997, 38, S173-S178.
40. Meisen A.; Shuai, X.S. Research and Development Issues in CO_2 Capture. Energy Conversion and Management, 1997, 38, S37-S42.
41. Beecy, D. The Role of Carbon Sequestration in a National Carbon Management Strategy. Am. Chem. Soc. Div. Fuel Chem. Prepr., 2001, 46 (1), 38-44.
42. Kane, R.; Klein, D. E. Opportunities for Advancements in Chemical Processes in Carbon Sequestration and Climate Change Mitigation. Am. Chem. Soc. Div. Fuel Chem. Prepr., 2001, 46(1), 275-277.
43. Riemer, P. W. F.; Ormerod, W. G. International Perspectives and the Results of Carbon-Dioxide Capture, Disposal and Utilization Studies. Energy Conversion and Management, 1995, 36 (6-9), 813-818.
44. Koros, W.J.; Mahajan, R. Pushing the Limits on Possibilities for Large Scale Gas Separation: Which Strategies?. J. Membrane Science, 2000, 175 (2), 181-196.

Downloaded by 217.66.152.143 on September 14, 2012 | http://pubs.acs.org
Publication Date: January 24, 2002 | doi: 10.1021/bk-2002-0809.ch001

45. (a) Song, C. Tri-reforming: A New Process for Reducing CO_2 Emissions. Chemical Innovation (formerly Chemtech, ACS), 2001, 31 (1), 21-26; (b) Song, C. Chemicals, Fuels and Electricity Co-generated from Coal. A Proposed Concept for Utilization of CO_2 from Power Plants. Proceedings of 16th Annual International Pittsburgh Coal Conference, Pittsburgh, PA, October 11-15, 1999, Paper No. 16-5.
46. Ferguson, J. E. Carbon Dioxide. MacMillan Encyclopedia of Chemistry. MacMillan References, New York, Vo. 1, 1997, pp. 302–308.
47. Lange's HDBK. Lange's Handbook of Chemistry, 13th Edition, McGraw-Hill, New York, 1985, p. 9-4 and p. 9-70.
48. CRC HDBK. CRC Handbook of Chemistry and Physics. 75th Edition, CRC Press, Boca Raton, FL, 1994, p.5-4.
49. Ormerod, W.; Riemer, P.; Smith, A. Carbon Dioxide Utilisation. IEA Greenhouse Gas R&D Programme, ISBN 1 898373 17 5, IEA, London, U.K., January 1995.
50. ACS. Facts & Figures for the Chemical Industry. Chem. Eng. News, June 26, 2000, 48-89.
51. ACS. Facts & Figures for the Chemical Industry. Chem. Eng. News, June 24, 1996, 38-79.
52. OTP (Office of technology Policy, U.S. Department of Commerce.). Meeting the Challenge: U.S. Industry Faces the 21st Century. Chemtech, 1996, 26, 46-54.
53. Audus H; Oonk H. An Assessment Procedure for Chemical Utilisation Schemes Intended to Reduce CO2 Emissions to Atmosphere. Energy Conversion and Management, 1997, 38, S409-S414.
54. Armor, J. N. Catalytic Fixation of CO_2, CO_2 Purity, Energy, and the Environment. Am. Chem. Soc. Div. Petrol. Chem. Prepr., 2000, 45 (1), 141-142.
55. Choudhary, V.R.; Mamman, A. S.; Uphade, B. S.; Babcock, R. E. CO_2 Reforming and Simultaneous CO_2 and Steam Reforming of Methane to Syngas over $Co_xNi_{1-x}O$ Supported on Macroporous Silica-Alumina Precoated with MgO. In *CO_2 Conversion and Utilization.* Song, C.; Gaffney, A. M.; Fujimoto, K.; Eds.; American Chemical Society, Washington DC, 2001, in press.
56. Aresta, M.; Quaranta, E. Carbon Dioxide: A Substitute for Phosgene. Chemtech, 1997, 27 (3), 32-40.
57. Aresta, M.; Dibenedetto, A.; Tommasi, I. Developing Innovative Synthetic Technologies of Industrial Relevance Based on Carbon Dioxide as Raw Material. Energy & Fuels, 2001, 15, 269-273.
58. Dibenedetto, A.; Aresta, M. Nb_2O_5 as Catalyst in the Oxidative Carboxylation of Olefins. Am. Chem. Soc. Div. Fuel Chem. Prepr., 2001, 46(1), 119-121.

Downloaded by 217.66.152.143 on September 14, 2012 | http://pubs.acs.org
Publication Date: January 24, 2002 | doi: 10.1021/bk-2002-0809.ch001

59. Markels, M.; Barber, R. T. Sequestration of Carbon Dioxide by Ocean Fertilization. Am. Chem. Soc. Div. Fuel Chem. Prepr., 2001, 46(1), 45-48.
60. Steinberg, M. CO_2 Mitigation and Fuel Production. Am. Chem. Soc. Div. Petrol. Chem. Prepr., 2000, 45 (1), 74-76.
61. Steinberg, M. CO_2 Mitigation and Fuel Production. In *CO_2 Conversion and Utilization*. Song, C.; Gaffney, A. M.; Fujimoto, K.; Eds.; American Chemical Society, Washington DC, 2001, in press.
62. Beecy, D.; Ferrell, F. M.; Carey, J. K. Advanced Concepts for CO_2 Conversion, Storage, and Reuse. Am. Chem. Soc. Div. Fuel Chem. Prepr., 2001, 46 (1), 99-100.
63. Mahajan, D.; Song, C.; Scaroni, A. W. Micro-reactor Study on Catalytic Reduction of CO_2 into Liquid Fuels: Simulating Reactions under Geologic Formation Conditions. Am. Chem. Soc. Div. Petrol. Chem. Prepr., 2000, 45 (1), 113-117.
64. Mahajan, D.; Song, C.; Scaroni, A. W. Catalytic Reduction of CO_2 into Liquid Fuels: Simulating Reactions under Geological Formation Conditions. . In *CO_2 Conversion and Utilization*. Song, C.; Gaffney, A. M.; Fujimoto, K.; Eds. American Chemical Society, Washington DC, 2001, in press.

Downloaded by 217.66.152.143 on September 14, 2012 | http://pubs.acs.org
Publication Date: January 24, 2002 | doi: 10.1021/bk-2002-0809.ch001

Downloaded by OHIO STATE UNIV LIBRARIES on September 16, 2012 | http://pubs.acs.org
Publication Date: January 24, 2002 | doi: 10.1021/bk-2002-0809.ch002

Chapter 2

CO_2 Mitigation and Fuel Production

M. Steinberg

Department of Applied Science, Brookhaven National Laboratory, Building 475,
Upton, NY 11973

CO_2 mitigation technologies deals with how to utilize fossil fuels, coal, oil and gas with reduced CO_2 emissions. Most development work to date has emphasized improving efficiency in generation and utilization of energy and in removal and recovery of CO_2 from central power stations followed by disposal in underground wells or in the ocean. The latter suffers from economic penalties and potential adverse environmental effects. CO_2 utilization for the chemicals industry is problematic because of the capacity mismatch between the gross CO_2 emission and the relatively smaller chemical products market. However, utilization Of CO_2 for conversion to alternative fuels for stationary and automotive power has potential of matching capacity between emissions and utilization. Although hydrogen-rich gaseous fuels such as methane and hydrogen can be used as alternative automotive liquid fuels which includes methanol and other higher oxygenates appear safer and fit in with the current liquid fuel infrastructure. The key for gas to liquid conversion utilizing CO_2 is the production of hydrogen for conversion with CO_2. The Carnol process, catalytically reacts CO_2 from coal fired plants with hydrogen from the thermal

The complete chapter is based on research from references 1 and 2.

In CO2 Conversion and Utilization; Song, C., et al.;
ACS Symposium Series; American Chemical Society: Washington, DC, 2002.

decomposition of methane while sequestering the elemental carbon, to produce methanol and higher oxygenated fuels. CO_2 emission reductions approaching 80% using fuel cell engines can be achieved compared to the conventional system of coal-fired power generating plants and gasoline-driven IC automotive engines.

Downloaded by OHIO STATE UNIV LIBRARIES on September 16, 2012 | http://pubs.acs.org
Publication Date: January 24, 2002 | doi: 10.1021/bk-2002-0809.ch002

The Carnol Process

The Carnol Process has been developed to convert CO_2 from coal burning power plants to produce liquid automotive fuel with reduced CO_2 emissions. The process is composed of three unit operations as follows:

1 . Carbon dioxide is extracted from the stack gases of coal fired power plants using monoethanolamine (MEA) solvent in an absorption-stripping operation. The technology for this operation is well known in the chemical industry for CO_2 recovery and has recently been significantly improved for extracting CO_2 from power plant stack gases. The power required to recover CO_2 from an integrated coal fired power plant to recover 90% of the CO_2 from the flue gas, has been reduced to about 10% of the capacity of the power plant. However, this energy requirement can be further reduced to less than 1% when the CO_2 recovery operation is integrated with a methanol synthesis step described in item 3 below.

2. Hydrogen is produced with CO_2 emission by the non-conventional method of thermally decomposing methane to carbon and hydrogen.

$$CH_4 = C + 2H_2$$

The energy requirement in conducting this process per unit of hydrogen is less than that required by the conventional steam reforming process. A fluidized bed reactor has been used to thermally decompose methane and more recently attempts are being made to improve reactor design by utilizing molten metal or salt reactors. The carbon is separated and either stored or can be sold as a materials commodity, such as in strengthening rubber for tires. The temperatures required for this operation are 800°C or above and pressures of less than 10 atm.

3. The third step in the process consists of reacting the hydrogen from step 2 with the CO_2 from step 1 in a conventional gas phase catalytic methanol synthesis reactor.

$$CO_2 + 3H_2 = CH_3OH + H_2O$$

This is an exothermic reaction so that the heat produced in this operation can be used to recover the stack gas CO_2 from the absorption/stripping operation described in step 1, thus reducing the energy required to recover the CO_2 from the power plan to less than 1% of the power plant capacity. This is an advantage compared to the energy cost in terms of derating the power plant when CO_2 is disposed of by pumping liquid CO_2 into the ocean in which case more than 20% of the power plant capacity is consumed. The gas phase methanol synthesis usually takes place at temperatures of 260°C and pressure of 50 atm using a copper catalyst. The synthesis can also be conducted in the liquid phase by using a slurry of zinc catalyst at a lower temperature of 120°C and 30 atm hydrogen pressure.

In its simplest form the Carnol Process is a two step operation. When hydrogen is used to supply the energy for the thermal decomposition of methane, then the CO_2 emission for methanol production is reduced to zero.

Methanol and Higher Oxygenates as Liquid Automotive Fuel

The Carnol Process can be considered as a viable coal-fired CO_2 mitigation technology because the resulting large production capacity of liquid methanol resulting from the large amount of CO_2 emitted can be utilized in a large capacity automotive fuel market. Most processes which utilize CO_2 produce chemical products which tend to swamp the market and thus cannot be used effectively. Methanol as an alternative automotive fuel has been used in internal combustion (IC) engines as a specialty racing car fuel for a long time. The EPA has shown that methanol can be used in IC engines with reduced CO and HC emissions and at efficiencies exceeding gasoline fuels by 30%. Methanol can also be used either directly or indirectly in fuel cells at several times higher conversion efficiency for automotive use. A great advantage of methanol is that, as a liquid, it fits in well with the infrastructure of storage and distribution compared to compressed natural gas and gaseous or liquid hydrogen, which are also being considered as alternative transportation fuels. Compared to gasoline, the CO_2 emission from methanol in IC engines is 40% less and over 70% less for fuel cell vehicles. However, other higher oxygenate fuels such as dimethyl

Downloaded by OHIO STATE UNIV LIBRARIES on September 16, 2012 | http://pubs.acs.org
Publication Date: January 24, 2002 | doi: 10.1021/bk-2002-0809.ch002

oxide which can be produced by catalytic Fisher-Tropsch reactions can be incorporated in the Carnol System. The thermodynamics o f these reactions and CO_2 emissions are shown in Table I. The entire Carnol System is shown in Figure 1.

It should also be pointed out that removal and ocean disposal of CO_2 is only possible for large central power stations which for the U.S. accounts for only 30% of the total CO_2 emission. For the dispersed industrial, domestic and transportation (automobiles) sectors, the Carnol Process provides the capability of CO_2 reduction in these sectors by supplying liquid methanol fuel to these numerous small dispersed CO_2 emitting sources.

Downloaded by OHIO STATE UNIV LIBRARIES on September 16, 2012 | http://pubs.acs.org
Publication Date: January 24, 2002 | doi: 10.1021/bk-2002-0809.ch002

Economics of Carnol Process

At $18/bbl oil, 90% refining gasoline yield and $10/bbl for refining cost, gasoline costs $0.78/gal, and methanol being 30% more efficient than gasoline, competes with gasoline at $0.57/gal methanol. Currently, the market for methanol is depressed because of over supply due to removal of mandatory requirements for MTBE oxygenation of gasoline.

In terms of the cost of reduction of CO_2 from power plants, with $2/MSCF natural gas, and a $0.55/gal methanol income the CO_2 reduction cost is zero. At $3/MSCF natural gas and $0.45/gal income from methanol, the CO_2 reduction or disposal cost is $47.70/ton CO_2, which is less than the maximum estimated for ocean disposal. More interesting, without any credit for CO_2 disposal from the power plant, methanol at $0.55/gal can compete with gasoline at $0.76/gal (~$18/bbl oil) when natural gas is at $2/MSCF. Any sale of elemental carbon reduces the cost for reducing CO_2 emissions.

CO_2 Emission Evaluation of Entire Carnol System

The entire Carnol System is evaluated in Table II in terms of CO_2 emissions and compared to the alternative methanol processes and to the base line case of conventional coal fired power plant and gasoline driven automotive IC engines and in fuel cell engines. All the cases are normalized to emissions from a 1 MMBTU of coal fired power plant, which produces CO_2 for a Carnol methanol plant equivalent to 1.27 MMBTU for use in automotive engines. The assumptions made are listed at the bottom of Table II The conclusions drawn from Table II are as follows:

Downloaded by OHIO STATE UNIV LIBRARIES on September 16, 2012 | http://pubs.acs.org
Publication Date: January 24, 2002 | doi: 10.1021/bk-2002-0809.ch002

Table I. Utilization of CO_2 for Oxygenates and Hydrocarbon Fuels

Process: H_2 Produced by Thermal Decomposition of Natural Gas
($CH_4 = C + 2\ H_2$) at 80% Efficiency
and Catalytic Reaction with CO_2 to Produce the Fuel Indicated

Fuel	*Reaction*	*Mol. Wt of Fuel*	*HT. of Form ΔH_F* Kcal/mol*	*HT. of React. ΔH_R ΔH_C Kcal/Mol*	*CO_2 Emission** Lbs CO_2/MMBTU*	*Heat of Combus. ΔH_C BTU/Lb*	*Carbon Sequestered Lbs C/MMBTU*
Methanol C_1	$1CO_2+3H_2=CH_3OH+H_2O$	32	-57	-31	22	10,000	56
Ethanol C_2	$2CO_2+6H_2=C_2H_5OH+3H_2O$	46	-66	-82	24	12,750	61
Propoanol C_3	$3CO_2+9H_2=C_3H_7OH+5H_2O$	60	-74	-130	24	14,580	62
Butanol C_4	$4CO_2+12H_2=C_4H_9OH+7H_2O$	74	-80	-180	24	15,800	62
Gasoline C_8-Octane	$8CO_2+25H_2=C_8H_{18}+16H_2O$	114	- 60	-396	25	20,600	64
Diesel C_{16}-Cetane	$16CO_2+49H_2=C_{16}H_{34}+32H_2O$	226	-149	-821	25	20,000	65
Dimethyl Ether C_2	$2CO_2+5H_2=C_2H_6O+2H_2O$	46	-51	-67	23	13,340	59

* Fuel and water in liquid state

**CO_2 emission is only for the conversion process. The emission from a conventional methane steam reforming plant for H_2 production ranges from 177 to 205 Lbs CO_2/MMBTU of oxygenated or hydrocarbon fuel which is 8 times higher than for the thermal decomposition of methane for hydrogen production shown above.

Downloaded by OHIO STATE UNIV LIBRARIES on September 16, 2012 | http://pubs.acs.org
Publication Date: January 24, 2002 | doi: 10.1021/bk-2002-0809.ch002

Table II. CO_2 Emission Comparison for Systems Consisting of Coal Fired Power Plant, Fuel Process Plant and Automotive Power Plant

Basis: 1 MMBTU for coal fired 900 MW(e) power plant
1.27 MMBTU of liquid fuel for IC engine – other fuel efficiencies proportions energy up and down
CO2 Emission units in lbs CO_2/MMBTU (multiply by 0.43 for KG/GJ)

System Unit	*Coal Fired Power Plan*	*Fuel Process Plant*	*IC Automotive Power Plant*	*Total System Emission*	*CO_2 Emission Reduction*
Basline Case; Coal Fired Power Plant and Gasoline Driven IC Engine	215	15	285	515	0%
Case 1A Coal Fired Power Plant with Conventional Steam Reformed Methanol Plant	215	56	175[2]	448	13%
Case 1B Coal Fired Power Plant with CO_2 Addition to Conventional Methanol Plant	161[4]	54	175	390	24%
Case 2 Coal Fired Power Plant with CARNOL Process Methanol Plant	21[1]	32	175	228	56%
Case 3 Coal Fired Power Plant with Biomass for Methanol Plant	0	43	175	219	57%
Case 4 Coal Fired Power Plant with CARNOL Methanol and Fuel Cell Automotive Power	11[5]	17	Fuel Cell 89[3]	117	77%

1) 90% recovery of CO_2 from coal fired plant.
2) Methanol is 30% more efficient than gasoline in IC engine.
3) Fuel cell is 2.5 times more efficient than conventional gasoline IC engine.
4) Only 25% reovery of CO_2 from coal plant is necessary for supplying CO_2 to conventional methanol plant.
5) Only 53% emissions of coal plant CO_2 is assigned to Carnol for fuel cells.

Downloaded by OHIO STATE UNIV LIBRARIES on September 16, 2012 | http://pubs.acs.org
Publication Date: January 24, 2002 | doi: 10.1021/bk-2002-0809.ch002

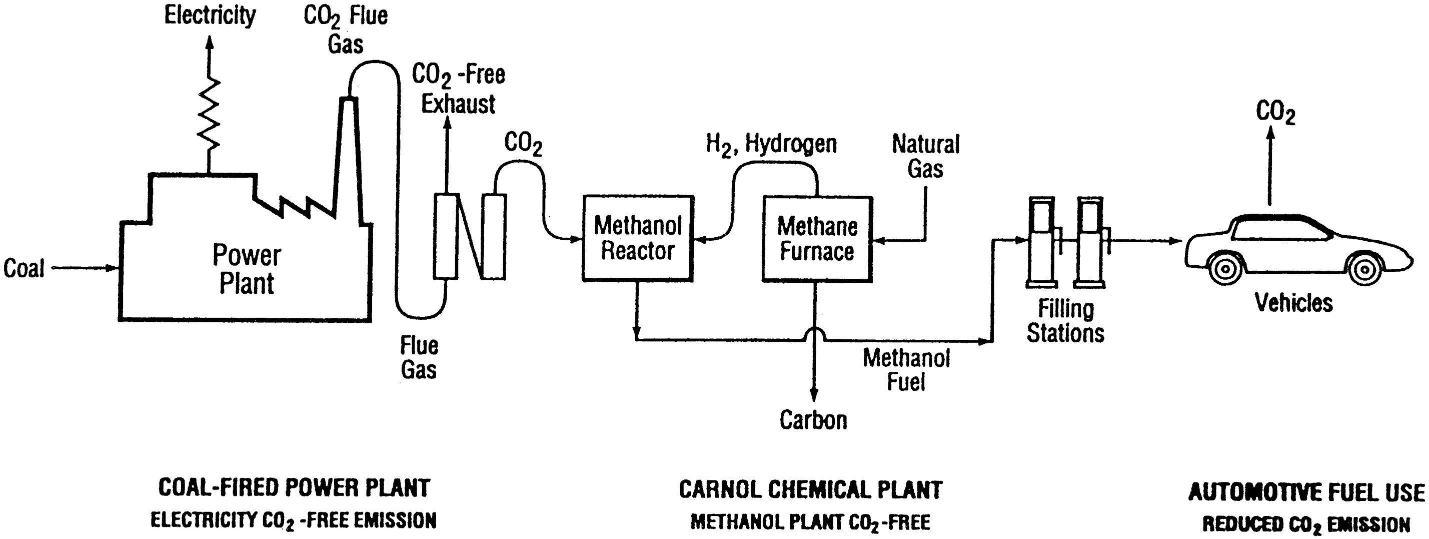
Electricity
CO2 Flue Gas
CO2 -Free Exhaust
CO2
H2, Hydrogen
Natural Gas
CO2
Coal
Power Plant
Methanol Reactor
Methane Furnace
Vehicles
Flue Gas
Methanol Fuel
Filling Stations
Carbon
COAL-FIRED POWER PLANT
ELECTRICITY CO2 -FREE EMISSION
CARNOL CHEMICAL PLANT
METHANOL PLANT CO2-FREE
AUTOMOTIVE FUEL USE
REDUCED CO2 EMISSION

Figure 1. Integrated System For CO_2 Emission Reduction Carnol Process

1. The use of conventional methanol reduces CO_2 by 13% compared to the gasoline base case and is mainly due to the 30% improved efficiency of the use of methanol in IC engines.

2. By addition of CO_2 recovered from the coal fired power plant to the conventional methanol process, the CO_2 from the power plant is reduced by about 25% (161 lbs/MMBTU compared to 215 lb CO_2/MMBTU) and the CO_2 emissions for the entire system is reduced by 24%. It should be pointed out that part of the CO_2 can also be obtained from the flue gas of the reformer furnace of the methanol plant.

3. The Carnol Process reduces the coal fired power plant CO_2 emission by 90% and the overall system emission is reduced by 56%.

4. Since the use of biomass is a CO_2 neutral feedstock, there is no emission from the power plants because the biomass feedstock comes from an equivalent amount of CO_2 in the atmosphere which has been generated from the coal fired power plant. Thus, the only net emission comes only from burning methanol in the automotive IC engine and thus, the CO_2 emission for the entire system is reduced by 57%, only slightly more than the Carnol System. However, the main point is that, at present, the cost of supplying biomass feedstock is higher than that of natural gas feedstock.

5. Another future system involves the use of fuel cells in automotive vehicles. The efficiency of fuel cells is expected to be 2.5 times greater than gasoline driven engines. Applying the Carnol Process to produce methanol for fuel cell engines reduces the CO_2 emission for the entire system by as much as 77%. Furthermore, because of the huge increase in efficiency, the capacity for driving fuel cell vehicles can be increased by 92% over that for conventional automobiles using the same 90% of the CO_2 emissions from the coal burning power plant.

Downloaded by OHIO STATE UNIV LIBRARIES on September 16, 2012 | http://pubs.acs.org
Publication Date: January 24, 2002 | doi: 10.1021/bk-2002-0809.ch002

REFERENCES

1. Meyer Steinberg "CO_2 Mitigation and Fuel Production", BNL 65454, Brookhaven National Laboratory, Upton, NY (1997).

2. Meyer Steinberg "Efficient Natural Gas Technologies: A Response to Global Warming", Chemtec 31-36 (January 1999).

Downloaded by UNIV OF GUELPH LIBRARY on September 16, 2012 | http://pubs.acs.org
Publication Date: January 24, 2002 | doi: 10.1021/bk-2002-0809.ch003

Chapter 3

CO_2 Emission Reductions: An Opportunity for New Catalytic Technology

Leo E. Manzer

**DuPont Central Research and Development, Experimental Station,
Wilmington, DE 19880–0262**

Summary

The theme of this symposium is related to reducing carbon dioxide emissions by conversion of the CO_2 to other products. While this is a worthwhile object, the real goal where possible, should be to avoid the production of CO_2 in the first place. It is the purpose of this paper to review processes that generate CO_2 and provide some opportunities for research, which ultimately will reduce CO_2 at the source to avoid end of pipe treatment.

Introduction

Catalytic oxidations are among the least selective of all catalytic reactions and the source of much of the carbon dioxide from chemical processes. These processes are often operated at very high temperatures, with selectivity to desired oxygenated products of less than 90%. The major byproduct is usually carbon dioxide. Table 1 shows typical selectivity to the major product in these large-scale commercial operations. Most of these processes have production capacities of several hundred million lb./year, so the amount of CO_2 generated is quite significant. For example, for a maleic anhydride plant operating at a capacity of 200-MM lb./year, with 60% selectivity, over 500-MM lb./year of carbon dioxide is produced. Therefore, there is a large incentive to improve yield to the hydrocarbon product in these processes. This can be done by improving the catalyst in these existing processes or by completely changing chemistry and engineering of existing processes. This paper will provide a brief overview of current trends and opportunities to reduce CO_2.

Table 1. Selectivity to Major Product for a few Commercial Catalytic Oxidation Reactions

Oxidation Process	Major Product	Selectivity
Butane Oxidation	Maleic Anhydride	60%
Propylene Oxidation	Acrolein/Acrylic Acid	75%
Propylene Ammoxidation	Acrylonitrile	80%
Ethylene Oxidation	Ethylene Oxide	88%

Discussion

2.1 Anaerobic vs. Aerobic Oxidations

It has been known for many years that in certain oxidation reactions the most selective catalysis occurs when the oxygen in the final product is derived directly from the lattice of the oxide catalyst.[1] However, most large-scale commercial processes are carried out in the non-flammable region, which often requires a feed of less <3% organic and the balance air. This large excess of gas-phase oxygen results in the low selectivity shown in Table 1. The Mars-van Krevelen mechanism suggests that a gain in selectivity is possible by keeping the gas phase oxygen from the process. The lattice oxygen of the catalyst is used in a stoichiometric reaction with a hydrocarbon to yield the oxygenated product. The reduced oxide catalyst is then transported to a separate zone and re-oxidized by air. The process is referred to as *anaerobic oxidation*.

For this complex engineering and catalysis to be successful and economically viable, several requirements must be met. First, there must be a selectivity improvement for the desired product by operating in this mode. If this is not seen in laboratory pulse experiments there is no sense in proceeding. Next, the catalyst must have a high oxygen carrying capacity per unit weight, to minimize the amount of catalyst circulated through the reactor. This is very important as the catalyst is often more expensive than the oxygenated product produced. Re-oxidation of the reduced catalyst in the regenerator should occur at a temperature similar to that of the oxidation step to minimize the need to heat or cool the catalyst solids (energy minimization). Finally, since the reaction is essentially stoichiometric between catalyst and organic, a large amount of solid is circulated around the reaction system. Therefore, the catalyst must be very resistant to attrition and must maintain structural integrity through many redox

Downloaded by UNIV OF GUELPH LIBRARY on September 16, 2012 | http://pubs.acs.org
Publication Date: January 24, 2002 | doi: 10.1021/bk-2002-0809.ch003

Downloaded by UNIV OF GUELPH LIBRARY on September 16, 2012 | http://pubs.acs.org
Publication Date: January 24, 2002 | doi: 10.1021/bk-2002-0809.ch003

Hydrocarbon Oxidation Step:

$$M_xO_y + C_4H_{10} \longrightarrow M_xO_{y-f} + C_4H_2O_3$$

Catalyst Regeneration Step:

$$M_xO_{y-f} + O_2 \longrightarrow M_xO_y$$

Figure 1. Mars-van Krevelen Oxidation of Butane to Maleic Anhydride

cycles. An excellent, early example of a two step, anaerobic oxidation, is the Lummus[2] process for ammoxidation of o-xylene to o-phalonitrile (dinitriles-DNs). A simplified schematic is shown in Figure 2. A higher selectivity is claimed for the two step process relative to the single stage, aerobic oxidation.

Another large development effort[3] was carried out by ARCO Chemical during the 1970's to couple methane to ethylene. The reaction occurred at a very high temperature of 850-900°C. Patent and literature references, which illustrate the use of a $Li_{0.5}B_{0.5}MnMg_{2.8}O_x/SiO_2$ catalyst, show that at a

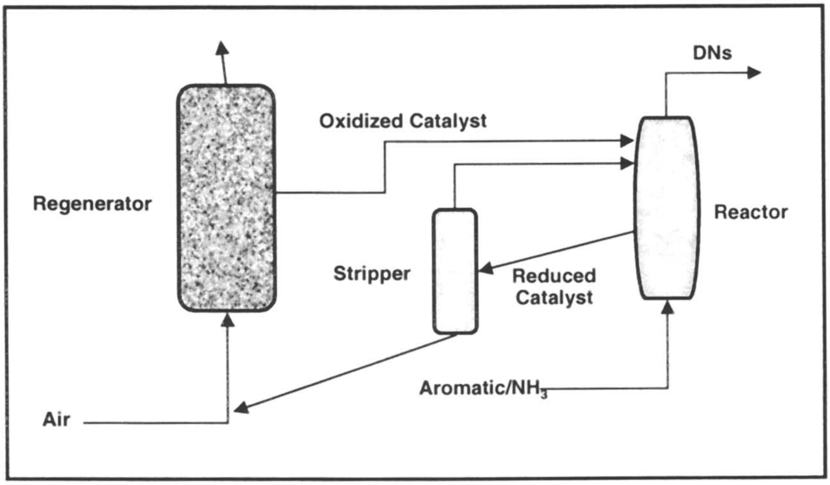

Figure 2. Simplified Schematic for the Two-Stage Oxidation of o-Xylene

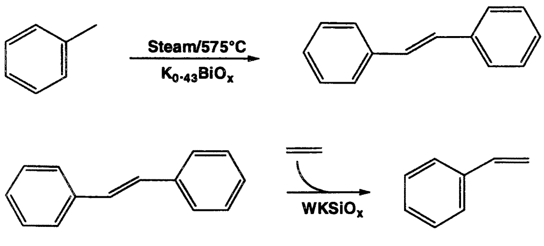

Figure 3. Monsanto Anaerobic Oxidative Coupling of Toluene

conversion of 22%, the selectivity to C_2s was about 60% under both aerobic and anaerobic conditions. However, the yield of CO_2 was reduced from 34 to 22% when the reaction was conducted in a cyclic mode, carrying out the oxidation under anaerobic conditions. A major development effort was terminated when the price of oil decreased.

Scientists and engineers at Monsanto[4] studied the oxidative dimerization of toluene to stilbene, as part of a new styrene process (Figure 3). In the first step, using a $K_{0.43}BiO_x$ catalyst at 575°C, the anaerobic process showed higher conversion (46 vs. 38%) and higher selectivity to stilbene (81.3 vs. 72.7%).

Catalytic research at Dow Chemical[5] on a new styrene process involved the oxidative dehydrogenation of butane to butadiene under anaerobic conditions using a $K/MoO_x/MgO$ catalyst. Under anaerobic conditions the conversion was 45% and selectivity to butadiene was 75%.

Emig[6] has recently studied the oxidative dimerization of isobutylene to 2,5-dimethylhexadiene (DMH). Under aerobic conditions a conversion of 24% was obtained with a selectivity of 38% to DMH giving a single-pass yield of 9.1%. Under anaerobic oxidation, the conversion dropped to 11%, the yield remained constant at 9.9%, while the selectivity to DMH increased from 38 to 90%. This is a remarkable example of CO_2 reduction using a two-step process.

A recent patent was issued to ATOCHEM[7] on the oxidation of propylene to acrolein and acrylic acid using a complex metal oxide catalyst in a circulating solids reactor (CSR). Under anaerobic conditions at 350°C, propylene conversion was 16% and selectivity was 95.5%. When air was introduced into the CSR, the conversion increased to 21% and selectivity dropped to 82%, once again showing the substantial advantage of keeping the gas phase oxygen out of the catalytic oxidation zone.

DuPont recently commercialized a new process for the oxidation of butane to maleic anhydride using a CSR[8]. The maleic anhydride is scrubbed from the reaction zone as maleic acid and then hydrogenated to tetrahydrofuran. The

Downloaded by UNIV OF GUELPH LIBRARY on September 16, 2012 | http://pubs.acs.org
Publication Date: January 24, 2002 | doi: 10.1021/bk-2002-0809.ch003

advantages have been well documented in the references. A key to this process was the development of an attrition resistant catalyst obtained by spray drying a solution of micronized VPO catalysts in polysilicic acid[9]. In the spray drier, a porous shell of very hard silica is formed to protect the soft VPO catalyst.

These few examples show an advantage of anaerobic oxidations for selected reactions, to minimize CO_2 formation. A few other opportunities for further study should include the oxidation of o-xylene to phthalic anhydride, oxidative dehydrogenation of ethylbenzene to styrene, oxidation of isobutylene to methacrolein and methacrylic acid and paraffin oxidative dehydrogenation to olefins.

2.2 Paraffin Oxidations

Currently, there are no commercial processes involving the direct gas-phase oxidation of paraffins to an oxygenated product or olefin. The conventional approach involves first, the endothermic dehydrogenation of paraffin, to the desired olefin, followed by oxidation to the desired product. This process generates CO_2 in the endothermic dehydrogenation step as a result of providing the heat for the reaction. By comparison, if direct oxidation of the paraffin to the desired oxygenates could be achieved at high selectivity, there would be a net reduction in CO_2 and the process, in fact, would export energy. A number of companies[10] have been very active in this area for many years.

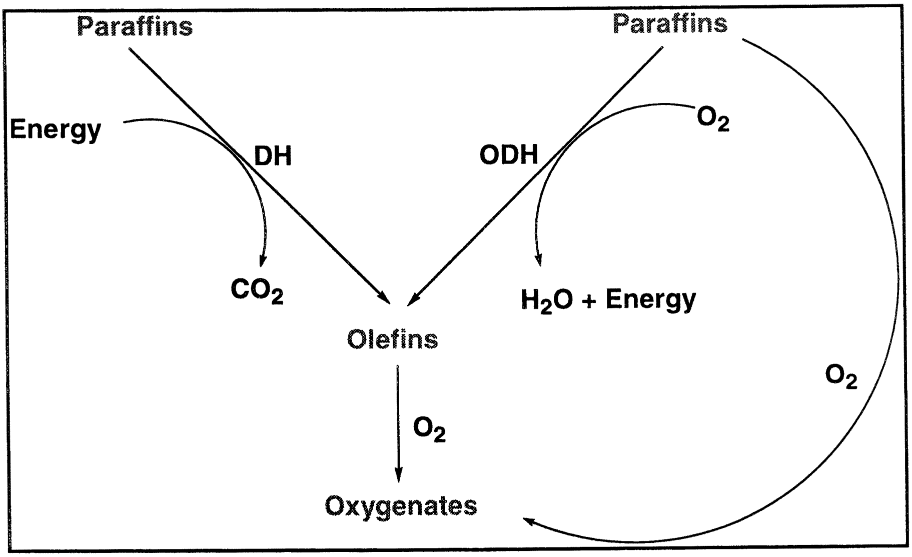

Figure 4. Incentive for Direct Oxidation of Paraffins

Downloaded by UNIV OF GUELPH LIBRARY on September 16, 2012 | http://pubs.acs.org
Publication Date: January 24, 2002 | doi: 10.1021/bk-2002-0809.ch003

The results from selected patents for the ammoxidation of propane to acrylonitrile are shown in Table 2. Significant advances have been made over the past 10 years. High conversions and selectivity approaching 64% have been obtained. BP has announced that a pilot plant is operational to collect basic data for commercial design. The stake is high for this development due to the lower cost of propane vs. propylene and a reduction in CO_2 emissions.

Table 2. Selected Results for the Ammoxidation of Propane to Acrylonitrile

Company	Catalyst	Conversion (%)	Selectivity (%)
BP	$VSb_{1.4}Sn_{0.2}Ti_{0.1}O_x$	30.5	58.3
Asahi	$NbSb_aCr_bX_yO_n$	29.1	30.7
Mitsui Toatsu	$V_1Li_{0.1}P_{1.1}O_x$	54.8	58.8
Mitsubishi	$MoV_xTe_{0.2}Nb_{0.1}O_{4.25}$	79.4	63.5

Another well-studied process, where significant progress has been made, involves the oxidation of propane to acrylic acid[11]. These results are quite impressive with selectivity reported in excess of 80%.

Table 3. Selected Results for the Oxidation of Propane to Acrylic Acid

Company	Catalyst	Conv %	Sel AA %
Wang (Fudan U)	$V1Zr_{0.5}P_{1.5}O_x$	18.3	81.0
	$Ce_{0.01}VPO$	27.2	68.3
Toa Gosei	$V/Sb/Mo/NbO_x$	30.9	29.4
Mitsubishi	$V_{0.3}Te_{0.23}Nb_{0.12}Bi_{0.017}MoO_x$	56.2	42.6
Rohm and Haas	V/Te/Nb/MoOx	71.0	59.0

By comparison, the direct catalytic oxidation of isobutane to methacrylic acid has been less developed[12]. Sumitomo has reported that 42% methacrylic acid can be obtained at 25% conversion.

Downloaded by UNIV OF GUELPH LIBRARY on September 16, 2012 | http://pubs.acs.org
Publication Date: January 24, 2002 | doi: 10.1021/bk-2002-0809.ch003

2.3 New Process Chemistry or Conditions

2.3.1 New Methylmethacrylate Process

Up to this point, the focus has been on improving the yield of the catalytic reaction to reduce CO_2 emissions. However it is important to consider entirely new process chemistry that might reduce the number of steps, lower the temperature, and as a result might also lower CO_2 production. An excellent example illustrating this point will involve the production of methylmethacrylate. Current commercial catalytic routes using a C_4 feedstock involve two high-temperature gas-phase catalytic steps followed by an esterification. The first two steps occur at >350°C and with an overall yield of about 75%. The main byproduct is carbon dioxide. A new process to methylmethacrylate is under development by Asahi Chemical[13]. Their new process combines the second and third steps into a single oxidative esterification step (Figure 5).

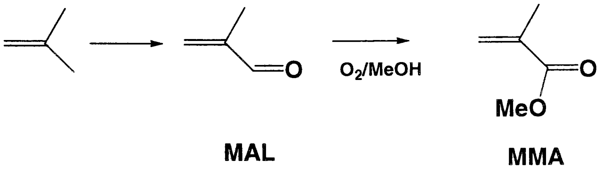

Figure 5. New Route to Methylmethacrylate

Using a $Pd/Pb/Mg\text{-}Al_2O_3$ catalyst, they report over 98% conversion of the methacrolein to methacrylic acid with a selectivity of >95%. The reaction occurs at mild 80°C, in a slurry phase reactor. The overall yield is significantly higher that the conventional process, less CO_2 is generated and capital investment is lower. A plant with a capacity of 135 million lbs. per year is currently under construction. Mitsubishi Rayon[14] has also been active in this area with a $Pd_5Bi_2Fe/CaCO_3$ catalyst giving over 97% selectivity to MMA at 76% conversion.

2.3.2 Chemistry Under Unusual Conditions

Normally intuition suggests that lower temperatures are required to achieve higher selectivity. However over the past decade, Schmidt[15] has found that by combining engineering, chemistry and catalysis, it is possible to achieve very high selectivity in a variety of oxidation reactions by going to very high

Downloaded by UNIV OF GUELPH LIBRARY on September 16, 2012 | http://pubs.acs.org
Publication Date: January 24, 2002 | doi: 10.1021/bk-2002-0809.ch003

temperatures and using very short contact times. Data from a recent example on the oxidative dehydrogenation of ethane to ethylene is shown in Table 4. Selectivity of 70% is achieved with a Pt-Sn catalyst supported on a monolith. Interestingly, addition of hydrogen gave a significant increase in selectivity. According to Schmidt the excess hydrogen rapidly reacts with oxygen, providing the necessary heat for the endothermic ethane dehydrogenation. As a result the excess oxygen is removed from the gas phase thus minimizing byproducts and combustion of the hydrocarbon. As a result ethylene selectivity goes up and CO_2 is reduced. Regarding safety, the ethane is reported to suppress H_2/O_2 flammability.

Table 4. Oxidative Dehydrogenation of Ethane to Ethylene (900-950°C)

Catalyst	Conversion(%)	Selectivity (%)
Pt/monolith	70	65
Pt-Sn/monolith	69	70
$H_2 + O_2$	73	85

2.4 Alternative Oxidants

Oxygen or air will likely be the preferred source of oxygen from an economic standpoint for many years. However, a growing number of developmental applications with hydrogen peroxide, nitrous oxide, and alkylhydroperoxides as the oxygen source are appearing in the literature. A relative comparison of cost for various oxygen sources is shown in Table 5. Clearly, from a cost standpoint, as an oxygen source, it will be difficult to justify new commodity chemical processes using on-purpose production of N_2O and H_2O_2. However for fine chemical applications like pharmaceuticals and agrochemicals, the cost may well be justified. Hydrogen and oxygen mixtures may well be economically justified although safety issues will likely require higher investment.

Panov has extensively studied the use of N_2O as a selective oxidant for aromatics[16]. Using zeolites, containing only small amounts of iron, he has shown that benzene can be oxidized to phenol with selectivity of >99% at temperatures around 300°C. Emig has studied the mechanism of this interesting reaction[17]. He proposes that in the absence of benzene at temperatures of <300°C, all the N_2O reacts with the surface to give an alpha-oxygen site which is very stable. Cooling the solid below room temperature and introducing benzene gives phenol in high selectivity. The lifetime of the site is 0.5 sec at 500°C and 1.75 seconds at 420°C.

Downloaded by UNIV OF GUELPH LIBRARY on September 16, 2012 | http://pubs.acs.org
Publication Date: January 24, 2002 | doi: 10.1021/bk-2002-0809.ch003

Downloaded by UNIV OF GUELPH LIBRARY on September 16, 2012 | http://pubs.acs.org
Publication Date: January 24, 2002 | doi: 10.1021/bk-2002-0809.ch003

Table 5. Cost of Various Oxygen Sources

Oxygen Source	$/lb.-mole	$/lb.
O_2	0.64	0.02
N_2O	7.5	0.17
H_2O_2	17	0.50
$H_2 + O_2$	0.65	0.02

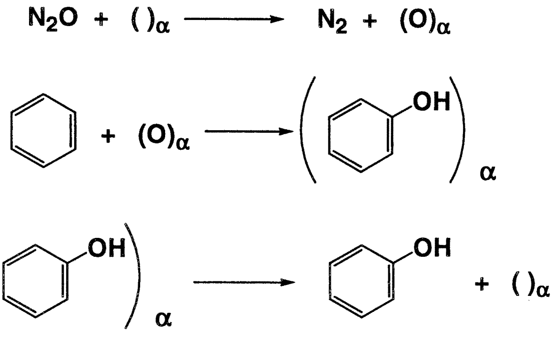

Figure 6. Proposed Mechanism for N_2O Oxidation of Benzene

Through a very extensive collaboration with Solutia[R]. this technology has been integrated into nylon intermediates manufacturing. Conventional technology for the production of adipic acid from cyclohexane provides cyclohexanone (K) and cylcohexanol (A) as intermediates. Nitric acid is used to oxidize the K/A to adipic acid and in that step significant amounts of N_2O are produced. Historically, the N_2O-containing gas stream has been vented to the atmosphere, but due to ozone depletion issues, most producers now abate the N_2O. Solutia[R] decided to separate the N_2O after the nitric acid oxidation of K/A and to react it with benzene to produce phenol, which can be hydrogenated to K and oxidized to adipic acid. This provides an opportunity to use the N_2O for expansion purposes and to provide a higher incremental yield to adipic acid. The process is reported to be in pilot plant production[18]. Application of this technology for uses other than retrofit options will be highly dependent on the cost of N_2O. Currently there are no simple high conversion, high selectivity, processes know for this reaction.

Titanosilicalites[19] are now well known to oxidize a wide variety of organics with hydrogen peroxide or alkylhydroperoxides (Figure 7). Selectivity is generally very high although utilization of the peroxide is often low. Due to the high cost of hydrogen peroxide (Table 5) commercial use will likely be restricted to fine chemical applications. However the use of hydrogen/oxygen mixtures is currently showing great promise.

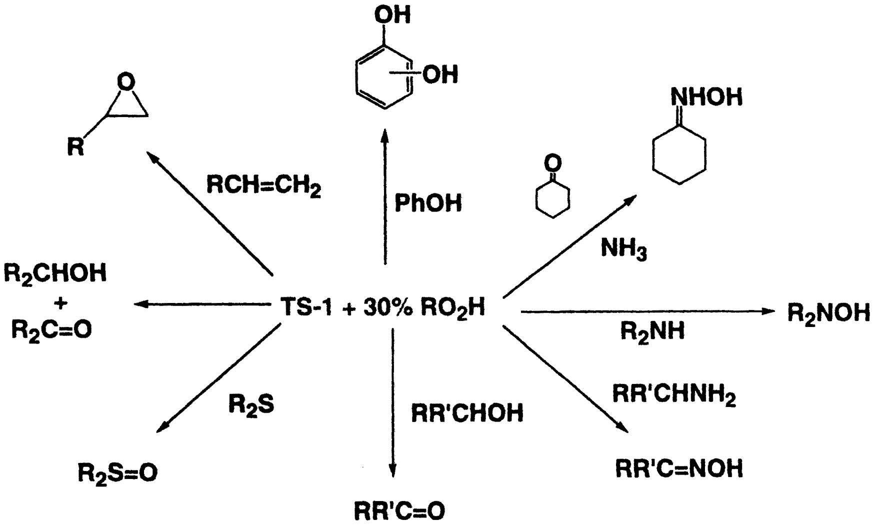

Figure 7 Products Available Using Titanosilicalite Oxidations.

For many years DuPont studied the direct catalytic combination of hydrogen and oxygen to hydrogen peroxide[20]. Platinum and palladium bimetallic catalysts on silica were studied extensively. Selectivity to hydrogen peroxide was highly dependent on the weight ratio of platinum to total metal loading on silica. Optimum ratios were 0.02-0.2, which yielded selectivity to H_2O_2 of about 70%. Very high pressures were reported and concentrations of hydrogen peroxide exceeded 20%. A key to achieving the high selectivity was the addition of a promoter such as Cl^- or Br^-.

Hoelderich[21] has been studying the epoxidation of propylene to propylene oxide using titano- or vanadio-silicate catalysts. Using a TS support with Pt/Pd and a NaBr promoter (Figure 8), with a mixture of hydrogen and oxygen, he was able to achieve selectivity to propylene oxide of 87.3% at 19.4% conversion. In the absence of the NaBr promoter, selectivity dropped to 34.1%. The result is an exciting development illustrating the potential for in-situ production of a peroxo species as a selective oxidant.

Downloaded by UNIV OF GUELPH LIBRARY on September 16, 2012 | http://pubs.acs.org
Publication Date: January 24, 2002 | doi: 10.1021/bk-2002-0809.ch003

Downloaded by UNIV OF GUELPH LIBRARY on September 16, 2012 | http://pubs.acs.org
Publication Date: January 24, 2002 | doi: 10.1021/bk-2002-0809.ch003

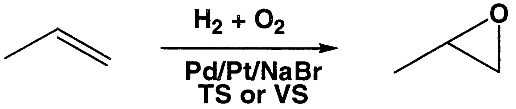

Figure 8. Preparation of Propylene Oxide from Hydrogen/Oxygen Mixtures

Recently, carbon dioxide has been reported to act as a mild oxidant with chromium-based catalysts at very high temperatures. Longya et al[22] has studied the oxidative dehydrogenation of ethane on modified chromium catalysts supported on silicalite-2. At 1073°K, good selectivity to ethylene is seen (Table 6). An evaluation of the data suggested that the overall chemistry is very complex (Figure 9) and that two successive coupling reactions occur. The first involves the dehydrogenation of ethane to ethylene and hydrogen. The second reaction involves the reverse water gas shift reaction, to form CO and water, thus allowing for a continuous removal of hydrogen during the dehydrogenation step. The process is reported to be commercial for the conversion of ethane to ethylene in a FCC tail-gas stream. The ethylene, produced is acceptable for the formation of ethylbenzene[23].

Table 6

Catalyst	Conv. (%)	Conv. (%)	Sel. (wt%)	Sel. (wt%)	Sel. (wt%)
	CO_2	C_2H_6	CH_4	C_2H_4	H_2/CO
Cr/Si-2	18.6	58.9	19.6	80.4	1.4
Cr-Mn/Si-2	22.2	62.4	18.4	81.6	1.4
Cr-Mn-Ni/Si-2	24.2	67.9	18.7	81.3	1.6
Cr-Mn-Ni-La/Si-2	20.5	64.2	13.8	86.2	1.4

$$16C_2H_6 + 9CO_2 \longrightarrow 14C_2H_4 + 12CO_2 + 6H_2O + 12H_2 + CH_4$$

$$C_2H_6 \longrightarrow C_2H_4 + H_2$$
$$CO_2 + H_2 \longrightarrow CO + H_2O$$

Figure 9. Oxidative Dehydrogenation of Ethane With CO_2

Recently Wang et al[24] have studied the effect of the support on the oxidative dehydrogenation of ethane with ethylene using carbon dioxide. The data is shown in Table 7. All data is at 600°C. Silica appears to be the optimum support in this study as well. Very high selectivity to ethylene is seen.

Table 7.

Catalyst	Conv. (%)	Conv. (%)	Sel. (wt%)	Sel. (wt%)	Sel. (wt%)
	CO_2	C_2H_6	CH_4	C_2H_4	H_2/CO
Cr_2O_3/TiO_2	0.8	0.9	6.3	93.7	4.2
Cr_2O_3	16.8	12.1	4.6	95.4	4.8
Cr_2O_3/Al_2O_3	4.9	12.6	2.3	97.6	5.6
Cr_2O_3/ZrO_2	19.2	37.9	25.3	74.6	3.2
Cr_2O_3/SiO_2	9.6	38.8	4.2	95.7	1.4

Downloaded by UNIV OF GUELPH LIBRARY on September 16, 2012 | http://pubs.acs.org
Publication Date: January 24, 2002 | doi: 10.1021/bk-2002-0809.ch003

Conclusions

The reduction in CO_2 emitted to the atmosphere is a desirable global goal. This symposium has provided a number of end-of-pipe opportunities to convert CO_2 into useful products. The ultimate goal is to eliminate the production of carbon dioxide in the first place for new processes. Clearly, it will be uneconomical to replace existing investment so end-of-pipe treatment is important. The purpose of this paper was to show that indeed there are a number of emerging new catalysts and catalytic processes that show higher selectivity to products, resulting in reduced production of CO_2. While most of these developments are only in the discovery or early development phases, there is sufficient progress to indicate that commercialization is a real possibility in the future. The key points of the paper are:

1. Anaerobic oxidation of hydrocarbons can offer significant reduction of CO_2 in several cases. However, several criteria must be met for economical viability.

2. Alternative oxidants such as H_2O_2, RO_2H and N_2O can provide higher selectivity in many reactions but economics are attractive in only a few isolated cases, currently.

3. The use of H_2 and O_2 mixtures is beginning to show promise as a replacement for H_2O_2 but safety issues will need to be seriously addressed.

4. Creative new catalytic technology can significantly reduce investment and carbon dioxide production through higher yields and few steps.

5. The direct use of CO_2 as a mild oxidant is an interesting new development that should be aggressively pursued.

References

[1] P. Mars and D. W. van Krevelen, Spec. Suppl. Chem. Eng. Sci., 3, (1954) 41

[2] M. C. Sze and A. P. Gelbum, Hydrocarbon Processing, February 1976, 103-106

[3] Gaffney, Anne M.; Jones, C. Andrew; Leonard, John J.; Sofranko, John A.. J. Catal. (1988), 114(2), 422-32

[4] S. J. Tremont, A. N. Williamson, US Patent 4,254,293 1981

[5] G. E. Vrieland and C. B. Murchison, *Applied Catalysis*, **1996**, 1 34, 101-121

[6] Oxidative Coupling of Isobutene in a Two Step Process, H. Hiltner and G. Emig, *3rd World Congress on Oxidation Catalysis*, **1997**, 593-602, Elsevier Science B. V.

[7] R. M. Contractor, M. W. Anderson, D. Campos, G. Hecquet, R. Kotwica, WO 99/03809 (1999)

[8] J. Haggin, *Chemical and Engineering News*, **1995,** April 3. Contractor, R. M.; Bergna, H. E.; Horowitz, H. S.; Blackstone, C. M.; Malone, B.; Torardi, C. C.; Griffiths, B.; Chowdhry, U.; Sleight, A. W., *Catal. Today* (1987), 1(1-2), 49-58, Contractor, R. M.; Bergna, H. E.; Horowitz, H. S.; Blackstone, C. M.; Chowdhry, U.; Sleight, A. W. **,** *Stud. Surf. Sci. Catal.* (1988), Volume Date 1987, 38 (Catalysis 1987), 645-54

[9] Bergna, Horacio E.. *ACS Symp. Ser.* (1989), Volume Date 1988, 411(Charact. Catal. Dev.), 55-64. CODEN: ACSMC8 ISSN: 0097-6156

[10] H. Kinoshita, T Ihara, (Mitsubishi Chemical Industries Ltd.) JP 98-294795;

[11] T Ushikubo, H. Nakamura, Y. Koyasu, S. Wajiki (Misubishi Kasei Corp.) US patent 5,380,933 **1995**; J. Harald, A. Tenten, S. Unverricht, A. Heiko, (BASF) WO 9920590, 1999; T. Shinrin, T. Mamoru, M. Ishii (Toa Gosei Chemical Industry Co., Ltd.) JP 09316023 1997; M. Lin, G. Buckley, (Rohm and Haas Ltd.) EP 0962253A2 1999,

[12] A. Okusako, T. Ui, K. Nagai (Sumitomo Chemical Co.) JP 95-171855 1997;

[13] T. Matsushita, T. Yamaguchi, S. Yamamatsu, H. Okamoto (Asahi Chemcial Industry Co., Ltd.)JP 10263399 (1998);

[14] Y. Mikami, A. Takeda, M. Okita JP 09216850A2 1997; Y. Mikami, A. Takeda, M. Ohkita DE 19734242A1 1999

[15] A. S. Bodke, D. A. Olschki, L. D. Schmidt and E. Ranzi, *Science*, **1999**, 712-715

[16] A. S. Kharitonov, G. I. Panov, K. G. Ione, V. N. Romannikov, G. A. Sheveleva, L. A. Vostrikova, V. I. Sobolev, US Patent 5,110,995 (1992)

[17] M. Hafele, A. Reitzmann, E. Klemm and G. Emig, *3rd World Congress on Oxidation Catalysis*, R. K. Grasselli, S. T. Oyama, A. M. Gaffney and J. JE. Lyons (Editors), Vol. 110, 847-856, **1997**, Elsevier Science B. V.

[18] A. K. Uriarte, M. A. Rodkin, M. J. Gross, A. S. Kharitonov and G. I. Panov, *3rd World Congress on Oxidation Catalysis*, R. K. Grasselli, S. T. Oyama, A. M. Gaffney and J. JE. Lyons (Editors), Vol. 110, 857-864, **1997**, Elsevier Science B. V.

[19] M. G. Clerici, *Heterogeneous Catalysis and Fine Chemicals III*, 21-33 (1993), M. Guisnet et al (Editors) Elsevier Science Publishers B. V.

20 L. W. Gosser US Patent 4,832,938 (1989)

Downloaded by UNIV OF GUELPH LIBRARY on September 16, 2012 | http://pubs.acs.org
Publication Date: January 24, 2002 | doi: 10.1021/bk-2002-0809.ch003

[21] W. Hoelderich, German Patent DE 98-19845975

[22] X. Longya, L. Liwu, W. Qingxia, Y. Li, W. Debao and L.Weichen, *NATURAL GAS CONVERSION V. Studies in Surface Science and Catalysis*, Vol. 119, 605-610 (1998), A. Parmaliana et al (Editors) Elsevier Science B. V.

[23] Wang Qingxia, Zhang Shurong, Cai Guangya, et al., CN 87105054.4, 1987

[24] S. Wang, K. Murata, T. Hayakawa, S. Hamakawa, K. Suzuki, *Applied Catalysis A: General*, 196 (2000) 1-8

Downloaded by UNIV OF GUELPH LIBRARY on September 16, 2012 | http://pubs.acs.org
Publication Date: January 24, 2002 | doi: 10.1021/bk-2002-0809.ch003

Downloaded by OHIO STATE UNIV LIBRARIES on September 16, 2012 | http://pubs.acs.org
Publication Date: January 24, 2002 | doi: 10.1021/bk-2002-0809.ch004

Chapter 4

Key Issues in Carbon Dioxide Utilization as a Building Block for Molecular Organic Compounds in the Chemical Industry

Michele Aresta* and Angela Dibenedetto

**Department of Chemistry, Campus Universitario, Via Orabona, 4 University of Bari,
70126 Barum Italy
*Fax: +39 080 5442429; email: miares@tin.it**

Carbon dioxide as a raw material for the Chemical and/or Energy Industry is receiving a growing attention because: i) if the recovery of CO_2 from flue gases will be implemented as a technology for controlling its accumulation in the atmosphere, the amount of carbon dioxide available for industrial utilisation may expand to unprecedented levels; ii) environmental issues urge to develop new processes/products which reduce the CO_2 emission. However transition metals systems are potential candidates for developing new processes. The knowledge of the behaviour of carbon dioxide and organic substrates towards metal centres plays a fundamental role for the exploitation of the chemical utilisation otpion.

In CO2 Conversion and Utilization; Song, C., et al.;
ACS Symposium Series; American Chemical Society: Washington, DC, 2002.

Downloaded by OHIO STATE UNIV LIBRARIES on September 16, 2012 | http://pubs.acs.org
Publication Date: January 24, 2002 | doi: 10.1021/bk-2002-0809.ch004

Introduction

The utilisation of carbon dioxide as a source of carbon in synthetic chemistry (*1, 2*) appears very attractive in view of the fact that, if recovery of carbon dioxide will be adopted as a technology for controlling its emission into the atmosphere, large amounts will be easily available. The products that can be conveniently obtained from carbon dioxide can be categorized as:

i) *Fine or commodity chemicals*, i.e. molecules containing functionalities such as: -C(O)O- acids, esters, lactones; -O-C(O)O- organic carbonates; -N-C(O)O- carbamates; -N-C(O)- ureas, amides;

ii) *Products for the energy industry*, i.e., energy-rich C1 molecules (HCOOH, CO, CH_3OH) and C_n hydrocarbons or their derivatives.

Developing industrial processes in these areas would produce the following advantages:

i) replacement of multistep processes with more direct synthetic procedures with waste reduction at source and atom economy, ii) implementation of alternative ways to processes presently based on more toxic or expensive materials, iii) raw materials diversification, and iv) recycling of carbon.

The overall CO_2 mass used in industrial (chemical and technological) applications is at present limited to ca. 100 Mt per year (*2*). Only four industrial processes based on carbon dioxide are on stream, two of which are more than one century old [synthesis of urea (*3*) and salicylic acid (*4*)] and do not require any catalyst. The two other processes are: the carboxylation of epoxides (*5*), and methanol synthesis (*6*), which require both metal catalysts.

The development of a "carbon dioxide-based industry" requires the discovery of new transition metal-assisted reactions. However, the modern carbon dioxide chemistry is very young, and has taken important steps since the first structural evidence of a "carbon dioxide molecule coordinated to a metal centre" was provided in 1975 (*7*).

A point that must be emphasized is that speaking of "avoided CO_2", one should consider not only the amount of CO_2 recycled through its fixation in chemicals, but also the amount of CO_2 not produced by implementing the atom efficiency and waste minimization principles (*1, 8*).

Energetics of Carbon Dioxide Utilising Reactions

The carbon dioxide-utilizing reactions mentioned so far, can be divided into two main categories from the energetic point of view.

Downloaded by OHIO STATE UNIV LIBRARIES on September 16, 2012 | http://pubs.acs.org
Publication Date: January 24, 2002 | doi: 10.1021/bk-2002-0809.ch004

Class 1

Reactions in which the whole carbon dioxide molecule is used. The substrate (amines, unsaturated hydrocarbons) is the energy vector and the amount of extra energy, if required, is usually very low. These reactions include the carboxylation reactions with the formation of a C-C or C-heteroatom bond (C-E; E=O, N, P, other element).

Class 2

Reduction reactions to C1 or C_n species, using dihydrogen, electrons, or heat as energy source.

All these reactions are common to, and very important in, biological systems (plants and bacteria), in which several enzymes involved in carbon dioxide utilisation are metal enzymes with the metal acting as the active site (*9*).

The Mechanism of CO_2 Conversion and the Role of Metal Systems

Carbon dioxide conversion requires an "acid-base", or in other terms, a "nucleophile-electrophile" catalysis. Metal centres may play a different role according to their oxidation state, which may produce an inversion of the role of the metal from electrophile to nucleophile.

Scheme 1. Role of the metal in CO_2 fixation

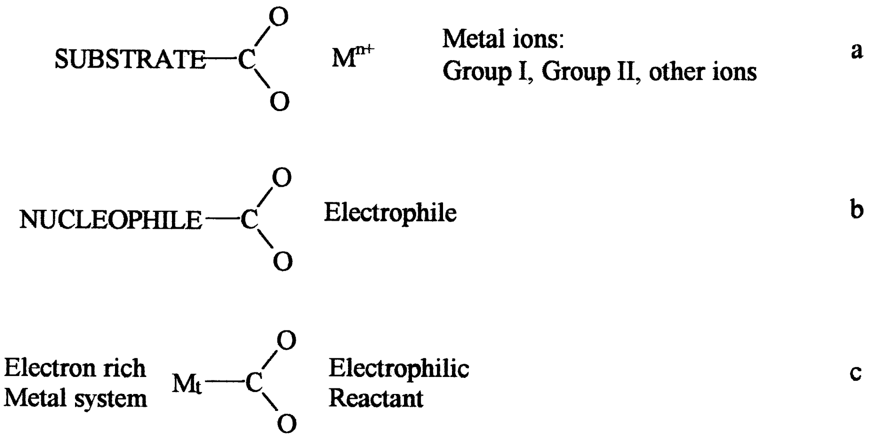
SUBSTRATE—C
O
O
M^n+
Metal ions:
Group I, Group II, other ions
a
NUCLEOPHILE—C
O
O
Electrophile
b
Electron rich
Metal system
Mt—C
O
O
Electrophilic
Reactant
c

Downloaded by OHIO STATE UNIV LIBRARIES on September 16, 2012 | http://pubs.acs.org
Publication Date: January 24, 2002 | doi: 10.1021/bk-2002-0809.ch004

A great emphasis has been put on elucidating the role of CO_2-metal complexes, in which CO_2 is either η^2-C, O or μ-bonded to one or more metal centres (*10*), in carbon dioxide reduction or in its reaction with olefins to afford carboxylates. This issue is relevant to the more general question if the coordination of CO_2 to a metal is a necessary prerequisite for CO_2 fixation onto an organic substrate. Available data suggest that such co-ordination is necessary in the reduction to CO (Scheme 2).

Scheme 2. Reactivity of the co-ordinated CO_2 molecule towards electrophile

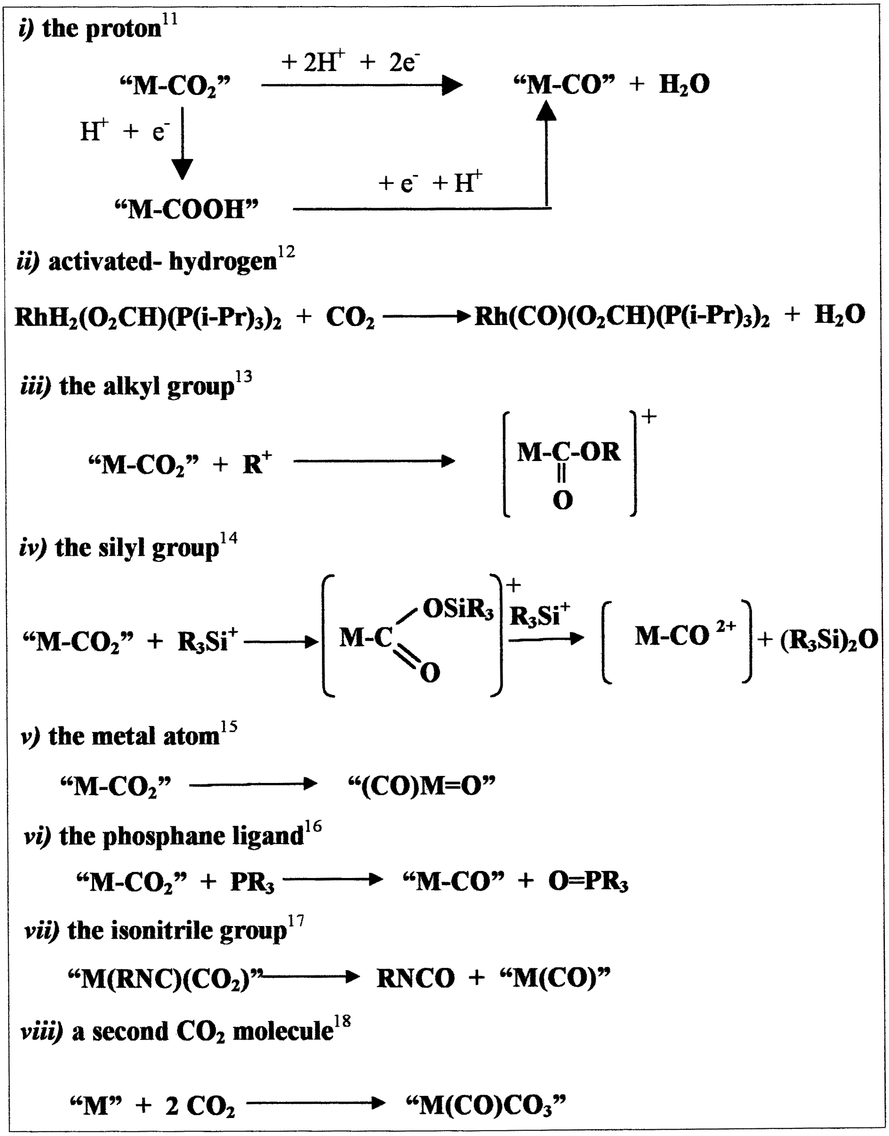
i) the proton[11]
"M-CO₂"
+ 2H⁺ + 2e⁻
"M-CO" + H₂O
H⁺ + e⁻
+ e⁻ + H⁺
"M-COOH"
ii) activated- hydrogen[12]
RhH₂(O₂CH)(P(i-Pr)₃)₂ + CO₂
Rh(CO)(O₂CH)(P(i-Pr)₃)₂ + H₂O
iii) the alkyl group[13]
"M-CO₂" + R⁺
M-C-OR
O
+
iv) the silyl group[14]
"M-CO₂" + R₃Si⁺
M-C
OSiR₃
O
+
R₃Si⁺
M-CO 2+
+ (R₃Si)₂O
v) the metal atom[15]
"M-CO₂"
"(CO)M=O"
vi) the phosphane ligand[16]
"M-CO₂" + PR₃
"M-CO" + O=PR₃
vii) the isonitrile group[17]
"M(RNC)(CO₂)"
RNCO + "M(CO)"
viii) a second CO₂ molecule[18]
"M" + 2 CO₂
"M(CO)CO₃"

Downloaded by OHIO STATE UNIV LIBRARIES on September 16, 2012 | http://pubs.acs.org
Publication Date: January 24, 2002 | doi: 10.1021/bk-2002-0809.ch004

In carboxylation reactions either the olefin is activated first, or a concerted three-centre mechanism may operate (Scheme 3).

Scheme 3. Carboxylation reactions

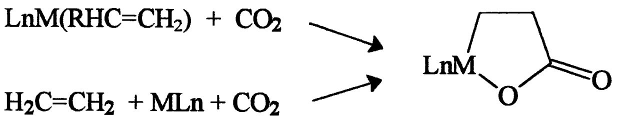
LnM(RHC=CH2) + CO2
H2C=CH2 + MLn + CO2
LnM
O
O

As a matter of fact, Ni-carbon dioxide complexes may react with olefins (*11, 19*) undergoing an exchange reaction (Scheme 4).

Scheme 4. Exchange reaction occurring when an olefin reacts with a Ni-CO2 complex

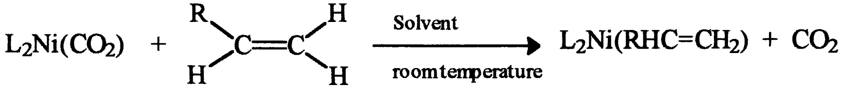
L2Ni(CO2) +
R
H
C=C
H
H
Solvent
roomtemperature
L2Ni(RHC=CH2) + CO2

Nevertheless, olefins and carbon dioxide, under the correct reaction conditions, react with low oxidation state metal systems to afford a metallacycle with the formation of a C-C bond, involving the C-atom of carbon dioxide, and the concurrent formation of a metal-oxygen bond.(Scheme 5a).

Scheme 5. Modes of interaction of M-olefin system with CO2

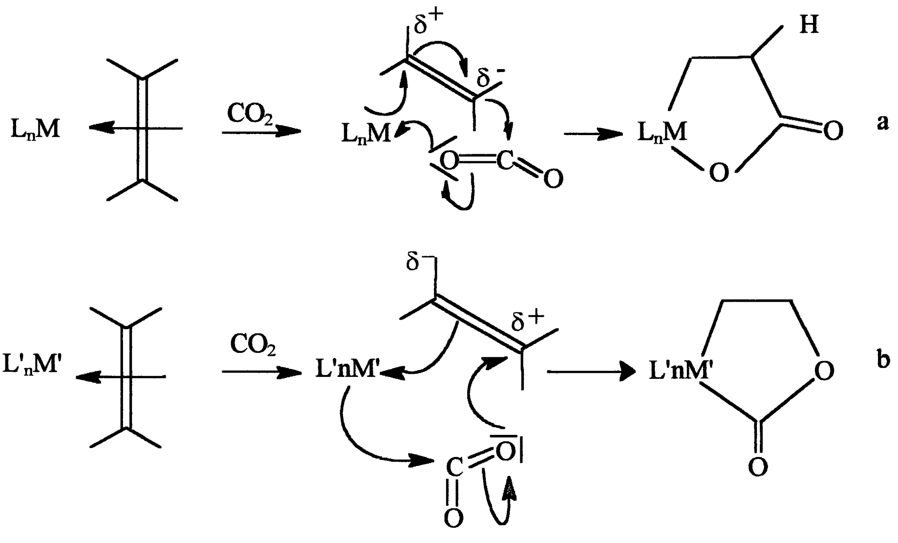
LnM
CO2
δ+
δ-
LnM
O=C=O
H
LnM
O
O
a
L'nM'
CO2
δ-
δ+
L'nM'
C
O
O
L'nM'
O
O
b

The reaction represented in scheme 5b has not been documented to date. The energy of the M-O bond results to be the TON limiting factor in catalysis, as it drives the elimination reaction that would afford the carboxylate product and regenerate the catalyst (Scheme 6).

Scheme 6. Elimination pathways from a metalla-carboxylate system

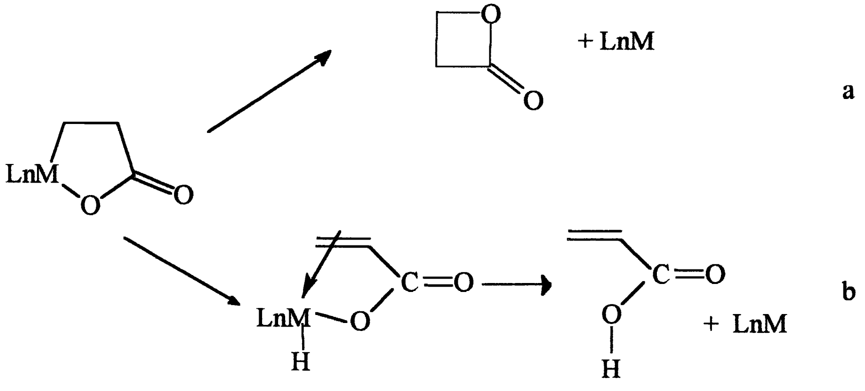

In fact, the free energy change of the elimination step according to 6a depends on the values reported in Eq. 1.

$$\Delta G = \Delta G(O\text{-}C)-[\Delta G(O\text{-}M) + \Delta G(M\text{-}C)] \quad (1)$$

The value of $\Delta G(O\text{-}M)$ can make the overall free energy change positive enough to prevent the elimination reaction. Kinetic and thermodynamic parameters play a key role

Also ancillary ligands play an important role. For example, the "dipyNi" moiety is by far more active than the "P_2Ni" unit in promoting the coupling and elimination reactions. In general, chelating ligands are better than monodentate. The ligand effect could be explained considering that CO_2 can act as oxidant of the phosphine [Scheme 2, (vi)] and this may change the nature of the catalyst.

However, the coordination of carbon dioxide in the η^2-C, O mode to a metal centre is not a necessary prerequisite for its transfer onto olefins, while it is necessary in order to promote the reduction of CO_2 through an electrophilic attack at the oxygen of carbon dioxide. The C-C bond formation, most probably goes through a nucleophilic attack at carbon dioxide, which requires a carbon atom not involved into a bonding to (or loosely bonded to) a metal-centre.

Downloaded by OHIO STATE UNIV LIBRARIES on September 16, 2012 | http://pubs.acs.org
Publication Date: January 24, 2002 | doi: 10.1021/bk-2002-0809.ch004

Downloaded by OHIO STATE UNIV LIBRARIES on September 16, 2012 | http://pubs.acs.org
Publication Date: January 24, 2002 | doi: 10.1021/bk-2002-0809.ch004

The comparative analysis of the role of metal centres in carbon dioxide fixation in natural and artificial systems (carboxylation of organic compounds) opens the question about the role of the metal in the two processes. Metal centres may present a different behaviour essentially linked to the oxidation state that may produce an inversion of the role from electrophile to nucleophile. Indeed, both natural and artificial carboxylation processes proceed through a "nucleophile-electrophile" concurrent catalytic action. (Scheme 1B).

In naturally occurring reactions, metal ions in the oxidation state (II) or (III) are involved; conversely, in artificial carboxylation, compounds containing the metal in low oxidation state (usually zero, more rarely one) are used. This fact inverts the role of the metal that in natural processes acts as an electron sink and concurs to stabilizing the carboxylate anion generated by the attack of electron rich species (amine-, hydroxo-, oxo-groups) to carbon dioxide or hydrogen carbonate (Scheme 1A), while in artificial systems the "electron rich" metal may act as nucleophile, attacking the carbon dioxide molecule at carbon (Scheme 1C). The latter reaction mechanism operates when a metal complex with the metal in a low oxidation state interacts with carbon dioxide: as a result, the further reaction of the co-ordinated carbon dioxide molecule to form a carbon-carbon bond is made difficult.

However, CO_2-metal complexes in which CO_2 is η^2-C,O bonded to the metal up to now have not shown a tendency to insert an olefin into the M-C bond of the co-ordinated CO_2. Conversely, when an olefin interacts first with the metal centre in a low oxidation state, the electron distribution can be changed: the electron rich centre is displaced from the metal to one of the carbon atoms of the coordinated olefin that can attack the carbon dioxide molecule at the carbon atom, producing a C-C bond with the concurrent formation of a metal-oxygen bond (Scheme 5b). The energy of this bond is the limiting factor for the elimination reaction (Scheme 6) that restores the catalyst, as discussed above.

The Carboxylation of Organic Substates

The carboxylation of unsaturated hydrocarbons (alkenes, alkynes, butadienes, allenes) has been recently developed with interesting yield and selectivity (>90%) using transition metal complexes as catalysts (*20*). In all cases the homo coupling of substrates is a concurrent process with the hetero-coupling substrate-CO_2. As homo-coupling reaction we mean the one in which two identical moieties are coupled: these can be either two "olefin" or two "carbon dioxide" molecules.

When two olefin molecules are considered, the result is the formation of dimers (or oligomers and/or polymers). If carbon dioxide is coupled with itself two routes are possible, bearing to either CO and carbonate (i) or oxalate (ii) (Scheme 7).

Scheme 7. Coupling of two molecules of CO_2

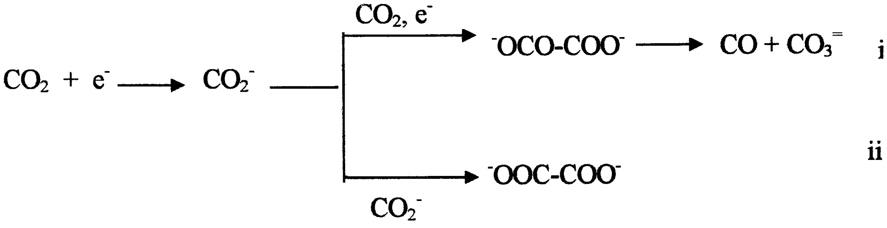

The solvent and the carbon dioxide concentration in solution play an important role in driving the reaction in either directions. It has been for a long time believed that a "one electron donor" would generate oxalate, while a "two electron donor" would produce CO and carbonate. It has been clearly stated that also in the electrochemical reduction of carbon dioxide (which is clearly a "one electron" transfer reaction) the formation of CO and carbonate is achieved, depending on parameters such as current density, carbon dioxide pressure, and solvent (*21*).

As a consequence, the formation of carboxylated products from olefins and carbon dioxide (hetero-coupling) is very often accompanied by homo-coupling products which, according to the experimental conditions, can also represent the most abundant fraction. The preliminary oligomerization of olefins is not a negative fact, as it can bear to the synthesis of long-chain carboxylic acids (Scheme 8) or ring-products starting from terminal mono-olefins or dienes.

To master this issue is of fundamental importance in order to develop processes which may have an industrial application.

The analysis of the literature data indicates that carbon dioxide-unsaturated hydrocarbon coupling (with a high TON) is driven by one of the following conditions: i) low energy of the M-O bond; ii) β-hydrogen shift from the hydrocarbon moiety to the metal, that can eventually produce an O-H bond in place of the O-M bond; iii) existence or generation of an allyl group that may assist the elimination through a σ-π interconversion.

The simple reductive elimination according to Scheme 6 has been observed in rare cases (22, *23*) and is not operative in processes with high TON.

Downloaded by OHIO STATE UNIV LIBRARIES on September 16, 2012 | http://pubs.acs.org
Publication Date: January 24, 2002 | doi: 10.1021/bk-2002-0809.ch004

However, to develop catalysts which produce acrylic acid from CO_2 and ethylene (Scheme 6b) or four membered ring lactones (Scheme 6a) would be of great industrial interest.

Scheme 8. Metal catalysis in butadiene-CO_2 chemistry

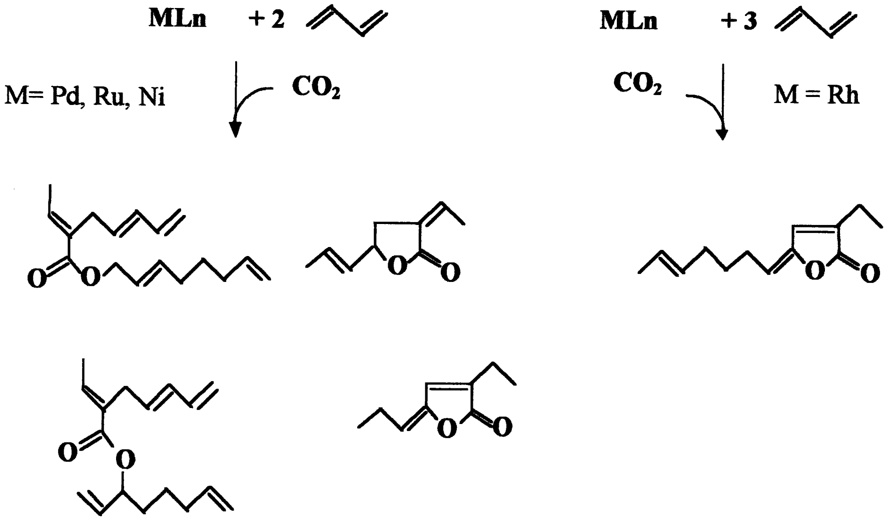

Insertion of CO_2 into C-C Bonds

The reaction of strained rings with CO_2 promoted by transition metal systems is of interest as it would be a way to synthesize lactones from cyclic hydrocarbons (or their derivatives) through a formal CO_2 insertion into a C-C bond. Rings of different size have been reacted with CO_2 in the presence of catalysts, both in thermal and light-driven reactions (*24, 25*). The size of the ring affects the reactivity. Cycloalkanes and cycloalkenes have different reactivity. As an example, the UV-visible irradiation of a solution of $RhCl(PMe_2Ph)_3$ at low temperature in presence of cyclopropane and carbon dioxide under pressure, produces butyrolactone (Scheme 9).

It is interesting to note that, as evidenziated in Scheme 9, light can promote reactions (i) different from heat (ii), which promotes phosphane oxidation with CO release, which changes the catalyst.

Synthesis of Carbonates

Organic carbonates can be synthesized from either carbon dioxide and epoxides, or olefins, dioxygen and carbon dioxide (*26*) (Scheme 10).

Downloaded by OHIO STATE UNIV LIBRARIES on September 16, 2012 | http://pubs.acs.org
Publication Date: January 24, 2002 | doi: 10.1021/bk-2002-0809.ch004

Scheme 9. Reactivity of cycloalkanes towards carbon dioxide

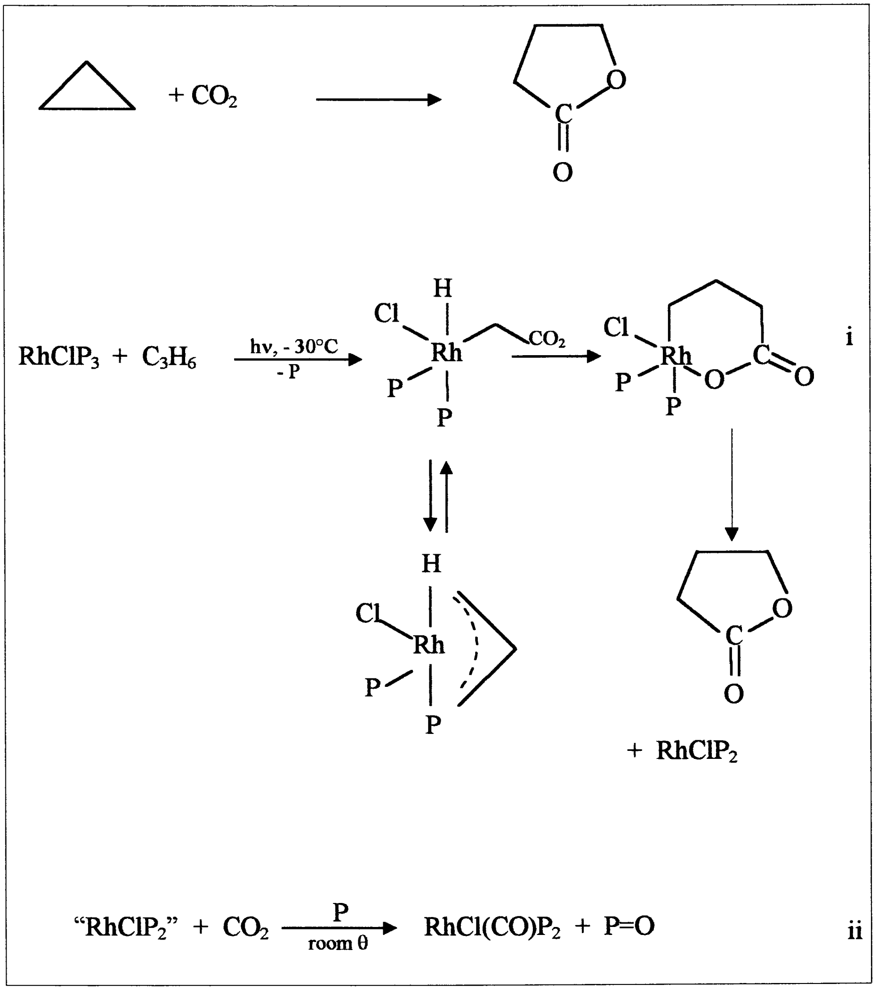
+ CO2
RhClP3 + C3H6
hν, - 30°C
- P
H
Cl
Rh
P
P
CO2
Cl
Rh
P
P
O
C
O
i
H
Cl
Rh
P
P
O
C
O
+ RhClP2
"RhClP2" + CO2
P
room θ
RhCl(CO)P2 + P=O
ii

Downloaded by OHIO STATE UNIV LIBRARIES on September 16, 2012 | http://pubs.acs.org
Publication Date: January 24, 2002 | doi: 10.1021/bk-2002-0809.ch004

Scheme 10. Syntheses of organic carbonates

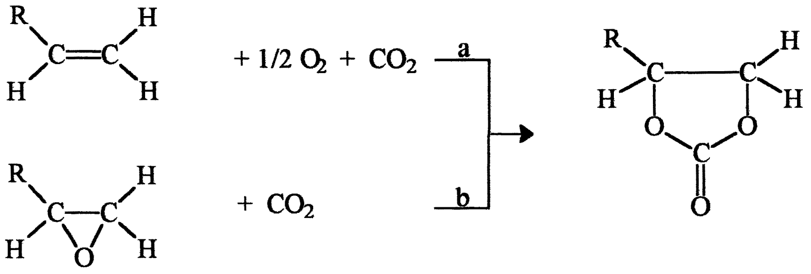

$$2\ ROH + CO_2 \xrightarrow{c} (RO)_2CO + H_2O$$

The two reactions (a, b) present different barriers to a full implementation. Because of their interest, a great effort is currently under way in order to understand the reaction mechanism for a full exploitation of the potential of these synthetic approaches.

Oxirane co-polymerization with CO_2 has been widely investigated as the way to polymers which may find large application (*27*). This approach is of interest as the products, besides their specific use, have a long life. Fixation of carbon dioxide in polymeric materials would be an example of quasi-perennial sequestration of the cumulene.

The most used catalysts use Zn-adducts or aluminium organometallic (*28*) systems [alkyl-Al or (porphyrin)-Al-derivatives]. These catalysts make the copolymerization easier to proceed, giving alternating polycarbonates, whose molecular mass ranges from 100 to 150 kDa.

The polycarbonates properties make them greatly interesting for their technological applications, being characterized by an high permeability to oxygen, low combustion heat, owing to the high oxygen content, low decomposition temperature, that ranges in very narrow intervals, high biodegradability.

Only few reports (*29, 30*) are in the literature on the direct synthesis of carbonates from olefins, dioxygen and carbon dioxide, despite the usefulness of this reaction, which avoids the preliminary synthesis of epoxides, well known

Downloaded by OHIO STATE UNIV LIBRARIES on September 16, 2012 | http://pubs.acs.org
Publication Date: January 24, 2002 | doi: 10.1021/bk-2002-0809.ch004

Downloaded by OHIO STATE UNIV LIBRARIES on September 16, 2012 | http://pubs.acs.org
Publication Date: January 24, 2002 | doi: 10.1021/bk-2002-0809.ch004

for their toxicity. $RhClP_3$ (P = PEt_2Ph, $PEtPh_2$) and $RhClL_2$ (L_2 = diphos, dipy) have been used as catalysts in styrene functionalization, affording a mixture of styrene oxyde, benzaldehyde, acetophenone, phenylacetaldehyde and styrene carbonate. (*31*) It has been ascertained that the product distribution is strongly dependent on the solvent used, the temperature, the ancillary ligand coordinated to rhodium, the ligand-to-Rh molar ratio and the pressure of the gas.

As epoxide is one of the oxidation products of styrene, it could be the origin of styrene carbonate. It has been ascertained that the formation of the carbonate from styrene, O_2 and CO_2 takes place at a higher rate than from styrene oxide and CO_2, in the presence of the same catalyst. This brings to the conclusion that the preliminary formation of the epoxide is not a necessary step for the synthesis of carbonate. Metal oxides appear to be more suitable catalysts due to their longer life (*26*).

Linear carbonates (Scheme 10c) are of remarkable importance as intermediates, solvents and reagents, and may find application as fuel additives.

Synthesis of Carbamates and Isocyanates

Carbamates can be prepared from carbon dioxide, amines and the proper alkylating agent (Scheme 11).

Scheme 11. Syntheses of carbamates

$$CO_2 + 2\,R'R''NH \longrightarrow R'R''NCOO^{-+}H_2NR'R''$$

$$R'R''NCOO^{-+}\,H_2NR'R'' + RX \xrightarrow[\text{yield} \cong 99\%]{\text{Crown-ether}} R'R''NCOOR + CE\,R'R''NH_2^{+}X^{-}$$

Primary amines can originate isocyanates (Scheme 12), which have a great importance in the chemical industry. Carbonates can be reacted with amines to generate carbamates, making the chemistry of carbamates, carbonates, and isocyanates fully integrated in a very interesting network of reactions (*31*). Transesterification reactions may play a very important role in synthetic chemistry.

Scheme 12. Transesterification reactions

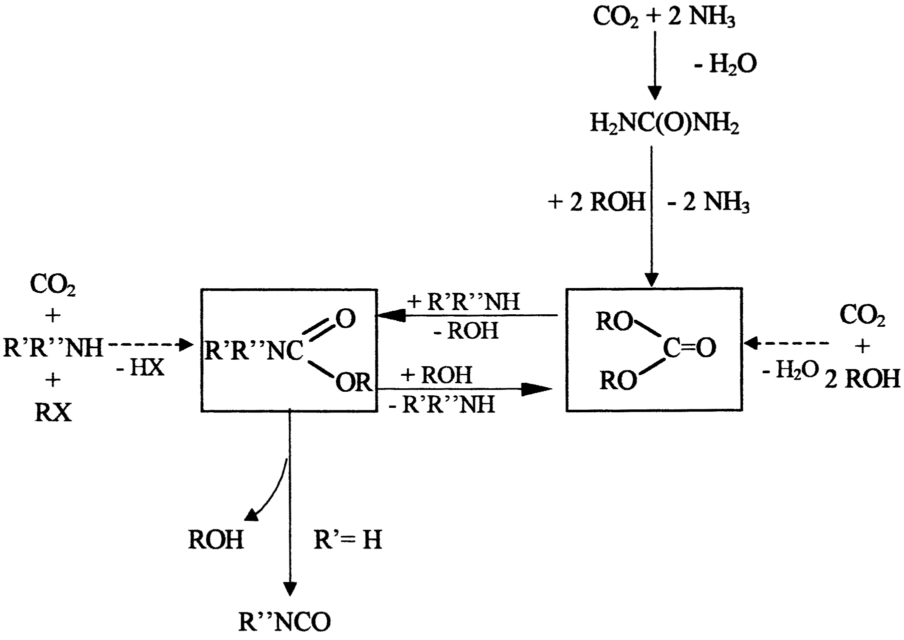

This approach is of great interest for the synthesis of several valuable chemicals which have a large market.

Coupling Chemistry with Biotechnology

Carboxylation reactions based on carbon dioxide have a great interest as the direct introduction of the carboxylic functionality represents, with respect to the conventional synthetic methodologies, a way for both saving energy and reducing the production of waste. Despite such aspects, which have a positive environmental impact, the only "direct carboxylation" process exploited at the industrial level is the more-than-one-hundred-years old Kolbe-Schmitt reaction. This process converts phenol (in the form of a Group 1 element salt) and carbon dioxide into a mixture of the o- or p-OH-benzoic acid. (Scheme 13)

The selectivity depends on the reaction conditions and the metal used (Na or K, respectively). This reaction has been recently revised (*32*) by several research groups and extended to other substrates.

Downloaded by OHIO STATE UNIV LIBRARIES on September 16, 2012 | http://pubs.acs.org
Publication Date: January 24, 2002 | doi: 10.1021/bk-2002-0809.ch004

Scheme 13. Kolbe-Schmitt reaction

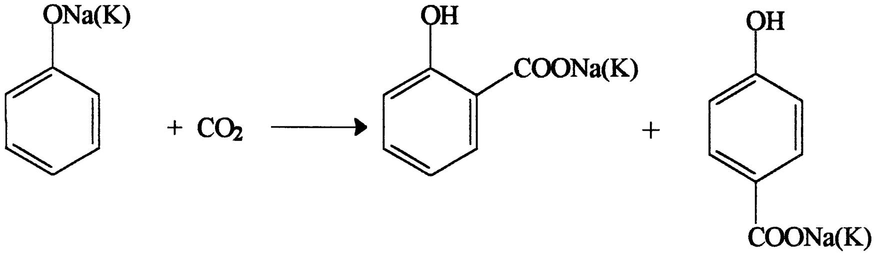
ONa(K)
+ CO2
OH
COONa(K)
+
OH
COONa(K)

The discovery of a Mn- and K-dependent Carboxylase enzyme (*33*) isolated from some anaerobic bacteria growing on phenol, stimulated our interest in enzymatic functionalization of phenol. The PC-enzyme converts, under mesophilic conditions, very specifically phenol into 4-OH-benzoate. (Scheme 14a).This is further dehydroxylated to benzoic acid and metabolized (Scheme 14b) (*33*).

Scheme 14. Enzymatic conversion of phenol to 4-OH-benzoate

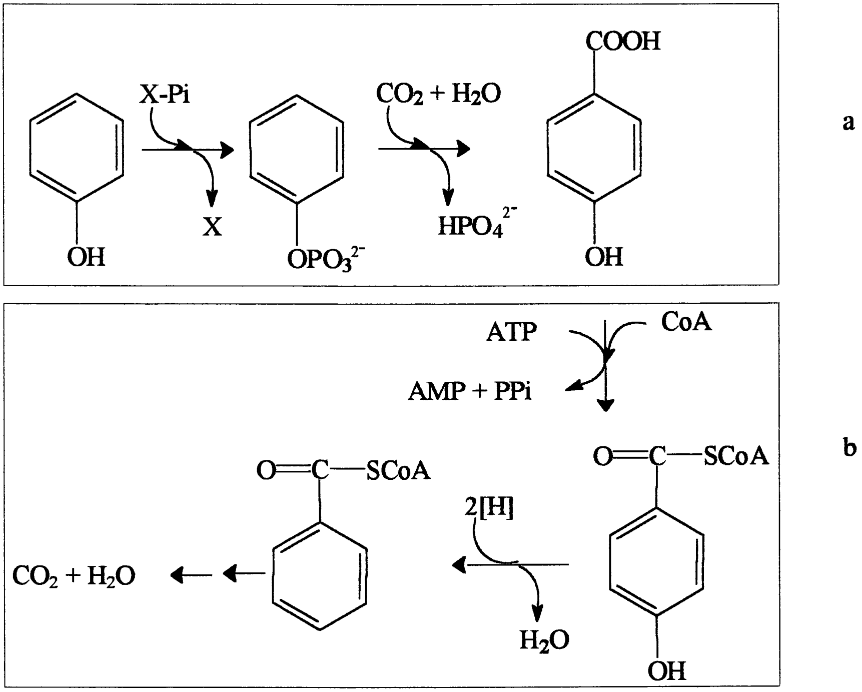
X-Pi
X
OH
OPO3 2-
CO2 + H2O
HPO4 2-
COOH
OH
a
ATP
CoA
AMP + PPi
O=C—SCoA
OH
2[H]
H2O
O=C—SCoA
CO2 + H2O
b

Downloaded by OHIO STATE UNIV LIBRARIES on September 16, 2012 | http://pubs.acs.org
Publication Date: January 24, 2002 | doi: 10.1021/bk-2002-0809.ch004

We decided to explore the possibility of using the purified enzyme (or the enzymatic pool) for catalyzing the net carboxylation of phenol. However, we have recently developed a quite interesting synthetic procedure that converts phenol into 4-OH-benzoate at room temperature and sub-atmospheric pressure of carbon dioxide. Either the enzymatic pool or the partially purified enzyme can be used, supported on low melting agar (that has been shown to be the best support) (*34*). As shown in Scheme 14a, in order to be carboxylated, phenol must be in the O-phosphorylated form. A rapid and inexpensive phosphorylation process of phenol has been developed (*34*) that occurs at room temperature (*34*). By passing the solution of the phosphorylated phenol on the supported enzyme the quantitative conversion of phenol into 4-OH-benzoate is observed. (Scheme 15)

Scheme 15. Biotechnological synthesis of 4-OH-benzoic acid

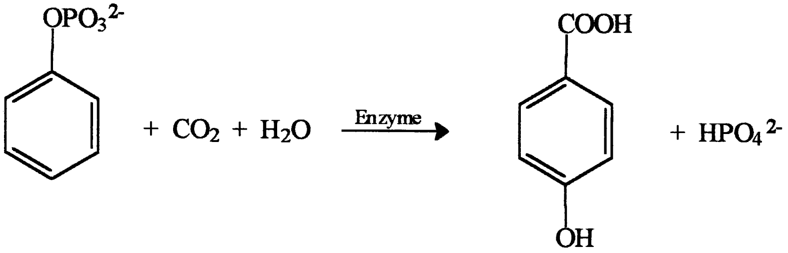

As the supported catalyst remains active for more than one week a TON of more than 10^4 moles of phenylphosphate carboxylated per mole of catalyst has been observed. This represents the first report on a supported Phenyphosphate Carboxylase protein and the unique demonstration of the use of a Carboxylase enzyme in synthetic application.

Conclusions

The utilisation of carbon dioxide in synthetic chemistry is a promising way for developing benign synthetic methodologies, avoiding toxic species and saving energy and carbon. New catalysts must be developed which are at the same time active and selective. Metal systems are excellent candidates for such reactions.

Downloaded by OHIO STATE UNIV LIBRARIES on September 16, 2012 | http://pubs.acs.org
Publication Date: January 24, 2002 | doi: 10.1021/bk-2002-0809.ch004

Nature provides very interesting examples of catalytic fixation of both the entire carbon dioxide molecule and its reduced forms. The utilisation of either biosystems or mimetic complexes is very challenging for chemists.

We have found that in some cases this approach can give interesting results that may find industrial interest.

References

1. Aresta, M.; Tommasi, I. *Energy Conv. Mgmt.*, **1997**, 38, S373.
2. Aresta, M.; Quaranta, E. *Chem. Tech.*, **1997**, 27, 32.
3. Fromm, D.; Lutzov, D. *Chem. Uns. Zeit.*, **1979**, 13, 78.
4. Kolbe, H.; Lautemann, *Ann.* **1980**, 113, 125.
5. Pacheco, M.A.,Marshall, C.L. *Energy&Fuels*, **1997**, 11, 2.
6. Ushikoshi, K.; Mori, K.; Watanabe, T.; Takeuchi, M.; Saito, M. *Advances Chemical Conversions for Mitigating Carbon Dioxide*, **1998**, 114, 357.
7. Aresta, M.; Nobile, F.; Manassero, M.; Albano, V.G.; Forni, E. *J. Chem. Soc. Chem. Commun.*, **1975**, 675.
8. Aresta, M.; Magarelli, A.; Tommasi, I. *Appl. Organmet. Chem.* **2000** in press.
9. Aresta, M.; Quaranta, E.; Tommasi, I.; Giannoccaro, P. *Gazz. Chim. Ital.*, **1995**, 125, 509.
10. Gibson D.H. *Chem. Rev.*, **1996**, 96, 2063.
11. Aresta, M.; Quaranta, E.; Tommasi, I. *J. Chem. Soc., Chem. Commun.*, **1988**, 450.
12. Yoshida T.; Thorn D.; Okano T.; Ibers J.A.; Yamamoto A. *J. Am. Chem. Soc.*, **1979**, 101, 4212.
13. Aresta M.; Nobile C.F. *Inorg. Chim. Acta*, **1977**, 24, L49.
14. Tsai J. C.; Khan M.; Nicholas K.M. *Organometallics*, **1989**, 8, 2967.
15. Demerseman B.; Bouquet G.; Bigorgne M. *J. Organometal. Chem.*, **1978**, 143, 151; Facchinetti G.; Floriani C.; Chiesi-Villa A. *J. Am. Chem. Soc.*, **1979**, 101, 176.
16. Aresta M.; Nobile C. F.; Albano V.G.; Forni E.; Manassero M. *J. Chem. Soc. Chem. Commun.*, **1975**, 675.
17. Tsuda T.; Sanada S.I.; Saegusa T. *J. Organometal. Chem.*, **1976**, 116, C10.
18. a) Chatt J.; Kubota M.; Leigh G.-J.; March F.C.; Mason R.; Yarrow D.J. *J. Chem. Soc. Chem. Commun.*, **1974**, 1033; b) Herskowitz T.; Guggenberger L.J. *J. Am. Chem. Soc.*, **1976**, 98(6), 1615-1616.
19. Aresta, M.; Quaranta, E.; Tommasi, I.; Gobetto, R. *Inorg. Chem.*, **1992**, 31, 4286.

Downloaded by OHIO STATE UNIV LIBRARIES on September 16, 2012 | http://pubs.acs.org
Publication Date: January 24, 2002 | doi: 10.1021/bk-2002-0809.ch004

20. Aresta, M.; Quaranta, E.; Tommasi, I. *New J. Chem.*, **1994**, 18, 133.
21. Vianello, E.; Isse, A.A.; Gennaro, A.; Severin, M.G. *Proceedings, International Conference on Carbon Dioxide Utilisation*, Bari, Italy, September 26-30, **1993**, 287.
22. Alvarez, R.; Carmona, E.; Cole-Hamilton, D.J.; Galindo, A.; Gutierrez-Puebla, E.; Monge, A.; Poveda, M.L.; Ruiz, C. *J. Am. Chem. Soc.*, **1985**, 107, 5529.
23. Aresta, M. in *Mechanistic Aspects of Molecular Catalysis, Education in Advanced Chemistry*, **1999**, 6, 21.
24. Aresta, M.; Quaranta, E.; Tommasi, I. *Photochemical Conversion and Storage of Solar Energy*, Kluwer Academic Publishers, **1991**, 517.
25. Aresta, M.; Quaranta, E.; Ciccarese, A.*C_1 Mol. Chem.*, **1985**, 1, 276, and references therein.
26. Aresta, M.; Dibenedetto, A.; Tommasi, I. *Appl. Organomet. Chem.*, **2000**, in press.
27. Inoue, S. *Copolymerization of Carbon Dioxide and Epoxide*, in *"Carbon Dioxide as a Source of Carbon"*, Aresta, M. and Forti, G. Eds., NATO-ASI Series C, **1987**, 206, 331.
28. Darensbourg, D. J.; Holtcamp, M.W. *Coordination Chem. Rev.*, **1996**, 153, 155.
29. Kao, J.L.; Wheaton, G.A.; Sheng M.N. U.S. Patent, 4, 224, 223; C.A. 95, 80926f **1981**.
30. Jacobsen, S.E. Eur. Pat. Appl. EP 118, 248; C.A., 102, 6460w, **1984**.
31. Aresta, M. *La chimica e l'Industria*, **1998**, 80, 1051, and references therein.
32. Bachmann, W.; Gnabs, C.; Janecka, K.; Mudlos, E.; Papenfuhs, T.; Waese, G. Ger. Offen. 2, 426, 850; C.A. 85, 20936t, **1976**.
33. Lack, A.; Tommasi, I.; Aresta, M.; Fuchs, G. *Eur. J. Biochem.*, **1991**, 197, 473.
34. Aresta, M.; Quaranta, E.; Liberio, R.; Dileo, C.; Tommasi, I. *Tetrahedron*, **1998**, 54, 8841.

Downloaded by OHIO STATE UNIV LIBRARIES on September 16, 2012 | http://pubs.acs.org
Publication Date: January 24, 2002 | doi: 10.1021/bk-2002-0809.ch004

Downloaded by UNIV OF GUELPH LIBRARY on September 16, 2012 | http://pubs.acs.org
Publication Date: January 24, 2002 | doi: 10.1021/bk-2002-0809.ch005

Chapter 5

Selective Conversion of Carbon Dioxide and Methanol to Dimethyl Carbonate Using Phosphoric Acid-Modified Zirconia Catalysts

Yoshiki Ikeda, Yutaka Furusawa, Keiichi Tomishige*, and Kaoru Fujimoto

**Department of Applied Chemistry, School of Engineering, The University of Tokyo,
7–3–1 Hongo, Bunkyo-ku, Tokyo 113–8656, Japan**

Direct synthesis of dimethyl carbonate from methanol and carbon dioxide was studied over heterogeneous catalysts. It is found that dimethyl carbonate can be synthesized selectively on zirconia catalysts. The additive effect of phosphates or sulfates to zirconia was investigated. Phosphoric acid was found to be very effective for the enhancement of the catalytic activity with high selectivity in this reaction. On zirconia and phosphoric acid-modified zirconia catalysts, the amount of by-products, dimethyl ether and carbon monoxide was below the detection limit. This reaction proceeded at much lower temperature on phosphoric acid-modified zirconia than on unmodified zirconia. It is suggested that DMC formation proceeds on the active sites derived from the interaction between phosphoric acid and zirconium hydoxide during the catalyst preparation.

In CO2 Conversion and Utilization; Song, C., et al.;
ACS Symposium Series; American Chemical Society: Washington, DC, 2002.

Downloaded by UNIV OF GUELPH LIBRARY on September 16, 2012 | http://pubs.acs.org
Publication Date: January 24, 2002 | doi: 10.1021/bk-2002-0809.ch005

Introduction

The development of CO_2-based methods for the synthesis of carbonic acid diesters is very attractive (*1*). Dimethyl carbonate (DMC), the lowest homologue of this family, is drawing attention as a safe, noncorrosive, and environmentally acceptable alternative to the carbonylating, carboxymethylating, and methylating agents $COCl_2$, $CH_3OC(O)Cl$, and dimethylsulfate or methyl halides, respectively. DMC has about 3 times the oxygen content as methyl *tert*-butyl ether and DMC has a good blending octane (*2*). DMC does not phase separate in a water stream like some alcohols do, and it is both low in toxicity and quickly biodegradable. DMC can also be used as an ocatne booster in gasoline. Furthermore the addition of DMC to the diesel fuel decreased the emission of the particulate matter. If DMC is used as the fuel additive, a large scale-up of current world DMC production would be necessary.

Three kinds of large-scale production methods of DMC have been developed. First method is the stoichiometric reaction of methanol and phosgene in a concentrated sodium hydroxide solution (*3*):

$$2CH_3OH + COCl_2 \rightarrow (CH_3O)_2CO + 2HCl$$

Second method is the oxidative carbonylation of CH_3OH with carbon monoxide and oxygen catalyzed by cuprous chloride in a slurry reaction system (*4-6*), where the reaction proceeds in the redox cycle of copper ions as follows:

$$2CuCl + 2CH_3OH + 1/2O_2 \rightarrow 2Cu(OCH_3)Cl + H_2O$$
$$2Cu(OCH_3)Cl + CO \rightarrow (CH_3O)_2CO + 2CuCl$$

Third is an excellent DMC synthesis process based on the oxidative carbonylation using a palladium catalyst and methyl nitrite promoter (*7*):

$$CO + 2CH_3ONO \rightarrow (CH_3O)_2CO + 2NO$$

Methyl nitrite used in this process is synthesized by the following reaction, which proceeds at room temperature without any catalyst:

$$2CH_3OH + 2NO + 1/2O_2 \rightarrow 2CH_3ONO + H_2O$$

There are some routes of DMC synthesis from CO_2. The reaction of alcohols with urea is one potential route to carbonates (*1*):

$$2CH_3OH + (NH_2)_2CO \rightarrow 2NH_3 + (CH_3O)_2CO$$
$$2NH_3 + CO_2 \rightarrow (NH_2)_2CO + H_2O$$

Ammonia is recycled to produce urea by reaction with CO_2. As a result, this process corresponds to the synthesis from CH_3OH and CO_2. There is another synthesis route of DMC via ethylene oxide route (*8*):

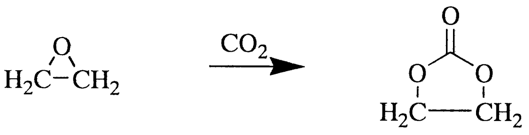

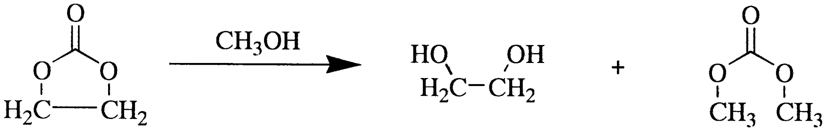

The reaction of epoxide with CO_2 is very rapid and high exothermic. This route produces ethylene glycol as a (1:1 molar) coproduct with DMC. This would limit the number of plants that could be built using this route.

Recently the selective DMC synthesis via the reaction of supercritical CO_2 and trimethyl orthoacetate using molecular catalyst $Bu_2Sn(OCH_3)_2$ has been reported (*9*):

$$CH_3C(OCH_3)_3 + CO_2 \rightarrow (CH_3O)_2CO + CH_3COOCH_3$$

It is known that DMC can be synthesized directly from CH_3OH and CO_2 in the presence of dialkoxydibutyltin (*10*). The reactions were carried out under pressure of CO_2. It is assumed that CO_2 is inserted into Sn-O bond of $Bu_2Sn(OCH_3)_2$ followed by alcoholysis yielding carbonate and $Bu_2Sn(OH)_2$. This species is again esterified by alcohol, so that the tin catalyst can be reused:

$$2CH_3OH + CO_2 \rightarrow (CH_3O)_2CO + H_2O$$

It has also been reported that DMC was synthesized from CH_3OH and CO_2 in the presence of Sn(IV) and Ti(IV) alkoxides and the metal acetates (*11*). These alkoxide catalysts react with the water produced with DMC and deactivate.

Recently we have reported that DMC was selectively synthesized from CH_3OH and CO_2 using zirconia catalysts (*12*). On some other catalysts, dimethyl ether (DME) was formed and DMC was not detected at all. It is characteristic that DME formation on ZrO_2 was below the detection limit. The amount of DMC formation showed the volcano-type dependence on the calcination temperature of zirconium hydroxide (*12*, *13*). It was found that the DMC formation rate was strongly dependent on the structure of ZrO_2. We calculated the equilibrium level of CH_3OH conversion under our reaction conditions to be

Downloaded by UNIV OF GUELPH LIBRARY on September 16, 2012 | http://pubs.acs.org
Publication Date: January 24, 2002 | doi: 10.1021/bk-2002-0809.ch005

around 1% (DMC = 0.96 mmol). This value is higher than the experimental results, but this seems to be because our calculation did not consider H_2O as an impurity. The reactor, reactants, and catalyst surface should contain H_2O as an impurity, the amount of which is difficult to estimate. H_2O as an impurity may decrease the equilibrium level of DMC formation (*12*). In this article, the modification effect of ZrO_2 with phosphates and sulfates in DMC synthesis from CH_3OH and CO_2 was investigated. Especially, the catalytic properties of phosphoric acid-modified ZrO_2 catalysts were focused.

Downloaded by UNIV OF GUELPH LIBRARY on September 16, 2012 | http://pubs.acs.org
Publication Date: January 24, 2002 | doi: 10.1021/bk-2002-0809.ch005

Experimental

ZrO_2 was prepared by calcining a commercially available zirconium hydroxide ($ZrO_2 \cdot xH_2O$) at 673 K for 3 h under air atmosphere. The calcination temperature was optimized by our privious study (*12*, *13*). Modified ZrO_2 catalysts were prepared by impregnating $ZrO_2 \cdot xH_2O$ with the aqueous solution of phosphates or sulfates. The solvent was removed by heating and the sample was dried at 393 K for 10 h, followed by calcining at different temperatures (573-923 K) for 3 h under air atmosphere. These catalysts are represented by $M_x(PO_4)_y/ZrO_2$ or $M_x(SO_4)_y/ZrO_2$ (M: H, K, Cs, Mg, Ce, Zn, Fe, x, y = 1, 2, 3). The loading of modification reagents is denoted as the molar ratio in parentheses; e.g. H_3PO_4/ZrO_2 (P/Zr = 0.05). Another preparation method was attempted. Phosphoric acid was loaded directly on ZrO_2 which had prepared by calcining $ZrO_2 \cdot xH_2O$ at 673 K for 3 h. After impregnation, the catalyst was prepared by the same procedure as described above. This catalyst is represented by H_3PO_4/ZrO_2(D).

The reaction was carried out in a stainless steel autoclave reactor with an inner volume of 70 ml. The standard procedure is as follows: 6.1 g CH_3OH (192 mmol) and 0.5 g catalyst were put into an autoclave, then the reactor was purged with CO_2. 8.8 g CO_2 (200 mmol) was introduced and the initial pressure was about 4 MPa at room temperature. The reactor was heated and magnetically stirred constantly during the reaction. The reaction was carried out at different temperatures (383-443 K) for 2 h. Products in both gas phase and liquid phase were analyzed by gas chromatograph (GC) equipped with FID and TCD. In this experiment the reproducibility is in the range of ±0.01 mmol. In the gas phase, no products were observed. CO was below the detection limit of FID-GC equipped with methanator. On ZrO_2 and H_3PO_4/ZrO_2 catalysts under all reaction conditions shown in this paper, DMC was the only product and DME was below the detection limit of FID-GC.

BET surface area, XRD spectra, and LRS spectra of the catalysts were measured with Gemini 2360 (Micromeritics, N_2 adsorption), RINT-2400 (Rigaku, Cu K_α), and LABRAM 1B (JOBIN-YBON, He-Ne laser), respectively.

Results and Discussion

The results of CH_3OH+CO_2 reaction over heterogeneous catalysts are listed in Table I. On some solid acid catalysts like Al_2O_3, TiO_2, H-ZSM-5, H-USY, H-Mordenite and H-β, DME was formed and DMC formation was not detected at all. DMC was formed selectively on ZrO_2 catalysts and SnO_2. On other catalysts, neither DMC nor DME was observed. The amount of DMC formation on ZrO_2 (calcined at 673 K) at 443 K for 40 h was 0.35 mmol, and DME formation was not detected at all. DME formation rate was extremely low (<0.0005 mmol/h·g-cat). On the other hand, DMC formation rate can be estimated to be 0.3 mmol/h·g-cat from the result that the amount of DMC formation was 0.3 mmol/0.5g-cat after 2 h reaction. From the comparison, the selectivity of DMC formation is >99%. It was found that ZrO_2 is an effective catalyst for the DMC synthesis from CH_3OH and CO_2. More details were described in our previous reports (*12*, *13*).

The effect of modified ZrO_2 catalysts calcined at 673 K and 923 K on DMC formation are shown in Table II and III, respectively. The modification with some phosphates and sulfates promoted the DMC formation. H_3PO_4 was found to be the most effective for the enhancement of the catalytic activity in this reaction at both calcination temperatures (*14*). DME was formed on $Ce_2(SO_4)_3/ZrO_2$ and $Fe_2(SO_4)_3/ZrO_2$ calcined at 923 K. This suggests that these catalysts have stronger acidity.

Figure 1 shows the dependence of DMC amount on reaction temperature over ZrO_2 and H_3PO_4/ZrO_2 (P/Zr = 0.025) calcined at 673 K. DMC formation on ZrO_2 is controlled by the reaction rate under these reaction conditions. The dramatic effect of the modification with H_3PO_4 was easily observed at all reaction temperatures. It seems that the amount of DMC on H_3PO_4/ZrO_2 (P/Zr = 0.025) at 443 K reached the equilibrium level. The DMC amount on H_3PO_4/ZrO_2 (P/Zr = 0.025) at 423 K became about four times larger than that on ZrO_2. The amount of DMC on H_3PO_4/ZrO_2 (P/Zr = 0.025) at 403 K was comparable to that on ZrO_2 at 443 K. While DMC formation was not observed on ZrO_2 at 383 K, 0.10 mmol DMC was formed on H_3PO_4/ZrO_2 (P/Zr = 0.025). It should be noted that the addition of H_3PO_4 to ZrO_2 promoted this reaction remarkably (*14*).

Figure 2 shows the dependence of DMC amount and BET surface area of H_3PO_4/ZrO_2 calcined at 673 K on H_3PO_4 loading. The amount of DMC and the surface area increased with the loading of H_3PO_4 in the range of low P/Zr. The amount of DMC reached a maximum at P/Zr = 0.05, and then decreased at P/Zr > 0.05. Especially, H_3PO_4/ZrO_2 (P/Zr = 0.3, 0.5) had high surface area, but exhibited very low activity for DMC formation (*14*).

XRD patterns of fresh H_3PO_4/ZrO_2 with various H_3PO_4 loadings are shown in Figure 3. On ZrO_2, both metastable tetragonal phase and monoclinic phase were observed. Metastable tetragonal phase gradually decreased and monoclinic

Downloaded by UNIV OF GUELPH LIBRARY on September 16, 2012 | http://pubs.acs.org
Publication Date: January 24, 2002 | doi: 10.1021/bk-2002-0809.ch005

Downloaded by UNIV OF GUELPH LIBRARY on September 16, 2012 | http://pubs.acs.org
Publication Date: January 24, 2002 | doi: 10.1021/bk-2002-0809.ch005

Table I. Results of CH_3OH+CO_2 reaction over heterogeneous catalysts

	Amount of formation / mmol		*BET surface area*
Catalyst	*DMC*	*DME*	*/ m^2g^{-1}*
ZrO_2 (calcined at 673 K)	0.30	n. d.	118
ZrO_2 (commercial)	0.22	n. d.	92
SiO_2	n. d.	n. d.	380
Al_2O_3	n. d.	0.11	100
TiO_2	n. d.	0.16	50
H-ZSM-5	n. d.	72.1	225
H-USY	n. d.	11.3	377
H-Mordenite	n. d.	11.6	239
H-β	n. d.	26.9	450
MgO	n. d.	n. d.	37
$CaCO_3$	n. d.	n. d.	1
$SrCO_3$	n. d.	n. d.	6
Y_2O_3	n. d.	n. d.	6
HfO_2	n. d.	n. d.	6
Nb_2O_5	n. d.	n. d.	5
MoO_3	n. d.	n. d.	1
SnO_2	0.14	n. d.	25
ZnO	n. d.	n. d.	4
Ga_2O_3	n. d.	n. d.	22
GeO_2	n. d.	n. d.	-
In_2O_3	n. d.	n. d.	9
Sb_2O_3	n. d.	n. d.	2
Bi_2O_3	n. d.	n. d.	1
La_2O_3	n. d.	n. d.	7
Pr_6O_{11}	n. d.	n. d.	-
$MgWO_3$	n. d.	n. d.	<1
$CaWO_3$	n. d.	n. d.	<1
$NiSO_4$ (calcined at 573 K)	n. d.	0.39	<1

n. d.: not detected.

Catalysts except ZrO_2 (calcined at 673 K) and $NiSO_4$ (calcined at 573 K): commercially available.

Reaction conditions: $CH_3OH:CO_2$=192 mmol:200 mmol, catalyst weight: 0.5 g, reaction temperature: 443 K, reaction time: 2 h.

Downloaded by UNIV OF GUELPH LIBRARY on September 16, 2012 | http://pubs.acs.org
Publication Date: January 24, 2002 | doi: 10.1021/bk-2002-0809.ch005

Table II. Effect of modified ZrO_2 catalysts calcined at 673 K on DMC formation

Catalyst	*Reaction temp.*	*Amount of DMC / mmol* 443 K	423 K	403 K	*BET surface area / m^2g^{-1}*
H_3PO_4/ZrO_2		0.44	0.42	0.26	189
H_2SO_4/ZrO_2		-	-	0.17	179
K_3PO_4/ZrO_2		0.33	-	-	185
K_2SO_4/ZrO_2		0.26	-	-	143
CsH_2PO_4/ZrO_2		0.43	0.35	0.18	185
Cs_2SO_4/ZrO_2		0.22	-	-	144
$MgSO_4/ZrO_2$		0.37	0.27	-	184
$Ce_2(SO_4)_3/ZrO_2$		0.44	-	0.20	178
$ZnSO_4/ZrO_2$		0.39	0.36	0.18	208
$Fe_2(SO_4)_3/ZrO_2$		0.40	0.36	0.20	195
ZrO_2		0.30	0.11	0.08	118

DME was not detected in all cases.

Reaction conditions: CH_3OH:CO_2=192 mmol:200 mmol, P/Zr=S/Zr=0.025, catalyst weight: 0.5 g, reaction time: 2 h.

Table III. Effect of modified ZrO_2 catalysts calcined at 923 K on DMC formation

Catalyst	*Amount of DMC / mmol*	*BET surface area / m^2g^{-1}*
H_3PO_4/ZrO_2	0.31	74
K_3PO_4/ZrO_2	n. d.	57
K_2SO_4/ZrO_2	0.18	36
CsH_2PO_4/ZrO_2	0.14	76
Cs_2SO_4/ZrO_2	0.07	39
$MgSO_4/ZrO_2$	0.14	54
$Ce_2(SO_4)_3/ZrO_2$	0.19 (0.28)[a]	73
$ZnSO_4/ZrO_2$	0.04	52
$Fe_2(SO_4)_3/ZrO_2$	n. d. (2.86)[a]	70
ZrO_2	0.12[b]	32

n. d.: not detected, *a*: DME formation amount, and DME was not detected except these cases, *b*: calcined at 873 K.

Reaction conditions: CH_3OH:CO_2=192 mmol:200 mmol, P/Zr=S/Zr=0.025, catalyst weight: 0.5 g, reaction temperature: 443 K, reaction time: 2 h.

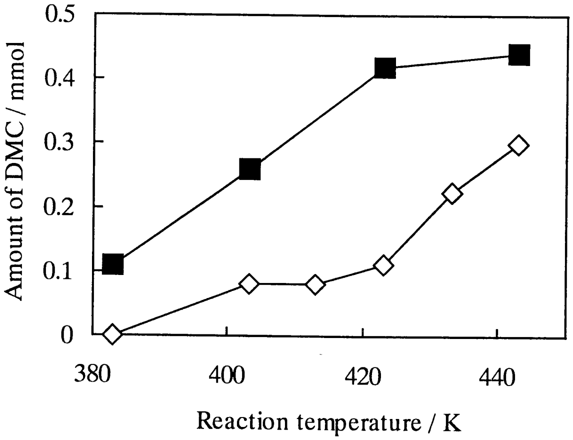

Figure 1. Dependence of DMC amount on reaction temperature over ZrO_2 (◇) and H_3PO_4/ZrO_2 (P/Zr = 0.025) (■) calcined at 673 K. Reaction conditions: $CH_3OH:CO_2$=192 mmol:200 mmol, catalyst weight: 0.5 g, reaction time: 2 h.

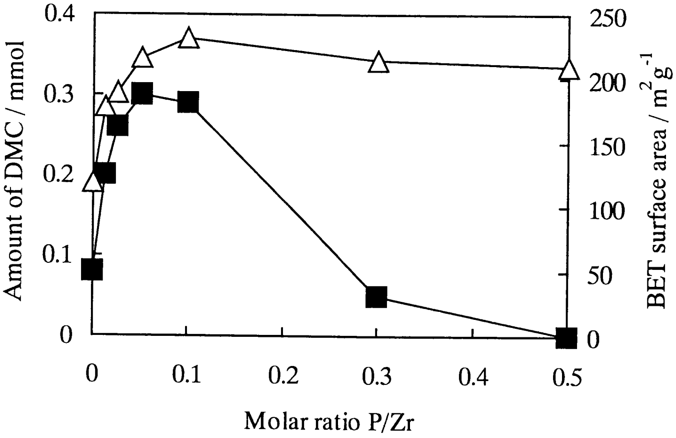

Figure 2. Dependence of DMC amount (■) and surface area (△) of H_3PO_4/ZrO_2 calcined at 673 K on H_3PO_4 loading. Reaction conditions: $CH_3OH:CO_2$=192 mmol:200 mmol, catalyst weight: 0.5 g, reaction temperature: 403 K, reaction time: 2 h.

Downloaded by UNIV OF GUELPH LIBRARY on September 16, 2012 | http://pubs.acs.org
Publication Date: January 24, 2002 | doi: 10.1021/bk-2002-0809.ch005

phase almost disappeared with the loading of H_3PO_4. Metastable tetragonal phase was predominantly formed on H_3PO_4/ZrO_2 (P/Zr = 0.05), which exhibited the highest activity as shown in Figure 2. H_3PO_4/ZrO_2 (P/Zr = 0.3, 0.5) did not show the diffraction patterns of either metastable tetragonal phase or monoclinic phase. It is suggested that zirconium ions and phosphate ions formed some salt compounds (*14*).

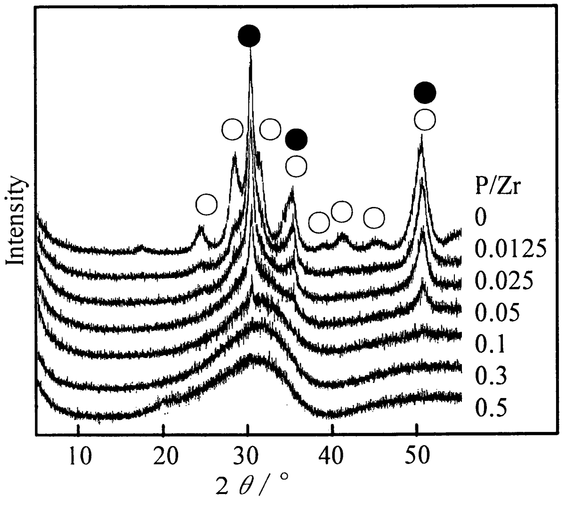

Figure 3. Cu K_α XRD patterns of fresh H_3PO_4/ZrO_2 with various H_3PO_4 loadings. Calcination temperature: 673 K. Crystal structure: metastable tetragonal (●), monoclinic (○).

Figure 4 shows the dependence of DMC amount and BET surface area on calcination temperature of H_3PO_4/ZrO_2 (P/Zr = 0.05). While BET surface area decreased with the calcination temperature, the amount of DMC formation was a maximum at 673 K. From the comparison between Figure 2 and Figure 4, the catalyst can be optimized. H_3PO_4/ZrO_2 (P/Zr =0.05) calcined at 673 K exhibited the highest performance in these catalysts. XRD patterns of fresh H_3PO_4/ZrO_2 (P/Zr=0.05) calcined at various temperatures are shown in Figure 5. Monoclinic ZrO_2 phase appeared on the catalysts calcined at 773 K and 923 K. It is suggested that the formation of monoclinic phase decreased BET surface area and DMC formation.

We also prepared H_3PO_4/ZrO_2(D) by the different method from H_3PO_4/ZrO_2. In stead of $ZrO_2 \cdot xH_2O$, ZrO_2 was impregnated with H_3PO_4. XRD patterns of fresh H_3PO_4/ZrO_2 (P/Zr = 0.05) prepared by different methods are shown in Figure 6. ZrO_2 and H_3PO_4/ZrO_2(D) (P/Zr = 0.05) exhibit almost the same diffraction patterns. Both metastable tetragonal phase and monoclinic phase

Downloaded by UNIV OF GUELPH LIBRARY on September 16, 2012 | http://pubs.acs.org
Publication Date: January 24, 2002 | doi: 10.1021/bk-2002-0809.ch005

Downloaded by UNIV OF GUELPH LIBRARY on September 16, 2012 | http://pubs.acs.org
Publication Date: January 24, 2002 | doi: 10.1021/bk-2002-0809.ch005

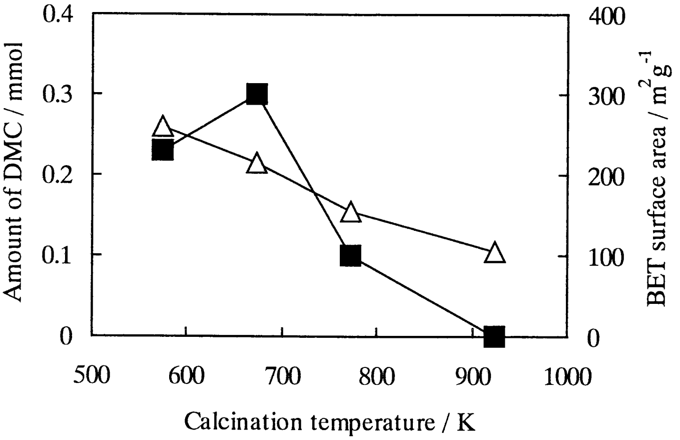

Figure 4. Dependence of DMC formation (■) and BET surface area (△) on calcination temperature of H_3PO_4/ZrO_2 (P/Zr = 0.05). Reaction conditions: $CH_3OH:CO_2$=192 mmol:200 mmol, catalyst weight: 0.5 g, reaction temperature: 403 K, reaction time: 2 h.

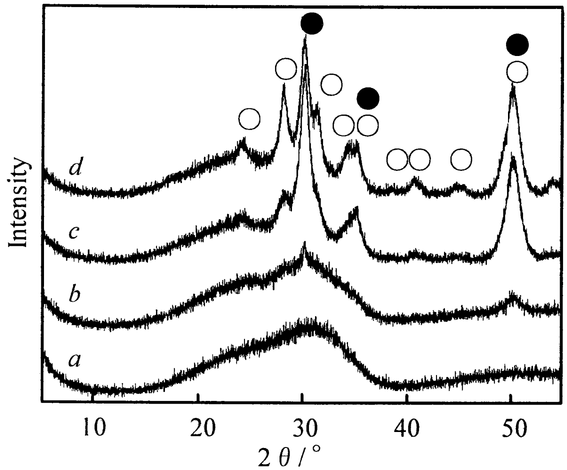

Figure 5. Cu K_α XRD patterns of fresh H_3PO_4/ZrO_2 (P/Zr = 0.05) calcined at various temperatures. a: 573 K, b: 673 K, c: 773 K, d: 923 K. Crystal structure: metastable tetragonal (●), monoclinic (○).

Downloaded by UNIV OF GUELPH LIBRARY on September 16, 2012 | http://pubs.acs.org
Publication Date: January 24, 2002 | doi: 10.1021/bk-2002-0809.ch005

were observed. LRS spectra of fresh H_3PO_4/ZrO_2 (P/Zr = 0.05) prepared by different methods are shown in Figure 7. It has been reported that the tetragonal phase of ZrO_2 exhibits typical Raman bands at 148, 263, 325, 472, 608, and 640 cm^{-1}. And the monoclinic phase of ZrO_2 exhibits bands at 140, 173, 185, 216, 260, 301, 328, 342, 378, 471, 499, 533, 553, 610, and 632 cm^{-1} (*15*, *16*). The LRS spectra of ZrO_2 and H_3PO_4/ZrO_2(D) (P/Zr = 0.05) are similar to each other. Both metastable tetragonal phase and monoclinic phase were formed on the surface as well as in the bulk of the two catalysts. All the peaks of the LRS spectrum of H_3PO_4/ZrO_2 (P/Zr = 0.05) can be assigned to tetragonal ZrO_2.

Table IV shows the effect of preparation method of H_3PO_4/ZrO_2 (P/Zr = 0.05) calcined at 673 K on DMC formation. H_3PO_4/ZrO_2(D) (P/Zr = 0.05) did not exhibit the activity for DMC formation, though 0.08 mmol DMC was formed on ZrO_2. It seems that H_3PO_4 poisoned the active sites in this preparation method. This suggests that the active sites are derived from the interaction between H_3PO_4 and $ZrO_2 \cdot xH_2O$. Similar tendency has been observed in the case of sulfated zirconia catalysts (*17*). Neighboring acid-base sites are important in this DMC synthesis as reported previously (*12*, *13*). However, when ZrO_2 is impregnated with H_3PO_4, H_3PO_4 interacts with base sites on ZrO_2 surface. On the other hand, when $ZrO_2 \cdot xH_2O$ is impregnated with H_3PO_4, highly active sites can be formed by the calcination of the catalyst, which are different from that on unmodified ZrO_2. The structure of the active sites and the role of the phosphoric species are not clear at the present stage. Further investigation and catalyst characterization are necessary.

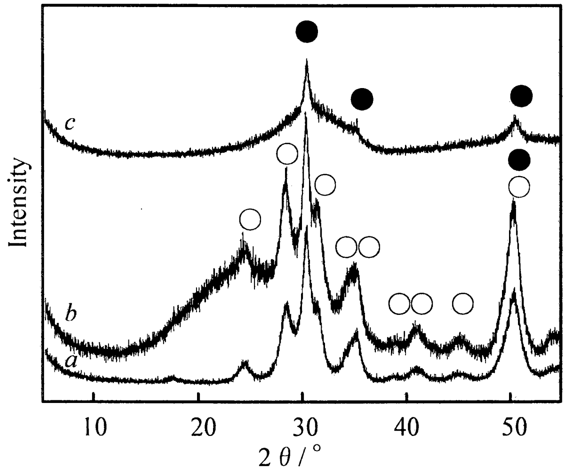

Figure 6. Cu K_α XRD patterns of fresh H_3PO_4/ZrO_2 (P/Z r = 0.05) prepared by different methods. a: ZrO_2, b: H_3PO_4/ZrO_2(D) (P/Zr = 0.05), c: H_3PO_4/ZrO_2 (P/Zr = 0.05). Calcination temperature: 673 K. Crystal structure: metastable tetragonal (●), monoclinic (○).

Downloaded by UNIV OF GUELPH LIBRARY on September 16, 2012 | http://pubs.acs.org
Publication Date: January 24, 2002 | doi: 10.1021/bk-2002-0809.ch005

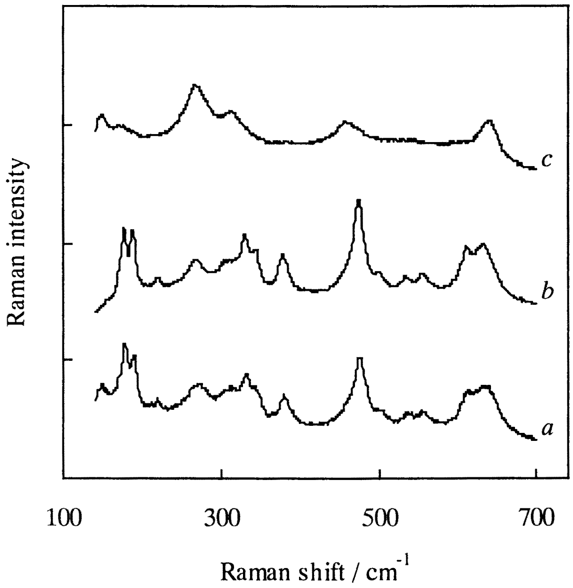

Figure 7. LRS spectra of fresh H_3PO_4/ZrO_2 (P/Zr = 0.05) prepared by different methods. a: ZrO_2, b: H_3PO_4/ZrO_2(D) (P/Zr = 0.05), c: H_3PO_4/ZrO_2 (P/Zr = 0.05). Calcination temperature: 673 K.

Table IV. Effect of preparation method of H_3PO_4/ZrO_2 (P/Zr = 0.05) calcined at 673 K on DMC formation

Catalyst	*Amount of DMC / mmol*	*BET surface area / m^2g^{-1}*
H_3PO_4/ZrO_2	0.30	216
H_3PO_4/ZrO_2(D)	not detected	106
ZrO_2	0.08	118

Reaction conditions: $CH_3OH:CO_2$=192 mmol:200 mmol, P/Zr=0.05, catalyst weight: 0.5 g, reaction temperature: 403 K, reaction time: 2 h.

Downloaded by UNIV OF GUELPH LIBRARY on September 16, 2012 | http://pubs.acs.org
Publication Date: January 24, 2002 | doi: 10.1021/bk-2002-0809.ch005

Conclusions

The addition of H_3PO_4 to ZrO_2 was found to be very effective for the enhancement of the catalytic activity with high selectivity in DMC synthesis from CH_3OH and CO_2. This modification could decrease the reaction temperature drastically compared to the unmodified ZrO_2. It is suggested that the active sites on H_3PO_4/ZrO_2 are derived from the interaction between H_3PO_4 and $ZrO_2 \cdot xH_2O$ during the catalyst preparation.

References

1. Aresta, M.; Quaranta, E. *CHEMTECH* **1997,** 32-40.
2. Pacheco, M. A.; Marshall, C. L. *Energy & Fuels* **1997,** *11,* 2-29.
3. Shaikh, A.-A. G.; Sivaram, S. *Chem. Rev.* **1996,** *96,* 951-976.
4. Romano, U.; Tesei, R.; Mauri, M. M.; Rebora, P. *Ind. Eng. Chem. Prod. Res. Dev.* **1980,** *19,* 396-403.
5. Molzahn, D.; Jones, M. E.; Hartwell, G. E.; Puga, J. U.S. Patent 5,387,708, 1995.
6. King, S. S. T.; Jones, M. E.; Olken, M. M. U.S. Patent 5,391,803, 1995.
7. Matsuzaki, T.; Nakamura, A. *Catal. Surv. Japan* **1997,** *1,* 77-88.
8. Peppel, W. J. *Ind. Eng. Chem.* **1958,** *50,* 767-770.
9. Sakakura, T.; Saito, Y.; Okano, M.; Choi, J.-C.; Sako, T. *J. Org. Chem.* **1998,** *63,* 7095-7096.
10. Sakai, S.; Fujinami, T.; Yamada T.; Furusawa, S. *Nippon Kagaku Kaishi* **1975,** *10,* 1789-1794.
11. Kizlink, J.; Pastucha, I. *Collect. Czech. Chem. Commun.* **1995,** *60,* 687-692.
12. Tomishige, K.; Sakaihori, T.; Ikeda, Y.; Fujimoto, K. *Catal. Lett.* **1999,** *58,* 225-229.
13. Tomishige, K.; Ikeda, Y.; Sakaihori, T.; Fujimoto, K. *J. Catal.* **2000,** *192,* 355-362.

14. Ikeda, Y.; Sakaihori, T.; Tomishige, K.; Fujimoto, K. *Catal. Lett.* **2000,** *66,* 59-62.
15. Yamamoto, T.; Tanaka, T.; Takenaka, S.; Yoshida, S.; Onari, T.; Takahashi, Y.; Kosaka, T.; Hasegawa, S.; Kudo, M. *J. Phys. Chem. B* **1999,** *103,* 2385-2393.
16. Mercera, P. D. L.; van Ommen, J. G.; Doesburg, E. B. M.; Burggraaf, A. J.; Ross, J. R. H. *Appl. Catal.* **1990,** *57,* 127-148.
17. Arata, K. *Adv. Catal.* **1990,** *37,* 165-211.

Downloaded by UNIV OF GUELPH LIBRARY on September 16, 2012 | http://pubs.acs.org
Publication Date: January 24, 2002 | doi: 10.1021/bk-2002-0809.ch005

Downloaded by PENNSYLVANIA STATE UNIV on September 16, 2012 | http://pubs.acs.org
Publication Date: January 24, 2002 | doi: 10.1021/bk-2002-0809.ch006

Chapter 6

Utilization of Carbon Dioxide for Direct, Selective Conversion of Methane to Ethane and Ethylene with Calcium-Based Binary Catalysts

Ye Wang[1,2] and Yasuo Ohtsuka[1,*]

[1]Research Center for Organic Resources and Materials Chemistry, Institute for Chemical Reaction Science, Tohoku University, Katahira, Aoba-ku, Sendai 980–8577, Japan
[2]Current address: Department of Applied Chemistry, Hiroshima University, Kagamiyama, Higashi-Hiroshima 739–8527, Japan

Utilization of CO_2 for the direct conversion of CH_4 to C_2H_6 and C_2H_4 has been studied under ambient pressure with a fixed bed quartz reactor. Ca-based binary catalysts, prepared by impregnating CeO_2, Cr_2O_3, or MnO_2 with $Ca(NO_3)_2$ solution, show remarkable synergistic effects on C_2 formation at 850°C. C_2 selectivity and C_2 yield increase with increasing partial pressure of CO_2, irrespective of the kind of catalyst, and the selectivity reaches 65 – 75% at 70 kPa. These catalysts provide stable performances with time on stream of 8 – 10 h. The TPD, XRD and XPS measurements strongly suggest that CO_2 first adsorbs on Ca^{2+} sites and the activation subsequently occurs on neighboring Ce^{3+}, Cr^{3+} or Mn^{2+} sites to yield active oxygen species, which work as the oxidant for selective formation of C_2 hydrocarbons.

In CO2 Conversion and Utilization; Song, C., et al.;
ACS Symposium Series; American Chemical Society: Washington, DC, 2002.

Downloaded by PENNSYLVANIA STATE UNIV on September 16, 2012 | http://pubs.acs.org
Publication Date: January 24, 2002 | doi: 10.1021/bk-2002-0809.ch006

Simultaneous activation and utilization of CH_4 and CO_2 have attracted increasing attention from environmental and practical points of view, since these gases show green house effects and natural gas frequently contains a high concentration of CO_2 in addition to CH_4. The present authors' group has been focusing on the novel use of CO_2 as an oxidant for the direct conversion of CH_4 to C_2H_6 and C_2H_4 (C_2 hydrocarbons) *(1-7)*. Although the oxidative coupling of CH_4 with O_2 has been studied extensively for the same purpose, the inevitable formation of CO_2 appears to be one of the most serious issues in this process *(8)*.

Overall equations for formation of C_2 hydrocarbons from CH_4 and CO_2 can be expressed as follows:

$$2CH_4 + CO_2 = C_2H_6 + CO + H_2O \quad (1)$$

$$2CH_4 + 2CO_2 = C_2H_4 + 2CO + 2H_2O \quad (2)$$

Figure 1 shows the results of thermodynamic considerations about these equations under total pressure of 0.1 MPa *(2,9)*. Yields of C_2H_6 and C_2H_4 at equilibrium depend on feed composition as well as reaction temperature and exceed 15% and 25% at CO_2/CH_4 ratio of 2 above 800°C, respectively. The sum of these values, if attainable, is comparable to the economically feasible C_2 yield, about 30% *(10)*, estimated for the oxidative coupling of CH_4 with O_2.

Our systematic study to identify the criteria for catalyst selection for the above reactions has shown that praseodymium and terbium oxides are more active among 30 metal oxides examined, but C_2 yield is as low as 1% *(1-3)*. As is seen in Figure 2 *(2)*, this pioneering work has also suggested that redox property of a metal oxide, such as, Ce, Cr, or Mn oxide, activates CH_4 and CO_2, and that its basicity affects C_2 selectivity. It is thus expectable that a combination of two metal oxides with the different functions leads to a binary catalyst effective for C_2 formation. The present paper features the catalytic performances of three binary systems prepared on this principle, clarifies the key factors controlling C_2 formation, and elucidates the reaction mechanisms.

Experimental Section

Catalyst Materials and Preparation

An alkaline earth metal nitrate, mainly $Ca(NO_3)_2$, was used as a precursor for one component of a binary catalyst, because the corresponding oxide formed after calcination has strong basicity. CeO_2, Cr_2O_3 or MnO_2 was selected as

Downloaded by PENNSYLVANIA STATE UNIV on September 16, 2012 | http://pubs.acs.org
Publication Date: January 24, 2002 | doi: 10.1021/bk-2002-0809.ch006

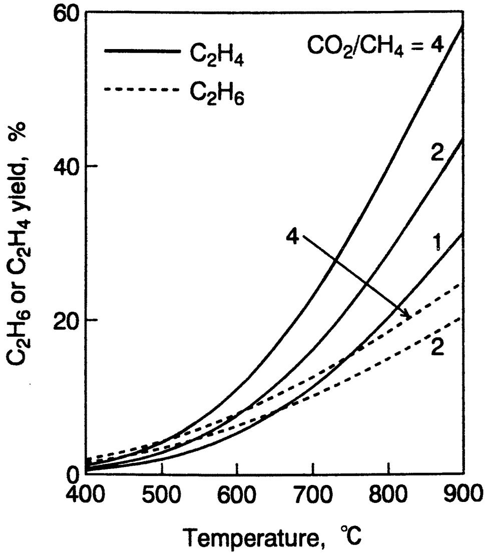

Figure 1. Dependence of yields of C_2H_6 and C_2H_4 at equilibrium on CO_2/CH_4 ratio and temperature.

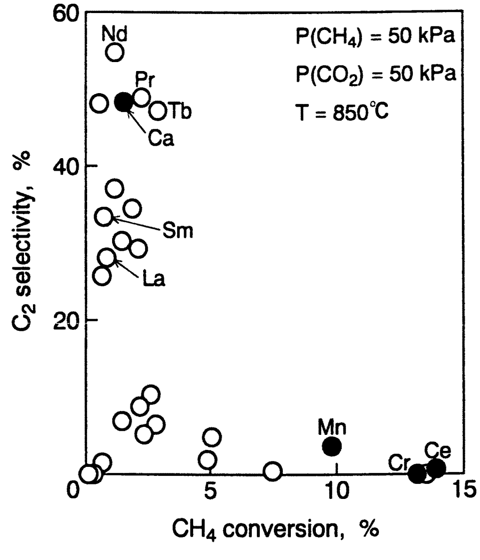

Figure 2. Relationship between CH_4 conversion and C_2 selectivity in the reaction of CH_4 and CO_2 with various metal oxides (Reproduced from reference 2 with permission from Elsevier Science).

another component, since they showed high conversions of CH_4 and CO_2 when used alone, as shown in Figure 2 *(2)*, and their valences are readily changeable.

The method of preparing a binary catalyst has been reported elsewhere *(4,6)* and is thus simply described. Powdery CeO_2, Cr_2O_3, or MnO_2, was impregnated with an aqueous solution of $Ca(NO_3)_2$, and then the resulting mixture was dried, followed by air calcination at 850°C. The calcined catalyst was sieved to 0.5 – 1 mm before use. A physical mixture of both CaO derived from $Ca(NO_3)_2$ and CeO_2 was also prepared as a reference of a Ca-Ce system.

Downloaded by PENNSYLVANIA STATE UNIV on September 16, 2012 | http://pubs.acs.org
Publication Date: January 24, 2002 | doi: 10.1021/bk-2002-0809.ch006

Catalytic Runs and Product Analysis

All runs were carried out with a fixed-bed quartz reactor under ambient pressure. The detailed procedure has been described elsewhere *(6)*. In a typical run, 2 g of the granular catalyst loaded onto quartz wool was calcined again under flowing air at 850°C, and, after complete replacement with high purity He (>99.9999%), a mixture of CH_4 (>99.999%) and CO_2 (>99.995%) was passed over the catalyst at 850°C. Partial pressure of CH_4 or CO_2, denoted as $P(CH_4)$ or $P(CO_2)$, was 30.3 or 70.7 kPa, respectively, unless otherwise stated. The effluent after removal of H_2O was sampled at 5-min intervals, and C_2H_6, C_2H_4, CO and H_2 as products were analyzed with a high-speed micro GC.

GC data were processed on the assumption that the C in CH_4 was converted to C_2H_6, C_2H_4, and CO, and the C in CO_2 to CO. Since CO is formed from CH_4 and CO_2, each contribution is separated by the previous method *(1)*, in which almost all of side reactions involving CH_4 and CO_2 are taking into account. CH_4 conversion and C_2 selectivity can thus be calculated by the following equations *(6)*, and C_2 yield is defined as the product of both values.

$$CH_4 \text{ conversion } (\%) = \{2[C_2H_6] + 2[C_2H_4] + [CO \text{ from } CH_4]\}/\{[CH_4] + 2[C_2H_6] + 2[C_2H_4] + [CO \text{ from } CH_4]\} \times 100$$

$$C_2 \text{ selectivity } (\%) = \{2[C_2H_6] + 2[C_2H_4]\}/\{2[C_2H_6] + 2[C_2H_4] + [CO \text{ from } CH_4]\} \times 100$$

Catalyst Characterization

Fresh and used catalysts were characterized by several methods, such as N_2 adsorption at 77 K, X-ray diffraction (XRD) with Ni-filtered Cu K_α radiation, and X-ray photoelectron spectroscopy (XPS) with Mg K_α radiation. Binary catalysts after 2 h reaction of CH_4 and CO_2 at 850°C were also subjected to the CO_2 temperature programmed desorption (TPD) measurements. In a TPD run, the catalyst after reaction under $P(CH_4)$ of 30.3 kPa and $P(CO_2)$ of 70.7 kPa was first quenched to 100°C in a stream of feed gas with the same composition, then held for 30 min at this temperature after replacement with pure He, and finally heated at 2.5°C/min up to 950°C under flowing a mixture of He and CO_2 with different $P(CO_2)$ in the range of 0 – 70.7 kPa. It took about 5 min for quenching the used catalyst to 100°C. The change in CO_2 concentration during the TPD run was monitored with the micro GC. The reproducibility of the change at a desorption peak was within ±5% under the highest $P(CO_2)$ of 70.7 kPa.

Downloaded by PENNSYLVANIA STATE UNIV on September 16, 2012 | http://pubs.acs.org
Publication Date: January 24, 2002 | doi: 10.1021/bk-2002-0809.ch006

Results and Discussion

Catalyst Composition

The effect of catalyst composition on the performance of binary Ca-Ce catalysts under $P(CH_4)$ of 30 kPa and $P(CO_2)$ of 30 kPa is illustrated in Figure 3, where the composition is expressed as [Ca/(Ca + Ce) × 100] in atomic percent (at%). CH_4 conversion was 12% or 0.1% with CeO_2 or CaO alone, respectively. The conversions over the binary catalysts were lower than the arithmetic mean of those over each component. C_2 selectivity was nearly zero with CeO_2 alone, but it steeply increased when a low content of CaO coexisted. C_2 selectivity was higher over the binary catalysts than over CaO alone. As shown in Figure 3B, C_2 yield was < 0.1% with CeO_2 or CaO alone, whereas it was much higher in the coexistence of both components. In other words, there was a synergistic effect on C_2 formation *(4,6)*. The maximal yield reached 3.2%, which was about 30 times that observed with the single oxide.

Table 1 summarizes the results when CeO_2 power was impregnated with other nitrate solutions than $Ca(NO_3)_2$. Surface areas of the binary oxides prepared, determined by the BET method, were almost independent of the kind of the alkaline earth metal. CH_4 conversion at 850°C increased in the sequence of Ba ~ Sr < Ca < Mg, whereas C_2 yield did in the order of Mg < Ba ~ Sr < Ca *(6)*. Thus, the Ca-Ce system showed the highest activity for C_2 formation. When CaO and CeO_2 were physically mixed at Ca/Ce ratio of 0.5, as shown in Table 1, surface area and CH_4 conversion were almost the same between the resulting mixture and the corresponding binary catalyst. On the other hand, C_2 yield was much higher with the latter. These observations indicate that catalyst preparation by the impregnation method is more effective for C_2 formation.

Downloaded by PENNSYLVANIA STATE UNIV on September 16, 2012 | http://pubs.acs.org
Publication Date: January 24, 2002 | doi: 10.1021/bk-2002-0809.ch006

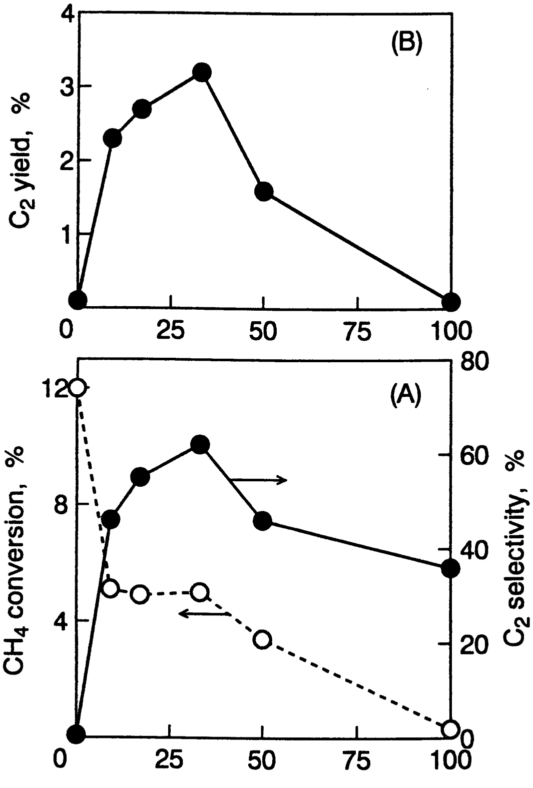

Figure 3. Effect of catalyst composition on the performance of binary Ca-Ce catalysts at 850°C.

On the basis of the results described above, the impregnation method using $Ca(NO_3)_2$ solution was used to prepare a binary catalyst containing Cr or Mn element. Figure 4 shows the effect of catalyst composition on CH_4 conversion at 850°C with the Ca-Cr *(5)* or Ca-Mn system. The conversion – composition profiles observed were quite similar as that (Figure 3) over the Ca-Ce catalyst; CH_4 conversion with Cr_2O_3 or MnO_2 alone decreased steeply by addition of a small amount of CaO and it leveled off with further increase in CaO. As is seen in Figure 5, C_2 yield with Cr_2O_3 or MnO_2 alone was low. On the other hand, Ca-Cr and Ca-Mn catalysts enhanced remarkably C_2 yields, which were at highest 4.0% and 4.7%, respectively. As observed in Figure 3. synergy also existed in C_2 formation over these binary systems.

It should be noted that the maximal C_2 yields over Ca-Ce, Ca-Cr, and Ca-Mn systems are 3 – 4 times those observed with the single Pr or Tb oxide that is most effective for C_2 formation *(3)*. With regard to a binary catalyst reported earlier, a PbO-MgO system enhanced C_2 yield in the oxidative coupling of CH_4 with O_2 in the coexistence of CO_2, but it readily lost the activity without O_2 *(11)*. Although a La_2O_3-ZnO system was also communicated to catalyze C_2 formation from CH_4 and CO_2 *(12)*, it was less active than the present binary catalysts. Since no mechanistic work to clarify not only the role of CO_2 but the reaction mechanism has been carried out so far, the following sections focus on them.

Downloaded by PENNSYLVANIA STATE UNIV on September 16, 2012 | http://pubs.acs.org
Publication Date: January 24, 2002 | doi: 10.1021/bk-2002-0809.ch006

Partial Pressure of CO_2

The profiles for the reaction of CH_4 alone with the Ca-Ce *(4)* or Ca-Cr system are illustrated in Figure 6, where CH_4 diluted with He is used at $P(CH_4)$ of 30 kPa. In the absence of CO_2, H_2 and CO were mainly produced with the molar ratio of approximately 2 by the reaction of CH_4 with lattice oxygen atoms, and formation rates of H_2 and CO finally approached to zero within 2 h. Figure 6 also revealed negligibly small amounts of C_2 hydrocarbons even at the early stage of reaction, which indicates that the lattice oxygen of these oxide systems does not work as an oxidant for C_2 formation.

In the presence of CO_2, C_2 formation proceeded readily. As shown in Figure 7, with the Ca-Ce catalyst, C_2 yield became steady immediately after the start of reaction and did not change even when time on stream was prolonged to 10 h *(6)*. Although it took 1 – 2 h for the yield to be steady with the Ca-Cr or Ca-Mn catalyst, their performances after the induction periods were sustainable, as with the Ca-Ce system. It is thus evident that oxygen species derived from CO_2 play a crucial role in coupling reactions of CH_4.

The effect of $P(CO_2)$ on CH_4 conversion and product selectivity over the Ca-Ce catalyst is provided in Figure 8, where $P(CH_4)$ is kept constant (30 kPa) and inert He is used as a balance gas *(6)*. The conversion increased steeply with

Downloaded by PENNSYLVANIA STATE UNIV on September 16, 2012 | http://pubs.acs.org
Publication Date: January 24, 2002 | doi: 10.1021/bk-2002-0809.ch006

Table I. Surface Areas and Catalytic Performances of Binary Oxides of Alkaline Earth Metal and Ce Elements

Alkaline earth metal	*M/Ce*[1]	*Surface area (m^2/g)*	*CH_4 conversion (%)*	*C_2 yield (%)*
Mg	0.2	1.4	11.6	0.2
Ca	0.2	0.6	4.9	2.5
Sr	0.2	n.a.[2]	3.1	1.6
Ba	0.2	0.5	2.8	1.3
Ca	0.5	0.4	5.8	3.2
Ca[3]	0.5	1.4	5.4	0.7

[1] Atomic ratio. [2] Not analyzed. [3] Physical mixture.

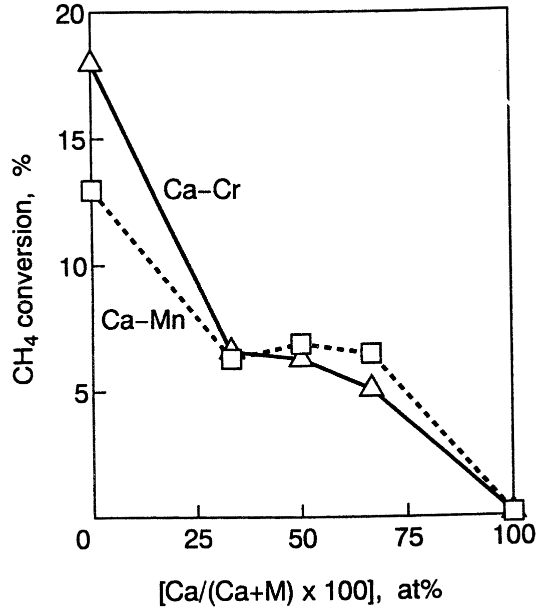

Figure 4. Effect of catalyst composition on CH_4 conversion with binary Ca-Cr and Ca-Mn catalysts at 850°C.

Downloaded by PENNSYLVANIA STATE UNIV on September 16, 2012 | http://pubs.acs.org
Publication Date: January 24, 2002 | doi: 10.1021/bk-2002-0809.ch006

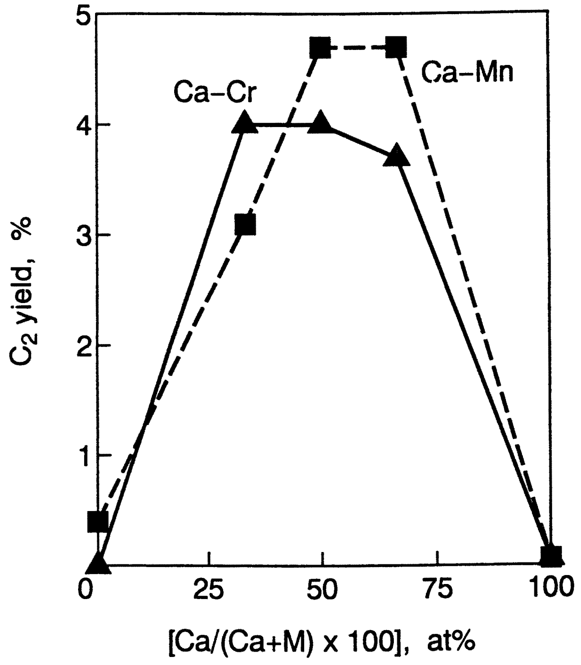

Figure 5. C_2 yield at 850°C over Ca-Cr and Ca-Mn catalysts with different compositions.

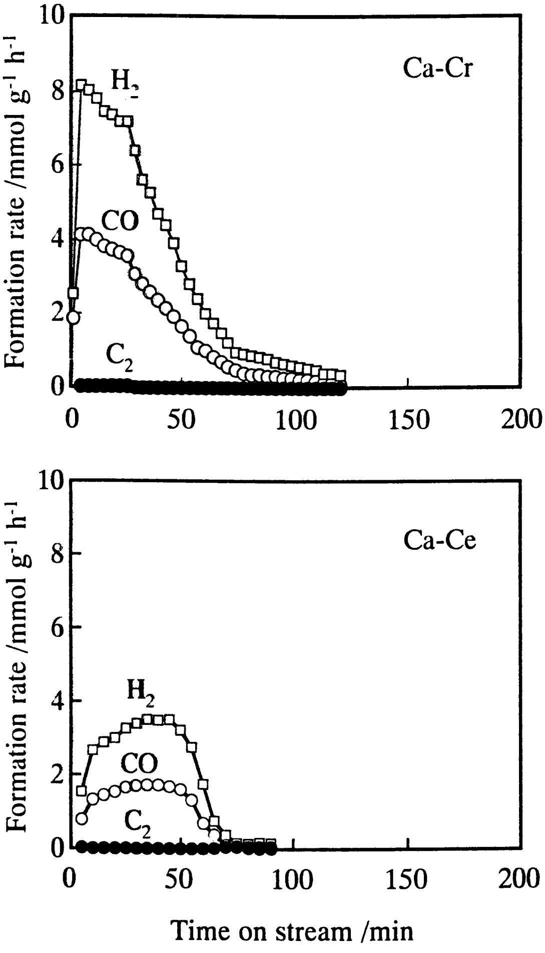

Figure 6. Formation rates of products in the reaction at 850°C of CH_4 alone with Ca-Ce and Ca-Cr oxides.

Downloaded by PENNSYLVANIA STATE UNIV on September 16, 2012 | http://pubs.acs.org
Publication Date: January 24, 2002 | doi: 10.1021/bk-2002-0809.ch006

Downloaded by PENNSYLVANIA STATE UNIV on September 16, 2012 | http://pubs.acs.org
Publication Date: January 24, 2002 | doi: 10.1021/bk-2002-0809.ch006

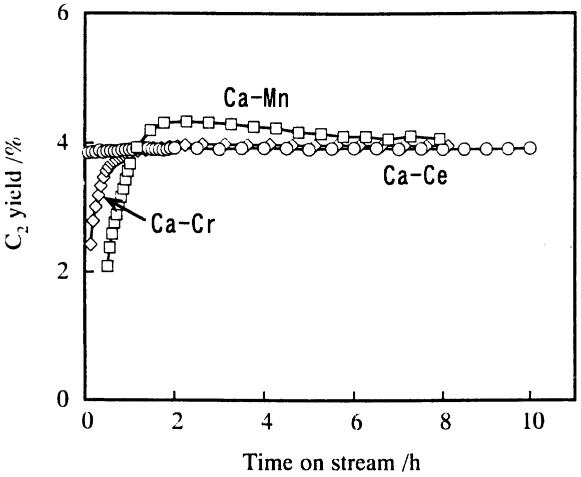

Figure 7. Effect of time on stream on C_2 yield at 850°C over Ca based binary catalysts.

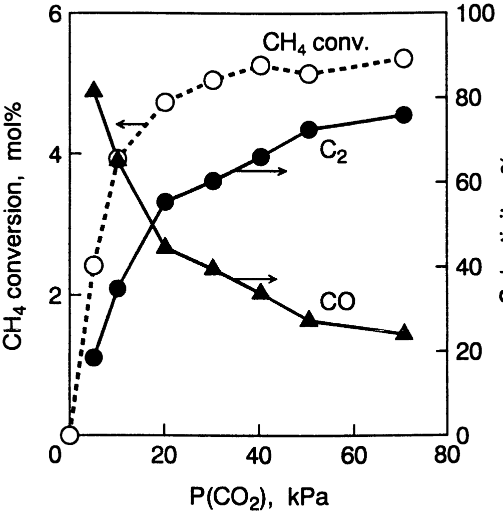

Figure 8. Dependence of CH_4 conversion and product selectivity on partial pressure of CO_2 over a Ca-Ce catalyst (Reproduced from reference 6 with permission from Academic Press).

increasing $P(CO_2)$ up to 10 kPa but leveled off beyond 20 kPa. This Langmuir-type curve indicates the involvement of CO_2 chemisorption in the present reaction. With product selectivity, CO formation was predominant at low $P(CO_2)$ below around 20 kPa, whereas C_2 selectivity increased with increasing $P(CO_2)$ and reached 70% at 70 kPa. As shown in Figure 9, the Ca-Cr and Ca-Mn catalysts showed the similar CH_4 conversion – $P(CO_2)$ curves as with the Ca-Ce system, that is, the Langmuir-type relationship between the two. Furthermore, the Ca-Cr or Ca-Mn system provided almost the same dependency of C_2 yield on $P(CO_2)$; the yield increased almost linearly with $P(CO_2)$. The observations in Figures 8 and 9 point out that high $P(CO_2)$ is essentially needed for selective formation of C_2 hydrocarbons.

Since CO_2 rather deactivates basic catalysts effective for the oxidative coupling of CH_4 with O_2 due to the strong adsorption ability, higher C_2 selectivity under higher $P(CO_2)$ is peculiar to the present reaction system. When time on stream was prolonged to 8 – 10 h, as shown in Figure 7, C_2 yields were almost unchanged except for the early stage of reaction, irrespective of the kind of a binary oxide system. Such the stable performances mean that there is no catalyst deactivation by CO_2 adsorption and carbon deposition.

Chemisorption of CO_2 and Catalyst State

In order to make clear the behavior of CO_2 adsorption upon C_2 formation, the three catalysts after reaction were subjected to the TPD runs. Figure 10 shows typical TPD profiles for the Ca-Ce system. The CO_2-desorption peak appeared at 730°C under flowing pure He and shifted to 810, 850, and 910°C in a stream of CO_2 with $P(CO_2)$ of 10, 30 and 70 kPa, respectively *(4,6)*. In other words, a pool of the CO_2 chemisorbed existed on the catalyst in the process of C_2 formation at 850°C under $P(CO_2)$ of 70 kPa, whereas it almost disappeared under $P(CO_2)$ of 10 kPa. The Ca-Cr and Ca-Mn catalysts after reaction also provided almost the same TPD profiles as in Figure 10. No significant desorption of CO_2 from any fresh catalysts were observed.

The comparison of Figures 8 and 10 suggests that the occurrence of CO_2 chemisorption leads to high C_2 selectivity. To ensure this point, the amount of CO_2 chemisorbed at 850°C was estimated by integrating the peak area observed in Figure 10 between 850°C and 950°C. The estimated value is plotted in Figure 11 as a function of $P(CO_2)$ used for the TPD run. The amounts chemisorbed on all of the binary catalysts showed almost the same dependencies on $P(CO_2)$; the values were very small at around 10 kPa but larger at higher $P(CO_2)$. It should be noted that such dependencies are quite similar as the C_2 selectivity – $P(CO_2)$ curves in Figure 8. It is thus likely that CO_2 chemisorption plays a key role in selective formation of C_2 hydrocarbons.

Downloaded by PENNSYLVANIA STATE UNIV on September 16, 2012 | http://pubs.acs.org
Publication Date: January 24, 2002 | doi: 10.1021/bk-2002-0809.ch006

Downloaded by PENNSYLVANIA STATE UNIV on September 16, 2012 | http://pubs.acs.org
Publication Date: January 24, 2002 | doi: 10.1021/bk-2002-0809.ch006

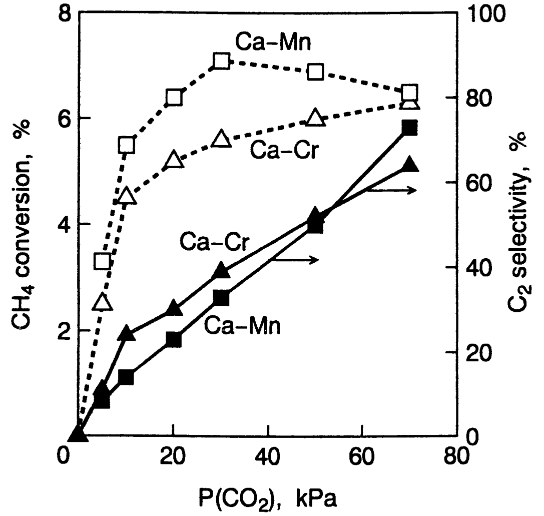

Figure 9. Dependence of CH_4 conversion and C_2 selectivity on partial pressure of CO_2 over a Ca-Cr or Ca-Mn catalyst.

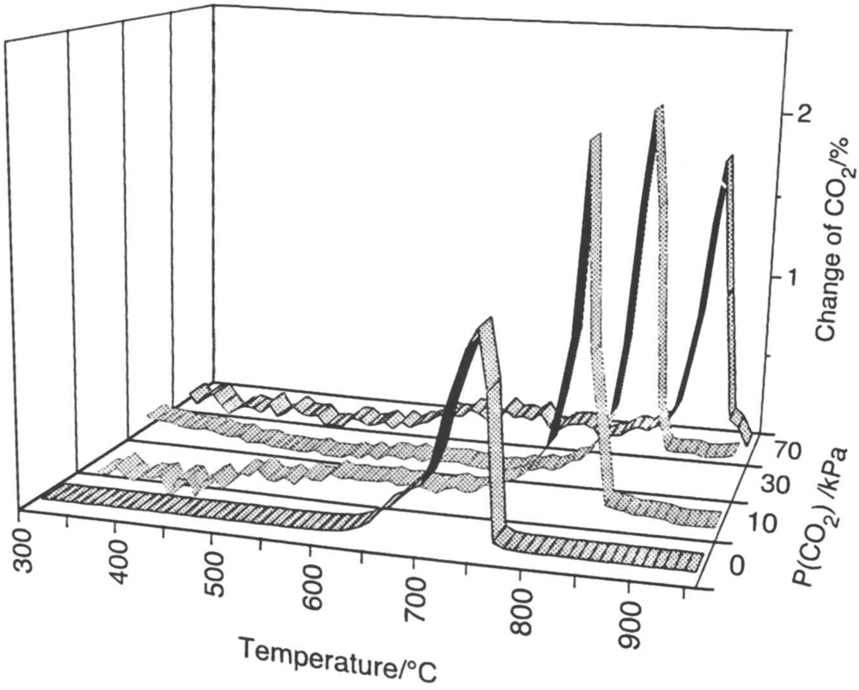

Figure 10. Profiles for CO_2 desorption during TPD measurements in different atmospheres of the Ca-Ce catalyst after the reaction of CH_4 and CO_2 at 850°C.

The largest amounts observed in Figure 11 were 0.8 – 1.1 mmol, which were only 10 – 15% of Ca contents. Since any CO_2 desorbed was not detectable with the used CeO_2, Cr_2O_3, or MnO_2 alone, Ca species on the surface layer of each binary catalyst must work as the sites for CO_2 chemisorption.

Table 2 summarizes the results of catalyst characterization. The XRD measurements showed that the Ca-Ce, Ca-Cr, or Ca-Mn catalyst before reaction existed mainly as $Ca_xCe_{1-x}O_{2-y}$, $CaCrO_4$, or $CaMnO_3$, respectively. The former was stable even when time on stream was prolonged to 10 h, whereas the latter two were transformed to $Ca(CrO_2)_2$ and $Ca_{0.48}Mn_{0.52}O$, which were unchanged after 8 h. This transformation took place at the early stage of reaction. The XPS spectra revealed the partial or complete transformation of Ce^{4+}, Cr^{6+}, and Mn^{4+} to the corresponding reduced species, such as Ce^{3+}, Cr^{3+} and Mn^{2+}. No XRD lines attributable to any carbonates were detectable with all of the three systems.

As is seen in Figure 7, the Ca-Cr and Ca-Mn catalysts showed the induction periods before the steady performances were attained. The XRD and XPS observations mentioned above suggest that the periods are caused by the changes in oxidation states at bulk phases, since any induction period was not observed with the Ca-Ce catalyst on which surface modification only took place (Table II).

Reaction Mechanisms Proposed

The different mechanisms under low and high $P(CO_2)$ may be proposed on the basis of the results mentioned above. At low $P(CO_2)$, the main product from CH_4 was CO (Figures 8 and 9), and the extent of CO_2 chemisorption was very low (Figure 11), irrespective of the kind of a binary catalyst. Since CH_4 reacted readily with the lattice oxygen to form CO and H_2 (Figure 6), this reaction may proceed predominantly at low $P(CO_2)$ through the following scheme:

$$CH_4 + CaMO_x \rightarrow CO + 2H_2 + CaMO_{x-1} \qquad (3)$$

$$CaMO_{x-1} + CO_2 \rightarrow CO + CaMO_x \qquad (4)$$

where M denotes Ce, Cr, or Mn element.

At high $P(CO_2)$ above 60 kPa, on the other hand, selective formation of C_2 hydrocarbons took place, and C_2 selectivity exceeded 60% on all of the binary catalysts examined (Figures 8 and 9). Almost the same dependencies of C_2 selectivity and CO_2 chemisorption on $P(CO_2)$, observed in Figures 8, 9, and 11,

Downloaded by PENNSYLVANIA STATE UNIV on September 16, 2012 | http://pubs.acs.org
Publication Date: January 24, 2002 | doi: 10.1021/bk-2002-0809.ch006

Downloaded by PENNSYLVANIA STATE UNIV on September 16, 2012 | http://pubs.acs.org
Publication Date: January 24, 2002 | doi: 10.1021/bk-2002-0809.ch006

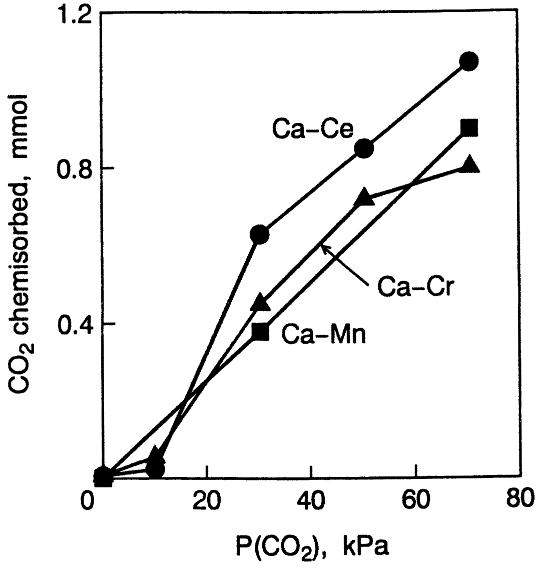

Figure 11. Amounts of the CO_2 chemisorbed on Ca-based binary catalysts after reaction under different partial pressures of CO_2.

Table II. Species Identified by XRD and XPS Measurements of Ca Based Binary Catalysts

Catalyst	*Before reaction*		*After reaction*[1]	
	XRD	*XPS*	*XRD*	*XPS*
Ca-Ce (0.5)[2]	$Ca_xCe_{1-x}O_{2-y}$, CaO[3]	Ce^{4+}	$Ca_xCe_{1-x}O_{2-y}$, CaO[3]	Ce^{4+}, Ce^{3+}
Ca-Cr (1.0)[2]	$CaCrO_4$	Cr^{6+}	$Ca(CrO_2)_2$, CaO[3]	Cr^{3+}
Ca-Mn (1.0)[2]	$CaMnO_3$	Mn^{4+}	$Ca_{0.48}Mn_{0.52}O$	Mn^{2+}

[1] At a steady state. [2] Atomic ratio. [3] With very small XRD intensities.

indicate that C_2 formation involves the chemisorption process. The following scheme may be proposed:

$$CO_2 \rightarrow CO_2\,(a) \rightarrow CO + O^* \tag{5}$$

$$CH_4 + O^* \rightarrow CH_3\bullet + OH\bullet \tag{6}$$

$$2CH_3\bullet \rightarrow C_2H_6 \rightarrow C_2H_4 \tag{7}$$

where CO_2(a) and O* designate chemisorbed CO_2 and active oxygen species, respectively. The CO_2 in feed gas first adsorbs on basic Ca^{2+} sites, and the reduced sites, such as Ce^{3+}, Cr^{3+} and Mn^{2+}, then activate the CO_2 chemisorbed to provide CO and active oxygen species adsorbed on the corresponding oxidized sites *(6)*. These sites appear to be near Ca^{2+}, since the three catalysts existed as the composite oxides (Table 2). According to equation (6), CH_4 reacts with the oxygen species to form methyl radicals, which subsequently undergo coupling reactions. In the former process, the regeneration of Ce, Cr, and Mn sites take place *(6)*. Since molar ratios of C_2H_4/C_2H_6 observed were almost independent on $P(CO_2)$, CO_2 seems to be hardly involved in the dehydrogenation of C_2H_6 to C_2H_4. Thus, C_2 formation at a steady state proceeds probably through a cycle mechanism between the reduced and oxidized site of Ce, Cr, or Mn species.

Conclusions

Binary catalysts of CaO and Ce, Cr, or Mn oxide show remarkable synergistic effects on formation of C_2 hydrocarbons from CH_4 and CO_2 at 850°C, and the maximal C_2 yields are 30 – 70 times that over each component. As partial pressure of CO_2 increases, C_2 selectivity over all catalysts increases and reaches 65 – 75% at 70 kPa. Their performances are stable during 8 – 10 h reaction. The TPD, XRD, and XPS measurements strongly suggest that CO_2 chemisorption on Ca sites and subsequent activation on neighboring Ce, Cr, or Mn sites provide active oxygen species that play a key role for selective formation of C_2 hydrocarbons.

Acknowledgement

The present work was supported in part by a Grant-in-Aid for Scientific Research (B) from the Ministry of Education, Science, Sports and Culture, Japan (No. 10555275).

Downloaded by PENNSYLVANIA STATE UNIV on September 16, 2012 | http://pubs.acs.org
Publication Date: January 24, 2002 | doi: 10.1021/bk-2002-0809.ch006

References

1. Asami, K.; Fujita, T.; Kusakabe, K.; Nishiyama.Y.; Ohtsuka, Y. *Appl. Catal. A: General* **1995,** *126*, 245
2. Asami, K.; K., Kusakabe, K.; Ashi, N.; Ohtsuka, Y. *Stud. Surf. Sci. Catal.* **1997**, *107*, 279.
3. Asami, K.; Kusakabe, K.; Ashi, N., Ohtsuka, Y. *Appl. Catal. A: General* **1997**, *156*, 43.
4. Wang, Y.; Takahashi, Y.; Ohtsuka, Y. *Appl. Catal. A: General* **1998**, *172*, 203.
5. Wang, Y.; Takahashi, Y.; Ohtsuka, Y. *Chem. Lett.* **1998**, 1209.
6. Wang, Y.; Takahashi, Y.; Ohtsuka, Y. *J. Catal.* **1999**, *186*, 160.
7. Wang, Y.; Ohtsuka, Y. *J. Catal.* **2000**, *192*, 252.
8. Lunsford, J.H. *Angew. Chem., Int. Ed. Engl.* **1995**, *34*, 970.
9. Ohtsuka, Y.; Asami, K.; Wang, Y. *J. Chin. Inst. Chem. Engrs.* **1999**, *30*, 439.
10. Kuo, J.W.; Kresge, C.T.; Palermo, R.E. *Catal. Today* **1989**, *4*, 470.
11. Nishiyama, N.; Aika, K. *J. Catal.* **1990**, *122*, 346.
12. Chen, C.; Xu, Y.; Li, G.; Guo, X.; *Catal. Lett.* **1996**, *42*, 149.

Downloaded by PENNSYLVANIA STATE UNIV on September 16, 2012 | http://pubs.acs.org
Publication Date: January 24, 2002 | doi: 10.1021/bk-2002-0809.ch006

Downloaded by PENNSYLVANIA STATE UNIV on September 16, 2012 | http://pubs.acs.org
Publication Date: January 24, 2002 | doi: 10.1021/bk-2002-0809.ch007

Chapter 7

Copolymerization of Carbon Dioxide, Propylene Oxide, and Cyclohexene Oxide by an Yttrium–Metal Coordination Catalyst System

Chung-Sung Tan, Char-Fu Chang, and Tsung-Ju Hsu

Department of Chemical Engineering, National Tsing Hua University, Hsinchu, Taiwan 30043, Republic of China

The catalyst system consisting of $Y(CF_3CO_2)_3$ (I), diethylzinc (II), and glycerine (III) in the solvent of 1,3-dioxolane was found to be very effective to carry out copolymerization of carbon dioxide, propylene oxide (PO), and cyclohexene oxide (CHO). At 353K, 27.2 atm., and a proper combination of the components I to III, the yield and weight-average molecular weight could be as high as of 7948 g/(mol of Y)/h and 2.53×10^5, respectively, for a 12 h operation. The IR and NMR spectra indicated that the resulting copolymer was an alternating polyethercarbonate. From the DSC analysis, it is observed that the copolymer resulting from an equal or a higher feed ratio of PO to CHO possessed two glass transition temperatures (T_g), otherwise only one T_g. The temperature at which 10 % weight loss occurred (T_{10}) of the resulting polyethercarbonate was also measured in this study. Both T_g and T_{10} were found to locate in a range between those of the copolymers generated from CO_2 and PO, and CO_2 and CHO.

In CO2 Conversion and Utilization; Song, C., et al.;
ACS Symposium Series; American Chemical Society: Washington, DC, 2002.

Downloaded by PENNSYLVANIA STATE UNIV on September 16, 2012 | http://pubs.acs.org
Publication Date: January 24, 2002 | doi: 10.1021/bk-2002-0809.ch007

The copolymerization of CO_2 with epoxides to result in polyethercarbonate is one of the possible means for utilization of CO_2. Besides, this means can avoid using more toxic compound such as phosgene in synthesis. But due to CO_2 is a relatively unreactive compound, an effective catalyst is generally required. For production of an alternating polyethercarbonate using PO or CHO as monomer, the catalyst systems consisting of dialkylzinc and a compound having two active hydrogens (1-5) as well as other synthesized zinc-based organometallic catalysts (6-12) have been extensively studied. Using these kinds of catalyst systems, a long reaction time is usually required and the yield needs to be improved. A ternary rare-earth-metal coordination system $Y(P_{204})_3$ -Al(i-Bu)$_3$-glycerine was reported recently to carry out the copolymerization of CO_2 and PO (13). Despite that a random polyethercarbonate was produced, a higher molecular weight with a narrower molecular weight distribution and a higher yield within a shorter reaction period could be obtained compared to the binary organometallic catalyst systems. When the ternary rare-earth-metal coordination system containing $Y(CF_3CO_2)_3$, $Zn(Et)_2$, and glycerine was used to proceed the copolymerization of CO_2 and PO, an alternating polycarbonate with a carbonate content of 95.6 % instead of a random polyethercarbonate could be generated (14). In addition to carbonate content, a much higher yield was also observed using this reaction catalyst system. For the copolymerization of CO_2 and CHO, this ternary yttrium-metal coordination catalyst system was also proved to be effective as well (15).

Though a high molecular weight of polyethercarbonate can be generated either by the copolymerization of CO_2 with PO or CHO using yttrium-metal coordination catalyst system, thermal properties of the resulting copolymers are quite different, for example, T_g are about 308 K and 385 K, and T_{10} are about 463 K and 555 K for the copolymers generated from CO_2 and PO and CO_2 and CHO, respectively. While the thermal properties of the resulting copolymer can be improved using CHO instead of PO as monomer, the mechanical properties were found to reduce. It seems to be rational to use both PO and CHO as monomer in copolymerization reaction to generate a polyethercarbonate with the desired thermal and mechanical properties. The objective of this paper is therefore to systematically study the copolymerization of CO_2, PO, and CHO catalyzed by a ternary yttrium-metal coordination catalyst system.

Experimental

Propylene oxide of a purity of 99.5 % (Janssen Chimica) and cyclohexene oxide of a purity of 98 % (Lancaster Synthesis) were treated by vacuum distillation before use. Diethylzinc, glycerine, and all the solvents, such as n-hexane, toluene, DMSO, 1,3-dioxolane, and THF, were of analytical reagent and used without further purification. CO_2 with a purity of 99.99 % (Air Product) was used as received. Yttrium trifluoroacetate, yttrium acetate, yttrium 2-ethylhexanonate, yttrium acetylacetonate, and yttrium nitrate purchased from Aldrich Chemical Co. were heated in vacuum at 353 K for 40 h before use.

The catalyst system containing yttrium compound, $Zn(Et)_2$, and glycerine was prepared in an atmosphere of purified argon. Glycerine was added dropwise to a solution of $Zn(Et)_2$ in solvent at room temperature. After ethane gas evolution had ceased, the solution containing white powders resulting from the reaction between $Zn(Et)_2$ and glycerine was heated at 333 K for 2 h. This solution was then added to an autoclave that contained a known amount of yttrium compound. The resultant catalyst was stirred at 353 K for 1 h prior to CO_2, PO, and CHO were introduced.

Copolymerization of CO_2, PO, and CHO was carried out in a 300 ml autoclave that was equipped with a magnetic stirrer (Autoclave Engineers Inc.). The spinning speed was kept at 1000 rpm. After a certain period of reaction time, the pressure in the autoclave was allowed to reduce to atmosphere. To collect the resulting copolymer in the autoclave, THF was introduced into the autoclave first to dissolve the copolymer and then the solution was added by an aqueous methanol solution to cause a precipitation. The copolymer reprecipitated was dried in vacuum at 303 K for 8 h before analysis.

To determine the structure and the composition of the copolymers generated, the ^1H and ^{13}C NMR spectra were measured by a Bruker AM-300 NMR spectrometer and the IR spectra by a Jasco J-0085 spectrometer. The molecular weights were determined by a gel permeation chromatography (Waters 150-CV). The glass transition temperature and T_{10} were measured by DSC (duPont 2900) and TGA (duPont 951).

Downloaded by PENNSYLVANIA STATE UNIV on September 16, 2012 | http://pubs.acs.org
Publication Date: January 24, 2002 | doi: 10.1021/bk-2002-0809.ch007

Results and Discussion

In the beginning of the study, screening of solvents was first performed. Table I indicates that a less polar solvent– n-hexane and a more polar solvent– DMSO were not a good candidate to make polyethercarbonate from CO_2, PO, and CHO. Regarding yield and molecular weight distribution, 1,3-dioxolane was found to be superior to toluene. At least 40 % increase in yield and a narrower molecular weight distribution of the resulting copolymer using 1,3-dioxolane were observed. These results indicate that a proper choice of solvent is essential in this kind of copolymerization. Since 1,3-dioxolane showed its excellence, it was used as solvent in the subsequent runs.

Table I. Effect of Solvent on Copolymerization of CO_2, PO, and CHO Using the Catalyst System $Y(CF_3CO_2)_3$-$Zn(Et)_2$-Glycerine*

Solvent	*yield, g/(mol of Y)/h*	*Mn* × 10^{-4}	*Mw* × 10^{-5}	*Mw/Mn*
1,3-Dioxolane	7948	5.5	2.53	4.63
Toluene	5152	3.4	2.13	6.20
n-Hexane	Trace	---	---	---
DMSO	Trace	---	---	---

* I = 0.0004 mol; II = 0.008 mol; III = 0.004 mol; T = 353 K; P = 27.2 atm; time = 12 h

Table II shows the experimental results using different yttrium coordination catalyst systems in 1,3-dioxolane at 353 K and 27.2 atm. Each experiment was performed in duplicate, the difference in yield was observed to be always less than 7.0 %. It is seen from Table II that the catalyst system $Y(CF_3CO_2)_3$-$Zn(Et)_2$ - glycerine provided the highest yield. It might be due to that fluorine induced more positive charge of yttrium, in a consequence, the coordination catalyst could adsorb CO_2 more easily. This catalyst system was also proved to be the most appropriate one for the copolymerization of CO_2 with PO or CHO (14, 15).

The IR, ^1H- and ^{13}C- NMR spectra of the resulting copolymer, shown in Figures 1 to 3, respectively, indicate that the copolymer was an alternating polyethercarbonate and the copolymerization reaction took place according to the following scheme,

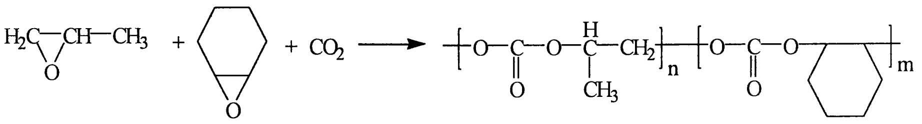

Since the poly(propylene oxide) and poly(cyclohexene oxide) contents in the resulting copolymer were small, sorption rate of CO_2 on the present catalyst was believed to be fast.

Downloaded by PENNSYLVANIA STATE UNIV on September 16, 2012 | http://pubs.acs.org
Publication Date: January 24, 2002 | doi: 10.1021/bk-2002-0809.ch007

Downloaded by PENNSYLVANIA STATE UNIV on September 16, 2012 | http://pubs.acs.org
Publication Date: January 24, 2002 | doi: 10.1021/bk-2002-0809.ch007

Table II. Copolymerization of CO_2, PO, and CHO by Different Catalyst Systems*

catalyst system			*Yield,*			
(I)	*(II)*	*(III)*	*g/(mol of Y)/h*	*Mn* × *10^{-4}*	*Mw* × *10^{-5}*	*Mw/Mn*
$Y(CF_3CO_2)_3$	$Zn(Et)_2$	Glycerine	7948	5.5	2.53	4.63
$Y(CH_3CO_2)_3$	$Zn(Et)_2$	Glycerine	Trace			
$Y(CH_3COCH{=}C(O\text{-})CH_3)_3$	$Zn(Et)_2$	Glycerine	5644	6.6	2.63	3.97
$Y(CH_3(CH_2)_3CH(C_2H_5)CO_2)_3$	$Zn(Et)_2$	Glycerine	6069	7.0	2.52	3.58
$Y(NO_3)_3$	$Zn(Et)_2$	Glycerine	6663	7.5	2.85	3.83

* I = 0.0004 mol; II = 0.008 mol; III = 0.004 mol; T = 353 K; P = 27.2 atm; time = 12 h

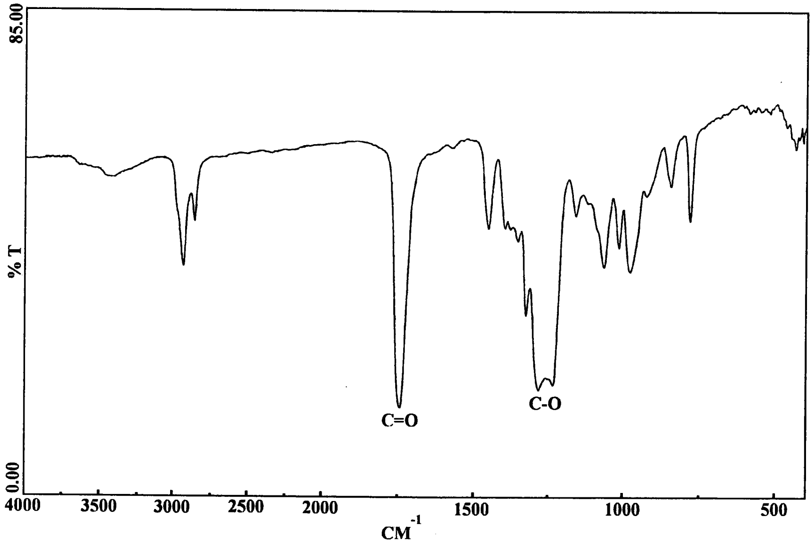

Figure 1. IR spectrum of the resulting copolymer.

Downloaded by PENNSYLVANIA STATE UNIV on September 16, 2012 | http://pubs.acs.org
Publication Date: January 24, 2002 | doi: 10.1021/bk-2002-0809.ch007

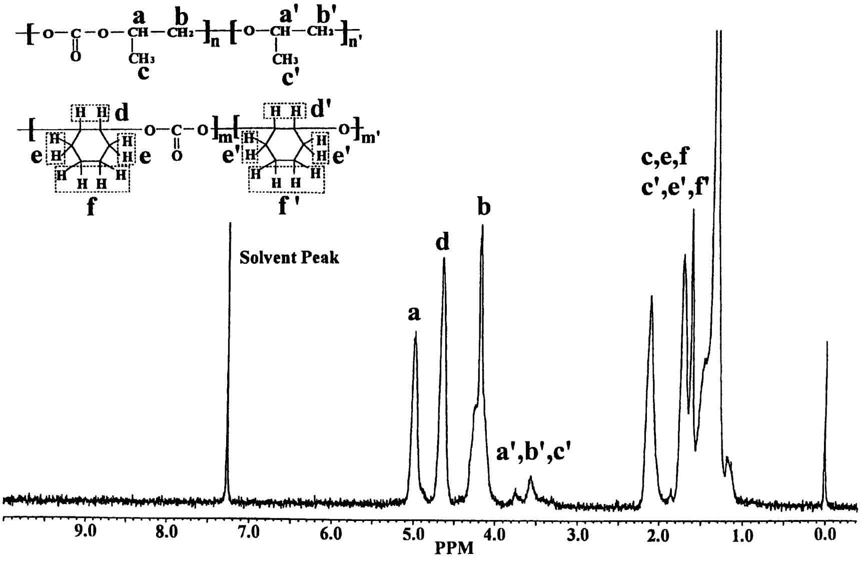

Figure 2. ^{1}H-NMR spectrum of the resulting copolymer.

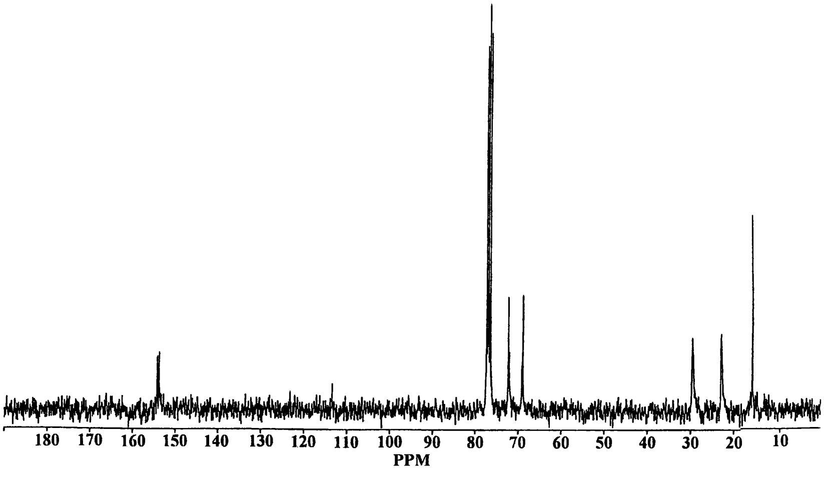

Figure 3. ^{13}C-NMR spectrum of the resulting copolymer.

When the molar ratios of II/I and III/II were maintained at 20 and 0.5, respectively, and the pressure was fixed at 27.2 atm., Table III shows that the yield increased with increasing temperature in a lower temperature range, reached a maximum at about 353 K, and then dropped as the temperature further increased. The existence of an optimum temperature in the copolymerization of CO_2, PO, and CHO is also observed in the copolymerization of CO_2 and PO (14)as well as CO_2 and CHO (15). According to the transition state theory (16), high-pressure operations are usually more favorable to polymerization reactions. For this copolymerization reaction, the yield was indeed enhanced with pressure as the pressure was less than 27.2 atm., but after that pressure was reached, the yield decreased with increasing pressure, shown in Table IV. One of the possible reasons for the decrease in yield is due to the decrease in solubility of copolymer resulted from the swelling of the solvent caused by the dissolution of CO_2.

Table III. Effect of Temperature on Copolymerization of CO_2, PO, and CHO*

T, K	*yield, g/(mol of Y)/h*	*Mn* × 10^{-4}	*Mw* × 10^{-5}	*Mw/Mn*
323	3475	7.4	5.02	6.94
333	6027	6.3	4.34	6.91
343	6792	6.0	3.78	6.33
353	7948	5.5	2.53	4.63
363	6046	4.2	2.46	5.88
373	5683	3.5	1.76	5.08

* I = 0.0004 mol; II = 0.008 mol; III = 0.004 mol; P =27.2 atm.; time = 12 h

Table IV. Effect of Pressure on Copolymerization of CO_2, PO, and CHO*

P, atm.	*yield, g/(mol of Y)/h*	*Mn* × 10^{-4}	*Mw* × 10^{-5}	*Mw/Mn*
20.4	6394	5.7	2.66	4.64
23.8	6717	6.0	3.81	6.34
27.2	7948	5.5	2.53	4.63
30.6	7710	5.3	2.95	5.58
34.0	7604	5.3	3.15	5.96
40.8	7210	5.9	3.29	5.55
47.6	7069	5.3	3.37	6.35

* I = 0.0004 mol; II = 0.008 mol; III = 0.004 mol; T = 353 K; time = 12 h

Downloaded by PENNSYLVANIA STATE UNIV on September 16, 2012 | http://pubs.acs.org
Publication Date: January 24, 2002 | doi: 10.1021/bk-2002-0809.ch007

Tan and Hsu (14) pointed out that the component ratios in a rare-earth-metal coordination catalyst system have significant effects on yield and molecular weight in copolymerization of CO_2 and PO, the same conclusion can be drawn here. From the experimental results over wide ranges of the molar ratios of II to I and III to II, it was observed that the II/I and III/II ratios of 20 and 0.5, respectively, provided the highest yield though not the largest molecular weight and the best Mw/Mn.

It is seen from Table V that only one T_g was observed when the feed contained more CHO than PO. On the other hand, two glass transition temperatures existed. This observation might provide two aspects: 1). a random polyethercarbonate or a block-polyethercarbonate could be produced by changing the monomer ratio in feed, 2). the ring-opening rate of CHO is faster than that of PO. At any ratio of PO to CHO, T_g of the resulting copolymers are all larger than those of the copolymer generated from CO_2 and PO but less than those of the copolymer generated from CO_2 and CHO. In addition, the T_{10} of the resulting copolymers were found to locate in a range between those of the copolymers generated by using PO or CHO as monomer.

Conclusion

Polycarbonate could be produced effectively from the copolymerization of carbon dioxide, propylene oxide, and cyclohexene oxide in 1,3-dioxolane with a catalyst system consisting of $Y(CF_3CO_2)_3$, diethylzinc, and glycerine. At a proper combination of temperature, pressure, and molar ratios of the catalyst components, a very high yield up to 7948 g/(mol of Y)/h and a molecular weight

Table V. Effect of Monomer ratio on Yield and Molecular Weight*

PO ml	*CHO ml*	*Yield g*	*Yield %*	*$Mn \times 10^{-4}$*	*$Mw \times 10^{-5}$*	*Mw/Mn*	*T_g, K*	*T_{10}, K*
10	20	33.24	76.72	9.3	3.72	4.02	343	549
10	30	40.32	68.94	6.4	2.08	3.23	371	545
10	40	47.75	64.82	8.3	3.88	4.67	390	550
15	15	38.15	90.34	5.5	2.53	4.63	313,370	543
20	20	40.67	72.23	5.2	1.75	3.40	319,371	552
20	10	28.59	69.50	5.3	1.66	3.13	319,361	533
30	10	35.56	65.71	3.5	1.06	3.03	320,357	544
40	10	37.51	55.90	6.5	2.29	3.52	319,368	528
30	20	44.78	64.51	7.1	2.55	3.58	321,371	540

* I = 0.0004 mol; II = 0.008 mol; III = 0.004 mol; P = 27.2 atm.; T = 353 K; time = 12 h

Downloaded by PENNSYLVANIA STATE UNIV on September 16, 2012 | http://pubs.acs.org
Publication Date: January 24, 2002 | doi: 10.1021/bk-2002-0809.ch007

as high as of 2.5 × 10 ^{5} were observed to obtain in a 12 h run in a batch-mode operation.

A copolymer containing random distribution of PO carbonate and CHO carbonate or a block-polyethercarbonate could be generated by varying the volume ratio of the monomers PO and CHO in feed. When the volume of CHO was greater than that of PO, only one T_g of the resulting copolymer existed, otherwise, two glass transition temperatures existed. All the T_g and T_{10} of the present copolymer were found to be present in a range between those of the copolymer generated from CO_2 and PO and CO_2 and CHO. This indicates that the thermal properties of the resulting polyethercarbonate can be modified by introducing two epoxides with different chemical structure.

Downloaded by PENNSYLVANIA STATE UNIV on September 16, 2012 | http://pubs.acs.org
Publication Date: January 24, 2002 | doi: 10.1021/bk-2002-0809.ch007

Acknowledgment

Financial support from the National Science Council of Republic of China, Grant NSC89-2214-E007-009, is gratefully acknowledged.

References

1. Inoue, S.; Koinuma, H.; Tsuruta, T., Makromol Chem., **1969**, 130, 210.
2. Yoshida, Y.; Inoue, S., Polym. J., **1980**, 12, 763.
3. Kuran, W.; Pasynkiewicz, S.; Skupinska, J., Makromol. Chem., **1977**, 178, 2149.
4. Hino, Y.; Yoshida, Y.; Inoue, S., Polym. J., **1984**, 16, 159.
5. Nishimura, M.; Kasai, M.; Tsuchida, E., Makromol. Chem., **1978**, 179, 1913.
6. Inoue, S.; Koinuma, H.; Yokoo, Y.; Tsuruta, T., Makromol. Chem., **1971**, 143, 97.
7. Darensbourg, D. J.; Holtcamp, M. W., Macromolecules, **1995**, 28, 7577.
8. Darensbourg, D. J.; Zimmer, M. S., Macromolecules, **1999**, 32, 2137.
9. Sarbu, T.; Beckman, E. J., Macromolecules, **1999**, 32, 6904.
10. Super, M.; Berluche, E.; Costello, C.; Beckman, E., Macromolecules, **1997**, 30, 368.
11. Ree, M.; Bae, J. Y.; Jung, J. H.; Shin, T. J., J. Polym. Sci. Polym. Chem., **1999**, 37, 1863.

12. Darensbourg, D. J.; Holtcamp, M. W.; Struck, G. E.; Zimmer, M. S.; Niezgoda, S. A.; Rainey, P.; Robertson, J. B.; Draper, J. D.; Reibenspies, J. H., J. Am. Chem. Soc., **1999**, 121, 107.
13. Chen, X.; Shen, Z.; Zhang, Y., Macromolecules, **1991**, 24, 5305.
14. Tan, C. S.; Hsu, T. J., Macromolecules, **1997**, 30, 3147.
15. Hsu, T. J.; Tan, C. S., submitted to J. Polymer Sci., 2000.
16. Savage, P. E.; Gopalan, S.; Mizan, T. I.; Martino, C. J.; Brock, E. C., AIChE J., **1995**, 41, 1723.

Downloaded by PENNSYLVANIA STATE UNIV on September 16, 2012 | http://pubs.acs.org
Publication Date: January 24, 2002 | doi: 10.1021/bk-2002-0809.ch007

Downloaded by PENNSYLVANIA STATE UNIV on September 16, 2012 | http://pubs.acs.org
Publication Date: January 24, 2002 | doi: 10.1021/bk-2002-0809.ch008

Chapter 8

The Role of CO_2 for the Gas-Phase O_2 Oxidation of Alkylaromatics to Aldehydes

Jin S. Yoo

Samsung Chemical Company, 2315 Mast Court, Flossmoor, IL 60422

Abstract: A synergistic cooperation between the guest moiety and the host matrix in the CVD Fe/Mo/DBH catalyst gave rise to a novel catalytic activity for the gas-phase O_2 oxidation of alkylaromatics. Para-selective property and activation of CO_2 to function as a co-oxidant are two key outstanding attributes exhibited by the catalyst. The oxidation mechanism was remarkably altered in the co-presence of CO_2 in the O_2 feed stream. The function of CO_2 not only enhanced the rate of reaction, but also improved the selectivity toward the aldehyde/oxygenate products. The peroxocarbonate complex has been postulated as an active catalytic species, which promoted the initial abstraction of hydrogen atom from the alkyl group in a much more effective manner than the usual O_2 oxidation.

During the last two decades, carbon dioxide has been attracting increasingly more attention worldwide for the green chemistry. Many homogeneous and heterogeneous catalysts have been reported for activation of the CO_2 molecule and its usage as an abundant inexpensive C_1-source for the chemical industry (1-10). The notable advances in its utilities include a one-oxygen transfer oxidant and a reaction modulating agent (11-14) for the synthesis of valuable commodity chemicals, fine and specialty chemicals containing the functional groups such as olefin (15-23), aldehyde, ketone, acid (24,25), epoxide, ester (26), carbonate (2,27), lactone, alcohol (28-31), carbamate (32-33), amide and other useful oxygenates (34). In light of the unique properties of CO_2 exhibited with a variety of catalysts, it deems

In CO2 Conversion and Utilization; Song, C., et al.;
ACS Symposium Series; American Chemical Society: Washington, DC, 2002.

appropriate to define the role of CO_2 as an oxidant more clearly for the organic syntheses as well as for green chemistry.

In the course of developing a new process for the selective synthesis of terephthaldehyde by the gas-phase O_2 oxidation of p-xylene over CVD Fe/Mo/DBH during late 1980s, it was unexpectedly discovered that the oxidation mechanism was drastically altered in the co-presence of CO_2 in the O_2 feed stream. This finding prompted us to continue to study the role of CO_2 for the gas-phase O_2 oxidation of various alkylaromatics to the corresponding aldehydes, oxygenates and, in some cases, olefins via oxidative dehydrogenation.

Downloaded by PENNSYLVANIA STATE UNIV on September 16, 2012 | http://pubs.acs.org
Publication Date: January 24, 2002 | doi: 10.1021/bk-2002-0809.ch008

Results and Discussion

The CVD Fe/Mo/DBH catalyst was prepared from $FeCl_3$, MoO_2Cl_2 or $MoCl_5$ and partially deboronated borosilicate molecular sieve known as HAMS-1B-3 (DBH) by the chemical vapor deposition technique based on a new catalyst concept in the late 1980s (1,35). The CVD Fe/Mo/DBH catalyst consisted of two guest phases of ferric molybdate, $Fe_2(MoO_4)_3$, and MoO_3 (a minor fraction) uniformly stabilized as nano-size particles within the main channel structure of the host MFI structure of the DBH matrix (36,37). A synergistic cooperation between guest nano-particles and the host matrix brought about novel catalytic activities, namely, para-selective property and a unique function of activating the CO_2 molecule to function as a co-oxidant for the gas-phase O_2 oxidation of a variety of alkylaromatics.

Oxidation of alkylaromatics over CVD Fe/Mo/DBH

Xylene isomers, pseudocumene, durene, mesitylne, substituted toluenes, ethylbenzene and substituted ethylbenzene derivatives were among a variety of alkylaromatics studied in this work. Besides an unexpected property of activating the CO_2 molecule (38), the catalyst also exhibited other interesting properties such as para-selectivity and catalyst stability for the oxidation reactions to produce aldehydes and/or oxygenates (39-46) as well as dehydrogenation of alkylbenzenes such as ethylbenzene, diethylbenzene, isopropyltoluene and ethyltoluene and alkanes to yield the corresponsing olefins (39, 43, 44).

Oxidation of p-Xylene over CVD Fe/Mo/DBH

In a typical gas-phase O_2 oxidation of p-xylene over the CVD Fe/Mo/DBH catalyst, terephthaldehyde and p-tolualdehyde were produced in a high yield despite the extremely high surface area of the catalyst (150-300 m^2/g). The co-presence of CO_2 not only enhanced the rate of oxidation, but also increased the selectivity and created a unique activity to alter the product distribution. The oxidation temperature was remarkably lowered as much as 150°C~200°C in the co-presence of CO_2 than that required to attain the same conversion of the p-xylene with O_2 alone.

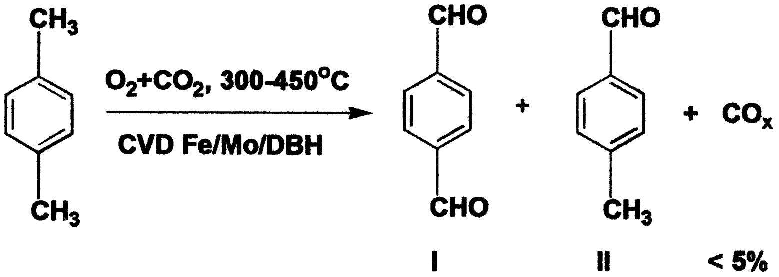

The experimental results on the p-xylene oxidation are summarized in Table I. The author has postulated two different active catalytic sites, "pair" and "single" sites, for the formation of terephthaldehyde (I) and p-tolualdehyde (II) elsewhere (1,27); The p-xylene molecule was aligned on the "pair sites" in a parallel fashion for activation, and one H-atom from each methyl group was simultaneously abstracted in a concerted manner to produce the stable diradical, which led to the aldehyde products via the peroxide intermediate. On the "single" sites, p-xylene was activated in the stand-on manner, and one H was abstracted from the activated methyl group to yield a single radical, which led to produce p-tolualdehyde (19). Further oxidation of p-tolualdehyde produced p-toluic acid instead of terephthaldehyde. Terephthaldehyde was not produced by the consecutive oxidation of p-tolualdehye. Instead, these were produced on two different active centers.

It became possible to control the molar ratio of terephthaldehyde to p-tolualdehyde in the product (I:II) in a wide range of 4:1 to 1:4 by adjusting factors such as the loading of the catalyst component, the acidity of the DBH host matrix, the atomic ratio of Fe/Mo in the guest moiety, the reaction temperature, and the composition of the feed. Among these factors, the co-presence of CO_2 in the O_2 feed stream appears to be the most dominant factor. It must fundamentally alter the reaction mechanism by affecting not only the oxidation rate, but also controlling the product yield.

These conclusions are also supported by the results plotted in Figure 1. The

Downloaded by PENNSYLVANIA STATE UNIV on September 16, 2012 | http://pubs.acs.org
Publication Date: January 24, 2002 | doi: 10.1021/bk-2002-0809.ch008

Downloaded by PENNSYLVANIA STATE UNIV on September 16, 2012 | http://pubs.acs.org
Publication Date: January 24, 2002 | doi: 10.1021/bk-2002-0809.ch008

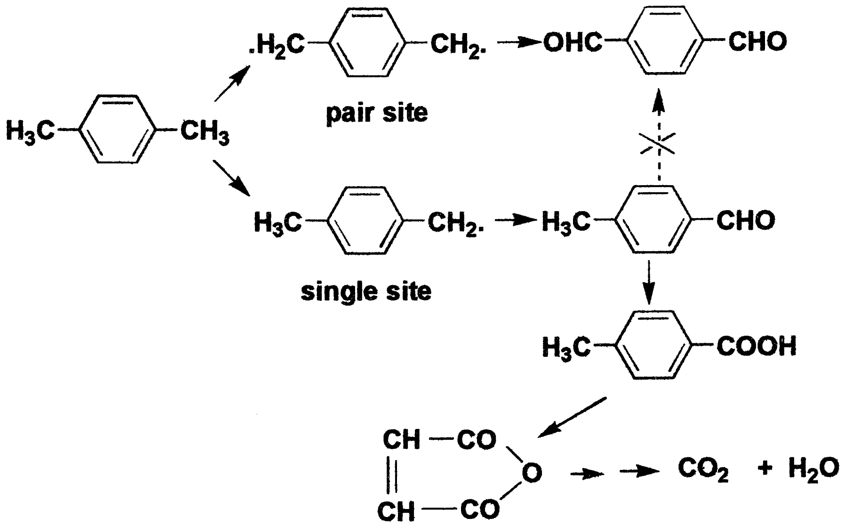
H3C CH3
.H2C CH2.
OHC CHO
pair site
H3C CH2.
H3C CHO
single site
H3C COOH
CH CO
CH CO
O
CO2 + H2O

Downloaded by PENNSYLVANIA STATE UNIV on September 16, 2012 | http://pubs.acs.org
Publication Date: January 24, 2002 | doi: 10.1021/bk-2002-0809.ch008

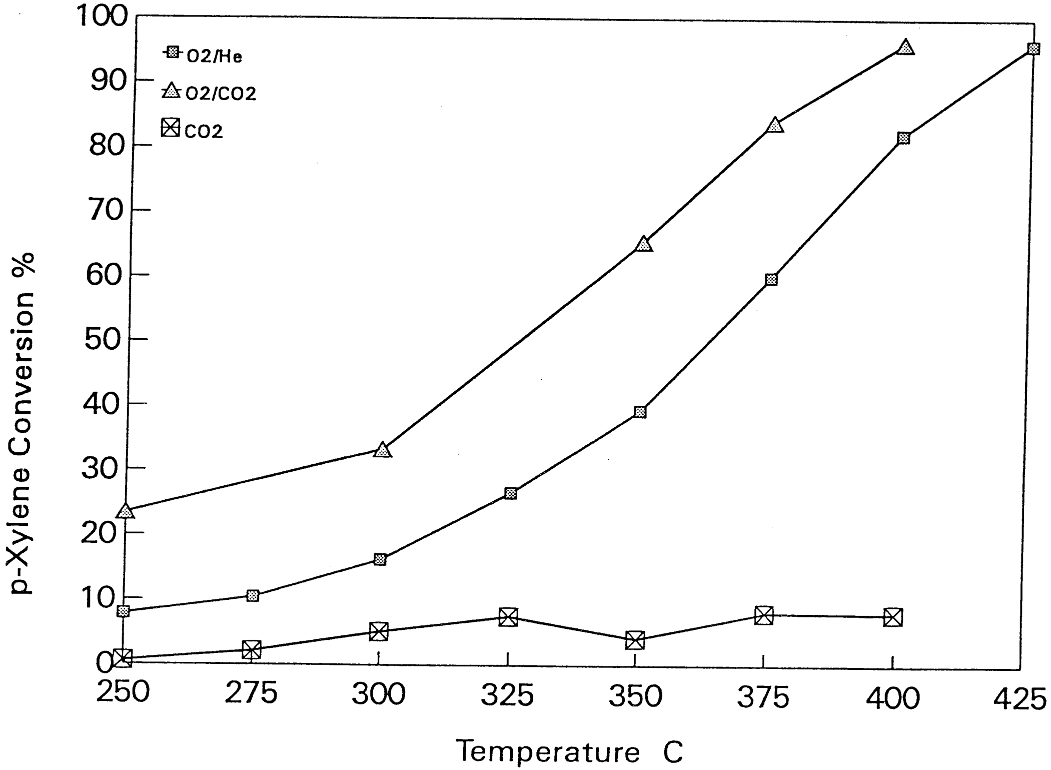

Figure 1. Effect of CO_2 on gas-phase oxidation of p-xylene over CVD Fe/Mo/DBH as a function of reaction temperature. Catalyst composition: 6.80% Mo, 1.88% Fe, 54 ppm B, the atomic ratio of Mo/Fe was altered from 2.11 for fresh non-activated system to 1.89 for the catalyst activated by prolonged air calcination. Reproduced with permission from reference 38. Elsevier 1993.

conversion of p-xylene was remarkably increased in the co-presence of CO_2 in the O_2 stream in comparison to that obtained in O_2 alone at the oxidation temperatures, 250~450°C. Under the anaerobic condition in the presence of CO_2 without O_2 in the feed stream (see Figure 2), the conversion of p-xylene was drastically reduced to a level of 5-6% and maintained at that level throughout a 45 hour run.

Table I. Gas-phase O_2 oxidation of p-xylene over CVD Fe/Mo/DBH
Reaction temperature: 350°C, the concentration of p-xylene in the O_2 feed stream: 0.1 mol%

Feed gas	p-xylene	Product selectivity mol%					
	Conversion %	I	II	byproduct[a]	others[b]	CO	CO_2
O_2	41.2	23.5	50.2	5.2	4.8	0.6	15.5
O_2+CO_2	65.5	33.6	40.9	5.4	8.7	3.4[c]	8.0
CO_2	5	14	69	17			

I:terephthaldehyde II:p-tolualdehyde a:hydrocarbon byproducts produced by the side reactions catalyzed by the acidic site of the DBH matrix b:further oxidized products c:most likely produced from the CO_2 feed instead of burning.

The selectivity of terephthaldehyde declined rapidly, and became nil in 10 hours on stream while the selectivity of p-tolualdeyde kept at an approximately 30% level. When the deactivated catalyst was calcined in the air, the selectivity to terephthaldehyde was restored again at a level of 10%, but it deactivated very quickly. However, the results shown in Figure 3 indicate that terephthaldehyde was not produced and even the selectivity of p-tolualdehyde, a sole aldehyde product, decreased extremely fast and became negligible in a flow of N_2 without CO_2 within a 5 hour period. These results suggest that CO_2 actually participates in the formation of active oxygen species even under the anaerobic condition although the process proceeds extremely slolowly.

The promoting phenomenon of CO_2 and para-selective activity were also observed with polymethylbenznes such as pseudocumene, durene, 2,6-dimethylnaphthalene and 4,4'-dimethylbiphenyl (41), substituted toluene derivatives (42), other types of alkylaromatics (43) with the CVD Fe/Mo/DBH catalyst. The same promoting function of CO_2 was also found for the gas-phase O_2 oxidation of alkane over both CVD Fe/Mo/DBH and CVD Zr/W/DBH (43).

Downloaded by PENNSYLVANIA STATE UNIV on September 16, 2012 | http://pubs.acs.org
Publication Date: January 24, 2002 | doi: 10.1021/bk-2002-0809.ch008

Downloaded by PENNSYLVANIA STATE UNIV on September 16, 2012 | http://pubs.acs.org
Publication Date: January 24, 2002 | doi: 10.1021/bk-2002-0809.ch008

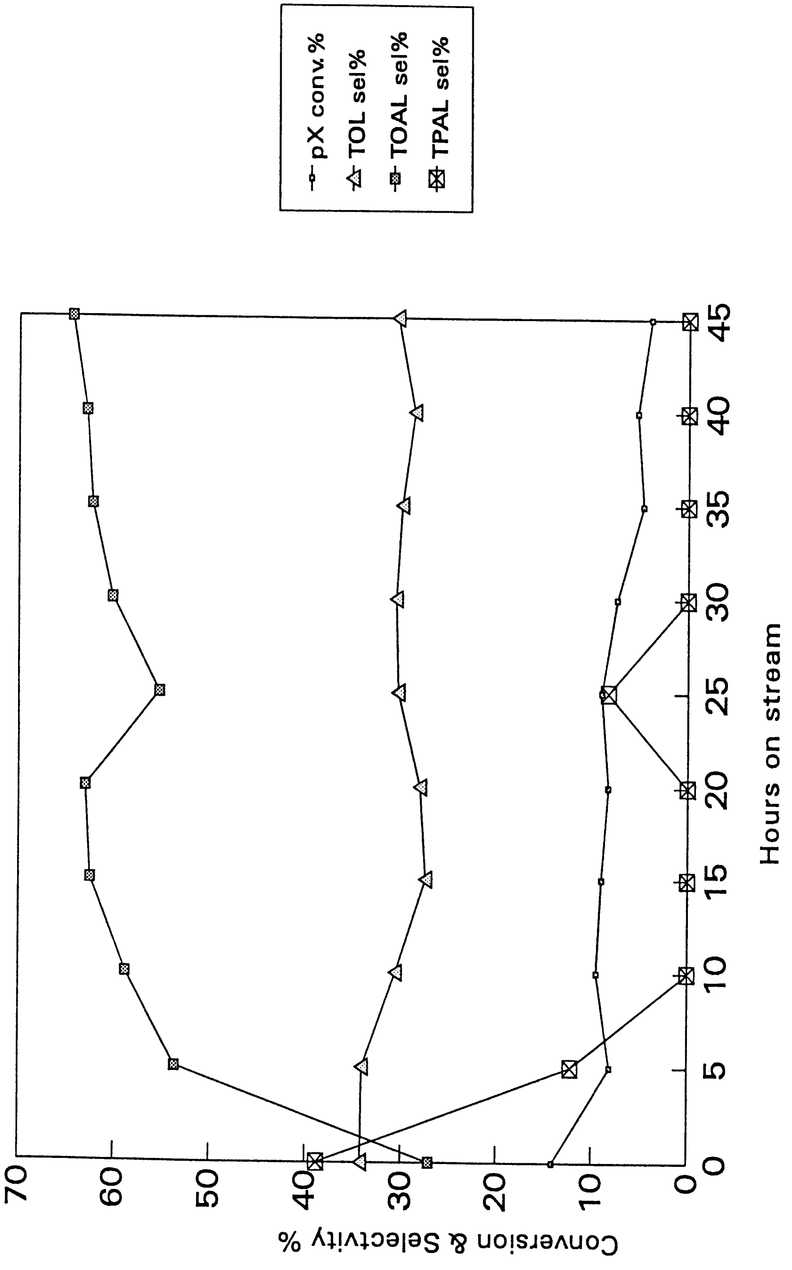

Figure 2. Oxidation of p-xylene in CO_2 alone over CVD Fe/Mo/DBH – conversion and selectivity vs hours on stream

Downloaded by PENNSYLVANIA STATE UNIV on September 16, 2012 | http://pubs.acs.org
Publication Date: January 24, 2002 | doi: 10.1021/bk-2002-0809.ch008

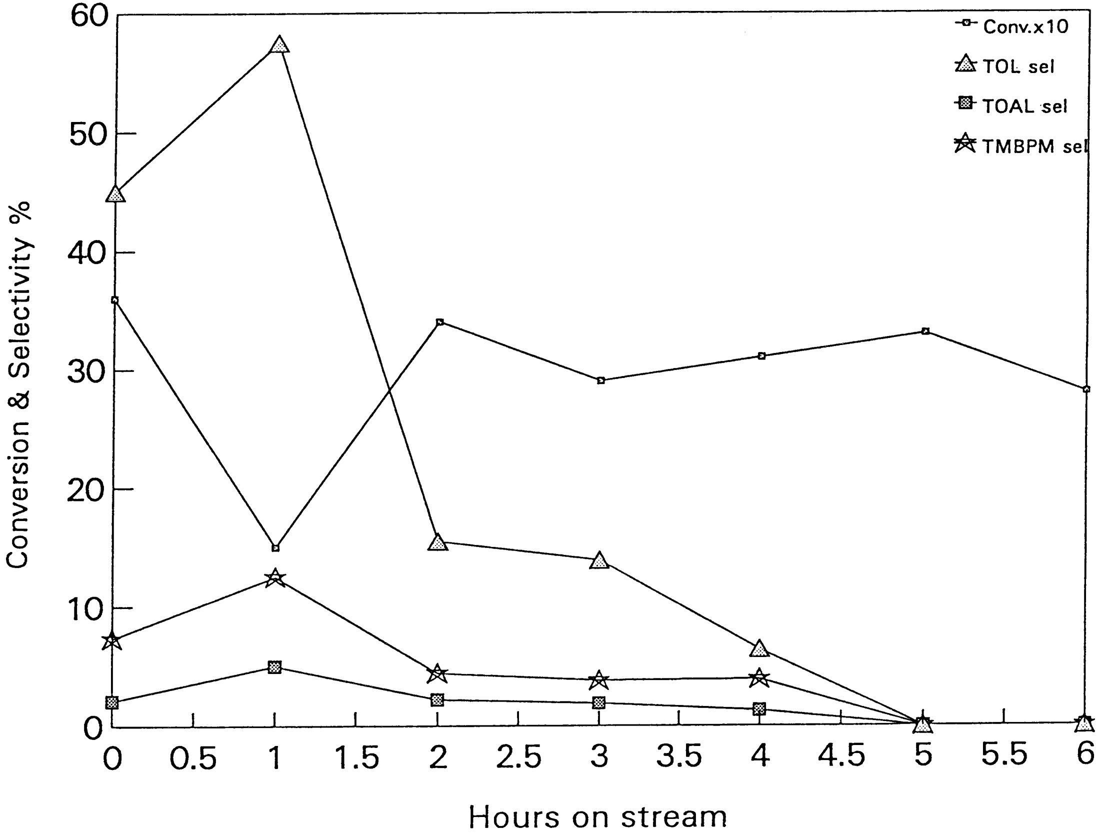

Figure 3. Reaction of p-xylene in N_2 over CVD Fe/Mo/DBH TMBPM: trimethylbiphenylmethane

Chemical modification of CVD Fe/Mo/DBH with silica deposition, Si/Fe/Mo/DBH

Attempts to characterize the active catalytic sites were made by the chemical modification techniques. The "single" site of the CVD Fe/Mo/DBH catalyst was more predominantly poisoned by depositing silica using $Si(OMe)_4$ via the chemical deposition method. As shown in Table II. the molar ratio of terephthaldehyde to p-tolualdehyde in the product remarkably increased from 0.51:1 with the unmodified system to 0.98:1 over the silica modified catalyst, CVD Si/Fe/Mo/DBH (39) for the oxidation of p-xylene. The catalytic activity was about the same (51~55% conversion) for both modified and unmodified original catalyst.

Downloaded by PENNSYLVANIA STATE UNIV on September 16, 2012 | http://pubs.acs.org
Publication Date: January 24, 2002 | doi: 10.1021/bk-2002-0809.ch008

Table II. Oxidation of p-xylene over silica modified catalyst, CVD Si/Fe/Mo/DBH

	CVD Si/Fe/Mo/DBH	CVD Fe/Mo/DBH
Temperature °C	350	350
p-Xylene conversion %	51.0	54.6
Selectivity (mol%)		
Terephthaldehyde (I)	32.2	24.9
p-Tolualdehyde (II)	32.7	48.4
Molar ratio of I : II	0.98 : 1	0.51 : 1

These results indicate that the selectivity to p-tolualdehyde was noticeably decreased by preferential poisoning of the "single" sites over the "pair" sites. It also suggests that the "single" sites may be mainly located on the exterior surface of the catalyst since the size of the $Si(OMe)_4$ is too big to get an access to the main channel structure of the host MFI matrix in the silica deposition procedure. It is likely that silica must be deposited on the exterior surface, while the guest $Fe_2(MoO_4)_3$ moiety inside the channel remains intact. Thus one could conclude that the "pair" sites are primarily located inside the channel: the limited space inside the channel structure of CVD Si/Fe/Mo/DBH may force the p-xylene molecule to align itself on the "pair" site in a parallel fashion for the concerted abstraction of one hydrogen atoms from two methyl groups to generate a stable diradical, •CH_2-C_6H_4-CH_2•, which leads to form terephthaldehyde via the peroxide radical intermediate, •O_2CH_2-C_6H_4-CH_2O_2•.

Chemical modification of CVD Fe/Mo/DBH with Ag-doping, Ag/Fe/Mo/DBH

Silver was doped at a level of 760 ppm on CVD Fe/Mo/DBH by using an aqueous solution of $Ag(NO_3)_3$ via the impregnation method to prepare the Ag/Fe/Mo/DBH catalyst. The original "pair" sites on the Fe/Mo/DBH catalyst were effectively poisoned by this procedure, and thus p-tolualdehyde became almost a sole product (45).

Table III. Oxidation of p-xylene over Ag/Fe/Mo/DBH

Catalyst	Ag/Fe/Mo/DBH		CVD Fe/Mo/DBH	
Surface area m^2/g	169		256	
Temperature °C	350		350	
Feed type	1	2	1	2
Conversion %	13.6	32.3[a]	41.2	65.6[a]
Product selectivity mol%				
p-Tolualdehyde	79.3	90.7	50.2	60.5
Terephthaldehyde	1.0	2.6	23.5	33.6
Benzaldehyde	0.4	0.4	2.4	2.7
Maleic anhydride	0	0	3.2	11.5
Toluene	0.8	1.2	3.5	4.8
Trimethylbiphenyl-methane(TMBPM)	0	0.1	1.7	0.6
CO	0	4.9	0.6	3.2
CO_2	18.5	-	15.6	-

a:excluding CO_2; feed 1:0.1% p-xylene, 1.0% O_2, 1.0% N_2 in He;
feed 2:0.1% p-xylene, 1.0% O_2, 1.0% N_2 in CO_2

The catalytic activity kept intact while the CO_2 promoting function still remained with Ag/Fe/Mo/DBH, as shown in Table III. However, another separate run with Si/Fe/Mo/DBH showed that the promoting function of CO_2 was suppressed by doping the silica on the CVD Fe/Mo/DBH catalyst.

Downloaded by PENNSYLVANIA STATE UNIV on September 16, 2012 | http://pubs.acs.org
Publication Date: January 24, 2002 | doi: 10.1021/bk-2002-0809.ch008

Oxidation of Ethylbenzene Derivatives

In the course of pursuing the selective oxidation of the xylene isomers containing ethylbenzene over the CVD Fe/Mo/DBH catalyst, we found that the catalyst exhibited an excellent activity to produce styrene as an initial product via the oxidative dehydrogenation reaction (44). If the alkyl groups in the alkylaromatics are ethyl or higher, dehydrogenation of the alkyl group to produce alkenylaromatics becomes the primary reaction with the catalyst under oxidation conditions similar to those for polymethylaromatics.

The similar promoting effect of CO_2 was also observed with ethylbenzene derivatives, in particular, ethylbenzene and p-ethyltoluene (see Table IV). Ethylbenzene was converted to styrene and the ethyl group in p-ethyltoluene was preferentially dehydrogenated to produce p-methylstyrene over the methyl group at the initial stage of the reaction. As soon as these styrene products were formed, they were very rapidly oxidized further to the corresponding aldehyde and oxygenates.

Downloaded by PENNSYLVANIA STATE UNIV on September 16, 2012 | http://pubs.acs.org
Publication Date: January 24, 2002 | doi: 10.1021/bk-2002-0809.ch008

Table IV. Oxidation of p-ethylbenzene and Styrene in CO_2 plus O_2 over CVD Fe/Mo/DBH

Substrate	p-Ethyltoluene		Styrene	
Temperature °C	375		300	
Feed type	1	2	1	2
Conversion %	39.0	60.0	34.5	26.5
	Product selectivity %			
p-Methylstyrene	7.3	6.4^a		
p-Tolualdehyde	17.2	20.0		
p-methylacetophpenone	6.9	6.7		
p-Toluic acid	23.0	34.8		
Terephthaldehyde	0.6	1.2		
Benzaldehyde			19.9	21.7^a
Phenylacetaldehyde			1.9	2.5
Acetophenone			6.5	7.7
Benzoic acid			57.3	60.5
CO	14.8	22.0^b	6.6	5.6^b

a:data exclude CO_2 (all data in the column), b:likely to be formed from CO_2 instead of burning source, Feed 1:O_2 alone, feed 2: CO_2 plus O_2

On the contrary, when styrene was subjected to the oxidation reaction over the same catalyst under similar conditions, the co-presence of CO_2 in the O_2 stream hampered the oxidation. In short, the CO_2 molecule participates in the abstraction of H from the methyl or alkyl group in the gas-phase O_2 oxidation to produce styrene at the initial stage, while it remained as an inert diluent for the subsequent oxidation of the styrene to other oxygenates in the second stage. The CO_2 plays a key role in the initial abstraction of H from methyl or alkyl group, but it becomes an inert gas for the oxidation of unsaturated substrates such as styrene and its derivatives. In this respect, the CVD Fe/Mo/DBH catalyst behaves quite differently from the homogeneous catalysts such as $[Rh(diphos)Cl].C_6H_6$ (11,12) and $Rh(bipy)(C_2H_4)Cl$ (11), which exhibited a remarkable role as a one-oxygen transfer oxidant as well as a modulating agent for the oxidation of styrene and tetrahydrofuran.

The Oxidation Mechanism

A synergistic interaction of the catalytic species with DBH

In order to understand the synergistic interaction between the guest catalytic moiety of $Fe_2MoO_4)_3$ and the host DBH matrix having an MFI structure stated in the front section of this paper, the catalytic behavior of the DBH matrix itself was investigated for the gas-phase O_2 oxidation of p-xylene. The borosilicate molecular sieve, HAMS-1B-3, was partially deboronated to prepare two DBH samples containing 1.0 wt% B (sample DBH I) and 52 ppm B (sample DBH II).

These samples were subjected to the p-xylene oxidation under the comparable reaction conditions. The results are compared with those obtained over CVD Fe/Mo/DBH (see in Table V.) The catalytic activity of the DBH sample depends on the acidity of the sample. It is in turn closely related to the boron content removed from the framework of the DBH. The byproducts such as toluene and pseudocumene were formed via disproportionation, and trimethylbiphenylmethane was produced via oxidative head-to-tail coupling of p-xylene. The acid sites of the catalyst are responsible for these side reactions.

However, it was surprising to observe that only p-tolualdehyde without accompanying terephthaldehyde was formed over these DBH samples, and that the oxidation was also promoted by the co-presence of CO_2 in the O_2 feed as well as under the anaerobic condition in the flow of CO_2 alone.

Since the specific acid sites on DBH which are responsible for the side reactions are assumed to be occupied by the catalytic guest moieties,

Downloaded by PENNSYLVANIA STATE UNIV on September 16, 2012 | http://pubs.acs.org
Publication Date: January 24, 2002 | doi: 10.1021/bk-2002-0809.ch008

$Fe_2(MoO_4)_3$ and MoO_3, during the catalyst preparation step, it is logical to believe that both "single" and "pair" sites are provided by the catalyst moiety rather than the DBH matrix itself with the CVD Fe/Mo/DBH catalyst.

The peroxocarbonate intermediate

The cyclic peroxocarbonate complex is proposed as an active species for the promoting function of CO_2 for the gas-phase O_2 oxidation of alkylaromatics based on the above results observed with CVD Fe/Mo/DBH(1,43,47). The nature of the peroxocarbonate anion (CO_4^-) has been disclosed for the liquid-phase oxidation of styrene and tetrahydrofuran by Aresta et al. (11-13) and for active metal oxide materials for selective oxidative coupling of methane by Dubois et al., (46,48,49).

Table V. Oxidation of p-Xylene over Deboronated HAMS-1B-3 (DBH) Host Matrix

Catalyst	DBH I		DBH II		CVD Fe/Mo/DBH	
Boron wt%	1.0		52 ppm		540 ppm	
Temperature °C	350		350		350	
Feed type	3	2	1	2	1	2
Conversion %	3.8	18.5	3.4	20.1	41.2	65.6
Product distribution (mole%)						
Toluene	67.6	48.4	51.1	48.7	3.5	4.8
Pseudocumene	11.6	4.5	12.7	8.7	0	0
Benzaldehyde	0	0	0	0	2.4	2.7
p-Tolualdehyde	13.2	28.2	10.3	20.9	50.2	40.9
Terephthaldehyde	0	0	0	0	23.5	33.6
Trimethylbiphenylmethane	7.6	5.0	25.9	21.7	1.7	0.6
CO	0	14.0	0	0	0.6	3.6
CO_2	-	-	-	-	15.6	-

feed 1:0.1% p-xylene, 1.0% N_2, 1.0% O_2 in CO_2; feed 2:1% p-xylene, 1.0% N_2 1.0% O_2 in He; feed 3: 0.1% p-xylene, 1.0% N_2, in CO_2 anaerobic condition.

As shown in scheme 1, it is thought that the metal-O_2 complex is initially

Downloaded by PENNSYLVANIA STATE UNIV on September 16, 2012 | http://pubs.acs.org
Publication Date: January 24, 2002 | doi: 10.1021/bk-2002-0809.ch008

formed on the $Fe_2(MoO_4)_3$ moiety (most likely on the four coordinated Mo center) when the CVD Fe/Mo/DBH catalyst is exposed to the feed stream containing both O_2 and CO_2. A CO_2 molecule is then inserted into the O-O bond on the resulting metal-O_2 complex to form an active peroxocarbonate species. It may play a key role in boosting the oxidation reaction as a one-oxygen transfer agent mimicking the mono-oxygenase enzyme. It has also been reported that the oxygen atoms directly bonded to the metal transfer to the oxophile (11) to form aldehyde and other oxygenates.

Downloaded by PENNSYLVANIA STATE UNIV on September 16, 2012 | http://pubs.acs.org
Publication Date: January 24, 2002 | doi: 10.1021/bk-2002-0809.ch008

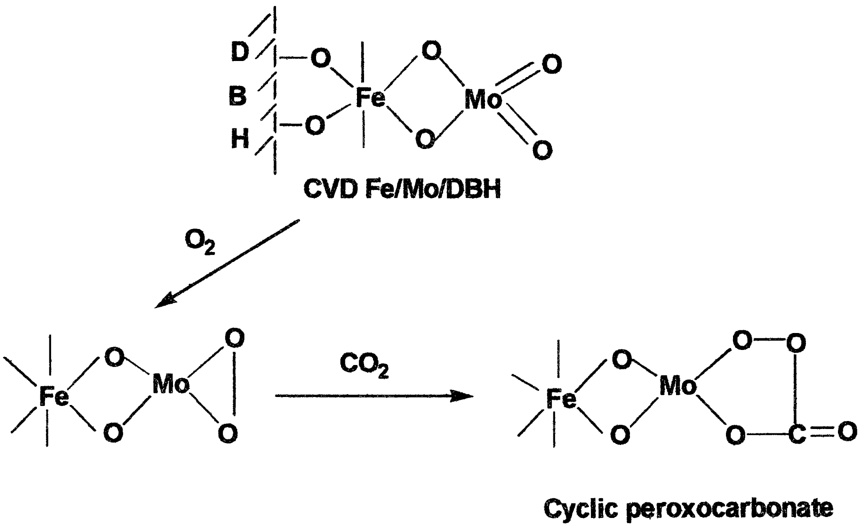

Scheme 1

Conclusions

A synergistic cooperation between the guest catalytic moiety, $Fe_2(MoO_4)_3$, with the host DBH matrix in CVD Fe/Mo/DBH gave rise to a novel catalytic activity for the gas-phase O_2 oxidation of alkylaromataics. The catalyst exhibited a unique property to activate CO_2 to function as a co-oxidant. The peroxocarbonate complex intermediate has been proposed to be an active species for the initial abstraction of H from the alkyl side chain substituents of alkylaromatics.

In a typical gas-phase O_2 oxidation run of p-xylene, the catalytic activity was remarkably enhanced in the co-presence of CO_2 in the O_2 feed gas stream. The CO_2 molecule functions not only to enchance the oxidation rate, but also to improve the selectivity to the aldehyde products by significantly lowering the reaction temperatures and suppressing the burning. It also plays a role as a reaction modulating agent to alter the product distribution.

Two active centers named "pair" site and "single" site have been postulated for the formation of terephthaldehyde and p-tolualdehyde respectively from the p-xylene. These sites were preferentially poisoned by the chemical modification techniques such as Ag-doping for the "pair" site and CVD silica deposition for the "single" site. The CO_2 promoting function remained intact with Ag/Fe/DBH while it disappeared almost completely over Si/Fe/Mo/DBH.

For the oxidation of ethylbenzene, the promoting function of CO_2 was effective for the initial abstraction of hydrogen causing dehydrogenation to produce styrene. Contrary to the homogenous catalysts studied previously for oxidation of styrene and tetrahydrofuran, carbon dioxide remained as an inert diluent over the CVD Fe/Mo/DBH catalyst. In short, the promoting function of CO_2 ties directly to the initial abstraction of hydrogen atom(s) from alkyl side chains of alkylaromatics with CVDFe/Mo/DBH.

References

1. Yoo, J.S.; Donohue, J.A. Kleefisch, M.S.; Lin, P.S.; Elfline, S.D. *Appl. Catal. A* **1993**, 105, 83
2. Aresta, M. et al. *Inorg. Chem.* 35(4), **1996**, 4254.
3. Kolomnikov, I.S.; Lysyak, T.V. *Russian Chem. Rev.* **1990**, 59(4), 344-360.
4. Wright, C.A.; Mathew, T.; McGill, J.W.; Gong, J.K. *Fourth Intern. Conf. on Carbon Dioxide Utilization,* Sept. 4-11, 1997, Kyoto, Japan, p-046,
5. Ishitani, O. et al. *J. Chem. Soc., Chem. Commun.* **1994**, 367.
6. Keene , F.R.et al. *Coord. Chem. Rev.* **1985**, 64, 247.
7. Jezowska-Trzebiatowska et al. *Organomet. Chem.* **1974**, 80, C27.
8. Galan. G. et al. *J. Phys. Chem.* **1997**, 101, 2626.
9. Mirzabekova. S.R. et al. *Kinet. and Catal.* **1995**, 36(1), 111.
10. Aida, T. *Shokubai.* **1991**, 33(3), 230.
11. Aresta, M.; Fragale, C.; Quaaranta, E.; Tommasi, I. *J. Chem. Soc., Chem. Commun.*,**1992**, 315.
12. Albano, P.; Aresta, M.; Manassero, M. *Inorg. Chem.* **1980**, 19, 1069
13. Aresta, M. et al. *Inorg. Chem.* **1996**, 35, 4254.
14. Nishiyama, T and Aika, K. *J. Catal.* **1990**, 122, 346.

Downloaded by PENNSYLVANIA STATE UNIV on September 16, 2012 | http://pubs.acs.org
Publication Date: January 24, 2002 | doi: 10.1021/bk-2002-0809.ch008

15. Tanaka, I.. et al., *Catal. Today,* **1998**, 45 (1-4), 55.
16. Nakagawa, K.; Kajita, C.; Okamura, M.; Kato, S.; Kasyua, H.; Ikenaga, N.;Kobayashi, T.; Suzuki, T. *Catal. Lett.* **2000**, 64, 214.
17. Mimura, N.; Saito, M. *Catal. Today* **2000**, 55, 173.
18. Minura N.; Takahara, I.; Saito, M.; Hattori, T.; Ohkuma, K.; Ando, M. *Fourth Intern. Conf. on CO_2 Utilization*, Kyoto, Japan, Sept. 4-11, 1997. P-024.
19. Chang, J-S.; Park, S.-E.; Park, M.S.; Anpo, M.; Yamaashita, H. *Fourth Intern. Conf. on CO_2 Utilization,* Kyoto, Japan, Sept. 4-11, 1997, P-013.
20. Hattori, T.; Yamauchi, S.; Komatsuki, M. *Proc. of the Intern. Symp. on Chemical Fixation of Carbon Dioxide*, Dec. 2-4. 1991, Nagoya, Japan, P 28; p 429,
21. Yamauchi, S. et al. *Sekiyu Gakkaishi*, **1994**, 37, 278.
22. Park, S-E et al. *Am. Chem. Soc. Meeting, Preprint, Fuel Div.* Paper C45, May 1997.
23. Hattori, T.; Yamaguchi, S.; Satsuma, A.; Murakami, Y. *Chem. Lett.*, **1992**, 629.
24. Llorca, J.; de la Piscina, R.; Sales, J.; Homs, N. *Fourth Intern. Conf. on Carbon Dioxide Utilization*, Sept. 7-11, 1997, Kyoto, Japan, O-03.
25. Hackerman, N. et al. *J. Electrochem.* Soc. **1984**, 131, 1511.
26. Yoshida, Y. and Ishii, S. *Proc. of the Intern. Symp. on Chemical Fixation of Carbon Dioxide*, Dec. 2-4. 1991, Nagoya, Japan, p 29; p 423.
27. Aresta, M. *J. Mol. Chem.* **1987**. 41. 355.
28. Kusama, H. et al. *Catal. Today*, **1996**, 28, 262.
29. Ihaara, T. et al. *Bull. Chem. Soc. Jpn.* **1996**, 69, 241.
30. Tominaga, K. et al. *Bull. Chem. Soc. Jpn.* **1995**, 68, 2837.
31. Inui et al., *Appl. Catal.* **1982**, 2, 389.
32. Aresta, M. Quaramta. E., *Chem. Tech.* **1997**, 27(3), 32.
33. Toda, T,; Yoshida, M.; Ohshima, M. *Proc. of the Intern. Symp. on Chemical Fixation of Carbon Dioxide;* Dec. 2-4. 1991, Nagoya, Jpn. B8, p 185.
34. Aresta, M, *Intern. Symp. on CO_2 Conversion and Utilization in Refinery and Chemical Processing, 219th National meeting, ACS,* San Francisco, CA, March 26-31, 2000, Preprint, Div. of Petrol. Chem., 45(no.1), 92.
35. Centi, G.; Misono, M., *Catal. Today*, **1998**, 41, 287.
36. Yoo, J.S.; Donohue, D.A.;Choi-Feng, C. *Advanced Catalysts and Nanostructured Materials*; Moser, W.R., Ed., Academic Press: New York, NY, 1996; Chapter 17, pp 453-477.
37. Zajac, G.W.; Choii-Feng, C.; Faber, J.; Yoo, J.S.; Patel. R.; Hochst, H. *J. Catal.* A **1995**, 151, 338.
38. Yoo, J.S.; Lin, P.S.; Elfline, S.D. *Appl. Catal.* A, **1993**, 106, 259.
39. Yoo, J.S.; Donohue, J.A.; Kleefisch, M.K. *Appl Catal.* A, **1994**, 110, 75.
40. Yoo, J.S.; Choi-Feng, C.; Donohue, J.A. *Appl. Catal.* A, **1994**, 118, 87.

Downloaded by PENNSYLVANIA STATE UNIV on September 16, 2012 | http://pubs.acs.org
Publication Date: January 24, 2002 | doi: 10.1021/bk-2002-0809.ch008

41. Yoo, J.S.; Lin, P.S.; Elfline, S.D. *Appl. Catal.* A, **1995**, 124, 139.
42. Yoo, J. S. *Appl. Catal.* A, **1996**, 135, 261.
43. Yoo, J. S. *Appl. Catal.* A, **1996**, 143, 20.
44. Yoo, J.S. *Appl. Catal.* A, **1996**, 142, 19.
45. Yoo, J.S.; Choi-Feng, C.; Zajac, G.W. *Appl. Catal.* A, **1999**, 184, 11.
46. Hayward, P.J. et al. *J. Am. Chem. Soc.* **1970**, 92(20), 5873.
47. Yoo, J.S. *Appl. Catal.* **1993**, 106, 259
48. Dubois, J.-L.; Bisiaux, M. Minoun, H.; Cameron, C.J. *Chem. Lett.* **1990**, 6, 967.
49. Dubois, J.-L.; Cameron, C.J. *Proceedings of the 10th Intern. Congr. On Catal. New Frontiers in Catal.* Guczi, L.; Solymosi, F; Tetenyi, P.; Ed.; Part-C, Akademiai Kiado, Budapest 1992, pp 2245-2252.

Downloaded by PENNSYLVANIA STATE UNIV on September 16, 2012 | http://pubs.acs.org
Publication Date: January 24, 2002 | doi: 10.1021/bk-2002-0809.ch008

Downloaded by PENNSYLVANIA STATE UNIV on September 16, 2012 | http://pubs.acs.org
Publication Date: January 24, 2002 | doi: 10.1021/bk-2002-0809.ch009

Chapter 9

Effective Conversion of CO_2 to Valuable Compounds by Using Multifunctional Catalysts

Tomoyuki Inui

Gas and Chemical Research Division, Air Water Inc., Sakai 592–8331, Japan
(Fax: (+81)–722–44–8085; email: inui-tom@awi.co.jp)

Indispensable conditions for CO_2 mitigation by catalytic conversion are enumerated. These are very rapid conversion rate and high selectivity to valuable compounds. Since reduction of CO_2 needs expensive hydrogen, the ways to get hydrogen inexpensively are described. One is the reduction of CO_2 by methane or natural gas instead of hydrogen. In order to realize this reaction without coke formation, the four-component composite catalyst, the Rh-modified Ni-based catalyst with Ce_2O_3 and Pt as additives has been developed by author et al. Another is the on-site heat supply by catalytic combustion to compensate the large endothermic heat of reforming of methane. Especially, the addition of more easily combustible hydrocarbons such as ethane, propane, and butane, which are contained in natural gas, made possible marked decrease in furnace temperature around as low as 570 - 600 K. Even such lower furnace temperatures, the catalyst temperature rises up to around 970 K and an equilibrium conversion of methane is observed even at a very short contact time such as 5 msec. Simultaneous reforming of methane with CO_2 and H_2O also achieved.

Ultra rapid methanation of CO_2 on the Ni-based three-component composite catalyst, Ni-La_2O_3-Ru, highly effective

In CO2 Conversion and Utilization; Song, C., et al.;
ACS Symposium Series; American Chemical Society: Washington, DC, 2002.

synthesis of methanol by CO_2 hydrogenation on the Pd-Ga-modified Cu-Zn-Cr-Al-Ox-Al-Ox catalyst, the effective synthesis of ethanol by CO_2 hydrogenation on the multifunctional catalyst are then summarized. Finally, highly effective syntheses of light olefins and gasoline via methanol synthesis from CO_2 hydrogenation using multi-step reactors connected in series are described.

The sequential results of these catalytic conversions of CO_2 shows a high potential to realize the processes for mitigation or recyclic use of CO_2.

Downloaded by PENNSYLVANIA STATE UNIV on September 16, 2012 | http://pubs.acs.org
Publication Date: January 24, 2002 | doi: 10.1021/bk-2002-0809.ch009

Hence carbon dioxide is the final combustion product of organic compounds, CO_2 itself has little value, and in order to obtain new products by chemical reduction, the large amount of additional energy, in particular expensive hydrogen, is necessary. However, the catalytic hydrogenation of CO_2 is superior to other chemical conversion methods for CO_2. Because, CO_2 can be converted with an extremely higher rate on the well designed solid catalysts than other chemical conversion methods, and desired compounds can be synthesized very selectively. The largest problem in the catalytic hydrogenation would be concentrated in the effective and economic production method of the huge amount of H_2 as the reducing reagent for CO_2. Development of the highly active Ni-based reforming catalyst which works at much lower temperatures than that of the conventional catalyst will be introduced first. Since the novel catalyst has high activity for not only steam-reforming but also CO_2-reforming of methane, H_2 for CO_2 hydrogenation could be replaced by CH_4 and H_2O. In this review paper, the focus will be concentrated to the CO_2 reduction by H_2 or CH_4 to synthesize highly valuable major building blocks for petrochemical industries such as ethylene, propylene, methanol, ethanol, and high quality gaseous and liquid fuels such as substituted natural gas and high octane-number gasoline. These high value products have a potential to partly compensate the cost of reducing reagents, hydrogen or methane, and these CO_2-conversion routes lead to a new paradigm for chemical industries and energy usage cycles in many fields.

Rapid CO_2-Reforming of Methane

The major conventional production method of H_2 is the steam reforming of saturated hydrocarbons, in particular natural gas or methane, on the stabilized supported Ni catalyst, and the reaction is operated at a high temperature around 1,170 K. In order to moderate the coke deposit, an excess concentration of steam than the stoichiometry of the reaction, Eq. [1] is added in the feed. As the conventional catalyst has no ability for CO_2

activation, CO_2 once formed by the shift reaction, Eq. [2] via Eq. [3] cannot be converted to other molecules by the reaction between CO_2 formed and methane unconverted as Eq. [4].

$$CH_4 + 2H_2O \rightarrow 4H_2 + CO_2, \quad \Delta H^\circ = 165\ kJ/mol \quad [1]$$
$$CO + H_2O \rightarrow H_2 + CO_2, \quad \Delta H^\circ = -41\ kJ/mol \quad [2]$$
$$CH_4 + H_2O \rightarrow 3H_2 + CO, \quad \Delta H^\circ = 206\ kJ/mol \quad [3]$$
$$CH_4 + CO_2 \rightarrow 2H_2 + 2CO, \quad \Delta H^\circ = 248\ kJ/mol \quad [4]$$

In recent years however, CO_2-reforming of methane as expressed by Eq. [4] has gathered a great deal of attention in the sequential international congresses on CO_2 mitigation and/or utilization (1-10). Reflecting these situations, several elaborative reviews on this subject have been made by Fox III (11) in 1993, Rostrup-Nielsen (12) in 1994, Ross et al. (13) in 1996, Halmann and Steinberg (14) in 1999, and Bradford and Vannice (15) in 1999. Especially, the last one (15) summarized as many as 190 papers including classic papers. The most recent 16 papers including in this review were published in 1997. The focus of this review is concentrated mainly on the fundamental aspects such as activation of CH_4 and CO_2, carbon deposition, kinetics, and reaction mechanisms. However, catalytic reaction-engineering aspects involving autothermal reforming and co-reforming such as CO_2 + O_2 and CO_2-H_2O-O_2 are not mentioned. From the view points of the rapid reforming, which is applicable to industrialization, these reaction-engineering aspects are indispensable, and indeed, in the most recent few years, the papers treated on these subjects are rapidly increasing (16-21).

Including the most recent papers published until middle of 2000, the review article written by the author (22) on "Reforming of CH_4 by CO_2 Associated with O_2 and /or H_2O" will be published from the Royal Society as Catalysis Vol. 16 in 2001. Therefore, here, only the essence of our recent research works on CO_2-reforming is described below.

It seems to be contradiction that in order to obtain H_2 for CO_2 hydrogenation, the additional fossil fuel is necessary to maintain the high reaction temperature, and moreover CO_2 is produced as the by-product. However, if by the innovative improvement in catalyst structure, on which no coke deposit occurs and exhibits a very high reaction rate even at the low temperature range around 600 K, situation would become different. Because the heat to maintain such a medium-range temperature could be supplied by the waste heat of large scale facilities of industries and even by the accumulated heat of solar energy. Furthermore, the large endothermic heat of reaction could be supplied on-site by the catalytic combustion of more easily combustible hydrocarbons and/or a part of methane fed on the same catalyst surface, on which methane reforming reactions are advancing.

In order to realize the rapid synthesis of hydrogen through methane reforming, the synergistic effect of composite catalysts and the combined reactions to compensate the large amount of endothermic heat were investigated. A Ni-based three-component catalyst such as Ni-Ce_2O_3-Pt

Downloaded by PENNSYLVANIA STATE UNIV on September 16, 2012 | http://pubs.acs.org
Publication Date: January 24, 2002 | doi: 10.1021/bk-2002-0809.ch009

supported on alumina-wash-coated ceramic fiber in a plate shape (23) was very suitable for the reforming of methane. The catalyst composition was set at 10 wt% Ni, 5.6 wt% La_2O_3, and 0.57 wt% Pt for example, or molar ratios of these components were 1: 0.2: 0.03. Even with such a low concentration, the precious metal enhanced the reaction rate markedly, and this synergistic effect was ascribed to the hydrogen spillover effect through the part of precious metal and it resulted in a more reduced surface of the main catalyst component. In particular, a marked enhancement in the reaction rate of CO_2-reforming of methane was observed by the modification of a low concentration Rh to the Ni-Ce_2O_3-Pt catalyst (24).

Fig. 1 shows that the four-component composite catalyst (⑥ in Fig. 1) exhibited a very high activity for CO_2-reforming of methane, Eq. [4], with the stoichiometric ratio of the products approaching to the reaction equilibrium even such as a high space velocity (SV) 730,000 h^{-1}, or a very short contact time of the reaction gas of 5 msec, on the basis of the net volume of the catalyst and its support.

The activity of the composite catalyst was much larger than the sum of the activities of the component catalysts, namely the Rh and the Ni-Ce_2O_3-Pt catalyst. This means that the composite catalyst involved a two-step spillover, i.e., hydrogen formed was adsorbed on the Rh part very rapidly, faster than on the Pt part, and then the spiltover hydrogen was abstracted by the Pt part, this being followed by its diffusion toward the major catalyst component, the Ni part. Consequently, the Ni part can be kept in a reduced surface state and the rapid reaction progress can occur on it. The role of Ce_2O_3 would be not only to promote dispersion of the Ni component, but also to act as a transporting media for spiltover hydrogen.

Hydrogen and CO were obtained in equivalent amounts by the reaction, and the space-time yield of H_2 and CO obtained at 873 K was 7,690 mol/l • h at 59% methane conversion.

In a reaction of CH_4-CO_2-H_2O-O_2 on the four components catalyst, an extraordinarily high space-time yield of hydrogen, 12,190 mol/l·h, could be realized under the conditions of very high space velocity (5 msec) (25).

In order to overcome the restriction in conversion of the reaction equilibrium, the combustion of more easily combustible hydrocarbons such as ethane or propane, which are involved in the natural gas, was then combined by adding these hydrocarbons and oxygen. The aimed reactions to produce only syngas are expressed as the following Equations [5] and [6], including generation and consumption of heat by combustion and reforming, respectively.

$$(x+5y)\ CH_4 + x\ CO_2 + y\ C_2H_6 + 3.5y\ O_2 \rightarrow (2x+7y)\ CO + (2x+13y)\ H_2$$

$$\Delta H_{773K} = 259x - 240y \text{ kJ/mol} \qquad [5]$$

$$(x+7z)\ CH_4 + x\ CO_2 + z\ C_3H_8 + 5z\ O_2 \rightarrow (2x+10z)\ CO + (2x+18z)\ H_2$$

$$\Delta H_{773K} = 259x - 375y \text{ kJ/mol} \qquad [6]$$

Downloaded by PENNSYLVANIA STATE UNIV on September 16, 2012 | http://pubs.acs.org
Publication Date: January 24, 2002 | doi: 10.1021/bk-2002-0809.ch009

Downloaded by PENNSYLVANIA STATE UNIV on September 16, 2012 | http://pubs.acs.org
Publication Date: January 24, 2002 | doi: 10.1021/bk-2002-0809.ch009

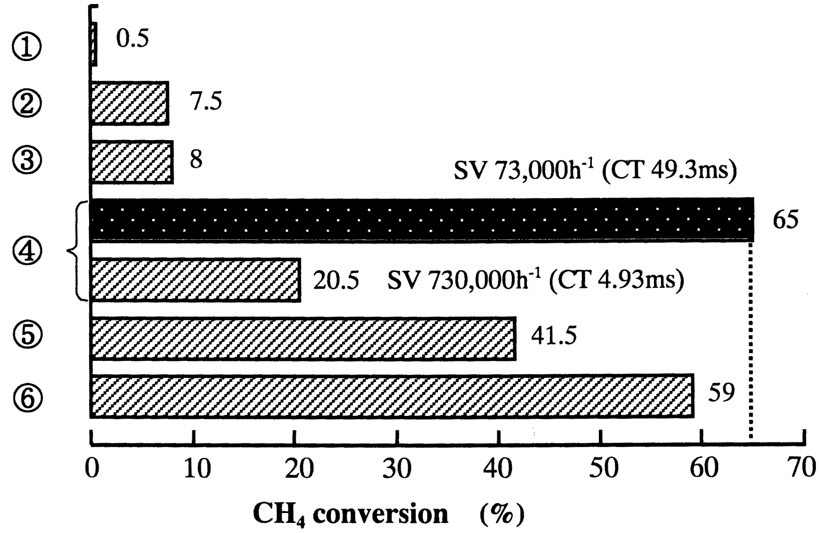

Figure 1. Synergistic effect in Rh-modified Ni-Ce_2O_3-Pt catalyst caused by combination with each ingredient upon the CO_2-reforming of methane

Catalyst supported on alumina washcoated ceramic fiber

① 10.0wt% Ni - 6.0wt% Ce_2O_3, ② 1.0wt% Pt, ③ 0.2wt% Rh,
④ 10.0wt% Ni - 6.0wt% Ce_2O_3 - 1.0wt% Pt,
⑤ 10.0wt% Ni - 6.0 wt% Ce_2O_3 - 0.2wt% Rh,
⑥ 10.0wt% Ni - 6.0 wt% Ce_2O_3 - 1.0wt% Pt - 0.2wt% Rh

Feed gas: 10 mol% CH_4 - 10 mol% CO_2 - 80mol% N_2

SV: ■ 73,000 h^{-1}; ▨ 730,000 h^{-1}

Dotted line: Equilibrium conversion level at 873 K

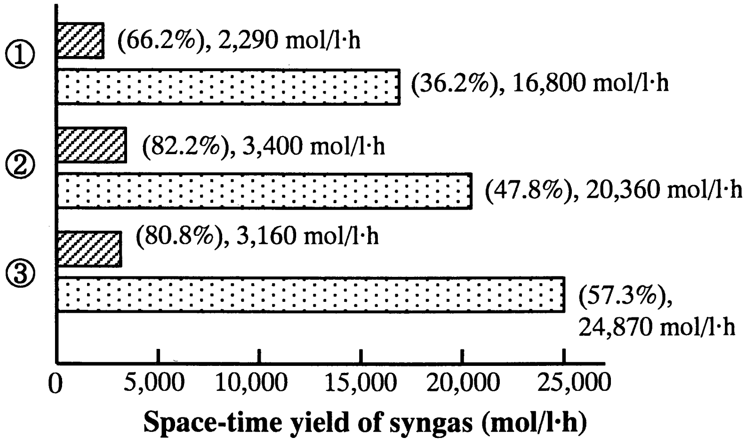

Figure 2. Effect of catalytic oxidation of ethane or propane on the CO_2 reforming of methane at two kinds of space velocities 73,000 and 730,000 h^{-1}
Catalyst: The Rh-modified four-component catalyst
Gas composition:
① 35% CH_4 - 10% CO_2 - 55% N_2
② 35% CH_4 - 10% CO_2 - 5% C_2H_6 - 17.5% O_2 - 32.5% N_2
③ 35% CH_4 - 10% CO_2 - 3.3% C_3H_8 - 16.5% O_2 - 35.2% N_2
Catalyst-bed temperature: 700 ℃ (Furnace temperature: 500 ℃) Pressure: 1 atm.
Numerals in parenthesis are methane conversion.

In case of ethane or propane addition in CO_2-reforming of methane, the catalyst temperature abruptly rose even at a very lower furnace temperature such as below 625 K, and it was maintained at much higher temperature than the furnace temperature, indicating that by the in-situ heat supply due to the catalytic combustion, the methane conversion was eventually induced at a very lower temperature range. As shown in Fig. 2, an extraordinarily high space-time yield of syngas, as high as 25,000 mol/l·h was obtained at a considerably low furnace temperature around 773 K (26).

Rapid CO_2-Methanation

Catalytic hydrogenation of carbon oxides was found by Sabatier and Senderens (27) at the beginning of twentieth century. Since then, a numerous studies have been done (28, 29). Industrially, this reaction has been applied to the purification of H_2-rich gas and production of substituted natural gas (30).

Two decades ago, methanation reactions, i.e., inverse reactions of Eqs. [3] and [1] were applied to energy saving devices and processes. A typical one known as EVA-ADAM process (30) was achieved in Germany. The

Downloaded by PENNSYLVANIA STATE UNIV on September 16, 2012 | http://pubs.acs.org
Publication Date: January 24, 2002 | doi: 10.1021/bk-2002-0809.ch009

process consists of two reaction systems. The one (EVA) is endothermic steam reforming of methane, i.e., Eqs. [1-3]. this requires a large amount of energy at a temperature level of more than 1,200K, which is supplied form the high temperature gas furnaces. Another one (ADAM) is exothermic methanation of CO and CO_2, i.e., inverse reaction of Eqs. [3] and [1], where heat is set free over a wide range of temperature. The energy taken up in EVA is transformed into a cold H_2-rich gas that is transported to ADAM, where heat is released according to the requirements of the heat market.

Recently, CO_2 methanation has had a new significant object concerning with the global warming problem. Since methanation of CO_2 needs four times molecules of H_2, it seems to be disadvantageous. However, as the rate of CO_2 methanation is far beyond all other methods for chemical conversion of CO_2 to hydrocarbons and oxygenates. The largest consumption of hydrogen per unit CO_2 mole equivalents to that the largest energy taking into methane molecules. Therefore, the methane synthesized by hydrogenation of CO_2 is expected as the transportation media of the energy injected to the reaction. When the rapid CO_2 methanation progress at a low temperature range around 470 - 570 K, the large exothermic reaction heat itself is available, and furthermore, when the methane formed is used as the fuel, a high temperature even 1,300 K can be obtained. Therefore, it is thought that the rapid CO_2-methanation is significant as one kind of the chemical heat pump, by which a low temperature, i.e., a low-value energy, can be transformed into a high temperature, i.e., a high-value energy, through chemical reactions.

Most recently, Halmann and Steinberg reviewed CO_2 methanation (32) in their monograph. As shown in this review, the most of the studies on CO_2 methanation used supported single component catalysts, except small number of studies, such as Co/Cu/K catalyst (33), $Rh/CeO_2/SiO_2$ (34), Fe-Mn doped with Rh and La (35), Fe-Zr-Ru (36), and Ni-La_2O_3-Ru supported on spherical silica or alumina reported by the author et al. (37). The last one had been developed more than two decades ago, however, this catalyst is regarded as one of the most active methanation catalysts among the whole catalysts, as recognized by Halmann and Steinberg in their review. The author has described in detail the sequential results on this catalytic performance and the reason of exerting the ultra-rapid reaction rate in the review article of "Methanation" in "Encyclopedia of Catalysis" (38), which is now under preparation with editing by Professor Horváth et al., and will be published soon. Therefore, here, only the essence of these works is described below.

The author et al. have studied on the CO_2 methanation since 1970's, and developed the Ni-based three components composite catalyst supported on the spherical silica support having meso-macro bimodal pore structure (37). The catalyst contained La_2O_3 by 1/5 mol of Ni, and Ru by 1/30 mol of Ni. As shown in Fig. 3, combination of these three kinds of catalyst components exerted an evident synergistic effect on the methanation rates of CO_2, and showed the high conversion rate to synthesize methane exclusively (24, 37).

Downloaded by PENNSYLVANIA STATE UNIV on September 16, 2012 | http://pubs.acs.org
Publication Date: January 24, 2002 | doi: 10.1021/bk-2002-0809.ch009

The catalyst made possible the CO-CO_2 co-methanation (39), and therefore, the process of CO_2 elimination in the conventional SNG process could be omitted. The cause of the high performance was elucidated as follows; the adsorption capacity of catalyst for CO_2 was increased by the weak basicity of La_2O_3, and hydrogen adsorption was markedly enhanced by combining Ru, which worked as the porthole of hydrogen spillover. The meso-macro bimodal pore structure has the roles of the supported bed for catalytic substances and the pass for quick diffusion of the reactants, respectively (37).

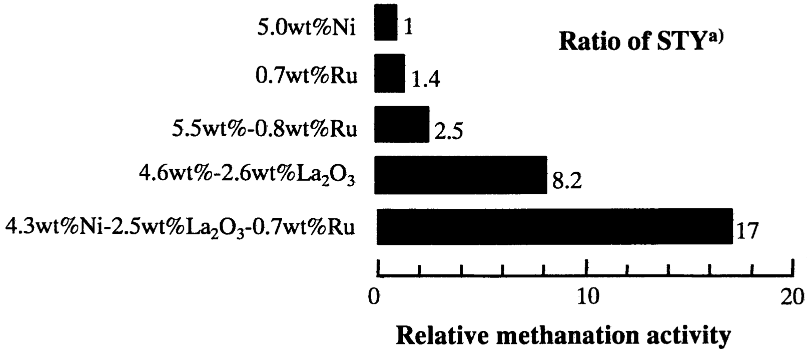

Figure 3. Activity of CO_2 methanation for the Ni-La_2O_3-Ru catalyst and catalysts of various combinations of the components a) Activity is expressed by the ratio of space-time yield (STY) of methane.
The activity ratio 1 is corresponds to methane STY 0.56 mol/l·h
Reaction conditions: 6mol% CO_2-18mol% H_2-76mol% N_2, Space velocity 10,000h^{-1}, Pressure 0.1 MPa, Temperature 500K.

In order to apply this catalyst to much higher space velocity of the reaction gas, the catalyst support and the reaction devises were investigated and increase in CO_2 methanation rate up to extraordinary high levels was observed (40). To reduce the resistance against high flow rates of reaction gases, Fiberflax (FF) of 1 mm thickness, produced by Toshiba Monoflax Co. LTD., was adopted as the catalysts support. The catalysts shaped in cross sheet was packed to the Pyrex glass tubular reactor of 10 mm inner diameter. The reaction gas composed of 12% CO_2, 88% H_2 was allowed to flow with the space velocities of 226,300 h^{-1} on the basis of the net catalyst volume eliminated the space of the super macro channel. When the SV was 226,300 h^{-1}, the CO_2 conversion reached as high as 96%, and at the very high

Downloaded by PENNSYLVANIA STATE UNIV on September 16, 2012 | http://pubs.acs.org
Publication Date: January 24, 2002 | doi: 10.1021/bk-2002-0809.ch009

SV 1,138,800 h^{-1} the CO_2 conversion at 723 K remained 67%, suggesting that the rate determined step was in the diffusion step. The corresponding space-time conversion of hydrogen was 15,390 mol/l·h.

Effective Methanol Synthesis by CO_2 Hydrogenation

In methanol synthesis by CO_2 hydrogenation, one oxygen remains in the objective product (methanol), therefore, it is regarded as the equivalent of the hydrocarbon synthesis from syngas, from the view point of energy balance. The demand of methanol is now increasing, and it would be possible to use as not only the fuel, for such as fuel cell, but also the alternative starting raw materials for the matured petrochemical industry, because methanol can be converted into a variety of important compounds. Methanol is now producing from syngas with large scale by using the Cu-Zn oxides-based precipitated catalysts. However, when the catalyst uses as it is to the CO_2 hydrogenation, the yield of methanol is much lower than that obtained from syngas conversion under the same temperature and pressure conditions. The equilibrium value for methanol synthesis from CO_2 is about one third, and moreover, below ca 520 K the yield of methanol hardly reaches to the equilibrium (41).

Recently, a number of papers concerned with methanol synthesis from CO_2-H_2 mixture have been presented, and the results were reviewed by Saito (42) and Halmann and Steinberg (44).

It is noteworthy that the world first demonstration pilot test-plant of a 50 kg/day methanol synthesis by CO_2 hydrogenation was achieved at the Research Institute of Innovative Technology for the Earth (RITE) in Kyoto, Japan (42, 44). The catalyst used was Cu-ZnO-based catalyst supported on alumina with modification of ZrO_2. A small concentration of silica addition prolonged catalyst life. The space-time yield of methanol around 600g/l·h was consistently obtained by circulating operation with 99.9% in selectivity for more than 8,000 h in the duration test under the conditions of 250℃ and 5MPa. The space-time yield of methanol obtained by the pilot plant at RITE is about several times of that obtained by the use of conventional methanol synthesis catalyst for syngas conversion. However, the author et al. developed much more highly active catalysts by introduction of new preparation method and concept for the working state as described below.

In our studies, Cu-Zn-Cr-Al mixed oxides catalyst was prepared by the uniform gelation method, in which the concentrated nitrate solution of the four components was changed into gel by the contact of NH_3 vapor, and followed by drying, thermal decomposition, calcination, and hydrogen reduction. As shown in Fig. 4 (45) the catalyst exhibited 50% higher activity for methanol synthesis from CO_2 than the catalyst which was prepared by the conventional precipitation method (46).

The methanol synthesis activity was markedly enhanced by the combination of La_2O_3 (41) and Pd or Ag (47). The reasons of those

Downloaded by PENNSYLVANIA STATE UNIV on September 16, 2012 | http://pubs.acs.org
Publication Date: January 24, 2002 | doi: 10.1021/bk-2002-0809.ch009

Downloaded by PENNSYLVANIA STATE UNIV on September 16, 2012 | http://pubs.acs.org
Publication Date: January 24, 2002 | doi: 10.1021/bk-2002-0809.ch009

Preparation and modification method	References	SV (h^{-1})	Pressure (atm)	Temp. (K)	Conversion to methanol (%)
Precipitation [a)]	(41)	4,700[d)]	50	523	7.3
Uniform gelation [a)]	(41)	4,700[d)]	50	523	10.5
Uniform gelation with Pd modification [a)]	(47)	4,700[d)]	50	523	21.2
Uniform gelation with La modification [a)]	(41)	4,700[d)]	80	523	28.5
Uniform gelation with Ga modification [b)]	(48)	18,800[e)]	80	543	12.8
Uniform gelation with Pd·Ga modification [b), c)]	(48)	18,800[e)]	80	563	25.1

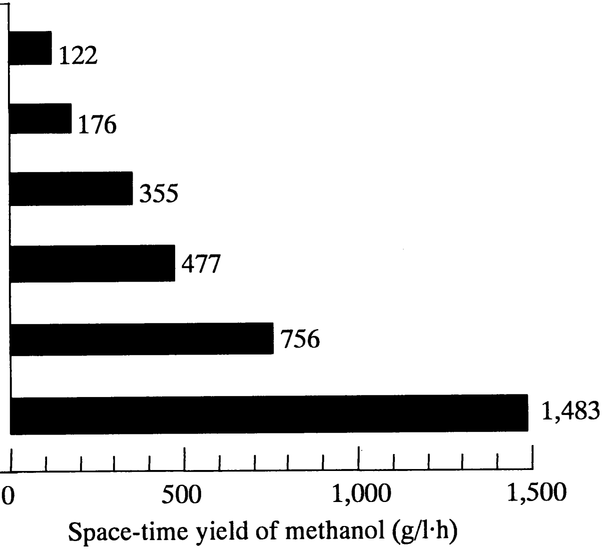

Figure 4. Methanol synthesis from CO_2 on catalysts with different composition and prepared by different method

a) CuO: ZnO: Cr_2O_3: Al_2O_3 = 25.0: 41.5: 1.2: 32.3 (wt%).

b) CuO: ZnO: Cr_2O_3: Al_2O_3 : Ca_2O_3 = 38.1: 29.4: 1.6: 13.1: 17.8 (wt%). c) Pd 1 wt%.

d) H_2/CO_2 = 75/25. e) H2: CO2: CO = 75: 22: 3.

improvements were considered as the weak basicity to increase of the adsorption capacity for acidic CO_2, and the effect of hydrogen spillover through the part of Pd or Ag, respectively. The hydrogen spillover gives an influence not only on the transportation rate of hydrogen as the reactant but also on the control of the reduction state of the catalyst surface during the reaction. In our more recent study (48), spillover effect with Pd and inverse-spillover effect with Ga, were then combined with an anticipation that the both effects could maintain with a good balance for the desired proper reduced state of the catalyst during the reaction giving the maximum methanol yield. The effect of Ga_2O_3 addition to the four component catalyst, by substituting Ga_2O_3 for Al_2O_3 was investigated. The addition of Ga_2O_3 markedly enhanced the methanol synthesis activity and retarded the CO formation, and a very high space-time yield (STY) of methanol, 1,483 g/l·h, was obtained at 563 K with a CO_2 conversion to methanol 25.1%. This value is as high as 12 times that of the catalyst prepared by conventional precipitation method.

It is noteworthy that the Pd-Ga-modified catalyst exhibited a very high activity for CO-rich syngas conversion. As shown in Table I, methanol STY in a CO-rich syngas can be obtained 4.4 and 4.8 times at 523 and 543K, respectively. Space velocity for CO-rich syngas could be increased two times as much as that for CO_2-rich syngas, without significant decrease in conversion (49). Space-time yield of methanol in the CO-rich syngas conversion on the catalyst is one order higher than that on conventional methanol synthesis catalysts.

Effective Alcohol Synthesis from CO_2-H_2 Mixture

Ethanol is produced industrially by hydration of ethylene using a phosphoric acid type catalyst with a space-time yield of ethanol below 0.2 kg/l·h. If ethanol could be directly produced by CO_2 hydrogenation with higher yield than the conventional method, it would have a potential as one of the alternative new route of ethanol synthesis. After the Oil Crisis, a number of studies on ethanol synthesis from syngas had been carried out. However, ethanol synthesis from CO_2 has not been studied extensively (50).

As compared in Fig. 5, Kusama et al. (51) and Fujiwara et. al. (52) observed fairly higher space-time yield of ethanol using Cu-Zn-Fe-K catalyst and Rh-Li-Fe/SiO_2 catalyst, respectively.

We have studied on the subject by our intrinsic principle for the catalyst design without use of expensive precious metals such as Rh, Ru, and Ir as the main catalyst component (45, 53). Iron-based composite catalyst (Cat. 1) for the role of carbon-carbon formation and Cu-Zn-based composite catalyst (Cat. 2) for the role of OH group formation were prepared by the uniform gelation method. The both were combined by various method with equivalent weight. As a result, 231 g/l·h ethanol was obtained (Fig. 5, third column from the top). Furthermore, the catalyst Rh/MFI-silicate (Cat. 3),

Downloaded by PENNSYLVANIA STATE UNIV on September 16, 2012 | http://pubs.acs.org
Publication Date: January 24, 2002 | doi: 10.1021/bk-2002-0809.ch009

Downloaded by PENNSYLVANIA STATE UNIV on September 16, 2012 | http://pubs.acs.org
Publication Date: January 24, 2002 | doi: 10.1021/bk-2002-0809.ch009

Table I. Methanol syntheses for both CO_2-rich and CO-rich syngas on the four-component composite catalyst

Reaction gas (%)	*SV (h^{-1})*	*Temp. (K)*	*Total Conv. (%)*		*Selectivity (C-mol %)*					*STY (g/l·h)*	
			CO_2	CO	MeOH	DME	HC	CO	CO_2	MeOH	MeOH + DME
22 % CO_2	18,000	523	22.3	---	19.2	---	0.1	3.0	---	1,230	---
3% CO											
75% H_2	18,000	543	26.1	---	22.0	---	0.2	3.9	---	1,410	---
30% CO	39,900	523	---	31.8	99.0	1.3	0.1	---	-0.4	5,380	5,430
3% CO_2											
7% H_2	39,900	543	---	41.1	95.8	4.1	0.4	---	-0.3	6,730	6,930

Catalyst: Cu: ZnO: Cr_2O_3: Al_2O_3: Ga_2O_3: Pd = 37.7: 29.1: 1.6: 13.0: 17.6: 1.0 (wt%)

Downloaded by PENNSYLVANIA STATE UNIV on September 16, 2012 | http://pubs.acs.org
Publication Date: January 24, 2002 | doi: 10.1021/bk-2002-0809.ch009

Catalyst	Ref.	SV ($x10^4h^{-1}$)	Pressure (atm)	Temp. (K)	Conv. of CO_2 (%)	Selectivity to EtOH (C-mol%)
Rh-Li-Fe/SiO_2	(51)		69	573	10.5	10.5
Cu-Zn-Fe-K	(52)		49	513-533	21.2	21.2
Fe-Cu-Zn-Al-K	(45)	2	80	583	28.5	28.5
(Rh/MFI-silicate)- (Fe-Cu-Zn-Al-K) packed in series	(53)	7	80	623	12.8	12.8
(Fe-Cu-Al-K) (Cu-Zn-Al-K·Ga·Pd) physically mixed	(53)	5	80	603	25.1	25.1

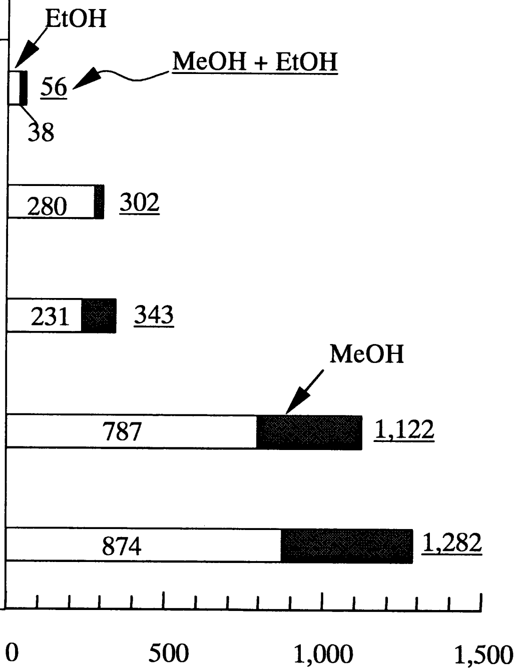

$H_2/CO_2 = 75/25$

Figure 5. Synthesis of ethanol from CO_2 on various catalysts

which has a function of partial reduction of CO_2 to CO, was combined with the iron-based catalyst (Cat. 1) in series, space-time yield of ethanol increased to 787 g/l·h. (Fig. 5, fourth column from the top). When the both catalysts used with physical mixing, space-time yield of ethanol was less than that of above mentioned case.

On the other hand, a physical mixture of a composite catalyst composed of Cu-Zn-Al-K-Ga-Pd, in which function of alcohol synthesis is promoted, with a composite catalyst composed of Fe-Cu-Al-K, exhibited space-time yield of ethanol 874 g/l·h (Fig. 5, the bottom column). In this case, the sum of methanol STY amount to 1,282 g/l·h and this volume is comparable to the maximum data of methanol synthesis mentioned above.

The reason for this difference can be understood by the comparison of temperature-programmed-reduction (TPR) profiles for Cat. 1 and Cats. (1+3). As is clearly compared in Fig. 6, the peak of the TPR profile for Cat. 1 is shifted to the 453 K lower side by the mixing with Cat. 3.

This change is attributed to the typical effect of hydrogen spillover through the Rh part as the porthole (24, 53). This indicates that, at the optimum reaction temperature for ethanol synthesis, 623 K, Fe component in Cat. 1 is reduced excessively and is far deviated from the optimum oxidation state for alcohol synthesis, as indicated in Fig. 6. Therefore, in this case, packing in series gives a better result.

In order to understand the inverse results shown in Fig. 5, TPR profiles for Cats. 1, 2, and (1+2) are compared in Fig. 7. Different from the case of Cats. (1+3) (Fig. 6), the profiles for Cats. (1+2) appeared in between the profiles for Cats. 1 and 2. The shift of the high temperature peak of Fe-based catalyst was fairly small, about 50 K, by the combination with Cu-based catalyst, and the peak for the mixed catalysts just fits into the optimum reaction temperature as indicated in Fig. 7. This indicates that the catalytic function of both catalysts can act favorably.

In the catalyst shown in the bottom column of Fig. 5, Pd and Ga were contained in the catalyst; however, these components have functions of spillover [41] and inverse spillover [48] of hydrogen, and as both functions were balanced, the basic property in the reduction could be regarded to be similar to that in Cat. 2.

Distribution of the alcohols formed on the three kinds of different catalyst is plotted in Fig. 8, and their SF plots are shown in Fig. 9. The catalysts used were the Fe-based catalyst (Cat. 1), a mixed catalyst of Fe-based and Cu-based catalyst, and Pd-Ga added Fe- and Cu-based catalyst. In every case, formation of ethanol was the largest among C_1 - C_6 alcohols formed, and ethanol formation increased with the use of catalysts in the order mentioned above. Especially, on the Pd-Ga combined catalyst, only ethanol formation deviated far from the SF plots and it was more than two times the value expected from the SF relation. As shown in the case of (c) in Figs. 8 and 9, only ethylene formation among C_2, C_3 hydrocarbons prominently decreased. This corresponds to the extraordinary high formation rate of

Downloaded by PENNSYLVANIA STATE UNIV on September 16, 2012 | http://pubs.acs.org
Publication Date: January 24, 2002 | doi: 10.1021/bk-2002-0809.ch009

Downloaded by PENNSYLVANIA STATE UNIV on September 16, 2012 | http://pubs.acs.org
Publication Date: January 24, 2002 | doi: 10.1021/bk-2002-0809.ch009

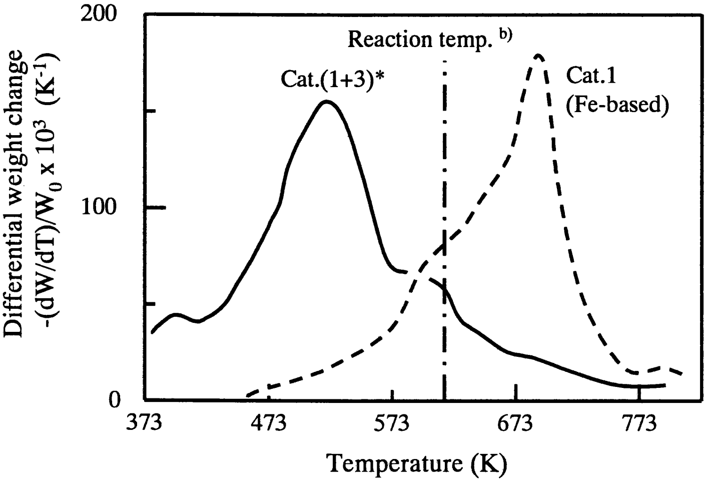

Figure 6. TPR profiles for Cat. 1 and Cats. (1+3)

5 mol% H_2 - 95 mol% N_2, 10 K min^{-1}; (a) physical mixing of the Rh catalyst (Cat. 3) with the Fe-based catalyst (Cat. 1); (b) optimum reaction temperature to give the maximum ethanol STY

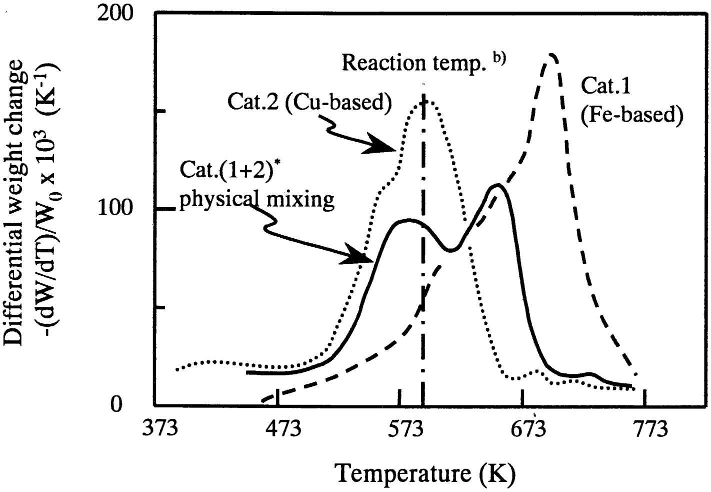

Figure 7. TPR profiles for Cats. 1, 2 and Cats. (1+2)

5 mol% H_2 - 95 mol% N_2, 10 K min^{-1} (a) physical mixing of the Cu-based catalyst with the Fe-based catalyst; (b) optimum reaction temperature to give the maximum ethanol STY.

Downloaded by PENNSYLVANIA STATE UNIV on September 16, 2012 | http://pubs.acs.org
Publication Date: January 24, 2002 | doi: 10.1021/bk-2002-0809.ch009

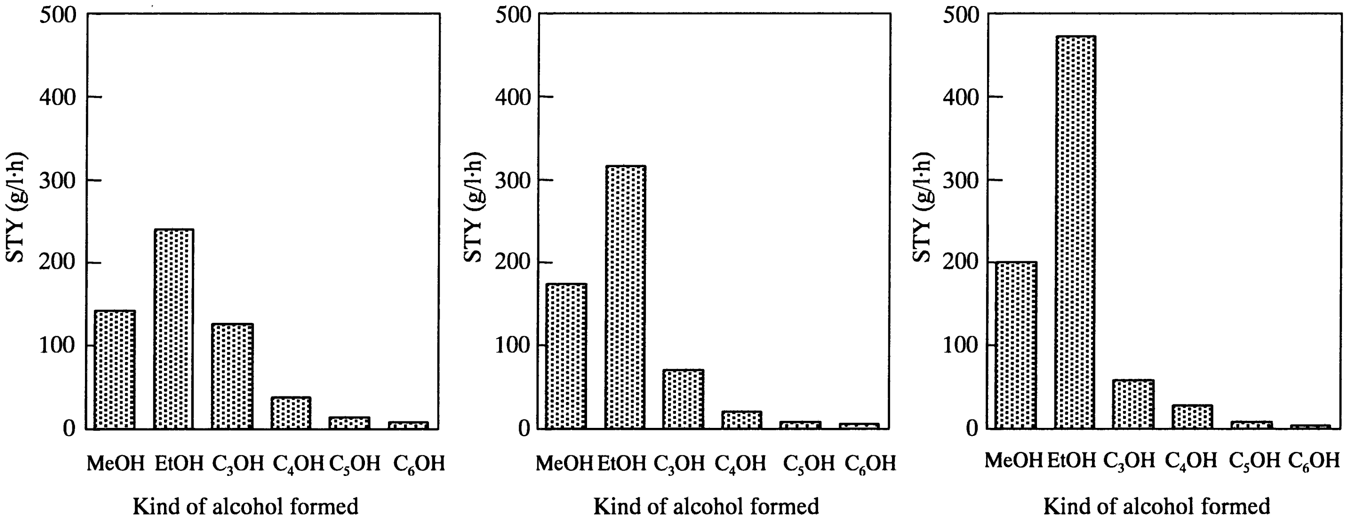

(a) Fe-based catalyst
Cat.1 Fe:Cu:Al:K = 1.0:0.03:2.0:0.7

(b) Physically mixed catalyst of Cat.1 and Cat.2 with an atomic ratio of Cu/Fe 0.53
Fe:Cu:Zn:Al:K=1.0:0.53:0.5:2.5:0.75

(c) Pd-Ga added physically mixed Fe-based (Cat. 2), Cu-based catalysts and 9.8 wt%Pd/1,060ºC calcined alumina with atomic ratios of Cu/Fe=0.53 and Pd/Fe=0.02
Fe:Cu:Zn:Al:K:Pd:Ga=1.0:0.53:0.5 : 2.75:0.75:0.02:0.16

Figure 8. Difference in alcohol distribution for different catalysts

Downloaded by PENNSYLVANIA STATE UNIV on September 16, 2012 | http://pubs.acs.org
Publication Date: January 24, 2002 | doi: 10.1021/bk-2002-0809.ch009

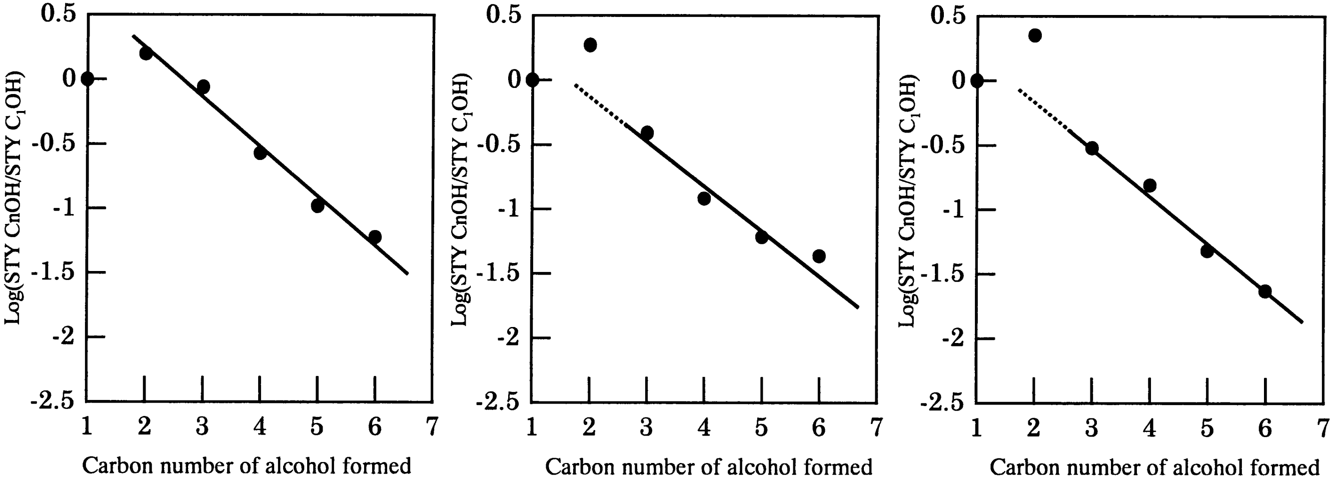

(a) Fe-based catalyst

(b) Physically mixed Fe-based and Cu-based catalysts

(c) Pd-Ga-combined Fe-based and Cu-based mixed catalyst

Figure 9. Schulz-Flory plots for the results shown in Fig. 8

ethanol, and it suggests that ethanol would be produced partly by hydration of ethylene in addition to the typical FT reactions.

Selective Synthesis of Light Olefins and Gasoline from CO_2-H_2 Mixture by One-pass Conversion via Methanol Synthesis

The classical Fischer-Tropsch synthesis catalysts such as Co-based and Fe-based catalysts produce a variety of hydrocarbons and oxygen-containing compounds, which obey the Schultz-Flory polymerization law, and when those kinds of catalyst use for CO_2 hydrogenation, only methane can be obtained exclusively, especially in higher CO_2 conversion levels. The zeolite ZSM-5 has been used for Mobil MTG process to produce aromatic-rich gasoline with light paraffinic hydrocarbons from methanol (54). When ZSM-5 is used for the conversion of methanol formed from syngas or CO_2-H_2 mixture, only a very little gasoline fraction is obtained (55). This is ascribed to the intrinsic property of H-ZSM-5, i.e. the strong hydrogen-shift function, and consequently intermediate olefins easily hydrogenated into light saturated hydrocarbons before oligomerized to gasoline range fraction.

Fujiwara and Souma et al. (56-59) presented results of their elaborated sequential studies on direct synthesis of hydrocarbons from CO_2 and H_2 mixtures. Their principle for CO_2 hydrogenation was the use of mixed catalyst prepared by mixing of Fischer•Tropsh-type catalysts or alcohol synthesis catalysts with HY-type zeolite. The feature of the products was light-olefin rich hydrocarbons, however, the reaction was operated at considerably low CO_2 conversion levels, and the space-time yields of hydrocarbons and their selectivities were not high enough.

Only the hydrogen inactive shape-selective microporous crystalline catalyst such as H-Fe-silicate having MFI structure and the similar MFI-type metallosilicate which has the hydrogen inverse-spillover function such as H-Ga-silicate (60) have a potential to produce gasoline fraction with a higher selectivity. For the selective olefin synthesis, the narrow pore microporous crystalline catalyst having weak acidity such as SAPO-34 (61) would be suitable, on which olefin oligomerization is prevented due to its weak acidity and ethylene and propylene could be obtained exclusively. The results are summarized in Fig.10 (8).

In case of the CO-rich syngas, methanol could be synthesized under rather moderate reaction conditions on the methanol synthesis catalyst. The methanol formed was totally converted in the 2nd-stage reactor packed with H-Fe-silicate at 573 K under atmospheric pressure to a gasoline fraction with 41.4% selectivity, and 1,170 g/l·h space-time yield. In stead of H-Fe-silicate, when H-Ga-silicate was used, gasoline fraction increased with a selectivity of 62.9% and STY of 1,860 g/l·h under the conditions of 593 K and 1.5 MPa. The contents of this gasoline fraction were mainly iso-mono-internal olefins, and other products in case of H-Fe-silicate still C_2 - C_4

Downloaded by PENNSYLVANIA STATE UNIV on September 16, 2012 | http://pubs.acs.org
Publication Date: January 24, 2002 | doi: 10.1021/bk-2002-0809.ch009

Downloaded by PENNSYLVANIA STATE UNIV on September 16, 2012 | http://pubs.acs.org
Publication Date: January 24, 2002 | doi: 10.1021/bk-2002-0809.ch009

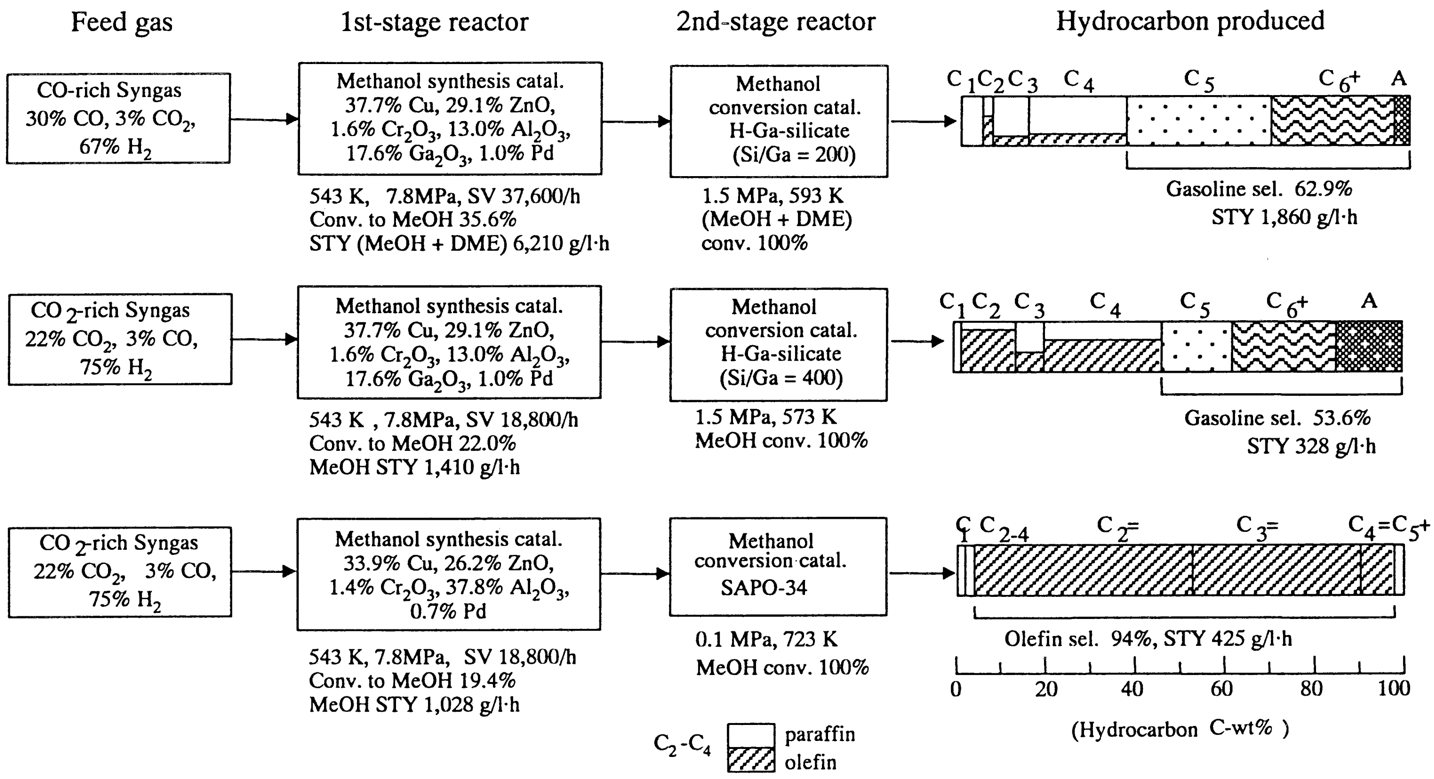
Feed gas
1st-stage reactor
2nd-stage reactor
Hydrocarbon produced
CO-rich Syngas
30% CO, 3% CO2,
67% H2
Methanol synthesis catal.
37.7% Cu, 29.1% ZnO,
1.6% Cr2O3, 13.0% Al2O3,
17.6% Ga2O3, 1.0% Pd
543 K, 7.8MPa, SV 37,600/h
Conv. to MeOH 35.6%
STY (MeOH + DME) 6,210 g/l·h
Methanol
conversion catal.
H-Ga-silicate
(Si/Ga = 200)
1.5 MPa, 593 K
(MeOH + DME)
conv. 100%
C1 C2 C3 C4 C5 C6+ A
Gasoline sel. 62.9%
STY 1,860 g/l·h
CO2-rich Syngas
22% CO2, 3% CO,
75% H2
Methanol synthesis catal.
37.7% Cu, 29.1% ZnO,
1.6% Cr2O3, 13.0% Al2O3,
17.6% Ga2O3, 1.0% Pd
543 K , 7.8MPa, SV 18,800/h
Conv. to MeOH 22.0%
MeOH STY 1,410 g/l·h
Methanol
conversion catal.
H-Ga-silicate
(Si/Ga = 400)
1.5 MPa, 573 K
MeOH conv. 100%
C1 C2 C3 C4 C5 C6+ A
Gasoline sel. 53.6%
STY 328 g/l·h
CO2-rich Syngas
22% CO2, 3% CO,
75% H2
Methanol synthesis catal.
33.9% Cu, 26.2% ZnO,
1.4% Cr2O3, 37.8% Al2O3,
0.7% Pd
543 K, 7.8MPa, SV 18,800/h
Conv. to MeOH 19.4%
MeOH STY 1,028 g/l·h
Methanol
conversion catal.
SAPO-34
0.1 MPa, 723 K
MeOH conv. 100%
C1 C2-4 C2= C3= C4=C5+
Olefin sel. 94%, STY 425 g/l·h
0 20 40 60 80 100
(Hydrocarbon C-wt%)
C2-C4
paraffin
olefin

Figure 10. Hydrocarbon synthesis from syngas having different contents of carbon oxides using two-stage series reactors packed with different types of catalysts.

olefins remained, which is markedly different from the results obtained by using H-ZSM-5.

Even in case of the CO_2-rich syngas, it is noteworthy that methanol formed in the first reactor transformed in similar way as the CO-rich syngas. As shown in Fig. 10, by selecting the kind of catalysts to be packed into the second reactor and corresponding reaction condition, gasoline or light olefins such as ethylene and propylene could be synthesized, respectively with considerably high selectivity and space time yields.

Downloaded by PENNSYLVANIA STATE UNIV on September 16, 2012 | http://pubs.acs.org
Publication Date: January 24, 2002 | doi: 10.1021/bk-2002-0809.ch009

Conclusion

The significance and the practical improvements in catalyst structure for the CO_2 hydrogenation to obtain the valuable compounds, such as methane, methanol, ethanol, ethylene, propylene, and gasoline were described. The rapid production of hydrogen or syngas by means of CO_2-reforming and/or steam reforming of natural gas must support realization of that CO_2-hydrogenation and the successive reactions. Especially, the development of new usage routes for huge amount methanol synthesized by CO_2 hydrogenation, and the rebuilding of a new paradigm for the use of waste heat come out from the large scale industries will be necessary to realize the new system for the CO_2 recycle.

Acknowledgement

The most part of data used in this paper is drawn from the studies done in Kyoto University before the author's retirement. I acknowledge all the co-authors appeared in the literatures cited.

The author also acknowledges all the publishing companies, who permit citation of the following Figures and Table in the author's papers for this review article. Reference numbers shown in below are the same as numbers shown in the Reference section in this paper. Figure 2 is drawn from Ref. 16 (John Wiley & Sons. Ltd.). Figure 3 is drawn from Ref. 24 (Elsevier Science). Figures 4 & 5 are drawn from Ref. 45 (Japan Petroleum Institute). Figures 6 - 9 are drawn from Ref. 53 (Elsevier Science). Figures 1 & 10 are drawn from Ref. 8 (Pergamon). Table I is drawn from Ref. 49 (VSP).

References

1. Seshan, K. and Lercher, J.A., in "Carbon Dioxide Chemistry: Environmental Issues," ed. Paul, J. and Prodier, C.-M., The Royal Soc. Chem., Cambridge, 1994, p.16-19.

2. Inui, T., in "Carbon Dioxide Chemistry: Environmental Issues," ed. Paul, J. and Prodier, C.-M., The Royal Soc. Chem., Cambridge, 1994, p.64-68.
3. Takayasu, O., Takegahara, Y., and Matsuura, I., *Energy Convers. Mgmt.*, 1995, *36*, 597.
4. Inui, T., Hara, H., Takeguchi, T., Ichino, K., Kim, J.B., Iwamoto, S., and Pu, S.B., *Energy Convers. Mgmt.*,1997, *38*, Suppl. S385.
5. Takayasu, O., Sato, F., Ota, K., Hitomi, T., Miyazaki, T., Osawa, T,, and Matsuura, I., *Energy Convers. Mgmt.,* 1997, *38*, Suppl., S391.
6. Park, S.E., Chang, S.E., Roh, H.S., Anpo, M., and Yamashita, H., *Stud. Surf. Sci. Catal.*, 1998, *114*, 395.
7. Aparicio, P.F., Baeza, B.B., Ruiz, A.G., and Ramos, I.R., *Stud. Surf. Sci., Catal.*, 1998, *114,* 399.
8. Inui, T., Green Gas Control Tech., ed. Riemer, P., Eliasson., B., and Wokaun, A., 1999, Pergamon, Amsterdam, p.331-336.
9. Schmitz, A.D. and Yoshida, T., Green Gas Control Tech., ed., Riemer, P., Eliasson., B., and Wokaun, A., 1999, Elsevier, Amsterdam, p.355-360.
10. Cheng, Z., Zhao, X., Liu, J., and Zhu, Q., Green Gas Control Tech., ed., Riemer, P., Eliasson., B., and Wokaun, A., 1999, Elsevier, Amsterdam, p.359-384.
11. Fox, J.M. III, *Catal. Rev.-Sci. Eng.*, 1993, *35(2)*, 169.
12. Rostrup-Nielsen, J.R., *Natural Gas Conv. II*, ed. Curry-Hyde and Howe, R.F., Elsevier, Amsterdam, 1994, p.25.
13. Ross, J.R.H., Van Keulen, A.N.J., Hegarty, M.E.S. and Seshan, K., *Catal Today,* 1996, *30*, 193 .
14. Halmann, M.M. and Steinberg, M., *Green Gas Carbon Dioxide Mitigation, Sci. Tech.*, Lewis Publishers, Boca Raton, 1999, p.315.
15. Bradford, M.C.J. and Vannice, M.A., *Catal. Rev. - Sci. Eng.*, 1999, *41(1)*, 1.
16. Inui, T., *J. Appl. Organomet. Chem.*, 2000, *14*, 1-8.
17. Tagawa, T., Ito, M., Goto, S., Preprints Fifth Intern. Confer. CO_2 Utilization, Karlsruhe, Sept. 1999, p.32. Full paper, *J. Appl. Organomet. Chem.* in press.
18. Inui, T., Preprints Symp. CO_2 Conversion and Utilization in Refinery and Chem. Process, ACS 219th Annual Meeting, San Francisco, 2000, p.113-117. Full paper ACS Symp. Series in press.
19. Song, C., ibid., p.159-163, Full paper, ACS Symp. Series, in press.
20. Choudhary, V.R., and Mamman, A.S., Uphade, B.S., and Babcolk, R.E., ibid., p.164-167, Full paper, ACS Symp. Series, in press.
21. Pan, W. and Song, C., ibid., p.168-171, Full paper, ACS Symp. Series in press.
22. Inui, T., Catalysis, 2001, 16, in press.
23. Inui, T., Miyamoto, Y., and Takegami, Y., *Stud. Surf. Sci. Catal.*, 1983, *17*, 181-190.

Downloaded by PENNSYLVANIA STATE UNIV on September 16, 2012 | http://pubs.acs.org
Publication Date: January 24, 2002 | doi: 10.1021/bk-2002-0809.ch009

24. Inui, T., *Stud. Surf. Sci. Catal.*, 1993, *77*, 17-26.
25. Inui, T., Saigo, K., Fujii, Y., and Fujioka, K., *Catal. Today*, 1995, *26*, 295-302.
26. Inui, T., Ichino, K., Matsuoka I., Takeguchi T., Iwamoto, S., Pu, S., and Nishimoto, S., Korean J. Chem. Eng., 1997, *14*, 441-444.
27. Sabatier, P., and Senderens, J.B., Hebd. Seances Acad. Sci. 1902, *134*, 514-516.
28. M. Greyson, Catalysis, 4, Emmett P.H. ed., Reinhold, New York, 1956, p.473-511.
29. Mills, G. A. and Steffgen, F.W., Catal. Rev., 1973, *8(2)*, 159-210.
30. Hegarty, W.P. and Moody, B.E., Chem. Eng. Progress, 1973, 69, 37-42.
31. Harth, R.E. and Baltendahl, U., Ind. Sci. Rev., 1981, 6, 221-228.
32. Halmann, M.H. and Steinberg, M., Greenhouse Gas carbon dioxide Mitigation, Lewis Publlishers, Boca.Taton, 1999, pp.334-343.
33. Baussart, H., Delobel, R. Le Bras, M., and Leroy, J.-M., J.C.s. Faraday Trans. I, 1987, 83, 1711-1718.
34. Trovarelli, A., De Leitenburg, C., and Dolcetti, G., J.C.S. Chem. Commun., 1991, 472-473.
35. Dziembay, R., Makowski, W., and Papp, H., J. Mol. Catl., 1992, 75, 81-99.
36. Tada, T., Habazaki, H., Akiyama, E., Kawashima, A., Asami, K., and Hashimoto, K., Mater. Sci. Eng., 1994, 182, 1133-1136.
37. Inui, T., Funabiki, M. Suehiro, M., and Sezume, T., J.C.S.. Faraday I, 1979, *75*, 787-802.
38. Inui, T., Encyclopedia of Catalysis, Horváth, I.T. ed, in press.
39. Inui, T., Funabiki, M., and Takegami, Y., I.E.C. Prod. Res. Dev., 1980, *19*, 385-388.
40. Inui, T., Catal. Today, 1996, *29*, 329-337.
41. Inui, T., Takeguchi, T., Kohama, A., and Tanida, K., Energy Convers. Mgmt., 1992, *33*, 513-520.
42. Saito, M., Fujitani, T., Takeuchi, M., and Watanabe, T., Appl. Catal. A: General, 1996, *138*, 311-318.
43. Halmann, M.H. and Steinberg, M., Greenhouse Gas Carbon dioxide Mitigation, Lewis Publishers, Boca Taton, 1999, pp. 344-355.
44. Ushikoshi, K., Mori, K., Watanabe, T., and Takeuchi, M., Stud. Surf. Sci. Catal., 1998, 114, 358-362.
45. Inui, T., Sekiyu Gakkaishi, 1997, *40*, 243-251.
46. Inui, T. and Takeguchi, T., Catal. Today, 1991, *10*, 95-106.
47. Inui, T., Takeguchi, T., Kohama, A. and Kitagawa K., Proc. 10th Intern. Congr. Catal., Guczi, L., Solymosi, F., and Tétényi. P. ed. Akadémiai Kiadó, Budapest, Hungary, 1993 Part B, pp. 1453-1466.
48. Inui, T., Hara, H., Takeguchi, T., and Kim, J., Catal. Today, 1997, *36*, 25-32.
49. Inui, T., Res. Chem. Intermed., 1998, *24*, 571-579.
50. Halmann, M.H. and Steinberg, M., Greenhouse Gas Carbon dioxide Mitigation, Lewis Publishers, Boca Taton, 1999, pp. 357-358.

Downloaded by PENNSYLVANIA STATE UNIV on September 16, 2012 | http://pubs.acs.org
Publication Date: January 24, 2002 | doi: 10.1021/bk-2002-0809.ch009

51. Kusama, H., Sayama, K., Okada, K., and Arakawa, H., Preprints 74th Annual Meeting Catalysis Soc. Jpn., 1994, p. 430.
52. Fujiwara, H. Okamoto, A., Takagawa, H., and Arakawa, H., Preprints 76th Annual Meeting Catalysis Soc. Jpn., 1995, p. 209.
53. Inui, T., Yamamoto, T., Inoue, M., Hara, H., Takeguchi, T., and Kim, J., Appl. Catal. A: General, 1999, *186*, 395-406.
54. Chang, C.D. and Silvestri, A.J., J. Catal., 1977, *47*, 249.
55. Inui, T., Kitagawa, K., Takeguchi, T., Hagiwara, T., and Makino, Y., Appl. Catal. A: General, 1993, *94*, 31-44.Inui,
56. Fujiwara, M., Kieffer, R., Ando, H., and Souma, Y., Appl. Catal. A. Gen., 1995, 121, 113-124.
57. Fujiwara, M., Ando, H., Tanaka, M., and Souma, Y., Appl. Catal. A. Gen., 1995, 130, 105-116.
58. Fujiwara, M., Ando, H., Matsumoto, M., Matsumura, Y., Tanaka, M., and Souma, M., Chem. Lett., 1995, pp.839-840.
59. Fujiwara, M., Kieffer, R., Ando, H., Xu, Q., and Souma, Y., Appl. Catal. A. Gen.. 1977, 154, 87-101.
60. Inui, T., Makino, T., Okazumi, F., Nagano, S., and Miyamoto, A., I.E.C. Res., 1987, *26*, 647-652.
61. Inui, T., Matsuda, H., Okaniwa, H., and Miyamoto, A., Appl. Catal., 1990, *58*, 155-163.

Downloaded by PENNSYLVANIA STATE UNIV on September 16, 2012 | http://pubs.acs.org
Publication Date: January 24, 2002 | doi: 10.1021/bk-2002-0809.ch009

Downloaded by NORTH CAROLINA STATE UNIV on September 16, 2012 | http://pubs.acs.org
Publication Date: January 24, 2002 | doi: 10.1021/bk-2002-0809.ch010

Chapter 10

Supported Copper and Manganese Catalyst for Methanol Synthesis from CO_2-Containing Syngas

K. Omata, G. Ishiguro, K. Ushizaki, and M. Yamada

Department of Applied Chemistry, Graduate School of Engineering, Tohoku University,
Aoba 07, Aramaki, Aoba-ku, Sendai 980–8579, Japan

Some supported copper and manganese oxide catalysts were found to show high activity for methanol synthesis from CO_2 containing syngas at 250°C, 10 atm, $H_2/CO/CO_2/N_2 = 60/30/5/5$. While copper and manganese oxide supported on Al_2O_3, SiO_2 and La_2O_3 showed low activity, those supported on ZrO_2 and TiO_2 showed higher activity. It was suggested that the spinel oxide of Cu/Mn=1/1 is formed on those supports to reveal the activity.

Methanol (MeOH) is one of the basic chemicals manufactured world-wide from synthesis gas (a mixture of $H_2/CO/CO_2$) in a large scale by using a Cu-Zn based oxide at 250-300°C and 50-100 atm (ICI process). In order to improve the catalysis (activity, selectivity or stability), the Cu-Zn is often modified with various metal oxides such as Zr, Cr, Ce, V, Ti, etc.. Among the additives, manganese is one of the promising promoters (*1-4*).

We reported the synergistic effect of Cu and Mn (*5*). The binary mixed oxide prepared by co-precipitation of mixed oxalate salts was found to show high activity for methanol synthesis from syngas at 250°C, 10 atm. The activity was highest when the Cu/Mn molar ratio was 1/1. Spinel type oxide was

In CO2 Conversion and Utilization; Song, C., et al.;
ACS Symposium Series; American Chemical Society: Washington, DC, 2002.

suggested to be related to the active site. Generally, we have two approaches to increase the activity of bulk oxide. One is to prepare the oxide from fine particle precursor to get high activity because of high surface area. The second one is to use high-surface-area support. If the catalysis of the oxide is not influenced by the support, an activity improvement can be expected if the oxide is synthesized on an appropriate support with high surface area. Perovskites are reported to show higher specific activity for oxidation (*6*).

This paper describes the latter approach. The role of spinel oxide in bulk catalyst and the activity of supported Cu-Mn catalyst is reported. An activity improvement can be expected if the spinel oxide is synthesized on an appropriate support with high surface area.

Experimental

Bulk catalysts were prepared by following procedure : metal nitrates in ethanol were mixed with oxalic acid/ethanol to precipitate oxalate salts. After centrifuging the precursor was dried and calcined. Cu-Mn oxide was also supported using impregnation method. Supports are listed in Table 1 with BET surface area which was measured by N_2 adsorption at –196°C. They were dried at 120°C and then impregnated in ethanol solution of nitrates. After removal of ethanol the precursor was calcined at 350°C. The content of Cu-Mn oxide were adjusted to form monolayer spinel oxide on the support. The weight of the unit lattice / the footprint is 4.67 mg-oxide / m^2.

Table I. List of Commercial Support.

Support (Surface Area (m^2/g))		Monolayer Loading (wt%)
AC(1651)	Shirasagi active carbon	66
Al_2O_3(321)	Nippon Ketjen	60
SiO_2(222)	Davison ID	51
TiO_2(51)	JRC-TIO-4	20
TiO_2(46)	JRC-TIO-3	18
ZrO_2(14)	JRC-ZRO-1	6.3
ZrO_2(5)	Wako	2.4
La_2O_3(8)	Wako	3.5

ZrO_2 and TiO_2 with high surface area are prepared according to scheme 1. Usually surface area of zirconium hydroxide decreases after calcination in air.

Downloaded by NORTH CAROLINA STATE UNIV on September 16, 2012 | http://pubs.acs.org
Publication Date: January 24, 2002 | doi: 10.1021/bk-2002-0809.ch010

But the addition of small amount of phosphoric acid disturbed the shrinkage (*7*). ZrO_2(81) was prepared by calcination of zirconium hydroxide ($Zr(OH)_4$(312)) at 450°C and 1 wt% phosphoric acid was supported on the $Zr(OH)_4$ followed by calcination at 450°C to prepare ZrO_2(214) (P). Almost same method was applied to prepare titania. As shown in scheme 1, titanium hydroxide was prepared from titanium alkoxide. Addition of silica or phosphoric acid was effective to get wide titania.

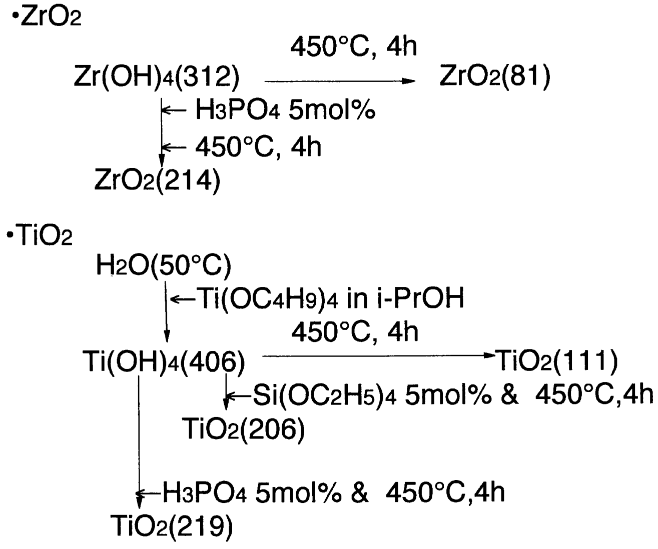
•ZrO2
450°C, 4h
Zr(OH)4(312)
ZrO2(81)
H3PO4 5mol%
450°C, 4h
ZrO2(214)
•TiO2
H2O(50°C)
Ti(OC4H9)4 in i-PrOH
450°C, 4h
Ti(OH)4(406)
TiO2(111)
Si(OC2H5)4 5mol% & 450°C,4h
TiO2(206)
H3PO4 5mol% & 450°C,4h
TiO2(219)

Scheme 1 Preparation of high surface area support.

Both type of catalysts (bulk and supported) were reduced and activated in the reaction gas. Activity tests were conducted in high pressure flow type fixed bed reactor or high-through-put reactor with which 12 catalysts can be tested parallelly (*5*). Reaction conditions were:10 atm, 250°C, $H_2/CO/CO_2/N_2$ = 60/30/5/5, W/F = 4gh/mol. Under this W/F, 1% COx conversion corresponds to STY 28 g-MeOHeq. /kg-cat/h. Product gas was analyzed by TCD and FID. Methanol was main product and small amount of dimethyl ether and methane were formed. Oxides were characterized by XRD (Rigaku CN-2125, Cu Kα, 40 kV-20 mA). Line broadening was corrected using CaF_2 single crystal powder. Copper surface area was determined by the technique of N_2O reactive

Downloaded by NORTH CAROLINA STATE UNIV on September 16, 2012 | http://pubs.acs.org
Publication Date: January 24, 2002 | doi: 10.1021/bk-2002-0809.ch010

chromatography. Estimation by Evans was used to calculate the surface area from N_2 formation (*8*).

Result and Discussion

Catalysis of Bulk Cu-Mn Oxide

Effect of Cu/Mn Ratio on Activity and Surface Area

As reported in the previous paper (*5*) the activity depends on the Cu/Mn ratio and synergy between Cu and Mn is observed as shown in Figure 1. Effect of copper content of bulk catalyst on the activity and the surface area are also shown. The surface area is not BET one but calculated from particle size by XRD, and copper metal area. When copper manganese ratio is 1 to 1, both activity and surface areas were highest. And activity per spinel-surface area or activity per copper metal area is almost same. This result strongly suggests that surface of spinel oxide is precursor of active site. So, if this spinel oxide spreads on high surface area support we can expect an active catalyst.

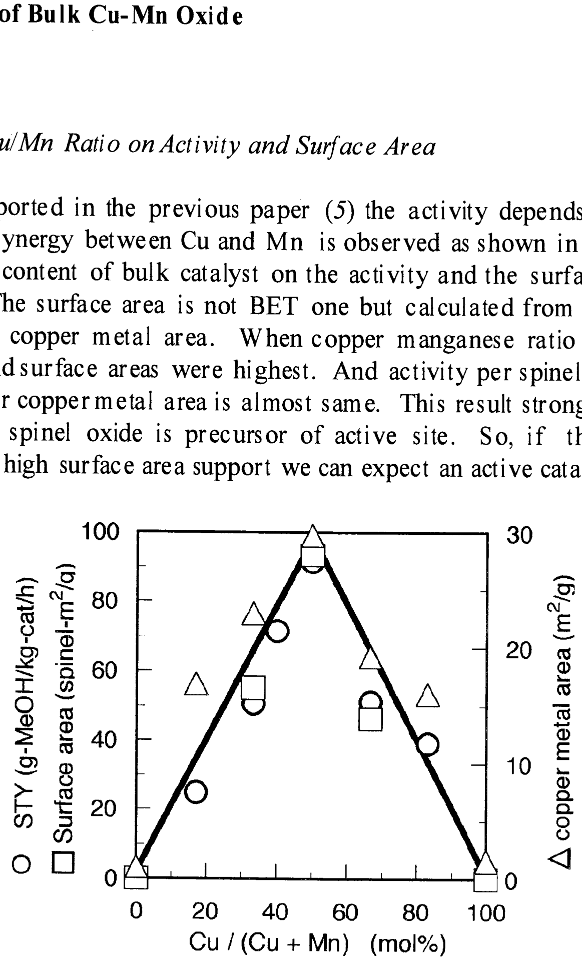

Figure 1. STY and surface area as a function of Cu content of Cu-Mn- Oxide.

Downloaded by NORTH CAROLINA STATE UNIV on September 16, 2012 | http://pubs.acs.org
Publication Date: January 24, 2002 | doi: 10.1021/bk-2002-0809.ch010

Effect of CO_2 on the Activity of Cu-Mn Oxide Bulk Catalyst

Isotopic tracer study of methanol formation from syngas has shown that, with Cu-Zn-Al catalyst, hydrogenation of CO_2 to methanol (eq. (1)) is predominant and that CO_2 is the main carbon source ofmethanol (*9*). By water-gas shift reaction between CO and water, produced as by-product of methanol synthesis from CO_2, regenerate CO_2 as shown in equation (2). The over-all reaction is apparently CO hydrogenation (eq. (3)) and the amount of CO_2 is unchanged during reaction. Therefore, activity of the Cu-Zn-Al catalyst for methanol synthesis from CO/H_2 is low and addition of CO_2 enhances the activity (*10*). The effect of CO_2, however, is sensitive to catalyst composition. For example activity of Cu/MgO decreases monotonously by addition of CO_2. It is concluded that only CO hydrogenation (eq. (3)) proceeds on Cu/MgO and CO is the main carbon source of methanol (*10*).

$$CO_2 + 3H_2 \rightarrow CH_3OH + H_2O \qquad (1)$$

$$CO + H_2O \rightarrow CO_2 + H_2 \qquad (2)$$

$$CO + 2H_2 \rightarrow CH_3OH \qquad (3)$$

As shown in Figure 2, activity of Cu-Mn-O for methanol synthesis from CO/H_2 is lower than that in Figure 1 from $CO/CO_2/H_2$. CO_2 enhances the activity of the oxide.

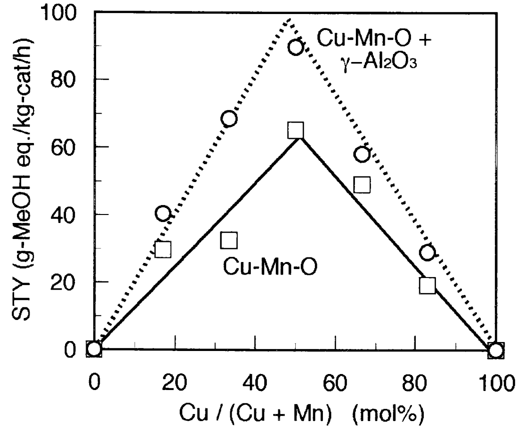

Figure 2. STY from CO/H_2 as a function of Cu Content of Cu-Mn Oxide.

In CO2 Conversion and Utilization; Song, C., et al.;
ACS Symposium Series; American Chemical Society: Washington, DC, 2002.

Downloaded by NORTH CAROLINA STATE UNIV on September 16, 2012 | http://pubs.acs.org
Publication Date: January 24, 2002 | doi: 10.1021/bk-2002-0809.ch010

On the other hand, Cu-Mn oxide was mixed with γ-alumina (1:1 by weight) and dimethyl ether was formed instead of methanol by the reaction (4).

$$2CH_3OH \rightarrow CH_3OCH_3 + H_2O \tag{4}$$

As shown in Figure 2, the activity was increased to the same level of methanol formation from $CO/CO_2/H_2$. The result suggests that water produced as by-product of reaction (4) is transformed quickly by water-gas shift reaction (eq.(2)) on the oxide and the produced CO_2 enhances the activity of Cu-Mn oxide. Like on Cu/Zn/Al catalyst, both reaction (1) and (2) proceeds on Cu-Mn oxide. Furthermore, activity of Cu-Mn oxide for methanol synthesis is proportional to Cu^0 area as shown in Figure 1, i.e., Cu^0 is active site of Cu-Mn oxide. It was reported that the active site for CO_2 hydrogenation is Cu^0 and that both Cu^0 and Cu^+ are necessary for CO hydrogenation (11). From these points of view, it can be concluded that hydrogenation of CO_2 is predominant on Cu-Mn oxide catalyst for methanol synthesis from syngas containing CO_2.

Downloaded by NORTH CAROLINA STATE UNIV on September 16, 2012 | http://pubs.acs.org
Publication Date: January 24, 2002 | doi: 10.1021/bk-2002-0809.ch010

Catalysis of Supported Cu-Mn Oxide

The activity of bulk catalyst prepared from oxalate salts was over 90g-MeOH /kg-cat/h as shown in Figure 3. The advantage of oxalate-ethanol method is clearly shown over nitrate method. The other activity than that of bulk oxide was calculated based on the loaded oxide weight. From this result zirconia and titania are good candidates. But unfortunately the surface area are not so high, so, the activity based on total weight is not good. High surface area for zirconia or titania is required.

Preparation of ZrO_2 and TiO_2 with High Surface Area

ZrO_2 with high surface area was prepared from zirconium hydroxide with the addition of small amount of phosphoric acid (*7*). In the case of titania, similar technique was available. After titanium hydroxide was first prepared from titanium alkoxide, the conditions for the hydrolysis was also optimized. The standard procedure is as follows: water was added at 55°C into 10mol% titanium butoxide in i-propanol to hydrolyze the butoxide. After centrifuge the precursor was calcined at 450 °C. As a result $TiO_2(111)$ was prepared.

As shown in Figure 4, while solvent for the butoxide, concentration of the butoxide and temperature for hydrolysis hardly influence on the surface of the

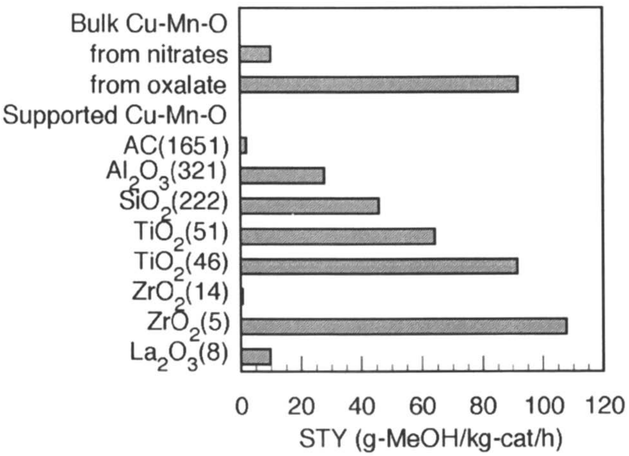

Figure 3 Activity of Cu-Mn-oxide on commercial support.

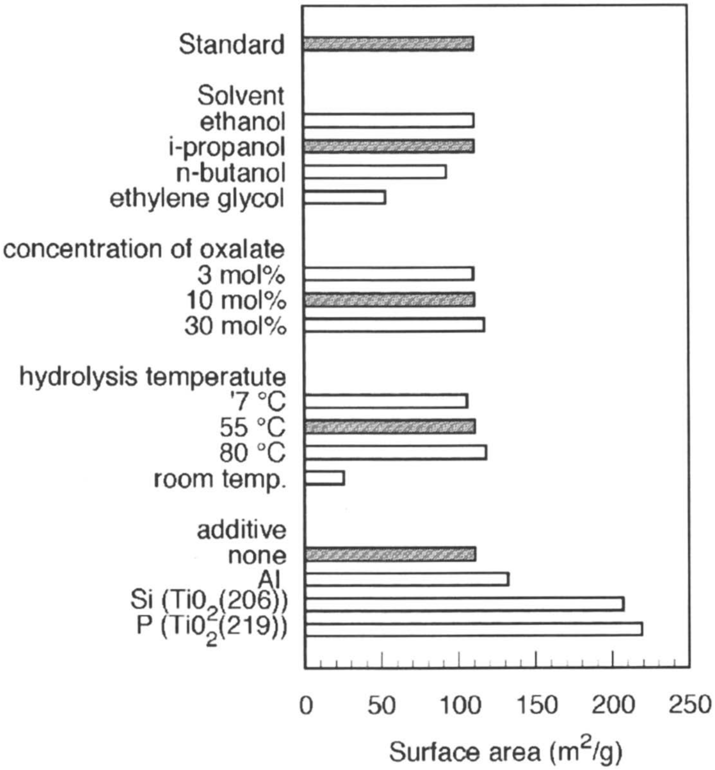

Figure 4. Preparation of TiO_2 support.

Downloaded by NORTH CAROLINA STATE UNIV on September 16, 2012 | http://pubs.acs.org
Publication Date: January 24, 2002 | doi: 10.1021/bk-2002-0809.ch010

resulting oxide, addition of Si or P gives good result. Thus TiO_2(206) and TiO_2(219) were prepared, respectively.

Catalysts of Cu-Mn-O / ZrO_2

In contradistinction to the activity of the bulk catalyst normalized by weight of Cu-Mn oxide, TiO_2 and ZrO_2 supported catalysts show good results as in Figure 3. Hereafter, the catalytic feature of ZrO_2 supported one was investigated. Figure 5 shows the effect of oxide content on ZrO_2(214) and ZrO_2 (81). The activity of the catalysts is almost same and increases in proportion to the oxide content under 30wt% which corresponds to the monolayer content of spinel on ZrO_2(81) support. Above 30wt% the activity of Cu-Mn oxide on ZrO_2 (214) increases on a proportional basis while that on ZrO_2(81) levels off. The result suggests that spinel oxide spreads in single-layer on the ZrO_2 surface until the whole surface is covered.

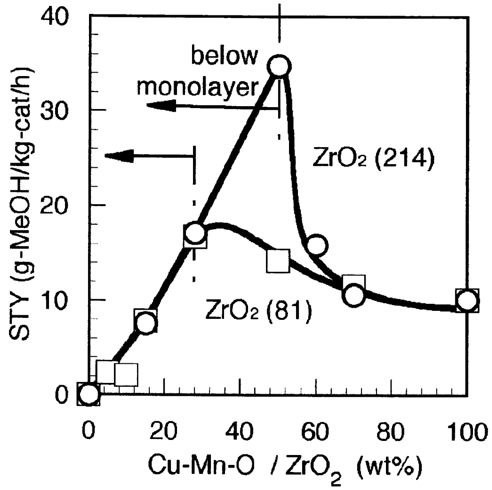

Figure 5. Effect of Cu-Mn-O loading on ZrO_2.

From XRD of the supported catalyst (Figure 6) no spinel oxide is found on zirconia and only copper oxide was observed. The result suggests that copper was sintered at high loading while manganese oxide was amorphous. Effect of Cu/Mn ratio was investigated on ZrO_2(214) which contains the same molar amount of Cu and/or Mn oxide with 50wt% Cu/Mn=1/1 oxide. Similar synergy is observed as shown in Figure 7 on the supported Cu-Mn oxide as the bulk Cu-Mn oxide and the activity shows maximum at Cu/Mn=1/1. The result strongly suggests that synergy between Cu and Mn appears on ZrO_2(214).

Downloaded by NORTH CAROLINA STATE UNIV on September 16, 2012 | http://pubs.acs.org
Publication Date: January 24, 2002 | doi: 10.1021/bk-2002-0809.ch010

Downloaded by NORTH CAROLINA STATE UNIV on September 16, 2012 | http://pubs.acs.org
Publication Date: January 24, 2002 | doi: 10.1021/bk-2002-0809.ch010

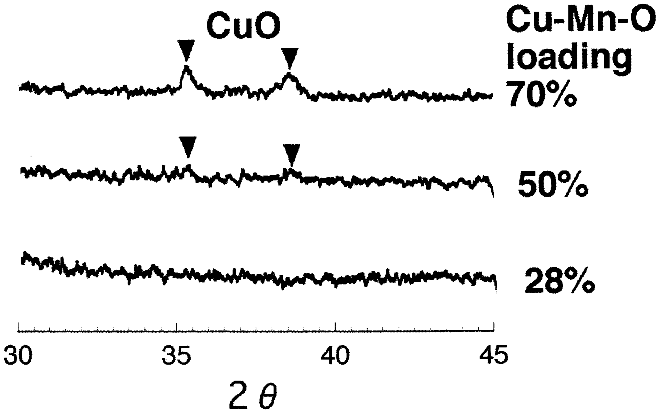

Figure 6. XRD of Cu-Mn-O on ZrO_2(214).

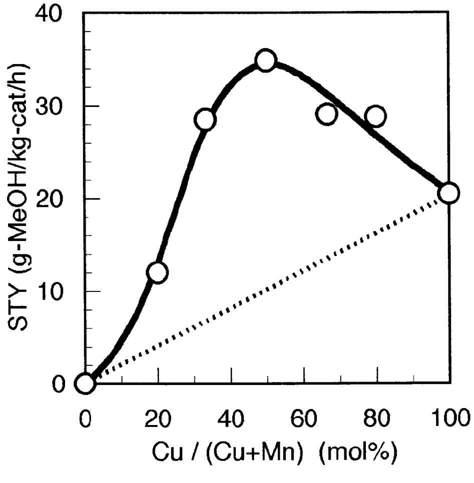

Figure 7. Cu-Mn synergy on ZrO_2(214).

Catalysts of Cu-Mn-O / TiO_2

On titania,synergy of copper and manganese was also observed. But the highest activity was achieved at Cu/Mn ratio 2 to 1 as shown in Figure 8.

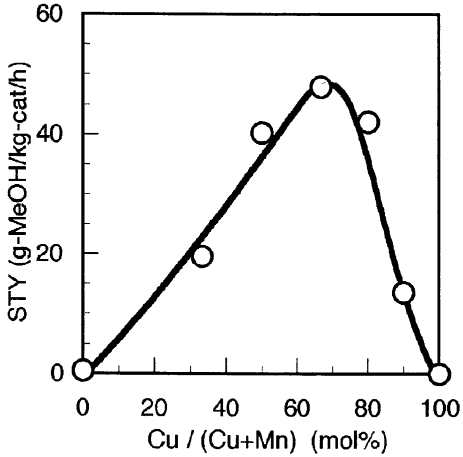

Figure 8. Cu-Mn synergy on TiO_2(219).

In the case of titania, XRD gave much information as shown in Figure 9. Titania is anatase type and all the particle size of TiO_2 was same after oxides were supported as shown above in Figure 10. The particle size was also same as calculated from BET surface area (72Å). This result suggests that most of titania is in anatase form without amorphous one. Other species was CuO. Intensity of CuO is low at low loading and increases above the monolayer loading rapidly while BET surface area decreases as shown below in Figure 10. Large particle of copper oxide may retard the reaction and decrease the activity.

The behavior of the activity of Cu-Mn-O/TiO_2(219) was almost same as on zirconia as shown in Figure 11. The activity increased with the amount of loading and it was highest at monolayer loading. From observation on XRD we can imagine what happened on these supports. When the activity as a function of oxide content is overlapped we can see that below monolayer loading the activity was almost same. But above it, the activity on zirconia decreases rapidly with increasing the oxide loading. Average particle size from BET surface of titania (72 Å) is almost two times larger than that of zirconia(48 Å). So plugging by CuO was serious problem for zirconia. Maybe this is because the low activity of zirconia at around these loading.

Downloaded by NORTH CAROLINA STATE UNIV on September 16, 2012 | http://pubs.acs.org
Publication Date: January 24, 2002 | doi: 10.1021/bk-2002-0809.ch010

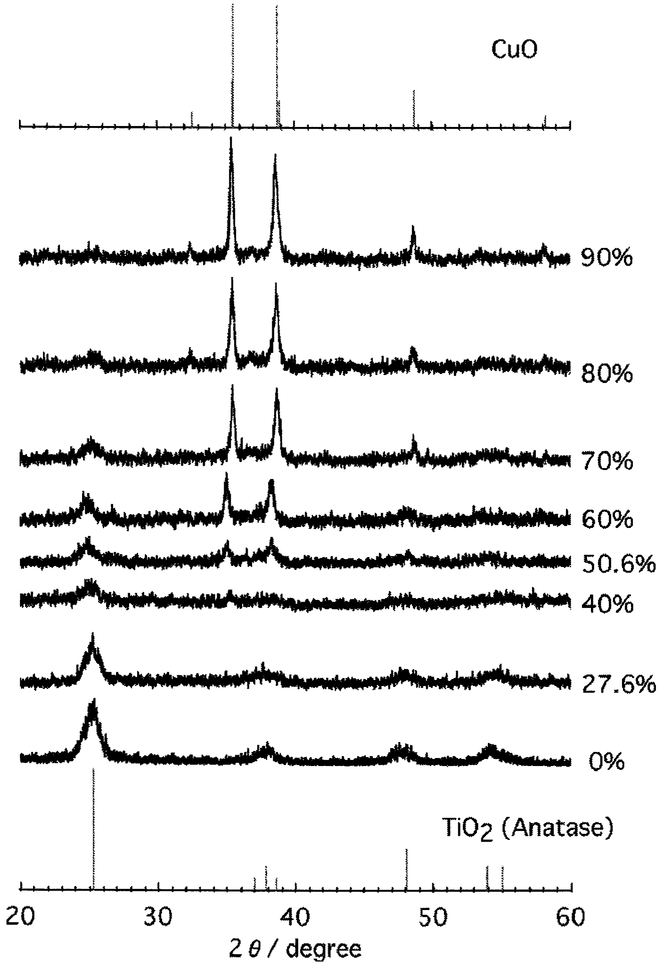

Figure 9. XRD of Cu-Mn-O on TiO_2(219).

Downloaded by NORTH CAROLINA STATE UNIV on September 16, 2012 | http://pubs.acs.org
Publication Date: January 24, 2002 | doi: 10.1021/bk-2002-0809.ch010

Downloaded by NORTH CAROLINA STATE UNIV on September 16, 2012 | http://pubs.acs.org
Publication Date: January 24, 2002 | doi: 10.1021/bk-2002-0809.ch010

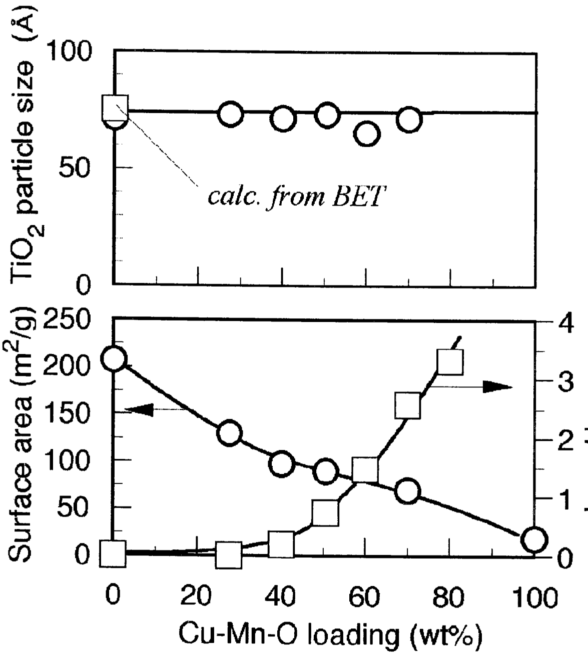

Figure 10. Effect of Cu-Mn-O loading on TiO_2(219).

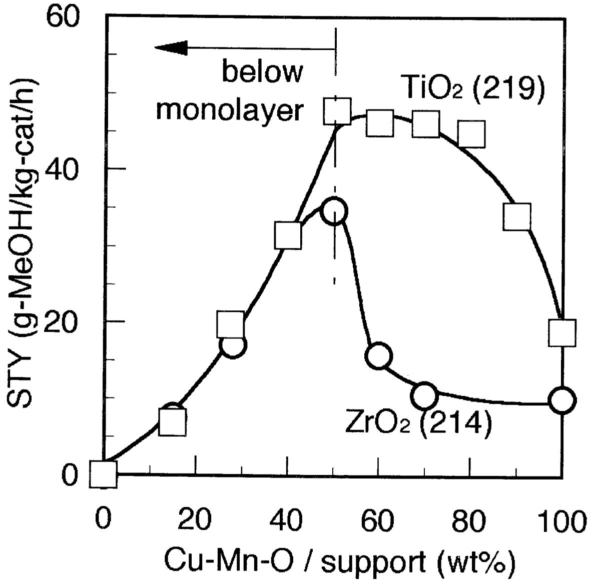

Figure 11. Comparison Cu-Mn-O loading effect.

Conclusion

Some supported copper and manganese oxide catalysts were found to show high activity for methanol synthesis from CO_2 containing syngas at 250°C, 10 atm, $H_2/CO/CO_2/N_2$ = 60/30/5/5. While copper and manganese oxide supported on Al_2O_3, SiO_2 and La_2O_3 showed lower activity than bulk spinel type oxide of copper and manganese prepared by co-precipitation of mixed oxalate salts, those supported on ZrO_2 and TiO_2 showed high activity. The activity was improved on ZrO_2 and TiO_2 with higher surface area.

Acknowledgement

This work was supported in part by Research for the Future Program of Japan Society for the Promotion of Science under the Project "Synthesis of Ecological High Quality of Transportation Fuels" (JSPS-RFTF98P01001) .

References

1. Audibert E. ; Raineau A. *Ind. Eng. Chem.*, **1929**, *20*, 880-885.
2. Li J.-L. ; Takeguchi T. ; Inui T. *Appl. Catal. A:General*, **1996**, *139*, 97-106.
3. Li J. ; Gao L. ; Zhang W. ; Lin J. ; Chen H. Y.; Tan K. L. *Chinese Sci. Bull.*, **1997**, *42*, 1100-1103.
4. Brown Bourzutschky J. A.; Homs N. ; Bell A. T. J. Catal., **1990**, *124*, 52-72.
5. Omata K. ; Ishiguro G.; Yamada M. *Sekiyu Gakkaishi*, **2000**, *43*, 317-319.
6. Mizuno N.; Fujii H.; Igarashi H. ; Misono M. *J. Am. Chem. Soc.*, **1992**, *114*, 7151-7151.
7. Tomishige K.; Ikeda Y.; Sakaihori T.; Fujimoto K. *J. Catal.*, **2000**, *192*, 355-362.
8. Evans J. W.; Wainwright M.S.; Bridgewater A.J. ; Young D.J. *Appl. Catal.*, **1983**, *7*, 75-83.
9. Kinnaird S. ;Webb G. ; Chinchen G.C. *J. Chem. Soc., Faraday Trans 1* , **1987**, 3399-3413.
10. Denise B. ; Cherifi O.; Bettahar M.M. ; Sneeden R.P.A. *Appl. Catal.*, **1989**, *48*, 365-372.
11. Brown Bourzutschky J. A.; Homs N. ; Bell A. T. J. Catal., **1990**, *124*, 73-85.

Downloaded by NORTH CAROLINA STATE UNIV on September 16, 2012 | http://pubs.acs.org
Publication Date: January 24, 2002 | doi: 10.1021/bk-2002-0809.ch010

Downloaded by STANFORD UNIV GREEN LIBR on September 16, 2012 | http://pubs.acs.org
Publication Date: January 24, 2002 | doi: 10.1021/bk-2002-0809.ch011

Chapter 11

Catalytic Reduction of CO_2 into Liquid Fuels: Simulating Reactions under Geologic Formation Conditions

D. Mahajan[1], C. Song[2], and A. W. Scaroni[2]

[1]Energy Sciences & Technology Department, Brookhaven National Laboratory, Building 815, Upton, NY 11973-5000
[2]Department of Energy and Geo-Environmental Engineering and the Energy Institute, Pennsylvania State University, University Park, PA 16802

In this paper, we describe two approaches that consider CO_2 recycle via utilization as a viable option to sequester carbon in CO_2. First, we summarize the results of our study of the integration of CO_2 capture with subsequent catalytic CO_2 hydrogenation to methanol for application to stationary CO_2-emitting sources. We carried out room temperature CO_2 solubility studies in amines and glycol solvents that are normally used to separate CO_2 from flue gas in power plants. In polyethylene glycol (Peg-400), the solubility data obey Henry's Law up to 4.5 MPa whereas in triethanolamine (TEA), the solubility is dominated by facile formation of the TEA.CO_2 adduct at CO_2 partial pressure as low as 0.33 MPa. Preliminary results on catalyst design and evaluation to affect the CO_2/H_2 reaction show that in these solvents, several transition metals are effective under mild conditions ($T < 150^\circ C$ and $P < 5$ MPa) for methanol synthesis though rates and product selectivity need further improvement. Second, we address the H_2-cost issue that implicates geologic formations as natural slurry reactors for CO_2 hydrogenation into liquid fuels wherein the needed H_2 is produced from H_2O by naturally occurring transition metals in these formations. A catalytic reaction then reduces the buried CO_2 into H_2-rich fuels. Successful development of the latter approach might close the natural carbon cycle in fossil fuels.

In CO2 Conversion and Utilization; Song, C., et al.;
ACS Symposium Series; American Chemical Society: Washington, DC, 2002.

Background

Carbon management with respect to CO_2 will define utilization of fossil fuels in the twenty-first century. A fundamental issue that will ultimately affect the implementation of any CO_2 sequestration technology is its cost. Several options to sequester CO_2 are described in the DOE technology roadmap entitled "Carbon Sequestration: State of the Science" (*1*). These options can be divided into two broad categories. These are: 1) CO_2 burial and 2) CO_2 recycle. The CO_2 burial category includes ocean sequestration, depleted oil and gas reservoirs, abandoned coal mines and deep geological formations. Of these, recovery of stranded CH_4 (by displacement with injected CO_2) from coal mines has the benefit of offsetting some of the overall cost of carbon sequestration. For the subterranean CO_2 sequestration options, the prohibitive cost remains an issue. Moreover, there is a growing concern about the long-term ecological impact of introducing large amounts of CO_2 in these formations. The second category involves use of CO_2 as a feedstock for making commodity products. This remediation option is attractive for its potential commercial value. One such preferred option involves recycling carbon in CO_2 by converting it in to H_2-rich synthetic fuels. Various aspects of thermal and photochemical activation of CO_2 by metal complexes have been studied (*2,3*). A significant amount of work has been carried out with variations of Fe catalysts for synthesis of hydrocarbons (Equation 1) via the Fischer-Tropsch (F-T) route (*4,5*), modified Cu-ZnO catalysts for methanol synthesis (Equation 2) or further conversion of methanol to gasoline (MTG) (*6*) with heterogeneous metal catalysts.

$$p\,CO_2 + q\,H_2 \rightarrow (\text{-}CH_2\text{-})_n + y\,H_2O + z\,CO_2 \qquad (1)$$

$$n\,CO_2 + (2n+1)\,H_2 \rightarrow C_nH_{2n+1}OH + n\,H_2O \qquad (2)$$

These energy intensive transformations utilize heterogeneous catalysts that operate between 250°C to 400°C. It is to be noted that any CO_2 transformation to H_2-rich fuels is highly endothermic (CO_2 is the thermodynamically stable product generated via combustion of fossil fuels). But it is the coproduction of H_2O that makes the overall reaction involving CO_2 feedstock (for example reactions (1) and (2)) exothermic. Thus, the production of large-volume fuels, namely hydrocarbons and alcohols (specifically methanol), is attractive in the overall CO_2 sequestration scheme but the cost of the required H_2 remains a key issue.

In this paper, we describe two research themes that relate to CO_2 conversion into liquid fuels. The first theme emphasizes integration of CO_2 capture with subsequent catalytic hydrogenation of CO_2 to methanol, a molecule that can be used as a building block for fuels and chemicals. Here, the key challenge was to develop a highly efficient catalyst that operates in an amine or glycol solvent

Downloaded by STANFORD UNIV GREEN LIBR on September 16, 2012 | http://pubs.acs.org
Publication Date: January 24, 2002 | doi: 10.1021/bk-2002-0809.ch011

that is normally used to separate CO_2 from the CO_2-emitting source. We, therefore, carried out CO_2 solubility studies in amines and glycol solvents. We also present here preliminary results on catalyst design and evaluation to affect the CO_2/H_2 reaction in these solvents under mild conditions of temperature and pressure. The second theme then outlines a concept to address the H_2-cost issue that implicates CO_2 reduction in geologic formations. The approach is to consider geologic formations as natural slurry reactors for CO_2 hydrogenation into liquid fuels wherein the needed H_2 is produced from H_2O by a natural phenomenon in the formations. A concomitant decrease in CO_2 concentration is achieved by catalytic reduction of the buried CO_2 into H_2-rich fuels.

Downloaded by STANFORD UNIV GREEN LIBR on September 16, 2012 | http://pubs.acs.org
Publication Date: January 24, 2002 | doi: 10.1021/bk-2002-0809.ch011

Experimental

Batch Unit

A commercially available AE Zipperclave stirred batch unit was modified at BNL and used in these studies. The unit consisted of a 0.55 L pressure vessel and was fitted with a dispersimax six-blade impeller, a removable metal ring, inserted into the vessel to break up any vortices, that might form during stirring. The unit had the following provisions: 1) heating/cooling through a Parr temperature controller and 2) several inlet and outlet ports for sampling of gases and liquids. The maximum working pressure and temperature were 20 MPa at 350°C. A dual channel Omega chart recorder was attached to the unit to monitor any change in temperature and pressure during a reaction.

Solubility Studies

In a typical run, a solvent of desired composition was purged with argon, loaded into the reactor and the reactor was sealed. CO_2 was slowly introduced in the reactor at room temperature over the liquid through one of the ports until the desired pressure was attained. The gas inlet valve was closed and the vessel was allowed to stabilize for one minute. The solution was stirred and the pressure drop was measured. Typically, the pressure drop was constant within ten seconds. The solubility data were then computed.

Catalyst Evaluation Studies

In a typical run, the selected metal catalyst, any additive, and solvent were loaded into the pressure vessel. The vessel was pressurized with feed gas containing CO_2 and H_2, heated to a desired temperature, and the pressure drop was followed as a function of time on the chart recorder. Gas and liquid samples were taken at the start, during and after the run. All samples were analyzed on gas chromatographs. For colored solutions, UV/VIS spectra were recorded on Perkin-Elmer Lambda 4B spectrophotometer

An Integrated Approach to Catalytic CO_2 Hydrogenation

Figure 1 outlines a general scheme for aquifer/ocean sequestration of CO_2. The steps involved are: 1) CO_2 is captured by using amines (typically mono or diethanolamines) or glycols in an exothermic reaction, 2) the captured CO_2 is released in a stripper by heating up to 150°C (an endothermic step) and the solvent recycled, and 3) free CO_2 is delivered via pipeline to a chosen site for deep burial. In the overall CO_2 sequestration scheme, the CO_2-capture step is the most energy-intensive step and accounts for up to 70% of the total sequestration cost (*1*). We propose to address the cost issue by integrating the CO_2-capture step with subsequent catalytic hydrogenation of CO_2 to methanol. The integrated scheme is shown in Figure 2. In this scheme, the stripper is replaced with a catalytic reactor wherein the heat is utilized to catalyze CO_2 hydrogenation to methanol. Note that H_2 needed for the reaction is assumed to be generated by direct CH_4 decomposition (C and $2H_2$) or from biomass (non-CO_2 sources). Our approach to develop an integrated system includes the following essential elements:

- Utilize amine, sodium or potassium carbonate or glycol solvents.
- H_2O is invariably produced as a byproduct during CO_2 transformations (Equations 1 and 2). Therefore, include H_2O as a cosolvent.
- Limit reaction temperature for catalytic CO_2 hydrogenation to <150°C.

The challenge then is to design a catalyst system for CO_2 hydrogenation that operates in a basic/ aqueous medium at low temperatures. Related to this, we have carried out preliminary work on two aspects. These are: 1) CO_2 solubility studies and 2) catalyst design for methanol synthesis.

CO_2 Solubility Studies

Solubility of gases is an important parameter in catalytic reactions that involve two-phase (gas/liquid) mixing. It is desirable to increase the solubility of gases in the solvent that may enhance reaction rates. We, therefore, undertook the solubility study to select a suitable solvent for the catalytic reaction.

Downloaded by STANFORD UNIV GREEN LIBR on September 16, 2012 | http://pubs.acs.org
Publication Date: January 24, 2002 | doi: 10.1021/bk-2002-0809.ch011

Downloaded by STANFORD UNIV GREEN LIBR on September 16, 2012 | http://pubs.acs.org
Publication Date: January 24, 2002 | doi: 10.1021/bk-2002-0809.ch011

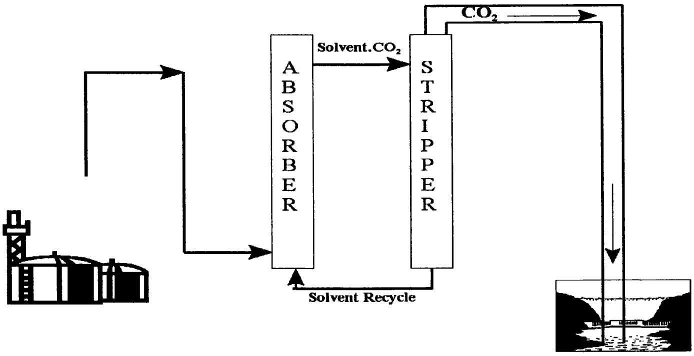
ABSORBER
Solvent.CO_2
STRIPPER
CO_2
Solvent Recycle

Figure 1. A general scheme for aquifer/ocean sequestration of CO_2.

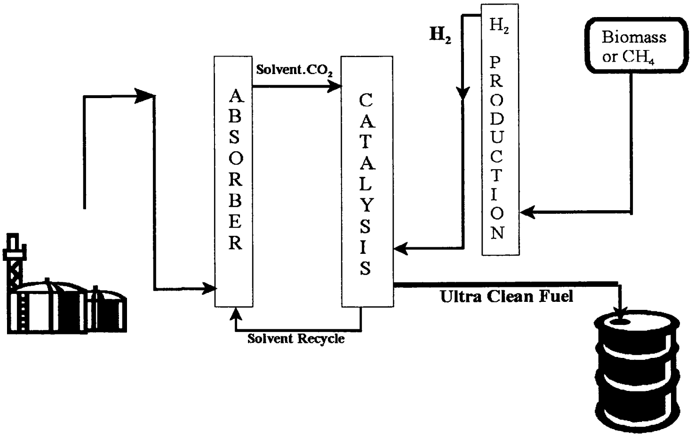
ABSORBER
Solvent.CO_2
CATALYSIS
H_2
H_2 PRODUCTION
Biomass or CH_4
Ultra Clean Fuel
Solvent Recycle

Figure 2. A proposed integrated system for the production of ultra clean fuels from CO_2.

Downloaded by STANFORD UNIV GREEN LIBR on September 16, 2012 | http://pubs.acs.org
Publication Date: January 24, 2002 | doi: 10.1021/bk-2002-0809.ch011

Aqueous solutions of alkanolamines, sodium or potassium carbonates, and glycols are commercially used to recover CO_2 from flue gases of power plants for various applications including the soft-drink bottling industry (*7*). With alkanolamines, the reaction is a simple adduct formation:

$$\text{AA} + CO_2 \Leftrightarrow \text{AA.}CO_2 + \Delta \qquad \text{(AA=alkanolamines)} \qquad (3)$$

The forward room temperature reaction involving the AA.CO_2 adduct formation is pressure dependent (0.1-1.0 MPa) and the reverse reaction is temperature dependent (80-150°C). Commercially, monoethanolamine (MEA) and diethanolamine (DEA) are amines of choice. These amines chemically react with CO_2 in a 1/0.5 mol ratio at ambient pressure via Reaction 4. For sterically hindered amines, reaction with H_2O increases the CO_2/amine ratio to 1/1 (Reaction 5).

$$2\,R\text{-}NH_2 + CO_2 \Leftrightarrow RNH_3^+ + R\text{-}NHCOO^- \qquad (4)$$

$$R\text{-}NH_2 + CO_2 + H_2O \Leftrightarrow RNH_3^+ + HCO_3^- \qquad (5)$$

For monoethanolamine (MEA), diethanolamine (DEA) and triethanolamine (TEA), the ease of adduct formation follows the order: MEA > DEA > TEA. Though both MEA and DEA operate at ambient pressure, the presence of terminal H is likely to make these amines more susceptible to degradation during the proposed catalytic CO_2 hydrogenation reaction. We, therefore, measured CO_2 solubility in TEA and polyethylene glycol (Peg-400) at room temperature as a function of pressure over a range of 0.3 to 5.2 MPa and these data are shown in Table I. For reference, the measured value in H_2O is also

Table I. CO_2 Solubility Data[1] in Various Solvents

Run	*Solvent*	*H_2O*	*Peq, MPa*	*χ_g*
1	--	100%	5.0	0.01
2	50% Peg-400	50%	5.13	0.11
3	50% TEA	50%	4.0	0.25
4	40% TEA	60%	0.33	0.78
5	40% TEA	60%	0.90	0.77
6	40% TEA	60%	1.69	0.75
7	40% TEA	60%	2.65	0.63

[1] 0.5 L AE Zipperclave batch unit; T=room temperature. Peg: polyethyleneglycol, TEA: triethanolamine.

Downloaded by STANFORD UNIV GREEN LIBR on September 16, 2012 | http://pubs.acs.org
Publication Date: January 24, 2002 | doi: 10.1021/bk-2002-0809.ch011

listed in Table I. It is known that the CO_3^{2-}/HCO_3^- equilibrium controls the CO_2 solubility in H_2O. The solubility in 40%TEA/60H_2O was measured as a function of CO_2 pressure. The notable observations from the TEA/H_2O/CO_2 system study at room temperature are: 1) the white TEA.CO_2 adduct forms readily with fast reaction rates ($t_{1/2}$ <1 min), 2) the adduct formation is ~ 80% complete even at ~0.3 MPa, and 3) this adduct readily dissociates if the gas-phase CO_2 is released. In the three solvents evaluated, the CO_2 solubility order is: TEOA > Peg-400 > H_2O.

The solubility data in Peg-400 as a function of pressure (0.4 – 4.5 MPa) were also collected at room temperature. Henry's Law holds in this solvent because unlike TEA, there is no chemical interaction (Figure 3). From the data in Figure 3, Henry's constant (H) was calculated to be 9.4 MPa.

For our proposed catalytic studies (vide infra), CO_2 solubility data as a function of temperature (25-150°C) and pressure (0.1-0.5 MPa) are needed. The measured data in Table 1 and Figure 3 can be used to extrapolate solubility values at higher temperatures in various solvents by literature methods (*8*).

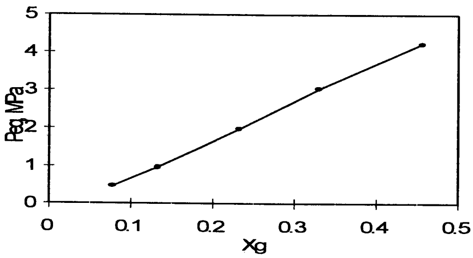

Figure 3. Equilibrium pressure-gas mol fraction isotherm for CO_2 solubility in Peg-400 at room temperature.

Specifically in water, the correlation for solubility as a function of temperature is based on the following equation (*9*):

$$\log xwt = A + B/T + C \log T + DT \qquad (6)$$

where xwt is weight fraction solubility of gases in water at 1 atm, T is absolute temperature, and A, B, C, and D are regression coefficients for CO_2. The corresponding correlation for Henry's Law constant (H) can be calculated:

$$\log H = A + B/T + C \log T + DT \qquad (7)$$

Methanol Synthesis Catalyst Design Considerations

It is known that catalytic hydrogenation of CO_2 produces several products (*10,11*). The products include formic acid, formaldehyde, CO, methanol, methane, higher alcohols and hydrocarbons that are thermodynamically related:

$$CO_2 \rightarrow CO \rightarrow HCOOH \rightarrow ROH \rightarrow RH \qquad (8)$$

We considered the following catalyst systems as the basis for our catalyst design.

- The homogeneous hydrogenation of CO_2 to formic acid can be catalyzed by [(dppp)Rh(hfacac)] (dppp is a bisphosphine ligand and hfacac is hexafluoroacetylacetonate) in dimethylsulfoxide solvent in the presence of triethylamine at 23°C and 40 atm pressure of CO_2/H_2 (1/1). The rate-determining step in the catalytic cycle appears to be the liberation of formic acid (*12*).
- One of the most active homogeneous catalyst systems for formic acid synthesis comprises of Ru-phosphine complexes in supercritical CO_2 solvent. At 50°C and 205 atm, turnover frequency (TOF) of 1400 h^{-1} has been reported (*13*). For comparison with the same catalyst in THF, the TOF is 80 h^{-1}.
- The $Ru_3(CO)_{12}/KI$ homogeneous catalyst system in N-methyl-2-pyrrolidone (NMP) solvent yields a mixture of CO, CH_3OH, and CH_4 at 240°C and under 8 MPa of CO_2/ H_2 (1/3) (*14*).
- Electrochemical reduction of CO_2 to CO catalyzed by Pd complexes has been reported (*15*).
- Photochemical reduction of CO_2 to formate catalyzed by metal complexes has been reported (*16*). The process uses a Ru^{2+} complex to capture sunlight and affect this transformation via electron relay, but the drawback is the consumption of expensive electron donor additives that are added to make the overall process catalytic.

The representative catalyst systems and the corresponding product selectivity are shown in Table II. It is clear that poor selectivity, low productivity, severe reaction conditions or other system limitations make these catalysts commercially unattractive. We specifically focused on developing catalysts that allow homogeneous liquid phase synthesis of methanol from CO_2:

Downloaded by STANFORD UNIV GREEN LIBR on September 16, 2012 | http://pubs.acs.org
Publication Date: January 24, 2002 | doi: 10.1021/bk-2002-0809.ch011

Downloaded by STANFORD UNIV GREEN LIBR on September 16, 2012 | http://pubs.acs.org
Publication Date: January 24, 2002 | doi: 10.1021/bk-2002-0809.ch011

Table II. Liquid Phase Catalytic Hydrogenation of CO_2/CO[1]

Catalyst	*Mode*	*Feedgas*			*Solvent*	*T*	*P*	*Product*	*Reference*
		%CO_2	*%CO*	*%H_2*		*°C*	*MPa*		
Lurgi	Slurry	50	-	50	Oil	260	5	CH_3OH > 99%	6
(dppp)Rh-(hfacac)	Homogeneous	50	-	50	DMSO/ Et_3N	23	4	HCOOH > 99%	13
Ru(acac)$_3$	Homogeneous	-	60	40	THF	270	130	CH_3OH > 80%	2
Ru(acac)$_3$	Slurry	-	60	40	THF	270	20	HC > 90%	2
NiL$_x$/KOR	Homogeneous	-	34	66	MeOH/ Glyme	120	2	CH_3OH > 99%	17
Fe/KOR	Highly dispersed slurry	9	25	66	E-164/ Peg-400	250	3	C_1-C_4-OH > 90%	25

[1] 0.5L AE Zipplerclave Reactor dppp = bis(diphenylphosphino)propane; hfacac = hexafluoroacetylacetonate; HC = hydrocarbons; L = Ligand; KOR = potassium alkoxide; E-flo-164 = C_{30} hydrocarbon solvent; Peg: polyethyleneglycol.

$$CO_2 + 3\,H_2 \rightarrow CH_3OH + H_2O \quad \Delta H^\circ_{298} = -\,52.8\ \text{kJ.mol}^{-1} \qquad (9)$$

Our approach to CO_2 hydrogenation is based on the liquid phase low temperature (LPLT) concept that was specifically developed at BNL to design enhanced carbon utilization catalyst for syngas conversion into methanol (*17*).

$$CO + 2\,H_2 \rightarrow CH_3OH \quad \Delta H^\circ_{298} = -\,128.6\ \text{kJ.mol}^{-1} \qquad (10)$$

With CO_2 as the reactant, the challenge was to initiate the water-gas-shift (WGS) reaction that can be combined with Reaction (10) to yield methanol. Since carbonyls of Mo, Co, Cu, Pt, Ru are known WGS catalysts, we conducted a preliminary screening study with these complexes to assess their ability to reduce CO to methanol. Peg-400/base or TEA itself provided the basic medium in these runs. The data are shown in Table III. Runs conducted in the batch unit with initial syngas (CO/H_2) charge of 5 MPa showed that except for Co, all other metal carbonyls evaluated consumed syngas. The gas consumption rate was 2 mmol/min at 130°C with Cu and 0.7 mmol/min at 150°C with Mo. The gas chromatographic analysis indicated that methanol was indeed formed in all these runs. Further work is underway to select the best metal that will yield high methanol selectivity under mild conditions of temperature (< 150°C) and pressure (< 5 MPa).

Table III. Catalytic hydrogenation screening runs[1]

Catalyst	*T, °C*	*Gas Consumed ,mmol*	*Rate, mmol/min*
$Cu(OMe)_2$	130	230	1.2
K_2PtCl_6	150	190	2.0
$Co_2(CO)_8$	130	--	0
$Ru_3(CO)_{12}$	160	185	1.2
$Mo(CO)_6$	150	201	0.7

[1] 0.5 L AE Zipperclave batch unit; catalyst: 1 mmol; Base: Potassium methoxide = 100 mmol; solvent: TEA or Glycol = 120 mL; Syngas: $H_2/CO \sim 2$; $P_I = 5$ MPa at room temperature.

Geologic Formations: The Ultimate Slurry Reactor for Catalytic CO_2 Reduction

In the previous section, we described the results of our laboratory study to develop a highly efficient catalyst for methanol synthesis via CO_2 hydrogenation

Downloaded by STANFORD UNIV GREEN LIBR on September 16, 2012 | http://pubs.acs.org
Publication Date: January 24, 2002 | doi: 10.1021/bk-2002-0809.ch011

that operates in an amine or a glycol solvent. Successful development of this novel system has the potential of lowering the cost of CO_2 sequestration by integrating the CO_2 capture and utilization aspects but the cost of H_2 remains an issue. Our aim is to design a highly effective catalyst for CO_2 hydrogenation in the laboratory and apply these results to ultimately conduct CO_2 reduction in geologic formations. Therefore, we envision geologic formations as slurry reactors to produce H_2 from H_2O that is subsequently utilized to hydrogenate CO_2 in these formations. We have based this approach on what is known about temperature and pressure conditions that exist in oil and gas reservoirs. We discuss below the basis of such an approach and the consequence of utilizing this pathway to recycle CO_2 by its conversion into fuels.

Downloaded by STANFORD UNIV GREEN LIBR on September 16, 2012 | http://pubs.acs.org
Publication Date: January 24, 2002 | doi: 10.1021/bk-2002-0809.ch011

Basis for the Proposed Approach

Oil and gas reservoirs have broad geographic distribution in the U.S. The porous and permeable reservoir rocks in oil and gas reservoirs include limestone, dolomite, and sandstone. The cap rock and basement rock which have a far lower permeability than the reservoir rock act as a seal to prevent the escape of oil and gas from the reservoir rock. Typical cap rock and basement rocks are clays and shale, that is, strata in which pores are much finer than those of reservoir rocks. The impermeable cap rock usually consists of shales that are clay minerals. The type of oil and gas reservoir depends on the boundary structure between the reservoir rocks and the cap rock. Many oil and gas accumulations (reservoirs) are trapped in either anticlines or salt domes.

The major metal elements found in reservoir rocks are Na, Ca and Mg. There are many other metal elements that occur in low concentrations in the rocks, including transition metals such as Fe, Ni, Mo, Pd. In essence, any element that has been identified in seawater can be found in the reservoir rocks.

Oil and gas reservoirs typically contain H_2O. The water may occur as wetting films around the sand grains as well as in some completely filled pores. The water in most oil and gas reservoirs is heavily salted and different in terms of detailed composition, but is generally neutral with a pH close to 7, as in most eastern reservoirs in the U.S. (*18*).

The temperature and pressure gradients of the earth vary regionally and vertically. The global average geothermal gradient is about 22°C/km, but ranges from as low as 10°C in old shield areas to as much as 50°C/km in active zones of sea floor spreading (*19*). Geothermal gradients in sedimentary basins generally range from 15-50°C/km; the average may be taken to be 30°C/km (*20*). The pressure gradients range from 0.434 psi for fresh water, 0.465 psi per foot for "standard" water containing 100 parts per thousand of dissolved solids, and 0.50-0.55 psi per foot for strong brines. The geostatic pressure depends on the bulk wet densities of the rocks including their fluids. The higher end of the overburden pressure gradient is 1 psi per foot (*21*). The estimated geologic conditions of many oil and gas reservoirs in Pennsylvania range from 1.1 to 5.7 miles in depth, 16°C to 150°C in temperature, and 17 to 86 MPa pressure.

The role of the sedimentary sulfur cycle in the diagenesis of organic matter is of wide interest. The sulfur content in crude oils varies from < 0.05 to 14 wt%. The subject has been reviewed in a recent book (*22*).

The foregoing discussion sets the stage for the proposed concept. The essential elements of a catalytic system that can convert the sequestered CO_2 into liquid fuels in geological formations are as follows:

- The cap rock and basement rock, which have a far lower permeability than the reservoir rock act as a seal to prevent the escape of fluids from the reservoir rock and can be viewed as a large natural reactor vessel.
- The reservoir rock must possess fluid-holding capacity (porosity) and fluid transmitting capacity (permeability). Transition metals such as Fe, Ni, Mo, Pd, that are normally found, though at ppm or ppb concentrations, in the reservoir rocks can be viewed as highly dispersed supported heterogeneous catalysts.
- The presence of oil and H_2O can be viewed as the available reaction solvents. H_2O will also serve as a natural source of H_2.
- The decreased concentration of O_2 as a function of depth provides a natural reducing atmosphere for the proposed consecutive reduction reactions, i.e. reduction of H_2O to H_2 followed by CO_2/H_2 conversion to H_2-rich fuels.
- At the reservoir depth of interest, the temperature and pressure range from: T: 16-150°C and P: 17-86 MPa.
- Sulfur could be implicated as a catalyst in the formation of hydrocarbons.

Some direct supporting evidence for the catalytic effects of certain metals in naturally occurring rocks and the feasibility of H_2 production from water by the action of transition metal species can be found in several recent papers (*23,24*). In these studies, it was shown during a one-year experiment that carbonaceous rocks (Monterey Formation, California, Eocene) that were low maturity and organic- rich (composition: 14 wt% total organic C, 7.5 wt% S, 350 ppm Ni and 560 ppm V) produced CH_4 from n-octadecene-1 and H_2 at 190°C. The reaction is believed to proceed via the hydrogenolysis of the C_{18} unsaturated hydrocarbon to CH_4 at a rate of ~10^{-7}g CH_4/g. rock/d. The addition of H_2O, up to ~ 2.5 wt%,

Downloaded by STANFORD UNIV GREEN LIBR on September 16, 2012 | http://pubs.acs.org
Publication Date: January 24, 2002 | doi: 10.1021/bk-2002-0809.ch011

appeared to increase both catalytic activity and product selectivity. It remains to be established the nature of the catalytically active species for H_2 production from H_2O, which is a key issue in the proposed CO_2 reduction scheme.

Effort at BNL AND PSU

The proposed concept integrates CO_2 sequestration with subsequent conversion in geologic formations. Catalytic activation of small gas molecules, namely CH_4, CO, CO_2 and H_2 that are major constituents of coal or natural gas-derived synthesis gas is a subject of ongoing efforts both at BNL and PSU (*25,26*). The new concept in the proposed research seeks to constitute a new and catalytic path for CO_2 conversion into reduced and useful products such as hydrocarbon fuels that only uses naturally available geothermal energy in oil and gas reservoirs following CO_2 sequestration in such geologic formations.

$$H_2O \rightarrow H_2 + (O)_{\mathrm{surroundings}} \qquad (11)$$

In Reaction 1, the O from H_2O is stabilized by naturally occurring materials in the surroundings. The produced H_2 then catalytically reacts with CO_2 to produce reduced products (according to Reactions (1) and (2)) that can be recovered after prolonged storage in geologic formations. The initial challenge is to demonstrate the reaction sequence for CO_2 to liquid fuels in micro pressure vessels under simulated geologic formation conditions in the laboratory. For this study, two Ni-rich natural rock samples, Niccolite (Ni_xAs_y) and Pentlandite $(Fe, Ni)_9S_8$, have been procured and their characterization is underway at the BNL National Synchrotron Light Source (BNL/NSLS). Runs are planned with these natural rocks in a micro-reactor to demonstrate: 1) catalytic production of H_2 from H_2O and 2) catalytic hydrogenation of CO_2 under the pressure and temperature conditions that are relevant to oil and gas reservoirs. The focus is on the feasibility of the production of liquid fuels from buried CO_2 under natural reservoir conditions. We then plan to utilize these laboratory data and design a system to selectively enhance the desirable reactions by adding trace amounts, in a vapor or a liquid form, to the "natural reactor" i.e., a selected geologic formation site. The proposed concept of seeding the geologic formation site with a highly active catalyst to enhance the H_2O to H_2 production and the subsequent CO_2/H_2 reaction to produce energy liquids closes the natural carbon cycle in fossil fuels. Interestingly, the concept is an alternative to "seeding the ocean with Fe to increase the growth of phytoplankton to enhance the CO_2 uptake.

Finally, it should be mentioned that there may be other undesirable reactions or more desirable reactions in geologic formations in addition to what

Downloaded by STANFORD UNIV GREEN LIBR on September 16, 2012 | http://pubs.acs.org
Publication Date: January 24, 2002 | doi: 10.1021/bk-2002-0809.ch011

we have considered; a number of issues need to be clarified, and many fundamental questions remain to be answered by further study.

Concluding Remarks

The production of H_2-rich synthetic fuels by catalytically recycling carbon in CO_2 is an attractive CO_2 sequestration option. In this paper, the CO_2-capture step that typically utilizes an amine or glycol solvent is integrated with subsequent catalytic hydrogenation of CO_2 to methanol. The challenge is to design a highly active catalyst that can produce methanol from CO_2/H_2 in basic medium under mild operating conditions. In the CO_2/H_2 system, CO_2 is first reduced to CO via the reverse water-gas-shift reaction. Preliminary data are presented for several metal catalysts that show activity for CO reduction. Further work is underway to select the best metal catalyst that will yield high methanol selectivity under mild conditions of temperature (< 150°C) and pressure (< 5 MPa).

Future work will extend these laboratory studies to address a key issue of H_2 cost in the overall scheme of CO_2 sequestration via CO_2 hydrogenation. Here, we envision geologic formations, specifically abandoned oil and gas reservoirs, as heated slurry reactors under pressure to catalytically produce H_2 from H_2O that is subsequently utilized to catalytically hydrogenate CO_2 in these formations. Knowledge gained from the laboratory studies will allow selection of active catalyst(s) that could be added to the formations to hasten reaction kinetics. This approach, if successful, holds an enormous potential for carbon sequestration.

Acknowledgments

We thank Dr. Arun C. Bose of the US Department of Energy (US DOE) National Energy Technology Laboratory (NETL) for his valuable input. This work was partially funded by US DOE under Contract No. DE-AC02-98CH10886.

References

1. *Carbon Sequestration: State of the Science.* Office of Science and Office of Fossil Energy, U.S. Department of Energy: Washington, DC, February **1999**.

Downloaded by STANFORD UNIV GREEN LIBR on September 16, 2012 | http://pubs.acs.org
Publication Date: January 24, 2002 | doi: 10.1021/bk-2002-0809.ch011

2. Hindermann, J. P.; Hutchings, G. J.; Kiennemann, A. *Catal. Rev.-Sci. Eng.* **1993,** *35(1)*, 1.
3. Hennig, H. *Coord. Chem. Rev.* **1999,** *182*, 101.
4. Ando, H.; Xu, Q.; Fujiwara, M.; Matsumura, Y.; Tanaka, M.; Souma, Y. *Catal. Today.* **1998,** *45*, 229..
5. Dry, M.E. *Catalysis Science and Technology, vol. 1*; Anderson , J. R.; Boudart, M., Eds.; Springer-Verlag, New York, **1981**; p 159.
6. Goehna, H.; Koenig, P. *CHEMTECH*, **1994,** *June*, 36.
7. *Kirk-Othmer Encyclopedia of Chemical Technology (4th ed.)*, **1991**, *1*, 38.
8. Fogg, P. G. T.; Gerrard, W. *Solubility of Gases in Liquids;* John Wiley & Sons Ltd.: New York, New York, **1991**.
9. Yaws, C. L. *Chemical Properties Handbook:* McGraw Hill: New York, New York, **1999**.
10. Jessop, P.G.; Ikariya, T.; Noyori, R. *Chem. Rev.* **1995,** *95(2*), 259.
11. Leitner, W. *Angew. Chem. Int. Ed. Engl.* **1995**, *34*, 2207.
12. Hutschka, F.; Dedieu, A.; Eichberger, M.; Fornika, R.; Leitner, W. *J. Am. Chem. Soc.* **1997,** *119*, 4432.
13. Jessop, P.G.; Ikarlya, T.; Noyori, R. *Nature* **1994,** *368*, 231.
14. Tominaga, K-I.; Sasaki, Y.; Kawai, M.; Watanabe, T.; Saito, M. *J. Chem. Soc. Chem. Commun.* **1993**, 629.
15. Dubois, D.L. *Comments Inorg. Chem.* **1997,** *19*, 307.
16. Lehn, J-M.; Ziessel, R., J. *Organomet. Chem.* **1990,** *382*, 157.
17. Wegrzyn, J.E.; Mahajan, D.; Gurevich, M. *Catal. Today* **1999**, *50*, 97.
18. Watson, R. Personal communication at Pennsylvania State University, October 26, **1999**.
19. Selley, R. C. *Applied Sedimentology;* Academic Press: London, **1998**. P 446.
20. North, F. K. *Petroleum Geology;* Allen & Unwin: Boston, **1985**; p 607.
21. Chapman, R. E. *Petroleum Geology*; Elsevier: Amsterdam, **1983**; p 415.
22. Vairavamurthy, M. A.; Schoonen, M. A. A. *Geochemical transformations of sedimentary sulfur;* ACS Symp. Ser.: American Chemical Society: Washington, D.C., **1995**.
23. Mango, F. D.; Hightower, J. W.; James, A. T. *Nature* **1994,** *368,* 536.
24. Mango, F. D. *Org. Geochem.* **1996,** *24*, 977.
25. Mahajan, D.; Vijayaraghavan, P. *Fuel* **1999,** *78*, 93.
26. Song, C.; Murata, S., S. T.; Srinivas, T. S.; Sun, L.; Scaroni, A. W. *Am. Chem. Soc.:* Div. Petrol. Chem. Prepr. **1999,** *44 (2)*, 160.

Downloaded by STANFORD UNIV GREEN LIBR on September 16, 2012 | http://pubs.acs.org
Publication Date: January 24, 2002 | doi: 10.1021/bk-2002-0809.ch011

Downloaded by NORTH CAROLINA STATE UNIV on September 16, 2012 | http://pubs.acs.org
Publication Date: January 24, 2002 | doi: 10.1021/bk-2002-0809.ch012

Chapter 12

Methane Dry Reforming over Carbide, Nickel-Based, and Noble Metal Catalysts

Abolghasem Shamsi

National Energy Technology Laboratory, U.S. Department of Energy, 3610 Collins Ferry Road, Morgantown, WV 26507

Carbide catalysts of molybdenum and tungsten were prepared and tested for reaction of methane with CO_2 at atmospheric pressure. At this pressure the catalysts were not stable and the tungsten carbide irreversibly deactivated after 35 hours on stream. The carbide catalysts produced lower H_2/CO ratios at lower temperatures of 650 and 750°C compared to noble metal or nickel-based catalysts. Tungsten carbide was partially oxidized to tungsten oxide during the reactions, resulting in lower catalytic activity. We also tested 1 wt% rhodium supported on alumina and two commercial Ni-based catalysts, R-67 and G-56B. Significant amounts of carbon formed on the commercial catalysts that plugged the reactor after 5 hours on stream.

U.S. government work. Published 2002 American Chemical Society

In CO2 Conversion and Utilization; Song, C., et al.;
ACS Symposium Series; American Chemical Society: Washington, DC, 2002.

Downloaded by NORTH CAROLINA STATE UNIV on September 16, 2012 | http://pubs.acs.org
Publication Date: January 24, 2002 | doi: 10.1021/bk-2002-0809.ch012

Introduction

Recently many researchers have concentrated their efforts toward catalytic reforming of methane with carbon dioxide. This process can be very useful for converting thermal energy into chemical energy. For example, energy losses in combustion/gasification systems and in advanced gas turbines can be captured by reacting natural gas with the by-product of combustion (CO_2) over a catalyst for producing syngas which can be converted into liquid fuels and chemicals, ultimately increasing the system efficiency. Although this concept has many environmental and economic incentives, unfortunately, there are no commercial processes for reforming of methane with CO_2 (1). The main problem is that there are several carbon-forming reactions associated with this concept that deactivate the conventional steam reforming, nickel-based, catalysts. Nickel catalyzes carbon formation via hydrocarbon decomposition and CO disproportionation reactions, which greatly contributes to catalyst deactivation.

Three phenomena are known to be responsible for the deactivation of nickel catalyst (2). 1) Carbon deposition, 2) metal sintering, and 3) phase transformation such as $NiAl_2O_4 \rightleftharpoons Ni/\gamma\text{-}Al_2O_3$. Choudhary et al. (3) reported that the pressure drop across a fixed bed reactor, containing NiO supported on CaO, increased rapidly due primarily to rapid coke formation on the catalyst surfaces. However, when they added steam to the reaction the amount of carbon was significantly reduced. Chang et.al. (4) found a coke formation rate of 7.0 wt% per hour for pentasil zeolite-supported nickel catalyst at 700°C. Furthermore, they indicated that addition of promoters such as potassium and calcium plus altering the preparation method reduced the coke formation rate to less than 0.1 wt% per hour. Addition of CaO to $Ni/\gamma\text{-}Al_2O_3$ catalyst is reported to improve the catalyst stability and also increases the reaction rate (5).

Operating conditions and catalyst support (6) also play an important role in catalyst particle size distribution, kinetics, and the reactivity of carbon deposited on the catalyst surfaces. Gadalla and Bower (7) recommended that a CO_2/CH_4 ratio of greater than one should be used for reducing carbon deposition. Furthermore, they have calculated the optimum range of temperatures for each feed composition and pressure in which carbon deposition and carbide formation are minimized.

It is reported (8) that the activity and stabilty of methane reforming catalysts are significantly affected by the support and by the active metals. Reducing the concentration of Lewis acid sites on the support and reducing nickle particle size will significantly lower carbon formation. Basini and Sanfilippo (9) studied the molecular aspects of syngas production and proposed that the formation of highly reactive oxidic species, formed from breaking one of the two CO_2 bonds, is responsible for inhibiting carbon formation on the surfaces of the dry reforming catalysts such as Rh, Ru, and Ir. The effect of the support on ruthenium catalyst, under dry reforming conditions, has also been studied (10) and the catalytic activity decreases in the following order: $Rh/Al_2O_3 > Rh/TiO_2 > Rh/SiO_2$.

Several studies (11-13) have shown that the high-surface area tungsten and molybdenum carbide materials are active for methane dry reforming reactions. These catalysts appeared to be stable at higher pressures without forming significant amounts of carbon on the catalyst surfaces. However, these catalysts are very sensitive to oxidation by oxygen or H_2O, forming oxides that are not active for dry reforming.

Review of the current literature indicates that developing an inexpensive catalyst, which exhibits a high selectivity toward hydrogen and carbon monoxide without forming carbon remains a challenge, specifically at higher pressure (14). In this paper, we report the preparation and testing of carbide, Ni-based and noble metal catalysts and compare catalytic activity, selectivity, and stability of these catalysts for reaction of methane with carbon dioxide.

Downloaded by NORTH CAROLINA STATE UNIV on September 16, 2012 | http://pubs.acs.org
Publication Date: January 24, 2002 | doi: 10.1021/bk-2002-0809.ch012

Experimental Section

The tungsten carbide catalyst was prepared as described (15) in U.S. patent 5321,161. The molybdenum carbide catalyst was prepared by temperature-programmed reduction (TPR) of molybdenum oxide in a flow of 11.6% ethane or methane in hydrogen at a flow rate of 55 ml/min. Molybdenum carbide supported on TiO_2 was prepared by mixing MoO_3 with TiO_2 in ethyl alcohol slurry. The dried mixture was reacted with 11.6 vol.% ethane in hydrogen to form carbide. More information on carbide preparation can be found in a paper published by Lee et.al. (16). The nickel-based catalysts were prepared from water soluble nitrate solutions with proper metal ratios. A 0.3-m long quartz reactor tube (6.35-mm o.d., 4.0-mm i.d.) with a quartz thermocouple well was used as a fixed-bed reactor with 0.5 grams of catalyst (-28/+48 mesh) held in place by quartz wool. Electronic mass flow controllers fed methane and carbon dioxide into the reactor, GHSV=5040 $cm^3.g^{-1}.h^{-1}$. The reactor was electrically heated to reaction temperatures. Products were analyzed by on-line gas chromatography (GC). Samples were analyzed for hydrogen, carbon monoxide, methane and carbon dioxide. A thermal conductivity detector was used with a 1-m by 3.2-mm-o.d. stainless steel molecular sieve 5A column and a 3.66-m by 3.2-mm-o.d. stainless steel HayeSep C (80/100 mesh) column at isothermal oven temperatures of 115 and 52°C, respectively. Argon was used as carrier gas at 20 ml/min.

Results and Discussion

A series of carbide, Ni-based, and noble metal catalysts were prepared and tested for methane dry reforming at a temperature range of 650-950°C and at atmospheric pressure. The results at 750 and 850°C are shown in Table I and the results at other temperatures are discussed in the text. Pure SiC was tested at 950°C and no significant methane or CO_2 conversion was observed. We also tested pure tungsten carbide and tungsten carbide supported on silica. Methane conversion of less than 41% was obtained for the supported catalyst at 950°C. The activity of the unsupported tungsten carbide was tested at 650, 750, and 850°C. At lower temperatures of 650 and 750°C, methane and CO_2 conversions were less than 15% with a H_2/CO ratio of 0.2. However, higher methane and CO_2 conversions with a H_2/CO ratio of 1.1 were obtained when the temperature was raised to 850°C, at which the reaction was continued for about 45 hours as shown in Figure 1. The catalyst irreversibly deactivated after 35 hours on stream and we were not able to regenerate it with flowing hydrogen or a mixture of 11.6% ethane in hydrogen over the catalyst. Identical results were obtained when a fresh catalyst, from the same batch, was tested at a similar reaction condition (not shown). Since the freshly prepared catalyst was very sensitive to air oxidation the reactor was loaded under an argon atmosphere in a glove box. Although we were not able to determine the exact cause of the sharp decrease in catalytic activity, characterization of the sample

Table I. Methane dry reforming over carbide and Ni-based catalysts

	% CH_4 Conversion		*% CO_2 Conversion*		*% CO Yield*		*H_2/CO ratio*	
Temperature, °C	750	850	750	850	750	850	750	850
Catalysts:								
Mo_2C (me)	18.3	92.1	37.3	99.8	37.3	96	0.3	1.0
Mo_2C (et)	36.9	89.5	59.1	99.9	51.6	89.4	0.7	1.1
Mo_2C/TiO_2	69.9	70.1	87.1	88.7	76.2	77.8	0.9	0.9
Tungsten carbide	5.4	90.7	12.0	99.7	13.4	86.6	0.2	1.1
R-67, Topsoe*	94.2	98.9	91.1	95.2	95.3	99.1	1.0	1.0
G-56B, UCI*	96.1	99.1	90.3	97.1	93.2	99.8	1.0	1.0

(me)- TPR of MoO_3 using 11.6% methane in H_2
(et) -TPR of MoO_3 using 11.6% ethane in H_2
* Plugged the reactor after 5 hours

Downloaded by NORTH CAROLINA STATE UNIV on September 16, 2012 | http://pubs.acs.org
Publication Date: January 24, 2002 | doi: 10.1021/bk-2002-0809.ch012

by X-ray diffraction after the reaction indicated that the tungsten carbide was partially oxidized to tungsten oxide, suggesting that some of the active sites had been destroyed.

Molybdenum carbide catalysts were prepared by temperature-programmed reduction of molybdenum oxide with a mixture of 11.6 vol.% methane or ethane in hydrogen. The catalyst prepared with methane mixture was tested at 750 and 850°C as shown in Table I. Methane and CO_2 conversions of less than 18% with a H_2/CO ratio of 0.3 were obtained at 650°C. At 850°C methane and CO_2 conversions were higher than 90% with a H_2/CO ratio of 1.0. Higher catalytic activity was observed for the catalyst prepared with ethane mixture compared to that prepared with methane mixture as shown in Table I. The carbide catalysts produced low H_2/CO ratios and deactivated rapidly at temperatures lower than 750°C. Molybdenum carbide prepared with ethane mixture was tested for 16 hours and the results are shown in Figure 2. After 10 hours the catalytic activity continuously decreased until the reaction was terminated. This could result from oxidation of carbide active sites into the oxide, which is inactive for dry reforming reactions as reported by Claridge et. al. (13).

Molybdenum carbide mixed with TiO_2 was tested at 650, 750, 850, and 900°C. Methane and CO_2 conversions of 21 and 42% with a H_2/CO ratio of 0.5 were obtained at 650°C. However, after 30 minutes on stream these numbers decreased to 9.5%, 21.8%, and 0.3, respectively. The results for the initial activity at 750 and 850°C are shown in Table I. The mixed catalyst was also unstable at temperatures of less than 850°C. Less deactivation was observed at higher temperatures and this could be due to higher stability of carbide catalyst at higher temperatures. Thermodynamically, the reduction of oxide into carbide is more favorable at higher temperatures while forming CO_2 as shown in Table II. The table shows the temperatures beyond which the equilibrium constants are greater than one (K>1). At 900°C a methane conversion of 95% and CO_2 conversion of 100% with a H_2/CO ratio of 1.0 were measured and the test was continued for 2.5 hours without a significant drop in catalytic activity or selectivity as shown in Figure 3. At temperatures of less than 850°C higher methane and CO_2 conversions with a higher H_2/CO ratio were obtained for molybdenum carbide mixed with TiO_2 than the sample without it. This shows that TiO_2 has a promoting effect on the catalytic activity of the carbide catalysts.

The tungsten carbide catalyst was characterized before and after reaction using X-ray diffraction, Scanning Electron Microscopy (SEM), and X-ray Photoelectron Spectroscopy (XPS). The X-ray diffraction patterns show that the carbide catalysts were partially oxidized to WO_2 during the reaction as shown in Figures 4. This is in good agreement with a study done by Clarige and his coworker (13), reporting that molybdenum and tungsten carbides were

Downloaded by NORTH CAROLINA STATE UNIV on September 16, 2012 | http://pubs.acs.org
Publication Date: January 24, 2002 | doi: 10.1021/bk-2002-0809.ch012

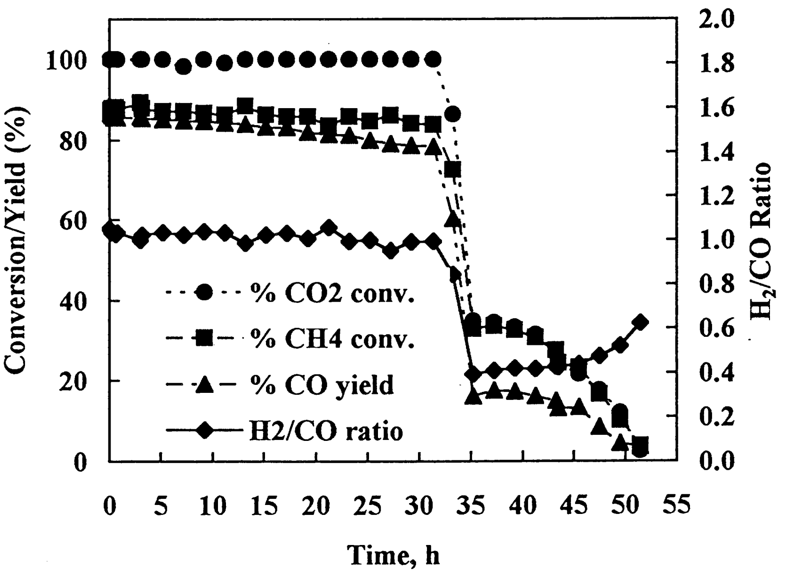

Figure 1. Dry reforming of methane over tungsten carbide at 850 °C, CH_4/CO_2 = 1.1

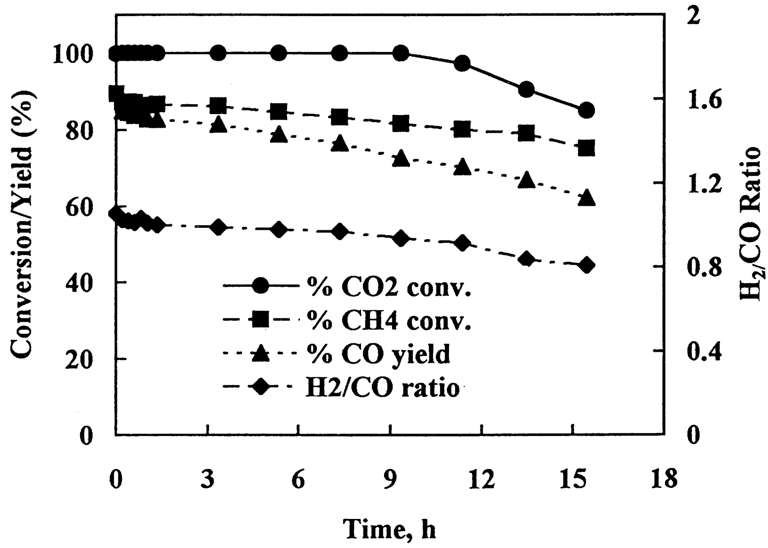

Figure 2. Dry reforming of methane over molybdenum carbide at 850 °C, CH_4/CO_2 = 1.16

Downloaded by NORTH CAROLINA STATE UNIV on September 16, 2012 | http://pubs.acs.org
Publication Date: January 24, 2002 | doi: 10.1021/bk-2002-0809.ch012

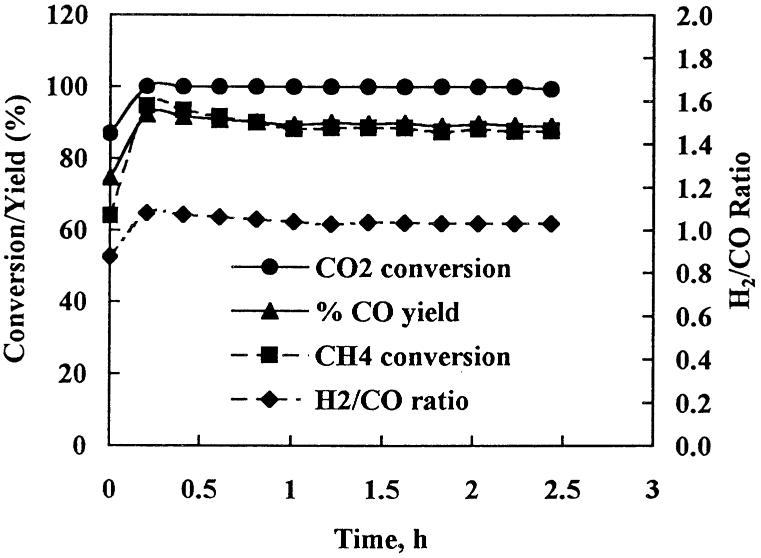

Figure 3. Dry reforming of methane over molybdenum carbide mixed with TiO_2, at 900 °C, CH_4/CO_2 = 1.12

Downloaded by NORTH CAROLINA STATE UNIV on September 16, 2012 | http://pubs.acs.org
Publication Date: January 24, 2002 | doi: 10.1021/bk-2002-0809.ch012

Downloaded by NORTH CAROLINA STATE UNIV on September 16, 2012 | http://pubs.acs.org
Publication Date: January 24, 2002 | doi: 10.1021/bk-2002-0809.ch012

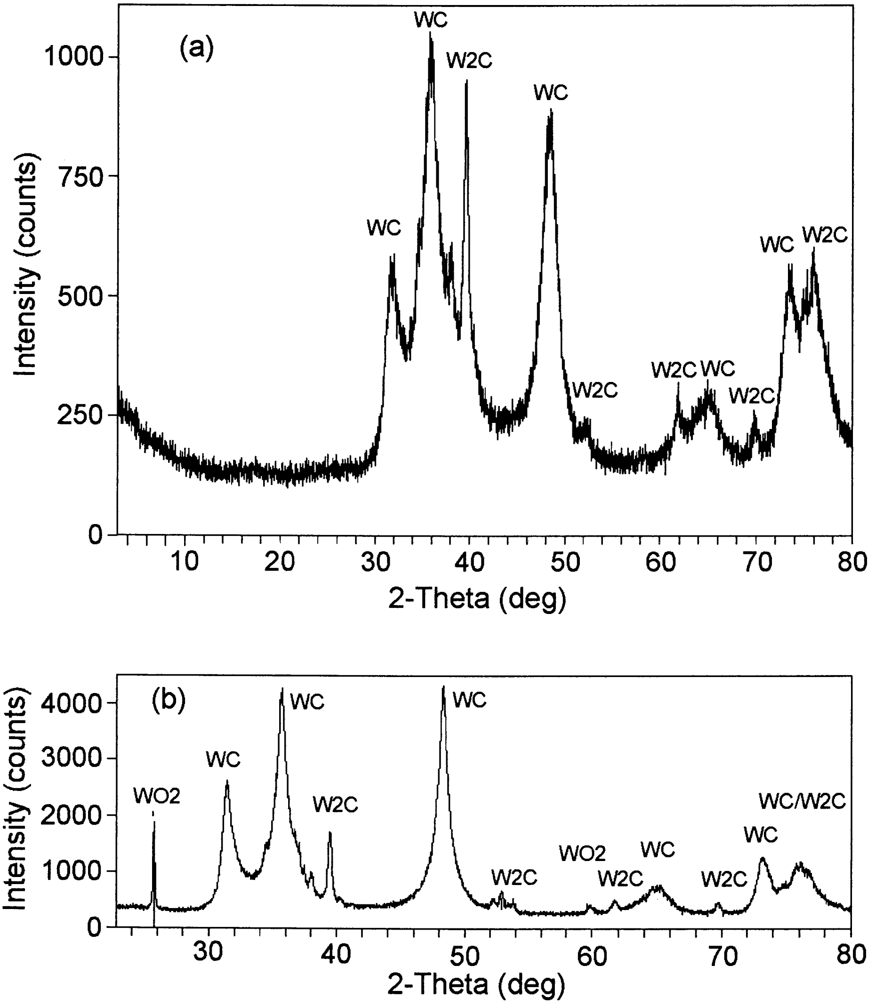

Figure 4. X-ray diffraction pattern of tungsten carbide catalyst: (a) before reaction and (b) after reaction at 850 °C, $CH_4/CO_2=1.15$

Downloaded by NORTH CAROLINA STATE UNIV on September 16, 2012 | http://pubs.acs.org
Publication Date: January 24, 2002 | doi: 10.1021/bk-2002-0809.ch012

Table II. Thermodynamic calculations for Molybdenum and Tungsten Carbide Species Found in the HSC Database†

Temperature °C	*Reaction*	*Equilibrium Constant (K)*
364	$2MoO_3 + 4CH_4 (g) = 3CO_2 (g) + Mo_2C + 8H_2 (g)$	1.087
379	$MoO_3 + 2.5CH_4 (g) = 1.5CO_2 (g) + MoC + 5H_2 (g)$	1.006
581	$MoO_2 + 2CH_4 (g) = CO_2 (g) + MoC + 4 H_2 (g)$	1.050
385	$3MoO_3 + 6.5 CH_4 (g) = 4.5CO_2 (g) + Mo_3C_2 + 13 H_2 (g)$	1.011
589	$2MoO_2 + 3CH_4 (g) = 2CO_2 (g) + Mo_2C + 6H_2 (g)$	1.067
604	$3MoO_2 + 5CH_4 (g) = 3CO_2 (g) + Mo_3C_2 + 10H_2 (g)$	1.024
549	$3WO_3 + 2.5CH_4 (g) = 1.5CO_2 (g) + WC + 5H_2 (g)$	1.032
567	$WO_2 + 2CH_4 (g) = CO_2 (g) + WC + 4H_2 (g)$	1.043
604	$2WO_3 + 4CH_4 (g) = 3CO_2 (g) + W_2C + 8H_2 (g)$	1.060
644	$2WO_2 + 3CH_4 (g) = 2CO_2 (g) + W_2C + 6H_2 (g)$	1.16

†Calculated using HSC Chemistry, Outokumpu Research Oy in Finland

converted to oxides during methane dry reforming. Further oxidation of the deactivated sample occurred when it was exposed to air. Tungsten carbides of W_2C and WC were detected in both samples. The SEM photographs of tungsten carbide catalyst, before and after reaction, clearly show differences between the two samples as shown in Figure 5. The particles in the sample before the reaction have sharper edges than the particles in the sample after the reaction, indicating that some of the active sites have been destroyed or covered with carbon during the reactions. The XPS analysis of tungsten carbide catalyst showed higher concentrations of carbon and oxygen on the surfaces of the sample after reaction compared to that before reaction. The ratio of carbon (C 1s) to tungsten (W 1s) increased from 7 to 50 while the ratio of oxygen (O 1s) to tungsten (W 1s) increased from 2.8 to 12.6 during 35 hours of reactions. Furthermore, no significant changes were observed for carbon (C 1s) or the oxygen (O 1s) peaks on these samples. The tungsten (W 1s) for both samples before and after the reactions is shown in Figure 6.

Two commercial nickel-based catalysts (R-67 and G-56B) were tested at 750 and 850°C as shown in Table I. Although these catalysts showed methane and CO_2 conversions of more than 90% at 750°C they produced significant amounts of carbon in the catalyst bed which eventually plugged the reactor and stopped the flow as shown in Figure 7.

Downloaded by NORTH CAROLINA STATE UNIV on September 16, 2012 | http://pubs.acs.org
Publication Date: January 24, 2002 | doi: 10.1021/bk-2002-0809.ch012

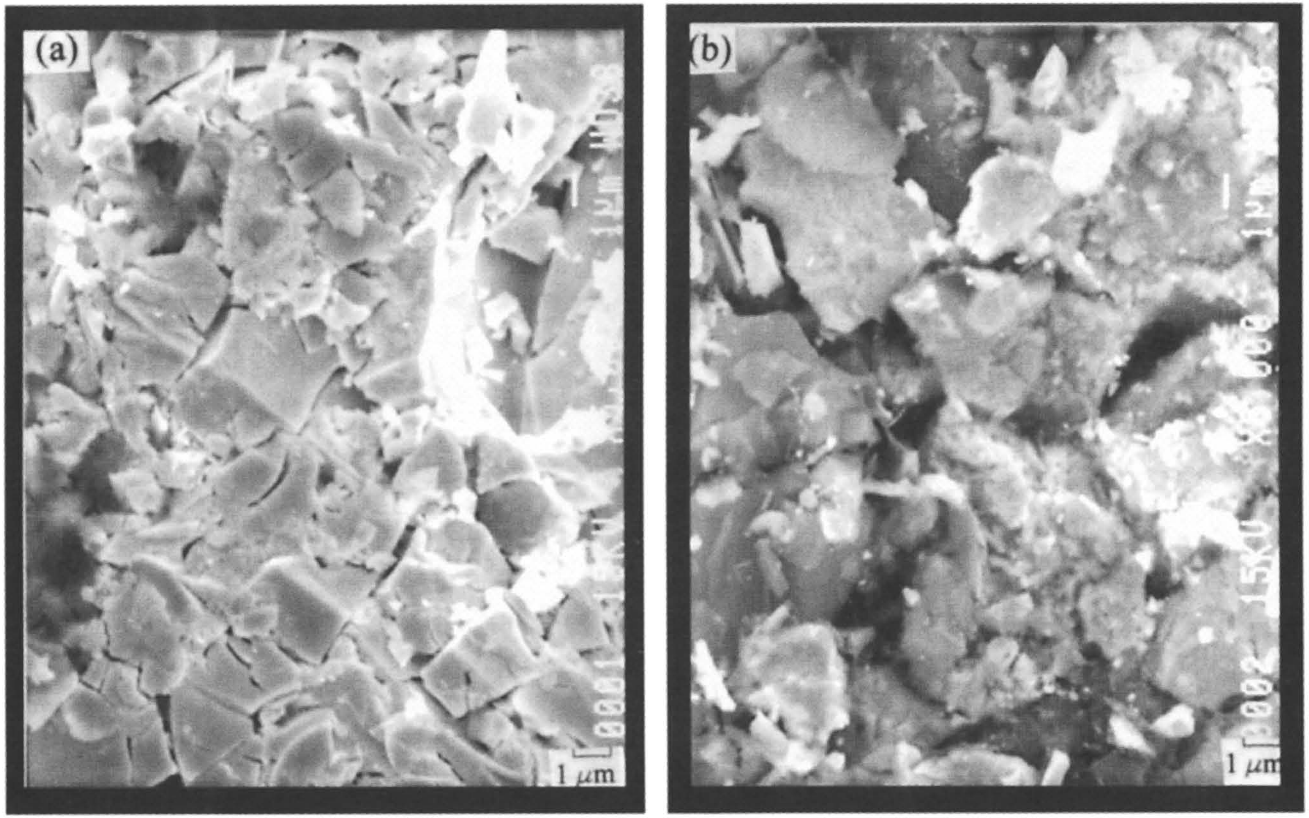

Figure 5. SEM photographs of tungsten carbide catalyst: (a) before reaction and (b) after reaction at 850 °C, CH_4/CO_2 = 1.15

Downloaded by NORTH CAROLINA STATE UNIV on September 16, 2012 | http://pubs.acs.org
Publication Date: January 24, 2002 | doi: 10.1021/bk-2002-0809.ch012

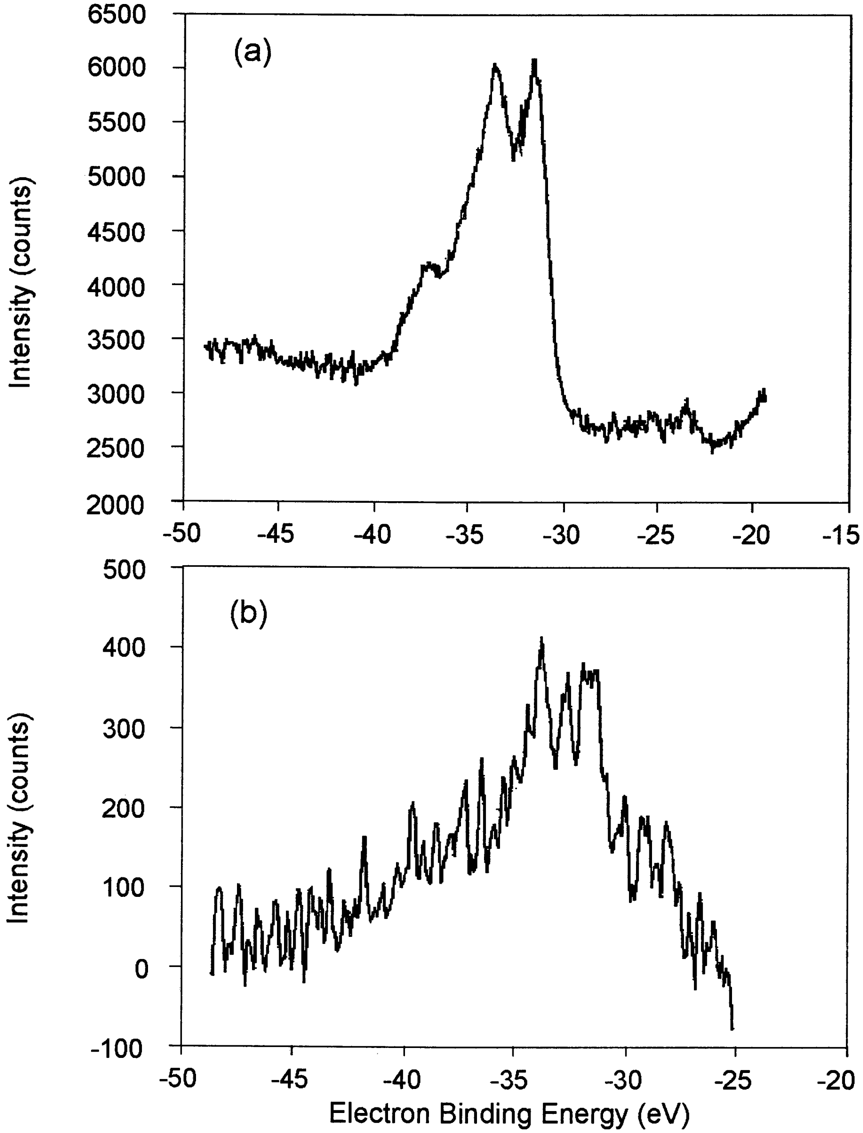

Figure 6. Photoelectron spectra of tungsten (W 1s) carbide catalyst: (a) before reaction and (b) after reaction at 850 °C, $CH_4/CO_2 = 1.15$

Downloaded by NORTH CAROLINA STATE UNIV on September 16, 2012 | http://pubs.acs.org
Publication Date: January 24, 2002 | doi: 10.1021/bk-2002-0809.ch012

A noble metal catalyst of 1% rhodium supported on alumina was tested at 650, 750, and 850°C and the results are listed in Table III. Methane and CO_2 conversions of more than 59% with a H_2/CO ratio of 0.9 were obtained at 650°C. At this temperature the catalyst showed higher activity, selectivity, and stability than carbide and Ni-based catalysts. The test was continued for more than 25 hours at 850°C, as shown in Figure 8, with no sign of deactivation or formation of significant amounts of carbon on the catalyst surface. When the space velocity (GHSV) was raised from 5040 to 7800 and 10200 $cm^3.g^{-1}.h^{-1}$ no significant changes in catalytic activity or selectivity were observed.

Table III. Methane dry reforming over 1% Rh/alumina catalyst

Temperature, °C	650	750	850	850	850
GHSV, $cm^3.g^{-1}.h^{-1}$	5040	5040	5040	7800	10200
H_2/CO ratio	0.9	1.0	1.0	1.0	1.0
% CO yield	65.6	88	95.7	96.1	94.7
% CH_4 conversion	59.2	86.9	97.2	97.2	95.9
% CO_2 conversion	65.2	88.1	97.4	93.0	92.3

The initial catalytic activity of carbide, Ni-based, and noble metal catalysts were similar at temperatures higher than 800°C. However, carbide catalysts were oxidized to oxide during the reaction and lost their catalytic activity after several days on stream. The commercial (Ni-based) catalysts formed significant amounts of carbon that plugged the reactor. Furthermore, at 650°C the initial activity of Ni-based and 1% Rh/alumina catalysts were significantly higher than the carbide catalysts. Although rhodium catalyst is much more expensive than nickel-based and carbide catalysts, it is more stable and produces little or no carbon during the reaction. Therefore, it is a good candidate for dry reforming reaction, producing syngas from methane and CO_2. The high cost of rhodium metal could be tolerated considering higher activity, low metal loading, and reduced carbon deposition. The existing nickel-based commercial catalysts are not suitable for dry reforming because significant amounts of carbon formed on the catalyst surfaces, plugging the reactor. We found that the carbide catalysts are also not reliable and deactivate irreversibly during the reaction at atmospheric pressure. However, it has been shown that these catalysts are much more stable at higher pressure (13).

Downloaded by NORTH CAROLINA STATE UNIV on September 16, 2012 | http://pubs.acs.org
Publication Date: January 24, 2002 | doi: 10.1021/bk-2002-0809.ch012

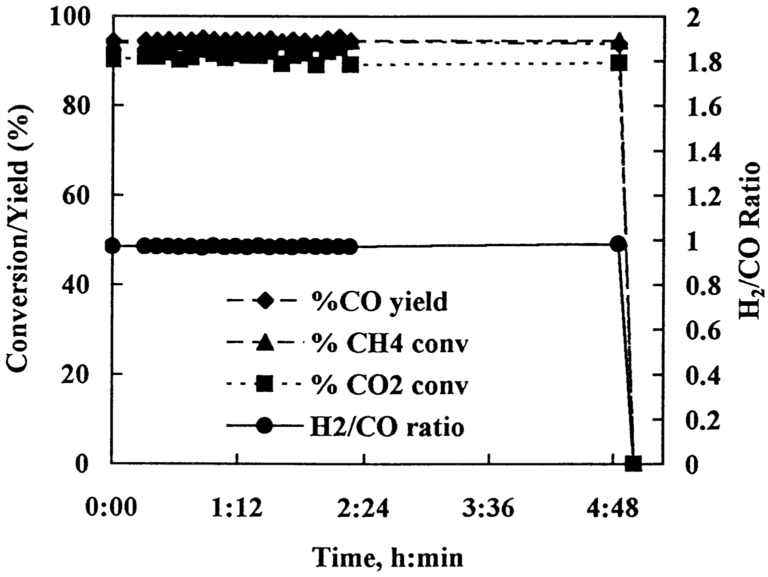

Figure 7. Dry reforming of methane over Ni-based catalyst (R-67) at 750 °C, $CO_2/CH_4 = 1.1$

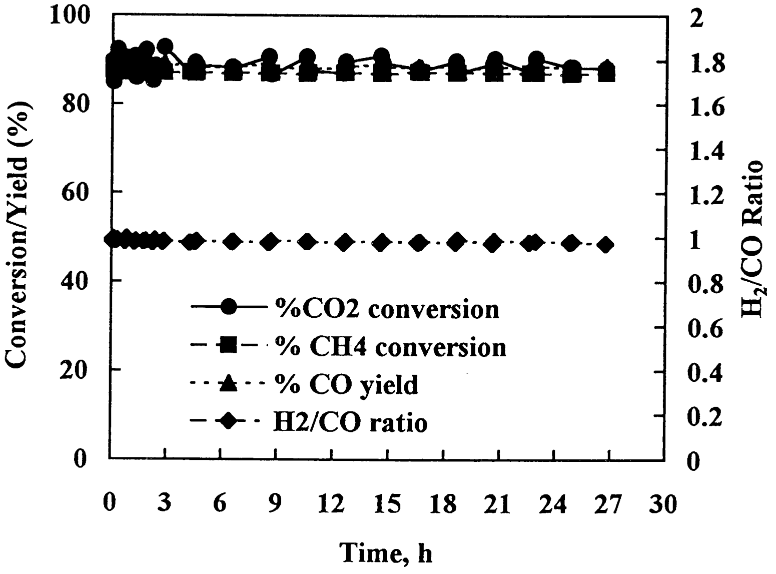

Figure 8. Dry reforming of methane over 1% Rh on alumina at 716 °C, $CO_2/CH_4 = 1.1$

Conclusion

Carbide catalysts of molybdenum and tungsten were prepared and tested for reaction of methane with CO_2. The catalysts were not stable at atmospheric pressure and irreversibly deactivated after several days on stream. The carbide catalysts produced a lower H_2/CO ratio than nickel-based and noble metal catalyst at lower temperatures of 650 and 750°C. The rhodium supported catalyst was active and more stable than the carbide and Ni-based catalysts at lower temperatures of 650 and 750°C. Significant amounts of carbon formed on the commercial catalysts, plugging the reactor after 5 hours on stream. Tungsten carbide catalyst was analyzed before and after methane dry reforming reactions using XRD, SEM, and XPS. The XRD and the XPS results showed that the tungsten carbide was partially oxidized to tungsten oxide during the reactions and may have resulted in the loss of some of the active sites.

Acknowledgment

Author acknowledges the Natural Gas Processing and Utilization team of National Energy Technology Laboratory for funding this work. He also thanks Dr. Ranjani V. Siriwardane, James A. Poston and Elizabeth A. Frommell for carrying out the XPS, SEM and XRD measurements.

References

1. Wang, S; Lu, G. Q. Carbon Dioxide Reforming of Methane to Produce Synthesis Gas over Metal-Supported Catalysts: State of the Art. *Energy & Fuels.* **1996**, 10, 896-904.
2. Tomishige, K.; Chen, Y-G.; Fujimoto, K. Studies on Carbon Deposition in CO_2 Reforming of CH_4 over Nickel-Magnesia Solid Solution Catalysts. *J. Catal.* **1999**, 181, 91-103.
3. Choudhary, V. R.; Rajput, A. M. Simultaneous Carbon Dioxide and Steam Reforming of Methane to Syngas over NiO-CaO Catalyst. *Ind. Eng. Chem. Res.* **1996**, 35, 3934-3939.
4. Chang, J-S.; Park, S-E.; Lee, K-W.; Choi, M. J. Catalytic Reforming of Methane with Carbon Dioxide over Pentasil Zeolite-Supported Nickel Catalyst. *Studies in Surface Science and Catalysis.* **1994**, 84, 1587-1594.
5. Zhang, Z. L.; Verykios, X. E. Carbon Dioxide Reforming of Methane to Synthesis Gas over Supported Ni Catalysts. *Catalysis Today.* **1994**, 21, 589-595.

Downloaded by NORTH CAROLINA STATE UNIV on September 16, 2012 | http://pubs.acs.org
Publication Date: January 24, 2002 | doi: 10.1021/bk-2002-0809.ch012

6. Goula, M. A.; Lemonidou, A. A.; Efstathiou, A. M. Characterization of Carbonaceous Species Formed During Reforming of CH_4 with CO_2 over Ni/CaO-Al_2O_3 Catalysts Studied by Various Transient Techniques. *J. Catal.* **1996**, 161, 626-640.
7. Gadalla, A. M.; Bower, B. The Role of Catalyst Support on the Activity of Nickel for Reforming Methane with CO_2. *Chem. Eng. Sci.* **1988**, 43 (11), 3049-3062.
8. Lercher, J. A.; Bitter, J. H.; Hally, W.; Niessen, W.; Seshan, K. Design of Stable Catalysts for Methane-Carbon Dioxide Reforming. *Studies in Surface Science and Catalysis.* **1996**, 101, 463-472.
9. Nakamura, J.; Aikawa, K.; Sato, K.; Uchijima, T. Role of Support in Reforming of CH_4 with CO_2 over Rh Catalysts. *Catalysis Letters.* **1994**, 25, 265-270.
10. Basini, L.; Sanfilippo, D. Molecular Aspects in Syn-Gas Production: The CO_2-Reforming Reaction Case. *J. Catal.* **1995**, 157, 162-178.
11. York, P. E.; Claridge, J.B.; Marquez-Alvarez C.; Brungs, A. J.; Green, M.L.H. Group (V) and (VI) Transition Metal Carbides as New Catalysts for the Reforming of Methane to Synthesis Gas. Prepr. Am. Chem. Soc., Div. Fuel Chem. **1997**, 42(2), 606-610.
12. York, A. P. E.; Claridge, J. B.; Brungs, A. J.; Tsang, S.C.; Green, M.L.H. Molybdenum and Tungsten Carbides as Catalysts for the Conversion of Methane to Synthesis Gas Using Stoichiometric Feedstock. *Chem. Commun.* **1997**, 39-40.
13. Claridge, J. B.; York, A.P.E.; Brungs, A. J.; Marquez-Alvarez, C.; Sloan, J.; Tsang, S.C.; Green, M.L.H. New Catalysts for the Conversion of Methane to Synthesis Gas: Molybdenum and Tungsten Carbides. *J. Catal.* **1998**, 180, 85-100.
14. Song, C.; Srimat, S. T.; Sun, L.; Armor, J. N. Comparison of High-Pressure and Atmospheric-Pressure Reactions for CO_2 Reforming of CH_4 over Ni/Na-Y and Ni/Al_2O_3 Catalysts Prepr. Am. Chem. Soc., Div. Petrol. Chem. **2000**, 45 (1), 143-148.
15. Vreugdenhil, W.; Sherif, F.G.; Burk, J.H.; Gadberry, J.F. U.S. Patent 5,321,161, **1994**.
16. Lee, J.S.; Oyama, S.T.; Boudart, M. Molybdenum Carbide Catalysts I. Synthesis of Unsupported Powders *J. Catal.* **1987**, 106, 125-133.

Downloaded by NORTH CAROLINA STATE UNIV on September 16, 2012 | http://pubs.acs.org
Publication Date: January 24, 2002 | doi: 10.1021/bk-2002-0809.ch012

Downloaded by STANFORD UNIV GREEN LIBR on September 16, 2012 | http://pubs.acs.org
Publication Date: January 24, 2002 | doi: 10.1021/bk-2002-0809.ch013

Chapter 13

A Highly Active and Carbon-Resistant Catalyst for CH_4 Reforming with CO_2: Nickel Supported on an Ultra-Fine ZrO_2

Jun-Mei Wei, Bo-Qing Xu, Jin-Lu Li, Zhen-Xing Cheng, and Qi-Ming Zhu

State Key Laboratory of C_1 Chemistry & Technology, Department of Chemistry, Tsinghua University, Beijing 100084, China

Ni supported on a specially prepared ultra-fine ZrO_2 is studied for activity and carbon-resistant ability in catalytic reforming of CH_4 with CO_2 to synthesis gas. This catalyst provides a space time yield of 46.7 g CO/h·g-cat at 1030 K and a catalyst life longer than 600 h without detectable deactivation. Possible reasons for the extremely high activity and stability of the catalyst are discussed.

Introduction

The catalytic reforming of CH_4 with CO_2 for producing synthesis gas ($CH_4 + CO_2 \rightarrow 2CO + 2H_2$) is one of the attractive routes for utilization of the two

In CO2 Conversion and Utilization; Song, C., et al.;
ACS Symposium Series; American Chemical Society: Washington, DC, 2002.

greenhouse gases. Moreover, this process can produce synthesis gas with a H_2/CO ratio less than a unity, which is more desirable for Oxo syntheses, and for the syntheses of oxygenates as well as long chain hydrocarbons. Numerous papers have been documented on the catalysis of this reaction in recent years, as were reviewed by Bradford and Vannice in 1999 [1]. It is commonly recognized that Ni-based catalysts are active for this reaction, but they deactivate rapidly due to carbon deposition via CO disproportionation and/or CH_4 decomposition [2]. Supported noble metal catalysts were found less sensitive to coking [3,4], but their practical utilization was restricted by the high cost and limited resource of the noble metals. In the search for highly active and carbon-resistant nickel-based catalysts, we showed very recently that an ultra-fine ZrO_2 (u-ZrO_2) supported Ni catalyst was very active and extremely stable for the reforming reaction [5-8]. The Ni loading in the catalyst system can be as high as 27% without degrading the catalyst. Besides, we have also found that u-ZrO_2 itself is somewhat active for this reaction. This presentation reports on the behavior of the catalysis.

Downloaded by STANFORD UNIV GREEN LIBR on September 16, 2012 | http://pubs.acs.org
Publication Date: January 24, 2002 | doi: 10.1021/bk-2002-0809.ch013

Experimental

The ultra-fine ZrO_2 with particle sizes around 6 nm and a specific surface area of 160 m^2/g was prepared with a precursor of drying an alcogel of $ZrO(OH)_2$ under conditions for supercritical ethanol (543 K, 8.0 MPa). The alcogel was obtained by washing with anhydrous ethanol of a $ZrO(OH)_2$ hydrogel prepared by addition of 0.17 M $ZrOCl_2$ solution into a 2.5 M ammonia water solution with careful control of pH=9~11. X-ray diffraction (XRD) measurement showed that the crystals of u-ZrO_2 were 22% monoclinic and 78% tetragonal. Ni/u-ZrO_2, Ni/Al_2O_3, Ni/TiO_2, and Ni/SiO_2 catalysts were prepared by impregnating the u-ZrO_2, Al_2O_3, TiO_2, and SiO_2 with an aqueous solution of nickel nitrate, followed by drying (at 383 K for 12 h) and calcining (at 923 K for 5 h). The three conventional supports were purchased from Tianjing Institute of Chemical Industry, China.

The catalytic reaction was performed under atmospheric pressure at 1030 K with a feed of 1:1 CH_4/CO_2 (GHSV=2.4×10^4 ml/h·g-cat). 200 mg catalysts diluted with 500 mg alfa-alumina or 200 mg supports with sizes ranging in 20-40 meshes were loaded into a fixed bed quartz tubular reactor for the activity and stability measurements. Before reaction, the samples were reduced in situ at 973 K with flowing 10% H_2/N_2 for 3 h. Ni loading in the catalysts was determined with XRF and expressed by weight percent.

Results and Discussions

Figure 1 shows CH_4 conversion versus reaction time on stream (TOS) over 5%Ni catalysts supported by different supports. The conversions of CH_4 and CO_2 and the selectivity to CO and H_2 at TOS=10 h are showed in Table 1. From figure 1 it can be seen that the initial activities over Ni/Al_2O_3, Ni/TiO_2, and Ni/u-ZrO_2 are all quite high and only Ni/SiO_2 shows poor activity. Although the initial activity over Ni/u-ZrO_2 is not the highest, it maintains its initial activity for longer than 200 h TOS without any deactivation. In contrast, the activity of the other catalysts declines rapidly. All these observations show that supports exert significant influence on activity and stability of the Ni-based catalyst.

Figure 2 shows CH_4 conversion versus TOS over Ni/u-ZrO_2 catalysts with different Ni loadings. It can be seen that the catalyst activity increases with the increase of Ni loadings and that the CH_4 conversion is close to the equilibrium value (87%) over the catalyst with a nickel loading of 27%. It can also be seen that all the Ni/u-ZrO_2 catalysts with different nickel loadings are very stable and that no deactivation occurs on the 27%Ni/u-ZrO_2 catalyst even after 600 h TOS. Besides, an obvious oscillation of CH_4 conversion on the three catalysts takes place.

Figure 3 shows CH_4 and CO_2 conversions versus TOS over u-ZrO_2 under conditions of atmospheric pressure, 1073 K, GHSV=2.4×10^4 ml/h·g-cat. Around 10% CH_4 conversion is obtained after an induction period and no deactivation happens after 50 h TOS. Besides, oscillation also occurs on the u-ZrO_2 sample. The conventional SiO_2, TiO_2, and Al_2O_3 supports with no Ni were also tested and all of them showed very low activity with CH_4 conversion being less than 1%.

The influence of space velocity (GHSV) on CH_4 conversion over the 27%Ni/u-ZrO_2 catalyst was also investigated under the conditions mentioned above except with varying GHSV. Table 2 shows that increasing the GHSV results in a decrease in CH_4 conversion, but the decreasing rate is so slow that the CH_4 conversion can still be near the equilibrium with a GHSV as high as 4.8×10^4 ml/h·g-cat, indicating very high activity of the catalyst. The present 27%Ni/u-ZrO_2 catalyst is more active than the $Ni_{0.03}Mg_{0.97}O$ catalyst reported by Fujimoto et al. [9]. CH_4 conversion over the latter catalyst is 82% at 1123 K and GHSV=1.8×10^4 ml/h·g-cat (W/F=1.2 h·g-cat/mol), corresponding to a STY of 11.9 g CO/h·g-cat. For comparison, the present catalyst provides 85% CH_4 conversion at 1030 K (ca.100 K lower than over $Ni_{0.03}Mg_{0.97}O$) and GHSV=4.8×10^4 ml/h·g-cat, corresponding to a STY of 46.7 g CO/h·g-cat.

The extremely high activity and stability of the Ni/u-ZrO_2 catalysts may be accounted for with the unique character of the u-ZrO_2 and the structure of the catalyst. On one hand, the u-ZrO_2 support is able to accommodate as high as near 30% Ni without degrading the catalyst. This is the reason why our catalyst is much more active than Fujimoto's, in which only 4.26 wt%Ni was contained.

Downloaded by STANFORD UNIV GREEN LIBR on September 16, 2012 | http://pubs.acs.org
Publication Date: January 24, 2002 | doi: 10.1021/bk-2002-0809.ch013

Downloaded by STANFORD UNIV GREEN LIBR on September 16, 2012 | http://pubs.acs.org
Publication Date: January 24, 2002 | doi: 10.1021/bk-2002-0809.ch013

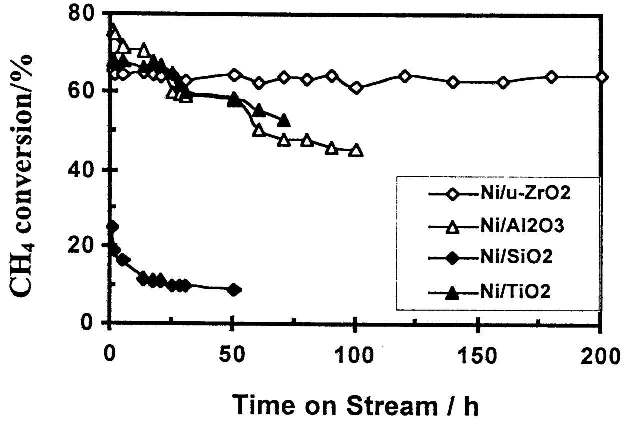

Figure 1: CH_4 conversion versus reaction time over Ni supported on different support

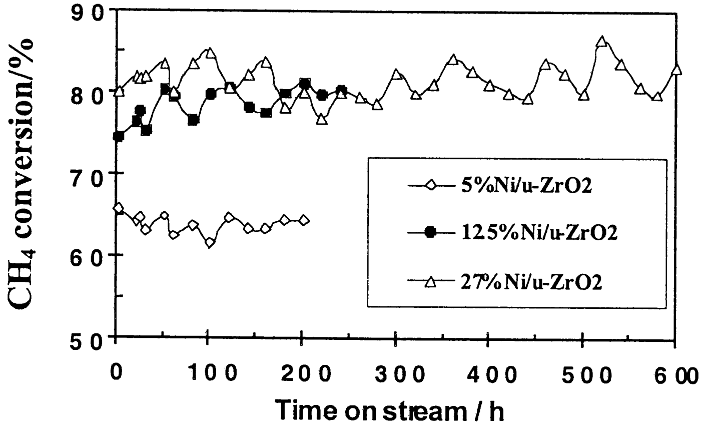

Figure 2: CH_4 conversion versus reaction time over Ni/u-ZrO_2 catalysts with different Ni loadings

Downloaded by STANFORD UNIV GREEN LIBR on September 16, 2012 | http://pubs.acs.org
Publication Date: January 24, 2002 | doi: 10.1021/bk-2002-0809.ch013

Table 1 Activity and selectivity of Ni-based catalysts for CH_4 reforming with CO_2 over different Ni-based catalysts

Catalyst	CH_4 Conv. / %[a]	CO_2 Conv. / %	TOF CH_4 / s^{-1a}	CO/H_2	CO Sel. / %	H_2 Sel. / %
Ni/γ–Al_2O_3	70.9	71.3	2.9	1.06	90.6	85.5
Ni/TiO_2	67.0	66.5	2.5	1.05	87.7	84.2
Ni/SiO_2	11.6	16.4	0.5	1.02	97.8	95.7
Ni/u-ZrO_2	65.0	67.8	1.1	1.18	98.7	85.9

[a]: The data represent the results at TOS=10 h

Reaction conditions: T=1030 K, P=0.1 MPa, GHSV=2.4×10^4 ml/g-cat·h, $CO_2/CH_4=1$

Table 2 Effect of GHSV on the activity and selectivity over 27%Ni/u-ZrO_2 catalyst

GHSV / 10^4 ml·h·g-cat	CH_4 Conv. / %	CO_2 Conv. / %	CH_4 TOF / s^{-1}	CO/H_2	CO Sel. / %	H_2 Sel. / %
1.2	88.7	100.0	0.5	1.17	97.6	83.4
2.4	86.2	88.3	1.0	1.20	95.4	79.5
3.6	85.9	86.7	1.5	1.10	96.7	87.9
4.8	85.8	86.4	2.0	1.23	97.3	83.2
7.2	79.7	81.2	2.8	1.08	98.4	91.1
9.6	79.1	77.5	3.7	1.10	95.2	86.6

Reaction temperature: 1030 K; The data represent the results at TOS=50 h.

Downloaded by STANFORD UNIV GREEN LIBR on September 16, 2012 | http://pubs.acs.org
Publication Date: January 24, 2002 | doi: 10.1021/bk-2002-0809.ch013

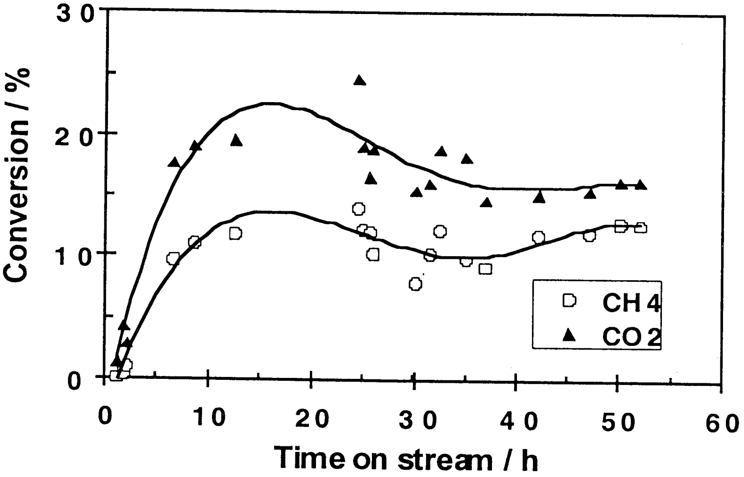

Figure 3: CH_4 and CO_2 conversions versus reaction time over u-ZrO_2 catalysts

In our Ni/u-ZrO_2 catalyst, Ni particles are dispersed among u-ZrO_2, there is no limitation to the loading of Ni, though there may be some interaction between Ni and u-ZrO_2. In fact, TEM and other characterization data show that the Ni/u-ZrO_2 catalyst can better be described as a nano-composite composed of nano-Ni metal and nano-ZrO_2 crystals. It is assumed that the nano-composite nature of the catalyst is essential for the long-lasting anti-carbon property of the catalyst. On the other hand, the fact that u-ZrO_2 itself possesses some activity for the desired reaction implies that, though being a support, it can activate both CH_4 and CO_2. This would appreciably increase the number of the active sites and therefore enhance the activity. In addition, surface oxygen formed by the dissociation of CO_2 on u-ZrO_2 at the interface between metal and support [5] facilitates the elimination of carbon, thereby the stability of the catalyst is enhanced. This mechanism could be effective for the present Ni/u-ZrO_2 catalyst because Ni and u-ZrO_2 particles are very tiny and therefore they are intimately dispersed and contacted. The large area of the interface and the close distance between Ni and u-ZrO_2 allow the surface oxygen to migrate onto the Ni surface and react with carbon easily.

Oscillation may stem from the alternative generation and elimination of carbon. Further investigations on this phenomenon are being made.

Downloaded by STANFORD UNIV GREEN LIBR on September 16, 2012 | http://pubs.acs.org
Publication Date: January 24, 2002 | doi: 10.1021/bk-2002-0809.ch013

Acknowledgement

This work was financially supported by the grants from the Fundamental Research Foundation of Tsinghua University and National Natural Science Foundation of China (NSFC, grant 0094).

References

1. Bradford, M.C.J., Vannice, M.A., Catal. Rev.-Sci. Eng.,**1999**, 41, 1.
2. Claridge, J.B., Green, M.L.H., Tsang, S.C., York A.P.E., Ashcroft A.T., Catal. Lett., **1993**, 22, 299.
3. Ashcroft, T., Cheetham, A.K., Greenand, M.L.H., Vernon, P.D.F., Nature, **1991**, 352, 225.
4. Bitter, J.H., Seshan, K., Lercher, J.A., J. Catal., **1998**, 176, 93.

5. Wei, J.M., Xu, B.Q., Li, J.L., Cheng, Z.X., Zhu, Q.M., Appl. Catal. A: General, **2000**, 196,L167.
6. Wei, J.M., Xu, B.Q., Cheng, Z.X., Li, J.L., Zhu, Q.M., Stud. Surf. Sci. Catal., **2000**, 130D, 3687
7. Wei, J.M., Xu, B.Q., Li, J.L., Cheng, Z.X., Zhu, Q.M., Fuel Chemistry Division preprint, **2001**, 46, xx
8. Xu, B.Q., Wei, J.M., Wang H.Y., Sun K.Q., Zhu, Q.M., Catal. Today, in press
9. Tomishige, K., Yamazaki, O., Chen, Y., Yokoyama, K., Li, X., Fujimoto K., Catal. Today, **1998**, 45, 35.

Downloaded by STANFORD UNIV GREEN LIBR on September 16, 2012 | http://pubs.acs.org
Publication Date: January 24, 2002 | doi: 10.1021/bk-2002-0809.ch013

Downloaded by COLUMBIA UNIV on September 16, 2012 | http://pubs.acs.org
Publication Date: January 24, 2002 | doi: 10.1021/bk-2002-0809.ch014

Chapter 14

CO_2 Reforming of Methane over Ru-Loaded Lanthanoid Oxide Catalysts

Kiyoharu Nakagawa[1,2], Shigeo Hideshima[1], Noriyasu Akamatsu[1], Na-oko Matsui[1], Na-oki Ikenaga[1], and Toshimitsu Suzuki[1,2,*]

[1]Department of Chemical Engineering, Faculty of Engineering, and [2]High Technology Research Center, Kansai University, Suita, Osaka 564–8680, Japan

CO_2 reforming of methane was carried out using ruthenium-loaded catalysts. The productivity of the synthesis gas from methane was strongly affected by support materials and pretreatment conditions. At 600 °C, methane conversion and yields of CO and H_2 were the highest with the Ru/Y_2O_3. CO_2 pretreatment at the reaction temperature were effective for the activation of Ru-loaded La_2O_3 and Y_2O_3 catalysts. During CO_2 pretreatment, loaded ruthenium species were transformed into metallic Ru and RuO_2. Coexistence of metallic Ru and RuO_2 might be important to exhibit high catalytic activity for the CO_2 reforming of methane.

In CO2 Conversion and Utilization; Song, C., et al.;
ACS Symposium Series; American Chemical Society: Washington, DC, 2002.

The production of synthesis gas from methane has been studied in three reactions that attract industrial interest; the partial oxidation of methane (reaction 1), steam reforming (reaction 2), and CO_2 reforming (reaction 3).

$$CH_4 + 1/2O_2 \rightarrow CO + 2H_2 \quad \Delta H^0_{298} = -36 \text{ kJ/mol} \quad (1)$$

$$CH_4 + H_2O \rightleftarrows CO + 3H_2 \quad \Delta H^0_{298} = +206 \text{ kJ/mol} \quad (2)$$

$$CH_4 + CO_2 \rightarrow 2CO + 2H_2 \quad \Delta H^0_{298} = +247 \text{ kJ/mol} \quad (3)$$

Among those, the CO_2-reforming of methane has recently attracted much attention (reaction 3) *(1-3)*. CO_2 reforming of methane to synthesis gas was first reported by Fischer and Tropsch *(4)*. This reaction can also contribute to the utilization of carbon dioxide as carbon sources. Since CO_2 and CH_4 are greenhouse gases, their conversion to synthesis gas could be a method of its reduction from the environment *(5)*.

The transition metals of the group VIII loaded on metal oxides have been widely examined as catalysts for the CO_2 reforming of methane *(6, 7)*, and in some cases the effect of the support on the catalytic activity has been reported. Rostrup-Nielsen *et al.* have shown the order of reactivity for CO_2 reforming to be Ru > Rh > Ni, Ir > Pt > Pd. This order is similar to the proposed order for steam reforming, but the superiority of Rh and Ru is less pronounced *(8)*. Solymosi *et al.* have reported the order of reactivity is Ru > Pd > Rh > Pt > Ir, when Al_2O_3 was used as a support *(9)*. Zhang *et al.* reported the effect of support on the Rh catalysts and concluded that the activity order is YSZ (yittria stabilized zirconia) > Al_2O_3 > TiO_2 > SiO_2 > La_2O_3 > MgO *(10)*. Nakamura *et al.* have investigated a significant effect of the support on the catalytic activity over Rh-loaded catalysts and the activity order is reported to be Al_2O_3 > TiO_2 > SiO_2 *(11)*. With the Pd catalysts, the activity order is reported to be TiO_2 > Al_2O_3 > SiO_2 > MgO *(12)*.

Carbon formation over metal catalysts during the CO_2 reforming has been observed *(13, 14)*. The deposited carbon is formed via different routes *(15)*. The conventional Ni based catalysts for steam reforming tend to be coked due to the formation of stable nickel carbide on the surface of the catalyst *(16)*. Zhaolong *et al.* *(16, 17)* reported that Ni/La_2O_3 catalyst exhibited high activity and long-term stability. On Ni/La_2O_3 catalyst, the rate increased during the initial 2-5 h of reaction and then became stationary value with time on stream. An X-Ray diffraction study revealed that a large amount of CO_2 was stored in the support as $La_2O_2CO_3$. Fujimoto *et al.* *(3, 18)* have found that $Ni_{0.03}Mg_{0.97}O$ and $Ni_{0.03}Ca_{0.13}Mg_{0.84}O$ solid solution catalysts which were reduced with hydrogen a

Downloaded by COLUMBIA UNIV on September 16, 2012 | http://pubs.acs.org
Publication Date: January 24, 2002 | doi: 10.1021/bk-2002-0809.ch014

high temperature, showed excellent activities and stabilities in a run for 100 h at 850 °C under 3.2 atm of total pressure and $CH_4/CO_2 = 1/1$.

We have reported in previous papers that the performance of iridium-loaded catalysts depended strongly upon the support materials in the methane to synthesis gas *(19)* and that the interaction between CO_2 and the support strongly affects the reactivity of Ir-loaded catalysts in the CO_2 reforming of methane *(20)*. In the CO_2 reforming of methane and heptane, Ru/La_2O_3 catalyst exhibited high activity *(21-23)*. To maintain a higher catalytic activity over Ru/La_2O_3 catalyst, the formation of $La_2O_2CO_3$ seemed to be essential. The interaction between CO_2 and the support over Ru-loaded catalysts in the pulsed reaction was discussed in previous papers *(22, 23)*.

In this paper, in order to exploit more active and stable catalyst for CO_2 reforming of methane we will discuss effect of support on the CO_2 reforming of methane over Ru loaded catalysts. It also describes studies of marked promoting effect of CO_2 pretreatment on the CO_2 reforming of methane over rare earth oxides-supported Ru catalysts.

Downloaded by COLUMBIA UNIV on September 16, 2012 | http://pubs.acs.org
Publication Date: January 24, 2002 | doi: 10.1021/bk-2002-0809.ch014

Experimental

The catalyst supports used were Al_2O_3 (JRC-ALO-4 the reference catalyst provided by the Catalyst Society of Japan), SiO_2, CaO (Wako Pure Chemical Industries. Ltd.), MgO (Ube Industry Co. Ltd.), TiO_2, ZrO_2 (Japan Aerosil Co.), Y_2O_3, La_2O_3, and Nd_2O_3 which were obtained by thermal decomposition of $Y_2(C_2O_4)_3 \cdot 4H_2O$ (Wako Pure Chemical Industries. Ltd.), $La(CH_3COO)_3 \cdot 1/2H_2O$, and $Nd_2(CO_3)_3$ (Nacalai tesque, Inc.), CeO_2 (Nacalai tesque, Inc.), Sm_2O_3, Eu_2O_3 (Anan Kasei. Co.), Pr_6O_{11}, Gd_2O_3, Tb_4O_7 (Santoku Kinzoku Industries Ltd.). The supported catalysts containing 0.5 wt% Ru metal were prepared by impregnation methods with an aqueous solution of $RuCl_3 \cdot H_2O$ (Mitsuwa pure chemicals) onto suspended supports, followed by evaporation-to-dryness. Loaded catalysts were calcined at 600 °C for 5 h in air. Prior to the reaction, the catalyst was pretreated with CH_4, H_2, or CO_2 at 400 or 600 °C for 1 h.

The reaction was carried out with a fixed-bed flow-type quartz reactor (300 x 8 mm) at 1 atmosphere pressure. The conditions for CO_2 reforming, using 100 mg of a catalyst and 300 mg of silica sand (Merck), 30 mL/min of CH_4 and 30 mL/min of CO_2 were introduced at 600 °C. Silica sand was used as a heat buffer for a large endothermic reforming reaction.

The reaction products (H_2, CO, CH_4, and CO_2) were analyzed by a gas chromatograph directly connected to the outlet of the reaction tube with a thermal conductivity detector (M200 chromato analyzer, Nippon Tyran Co.), which can separate H_2, CO, CH_4, and CO_2, within a few hundred seconds.

The specific surface areas of catalysts were measured with the BET method using N_2 at -196 °C with an automatic Micromeritics Gemini model 2375.

Powder X-ray diffraction (XRD) patterns were measured by a Simadzu XRD-6000 using monochromatized Cu-K α radiation.

Results and discussion

Table I and Figure 1 show the product distributions and effect of time on stream on the CH_4 conversion over various metal oxide Ru-loaded catalysts. In all cases, the CO_2 conversion was higher than that of CH_4. The support activity order at 600 °C was $Y_2O_3 \geqq La_2O_3 \geqq Nd_2O_3 > Pr_6O_{11} \geqq Sm_2O_3 \geqq Sc_2O_3 \geqq Gd_2O_3 > CeO_2 > MgO \geqq TiO_2 > CaO \geqq Tb_4O_7, Al_2O_3 > SiO_2$. The performance of the catalyst depended strongly upon support materials. At 600 °C, methane conversion and yields of CO and H_2 were the highest with the Y_2O_3-supported Ru catalyst, providing an H_2 to CO ratio of 0.83. La_2O_3 and Nd_2O_3 supports also exhibited high activities at 600 °C. Characteristic features of the rare earth oxide supports exhibited relatively high activities irrespective of the surface area. In addition, no carbon deposition was observed. CH_4 conversions gradually increased with time-on-stream over Ru-loaded Y_2O_3 and La_2O_3 catalysts. On other supports, CH_4 conversions gradually decreased with time on stream. The significant effect of the support might be ascribed to the activation of CO_2 with metal oxides used as a support. Similar results have been obtained in the CO_2 reforming of heptane using a Ru-loaded catalyst *(21)*. To achieve a higher activity in the CO_2 reforming, the activation of CO_2 on the support would be one important factor, in addition to the activation of methane on the transition metal surface. Nakamura *et al. (11)* have reported the effects of supports on catalytic activities in the CO_2 reforming of methane. They obtained an enhanced catalytic activity by mixing MgO with Rh/SiO_2, concluding that promoted activity is ascribed to the dissociation of CO_2 on the surface of Rh enriched with the CO_2 adsorbed on MgO. This suggests that CO_2 dissociation is the rate-determing step of this reaction.

CH_4 conversion with Al_2O_3, TiO_2, and SiO_2-supported catalyst decreased gradually with increasing reaction time, presumably due to the accumulation of carbonaceous material on the catalyst surface. Carbon deposition through the Boudouard reaction (reaction 4) or methane decomposition (reaction 5) is thermodynamically favorable below 900 °C *(15, 24)*.

$$2CO \rightleftarrows C + CO_2 \quad \Delta H^0_{298} = -173 kJ/mol \quad (4)$$

$$CH_4 \rightleftarrows C + 2H_2 \quad \Delta H^0_{298} = +75 kJ/mol \quad (5)$$

Downloaded by COLUMBIA UNIV on September 16, 2012 | http://pubs.acs.org
Publication Date: January 24, 2002 | doi: 10.1021/bk-2002-0809.ch014

Table I. Effect of supports of Ru(0.5 wt%) catalyst on the CO_2 reforming of methane at 600 °C

Catalyst	S. A.	Conversion		Yield		H_2/CO
		CH_4	CO_2	H_2	CO	
	(m^2/g)	(%)		(%)		(ratio)
Y_2O_3	12.9	29.9	35.5	27.1	32.7	0.83
La_2O_3	23.7	28.0	33.0	25.4	30.5	0.83
Nd_2O_3	4.6	27.2	36.1	22.7	31.6	0.72
Pr_6O_{11}	9.9	22.8	29.7	19.3	26.3	0.73
Sm_2O_3	3.2	21.6	29.2	17.7	25.4	0.70
Sc_2O_3	27.1	19.3	26.6	15.7	23.0	0.68
Gd_2O_3	1.4	17.8	26.3	13.6	22.1	0.62
CeO_2	50.7	15.0	23.4	10.8	19.2	0.56
MgO	32.1	12.7	20.2	8.9	16.4	0.54
TiO_2	41.2	12.3	18.7	9.2	15.5	0.66
CaO	4.6	9.5	15.8	6.3	12.6	0.50
Tb_4O_7	13.5	9.3	17.5	5.1	13.4	0.38
Yb_2O_3	2.8	7.2	16.0	2.8	11.6	0.24
Al_2O_3	174.0	6.8	14.3	3.0	10.5	0.28
SiO_2	151.6	4.7	11.3	1.4	8.0	0.18

Catalyst, 0.100g; Silica sand, 0.300g; Space velocity=36,000h^{-1}mL g-cat^{-1}
Flow rate, 60.0mL/min(CH_4/CO_2=1.0); Reaction time = 2 h

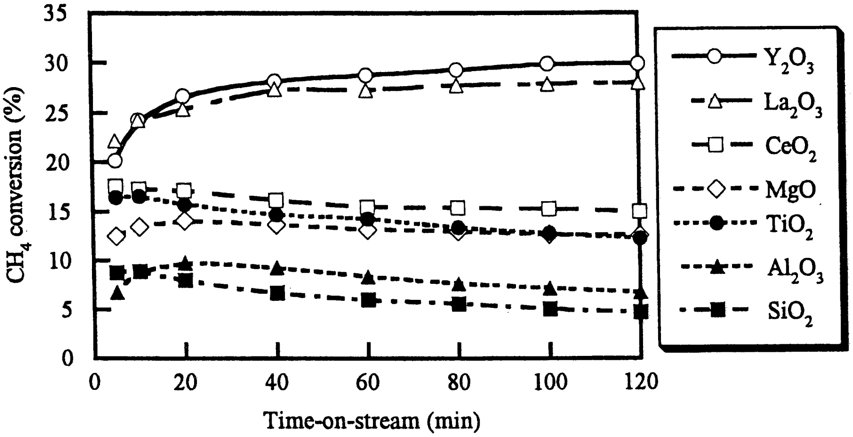

Figure 1. Effect of time-on-stream on the conversion of CH_4 for CO_2 reforming of methane over Ru loaded catalysts. Reaction temperature = 600 °C , Catalyst = 100 mg + 300 mg of silica sand, Ru loading level = 0.5 wt%, Flow rate = 60.0 mL/min (CH_4/CO_2 = 1.0), Space velocity = 36000 h^{-1} ml/g-catalyst

Downloaded by COLUMBIA UNIV on September 16, 2012 | http://pubs.acs.org
Publication Date: January 24, 2002 | doi: 10.1021/bk-2002-0809.ch014

Downloaded by COLUMBIA UNIV on September 16, 2012 | http://pubs.acs.org
Publication Date: January 24, 2002 | doi: 10.1021/bk-2002-0809.ch014

Kinetically, both the Boudouard reaction (reaction 4) and the methane decomposition reaction (reaction 5), which give undesirable carbon, are known to be exceptionally slow in the absence of a catalyst, but both can be readily catalyzed by many transition metals.

Figure 2 shows XRD analyses of Ru(5.0wt%)/La_2O_3 catalyst after the reaction. Lanthanum oxide was transformed into $La_2O_2CO_3$ during reaction. Similar results were reported *(16, 21)*. In addition, metallic Ru and RuO_2 were detected. This result would suggest that to exhibit high activity for CO_2 reforming of methane over Ru/La_2O_3, formation of $La_2O_2CO_3$ and coexistence of metallic Ru and RuO_2 were important.

In Ru-loaded Y_2O_3 and La_2O_3 catalysts, CH_4 conversions gradually increased with time on stream. To investigate increased CH_4 conversions, effect of pretreatment on the CO_2 reforming of methane was carried out with Ru loaded catalysts, and the relations between the activity and product distributions were examined. Figures 3 and 4 show the effect of various pretreatment conditions on the catalytic activity over Ru/La_2O_3 and Ru/Y_2O_3 catalysts. H_2 reduction, CO_2 pretreatment, and CH_4 pretreatment were carried out at 600 °C for 1h, respectively. H_2 reduction followed by CO_2 pretreatment was carried out, at first H_2 reduction for 1h, following CO_2 pretreatment for 1h at 600 °C. Similar results were obtained using La_2O_3 and Y_2O_3 supports. When Ru/La_2O_3 and Ru/Y_2O_3 catalysts were pretreated with CH_4, they were not these catalysts activated for CO_2 reforming of methane. CO_2 pretreatment or H_2 reduction were effective pretreatments for La_2O_3 and Y_2O_3 supports. Most effective pretreatment was H_2 reduction followed by CO_2 pretreatment.

Table II shows effect of pretreatment on the activity for the CO_2 reforming of methane over various metal oxide supported Ru catalysts. CH_4 and CO_2 conversions were greatly affected by the support materials. In all the cases, the CO_2 conversion was higher than that of CH_4. In La_2O_3, Y_2O_3, TiO_2, and SiO_2-supported cases, H_2 yield and H_2/CO ratio after CO_2 pretreatment were higher than that without pretreatment. At 600 °C, all the Ru-loaded catalysts without CO_2 pretreatment afforded a lower H_2/CO ratio than the stoichiometric ratio of unity. Low H_2/CO ratios over Ru-loaded catalysts could be attributed to the reverse water-gas shift reaction shown below:

$$CO_2 + H_2 \rightleftarrows CO + H_2O \quad \Delta H^0_{298} = +41 kJ/mol \quad (6)$$

The excess CO may come from this reaction, and H_2 was consumed to increase CO_2 conversion. This reaction seems to be faster than the CH_4-CO_2 reaction. In contrast, in cases of CO_2 pretreatment, H_2/CO ratio was remarkably improved. It seemed that CO_2 pretreatment suppressed the reverse water-gas shift reaction.

Downloaded by COLUMBIA UNIV on September 16, 2012 | http://pubs.acs.org
Publication Date: January 24, 2002 | doi: 10.1021/bk-2002-0809.ch014

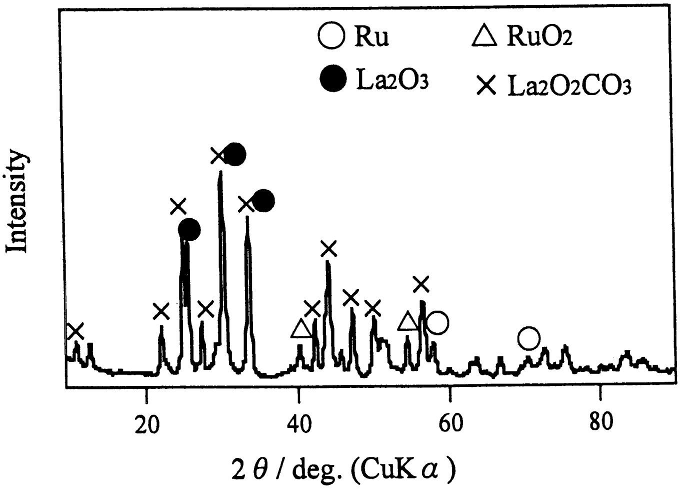

Figure 2. XRD pattern of Ru(5.0 wt%)/La$_2$O$_3$ catalyst after reaction. Ru(5 wt%)/La$_2$O$_3$ was reacted at 600 °C for 1h.

Downloaded by COLUMBIA UNIV on September 16, 2012 | http://pubs.acs.org
Publication Date: January 24, 2002 | doi: 10.1021/bk-2002-0809.ch014

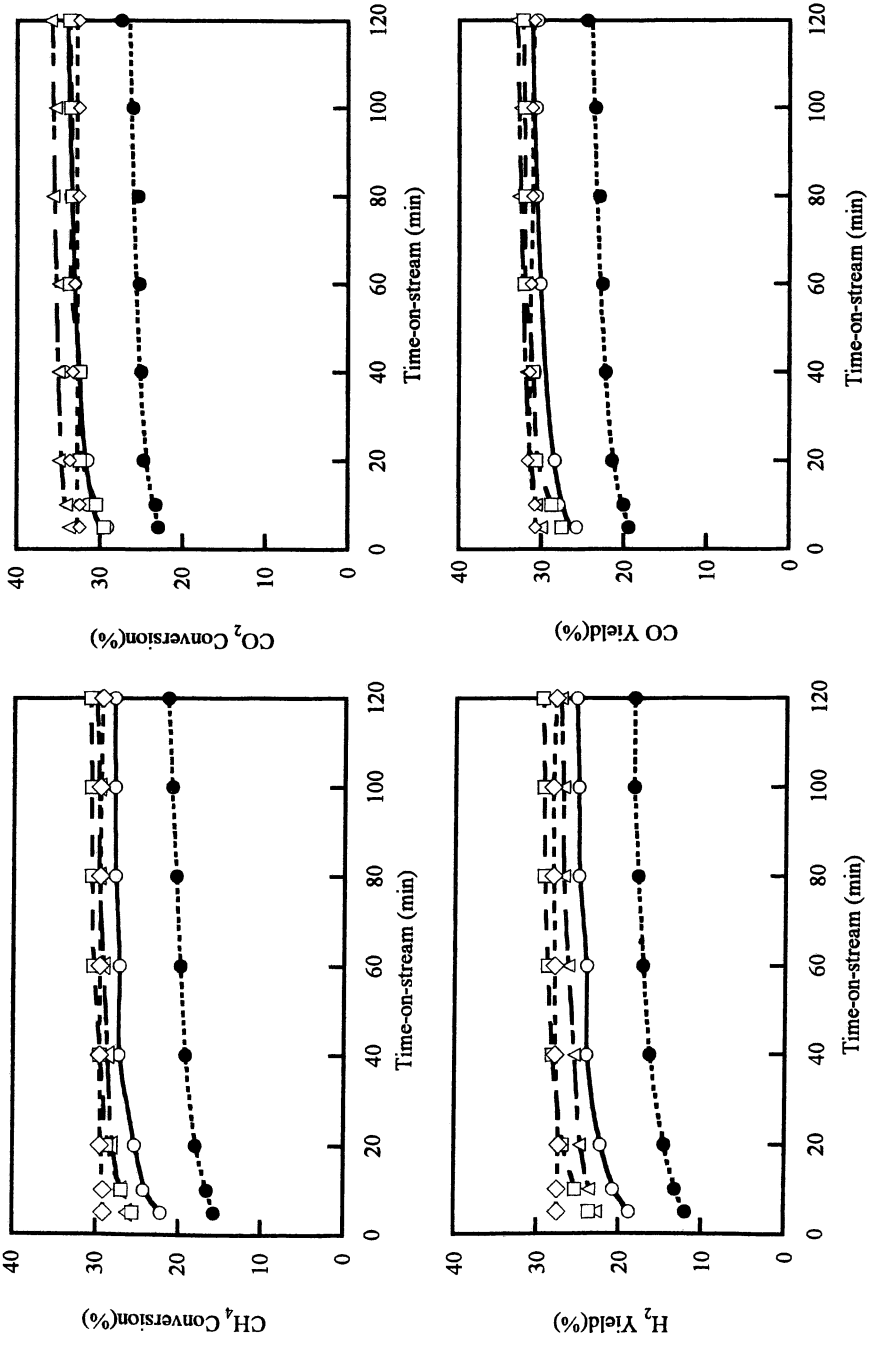

Downloaded by COLUMBIA UNIV on September 16, 2012 | http://pubs.acs.org
Publication Date: January 24, 2002 | doi: 10.1021/bk-2002-0809.ch014

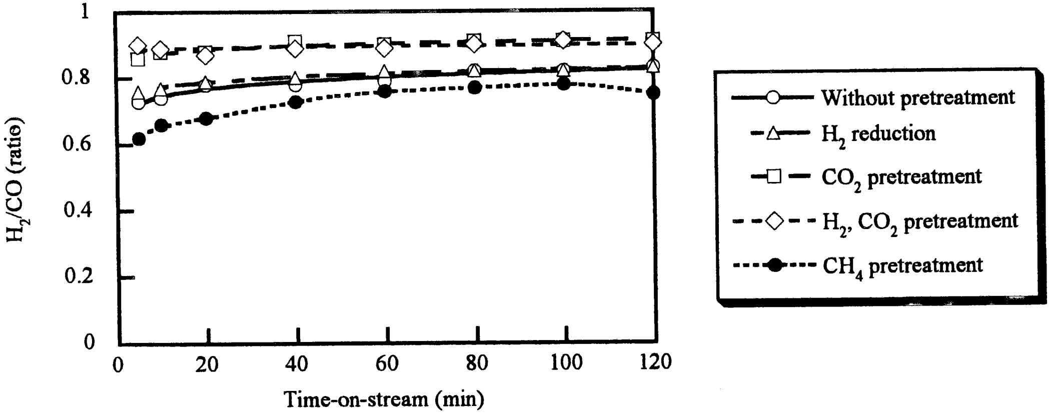

Figure 3. Effect of pretreatment gases on the activity of CO_2 reforming of methane over Ru/La_2O_3 catalyst. Reaction temperature = 600 °C, Catalyst = 100 mg + 300 mg of silica sand, Ru loading level = 0.5 wt%, Flow rate = 60.0 mL/min (CH_4/CO_2 = 1.0), Space velocity = 36000 h^{-1}ml/g-catalyst

Downloaded by COLUMBIA UNIV on September 16, 2012 | http://pubs.acs.org
Publication Date: January 24, 2002 | doi: 10.1021/bk-2002-0809.ch014

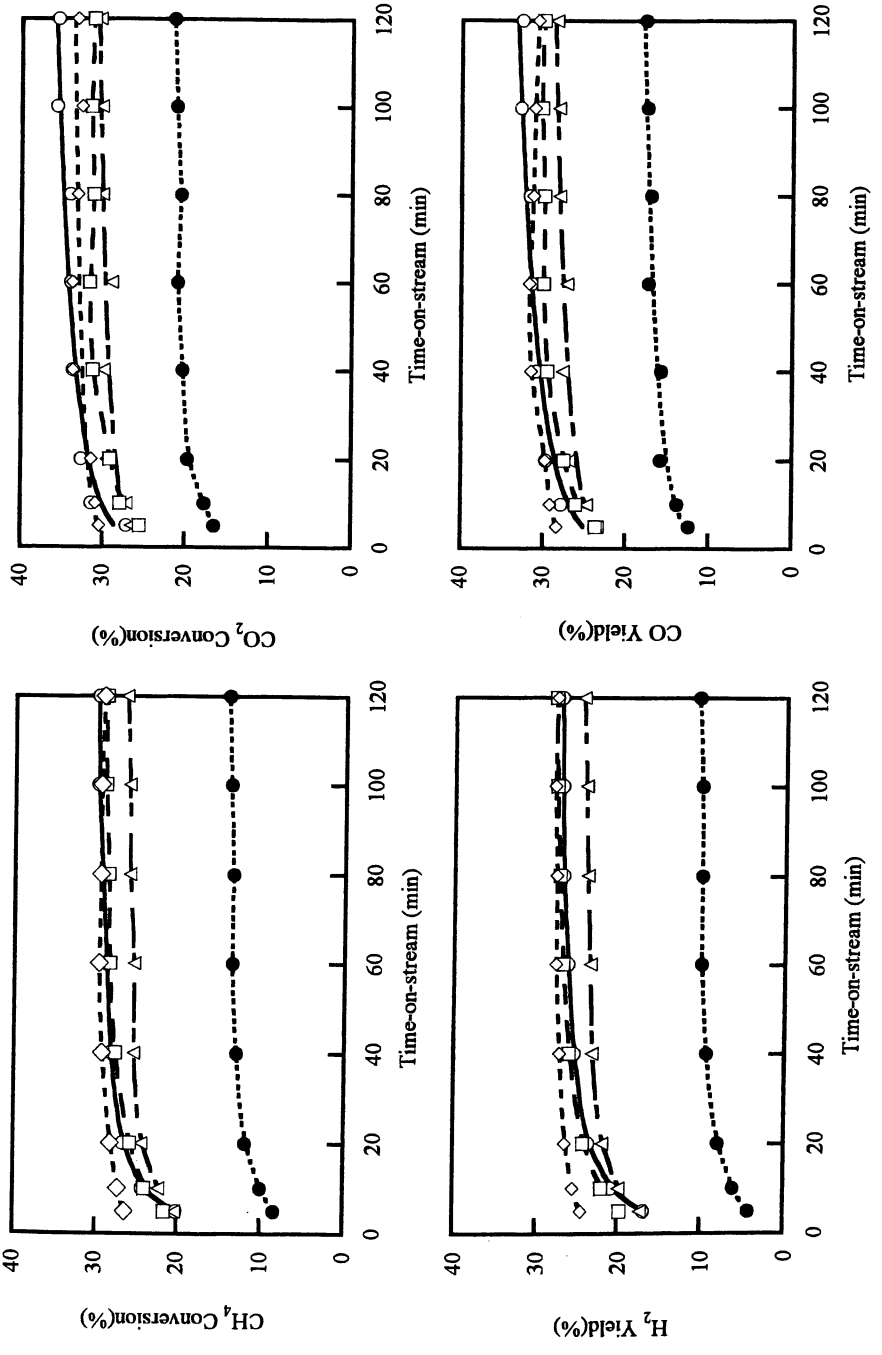

Downloaded by COLUMBIA UNIV on September 16, 2012 | http://pubs.acs.org
Publication Date: January 24, 2002 | doi: 10.1021/bk-2002-0809.ch014

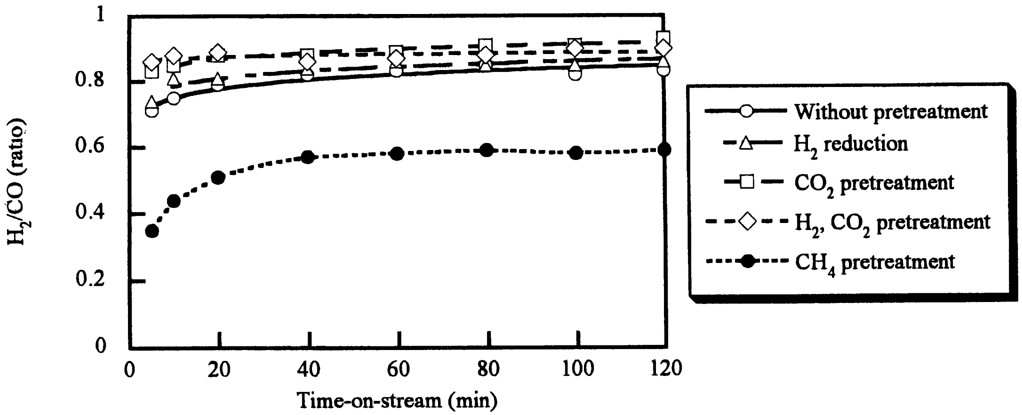

Figure 4. Effect of pretreatment gases on the activity of CO_2 reforming of methane over Ru/Y_2O_3 catalyst. Reaction temperature = 600 °C, Catalyst = 100 mg + 300 mg of silica sand, Ru loading level = 0.5 wt%, Flow rate = 60.0 mL/min (CH_4/CO_2 = 1.0), Space velocity = 36000 h^{-1}ml/g-catalyst

Downloaded by COLUMBIA UNIV on September 16, 2012 | http://pubs.acs.org
Publication Date: January 24, 2002 | doi: 10.1021/bk-2002-0809.ch014

Table II. Effect of pretreatment on the activity for CO_2 reforming of CH_4 at 600 °C over Ru(0.5wt%)-loaded various supports

Catalyst	Reaction	Conversion		Yield		H_2/CO
	time	CH_4	CO_2	H_2	CO	
	(min)	(%)		(%)		(ratio)
La_2O_3	5	22.2	29.1	18.8	25.7	0.73
Without pretreatment	60	27.3	33.1	24.4	30.2	0.81
	120	28.0	33.0	25.4	30.5	0.83
La_2O_3	5	25.5	29.5	23.6	27.6	0.86
CO_2-pretreatment	60	30.4	33.7	28.8	32.1	0.90
	120	30.9	33.7	29.5	32.3	0.91
Y_2O_3	5	20.2	27.1	16.8	23.7	0.71
Without pretreatment	60	28.8	34.0	26.2	31.4	0.83
	120	29.9	35.5	27.1	32.7	0.83
Y_2O_3	5	21.7	25.6	19.7	23.6	0.83
CO_2-pretreatment	60	28.4	31.6	26.8	30.0	0.89
	120	28.9	31.2	27.8	30.0	0.93
Al_2O_3	5	6.8	13.2	3.6	10.0	0.37
Without pretreatment	60	8.4	15.9	4.7	12.2	0.39
	120	6.8	14.3	3.0	10.5	0.28
Al_2O_3	5	7.1	11.8	4.7	9.5	0.49
CO_2-pretreatment	60	5.5	11.6	2.5	8.6	0.29
	120	4.2	10.1	1.3	7.2	0.18
TiO_2	5	16.5	23.1	13.3	19.8	0.77
Without pretreatment	60	14.3	21.1	11.0	17.7	0.75
	120	12.3	18.7	9.2	15.5	0.77
TiO_2	5	26.5	29.1	25.2	27.8	0.91
CO_2-pretreatment	60	20.9	23.9	19.5	22.4	0.87
	120	17.6	21.4	15.8	19.5	0.81
SiO_2	5	8.8	16.1	5.1	12.5	0.38
Without pretreatment	60	6.0	13.0	2.5	9.5	0.47
	120	4.7	11.3	1.4	8.0	0.43
SiO_2	5	17.2	19.9	15.9	18.6	0.85
CO_2-pretreatment	60	8.7	13.7	6.3	11.2	0.56
	120	6.3	11.1	3.9	8.7	0.45

Flow rate, 60.0mL/min(CH_4/CO_2=1.0); Reaction time = 2h
Catalyst, 0.10g; Silica sand, 0.300g; Space velocity=36,000h^{-1}mL g-cat^{-1}

Downloaded by COLUMBIA UNIV on September 16, 2012 | http://pubs.acs.org
Publication Date: January 24, 2002 | doi: 10.1021/bk-2002-0809.ch014

Figures 5, 6, and 7 show XRD analyses of Ru(5.0wt%)/Y_2O_3 and Ru(5.0wt%)/Al_2O_3 catalysts before and after Ar or CO_2 pretreatments. All catalysts were calcined in air at 600 °C for 5h before the pretreatment. Therefore, at first, RuO_2 was formed in the major phase of Ru species. In the Ru/Y_2O_3 catalyst, the chemical species of ruthenium after CO_2 pretreatment were observed both metallic ruthenium and RuO_2. Co-existence of Ru metal and Ru oxide were more effective for CO_2 reforming of methane than single species of metallic Ru or Ru oxide (see Fig. 2). It seems that co-existence of metallic Ru and Ru oxide would play important roles for CO_2 reforming of methane. Thus higher catalytic activity would be exhibited after CO_2 pretreatment over Ru/Y_2O_3 catalyst. After Ar pretreatment, coexistence of Ru metal and Ru oxide was not detected. In the Ru/Y_2O_3 catalyst, CO_2 pretreatment greatly enhanced formation of metallic Ru. During the CO_2 pretreatment, CO was observed, and CO might react with RuO_2 to give metallic Ru. In contrast, in the Ru/Al_2O_3 catalyst, where catalytic activity was not improved by CO_2 pretreatment, Ru metal was not detected after CO_2 pretreatment. Therefore, higher catalytic activity would not be exhibited. In addition, X-ray photoelectron spectroscopic (XPS) analysis also indicated that ruthenium species of the pretreated Ru/Y_2O_3 catalyst was found to be more reduced state than the untreated Ru/Y_2O_3 catalyst. Previously, CO_2 was behaved to be an oxidant of several lower valent transition metal oxides (Fe_3O_4/activated carbon *(25)*, V_2O_4/MgO *(26)*). Such, reducing effect of CO_2 is not consistent with previous results. However, such reducing effect of CO_2 was only observed over La_2O_3 and Y_2O_3 supports, which were basic oxides and were partially transformed into carbonate, to give strongly adsorbed CO_2 species. Electron transfer from these species might have affected oxidation state of ruthenium species.

Table III lists effect of pretreatment on the activity for the CO_2 reforming of methane over noble metal-loaded Y_2O_3 catalysts. Except Ir case, the CH_4 conversion, synthesis gas yield and H_2/CO ratio after CO_2 pretreatment were higher than that of without pretreatment. Especially, in the case of Rh/Y_2O_3 catalysts, the CH_4, CO_2 conversion, and synthesis gas yield remarkably increased. To improve a higher activity in the CO_2 reforming of methane, the activation of CO_2 on the Y_2O_3 support would be one of important factors, in addition to the modification of surface metal spices.

Conclusions

CO_2 reforming of methane with supported Ru catalysts was strongly affected by support oxides and pretreatment. At 600 °C, Ru/Y_2O_3 catalyst showed the highest catalytic activity without pretreatment. CO_2 pretreatment or H_2 reduction were effective pretreatment for La_2O_3 and Y_2O_3 supported Ru catalysts. During CO_2 pretreatment, co-existence of metallic Ru and RuO_2 were

Downloaded by COLUMBIA UNIV on September 16, 2012 | http://pubs.acs.org
Publication Date: January 24, 2002 | doi: 10.1021/bk-2002-0809.ch014

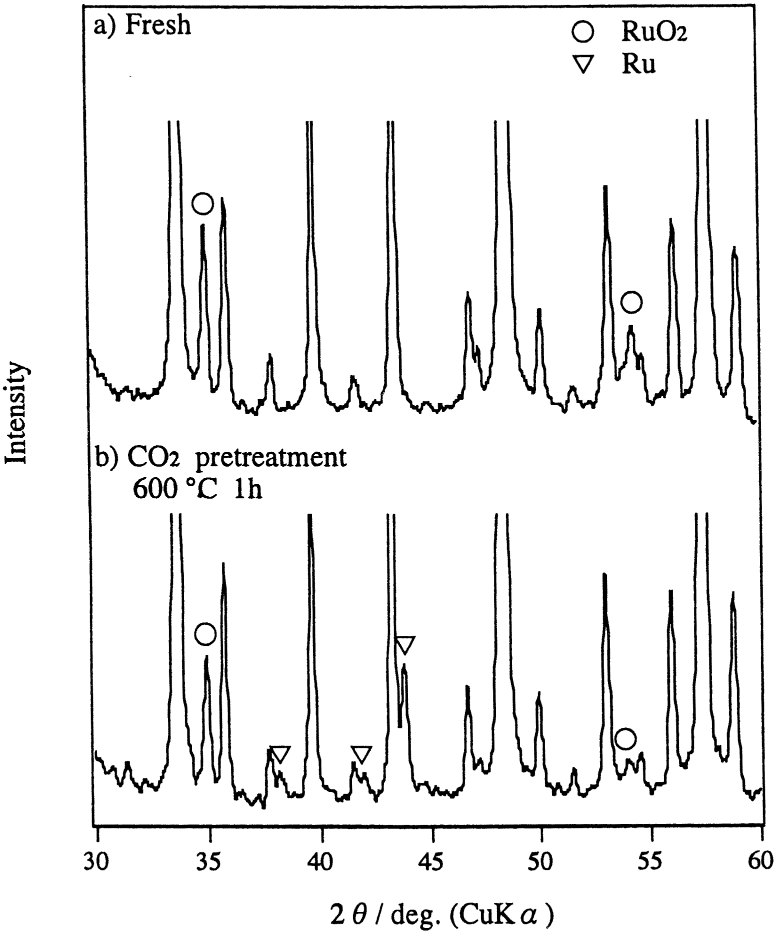

Figure 5. XRD patterns of Ru(5.0 wt%)/Y_2O_3 catalyst before and after heat treatment under CO_2. a)Ru(5.0 wt%)/Y_2O_3 was calcined at 600 °C in air. b) CO_2 pretreatment at 600 °C for 1h.

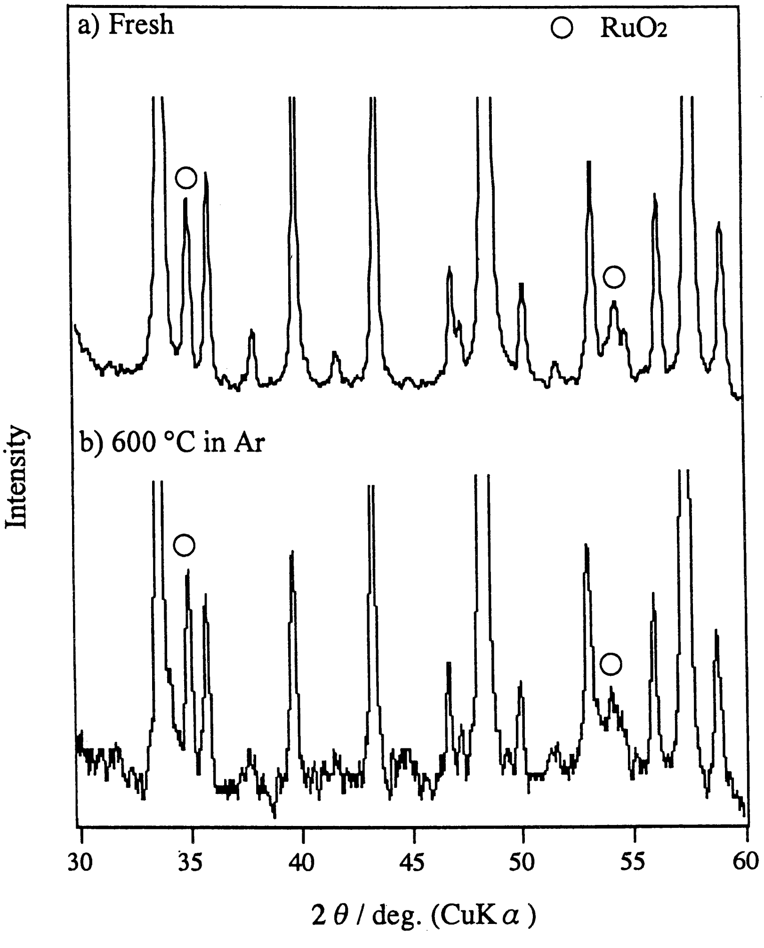

Figure 6. XRD patterns of Ru(5.0 wt%)/Y_2O_3 catalyst before and after heat treatment under Ar. a)Ru(5.0 wt%)/Y_2O_3 was calcined at 600 °C in air. b) Ar pretreatment at 600 °C for 1h.

Downloaded by COLUMBIA UNIV on September 16, 2012 | http://pubs.acs.org
Publication Date: January 24, 2002 | doi: 10.1021/bk-2002-0809.ch014

Downloaded by COLUMBIA UNIV on September 16, 2012 | http://pubs.acs.org
Publication Date: January 24, 2002 | doi: 10.1021/bk-2002-0809.ch014

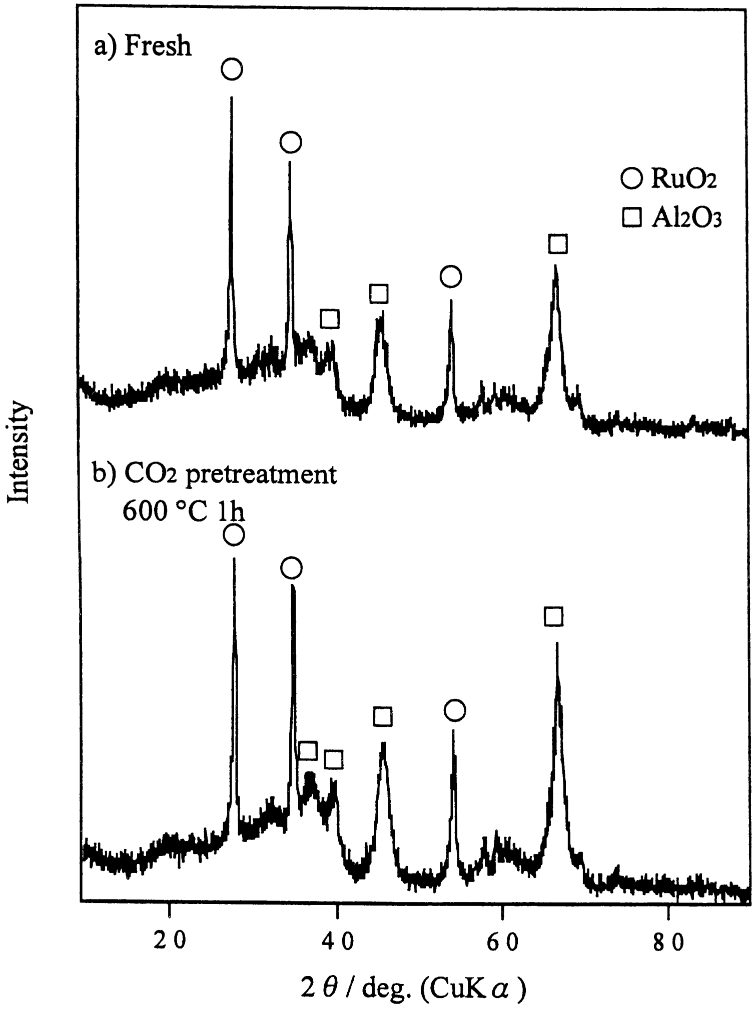

Figure 7. XRD patterns of Ru(5.0 wt%)/Al_2O_3 catalyst before and after heat treatment under CO_2. a)Ru(5.0 wt%)/Al_2O_3 was calcined at 600 °C in air. b) CO_2 pretreatment at 600 °C for 1h.

Table III. Effect of pretreatment on the activity for CO_2 reforming of CH_4 at 600 °C over variours metals-loaded Y_2O_3 catalysts

Catalyst	Reaction	Conversion		Yield		H_2/CO
	time	CH_4	CO_2	H_2	CO	
	(min)	(%)		(%)		(ratio)
Ru(0.5wt%)/Y_2O_3	5	20.2	27.1	16.8	23.7	0.71
Without pretreatment	60	28.8	34.0	26.2	31.4	0.83
	120	29.9	35.5	27.1	32.7	0.83
Ru(0.5wt%)/Y_2O_3	5	21.7	25.6	19.7	23.6	0.83
CO_2-pretreatment	60	28.4	31.6	26.8	30.0	0.89
	120	28.9	31.2	27.8	30.0	0.93
Rh(0.5wt%)/Y_2O_3	5	18.9	23.8	16.4	21.3	0.77
Without pretreatment	60	19.5	25.0	16.8	22.3	0.75
	120	18.1	22.6	15.8	20.4	0.77
Rh(0.5wt%)/Y_2O_3	5	31.2	35.1	29.3	33.1	0.89
CO_2-pretreatment	60	31.2	35.5	29.1	33.4	0.87
	120	30.1	33.7	28.3	31.9	0.89
Pt(0.5wt%)/Y_2O_3	5	18.9	23.8	16.4	21.3	0.77
Without pretreatment	60	19.5	25.0	16.8	2.3	0.75
	120	18.1	22.6	15.8	20.4	0.77
Pt(0.5wt%)/Y_2O_3	5	21.6	26.2	19.3	23.9	0.81
CO_2-pretreatment	60	20.6	24.7	18.5	22.7	0.81
	120	19.9	24.4	17.7	22.2	0.80
Ir(0.5wt%)/Y_2O_3	5	11.0	18.4	7.3	14.7	0.50
Without pretreatment	60	9.1	16.4	5.5	12.8	0.43
	120	8.5	15.9	4.8	12.2	0.39
Ir(0.5wt%)/Y_2O_3	5	8.7	16.0	4.9	12.3	0.40
CO_2-pretreatment	60	8.0	15.9	4.1	11.9	0.34
	120	7.7	15.4	3.8	11.5	0.33
Pd(0.5wt%)/Y_2O_3	5	8.4	16.0	4.6	12.2	0.38
Without pretreatment	60	8.9	15.3	5.7	12.1	0.47
	120	7.5	13.5	4.5	10.5	0.43
Pd(0.5wt%)/Y_2O_3	5	14.0	21.5	10.3	17.8	0.58
CO_2-pretreatment	60	12.1	19.1	8.6	15.6	0.55
	120	10.6	17.7	7.1	14.1	0.50

Flow rate, 60.0mL/min(CH_4/CO_2=1.0); Reaction time = 2h
Catalyst, 0.10g; Silica sand, 0.300g; Space velocity=36,000h^{-1}mL g-cat^{-1}

Downloaded by COLUMBIA UNIV on September 16, 2012 | http://pubs.acs.org
Publication Date: January 24, 2002 | doi: 10.1021/bk-2002-0809.ch014

detected. In order to achieve a high catalytic activity, co-existence of metallic Ru and RuO_2 might be important.

Acknowledgements

This work was has been carried out as a research project of The Japan Petroleum Institute commissioned by the Petroleum Energy Center with the subsidy of the Ministry of International Trade and Industry, Japan. K. Nakagawa is grateful for his fellowship from the Japan Society for the Promotion of Science (JSPS) for Young Scientists.

References

1. Richardson, J. T.; Paripatyadar, S. A. *Appl. Catal.* **1990,** 61. 293.
2. Ashcroft, A. T.; Cheetham, A. K.; Green, M. L. H.; Vernon, D. D. F. *Nature.* **1991,** 352. 18.
3. Tomishige, K.; Fujimoto, K. *Catal. Surv. Jpn.* **1998,** 2. 3.
4. Fischer, F.; Tropsch, H. *BrennstoffChem.* **1928,** 9. 39.
5. Rostrup-Nielsen, J.R. *Stud. Surf. Sci. Catal.* **1994,** 81. 25.
6. Sodwsawa, T.; Dobashi, A.; Nozaki, F.; *React. Kinet. Catal. Lett.* **1979,** 12. 107.
7. Erdöhelyi, A.; Cserényi , J.; Solymosi, F. *J. Catal.* **1993,** 141. 287.
8. Rostrup-Nielsen, J.R.; Hansen, J.H.B. *J. Catal.* **1993,** 144. 38.
9. Solymosi, F.; Kutsan, G.; Erdöhelyi, A. *Catal. Lett.* **1991,** 11. 149.
10. Zhang, Z.L.; Tsipouriari, V.A.; Efstathiou, A.M.; Verykios, X.E. *J. Catal.* **1996,** 158. 51.
11. Nakamura, J.; Aikawa, K.; Sato, K.; Uchijima, T. *Catal. Lett.* **1994,** 25. 265.
12. Erdöhelyi, A.; Cserényi, J.; Papp, E.; Solymosi, F. *Appl. Catal. A.* **1994,** 108. 205.
13. Vernon, P.D.F.; Green, M.L.H.; Cheetham, A.K.; Ashcroft, A.T. *Catal. Today.* **1992,** 13. 417.
14. Rostrup-Nielsen, J.R. *Catal. Today.* **1993,** 18. 305.
15. Rostrup-Nilsen, J.R. in *Catalysis, Science and Tecnology*, edited by Anderson, J.R.; Boudart, M. Springer, Berlin, 1984; Vol. 5, pp 1-117.
16. Zhang, Z.L.; Verykios, X.E. *Appl. Catal. A.* **1995,** 138. 109.
17. Zhang, Z.L.;Verykios, X.E.;MacDonald, S.M.; Affossman, S. *J. Phy. Chem.* **1996,** 100. 744.
18. Yamazaki, O.; Nozaki, T.; Omata, K.; Fujimoto, K. *Chem. Lett.* **1992,** 1953.
19. Nakagawa, K.; Ikenaga, N.; Suzuki, T.; Kobayashi, T.; Haruta, M. *Appl. Catal. A.* **1998,** 169. 281.
20. Nakagawa, K.; Anzai, K.; Matsui, N.; Ikenaga, N.; Suzuki, T.; Teng, Y.; Kobayashi, T.; Haruta, M. *Catal. Lett.* **1998,** 51. 163.

Downloaded by COLUMBIA UNIV on September 16, 2012 | http://pubs.acs.org
Publication Date: January 24, 2002 | doi: 10.1021/bk-2002-0809.ch014

21. Fujimura, S.; Nakagawa, K.; Ikenaga, N.; Suzuki, T. *Sekiyu Gakkaishi.* **1997,** 4. 179.
22. Matsui, N.; Anzai, K.; Akamatsu, N.; Nakagawa, K.; Ikenaga, N.; Suzuki, T. *Appl. Catal. A.* **1999,** 179. 247.
23. Matsui, N.; Nakagawa, K.; Ikenaga, N.; Suzuki, T. *J. Catal.* **2000,** 194. 115.
24. Tsang, S.C.; Claridge, J.B.; Green, M.L.H. *Catal. Today.* **1996,** 23. 3.
25. Sugino, M.; Shimada, H.; Tsuruda, T.; Miura, H.; Ikenaga, N.; Suzuki, T. *Appl. Catal. A.* **1995,** 121. 125.
26. Sakurai, Y.; Suzaki, T.; Nakagawa, K.; Ikenaga, N.; Aota, H.; Suzuki, T. *Chem. Lett.* **2000,** 526.

Downloaded by COLUMBIA UNIV on September 16, 2012 | http://pubs.acs.org
Publication Date: January 24, 2002 | doi: 10.1021/bk-2002-0809.ch014

Downloaded by OHIO STATE UNIV LIBRARIES on September 16, 2012 | http://pubs.acs.org
Publication Date: January 24, 2002 | doi: 10.1021/bk-2002-0809.ch015

Chapter 15

CO_2 Reforming and Simultaneous CO_2 and Steam Reforming of Methane to Syngas over $Co_xNi_{1-x}O$ Supported on Macroporous Silica–Alumina Precoated with MgO

V. R. Choudhary[1], A. S. Mamman[1], B. S. Uphade[1], and R. E. Babcock[2]

[1]Chemical Engineering Division, National Chemical Laboratory, Pune 411 008, India
[2]Chemical Engineering Department, University of Arkansas, 3202 Bell Engineering Center, Fayetteville, AR 72701

Reaction of CO_2 with methane in the absence and presence of steam over Co_xNiO_{1-x} ($x = 0.0$-0.5) supported on commercial macroporous silica-alumina catalyst carrier (SA-5205, obtained from M/S Norton Co. U.S.A.) precoated with MgO at different temperatures (700°-900°C) and contact times (0.03-0.3 s at STP) has been investigated. With the increasing Co/Ni ratio of the catalyst, its surface area is decreased and its degree of reduction by H_2 at 900°C (for 1h) is increased. TPR (from 100° to 900°C) of the catalysts indicated that the NiO-CoO-MgO in the catalyst exists as a solid solution. The influence of Co/Ni ratio of the catalyst and feed ratios [$CO_2/CH_4 = 0.8 - 1.2$ in the CO_2 reforming and $(CO_2+H_2O)/CH_4 = 1.2$ and $CO_2/H_2O = 0.4 - 2.0$ in the simultaneous CO_2 and steam reforming] on the conversion and selectivity or H_2/CO product ratio has also been thoroughly investigated. When the Co/Ni ratio is increased, in the CO_2 reforming, the carbon deposition on the catalyst is reduced drastically and the conversion of methane and CO_2, H_2 selectivity and H_2/CO ratio is passed through a maximum. The conversion in the simultaneous CO_2 and steam reforming is also passed through a maximum, at the Co/Ni ratio of about 0.17. The supported catalyst with Co/Ni ratio of 0.17 shows high methane conversion activity (methane conversion > 95%) and 100% selectivity for both CO and H_2 with H_2/CO ratio varying from 1.2 - 2.2 in the simultaneous CO_2 and steam reforming processes at a high space velocity. The H_2/CO ratio can be controlled by manipulating the H_2O/CO_2 ratio in the feed; it is increased with increasing the H_2O/CO_2 ratio and vice versa.

Downloaded by OHIO STATE UNIV LIBRARIES on September 16, 2012 | http://pubs.acs.org
Publication Date: January 24, 2002 | doi: 10.1021/bk-2002-0809.ch015

Release of large quantities of CO_2 in the atmosphere has created a large greenhouse effect causing a global warming. Hence worldwide efforts are being made for conversion of CO_2 to useful products. One of the ways of activating CO_2 is its reaction with methane to carbonmonoxide and hydrogen, commonly known as CO_2 reforming of methane. In the last few years, the research activities on the CO_2 reforming of methane have gained a lot of momentum (1). Several studies on this reaction over different catalysts, such as supported Pt group metals (2-10), Ni/MgO (6, 11), Ni/Al_2O_3 (12), Ni/MgO-CaO (13), NiO-CaO (14) and NiO/MgO/SA-5205 (15), have been reported. A rapid coke deposition on the catalyst is, however, a serious problem in the CO_2 reforming of methane, particularly when Ni- containing catalyst is used (6, 14). CO_2 reforming simultaneously with steam reforming and/or oxidative conversion of methane over NiO-CaO (14, 16, 17), NiO-MgO (11) and $LaNiO_3$ (18), Ni/ALPO-5 (19) and NiO/MgO/SA-5205 (15) catalysts have also been reported earlier. The coke formation in CO_2 reforming over NiO-CaO catalyst was reduced drastically by carrying out the CO_2 reforming simultaneously with steam reforming (14) or oxidative conversion (17) of methane to syngas.

Our earlier study (20) revealed that the addition of cobalt to unsupported Ni-containing catalyst causes a drastic reduction in the carbon formation in the oxidative conversion of methane to syngas. It is, therefore, interesting to study the effect of cobalt addition to Ni-containing catalysts on carbon deposition on them in the CO_2 reforming. Also, in our earlier studies, NiO supported on a low surface area macroporous silica-alumina catalyst carrier precoated with MgO showed high activity and selectivity in the steam reforming, CO_2 reforming and simultaneous steam and CO_2 reforming of methane to syngas in the presence or absence of O_2 (15, 21) .The present work was undertaken for studying the influence of cobalt addition to this catalyst on its activity and selectivity and also on the filamental carbon formation in the CO_2 reforming with or without simultaneous steam reforming at different process conditions.

Experimental

Supported $Co_xNi_{1-x}O$ (14.0 ± 0.5 wt%)/MgO/SA-5205 (x = 0.0, 0.05, 0.15, 0.29, and 0.5) catalysts (Table 1) were prepared by depositing mixed nitrates of

Ni and Co with desired Co/Ni ratio (0.0, 0.053, 0.17, 0.41, or 1.0) from their aqueous solution on 22-30 mesh size particles of commercial catalyst carrier, SA-5205 [sintered low surface area macroporous support, obtained from M/S Norton Co. USA] precoated with MgO, using an incipient wetness impregnating technique, followed by drying and decomposing(or calcining) in air at 900°C for 4h. The catalyst carrier was precoated with MgO by impregnating the carrier with Mg-nitrate, drying and decomposing as above. The support consists mainly of alumina (86.1%) and silica (11.8 wt%) and its surface area, porosity, pore volume and average pore size are <0.01 m^2 g^{-1}, 54%, 0.35 cm^3 g^{-1} and 200 μm, respectively.

The catalyst was characterized for its surface area by the single point BET method, using a Monosorb Surface Area Analyzer (Quanta Chrome Corp., USA). The catalyst was also characterized by its temperature programmed reduction (TPR) from 100° to 900°C with a linear heating rate of 20°C min^{-1} in a flow of H_2-Ar (3.7 mol% H_2) mixture (space velocity = 6,000 $cm^3.g^{-1}.h^{-1}$) in a quartz reactor (i.d. 4 mm) having a low dead volume. The hydrogen consumed in the TPR was measured quantitatively by a thermal conductivity detector (TCD). Before the TPR, the catalyst was pretreated in a flow of He at 900°C for 1h.

The catalytic reactions for CO_2 reforming and simultaneous steam and CO_2 reforming of methane over the catalysts were carried out at the atmospheric pressure in a continuous flow quartz reactor (i.d. 9 mm) packed with 0.3 g catalyst and provided with a chromel-alumel thermocouple located in the center of the catalyst bed. The feed was a mixture of pure methane (> 99.95 %), CO_2 and (99.99 %) with or without steam. Water was added to the feed using a SAGE syringe pump and a specially designed evaporator. Before carrying out the reaction, the catalyst was heated insitu at 900°C in a flow (50 $cm^3.min^{-1}$) of moisture-free nitrogen for 1 h. The catalytic reactions were carried out at different temperatures, gas hourly space velocities (GHSV, measured at 0°C at 1 atm) and relative concentrations of methane, steam, CO_2 in the feed. The product gases (after condensation of the water from them at 0°C) were analyzed by an on-line gas chromatography with TCD, using a Spherocarb column and He as a carrier gas. The conversion/selectivity data were collected after a reaction period of 30 min. For the CO_2 reforming reaction, a fresh catalyst was used for every experiment. The H_2 and CO selectivities reported in this paper are based on the methane conversion.

Downloaded by OHIO STATE UNIV LIBRARIES on September 16, 2012 | http://pubs.acs.org
Publication Date: January 24, 2002 | doi: 10.1021/bk-2002-0809.ch015

Results

Catalyst Characterization

Results showing the influence of Co/Ni ratio in the catalyst on surface area are given in Table 1. The surface area is decreased appreciably with increasing the Co/Ni ratio in the catalyst.

Figure 1 shows curves for the TPR (by H_2) from 100° to 900°C of the catalyst with different Co/Ni ratios (0.05 - 1.0). The TPR of the catalyst without cobalt (NiO/MgO/SA-5205) is given earlier (15). The TPR curves are quite similar to that observed for the catalyst without cobalt (15, 21) and also for a NiO-MgO solid solution (22, 23), except for a small hump between 400° and 650°C (Fig. 1). The hump is more pronounced for the catalyst with higher Co/Ni ratios and it is shifted towards the lower temperature side with increasing the Co/Ni ratio. The peak maximum temperature for all the TPR curves is 900°C. However, this is not a true peak maximum temperature as the maximum temperature chosen for the TPR itself is 900°C. Hence, true maximum temperature is expected to be above 900°C.

The degree of reduction of $Co_xNi_{1-x}O$ from the catalyst is increased with increasing its Co/Ni ratio (Table 1). The degree of reduction was estimated from the knowledge of the concentration of CoO and NiO in the catalyst and the amount of H_2 consumed in the TPR, and assuming the reaction stoichiometry (CoO or NiO + $H_2 \rightarrow Co^o$ or $Ni^o + H_2O$).

TABLE I. Surface Area and Degree of Reduction (in the TPR) of the $Co_xNi_{1-x}O$/MgO/SA-5205 (x = 0.0-0.5) Catalysts

x	*Co/Ni Mol ratio*	*Surface area ($m^2\ g^{-1}$)*	*Degree of reduction (%)*
0.0	0.0	2.0	34.5
0.05	0.053	1.9	49.7
0.15	0.17	1.6	61.7
0.29	0.41	1.3	65.1
0.50	1.0	1.1	72.5

Downloaded by OHIO STATE UNIV LIBRARIES on September 16, 2012 | http://pubs.acs.org
Publication Date: January 24, 2002 | doi: 10.1021/bk-2002-0809.ch015

Downloaded by OHIO STATE UNIV LIBRARIES on September 16, 2012 | http://pubs.acs.org
Publication Date: January 24, 2002 | doi: 10.1021/bk-2002-0809.ch015

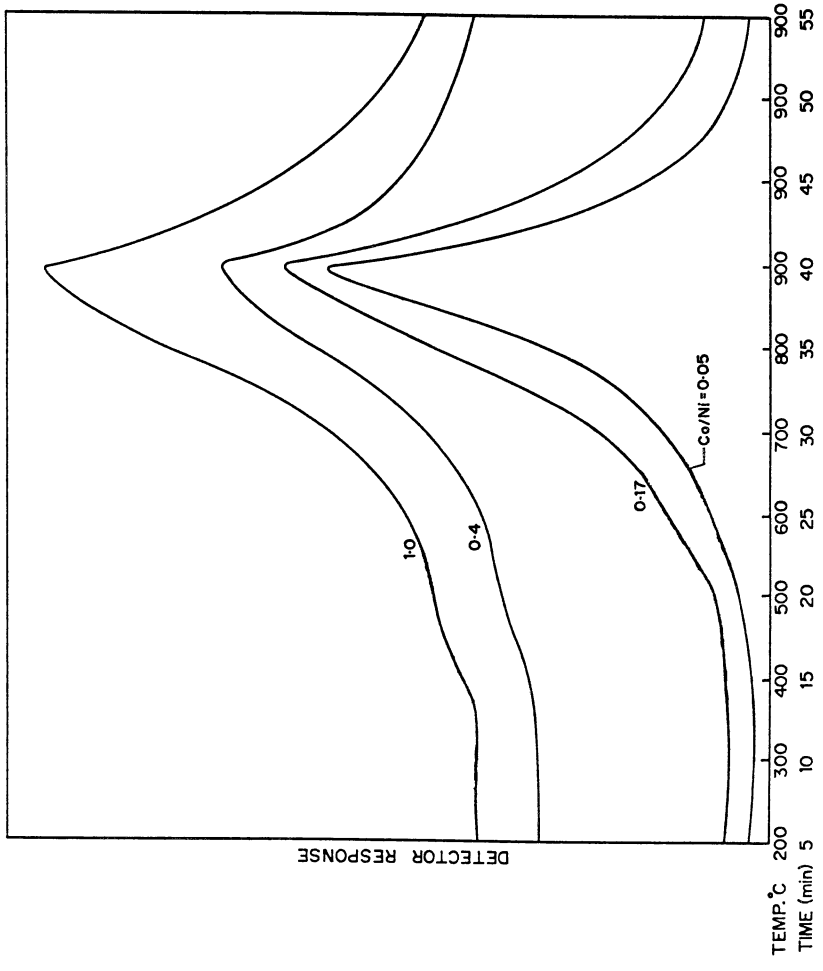

Figure 1. TPR of the catalysts with different Co/Ni ratios.

CO_2 Reforming of Methane

In order to find the influence of Co/Ni ratio on the extent of filamental carbon formation on the catalyst, particularly in the CO_2 reforming of methane at different temperatures, a pressure drop across the catalyst bed after a reaction period of 1.0 h was measured. Results showing the influence of Co/Ni ratio on the pressure drop across the catalyst bed due to filamental carbon formation in the CO_2 reforming at different temperatures (700°-900°C) are presented in Fig.2. At all the temperatures the pressure drop and consequently the extent of filamental carbon formation on the catalyst is decreased exponentially with increasing the Co/Ni ratio. It is also strongly influenced by the reaction temperature; it is increased with increasing the temperature. The pressure drop in all the cases was reduced to its original value after oxidative removal of the carbon from the catalyst in a flow of nitrogen-air mixture (25% air) at 500°-600°C.

Results showing the influence of Co/Ni ratio of the catalyst on the conversion, H_2 selectivity, and H_2/CO product ratio in the CO_2 reforming of methane to syngas for a low contact time (high space velocity) are presented in Fig. 3. At all the temperatures, the conversion, selectivity and H_2/CO ratio are passed through a maximum at the Co/Ni ratio of about 0.17. This indicates that at this optimum Co/Ni ratio, the catalyst shows the best performance in the CO_2 reforming. The performance of the catalyst with the optimum Co/Ni ratio (0.17) in the CO_2 reforming of methane at different process conditions is presented in Fig. 4. Figure 4 also shows the influence of temperature, space velocity and CH_4/CO_2 feed ratio on the conversion of both methane and CO_2, H_2 selectivity and H_2/CO product ratio in the process.

Following general observations can be made from the results (Figs. 3 and 4):

- The conversion of CO_2 is higher than that of CH_4.
- The H_2 selectivity and H_2/CO ratio (except at 900°C for the intermediate Co/Ni ratios) are less than 100% and 1.0, respectively.

These observations indicate that, along with the CO_2 reforming of methane ($CH_4+CO_2 \rightarrow 2CO+2H_2$), a reverse water gas shift reaction, ($CO_2+H_2 \rightarrow CO+H_2O$) also occurs simultaneously, depending upon the process conditions. This side reaction is favored at lower temperature, higher space velocity and higher CO_2/CH_4 ratio; the H_2/CO ratio is increased with increasing temperature but decreased with increasing space velocity and CO_2/CH_4 feed ratio (Fig. 4).

Downloaded by OHIO STATE UNIV LIBRARIES on September 16, 2012 | http://pubs.acs.org
Publication Date: January 24, 2002 | doi: 10.1021/bk-2002-0809.ch015

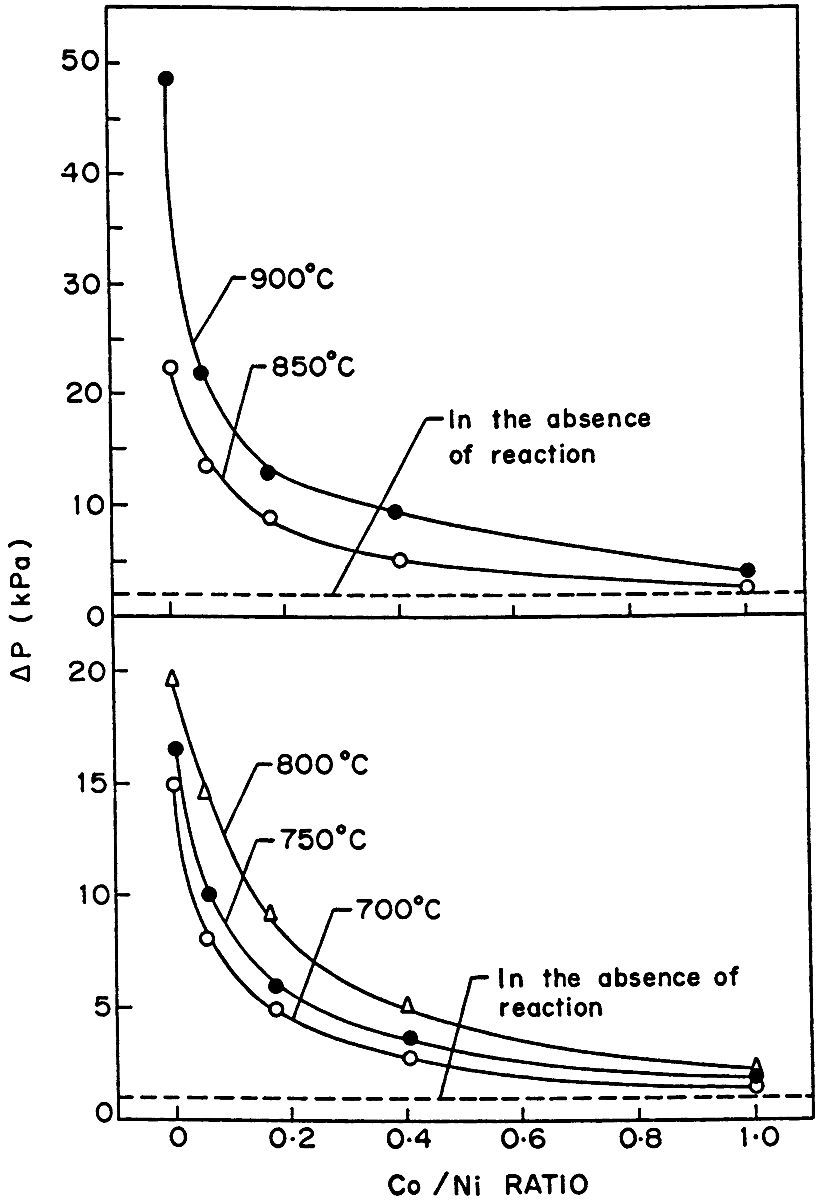

Figure 2. Influence of Co/Ni ratio in the catalyst on the pressure drop across the catalyst bed in the CO_2 reforming of methane over the catalysts at different temperatures (CO_2/CH_4 feed ratio = 1.0 and GHSV = 3.9×10^4 cm^3 g^{-1} h^{-1}).

Downloaded by OHIO STATE UNIV LIBRARIES on September 16, 2012 | http://pubs.acs.org
Publication Date: January 24, 2002 | doi: 10.1021/bk-2002-0809.ch015

Downloaded by OHIO STATE UNIV LIBRARIES on September 16, 2012 | http://pubs.acs.org
Publication Date: January 24, 2002 | doi: 10.1021/bk-2002-0809.ch015

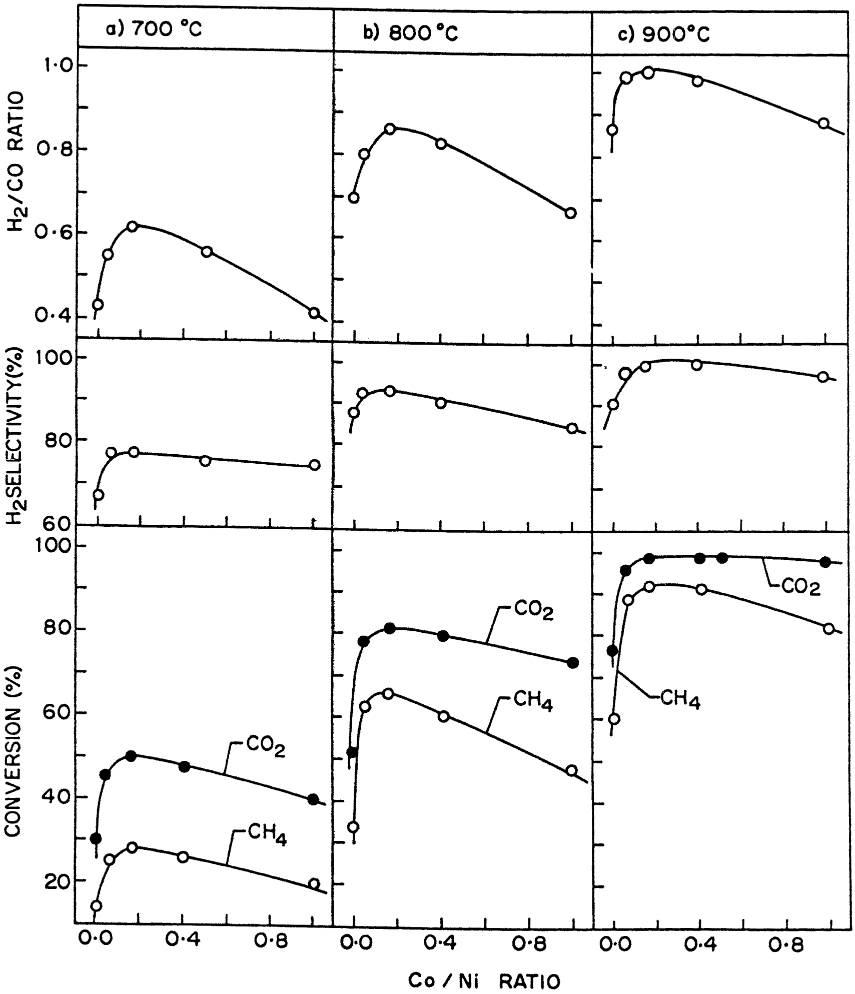

Figure 3.Influence of Co/Ni ratio in the catalyst on its performance in the CO_2 reforming of methane at different temperatures (CO_2/CH_4 feed ratio = 1.0 and GHSV = 3.9 x 10^4 cm^3 g^{-1} h^{-1}).

Downloaded by OHIO STATE UNIV LIBRARIES on September 16, 2012 | http://pubs.acs.org
Publication Date: January 24, 2002 | doi: 10.1021/bk-2002-0809.ch015

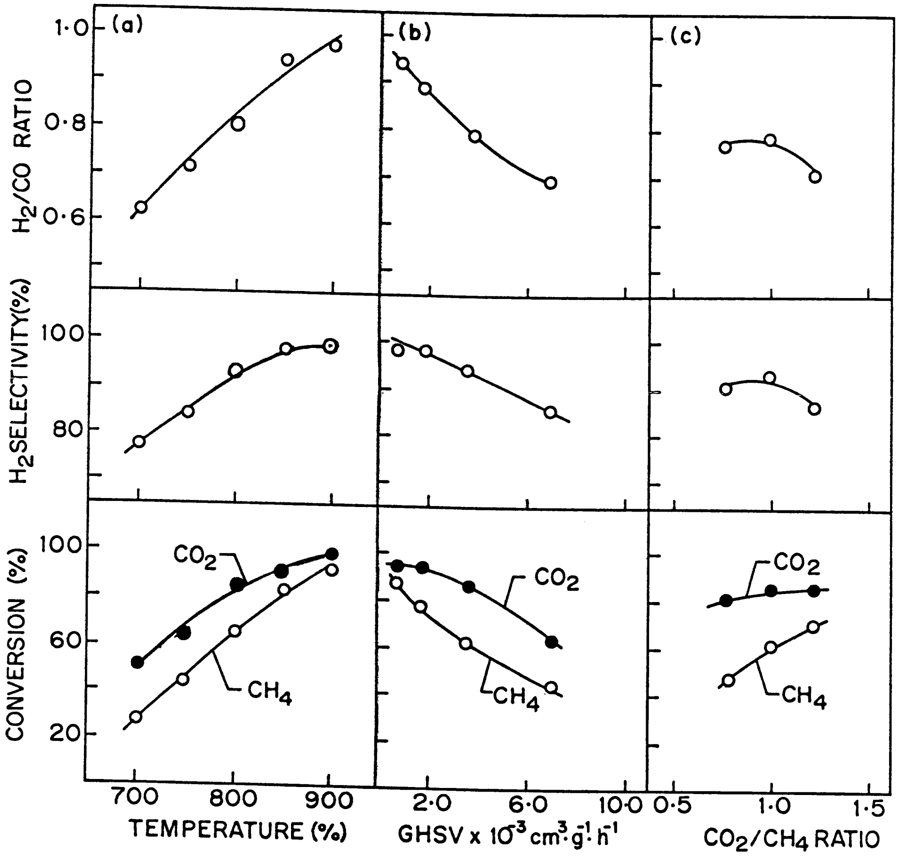

Figure 4.Influence of a) reaction temperature (CH_4/CH_4 = 1.0 and GHSV = 3.9 x 10^4 cm^3 g^{-1} h^{-1}) b) space velocity (at 800°C and CO_2/CH_4 = 1.0) and c) CO_2/CH_4 ratio (at 800°C and GHSV = 3.9 x 10^4 cm^3 g^{-1} h^{-1}) on the conversion, CO selectivity and H_2/CO product ratio in the CO_2 reforming of methane over the catalyst with Co/Ni ratio of 0.17.

Simultaneous CO_2 and Steam Reforming of Methane

Figure 5 shows the influence of Co/Ni ratio on the catalyst performance (conversion of methane, CO_2 and water and H_2/CO product ratio) in the simultaneous CO_2 reforming ($CH_4+CO_2 \rightarrow 2CO+2H_2$) and steam reforming ($CH_4+ H_2O \rightarrow CO+3H_2$). The catalyst performance is strongly influenced by the Co/Ni ratio, similar to that was observed for the CO_2 reforming of methane. In this case also, the catalyst shows highest activity when its Co/Ni ratio is 0.17; the conversion of all the reactants is passed through a maximum for the catalyst with (Co/Ni ratio = 0.17). The H_2/CO ratio is, however, passed through a minimum at this Co/Ni ratio (Fig. 5).

Results showing the performance of the catalyst with its optimum Co/Ni ratio in the simultaneous CO_2 and steam reforming process at different process conditions are presented in Figs. 6 and 7.

Results in Fig. 6 show a strong influence of space velocity on the conversion of all the reactants but almost no effect on the H_2/CO ratio. The H_2/CO ratio is, however, decreased markedly with increasing the CO_2/H_2O feed ratio for a constant $(CO_2+H_2O)/CH_4$ feed ratio (Fig. 7).

The pressure drop across the catalyst bed for all the catalysts at the different process conditions was negligibly small, indicating a little or no formation of the filamental carbon on the catalyst during the simultaneous CO_2 and steam reforming process.

Discussion

The above results reveal that the surface properties, filamental carbon formation in the CO_2 reforming of methane and catalytic activity in the CO_2 and/or steam reforming of methane are strongly influenced by increasing the Co/Ni ratio of the catalyst.

The decrease in the surface area with increasing the Co/Ni ratio (Table 1) indicates that the addition of cobalt causes sintering or crystal growth of the catalyst. Since, the surface area of the support is very low ($0.01\ m^2\ g^{-1}$), the observed surface area of the catalyst is mainly because of the active catalytic components (i.e. oxides of nickel and Co and MgO) deposited on the support.

The dependence of the trend of the TPR curves (Fig. 1) and degree of catalyst reduction (Table 1) on the Co/Ni ratio shows that the rate of catalyst reduction is enhanced because of the addition of cobalt to the catalyst. The observed hump at low temperature may be due to a faster reduction of that of cobalt oxide, which has not formed a solid solution in the MgO. Both NiO and CoO can form a complete solid solution in MgO (22). However, since the ionic

Downloaded by OHIO STATE UNIV LIBRARIES on September 16, 2012 | http://pubs.acs.org
Publication Date: January 24, 2002 | doi: 10.1021/bk-2002-0809.ch015

Downloaded by OHIO STATE UNIV LIBRARIES on September 16, 2012 | http://pubs.acs.org
Publication Date: January 24, 2002 | doi: 10.1021/bk-2002-0809.ch015

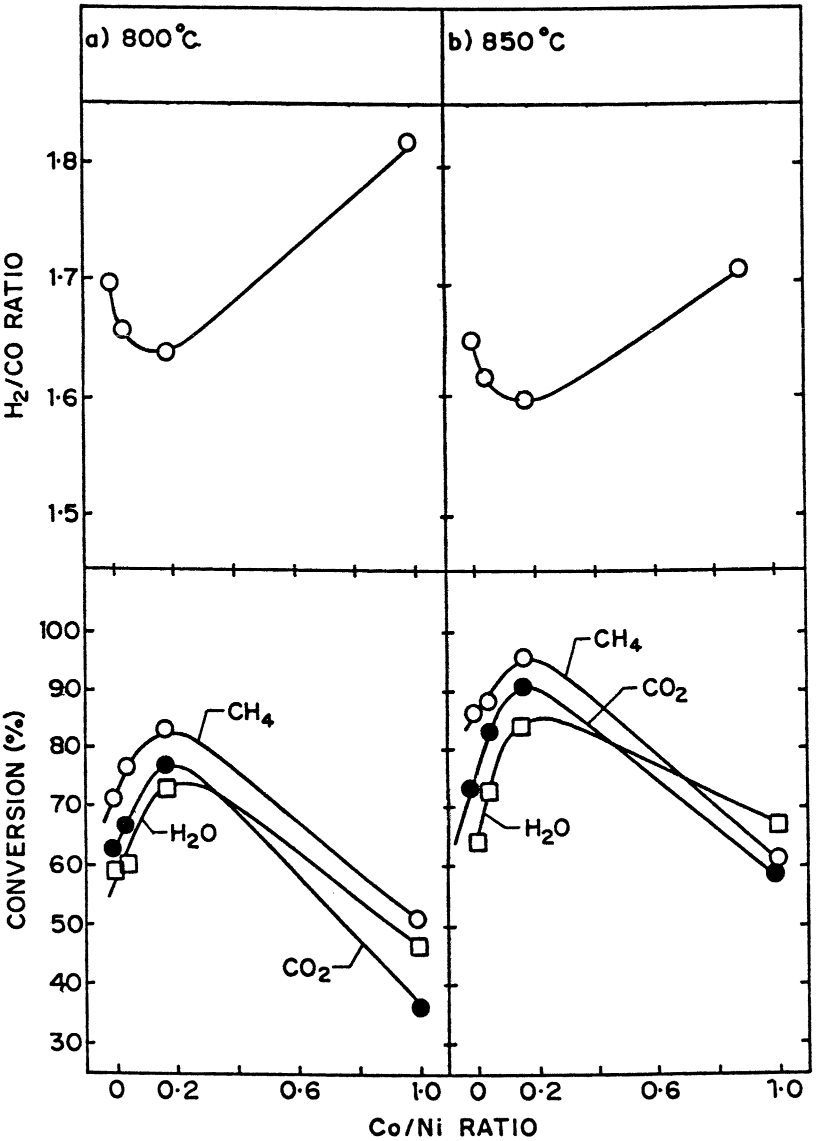

Figure 5.Influence of Co/Ni ratio in the catalyst on its performance in the simultaneous CO_2 and steam reforming of methane at 800^0 and $850^0C(CO_2/CH_4$ feed ratio = 0.55, H_2O/CH_4 feed ratio = 0.57 and GHSV = 5.1 x 10^4 cm^3 g^{-1} h^{-1}).

Downloaded by OHIO STATE UNIV LIBRARIES on September 16, 2012 | http://pubs.acs.org
Publication Date: January 24, 2002 | doi: 10.1021/bk-2002-0809.ch015

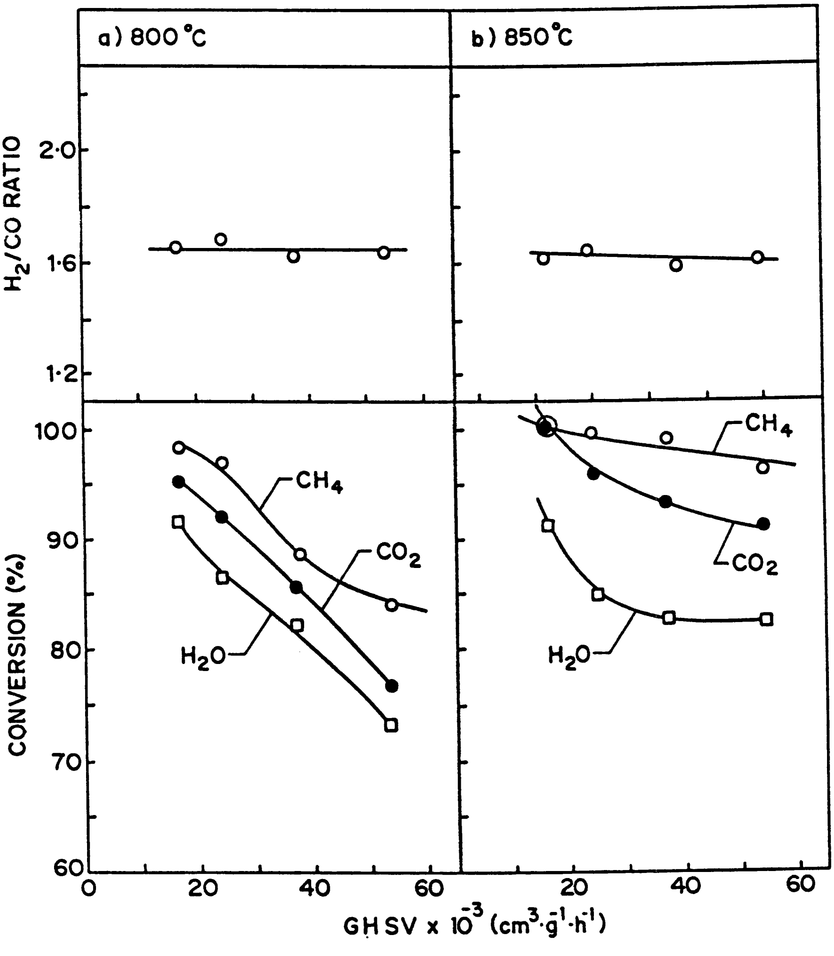

Figure 6. Influence of GHSV on the conversion and H_2/CO product ratio in the simultaneous steam and CO_2 reforming of methane over the catalyst with Co/Ni ratio of 0.17 at 800° and 850°C (CO_2/CH_4 and H_2O/CH_4 feed ratios = 0.57 and 0.57, respectively).

Downloaded by OHIO STATE UNIV LIBRARIES on September 16, 2012 | http://pubs.acs.org
Publication Date: January 24, 2002 | doi: 10.1021/bk-2002-0809.ch015

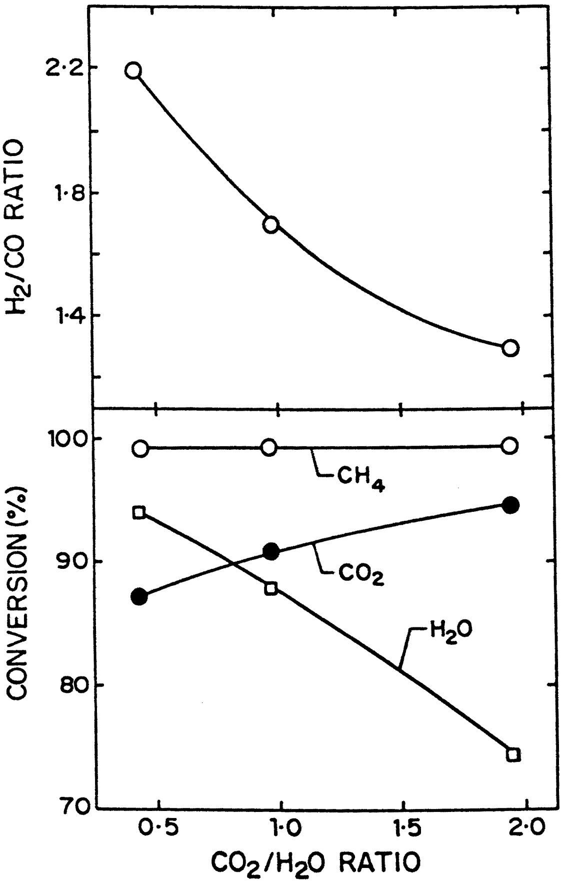

Figure 7.Influence of CO_2/H_2O feed ratio on the conversion and H_2/CO product ratio in the simultaneous CO_2 and steam reforming of methane over the catalyst with Co/Ni ratio of 0.17 at 850^oC $[(CO_2 + H_2O)/CH_4$ feed ratio = 1.2 and GHSV = 2.3×10^4 cm^3 g^{-1} $h^{-1}]$.

radius of Co^{2+} (0.72°A) is larger than that of Ni^{2+} (0.69°A) (the ionic radius of Mg^{2+} is 0.66°A), the formation of solid solution of CoO in MgO is difficult as compared to that of NiO in MgO.

The higher pressure drop across the reactor for the catalyst containing nickel alone (i.e. without cobalt) is resulted form the filamental (whisker) carbon on the catalyst (24,25) leading to plugging of the catalyst bed. The carbon formation can be due to the Boudouard reaction ($2CO \rightarrow C+CO_2$), methane decomposition ($CH_4 \rightarrow C+2H_2$) and CO reduction ($CO+H_2 \rightarrow C+H_2O$), occurring simultaneously. The observed large decrease in the filamental carbon formation with increasing the Co/Ni ratio of the catalyst (Fig. 2) is attributed mostly to its reduced activity for the above carbon forming reactions. Such beneficial effect was also observed earlier in case of the oxidative conversion of methane to syngas over Ni and Co containing Yb_2O_3, ZrO_2 and ThO_2 catalysts (20). Work is in progress for understanding this beneficial effect of the cobalt addition.

The nickel and cobalt oxides in the catalyst are reduced to their metallic form in the initial short reaction period (< 30 min.), first by methane and then by hydrogen produced in the reforming of methane over the partially reduced catalyst.

In the CO_2 reforming and simultaneous CO_2 and steam reforming processes, the catalyst shows best performance at the optimum Co/Ni ratio (0.17) (Figs. 3 and 5). Thus, the addition of cobalt to the catalyst at the optimum concentration has also another beneficial effect in these processes; not only it reduces drastically the filamental coke formation but it also enhances the catalytic activity and increases the selectivity, particularly for the CO_2 reforming reaction. It may be noted that, in the simultaneous CO_2 and steam reforming processes, there is no formation of any side product and hence, as long as the conversion of both CO_2 and water is positive, the selectivity for H_2 and CO in the conversion of methane to syngas is always 100%.

The results reveal that the catalyst with optimum Co/Ni ratio of 0.17 is a highly promising catalyst for the CO_2 reforming process and also for the simultaneous CO_2 and steam reforming process, showing high activity for the conversion of methane to CO and H_2 at a low contact time (high space velocity) with little or no carbon formation on the catalyst.

Among the two processes, the simultaneous CO_2 and steam reforming process is of great practical importance because of its following interesting features:

- Unlike the CO_2 reforming process, the carbon formation on the catalyst is much less and the H_2 selectivity (based on methane conversion) is always 100% as long as the conversion of both CO_2 and water is $\geq$ zero.

Downloaded by OHIO STATE UNIV LIBRARIES on September 16, 2012 | http://pubs.acs.org
Publication Date: January 24, 2002 | doi: 10.1021/bk-2002-0809.ch015

- Unlike the steam reforming process, there is no formation of undesired product such as CO_2 (which has high green house effect), and hence the CO selectivity (based on methane conversion) is 100%.
- The H_2/CO product ratio can be varied between 1.0 and 3.0 by simply manipulating the CO_2/H_2O feed ratio.

Conclusions

From this investigation, following important conclusions have been drawn:

1. The surface and reduction properties, filamental carbon formation in the CO_2 reforming of methane, and methane-to-syngas conversion activity (in the steam and/or CO_2 reforming of methane) over the $Co_xNi_{1-x}O/MgO/SA$-5205 catalyst (x = 0-0.5) are strongly influenced by the Co/Ni ratio in the catalyst.

2. The addition of cobalt to the supported nickel catalyst has following beneficial effects:

    - Formation of filamental carbon in the CO_2 reforming of methane is drastically reduced with increasing the Co/Ni ratio in the catalyst.
    - The methane conversion activity of the catalyst in both the CO_2 reforming and simultaneous CO_2 and steam reforming reactions is increased; it is maximum for the Co/Ni ratio of 0.17.

3. The supported Co-Ni containing catalyst with an optimum Co/Ni ratio of 0.17 is a highly promising catalyst for the conversion of methane to syngas, particularly by the simultaneous CO_2 and steam reforming process; the NiO, CoO and MgO in the catalyst exist as a solid solution.

References

1. Edwards, J. H; Maitra, A.M. The chemistry of methane reforming with CO_2 and its current and potential applications. *Fuel Processing Technol.* **1995,** *42,* 269–289.
2. Richardson, J.T. and Patipatyadar, S.A. Carbon dioxide reforming of methane with supported rhodium. *Appl.Catal.* **1990,** *61,* 293–309.
3. Solymosi, F., Kutsan, Gy. and Erdohelyi, A. Catalytic reaction of CH_4 with CO_2 over alumina-supported Pt metals. *Catal. Lett.* **1991,** *11,* 149–156.

Downloaded by OHIO STATE UNIV LIBRARIES on September 16, 2012 | http://pubs.acs.org
Publication Date: January 24, 2002 | doi: 10.1021/bk-2002-0809.ch015

4. Perera, J. H. S. Q., Couves, J. W., Sankar, G. and Thomas, J. M. The catalytic activity of Ru and Ir supported on Eu_2O_3 for the reaction, $CO_2+CH_4\rightarrow 2H_2+2CO$; a viable solar-thermal energy system. *Catal. Lett.* **1991,** *11,* 219–226.
5. Ashcroft, A. T., Cheetham, A. K., Green, M. L. H. and Vernon, P. D. F. Partial oxidation of methane to synthesis gas using carbon dioxide. *Nature* **1991,** *352,* 225–226.
6. Rostrup-Neilsen, J. R. and Bak-Hansen, J. H. CO_2 reforming of methane over transition metals. **1993,** *144,* 38–49.
7. Erodohelyi, A., Csernyi, J. and Solymosi, F. Catalytic activation of CH_4 with CO_2 over alumina-supported Pt metals. *J. Catal.* **1993,** *25,* 265–270.
8. Nakamura, J., Aiakwa, A., Sato, K. and Uchijima, T. Role of support in the reforming of CH_4 with CO_2 over Rh catalysts. *Catal. Lett.* **1994,** *25, 265–270.*
9. Vernon, P. D. F., Green, M. L. H., Cheetham, A. K. and Ashcroft, A. T. Partial oxidation of methane to synthesis gas and carbon dioxide as an oxidising agent for methane conversion. *Catal. Today* **1992,** *13,* 417–426.
10. Masai, M., Kudo, H., Miyake, A., Nishyama, S. and Suruya, *S.* Methane reforming by carbon dioxide and steam over supported Pd, Pt and Rh catalysts. *Stud. Surf. Sci. Catal.* **1988,** *36,* 67–71.
11. Choudhary, V. R. and Mamman, A. S. Oxidative conversion of methane to syngas over noble metal supported MgO, CaO and rare earth oxides. *Fuel.* **1998,** *77,* 1477-1488.
12. Chen, Y. and Ren. Conversion of methane and carbon dioxide into synthesis gas over alumina-supported nickel catalysts. Effect nickel-alumina interactions. *J. Catal. Lett.* **1994,** *29,* 39–48.
13. Yamazaki, O., Nozaki, T., Omata, K. and Fujimoto, K. Reduction of carbon dioxide by methane with Ni on MgO-CaO containing catalysts. *Chem. Lett.* **1992,** 1953–1954.
14. Choudhary, V. R. and Rajput, A. M. Simultaneous carbon dioxide and steam reforming of methane to syngas over NiO-CaO catalyst. *Ind. Eng. Chem. Res.* **1996,** *35,* 3934–3939.
15. Choudhary, V. R., Uphade, B.S. and Mamman, A. S. Simultaneous steam and CO_2 reforming of methane to syngas over NiO/MgO/SA-5205 in presence and absence of oxygen. *Appl. Catal. A:* **1998,** *168,* 33–46.
16. Choudhary, V. R. and Rajput, A. M.and Prabhakar, B. Coupling of exothermic oxidative conversion and endothermic CO_2 and steam reforming of methane to syngas over NiO-CaO catalyst. *Angew. Chem. Intl. Ed. Engl.* **1994,** *33,* 2104–2106.
17. Choudhary, V. R. and Rajput, A. M.and Prabhakar, B. Energy efficient methane-to-syngas conversion with low H_2/CO ratio by simultaneous

Downloaded by OHIO STATE UNIV LIBRARIES on September 16, 2012 | http://pubs.acs.org
Publication Date: January 24, 2002 | doi: 10.1021/bk-2002-0809.ch015

catalytic reaction of methane with CO_2 and oxygen over NiO-CaO. *Catal. Lett.* **1995,** *32,* 391–396.

18. Choudhary, V. R., Uphade, B.S. and Belhekar, A. Oxidative conversion of methane to syngas over $LaNiO_3$ perovskite with or without simultaneous steam and CO_2 reforming reactions. *J. Catal.* **1996,** *163,* 312–318.
19. Choudhary, V. R., Uphade, B. S. and Mamman, A. S. Partial oxidation of methane to syngas with or without simultaneous CO_2 & steam reforming reactions over Ni/AlPO-5. *Microporous and Mesoporous Mater.* **1998,** *23,* 61-66.
20. Choudhary, V. R., Rane, V. H. and Rajput, A. M. Beneficial effects of cobalt addition to Ni-catalyst for oxidative conversion of methane to syngas. *Appl. Catal. A*: **1997,** *162,* 235–238.
21. Choudhary, V. R., Uphade, B. S. and Mamman, A. S. Oxidative conversion of methane to syngas over nickel supported on low surface area porous catalyst carriers precoated with alkaline and rare earth oxides. *J. Catal.* **1997,** *172,* 281–293.
22. Highfield, J. G., Bossi, A. and Stone, F. S. Preparation of catalysts III. Scientific bases for the preparation of heterogeneous catalysts. Proceedings of Third International Symposium, Louvain-la-Neuve, Sept. 6-9, 1982. Eds. Poncelet, G., Grange, P, Jacobs, P. A. *Stud. Surf. Sci. Catal.* **1983,** *16,* 181–192.
23. Parmaliana, A., Arena, A., Frusteri, N. and Giordano, N. J. Temperature-programmed reduction NiO-MgO interactions in magnesia supported Ni catalysts and NiO-MgO physical mixtures. *Chem. Soc. Faraday Trans.* **1990,** *86,* 2663–2669.
24. Rostrup-Nielsen, J. R. Production of synthesis gas. *Catal. Today* **1993,** *18,* 305–324.
25. Tsang, S. C., Claridge, J. B. and Green M. L. H. Recent advances in the conversion of methane to syngas. *Catal. Today,* **1995,** *23,* 3–15.

Downloaded by OHIO STATE UNIV LIBRARIES on September 16, 2012 | http://pubs.acs.org
Publication Date: January 24, 2002 | doi: 10.1021/bk-2002-0809.ch015

Downloaded by COLUMBIA UNIV on September 16, 2012 | http://pubs.acs.org
Publication Date: January 24, 2002 | doi: 10.1021/bk-2002-0809.ch016

Chapter 16

Low-Temperature CH_4 Decomposition on High-Surface Area Carbon Supported Co Catalysts

Z.-G. Zhang, K. Haraguchi, and T. Yoshida

Hokkaido National Industrial Research Institute, 2–17 Tsukisamu-Higashi, Toyohira-ku, Sapporo 062–8517, Japan

High surface area carbon supported Co catalysts with loading up to 35wt% were prepared for converting CH_4 to C_2^+ hydrocarbons with the two-step reaction sequence. The catalysts were characterized by N_2 adsorption, XRD analysis, TPR and TPD techniques. The activity of the catalysts in the CH_4 decomposition was examined in a temperatures range of 300-450°C, while the subsequent hydrogenation in the second step was conducted at 100°C. It was found that the carbon supported catalysts provided higher Co dispersions than SiO_2 supported one, and therefore exhibited higher CH_4 decomposition activities. Moreover, the molar ratio of produced H_2 to consumed CH_4 in the decomposition indicated that CH_x formed at lower temperatures tended to contain more hydrogen. The production of C_2^+ in the hydrogenation step provided further evidence for the CH_x formation in the decomposition and exhibited potential of the carbon supported catalysts to be used in the two-step CH_4 reaction.

In CO2 Conversion and Utilization; Song, C., et al.;
ACS Symposium Series; American Chemical Society: Washington, DC, 2002.

Introduction

Increasing attention has been paid recently to the two-step reaction of CH_4 to produce higher hydrocarbons (C_2^+). In this reaction, CH_4 is first activated on suitable metal catalysts at mild temperatures (<=450°C) to form carbonaceous species (CH_x) and then these species are hydrogenated at the same (*1-3*) or lower (*4-6*) temperatures to produce C_2^+ hydrocarbons. Compared with CH_4 oxidative coupling or partial oxidation, the most important advantage of this two-step procedure is not to produce either CO or CO_2, that is, not to waste CH_4.

Previous studies have demonstrated that supported Pt, Ru and Co metal catalysts are effective to produce C_2^+ hydrocarbons with the two-step reaction sequence and C_2^+ yield strongly depends on the reactivity of CH_x species formed on the catalyst surface in the activation step (*2,5,7*). In order to increase C_2^+ yield, some effort has been made to increase the surface concentration of CH_x species by modifying the reaction conditions (*8,9*) or by using a circulating or static reactor system with H_2 trap or acceptor (*10-12*). However, there is a limitation in doing this, because CH_4 decomposition occurs in principle only on the metal surface and will cease when the surface is fully covered by CH_x species and/or deposit carbon. Therefore, to produce CH_x species as much as possible with a given catalyst, it is also necessary to increase its metal surface area itself, that is, the metal dispersion.

A high metal dispersion can generally be obtained by using a high surface area material as support. Various supports, such as SiO_2, Al_2O_3 and so on, have been investigated in the CH_4 decomposition related to the two-step reaction (*13-16*), but no contribution is found to pay an attention to carbon support. In this study, therefore, a high surface area carbon was used as support in an attempt to prepare highly active catalysts for the two-step CH_4 reaction.

The aim of the present paper is to demonstrate that Co supported on the high surface area carbon is highly dispersed and that the catalytic activity of this carbon-supported catalyst is much higher than that of SiO_2-supported one in the decomposition of CH_4 at the temperatures of 300-450°C. The formation of CH_x species on the catalyst in the decomposition is also confirmed by the production of C_2^+ in the subsequent hydrogenation step.

Experimental

Catalyst preparation

A microporous carbon referred to as PRC20 (Kurare Chemical Co.) as well as a commercial SiO_2 (Nikki Chemical Co.) for comparison was used as support for preparing Co catalysts. PRC20 was prepared from phenol resin and is essentially ash free. Its BET surface area, pore volume and mean pore size

Downloaded by COLUMBIA UNIV on September 16, 2012 | http://pubs.acs.org
Publication Date: January 24, 2002 | doi: 10.1021/bk-2002-0809.ch016

were measured to be 1770 m^2/g, 0.75 ml/g and 0.77 nm, respectively. On the other hand, the surface area and pore size of SiO_2 were 330 m^2/g and 18 nm, respectively.

The Co catalysts with loading in a range of 4-35wt% (determined by ICP analysis) were prepared by aqueous impregnation of $Co(NO_3)_2 \cdot 6H_2O$ (98%) onto the supports according to the conventional technique. After preparation, the catalysts were dried in air at 110°C for 1 h, and then heated linearly up to 300°C under a pure N_2 flow and kept there for 30 min. For the catalysts with higher loadings (28 and 35wt%), temporarily abrupt increases of catalyst bed temperature up to 350°C were observed during the heating as $Co(NO_3)_2$ began to decompose around 200°C.

Apparatus

A flow type temperature programmed desorption (TPD) apparatus (TPD-1-A, Bel Japan, Inc.) was used for all temperature programmed reduction (TPR), TPD of adsorbed H_2 and CH_4 decomposition experiments in this study. The apparatus mainly consists of five mass flow meters for the controlling of feed gases, a four-way autovalve for the switching of feed gas without pressure shock, a fixed-bed micro reactor made of quartz tube (6 mm i.d.) and a quadrupole mass spectrometer (QMS) for the analysis of exit gas.

The catalyst particles in this system were held at a right place in the reactor with quartz wool. The reactor temperature was measured by a thermocouple fixed inside an in-bed thermowell and controlled by a linear temperature-programmable controller. The gas sampling was taken just at the outlet of the reactor by a rotary pump. A small portion of exit gas was first introduced to a vacuumed sub-line, and then its tiny fraction was sampled through a leaking valve into the mass spectrometer chamber for analysis. The intensity of signals (m/z = 2 and 16) was calibrated by using a pre-mixed standard gas on the basis of helium (around 1vol% each for H_2 and CH_4) after each measurement. In addition, all gases used in this study were high purity and were further purified by passage through moisture and then oxygen filters (GL Sciences Inc., Japan) before being fed.

Catalyst characterization

The surface area of the supports and catalysts was measured by N_2 adsorption (–196°C) according the BET method, using an automated analyzer (Belsorb 28,Bel Japan, Inc.). Samples were degassed for 4 h at 130°C prior to analysis. X-ray diffraction (XRD) pattern of the catalysts was obtained on a powder diffractormeter (Rigaku RAD-3C) using Cu Kα radiation. The X-ray tube was operated at 35kV and 20mA, and the X-ray diagram was scanned with a step size of 0.02 (2θ) from 10 to 80° (2θ).

Downloaded by COLUMBIA UNIV on September 16, 2012 | http://pubs.acs.org
Publication Date: January 24, 2002 | doi: 10.1021/bk-2002-0809.ch016

The TPR profile was obtained by heating 100 mg of pre-dried catalyst from 120 to 600°C at a heating rate of 10°C /min in a stream of 1% H_2 in He (100 ml/min). On the other hand, the TPD experiment for the measurement of hydrogen chemisorbed on the catalysts was performed from room temperature to 450°C in pure He (100 ml/min). Prior to TPD, the catalysts were first reduced in situ at desired temperatures (350-500°C) for desired periods of time (10-120 min) in a stream of 20% H_2 in He (100 ml/min), then purged with 100 ml/min of He at 450°C for 30min, and finally submitted at 100°C to a flow of 1vol% H_2 in He (100ml/min) for chemisorption. The purge performed at the temperature of 450°C after the reduction was to clean the Co surface of catalyst and to remove hydrogen which might migrate to support surface by spillover mechanism during the reduction (*17,18*). On the other hand, the temperature of 100°C chosen for hydrogen adsorption was to obtain a maximum surface coverage of Co metal (*19*).

Downloaded by COLUMBIA UNIV on September 16, 2012 | http://pubs.acs.org
Publication Date: January 24, 2002 | doi: 10.1021/bk-2002-0809.ch016

Catalytic activity

The CH_4 decomposition activity of the catalysts was tested at temperatures ranging from 300 to 450°C, isothermally, with a diluted CH_4 mixture (1%CH_4 in He, 100 ml/min) as feed. After the reduction with 20% H_2 in He (100 ml/min) at 450°C for 30 min and then helium purge at the same temperature for another 30 min, the catalyst (50 mg) was kept at 450°C or cooled to desired temperatures for a 10 min decomposition of CH_4. During the period, the concentration of both produced H_2 and unreacted CH_4 in the flow out of the reactor was continuously analyzed by QMS and then calibrated by using the standard gas as described above. Therefore, a quantitative comparison of catalytic activity could be made.

Results and Discussion

Catalyst characterization

Very high metal dispersion can be easily achieved by using high surface area active carbons as supports (*20*). To confirm that it was also true in the present cases, the catalysts prepared were first characterized by N_2 adsorption, XRD, TPR and TPD techniques.

Physical characteristics of catalysts

In addition to the BET surface areas, the pore volumes and mean pore sizes of all the carbon supported catalysts were also estimated by the application of t-method to the corresponding N_2 adsorption isotherms (Table I). In comparison with the characteristics of carbon support itself described above, the data in

Table I shows that the loading of Co on the high surface area carbon resulted in a significant decrease in both surface area and pore volume, and that the degree of the decrease increased essentially with loading. These clearly indicate the blocking of micropores of carbon support by Co species. The extent of decrease in the pore volume of each carbon supported catalyst was calculated to exceed greatly the theoretical volume of the supported Co phase being Co_3O_4 (for example, 0.19 to about 0.04 ml/g for 18%Co/PRC20), further supporting this conclusion. In addition, for 28% and 35%Co/PRC20, apparently larger mean pore sizes were resulted. This is an unexpected result and it may be related to the temporarily abrupt temperature increases observed in the heating process of these two catalysts in preparation. Their higher Co loadings mean that more $Co(NO_3)_2$ was contained in the correspondingly impregnated samples. Thus, in the followed heating process, more NO_2, that is, higher local NO_2 concentrations were produced as $Co(NO_3)_2$ decomposed. Due to this, the consuming oxidation of inner wall carbon of support's micropores could occur more intensely. As results, the bed temperatures increased and the pores of the catalysts were enlarged.

Co dispersion

Co state and its particle size of the catalysts were first examined by XRD analysis. As shown in Figure 1, Co_3O_4 was an only Co phase detected in the catalysts of 4%, 9% and 18%Co/PRC20 as well as 18%Co/SiO_2. Compared with the case of SiO_2 supported catalyst, the peaks of Co_3O_4 observed from these three carbon supported catalysts were much weaker and broader, indicating that these catalysts have much smaller Co_3O_4 particles with them. Application of the Scherrer line broadening equation to the peaks at about 36.9° yielded average crystallite sizes of ≤ 7 nm for all the three, much smaller than that of 17 nm determined for 18%Co/SiO_2.

On the other hand, for the higher loading catalysts (28% and 35%Co/PRC20), CoO and γ-Co, instead of Co_3O_4, were the main phases of Co. This fact implies that the partial reduction of Co_3O_4 by the support carbon took place in the preparation of these two catalysts. Again, this was ascribed to the temporarily abrupt increases of their bed temperatures occurred in the heating process. If these temporary temperature increases, as discussed above, were caused by the carbon oxidation, the inner temperature of catalyst particles would be much higher than the bed temperature. In the present two cases, it possibly reached 550°C or higher. Otherwise, γ-Co would not be produced. Simultaneously, the higher inner temperatures would also enhance the local sintering of Co phases. This might be why the sharper XRD peaks were observed with both catalysts. Again, by applying the Scherrer line broadening equation, average particle sizes of CoO and γ-Co in these two catalysts were determined to be 20 and 17 nm for 28%, and 22 and 24 nm for 35%Co/PRC20, respectively. Here, it should be noted that these slightly higher values in particle size do not absolutely mean that Co dispersion in these two catalysts is

Downloaded by COLUMBIA UNIV on September 16, 2012 | http://pubs.acs.org
Publication Date: January 24, 2002 | doi: 10.1021/bk-2002-0809.ch016

Table I. Characteristics and Activities of the Catalysts

Catalyst	*Surface Area* ($m^2 g^{-1}$)	*Pore Volume* ($ml\ g^{-1}$)	*Pore Size* (nm)	*Relative Dispersion* (-)	*H_2 Production Rate*[a] ($mmol\ h^{-1} g\text{-}Co^{-1}$)
4%Co/PRC20	1680	0.71	0.77	1730	850
9%Co/PRC20	1370	0.68	0.77	1130	440
18%Co/PRC20	1140	0.56	0.78	780	250
28%Co/PRC20	950	0.47	0.81	370	140
35%Co/PRC20	790	0.42	0.86	230	100
18%Co/SiO_2	250	n.d.	18[b]	100	100

[a] at 450°C and 100 s.

[b] Determined by Dollimore-Heal method.

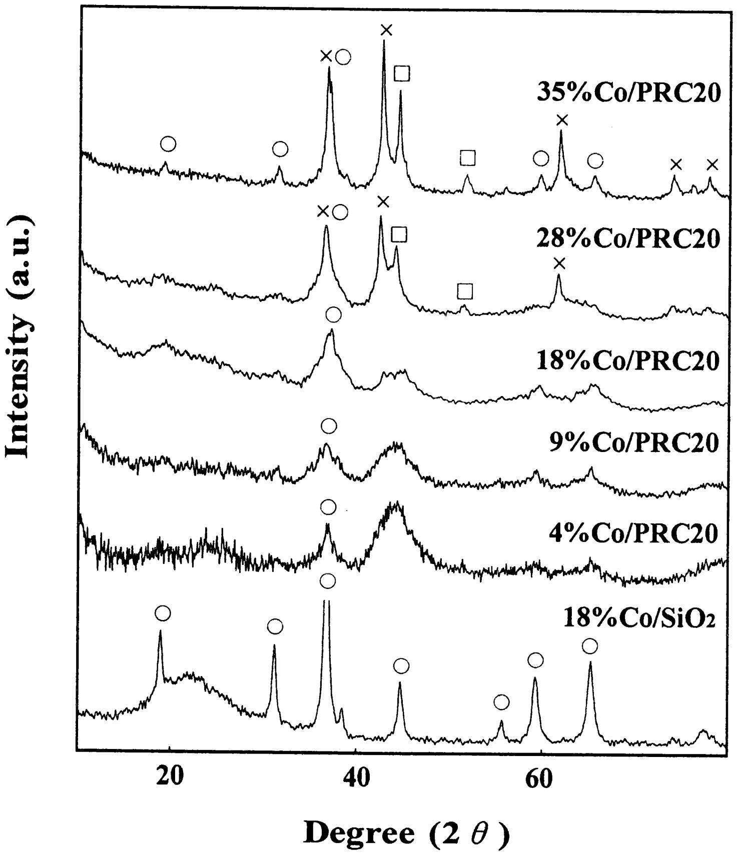

Figure 1. XRD patterns of the supported Co catalysts with different loading.

Downloaded by COLUMBIA UNIV on September 16, 2012 | http://pubs.acs.org
Publication Date: January 24, 2002 | doi: 10.1021/bk-2002-0809.ch016

higher than that of 18%Co/SiO_2 having an average Co_3O_4 size of 18 nm. Their weaker XRD peaks indicate that a significant amount of Co in these two higher loading catalysts is dispersed finely and was not detected in the XRD measurement.

Next, Co dispersion of the catalysts was examined by the shift of reduction temperature of Co_3O_4 in their TPR profiles. Figure 2 shows the TPR profiles obtained with all the catalysts. In each of them, two clear hydrogen consumption peaks were observed. By comparing with literature data (*21,22*) and using a mixture of pure Co_3O_4 with PRC20 as well as SiO_2, the two peaks in all the cases were ascribed to the reduction of Co_3O_4 to CoO and that of CoO to metallic Co, respectively. All the carbon supported catalysts exhibited quite lower Co_3O_4 and CoO reduction temperatures than 18%Co/SiO_2, indicating their average smaller Co_3O_4 and CoO particle sizes. This is essentially in agreement with the XRD results. Moreover, the rather stronger first peaks were observed for 28% and 35%Co/PRC20 catalysts. This reveals that a substantial amount of finely dispersed Co_3O_4 indeed existed in these two higher loading catalysts, further supporting the above conclusion reached from their XRD results. Furthermore, an expected but very limited shift in the first peak temperature was also observed, as the Co loading in the carbon supported catalyst was increased.

Finally, the TPD pattern of hydrogen chemisorbed on each of the catalysts was measured to evaluate its relative Co dispersion quantitatively. Figure 3 presents the TPD patterns of hydrogen obtained with all the catalysts, which experienced H_2 adsorption at 100°C after being reduced at 450°C. A comparison of the patterns of the carbon and SiO_2 supported catalysts indicates

Downloaded by COLUMBIA UNIV on September 16, 2012 | http://pubs.acs.org
Publication Date: January 24, 2002 | doi: 10.1021/bk-2002-0809.ch016

Downloaded by COLUMBIA UNIV on September 16, 2012 | http://pubs.acs.org
Publication Date: January 24, 2002 | doi: 10.1021/bk-2002-0809.ch016

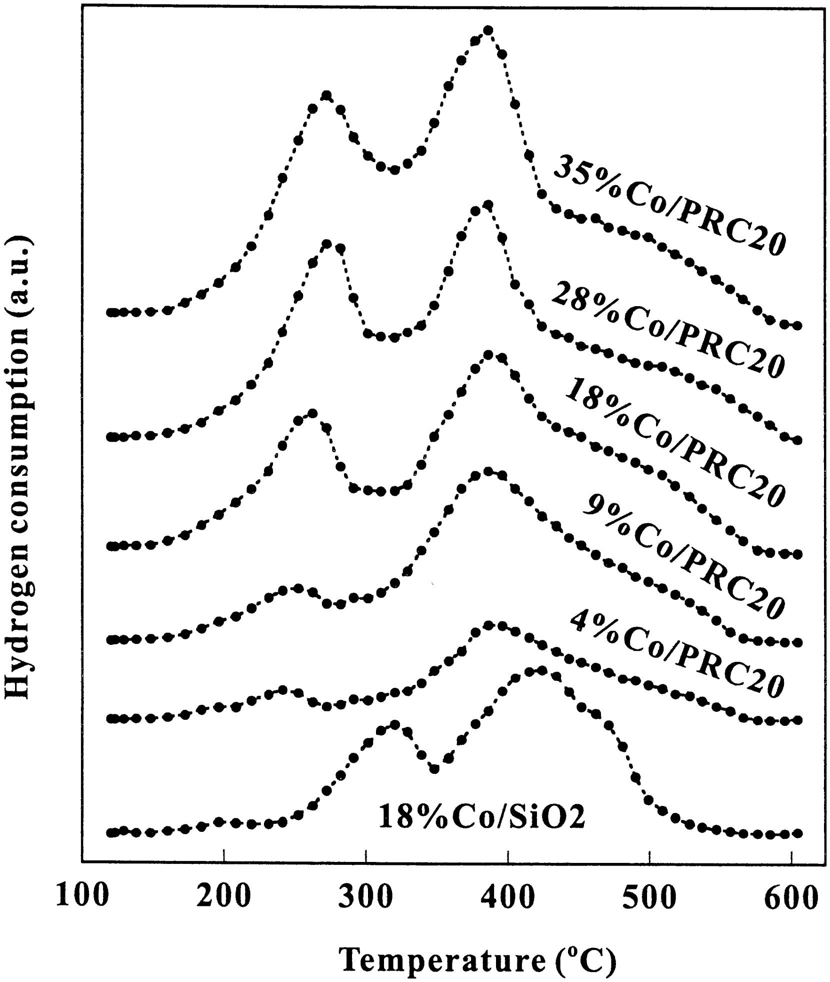

Figure 2. TPR profiles in 1% H_2/He at 10°C /min of the supported Co catalysts with different loading.

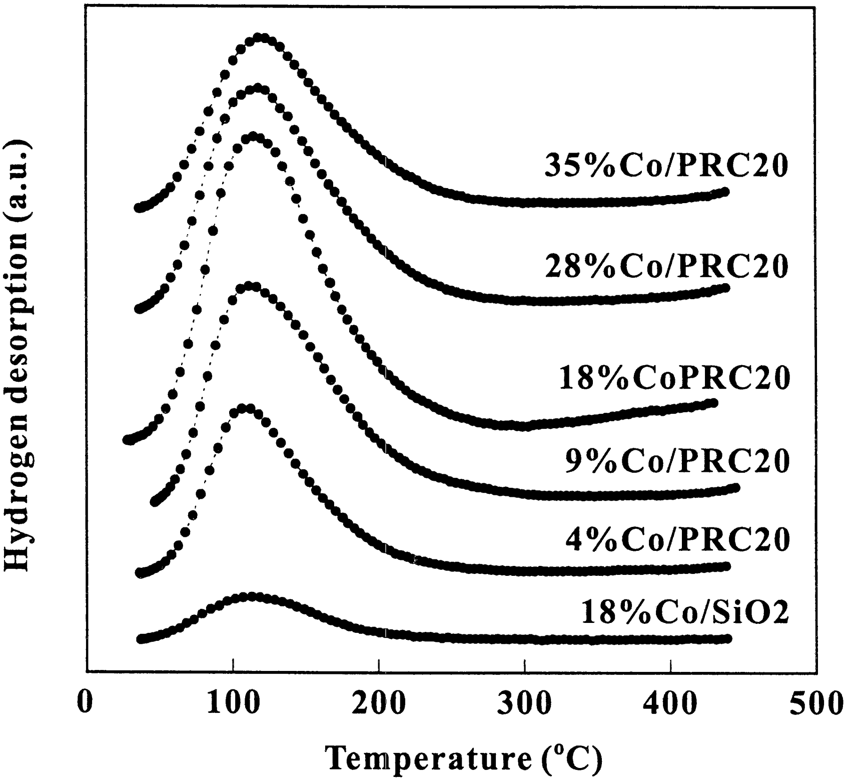

Figure 3. TPD patterns of hydrogen chemisorbed on the supported Co catalysts with different loading.

Downloaded by COLUMBIA UNIV on September 16, 2012 | http://pubs.acs.org
Publication Date: January 24, 2002 | doi: 10.1021/bk-2002-0809.ch016

As shown in Table II, the condition of 450°C /30min, which was used in this study for the reduction of all the catalysts exposed to the CH_4 decomposition, produced the highest relative Co dispersion. The relative dispersion decreased with longer periods of reduction time or at a higher temperature (500°C), suggesting the sintering of reduced Co. On the other hand, the low values obtained at a lower temperature (350°C) might result from the incomplete reduction of Co_3O_4.

Catalytic activity

The activity of the prepared catalysts in the decomposition of CH_4 was tested at 450°C isothermally. During 10 min decompositions, very similar profiles of concentrations of produced H_2 and unreacted CH_4 were obtained for all the catalysts. As shown in Figure 4, H_2 concentration quickly reaches a maximum at about 100 s after CH_4 was introduced into the reactor, and then decreases slowly until the CH_4 feeding is stopped. In contrast, the concentration of unreacted CH_4 exhibits a slow increase after a sharp appearance within the first 100 s. In terms of CH_4 consumption, its rate slowly decreases after a rapid drop at the initial stage. This is different from the result obtained for SiO_2 supported Co catalyst in a previous study that a longer period of constant and low reaction rate was observed for CH_4 consumption after a short period of high reaction rate at very initial stage (*16*). It seems that the continuous decrease of CH_4 consumption observed in the present study is very reasonable, since the catalyst would continuously lose its activity as the accumulation of carbon deposit on the metal surfaces proceeds with the CH_4 decomposition.

As demonstrated in previous studies (*2,8,9,16*), a very short period of time is desirable for CH_4 decomposition to form the most reactive surface CH_x species that, upon hydrogenation in the second step, could be converted to the desired higher hydrocarbons. Therefore, the initial activity of catalyst is of great importance. From the concentration profiles recorded, the rates of produced H_2 and decomposed CH_4 were obtained. Table I shows the H_2 production rate measured for all the catalysts at 100s after CH_4 is introduced at 450°C. On the basis of per unit mass of Co, the rate became greater in the order of 18%Co/SiO_2 = 35% < 28% < 18% < 9% < 4%Co/PRC20. This order, except the case of 35%Co/PRC, is in very good agreement with that of the relative dispersion of the catalysts, suggesting that the initial activity of the catalysts in the CH_4 decomposition strongly depends on their dispersions. On the other hand, when the rate was calculated on the basis of per unit mass of catalyst, the highest value was reached with 18%Co/PRC20, which exhibited the largest surface area of metallic Co.

Downloaded by COLUMBIA UNIV on September 16, 2012 | http://pubs.acs.org
Publication Date: January 24, 2002 | doi: 10.1021/bk-2002-0809.ch016

Downloaded by COLUMBIA UNIV on September 16, 2012 | http://pubs.acs.org
Publication Date: January 24, 2002 | doi: 10.1021/bk-2002-0809.ch016

Table II. Effect of Reduction Condition on the Relative Dispersion of 18%Co/PRC20 Catalyst

Condition		*Relative*	*Condition*		*Relative*
Temperature (°C)	*Time (min)*	*Dispersion (-)*	*Temperature (°C)*	*Time (min)*	*Dispersion (-)*
350	10	230	450	30	780
350	60	320	450	60	690
400	10	400	450	120	500
400	60	640	500	10	730
450	10	660			

Dispersion: relative to that of 18%Co/SiO2 listed in Table I.

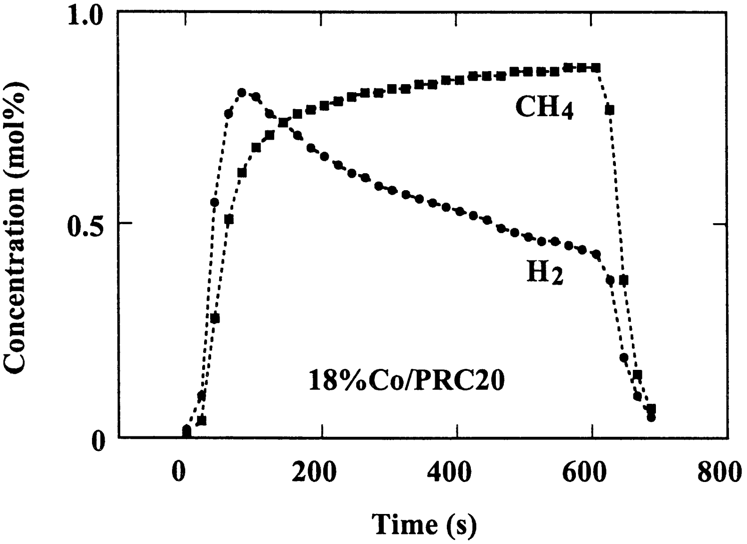

Figure 4. Concentration changes of produced H_2 and unreacted CH_4 in a 10 min CH_4 decomposition at 450°C over 18%Co/PRC20 catalyst.

Additionally, the use of lower temperatures in the decomposition step of the two-step CH_4 conversion process is also desirable from the viewpoint of suppressing or avoiding the formation of inactive carbon that may not be removed in the subsequent hydrogenation step (*2,9*). Therefore, the CH_4 decomposition activity of 18%Co/PRC20 was also compared with that of 18%Co/SiO_2 at lower temperatures. As shown in Figure 5, the carbon supported catalyst at either 300 or 350°C provided much higher H_2 production than SiO_2 supported one, again demonstrating its superior performance in the CH_4 decomposition. Moreover, the H_2 productions greatly decreased in both cases as the decomposition temperature was lowered, indicating the strong temperature dependence of CH_4 decomposition (*5*).

To get a better understanding of CH_4 decomposition behavior, the molar ratio of produced H_2 to decomposed CH_4 in the decomposition was also calculated against reaction time. As shown in Figure 6, at 450°C the molar ratio obtained over 20%Co/PRC20 reached 2 quickly, and then kept constant essentially until the CH_4 feeding was stopped. The value of less than 2 was observed only within the first 100 s, indicating that CH_x forms only at the very initial stage of the decomposition. As the decomposition temperature decreased, the period with the ratio less than 2 became longer, being about 200 s at 350°C. This means that controlling the formation of CH_4 on the Co surface of the catalyst through varying reaction time would become easier at lower temperatures. When the temperature was further decreased to 300°C, the molar ratio was estimated never to reach 2 in the 10 min decomposition. At this low temperature, CH_4 decomposition proceeded very slowly possibly due to its low sticking coefficient and produced the surface CH_x with more hydrogen.

Finally, some preliminary hydrogenation experiments were also performed with 18%Co/PRC20 to confirm that CH_x species was indeed formed on the Co surface of the carbon supported catalysts in the CH_4 decomposition and then it could be hydrogenated in the second step to C_2^+ hydrocarbons. The reactor system used for these experiments was very similar to the one described above for the CH_4 decomposition, except C_2^+ products were sampled through a sampler with 16 loops at the atmospheric pressure and then analyzed by a GC with FID detector. In these series of experiments, 300 mg of the catalyst was first reduced at 450°C following the same procedure as above and then exposed to 50ml/min CH_4 (7% in Ar) at 350°C for 5 min to produce surface CH_x species. Next, the catalyst was cooled rapidly in an Ar flow to 100°C and exposed at that temperature to 30ml/min H_2 for a 10 min hydrogenation to produce C_2^+ hydrocarbons. Figure 7 shows a typical profile of CH_4, C_2H_4 and C_3H_8 production as a function of hydrogenation time. Although no alkane $\geq C_4^+$ was observed (*2,5*), the present result shows that the carbon supported Co catalyst has potential to be used for the low temperature conversion of CH_4 to C_2+ alkanes by the two-step reaction sequence. Detailed investigation on the hydrogenation of CH_x species using the carbon supported Co catalysts is underway.

Downloaded by COLUMBIA UNIV on September 16, 2012 | http://pubs.acs.org
Publication Date: January 24, 2002 | doi: 10.1021/bk-2002-0809.ch016

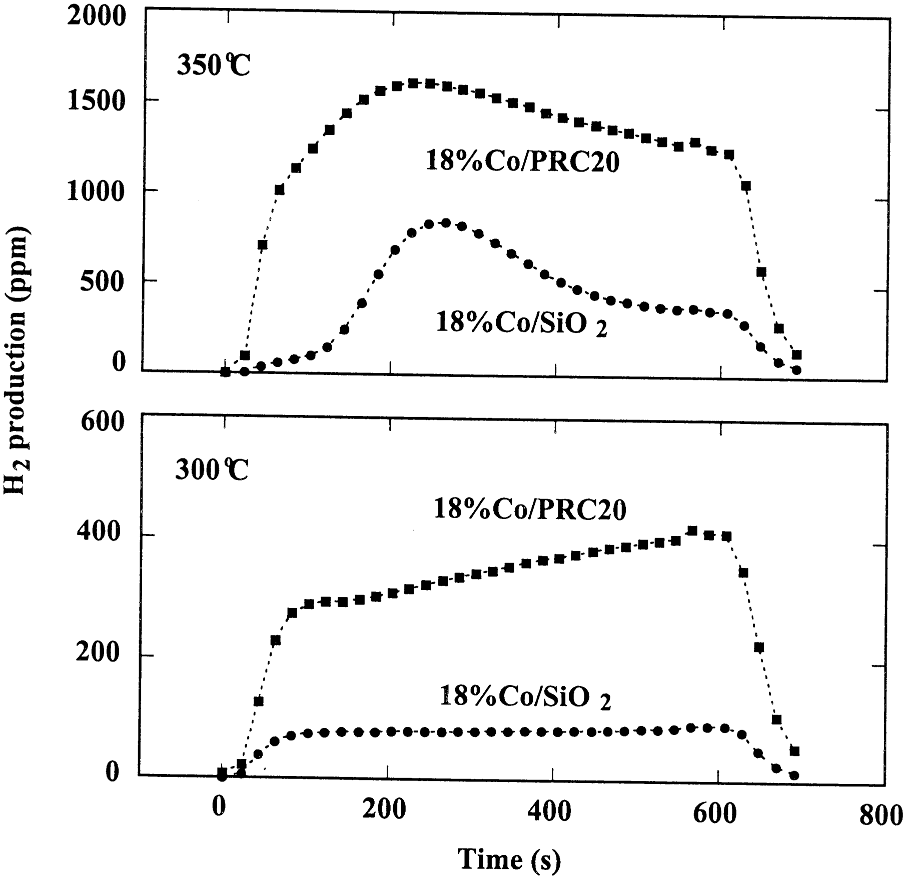

Figure 5. Activity Comparison of 18%Co/PRC20 and 18%Co/SiO2 Catalysts.

Downloaded by COLUMBIA UNIV on September 16, 2012 | http://pubs.acs.org
Publication Date: January 24, 2002 | doi: 10.1021/bk-2002-0809.ch016

Downloaded by COLUMBIA UNIV on September 16, 2012 | http://pubs.acs.org
Publication Date: January 24, 2002 | doi: 10.1021/bk-2002-0809.ch016

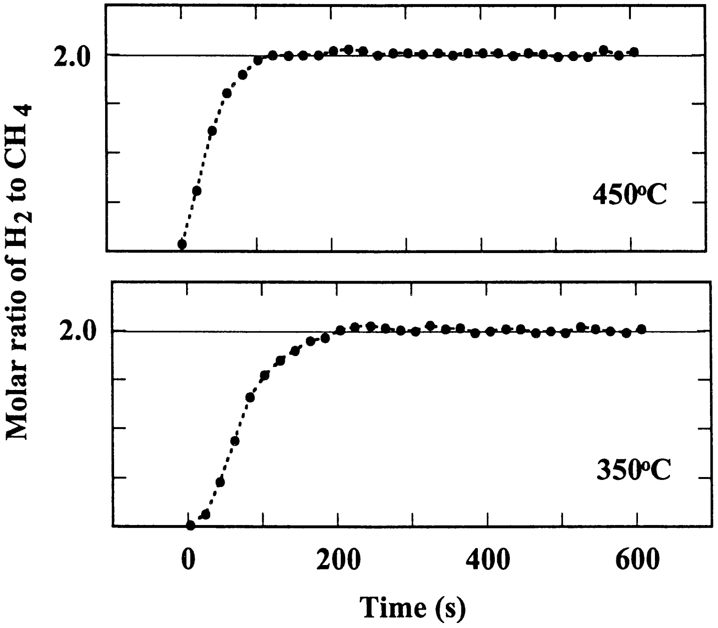

Figure 6. Change in the molar ratio of produced H_2 to decomposed CH_4 in the decomposition over 18%Co/PRC20 catalyst.

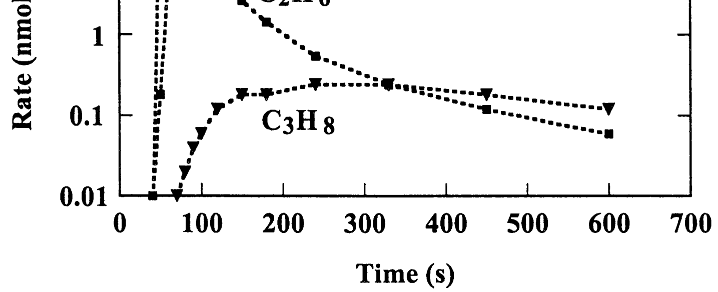

Figure 7. Formation of C_2H_6 as well as C_3H_8 in the hydrogenation of surface CH_x created from CH_4 decomposition at 350°C on 18%Co/PRC20 catalyst.

Conclusions

The characterization of the catalysts has shown that Co impregnated onto on a high surface area carbon was highly dispersed in a loading range of 4-35wt%, in comparison with that of the SiO_2 supported catalyst. Due to their higher dispersions, these carbon supported catalysts (except 35%Co/PRC20) exhibited higher activity in the CH_4 decomposition. Moreover, the molar ratio of produced H_2 to consumed CH_4 measured in the decomposition suggests that the formation of CH_x species on the carbon supported catalysts was an activated process and that CH_x produced at lower temperatures might contain more hydrogen. Finally, the production of C_2H_6 as well as C_3H_8 in the subsequent hydrogenation step confirmed the formation of CH_x species on the Co surface of carbon supported catalysts and simultaneously exhibited potential of the carbon supported Co catalysts to be used in the low temperature, two-step CH_4 conversion process.

Downloaded by COLUMBIA UNIV on September 16, 2012 | http://pubs.acs.org
Publication Date: January 24, 2002 | doi: 10.1021/bk-2002-0809.ch016

References

1. Belgued, M.; Pareja, P.; Amariglio, A.; and Amariglio, H. *Nature* **1991**, *352*, 789.
2. Belgued, M.; Amariglio, H.; Pareja, P.; Amariglio, A.; Saint-Just., J. *Catal.Today* **1992**, *13*, 437.
3. Solymosi, F.; Erdohelyi, A.; Cserenyi, J. *Catal. Lett.* **1992**, *16*, 399.
4. Koerts, T.; van Santen, R.A. *J. Chem. Soc. Chem. Commun.* **1991**, 1281.
5. Koerts, T.; Deelen, M.J.A.G.; van Santen, R. A. *J. Catal.* **1992**,*138*, 101.
6. Lenz-Solomun, P.; Wu, M.-C.; Goodman, D. W. *Catal. Lett.* **1994,** *25*,75.
7. Carstens, J.N.; Bell, A.T. *J. Catal.* **1996**,*161*, 423.
8. Koranne, M. M.; Goodman, D. W.; Zajac, G. W. *Catal. Lett.* **1995**, *30*, 219.
9. Soltan Mohammad Zadeh, J.; Smith, K.J. *J. Catal.* **1999**, *183*, 232.
10. Pareja, P.; Amariglio, A.; Belgued, M.; Amariglio, H. *Catal. Today* 1994, 21, 423.
11. Amariglio, A.; Pareja, P.; Belgued, M.; Amariglio, H. *J. Chen Soc. Chem Commun.* **1994**, 561.
12. Pareja, P.; Mercy, M.; Gachon, J.- C.; Amariglio, A.; Amariglio, H. *Ind. Eng. Chem. Res.* **1999**, *38*, 1163.
13. Solymosi, F.; Erdohelyi, A.; Cserenyi, J.; Felvegi, A. *J. Catal.* **1994**, *147*, 272.
14. Ferreira-Aparicio, P.; Rodriguez-Ramos, I.; Guerrero-Ruiz, A. *Appl. Catal. A* **1997**, *148*, 343.
15. Guczi, L.; Sarma, K.V.; Borko, L. *J. Catal.* **1997**, *167*, 495.
16. Soltan Mohammad Zadeh, J.; Smith, K.J. *J. Catal.* **1998**, *176*, 115.
17. Ming H.; Baker, B. G. *Appl. Catal. A* **1995**, *123*, 23.

18. Fujimoto, K. *J. Japan Petrol. Inst.* **1984**, *27*, 463.
19. Reuel, R. C.; Bartholomew, C. K. *J. Catal.* **1984**, *85*,63.
20. Daza, L.; Gonzalez-Ayuso, T.; Mendioroz, S.; Pajares, J. A. *Appl. Catal.* **1985**, *13*, 295.
21. van Steen, E.; Sewell, G. S.; Makhothe, R. A.; Micklethwaite, C.; Manstein, H; de Lange, M.; O'Connor, C. T. *J. Catal.* **1996**, *162*, 220
22. Lapidus, A.; Krylova, A.; Kazanskii, V.; Borovkov, V.; Zaitsev, A. *Appl. Catal.* **1991**, *73*, 65.

Downloaded by COLUMBIA UNIV on September 16, 2012 | http://pubs.acs.org
Publication Date: January 24, 2002 | doi: 10.1021/bk-2002-0809.ch016

Downloaded by OHIO STATE UNIV LIBRARIES on September 16, 2012 | http://pubs.acs.org
Publication Date: January 24, 2002 | doi: 10.1021/bk-2002-0809.ch017

Chapter 17

Effects of Pressure on CO_2 Reforming of CH_4 over Ni/Na-Y and Ni/Al_2O_3 Catalysts

Chunshan Song[1,*], Srinivas T. Srimat[1], Satoru Murata[1], Wei Pan[1], Lu Sun[1], Alan W. Scaroni[1], and John N. Armor[2]

[1]**Clean Fuels and Catalysis Program, The Energy Institute, and Department of Energy and Geo-Environmental Engineering, Pennsylvania State University, 209 Academic Projects Building, University Park, PA 16802**
[2]**Corporate Science and Technology Center, Air Products and Chemicals Inc., Allentown, PA 18195**
***Corresponding author: fax: 814–865–3248; email: csong@psu.edu**

CO_2 reforming of CH_4 was studied over Ni/Na-Y and Ni/Al_2O_3 catalysts at atmospheric pressure as well as high pressure (27 atm). Both types of catalysts showed high conversion at atmospheric pressure whereas both CO_2 conversion and CH_4 conversion decreased drastically at high pressure. Higher extent of carbon formation was observed at high pressure compared to the runs at atmospheric pressure over both laboratory and commercial Ni-based catalysts.

CO_2 reforming of CH_4 is a promising alternate process for production of CO-rich syngas from natural gas (1-3). It is also a potential reaction process for conversion of CO_2-rich natural gas into syngas. Most previous studies reported in the literature regarding CO_2 reforming of CH_4 were carried out at atmospheric pressure (4-11). However, industrial operation would prefer high-pressure conditions (25 to 45 atm) for CO_2 reforming of CH_4 in terms of higher process

In CO2 Conversion and Utilization; Song, C., et al.;
ACS Symposium Series; American Chemical Society: Washington, DC, 2002.

efficiency (3). This paper reports for the first time results obtained on CO_2 reforming of CH_4 at high pressure over Na-Y and Al_2O_3-supported Ni catalysts as well as several Ni-based commercial steam-reforming catalysts. The laboratory-prepared Ni catalysts were evaluated under atmospheric pressure (14.7 psi or 1 atm) as well as high pressure (400 psi or 27 atm) in a fixed-bed flow reactor.

Remarkable differences in conversion and selectivity as well as the amount of coke formed were observed at high pressure when compared to reactions at atmospheric pressure. Both catalysts give >90% conversion of CH_4 and CO_2 and high selectivity to CO and H_2 at atmospheric pressure. However, at high pressure a drastic decrease in conversion, a significant change in selectivity to H_2 and CO and substantial carbon formation were observed with both catalysts.

Downloaded by OHIO STATE UNIV LIBRARIES on September 16, 2012 | http://pubs.acs.org
Publication Date: January 24, 2002 | doi: 10.1021/bk-2002-0809.ch017

Experimental

Two series of catalysts, Ni/Na-Y and Ni/Al_2O_3, were prepared by incipient wet impregnation method using Na-Y zeolite (LZ-Y52, SiO_2/Al_2O_3 molar ratio: 5; Surface area: 826 m^2/g) and γ-Al_2O_3 support (S-1/KF; 203 m^2/g), respectively. A weighed amount of nickel nitrate to yield the desired loading is dissolved in distilled water. Then the precursor salt solution was added dropwise to the support while stirring. After the impregnation, the resulting powder was dried in an oven for 16 h at 110°C. The samples were calcined at 450°C for 4 h in an air-circulating oven (air flow rate 100 ml/min). The finished catalysts were sealed in sample bottles and kept in a desccicator before use.

The BET surface areas of the supports and catalysts were determined by nitrogen adsorption using a GEMINI system (Micromeritics, USA) at -196°C. H_2 and CO chemisorption measurements of catalysts were carried out on an AutoChem 2910 (Micromeritics, USA) analyzer using pulse chemisorption. Temperature programmed oxidation (TPO) of carbon species on the catalysts after the CO_2 reforming of CH_4 reaction was carried out on a thermogravimetric analyzer (Mettler TG-50). Scanning electron microscopic analysis was conducted on fresh and used catalysts in CO_2 reforming of CH_4 to investigate the structure of carbon deposits. DS 130 dual stage SEM (ISI, USA) was used for this purpose.

The reaction of CO_2 reforming of CH_4 was studied at a temperature of 750°C or 800°C under atmospheric pressure (1 atm) and high pressure (400 psi or 27 atm) with the feed CO_2/CH_4 molar ratio of 1.0. Ultra-high-purity gases were used in all experiments. Mass flow controllers allow exact control of the volumes of CH_4, CO_2 and Ar into the reactor at a space velocity (WHSV) of 30,000 $cm^3.g^{-1}.h^{-1}$. The calcined Ni/Na-Y catalyst sample was mixed with 20 wt% of alumina binder (Catapal B), pressed at 5000 psi for 1 min, and sieved between 0.5 to 1 mm. Ni/Al_2O_3 catalyst was used without binder. About 0.1 g

Downloaded by OHIO STATE UNIV LIBRARIES on September 16, 2012 | http://pubs.acs.org
Publication Date: January 24, 2002 | doi: 10.1021/bk-2002-0809.ch017

of the catalyst was used in each run. The catalyst sample (0.1 g) was placed in an Inconel 800 H alloy tubular reactor (0.54" OD x 0.375" i.d. and about 16" in length) for high pressure reaction and quartz reactor with similar dimensions for atmospheric reaction. A quartz wool plug was placed at the base of the reactor to support the reactor packing material. Atop the quartz wool plug a bed of α-Al_2O_3 spheres (2 mm diam) were filled up to the lower 1/3rd of the reactor on which the catalyst was loaded between two quartz wool plugs. Above the catalyst bed α-Al_2O_3 spheres were filled to form a pre-heat bed. A plug of the quartz wool was placed in the inlet of the reactor to hold the beds in place.

The catalyst bed temperature was monitored by using a chromel/alumel thermocouple placed in the center of the catalyst bed and a temperature controller. Simultaneously the furnace temperature was also monitored with the help of a separate temperature indicator. The pressure in the reactor was maintained and monitored by using a backpressure regulator and high-pressure transducer, respectively. Before admitting the reactants the catalysts were pretreated in Ar gas flow (30 ml/min) [without or with H_2 addition at 450°C] by using the following temperature program: 100°C with 15 min hold, 450°C with 75 min hold, and at reaction temperature (750°C or 800°C) with a 15 min hold. [The heat up from 100°C to 450°C, and that from 450 to 750°C or 800°C were completed in about 15 min each]. The Na-Y supported catalyst was pretreated in Ar without H_2, while the Al_2O_3-supported catalyst was pretreated in the same temperature program but with addition of H_2 flow at 450°C [10 ml/min H_2 plus 30 ml/min Ar] and with H_2 flow stopped at the end of 75 min at 450°C, because such pretreatment procedures give the best catalyst performance for both types based on our previous research (11). The commercial alumina-supported Ni catalysts were pretreated in the same way as the laboratory-prepared Al_2O_3-supported catalyst. After this catalyst pretreatment the reaction run was started by introducing CH_4 and CO_2 into the reactor (feed: CH_4=10 ml/min, CO_2=10 ml/min and Ar=30 ml/min).

The reactor system was connected to a gas chromatograph (GC) (SRI GC 8610C, Torrance, CA, USA) on line. The analysis of the reaction products was carried out by using a packed silica gel column and thermal conductivity detector (TCD). After the steady state conditions were reached (15-30 min) the reaction products were analyzed by on-line GC every 30 min during a time-on-stream (TOS) period of 300 min. H_2 and CO yields were calculated from the number of moles of CO or H_2 produced based on the total number of moles of feed (CH_4+CO_2).

Results and Discussion

Table I shows the physicochemical properties of the Ni catalysts supported on Na-Y and γ-Al_2O_3 prepared by incipient wetness impregnation method (IWI). The surface area of 8 wt% Ni/Na-Y catalyst is much higher than that of 6.6 wt% Ni/Al_2O_3 catalyst, as expected from the difference between the surface areas of

Na-Y support (826 m^2/g for LZ-Y52) and γ-Al_2O_3 support (203 m^2/g for S-1/KF). Measurements of Ni dispersion from both CO and H_2 chemisorption are based on the standard stochiometry of H/Ni or CO/Ni as unity (12). Both H_2 and CO pulse chemisorption measurements indicate that the Ni metal dispersion is better on the zeolite Na-Y than on amorphous γ-Al_2O_3.

Table I: Physicochemical properties of Ni/Na-Y and Ni/Al_2O_3 fresh catalysts prepared by IWI method

Fresh Catalysts	*Ni/Na-Y*	*Ni/Al_2O_3*
Ni loading (wt%)	8.0	6.6
BET area ($m^2.g^{-1}$-cat.)	476	185
H/Ni (fresh catalyst)	0.38	0.27
CO/Ni (fresh catalyst)	0.35	0.23

Downloaded by OHIO STATE UNIV LIBRARIES on September 16, 2012 | http://pubs.acs.org
Publication Date: January 24, 2002 | doi: 10.1021/bk-2002-0809.ch017

Figure 1 shows CO_2 conversion for Ni/Na-Y catalyst at 750°C at atmospheric pressure (1 atm) and high pressure (400 psi or 27 atm). The 8 wt% Ni/Na-Y prepared by incipient wet impregnation (IWI) is one of the better Ni catalysts among various Ni catalysts that we have prepared using different types of zeolites or amorphous supports and different preparation methods. Table II lists the conversion data corresponding to a time-on-stream (TOS) of 90 min. It can be seen from Figure 1 and Table II that CO_2 conversion over 8 wt% Ni/Na-Y at atmospheric pressure is fairly high, and remains steady at 91% over 6 h. The corresponding CH_4 conversion, 89%, is slightly lower than that of CO_2. It is worth mentioning here that several runs at atmospheric pressure were carried out in an Inconel steel reactor [with 8 wt% Ni/Na-Y (IWI), 6.6 wt% Ni/Al_2O_3 (IWI) catalysts] as well as in quartz reactor [with 7.9 wt% Ni/Na-Y (WI), 6.6 wt% Ni/ Al_2O_3 (WI) catalysts prepared by wet impregnation method (WI)]. The differences in CO_2 and CH_4 conversions for similar catalysts with the two different reactors under otherwise identical conditions were generally <5%.

However, when pressure was increased from atmospheric pressure (1 atm) to 27 atm (400 psi), drastic decreases in CO_2 conversion (from 91.1 to 46.2%) and in CH_4 conversion (from 89.1 to 29.1%) were observed. CH_4 conversion decreased more than that of CO_2 with increasing pressure. Consequently, the yields of H_2 and CO also decreased, but not in the same proportion to the decrease in conversion; CO yield decreased more than that of H_2 yield. As a result, the H_2/CO ratio increased from 0.80 to 0.96 with increasing reaction pressure from 1 to 27 atm.

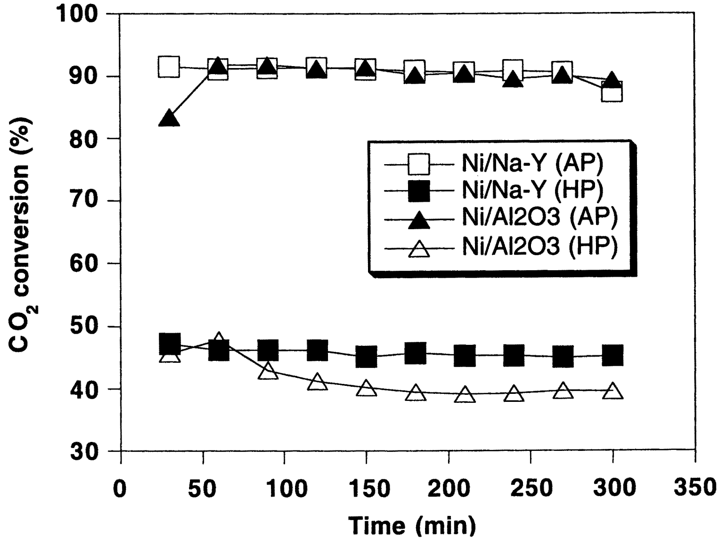

Figure 1. *CO_2 conversion as a function of TOS for 8 wt% Ni/Na-Y (IWI) and 6.6 wt% Ni/Al_2O_3 (IWI) catalysts during CO_2 reforming of CH_4 at 750 °C under 1 atm (AP) and 27 atm (HP).*

In the case of Ni/Al_2O_3 catalyst which is more (compared to Ni/Na-Y) similar to commercial Ni-based steam-reforming catalysts, CO_2 and CH_4 conversions at 750°C at atmospheric pressure are similar to those over Ni/Na-Y catalyst at atmospheric pressure. The stability of the Ni/Al_2O_3 catalyst is not as good as that of Ni/Na-Y due to extensive carbon formation at atmospheric pressure. When the system pressure was increased from 1 to 27 atm, dramatic decreases in CO_2 and CH_4 conversions were observed. Table II shows that increasing pressure caused more reduction in CH_4 conversion (89.1 to 29.1%) than that of CO_2 (91.1 to 46.2%).

These results show that the CO_2 reforming system at high pressure is considerably different from that at atmospheric pressure. The changes in conversions, the product yields and composition can not be represented by a linear function of reaction conditions. The changes in product composition and H_2/CO ratios are critical factors since they determine how the reaction could be used or integrated into a processing scheme.

Downloaded by OHIO STATE UNIV LIBRARIES on September 16, 2012 | http://pubs.acs.org
Publication Date: January 24, 2002 | doi: 10.1021/bk-2002-0809.ch017

Table II: Conversion and product yields for CO_2 reforming of CH_4 on 8 wt% Ni/Na-Y and 6.6 wt% Ni/Al_2O_3 catalysts prepared by IWI method

Catalyst	*8 wt% Ni/Na-Y*	*8 wt% Ni/Na-Y*	*6.6 wt% Ni/Al_2O_3*	*6.6 wt% Ni/Al_2O_3*
Pressure-Temp	1 atm-750°C	27 atm-750°C	1 atm-750°C	27 atm-750°C
CO_2 conversion (%)	91.1	46.2	91.8	43.0
CH_4 conversion (%)	89.1	29.1	95.3	33.3
CO yield (%)	85.6	42.6	81.9	57.9
H_2 yield (%)	68.9	40.7	66.3	29.6
H_2/CO	0.80	0.96	0.81	0.51

Note: Conversion and product yields at TOS of 90 min.

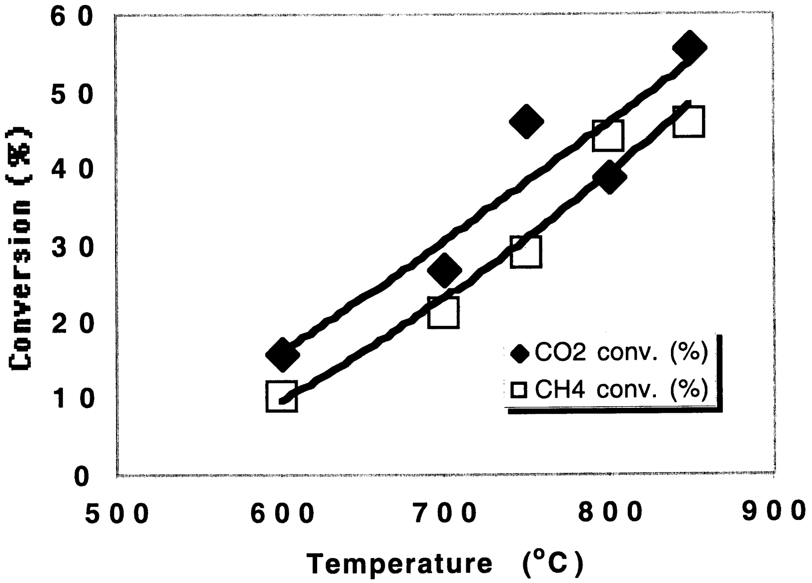

***Figure 2.** Effect of reaction temperature on CO_2 and CH_4 conversion in CO_2 reforming of CH_4 on 8 wt% Ni/Na-Y (IWI) catalyst at 400 psi (TOS: 90 min).*

Downloaded by OHIO STATE UNIV LIBRARIES on September 16, 2012 | http://pubs.acs.org
Publication Date: January 24, 2002 | doi: 10.1021/bk-2002-0809.ch017

Downloaded by OHIO STATE UNIV LIBRARIES on September 16, 2012 | http://pubs.acs.org
Publication Date: January 24, 2002 | doi: 10.1021/bk-2002-0809.ch017

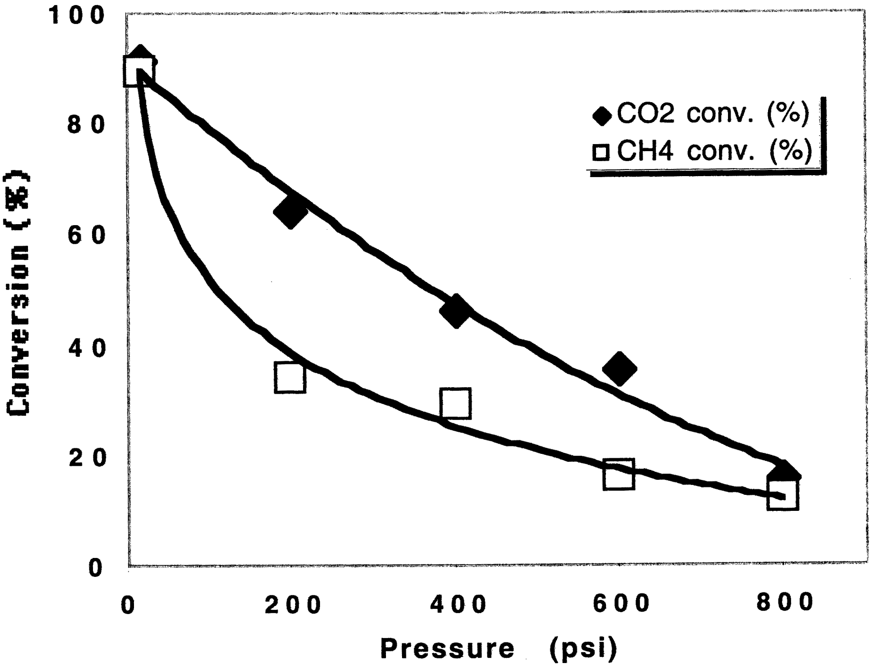

Figure 3. Effect of reaction pressure on CO_2 and CH_4 conversion in CO_2 reforming of CH_4 on 8 wt% Ni/Na-Y (IWI) catalyst at 750°C (TOS: 90 min).

We have studied the effect of temperature and pressure on CO_2 reforming of CH_4 on 8 wt% Ni/Na-Y catalyst. Figure 2 shows the effect of temperature on CO_2 and CH_4 conversion on 8 wt% Ni/Na-Y (IWI) catalyst at 400 psi (and different reaction temperatures between 600 to 850°C). It can be seen from Figure 2 that both CO_2 and CH_4 conversions increase with increasing reaction temperature, and CO_2 conversion is always higher than CH_4 conversion. Increasing CO and H_2 yields were observed with increasing reaction temperature (CO yield 21.1% at 600°C to 55.3% at 850°C; H_2 yield 16.8% at 600°C to 40.4 at 850°C), and H_2/CO ratio varied between 0.7 to 1.4 within the temperatures studied.

Figure 3 shows the effect of pressure on catalyst activity at 750°C (at different pressures 15 psi (1 atm), 200, 400, 600 and 800 psi). It can be seen from Figure 3 that CO_2 reforming of CH_4 at atmospheric pressure gives highest conversion (>90%) of CO_2 and CH_4, whereas conversions drops with increasing pressure. At all pressures CO_2 conversion was higher than CH_4 conversion. CO yields decreased with increasing pressure (CO yield: 59.2% at 200 psi to 32% at

800 psi), whereas H_2 yield increased with increasing pressure up to 400 psi and beyond which it decreased (H_2 yield: 27.9% at 200 psi to 25% at 800 psi with a maximum of 40.7% at 400 psi). H_2/CO ratio remained close to unity at all pressures except at 200 psi where it was 0.47. It is worth mentioning again that at atmospheric pressure maximum CO_2 and CH_4 conversions and CO and H_2 yields were obtained. Increasing pressure decreases catalytic conversion but increasing temperature increases CH_4 and CO2 conversion. Based on these results if we select a moderate pressure (for example 200 or 400 psi) and relatively high temperature (800-850°C), higher CO_2 and CH_4 conversions may be achieved.

Downloaded by OHIO STATE UNIV LIBRARIES on September 16, 2012 | http://pubs.acs.org
Publication Date: January 24, 2002 | doi: 10.1021/bk-2002-0809.ch017

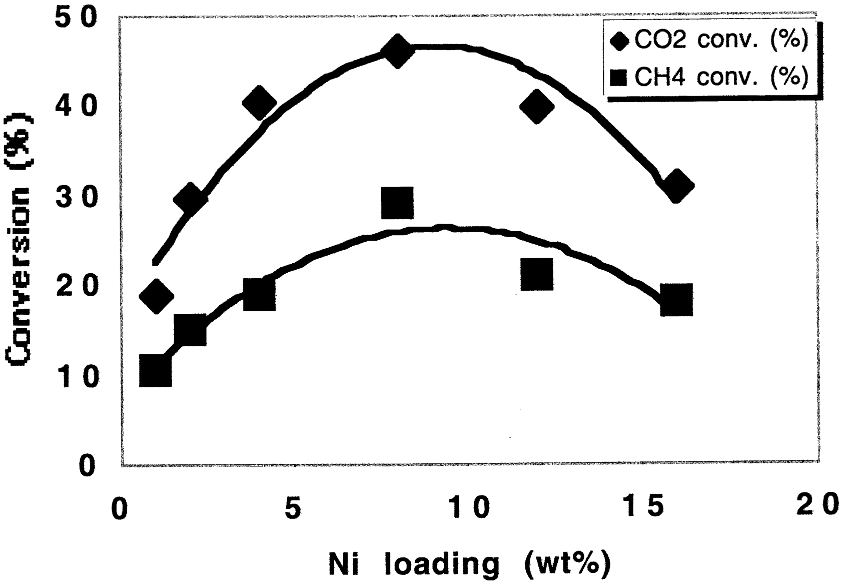

Figure 4. Effect of Ni loading on CO_2 and CH_4 conversion over Ni/Na-Y (IWI) catalyst in CO_2 reforming of CH_4 at 27 atm and 750°C (TOS: 90 min).

Figure 4 shows the effect of Ni loading in Ni/Na-Y (IWI) catalysts on CH_4 and CO_2 conversion in CO_2 reforming of CH_4 at 27 atm and 750°C. The catalytic activity strongly depends on Ni loading, and maximum CO_2 and CH_4 conversion was obtained at 8wt% Ni loading. Both CO_2 and CH_4 conversions increased with increasing Ni loading up to 8 wt% Ni, beyond that the conversions decreased with further increasing Ni loading. It can be seen from Figure 4 that CO_2 conversion is higher than CH_4 conversion for all Ni loadings. CO and H_2 yield were also increased with increased Ni loading giving an optimum at 8 wt% Ni loading (CO yield: 42.6%; H_2 yield: 40.7%), whereas

H_2/CO ratio remained around unity (between 0.78 to 0.93 from 1 wt% to 12 wt% Ni and 1.5 at 16 wt% Ni loading).

We have found that Ni/Na-Y prepared by incipient wetness impregnation (IWI) is much better than that by ion-exchange (IE) method for CO_2 reforming of CH_4 (11). For Ni loaded on Na-Y support by IWI, isolation of Ni particles in a three-dimensional structure of Na-Y zeolite surface with Na ion between Ni may inhibit bridged CO chemisorption and suppresses carbon formation. In fact, the carbon formation on Ni/Na-Y catalyst prepared by IWI method was much less than that on the corresponding catalyst prepared by ion-exchange method, and also less than that formed on Ni/Al_2O_3 catalyst. However, even with Ni/Na-Y prepared by IWI, the carbon formation problem was exacerbated significantly with increasing pressure from atmospheric pressure to 27 atm, which falls into the range of the common pressure range in industrial syngas manufacture. On the other hand the Ni/Al_2O_3 catalyst suffers from severe coking in both atmospheric- and high-pressure runs, but the difference in total amount of carbon formation due to pressure change appears to be smaller than that observed for Ni/Na-Y (IWI). The deactivation of the Ni/Al_2O_3 catalyst is more rapid during high-pressure reforming, as can be seen from Figure 1.

Table III: Analysis of used Ni/Na-Y and Ni/Al_2O_3 catalysts after CO_2 reforming at 750°C at atmospheric pressure

Used Catalysts	*8 wt% Ni/Na-Y (IWI)*	*6.6 wt% Ni/Al_2O_3 (IWI)*
H/Ni (Ni dispersion from H_2)	0.32	0.08
CO/Ni (Ni dispersion from CO)	0.3	0.05
Carbon deposit (wt%)	27.5 [66.3]*	82.3 [84.5]*

* Values outside brackets are after A-P reforming (1 atm) at 750 °C for 300 min, and those in brackets are after H-P reforming (27 atm) at 750 °C for 300 min.

We also analyzed the used Ni catalysts after the CO_2 reforming. Table III lists the metal dispersion data from H_2 and CO chemisorption, and the amount of coke determined by temperature programmed oxidation (TPO). Both H_2 and CO chemisorption data indicate that the metal dispersion was better maintained on Ni supported on Na-Y prepared by IWI. The metal dispersion data for used Ni/Al_2O_3 catalyst was much lower after 300 min TOS as compared to the fresh catalyst (Table I). This may be a result of both the change in catalytic metal species (metal sintering) and the surface carbon deposition. Despite the known uncertainties in the stochiometric ratio of CO/Ni and the possible occurrence of CO disproportionation (12), the results obtained by CO chemisorption are in good agreement with H_2 chemisorption. This may suggest the dominance of CO

Downloaded by OHIO STATE UNIV LIBRARIES on September 16, 2012 | http://pubs.acs.org
Publication Date: January 24, 2002 | doi: 10.1021/bk-2002-0809.ch017

chemisorption in the form of linearly-bound CO ($CO/Ni_{surface}=1$) in the case of CO chemisorption.

Temperature programmed oxidation (TPO) was carried out for selected catalysts before and after the reforming reaction. The results obtained after reaction at 1 atm and 27 atm at 750°C are presented in Figure 5. It can be seen from Figure 5 that there was severe carbon formation on Ni/Al_2O_3 catalyst both at atmospheric pressure (82.3% in terms of weight loss from TPO) and high pressure (84.5 % in terms of weight loss from TPO). Extent of carbon formation is less on Ni/Na-Y catalyst at high pressure (66.3%) compared to Ni/Al_2O_3 catalyst. Ni/Na-Y gives 27.3% carbon formation at atmospheric pressure reaction.

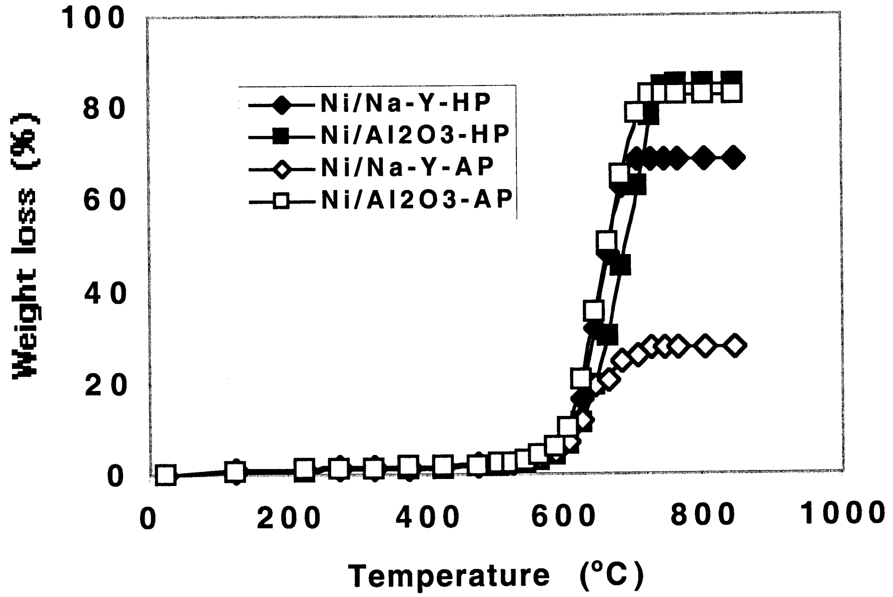

Figure 5. Temperature programmed oxidation profiles from TGA of used 8 wt% Ni/Na-Y, 6.6 wt% Ni/Al_2O_3 catalysts after CO_2 reforming of CH_4 at 1 atm (AP) and 27 atm (HP) and 750°C (used after TOS of 300 min).

Figure 6 shows the SEM photographs of Ni catalysts before and after use in CO_2 reforming at 27 atm at 750°C. The catalysts examined were 8 wt% Ni/Na-Y (IWI) (fresh catalyst and used catalyst: a, b), Ni/Na-Y (ion-exchange, IE) (fresh and used catalyst: c, d) Ni/Al_2O_3 (IWI) (fresh catalyst and used catalyst: e, f). It

Downloaded by OHIO STATE UNIV LIBRARIES on September 16, 2012 | http://pubs.acs.org
Publication Date: January 24, 2002 | doi: 10.1021/bk-2002-0809.ch017

Downloaded by OHIO STATE UNIV LIBRARIES on September 16, 2012 | http://pubs.acs.org
Publication Date: January 24, 2002 | doi: 10.1021/bk-2002-0809.ch017

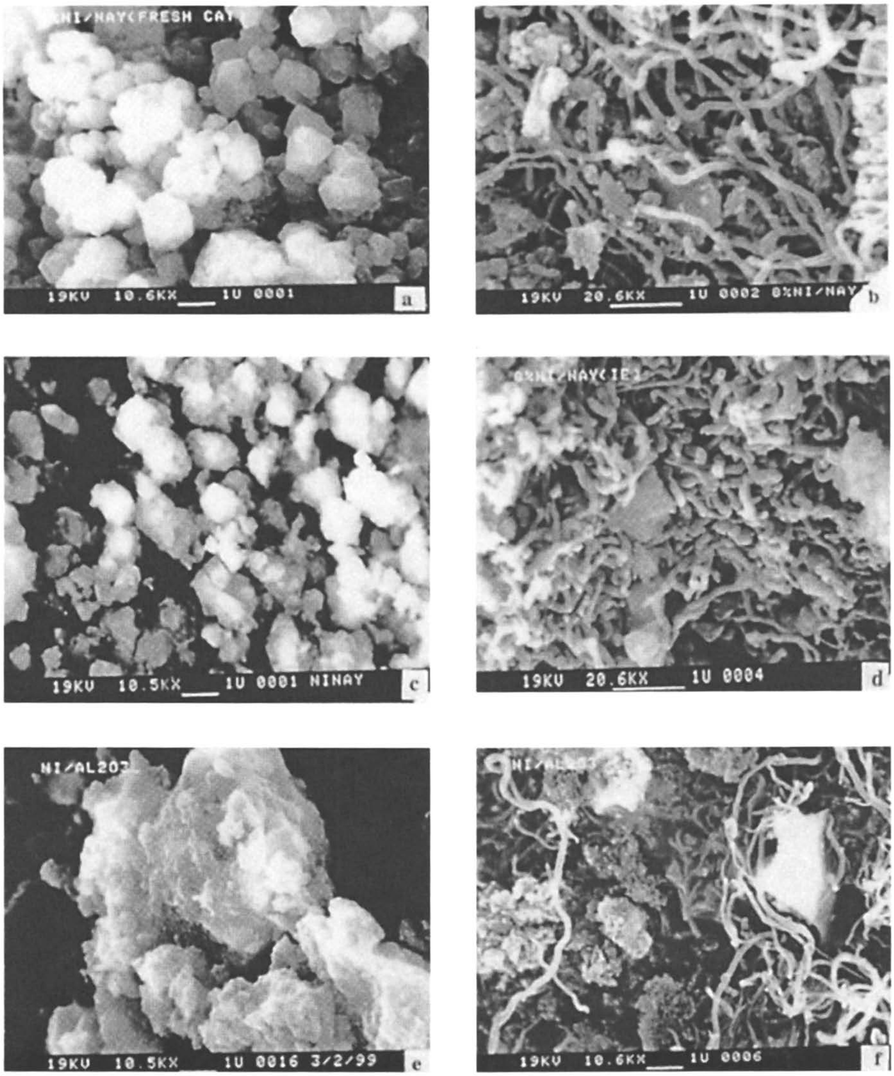
NI/NAY(FRESH CA
19KU 10.6KX 1U 0001
a
19KU 20.6KX 1U 0002 8%NI/NAY
b
19KU 10.5KX 1U 0001 NINAY
c
8%NI/NAY(IE)
19KU 20.6KX 1U 0004
d
NI/AL2O3
19KU 10.5KX 1U 0016 3/2/99
e
NI/AL2O3
19KU 10.6KX 1U 0006
f

Figure 6. *SEM photographs of fresh and used catalysts after CO_2 reforming of CH_4 at 27 atm and 750°C (after TOS of 300 min): 8 wt% Ni/Na-Y (IWI; a: fresh; b: used), 7.9 wt% Ni/Na-Y (IE; c: fresh; d: used), 6.6 wt% Ni/Al_2O_3 (IWI; e: fresh; f: used).*

is worth to mention here that the SEM photographs shown for each catalyst are representative, since several photographs of the same catalysts samples were considered in this regard. In the case of fresh catalysts crystallites of Na-Y can be seen with finely dispersed Ni-zeolite particles. In the used Ni/Na-Y (IWI) catalyst, carbon deposits in the form of carbon filaments can be clearly seen. On the other hand SEM photograph of Ni/Na-Y (IE) used catalyst shows dense carbon filamentous growth compared to Ni/Na-Y (IWI) catalyst. Inspite of severe carbon filament growth, Ni/Na-Y catalyst exhibited reasonably good activity and selectivity in CO_2 reforming of CH_4 till the end of the 300-min run. This may be due to the unique three-dimensional structure of Na-Y zeolite, wherein the Ni particles located in zeolite cage can be protected from carbon deposition, whereas the Ni particles located on the outer surface of Na-Y zeolite suffer from carbon deposition.

It appears from Figure 6 that apart from filamentous carbon some amorphous carbon can also be found on the catalysts surface. On used Ni/Al_2O_3 catalyst, the amount of amorphous carbon is more than the filamentous carbon (16). Different types of carbon have been observed on "coked" catalysts ranging from amorphous or microcrystalline species to highly aromatic/graphitic carbons and to carbides [17]. These usually result from polymerization and/or cracking of hydrocarbons. In the presence of CH_4 in its CO_2 reforming, CH_4 disproportionation as well as CH_4-CH_4 coupling may give rise to filamentous carbon growth on Ni particles [18]. The reactant adsorption effects may also greatly influence the carbon formation on metal catalysts [19].

The origin of carbon formation during CO_2 reforming of CH_4 may be from carbon monoxide disproportionation [$2\ CO = C + CO_2$] and/or methane decomposition [$CH_4 = C + 2\ H_2$], depending on the reaction conditions, the type of surface metal species, and the structure of catalyst surface.

$$2CO + * \rightarrow CO_2 + C^* \qquad (1)$$

$$CH_4 + * \rightarrow C^* + 2H_2 \qquad (2)$$

Carbon monoxide disproportionation is exothermic whereas methane decomposition is endothermic. The former is favored by higher pressure and lower temperature, while the latter is favored by higher temperature and lower pressure. The reactant adsorption effects may also influence the carbon formation on metal catalysts (13). The movement of catalyst particles is a known phenomenon and surface diffusion, temperature driven dissolution-precipitation have been reported to be responsible for carbon formation (14). In surface diffusion, surface migration of adsorbed species is an established mechanism. Thus adsorption of a hydrocarbon on a clean metal surface may lead to the diffusion of hydrocarbon or its fragments across the surface to the carbon-metal interface, where decomposition occurs to give growth of the

Downloaded by OHIO STATE UNIV LIBRARIES on September 16, 2012 | http://pubs.acs.org
Publication Date: January 24, 2002 | doi: 10.1021/bk-2002-0809.ch017

Downloaded by OHIO STATE UNIV LIBRARIES on September 16, 2012 | http://pubs.acs.org
Publication Date: January 24, 2002 | doi: 10.1021/bk-2002-0809.ch017

filament. From studies of Boudouard reaction, it was observed that nucleation of carbon occurred on specific steps and kinks of the nickel surface (15). Alternatively, adsorption of carbon may be followed by decomposition and by diffusion of carbon to the growing filament (15). At high-pressure conditions, the overall carbon concentration (from reactants) is high compared with that at atmospheric pressure, which could increase the rate of methane and carbon dioxide decomposition on surface.

The computational analysis of the thermodynamics indicated that the equilibrium conversions of CH_4 and CO_2 decrease significantly with increasing reaction pressure (21). The data in Table 1 show that more carbon deposits were formed during high-pressure CO_2 reforming compared to atmospheric-pressure reactions. The carbon formation is enhanced at high pressure according to our computational thermodynamic analysis (21). Apart from carbon formation, CO_2 and CH_4 conversions are governed by equilibrium limitations. The calculated equilibrium conversions of CO_2 at 750°C under 1 atm are around 92% and 85%, respectively, for the cases without and with carbon formation incorporated in computational analysis (21). The calculated equilibrium conversions of CO_2 at 750°C under 27 atm are around 56% and 53%, respectively, for the cases without and with carbon formation incorporated in computational analysis (21).

Some recent reports have indicated that Ni/MgO (22,23) or Ni/CaO catalysts (24) as well as Ni catalysts supported on MgO- or CaO-precoated Al_2O_3 (25) are more resistant to coke formation during CO_2 reforming of CH_4 at atmospheric pressure. On the other hand, commercial Ni-based steam-methane reforming (SMR) catalysts generally have alkali earth promoters such as MgO and CaO; and in some cases with additional alkali promoters such as K; many commercial SMR catalysts contain Ni supported on modified alumina or calcium aluminate or magnesium aluminate (26, 27). Such catalysts have been used in industrial SMR processes at high pressures, and thus it would be interesting to examine such catalysts for CO_2 reforming of CH_4 at high pressure.

We have obtained several SMR catalysts from Haldor-Topsoe A/S, United Catalyst Co. and ICI Katalco. They are commercially available samples (27) of Ni-based SMR catalysts containing MgO or CaO that were supplied together with a nominal range of composition. Table IV shows the results of performance tests with some commcercial Ni-based catalysts for CO_2 reforming at 800°C at 27 atm with CO_2/CH_4 feed ratio of 1.0 and WHSV of 30,000 $cm^3.g^{-1}.h^{-1}$. We also tested our laboratory-prepared catalysts [8 wt% Ni/Na-Y and 6.6 wt% Ni/Al_2O_3] under the same conditions using the same reactor, and the results are shown in Table IV for comparison.

Among the three commercial catalysts shown in Table IV, the Ni catalyst R-67 containing MgO and the Ni catalyst G-91 containing CaO appear to be more active than the Ni catalyst C11-9-02 for CO_2 reforming of CH_4 at 800°C under 27 atm. The laboratory-prepared catalysts give similar range of CO_2 and CH_4 conversion at 800 °C under 27 atm when compared to the two commercial catalysts R-67 and G-91. The comparison of high-pressure and atmospheric-pressure tests over the laboratory catalysts again demonstrate that increasing

Downloaded by OHIO STATE UNIV LIBRARIES on September 16, 2012 | http://pubs.acs.org
Publication Date: January 24, 2002 | doi: 10.1021/bk-2002-0809.ch017

Table IV: Commercial SMR and Laboratory Ni Catalysts Tested for CO_2 Reforming of CH_4 at 800°C under High Pressure (27 atm) (Corresponding TOS of 90 min for the Data Reported).

Catalyst Type	Commercial Cat	Commercial Cat	Commercial Cat	Laboratory Cat	Laboratory Cat	Laboratory Cat	Laboratory Cat
Catalyst ID	Haldor-Topsoe R-67 Ni/Al_2O_3-MgO	United Catalyst G-91 Ni/Al_2O_3-CaO	United Catalyst C11-0-02 Ni/Al_2O_3	PSU /ACEL, IWI 6.6 wt% Ni/Al_2O_3	PSU /ACEL, IWI 8 wt% Ni/Na-Y	PSU/ACEL IWI 6.6 wt% Ni/Al_2O_3	PSU/ACEL IWI 8 wt% Ni/Na-Y
Nominal range of composition data supplied by vendors	NiO (15-20%), MgO (20-25%), Al_2O_3 Al_2O_3 (55-60%)	NiO (15-25%), CaO (5-15%), $CaAlO_4$ (5-15%), Al_2O_3 (55-60%), K_2O (1-10%)	NiO (10-30%), Al_2O_3 (70-90%)	Laboratory-prep'd, IWI on S-1/KF g-Al_2O_3 support 6.6 wt% Ni	Laboratory-prep'd, IWI on LZ-Y52 Na-Y support 8 wt% Ni	Laboratory-prep'd, IWI on S-1/KF g-Al_2O_3 support 6.6 wt% Ni	Laboratory-prep'd, IWI on LZ-Y52 Na-Y support 8 wt% Ni
Press-Temp	27 atm-800°C	27 atm-800°C	27 atm-800°C	27 atm-800°C	27 atm-800°C	1 atm-800°C	1 atm-800°C
CO_2 conv (%)	55.7	53.3	31.9	43.9	38.6	93.1	92.3
CH_4 conv (%)	49.4	59.8	36.8	34.9	43.8	89.4	95.6
CO yield (%)	48.1	58.0	25.5	46.3	40.6	89.9	73.9
H_2 yield (%)	40.8	45.2	25.8	42.0	42.9	69.4	67.4
H_2/CO	0.85	0.78	1.01	0.91	1.06	0.68	0.91

pressure can decrease CO_2 and CH_4 conversions dramatically, cause product yields to decrease and change H_2/CO ratios.

The performance of C11-9-02 was poor in terms of lower CO_2 conversion compared to other commercial or laboratory catalysts. Our analysis of used catalysts by TPO, however, revealed severe carbon formation on all these commercial SMR catalysts under high-pressure CO_2 reforming conditions employed, with all the used catalysts after 300 min TOS containing over 60 wt% carbon deposits. It should be mentioned that these commercial catalysts were designed and optimized for steam reforming of natural gas and hydrocarbons, and our results in Table IV only reflect on their performance for CO_2 reforming of CH_4 under the conditions employed here in a small laboratory reactor.

Besides the effects of temperature and pressure, the level of carbon formation will be very dependent upon the ratios of steam/CO_2/CH_4.

Concluding remarks

Remarkable differences in CO_2 reforming of CH_4 at atmospheric pressure and high pressure were observed. The differences in catalyst conversions at 1 atm and 27 atm are in large part due to thermodynamic limitations.

Both Ni/Na-Y and Ni/Al_2O_3 were reasonably active at atmospheric pressure with high CO_2 and CH_4 conversion (>89%). The conversions over the same catalysts show a drastic decrease at high pressure (27 atm), but the change in pressure had different impacts on CO_2 and CH_4 conversions, and varied effects on H_2/CO ratios of the syngas products.

Carbon formation on some catalysts that display a superior performance at atmospheric pressure may be exacerbated at high pressure.

Low conversions of CO_2 and CH_4 and low yields of CO and H_2 were obtained from CO_2 reforming of CH_4 at high pressure of 27 atm with both laboratory and commercial Ni-based steam reforming catalysts, and all the catalysts suffered significant carbon formation within 300 min of TOS at high pressure.

Increasing reaction temperature increased catalytic conversion whereas increasing pressure has an opposite effect. On Ni/Na-Y, significant effects of Ni loadings on catalyst activity were observed; among the catalysts 2ith 1-16 wt% Ni loading, the 8 wt% Ni loading on Na-Y by IWI method gives optimum catalyst activity.

TPO characterization of carbon deposits in used catalysts showed that more severe carbon formation occurs at high pressure in the case of Ni/Na-Y (IWI), whereas the use of Ni/Al_2O_3 results in severe carbon formation both at

Downloaded by OHIO STATE UNIV LIBRARIES on September 16, 2012 | http://pubs.acs.org
Publication Date: January 24, 2002 | doi: 10.1021/bk-2002-0809.ch017

atmospheric as well as high pressure CO_2 reforming of CH_4. SEM investigation of used catalysts reveals that there are remarkable effects of type of support (Na-Y or Al_2O_3) used and catalyst preparation method on the structure of carbon deposits.

Acknowledgment

We are pleased to acknowledge the start-up funding provided to CS for this work by the Energy Institute (for purchasing reactor parts) and the Department of Materials Science and Engineering (for purchasing mini-GCs) of the Pennsylvania State University. We thank Air Products & Chemicals Inc. and members of APCI/PSU SAMCOM for funding the work on high-pressure CO_2 reforming of CH_4. We are grateful to Prof. Harold H. Schobert for his encouragement for this work, and to Mr. Ron M. Copenhaver and Dr. Jian-Ping Shen for assistance in setting up the flow reactor and on-line GC. We would like to acknowledge the Haldor-Topsoe A/S, United Catalyst Co. and ICI Katalco for graciously providing their commercial samples of steam hydrocarbon reforming catalysts with nominal compositional data.

References

1. Gunardson, H.H.; Abrardo, J.M. Hydrocarbon Processing, April 1999, p 87.
2. Armor, J.N. Appl. Catal A: **1999**, *176*, 159.
3. Rostrup-Nielsen, J.H.; Hansen, J.H.B. J. Catal. **1993**, *144*, 38.
4. Ross, J.R.H.; van Keulen, A.N.J.; Hegarty, M.E.S.; Seshan, K. Catal. Today. **1996**, *30*, 193.
5. Wang, S.; Lu, G. Q. CHEMTECH, **1999**, *29*,37.
6. Xu, X.; J. A. Moulijn. Energy & Fuels, **1996**, *10*, 305.
7. Bradford, M.C.J.; Vannice, M.A. J.Catal. **1998**, *173*, 157.
8. Chang, J. -S.; Park, S. -E.; Chon, H. Appl. Catal. A. **1996**, *145*,111.
9. Bhat, R. N.; Sachtler, W. M. H. Appl. Catal. A. **1997**, *150*, 279.
10. Ruckenstein, E.; Hu, Y.H. Ind.Eng.Chem. Res. **1998**, *37*, 1744.
11. Song, C.; Murata, S.; Srinivas, S.T.; Sun, L.; Scaroni, A.W. Am. Chem. Soc. Div. Petrol. Chem. Prepr., **1999**, *44*, 160.
12. Zhang, Z.; Verykios, X.E. Appl. Catal. **1996**, *138*, 109.
13. Nishiyama, Y.; Tamai, Y. Carbon, **1976**, *14*, 13.
14. Rostrup-Nielsen, J.; Trimm, D.L. J. Catal. **1997**, *48*, 155.
15. Gadalla, A.M.; Bower, B. Chem. Eng. Sci.,**1988**, *35*, 3049.
16. Srinivas, S.T.; Song, C.; Pan, W.; Sun, L. Am. Chem. Soc. Div. Petrol. Chem. Prepr., **2000**, *45*, 348.
17. Lobo, L.S.; Trimm, D.L. J. Catal., **1973**,*29*, 15.
18. Bernardo, C.; Trimm, D.L. Carbon, **1976**, *14*, 225.

Downloaded by OHIO STATE UNIV LIBRARIES on September 16, 2012 | http://pubs.acs.org
Publication Date: January 24, 2002 | doi: 10.1021/bk-2002-0809.ch017

19. Nishiyama, Y.; Tamai, Y. Carbon, **1976**,*14*, 13.
20. Rostrup-Nielsen, J. Stud. Surf. Sci. Catal., **1994**, *81*, 25.
21. Pan, W.; Srinivas, T.S.; Song, C. 16 th International Pittsburgh Coal Conference, Pittsburgh, USA, October 11-15, 1999, Paper No. 26-2. CD-ROM ISBN 1-890977-16-0 1999.
22. Tomishige, K.; Chen, Y.; Li, X.; Yokoyama, K.; Sone, Y.; Yamazaki, O.; Fujimoto, K. Stud. Surf. Sci. Catal. **1998**, *114*, 375.
23. Ruckenstein, E.; Hu, Y.H. Catal. Lett.**1998**, *51*, 183.
24. Cheng Z.X.; Wu Q.L.; Li J.L.; Zhu, Q. Catal. Today, **1996**, *30*, 147.
25. Choudhary, V.R.; Uphade B.S.; Mamman A.S. Catal. Lett. **1995**, *32*, 387.
26. Gunardson, H. Industrial Gases in Petrochemical Processing, Marcel Dekker, New York, 1998, p 46.
27. OGJ Special. Oil Gas J., Sept 27, 1999, p 63.

Downloaded by OHIO STATE UNIV LIBRARIES on September 16, 2012 | http://pubs.acs.org
Publication Date: January 24, 2002 | doi: 10.1021/bk-2002-0809.ch017

Downloaded by STANFORD UNIV GREEN LIBR on September 16, 2012 | http://pubs.acs.org
Publication Date: January 24, 2002 | doi: 10.1021/bk-2002-0809.ch018

Chapter 18

A Comparative Study on CH_4-CO_2 Reforming over Ni/SiO_2–MgO Catalyst Using Fluidized- and Fixed-Bed Reactors

A. Effendi, Z.-G. Zhang, and T. Yoshida

Resource and Energy Division, Hokkaido National Industrial Research Institute,
2–17 Tsukisamu-Higashi, Toyohira-ku, Sapporo 062-8517, Japan
(email: tadashi@hniri.go.jp)

CH_4-CO_2 reforming to syngas was studied by using micro-fluidized- and fixed-bed reactors over Ni/SiO_2-MgO at 700 °C, 1 atm with CO_2/CH_4 =1. The catalytic activity in the fluidized-bed reforming showed higher CH_4 and CO_2 conversions and larger H_2/CO ratio compared to those in the fixed-bed reforming. An efficient contact between reactants and catalyst in the fluidization was suggested to be partly responsible for the enhancements. Moreover, the fluidization minimized a temperature gradient of the catalyst bed and a concentration gradient of the reactant gases. Although only a limited amount of carbon, which consisted of amorphous and crystallized forms, was deposited on spent catalysts, a relatively higher XPS intensity of crystallized carbon was observed on the fixed-bed catalyst than that on the fluidized-bed one. This suggested a faster deactivation of the catalyst in the fixed-bed reactor. In addition, an uneven coke deposit was observed along fixed-bed positions.

In CO2 Conversion and Utilization; Song, C., et al.;
ACS Symposium Series; American Chemical Society: Washington, DC, 2002.

Introduction

Catalytic CO_2 reforming of CH_4 (Eq. 1) has been renewed as an attractive route for direct production of synthesis gas. Under the given conditions, however, a competitive coke formation occurs as results of CH_4 decomposition (Eq. 2) and CO disproportionation (Eq. 3), causing a catalyst deactivation. In addition, a reverse water-gas-shift (RWGS) reaction (Eq. 4) occurs simultaneously during the reforming.

$$CH_4 + CO_2 \rightarrow 2CO + 2H_2 \qquad \Delta_r H_{298} = +247.9 \text{ kJ/mol} \quad (1)$$

$$CH_4 \rightarrow C + 2H_2 \qquad \Delta_r H_{298} = +75.0 \text{ kJ/mol} \quad (2)$$

$$2CO \rightarrow C + CO_2 \qquad \Delta_r H_{298} = -172.0 \text{ kJ/mol} \quad (3)$$

$$CO_2 + H_2 \rightarrow CO + H_2O \qquad \Delta_r H_{298} = +41.0 \text{ kJ/mol} \quad (4)$$

Ni-based material has been considered as potential catalysts for industrial applications, and their modifications to high resistant coke ones by adding basic oxides such as MgO have been widely investigated. A loading of 5 wt % Ni exhibited a high activity and much less magnitude of coke deactivation (1-4).

Beside the massive coke deposition, performing CH_4-CO_2 reaction by using a fixed-bed reactor has limitations due to its high endothermicity. Poor heat-transfer can cause a temperature gradient across a fixed-bed, creating a cool-spot. To minimize these difficulties, the use of a fluidized-bed reactor has been approached (1,5,6). A fluidized reforming allowed catalyst-circulations, resulting in almost isothermal reactor operation, less concentration gradient of reactant gases and lower deactivation of catalysts (1,5,6). Lab-scale experiments showed that thermodynamic equilibrium could be achieved (5). On the other hand, a mechanical loss due to catalyst attrition during the fluidization might take place.

In the present work, the catalytic CH_4-CO_2 reforming has been examined by using a micro fluidized-bed reactor over Ni/SiO_2-MgO at 700 °C, 1 atm with $CO_2/CH_4=1$. For a comparison, fixed-bed experiments on the reforming were carried out under the same conditions. In both reactions, catalytic parameters such as CO_2 and CH_4 conversions as well as H_2/CO ratio were investigated. Coke deposits on spent catalysts were also characterized.

Downloaded by STANFORD UNIV GREEN LIBR on September 16, 2012 | http://pubs.acs.org
Publication Date: January 24, 2002 | doi: 10.1021/bk-2002-0809.ch018

Experimental

Catalyst Preparation and Characterization

A catalyst with a loading of 4.5 wt % NiO on SiO_2-MgO (Nikki Chemicals Co. Inc., 75.6 wt % SiO_2, 21.3 wt % MgO and particle size of 45-88 μm) was prepared by a multiple impregnation using an aqueous solution of nickel nitrate precursor. The support containing the active metal was dried at 70 °C between impregnation steps, then at 110 °C overnight and finally calcined in air at 550 °C for 4 hrs. Bulk compositions were determined by using ICP-AES (Shimadzu GV-1000P), whereas the surface by XPS analysis (VG ESCALAB 2201XL). Surface area (70.8 m^2/g) and average pore volume (16.2 cm^3/g) were measured by N_2 adsorption according to the BET method (Belsorb 28 apparatus, Bel Japan, Inc.). Prior to the analysis, samples were degassed at 200°C for 4 hrs. Phase analysis of powder catalysts was done by XRD (Rigaku Ltd.) using CuKα radiation (35 kV, 20 mA). Samples for TEM (JEM2010, JEOL Ltd.) were powdered and dispersed in ethanol to prepare suspensions, then applied to sample grids for this analysis. Crystallites of NiO with average particle sizes of 100-130 Å were observed from latter analyses.

Apparatus and Conditions of Reforming

A quartz micro-reactor (id of 9 mm) was applied for fluidized- and fixed-bed experiments. A thermocouple inserted inside a thermowell was used for measuring the catalyst-bed temperature and the furnace temperature was controlled by another thermocouple placed outside the wall of the reactor. A power supply (Chino SU KP3000) equipped to a tubular gold-coated glass furnace was employed. This furnace allowed an even heat distribution through the reactor-wall. Gases (CH_4, CO_2, and Ar) were purified by passage through appropriate adsorbents, and delivered to the reactor through mass flow controllers (Tokyo Keiso Co. Ltd.). Both reactions were performed under same conditions, namely at a furnace temperature of 700 °C, 1 atm with a $CO_2/CH_4=1$, and equal contact time (88 ml/min, STP, 150 mg catalyst, so W/F= 0.64 g.h/mol). In the case of the fluidized-bed experiments, the feed was supplied up-flow through a porous quartz disc. A down-flow gas stream was employed for fixed-bed experiments. Initially, the catalyst was purged with Ar (40 ml/min, STP) up to 700 °C, and then CO_2/CH_4 gases were switched to the reactor. Gases were analyzed on-line by a GC (Yanaco G3800 GC) using a 2m x 3mm id activated carbon column at isothermally 110 °C and 50 Nml/min Ar carrier. Reactants and products (CO, H_2O and H_2) from the reactor effluent were passed through a condenser and anhydrous $Mg(ClO_4)_2$ sorbent to trap residual moisture. Amount of condensed water as well as the total flow rate of effluent-gas was quantified.

Downloaded by STANFORD UNIV GREEN LIBR on September 16, 2012 | http://pubs.acs.org
Publication Date: January 24, 2002 | doi: 10.1021/bk-2002-0809.ch018

A catalytic test using the support alone resulted in below 0.1 % of CO and H_2 yields, showing a negligible activity.

Coke Determination

Coke amount on spent catalysts after reaction tests was determined by using a TG analyzer (Shimadzu DT40). Approximately 15 mg sample was pre-dried up to 110°C under 10% O_2/Ar (30 ml/min) for 10 min and a weight-loss profile was recorded from this temperature to 825°C with a heating rate of 10°C/min. Then, the profile was corrected with a baseline measured from a blank test. XPS surface analysis with C1s spectra was used to examine the nature of carbonaceous species. The AlKα was used as an energy source (1486.6 eV), operated at 10 kV, 15 mA and mainly an energy pass of 30 eV. As a reference line, the Au4$f_{7/2}$ spectrum with a binding energy (BE) of 84.0 eV was used for all measurements of pelletized samples. Moreover, changes in surface compositions of metal atoms were also examined.

Results and Discussion

Conditions for Fluidized- and Fixed-Bed Experiments

Choice of the present experimental conditions was based on results given in Fig. 1. The figure shows conversions of CO_2, CH_4 and H_2/CO ratio as a function of space velocity (W/F) using a fixed-bed reactor. Both conversions increased with the increase in W/F, then unchanged beyond 1.30 g.h/mol. Similar tendency was also obtained for the H_2/CO ratio. The suppression of their conversions in a range beyond 1.30 g.h/mol suggested that the reforming was strongly influenced by the diffusion of the reactant gases at the interphase of catalyst particles. Thus, W/F=0.64 g.h/mol was chosen for both experiments, in which the diffusion effect was considered to be less significant and the requirement for a minimum fluidization was met. Consequently, the fluidized-bed of 150 mg catalyst achieved a minimum height of $H_{mf} \approx 4$ mm, velocity of $u_{mf} \approx 47$ ml/min, STP, as visually measured and the u/u_{mf} of > 1.5 was employed.

Catalytic Activity using Fluidized- and Fixed-Bed Reactors

All catalytic activities on CH_4-CO_2 reforming were tested at 700 °C, with CO_2/CH_4 = 1.0, 1 atm for 30 hrs time-on-stream (tos) and the results are shown in Fig. 2 and Table I. Catalytic activity obtained from the fluidized-bed

Downloaded by STANFORD UNIV GREEN LIBR on September 16, 2012 | http://pubs.acs.org
Publication Date: January 24, 2002 | doi: 10.1021/bk-2002-0809.ch018

Downloaded by STANFORD UNIV GREEN LIBR on September 16, 2012 | http://pubs.acs.org
Publication Date: January 24, 2002 | doi: 10.1021/bk-2002-0809.ch018

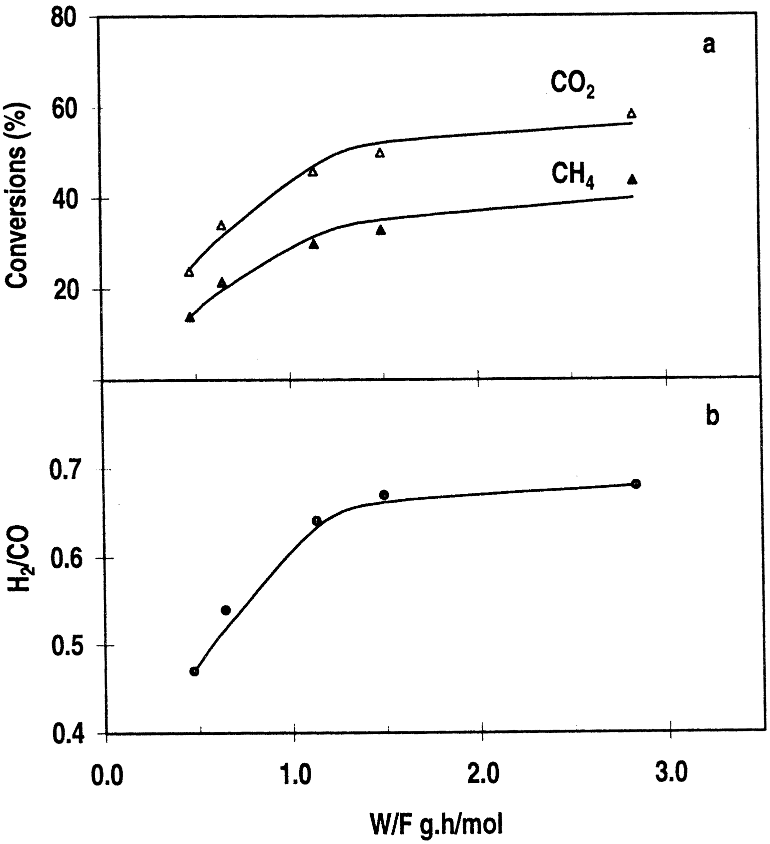

Figure 1. Conversions of CH_4 and CO_2 (a) and H_2/CO (b) over Ni/SiO_2-MgO in a fixed-bed reactor as a function of W/F

experiment showed superiority on conversions as well as H_2/CO ratio compared to that from the fixed-bed one. The conversions of CH_4 and CO_2 were higher by 16 and 19 %, whereas the H_2/CO indicated 0.69 and 0.54 for the fluidized- and fixed-bed reactions, respectively. For all cases, CO_2 conversions were always higher than the CH_4 ones, moreover, the resulted H_2/CO and CO_2/CH_4 ratios were differed from the stoichiometric values due to the occurrence of accompanied reactions (Eq. 2-4). The higher H_2/CO ratio obtained from the fluidized-bed reaction was attributed to relatively less selectivity towards the RWGS reaction, as the water yield (3.4 mol %) was lower than that from the fixed-bed one (3.8 mol %).

To elucidate the catalytic activity difference using both type reactors, particular parameters such as catalyst-bed temperatures, pressure-drops over the reactors, and coke deposits were further discussed.

Effects of Catalyst-bed Temperature

Due to the highly endothermic reforming, the catalyst-bed temperature gradient and its effect on the catalytic activity were a major importance to investigate. Under Ar alone at 700 °C, no temperature difference was observed between the catalyst-bed and furnace for both cases. However, when the supply of a CO_2/CH_4 mixture started, the bed temperature was gradually decreased and remained constant after 1 hr tos.

Table I. Results of CH_4-CO_2 reforming over Ni/SiO_2-MgO catalyst

Bed reactor	*Tb (°C)*	*CO_2/CH_4*	*H_2/CO*	*Conversions (%)*		*Coke*
				CH_4	*CO_2*	*wt %*
Fluidized	695	0.84	0.69	37.7	52.7	1.5
Fixed	684	0.77	0.54	21.5	34.0	1.6
Fluidized at 684 °C	684	0.78	0.68	37.5	51.9	nd[1]
Fixed-fluidized[2]	696	0.81	0.63	23.2	37.9	nd

[1] not determined [2]for 1.5 hrs in fixed-bed, then fluidized mode for 4.0 hrs tos

Although an axial temperature gradient over catalyst-beds was not determined, measuring temperatures at the center of the catalyst-bed might reflect a thermal reaction behavior in fluidized- and fixed-bed reactors. As shown in Fig. 3, the fluidized-bed temperature increased to 695 °C, then attained a steady state, whereas the fixed-bed temperature showed a slight increase, and remained unchanged at 684 °C. As the temperature difference was related to the thermal behavior, this might also reflect a measure of the overall change in enthalpy (7). According to this approach, the bed temperatures showed different reaction-heats, so a lower catalyst temperature of the fixed-bed indicated a larger reaction-heat absorbed for this catalytic reforming. The fixed-bed disfavored the thermal efficiency due to an inferior heat-transfer, as consequence lowering the

Downloaded by STANFORD UNIV GREEN LIBR on September 16, 2012 | http://pubs.acs.org
Publication Date: January 24, 2002 | doi: 10.1021/bk-2002-0809.ch018

Downloaded by STANFORD UNIV GREEN LIBR on September 16, 2012 | http://pubs.acs.org
Publication Date: January 24, 2002 | doi: 10.1021/bk-2002-0809.ch018

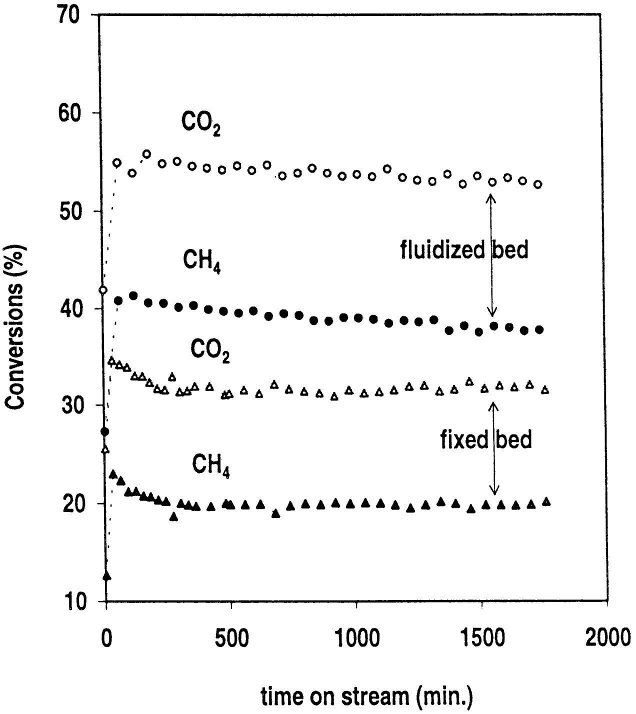

Figure. 2. Conversions of CH_4 and CO_2 over Ni/SiO_2-MgO resulted from the reforming using fixed and fluidized-bed reactors

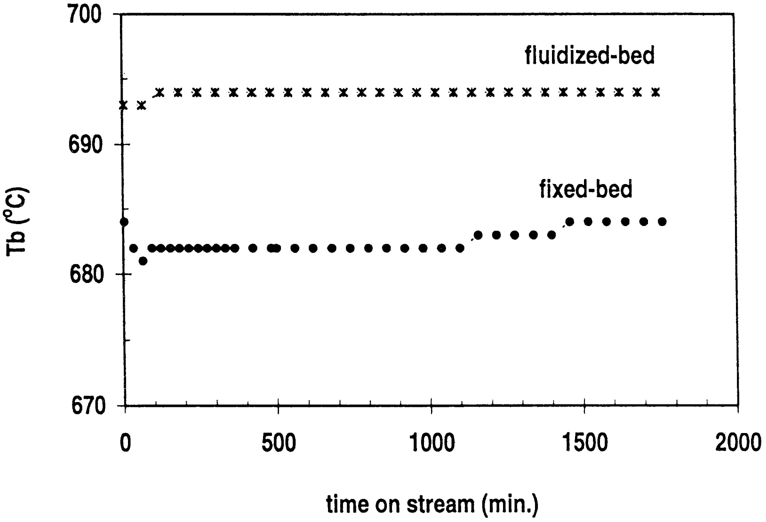

Figure. 3. Catalyst-bed temperature profiles of fluidized- and fixed reactors during CH_4-CO_2 reforming over Ni/SiO_2-MgO

Downloaded by STANFORD UNIV GREEN LIBR on September 16, 2012 | http://pubs.acs.org
Publication Date: January 24, 2002 | doi: 10.1021/bk-2002-0809.ch018

overall bed temperature. In the case of the fluidized-bed, the catalyst circulation in gases led to less heat-transfer resistance, and the absorbed-heat for the endothermic reforming was favored. Moreover, an even-heating bed was possibly achieved assuring an isothermal region, inhibiting a temperature gradient.

The above temperature difference of 11 °C might represent their variance in the catalytic activities. To examine the influence of the bed-temperatures, the fluidized-bed reforming at 684 °C was also conducted. Table I shows that lowering the catalyst-bed temperature to 684°C, which was the same bed-temperature as that of the fixed-bed applied, did not decrease significantly the catalytic activity, and the conversion levels remained close to those resulted at 695 °C. Hence, this temperature variation did not cause the difference in the catalytic activity between the fluidized- and fixed-bed reactions.

Profiles of Pressure-drop

Pressure-drop over both reactors was monitored for 30 hrs tos in which its alteration might reflect coke amount. At both initial activity tests, the pressure-drops increased slightly, and then remained significantly unchanged for 30 hrs tos. This was possibly associated to the limited amount of coke formed, ≈1.5 wt %, analyzed by the TG as shown in Table I.

Deposited Coke

Evidence of a Rapid Catalyst Deactivation in Fixed-bed. The lower catalytic activity in the fixed-bed might be related to a rapid coke formation at initial stages. To understand coke poisoned-levels on the catalyst deactivation in the fixed-bed, a short run of a catalytic test was carried out firstly in a fixed-bed for 1.5 hrs, then immediately switched to a fluidized-mode for 4 hrs. As shown in Fig. 4, the catalytic activity was lowered in the fixed-bed reaction, and then was recovered when switched to a fluidized-mode. However, the final CH_4 and CO_2 conversions appeared to be slightly higher than the result obtained from the fixed-bed mode, and much smaller than their conversions obtained by the fluidized-bed experiment alone (see Table I). It suggests that the formation of coke at the initial stage of the fixed-bed reaction gave decisive effects on lowering the catalytic activity.

Characterization on the nature of coke. Since the coke amount of both spent catalysts indicated insignificant difference, the XPS analysis was applied to distinguish the nature of the surface carbonaceous species. Figure 5 shows the C1s spectra for the fresh and spent catalysts. C1s line of the fresh catalyst

Downloaded by STANFORD UNIV GREEN LIBR on September 16, 2012 | http://pubs.acs.org
Publication Date: January 24, 2002 | doi: 10.1021/bk-2002-0809.ch018

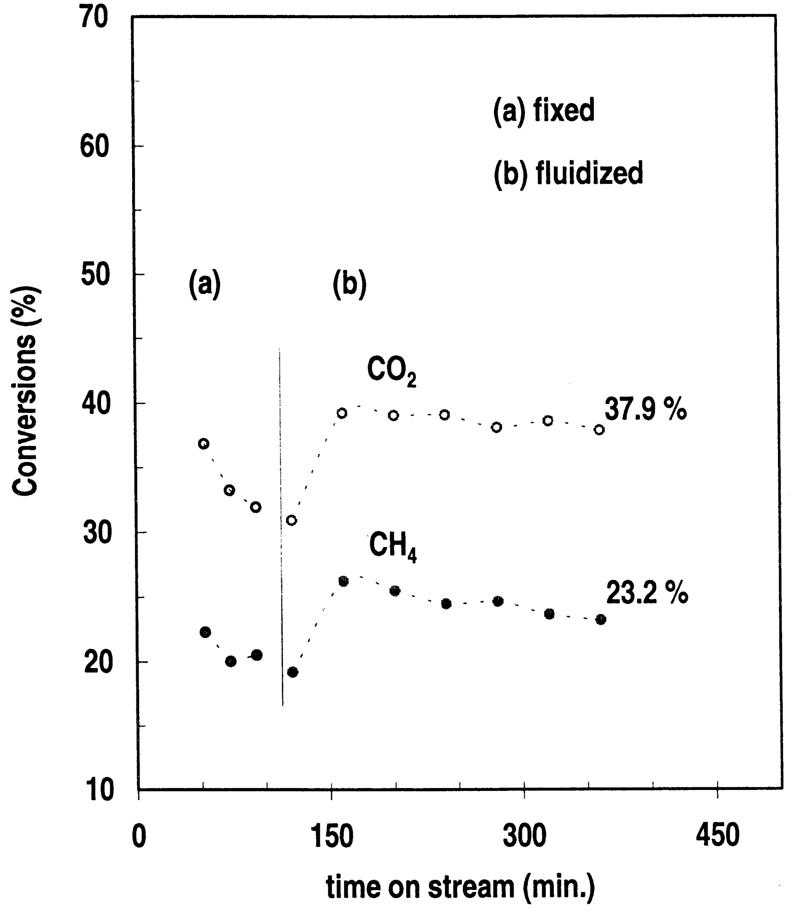

Figure. 4. Conversions of CH_4 and CO_2 over Ni/SiO_2-MgO obtained from the fluidized reforming after experiencing the fixed-bed mode

Downloaded by STANFORD UNIV GREEN LIBR on September 16, 2012 | http://pubs.acs.org
Publication Date: January 24, 2002 | doi: 10.1021/bk-2002-0809.ch018

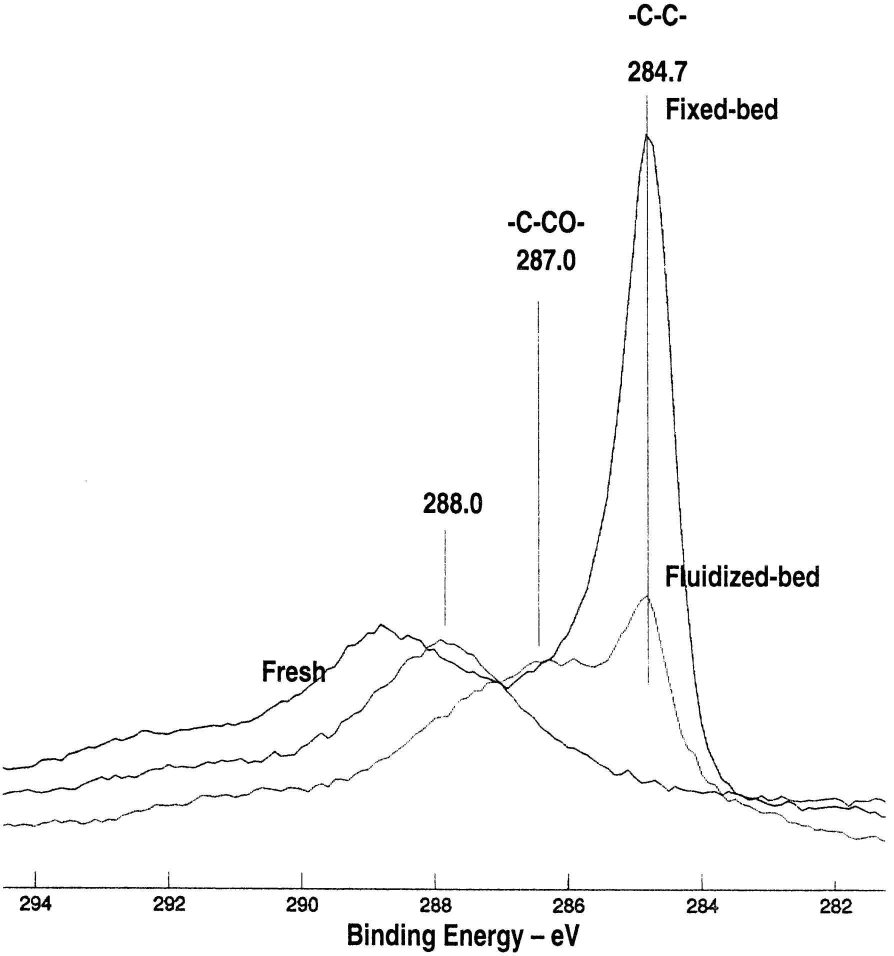

Figure. 5. XPS C1s spectra of fresh Ni/SiO$_2$–MgO and spent catalysts resulted from fluidized- and fixed-bed reforming

demonstrated a main peak with a BE of 290 eV assigned to carbonate, CO_3^- species possibly due to the exposure to air containing CO_2. Whereas, C1s lines of both spent catalysts presented peak-maxima at 287.0 and 284.7 eV, indicating the presence of amorphous (-C-CO-) and crystallized (-C-C-) structures, respectively. In the case of the fluidized-bed sample, the crystallized one was relatively a minor species. On the other hand, the average fixed-bed sample showed that the crystallized carbon became a major species and the amorphous form was less pronounced. Table II shows the relative intensity of the crystallized to amorphous forms.

According to the temperature-programmed oxidation (TPO) studies (2-4,6,9,10), it is well known that crystallized form is a less reactive carbon and usually oxidized at higher temperatures, whereas the highly reactive amorphous carbon is readily oxidized at lower temperatures. This kind of reactive species would be formed at initial stages of catalytic runs, then could be removed by gasifying with CO_2. At the same time, a possible remaining carbon would be gradually converted to a crystallized form. It became a major species on Ni catalyst after 1 hr (2-5).

Table II. XPS relative intensities of crystallized to amorphous forms and surface elemental compositions (atomic %) of Ni/SiO_2–MgO catalysts

Catalyst	I_{-C-C-}/I_{-C-CO-}	*O*	*Ni*	*Si*	*Mg*	*C*
Fresh	-	63.8	2.5	19.5	4.5	9.7
Spent (fluidized-bed)	0.67	58.6	0.7	16.4	3.0	21.3
Spent (fixed-bed)	1.93	55.4	1.1	16.0	2.8	24.7

In the catalyst fluidization, a concentration gradient of the reactant gases and an accumulation of less reactive carbon leading to the formation of crystallized carbon could be prevented. During the CH_4-CO_2 reforming, the formation of carbon by CH_4 cracking and its gasification with CO_2 were in balance and these occurred simultaneously. When the carbon was formed, it would be immediately gasified by CO_2, so this process inhibited a conversion of less reactive to crystallized forms.

Table II shows that on both spent catalysts, the surface concentrations of metals and oxygen decreased as carbon was accumulated. As more crystallized species was observed on the fixed-bed spent catalyst, which suggested to be a primary cause for the catalyst deactivation due to a poisoned encapsulation of Ni particles (3,4,9,10). Therefore, the catalyst deactivation was relatively faster in the fixed-bed reaction.

Carbonaceous species along the fixed-bed. As the color intensity of the spent catalyst resulted from the fixed reactor increased from dark gray to black with bed-positions, this might reflect its coke distribution. Accordingly, a separate experiment on a longer fixed-bed (10 mm) was carried out by using a

Downloaded by STANFORD UNIV GREEN LIBR on September 16, 2012 | http://pubs.acs.org
Publication Date: January 24, 2002 | doi: 10.1021/bk-2002-0809.ch018

Downloaded by STANFORD UNIV GREEN LIBR on September 16, 2012 | http://pubs.acs.org
Publication Date: January 24, 2002 | doi: 10.1021/bk-2002-0809.ch018

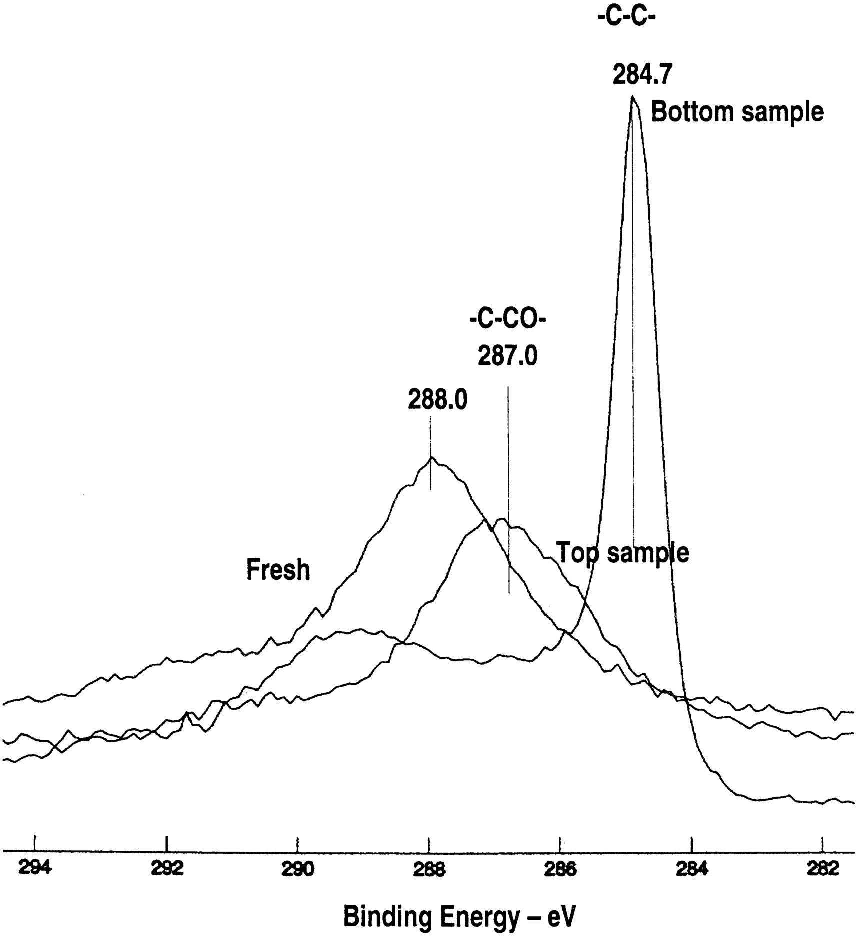

Figure. 6. XPS C1s spectra of spent catalysts sampled at top and bottom of the fixed-bed

smaller reactor (id of 4 mm) under the same condition. Figure 6 demonstrates C1s spectra of the top and bottom samples recovered after 5 hrs tos. The carbonaceous species from the top sample was dominated by a species with a BE of 287.0 eV, whereas the crystallized carbon positioned at 284.7 eV was a significant species from the bottom sample. Hence, various carbonaceous species was distributed as a function of bed positions.

It was previously suggested (2-4,9,10) that the formation of amorphous species was associated with CH_4 decomposition. In the bottom of the fixed-bed reactor, the CH_4 concentration was higher than that of CO_2, as a result, the CO_2/CH_4 ratio was less than unity. The concentration gradient of CO_2 was possibly caused by the progress of the reforming with fixed-bed positions. At the bottom of the catalyst bed, the CO_2 concentration would be minimum, leading to the suppression of the carbon gasification with CO_2. Thus, the carbon concentration increased continually with fixed-bed positions and was relatively higher on catalysts in the bottom of the bed. Moreover, since the presence of CO_2 was insufficient to remove all carbon formed, CO disproportionation (Eq.3) would possibly take place.

Downloaded by STANFORD UNIV GREEN LIBR on September 16, 2012 | http://pubs.acs.org
Publication Date: January 24, 2002 | doi: 10.1021/bk-2002-0809.ch018

Conclusions

A comparative study on the CH_4-CO_2 reforming using two different reactor types leads to the following conclusions. Conducting of the CH_4-CO_2 reforming in a fluidized-bed reactor increased the performance of the catalytic activity and H_2/CO ratio, compared to that in the fixed-bed one. Amorphous and crystallized forms were observed on the spent catalysts in the fluidized- and fixed-bed reactions. The presence of the crystallized form was a major carbon species in the fixed-bed sample, as the result, the catalyst deactivation in the fixed-bed reforming was relatively faster. In addition, a concentration gradient of the reactant gases over the fixed-bed resulted in uneven carbon distribution.

Acknowledgements

We acknowledge the financial support by the Japan International Science and Technology Exchange Corporation under the Science and Technology Fellowship Program. We also thank N. Imai for TPR, TG measurements, and Mr. O. Nishimura (HNIRI, Sapporo) for XPS analysis.

References

1. Effendi, A., Z-G. Zhang, M. Sahibzada, T. Yoshida, Am. Chem. Soc. Div. Petrol. Chem. Prepr., 45(135-137) **(2000)**
2. Schmitz, A. D. and T. Yoshida, "*Greenhouse Gas Control Technologies*", Pergamon **(1999)** 355

3. Wang, S. and G. Q. Lu, *Ind. Eng. Chem. Res.*, 38 **(1999)**, 2615-2625
4. Lu, G. Q. and S. Wang, *Chem.Tech.*, January **(1999)** 37-43
5. Mlecko, L., S. Malcus and T. Wurzel, *Ind. Eng. Chem. Res.*, 36 **(1997)** 4459-4465
6. Olbye, O., L. Mlecko and T. Wurzel, *Ind. Eng. Chem. Res.*, 36 **(1997)** 5180-5188
7. Gadalla, A. M. and B. Bower, *Chem. Eng. Sci.* 42**(1988)**, 3049-3062
8. Kunii, D. and O. Levenspiel, Fluidization Engineering 2nd edition, Butterworth-Heinemann **(1991)**
9. Himeno, Y., K. Tomoshige, K. Fujimoto, *Sekiyu Gakkashi*, 42(4) **(1999)**, 252-257
10. Wang, S., G. Q. Lu, G. J. Millar, *Energy and Fuels*, 10 **(1996)**, 896-904

Downloaded by STANFORD UNIV GREEN LIBR on September 16, 2012 | http://pubs.acs.org
Publication Date: January 24, 2002 | doi: 10.1021/bk-2002-0809.ch018

Downloaded by UNIV MASSACHUSETTS AMHERST on September 16, 2012 | http://pubs.acs.org
Publication Date: January 24, 2002 | doi: 10.1021/bk-2002-0809.ch019

Chapter 19

Effects of Pressure on CO_2 Reforming of CH_4 over Rh/Na-Y and Rh/Al_2O_3 Catalysts

Srinivas T. Srimat and Chunshan Song*

Clean Fuels & Catalysis Program, The Energy Institute, and Department of Energy and Geo-Environmental Engineering, Pennsylvania State University, 209 Academic Projects Building, University Park, PA 16802
***Corresponding author: fax: 814–865–3248; email: csong@psu.edu**

Laboratory-prepared Rh/Na-Y and Rh/Al_2O_3 catalysts were examined in CO_2 reforming of CH_4 at atmospheric pressure (1 atm) and high pressure (27 atm). It was found that the use of higher pressure substantially decreased CO_2 and CH_4 conversion and increased catalyst deactivation during CO_2 reforming of CH_4, compared to runs at 1 atm for both Rh/Na-Y and Rh/Al_2O_3 catalysts. Deactivation was related to carbon formation, and the type of support also affects both the amount and structure of carbon deposits.

Reforming of methane by carbon dioxide yields synthesis gas with a low H_2/CO ratio close to unity, which is suitable for adjusting H_2/CO ratio for certain synthetic applications such as oxo synthesis and Fischer-Tropsch synthesis (1-3). This reaction has received increasing attention in the past decade (2-14).

In CO2 Conversion and Utilization; Song, C., et al.;
ACS Symposium Series; American Chemical Society: Washington, DC, 2002.

Many catalysts tested for CO_2 reforming of CH_4 are based on Ni supported systems (4-6) that are similar to steam-reforming catalysts. Noble metals have been reported to be more resistant to coking than Ni at 1 atm (7-10) for reactions at atmospheric pressure. On the other hand, the industrial application of this reaction would require high-pressure conditions at 20 atm or higher (2,3). Under high-pressure conditions catalysts may be more susceptible to carbon formation (1). Hence a study was carried out in our laboratory to examine the behavior of Rh catalysts supported on zeolites and on amorphous materials for high-pressure CO_2 reforming of CH_4. This paper reports the results obtained on Rh catalysts for CO_2 reforming of CH_4 at 1 atm and 27 atm. Pressure significantly affects the conversion over Rh catalysts and selectivity to H_2 and CO. At similar reaction conditions, Rh supported on Na-Y and Al_2O_3 exhibit comparable activity and selectivity to Ni catalysts supported on Na-Y and Al_2O_3.

Downloaded by UNIV MASSACHUSETTS AMHERST on September 16, 2012 | http://pubs.acs.org
Publication Date: January 24, 2002 | doi: 10.1021/bk-2002-0809.ch019

Experimental

Various catalysts with Rh supported on Na-Y zeolite (LZ-Y52, SiO_2/Al_2O_3 molar ratio: 5; Surface area: 826 m^2/g) and γ-Al_2O_3 (S-1/KF; 203 m^2/g) were prepared by incipient wetness impregnation (IWI) method. In a typical preparation, a weighted amount of rhodium chloride to yield desired loading (1 wt% Rh) was dissolved in distilled water. Then the precursor salt solution was added drop-wise to Na-Y or γ-Al_2O_3 support while stirring. After the impregnation, the resulting powder was dried in oven for 16 h at 110°C. Then the samples were calcined at 450°C for 4 h in an air-circulating oven (flow rate 100 ml/min). For comparison purpose, different rhodium precursor and different preparation procedure were also employed in some catalyst preparation and reforming experiments (see below). The finished catalysts were sealed in sample bottles and kept in desccicator before use.

BET surface areas of supports and catalysts were determined by nitrogen adsorption using a GEMINI system (Micromeritics, USA) at -196°C. Rh dispersion was determined from H_2 and CO chemisorption of catalysts carried out on a Micromeritics 2910 AutoChem (USA) analyzer using a pulse chemisorption method. Carbon deposits on the catalysts after the reaction were determined by temperature programmed oxidation using TGA (Mettler TG-50). Scanning electron microscopy was used on fresh and used catalysts after CO_2 reforming of CH_4 to investigate the structure of carbon deposits. DS 130 dual stage SEM (ISI, USA) was used.

The reaction of CO_2 reforming of CH_4 was studied at a temperature of 750°C or 800°C at atmospheric pressure (1 atm) and at high pressure of 27 atm (400 psi) with a feed CO_2/CH_4 molar ratio of 1.0. Ultra-high-purity gases were used in all experiments. Mass flow controllers allow exact control of the volumes of CH_4, CO_2 and Ar into the reactor at a space velocity (WHSV) of 30,000 $cm^3 \bullet g^{-1} \bullet h^{-1}$. The calcined Rh/Na-Y catalyst sample was mixed with 20 wt% of binder alumina (Catapal B), pressed up to 5000 psi for 1 min, and sieved (between 0.5 to 1 mm), and Rh/Al_2O_3 catalyst was used without binder. About 0.1 g of the catalyst was used in reaction runs. The catalyst sample (0.1 g) was placed between two quartz wool plugs in an Inconel 800 H alloy tubular reactor (0.54” OD x 0.375” i.d. and about 16” in length). A quartz wool plug was placed at the base of the reactor to support the reactor packing material. Apart from the catalyst bed the reactor was packed with α-Al_2O_3 spheres (2 mm dia). Temperature of the reactor was monitored by using a chromel/alumel thermocouple placed in the center of the catalyst bed and a temperature controller and the furnace temperature was monitored with the help of a separate temperature indicator. The pressure in the reactor was maintained and monitored by using a backpressure regulator and pressure transducer, respectively.

The reactor system, the procedure for CO_2 reforming and the on-line GC used in this work are the same as described in another paper from our laboratory (11) was connected to GC (SRI GC 8610C, Torrance, CA, USA) on line. Before admitting the reactants the catalysts were treated in Ar flow (30 ml/min) [without or with the addition of H_2 at 450°C] by using the following temperature program: 100°C, 15 min hold-450°C, 75 min hold-750°C, 15 min hold. The zeolite-supported Rh catalysts prepared by impregnation or ion-exchange were pretreated in Ar without H_2, while the Al_2O_3-supported Rh catalysts were pretreated with the addition of H_2 (10 ml/min plus 30 ml/min Ar) at 450°C for 75 min. After this catalyst pretreatment the reaction run was started by introducing feed (CH_4=10 ml/min, CO_2=10 ml/min and Ar=30 ml/min) into the reactor. After the steady state conditions were reached (15-30 min) the reaction products were analyzed by on-line GC every 30 min during a time-on-stream (TOS) period of 300 min. H_2 and CO yields were calculated based on number of moles of CO or H_2 produced to total number of moles of feed (CH_4+CO_2).

Results and Discussion

Table I shows the physico-chemical properties of the 1 wt% Rh/Na-Y and 1 wt% Rh/Al_2O_3 catalysts prepared by IWI using rhodium chloride precursor. Figure 1 shows the CO_2 conversion for atmospheric-pressure and high-pressure runs over Rh/Na-Y and Rh/Al_2O_3 catalysts. The activity data for the Rh catalysts at TOS of 90 min are presented in Table II for comparison. Rh/Na-Y gives 90.4 % CO_2 conversion at 1 atm whereas the CO_2 conversion drops to 52.3% at 27 atm. Similarly, Rh/Al_2O_3 gives 91.3% CO_2 conversion at 1 atm while it decreased to 45% at 27 atm. Thus high CO_2 conversions were achieved with both catalysts at atmospheric pressure, but with increasing pressure both the conversion and product yields dropped significantly. Similar trends of differences in CH_4 conversion between runs at 1 atm and 27 atm were observed, as can be seen in Table II.

CO and H_2 yields for Rh/Na-Y and Rh/Al_2O_3 are shown in a bar graph (Figure 2). Both H_2 and CO yields are lower from reforming at higher pressure. However, increasing pressure decreased more of H_2 formation over Rh catalysts,

Downloaded by UNIV MASSACHUSETTS AMHERST on September 16, 2012 | http://pubs.acs.org
Publication Date: January 24, 2002 | doi: 10.1021/bk-2002-0809.ch019

and consequently this resulted in a lower H_2/CO ratios at high pressures with both Rh/Na-Y and Rh/Al_2O_3 catalysts.

Table I: Physicochemical properties of 1 wt% Rh/Na-Y and 1 wt% Rh/Al_2O_3 catalysts prepared by IWI using rhodium chloride precursor supported on Na-Y and Al_2O_3

Catalyst Precursor	*Rh chloride*	*Rh chloride*
Fresh Catalyst	Rh/Na-Y	Rh/Al_2O_3
Metal loading (wt%)	1.0	1.0
BET area ($m^2.g^{-1}$-cat.)	628	177
H/M (fresh catalyst)	0.66	-
CO/M (fresh catalyst)	0.55	-
Used Catalyst		
H/M (used catalyst)	0.42	-
CO/M (used catalyst)	0.4	-
Carbon deposit (wt%)*	5.3 [7.4]*	0.5 [1.4]*

NOTE: * Values outside brackets are after A-P reforming (1 atm; 750 °C; TOS:300 min); values inside brackets are after H-P reforming (27 atm; 750°C; TOS:300 min).

Downloaded by UNIV MASSACHUSETTS AMHERST on September 16, 2012 | http://pubs.acs.org
Publication Date: January 24, 2002 | doi: 10.1021/bk-2002-0809.ch019

The decrease in the activity between atmospheric-pressure (1 atm) and high-pressure (27 atm) operations can be attributed to several factors including equilibrium limitations of the reaction and carbon formation, and possibly some other issues associated with pressure change. We have calculated equilibrium conversions for CO_2 and CH_4 at 1 atm and 27 atm in the presence and absence of carbon formation (12). The calculated equilibrium conversions for CO_2 at 750 °C under 1 atm are, 92% and 85% respectively, for cases without and with carbon formation incorporated in computational analysis. At the same reaction temperature under 27 atm, equilibrium conversions for CO_2 are 56% and 53% respectively, for cases without and with carbon formation incorporated in computational analysis (12). The calculated equilibrium conversions of CH_4 at 750°C under 1 and 27 atm incorporating the carbon formation are around 95% and 68%, respectively. The calculated equilibrium conversions of CH_4 at 750°C under 1 and 27 atm without incorporating the carbon formation are around 88% and 34%, respectively (12). It can be seen from equilibrium conversions that in the case of CO_2, decrease in conversion is small with considering carbon formation and without considering carbon formation at both 1 atm and 27 atm, whereas higher decrease in equilibrium CH_4 conversion can be seen calculated

Table II: Conversion and product yields for CO_2 reforming at 750°C over 1 wt% Rh/Na-Y and 1 wt% Rh/Al_2O_3 catalysts prepared by IWI using rhodium chloride precursor (TOS: 90 min)

Rh precursor	Rh Chloride, IWI	Rh Chloride, IWI	Rh Chloride, IWI	Rh Chloride, IWI
Catalyst	1 wt% Rh/Na-Y	1 wt% Rh/Na-Y	1 wt% Rh/Al_2O_3	1 wt% Rh/Al_2O_3
Pressure-Temp	1 atm-750°C	27 atm-750°C	1 atm-750°C	27 atm-750°C
CO_2 conv.(%)	90.4	52.3	91.3	45.0
CH_4 conv. (%)	89.1	24.2	89.1	21.5
CO yield (%)	78.6	25.7	82.1	51.6
H_2 yield (%)	60.9	17.9	60.9	31.7
H_2/CO ratio	0.77	0.69	0.74	0.61

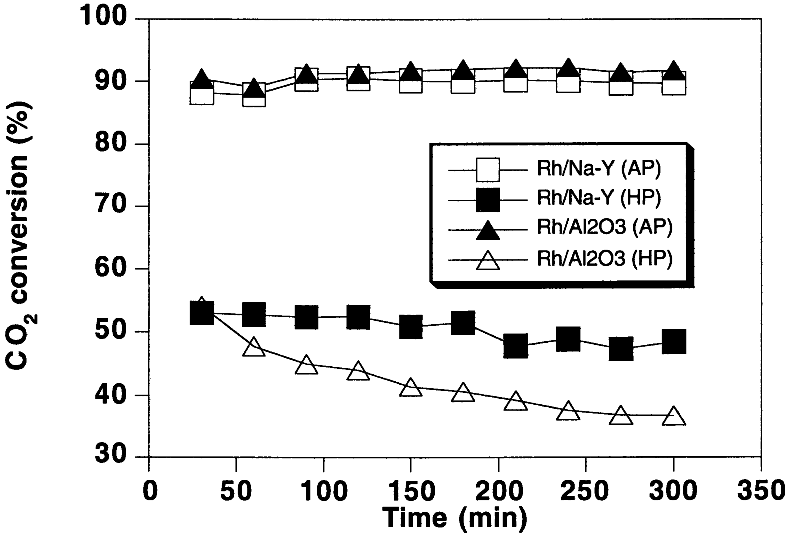

Figure 1. CO_2 conversion for 1 wt% Rh/Na-Y and 1 wt% Rh/Al_2O_3 at 1 atm (AP) and 27 atm (HP) at 750 °C. (Rh chloride was used for IWI).

Downloaded by UNIV MASSACHUSETTS AMHERST on September 16, 2012 | http://pubs.acs.org
Publication Date: January 24, 2002 | doi: 10.1021/bk-2002-0809.ch019

under similar conditions. This shows that carbon formation results from CH_4 decomposition and is in agreement with previous literature reports (5-9, 13,14). Thus our experimental data is in agreement with computational thermodynamic calculations showing that the reaction is governed by equilibrium limitations and influences catalyst activity at atmospheric and high pressure apart from carbon formation.

The TOS profiles in Figure 1 illustrate that the Rh catalysts display a stable performance against deactivation at the atmospheric pressure, but begin to deactivate within the first few hours at high pressure of 27 atm. The deactivation is more rapid with Rh/Al_2O_3 catalyst than with Rh/Na-Y catalyst during high-pressure CO_2 reforming. Relative to the runs at atmospheric pressure, the more pronounced decrease in catalyst activity with time on stream at 27 atm can be attributed mainly to enhanced carbon formation. On Na-Y, Rh is dispersed on the outer surface of the zeolite as well as in its inner pores. Carbon formation that takes place on the outer surface of the catalyst can block the active sites.

Downloaded by UNIV MASSACHUSETTS AMHERST on September 16, 2012 | http://pubs.acs.org
Publication Date: January 24, 2002 | doi: 10.1021/bk-2002-0809.ch019

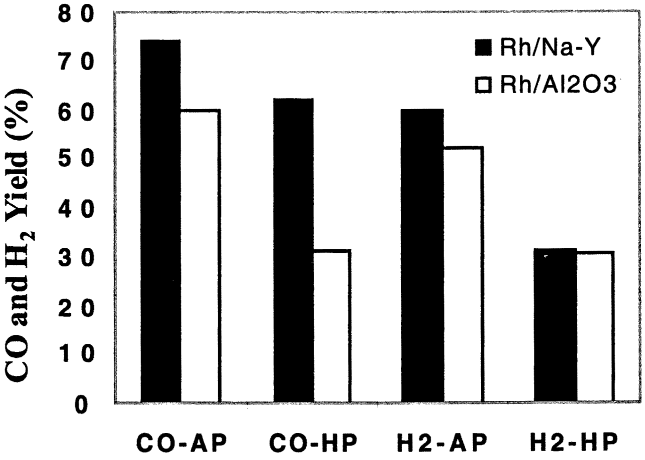

Figure 2. CO and H_2 yields for 1 wt% Rh/Na-Y and 1 wt% Rh/Al_2O_3 at 1 atm (AP) and 27 atm (HP) at 750 °C. (Rh chloride was used for IWI) (TOS: 90 min).

We also analyzed the 1 wt% Rh/Na-Y (prepared using $RhCl_3$) by H_2 and CO pulse chemisorption before and after the CO_2 reforming at 750°C (after TOS of 300 min). It can be seen from the data for used catalyst in Table I that after 300 min reaction at 750°C, Rh dispersion in Rh/Na-Y decreased by about 10%. The chemisorption data for the 1 wt% Rh/Al_2O_3 catalyst are not available at this time. On the other hand, we have observed a significant loss of the apparent Rh dispersion in a 2.5 wt% Rh/Al_2O_3 catalyst after the CO_2 reforming reaction at 750°C (eg. CO/Rh before reaction=0.27; CO/Rh after reaction at 27 atm=0.09).

Table III: Comparision of CO and H_2 yields in CO_2 reforming at 750°C over Rh catalysts (prepared from Rh chloride) and Ni catalysts (prepared from Ni nitrate) supported on Na-Y and Al_2O_3 (TOS: 90 min)

Catalyst	*H_2 yield . (%)*	*H_2 yield (%)*	*CO yield (%)*	*CO yield. (%)*
Pressure-Temp	1 atm-750°C	27 atm-750°C	1 atm-750°C	27 atm-750°C
1 wt% Rh/Na-Y (IWI)	60.9	17.9	78.6	25.7
1 wt% Rh/Al_2O_3 (IWI)	60.9	31.7	82.1	51.6
8wt% Ni/Na-Y (IWI)	68.9	40.7	85.6	42.6
6.6 wt% Ni/Al_2O_3 (IWI)	66.3	29.6	81.9	57.9

We have also examined the performance of several supported Ni catalysts for atmospheric-pressure (6) and high-pressure (11) CO_2 reforming at 750°C as well as 800°C. At high pressure of 27 atm, in general, the Rh catalysts showed no better catalyst performance than the Ni/Na-Y catalysts on similar supports under comparable conditions, both in terms of CH_4 and CO_2 conversions and catalyst stability at 27 atm. At atmospheric pressure and 750°C, 90% CH_4 and CO_2 conversions were obtained on Rh as well as Ni catalysts supported on Na-Y and Al_2O_3. At high pressure and 750°C, both CH_4 and CO_2 conversions drop but remained in similar range for all catalysts. CO_2 conversion (%) for various catalysts follows: Ni/Na-Y (46.2), Ni/Al_2O_3 (43), Rh/Na-Y (52.3) and Rh/Al_2O_3 (45); CH_4 conversion (%) for various catalysts follows: Ni/Na-Y (29.1), Ni/Al_2O_3 (33.3), Rh/Na-Y (24.2), Rh/Al_2O_3 (21.5). However, both Rh/Na-Y and Rh/Al_2O_3 appear to be much more resistant to carbon formation than Ni/Na-Y and Ni/Al_2O_3 catalysts, since the amounts of carbon accumulated on the catalysts during 300-min runs were found to be much smaller on the former (Table I) than on the latter (11), by an order of magnitude.

Downloaded by UNIV MASSACHUSETTS AMHERST on September 16, 2012 | http://pubs.acs.org
Publication Date: January 24, 2002 | doi: 10.1021/bk-2002-0809.ch019

Table III shows CO and H_2 yields on Rh catalysts (prepared from chloride precursor) and Ni catalysts (prepared from nitrate precursor) at 750°C and atmospheric pressure (1 atm) as well as at high pressure (27 atm). It can be seen from Table III that both H_2 and CO yields are similar on Rh and Ni catalysts supported on Na-Yand Al_2O_3 at atmospheric pressure (1 atm) and 750°C. On the other hand Ni/Na-Y gives more H_2 yield than Rh/Na-Y catalyst at high pressure (27 atm) and 750°C. Where as both Rh and Ni supported on Al_2O_3 give similar H_2 yields at high pressure. Similar trends were observed in CO yields obtained at high pressure.

Bhat and Sachtler (7) have reported on the superior performance of 0.93 wt% Rh/Na-Y catalyst prepared by ion exchange when compared to other Rh catalysts on amorphous supports for CO_2 reforming at atmospheric pressure. We also prepared a Rh/Na-Y (IE) with 1 wt% Rh by ion-exchange method following the method and procedure reported by Bhat and Sachtler (7) using rhodium amine precursor and Na-Y support [LZ-Y52]. In addition, we also prepared a Rh/Na-Y (IWI) catalyst using the same rhodium amine precursor and Na-Y support but by incipient wetness impregnation method.

Downloaded by UNIV MASSACHUSETTS AMHERST on September 16, 2012 | http://pubs.acs.org
Publication Date: January 24, 2002 | doi: 10.1021/bk-2002-0809.ch019

Table IV: Conversion and product yields for CO_2 reforming at 800°C over 1 wt% Rh/Na-Y (IE) and 1 wt% 1 wt% Rh/Na-Y (IWI) catalysts prepared using rhodium amine complex precursor

Rh precursor	Rh Amine Complex (IE)	Rh Amine Complex (IE)	Rh Amine Complex (IWI)	Rh Amine Complex (IWI)
Catalyst	1 wt% Rh/Na-Y	1 wt% Rh/Na-Y	1 wt% Rh/Na-Y	1 wt% Rh/Na-Y
Pressure-Temp	1 atm-800°C	27 atm-800°C	1 atm-800°C	27 atm-800°C
CO_2 conv. (%)	94.0	58.5	93.5	53.7
CH_4 conv. (%)	91.3	35.0	90.3	49.4
CO yield (%)	77.8	42.9	74.1	62.0
H_2 yield (%)	62.2	27.1	59.9	31.5
H_2/CO	0.81	0.63	0.81	0.51

Table IV shows the results for conversion and product yields for atmospheric-pressure and high-pressure CO_2 reforming at 800°C over 1 wt% Rh/Na-Y (IE) and 1 wt% Rh/Na-Y (IWI) catalysts prepared using rhodium amine complex precursor. For the runs under atmospheric pressure, both Rh catalysts give high CO_2 and CH_4 conversions, and the catalyst performance seems to be stable. These observations are similar to those reported by Bhat and

Sachtler (7). However, when the pressure is increased to 27 atm, the conversion dropped significantly, and so did the yields of CO and H_2. Moreover, the

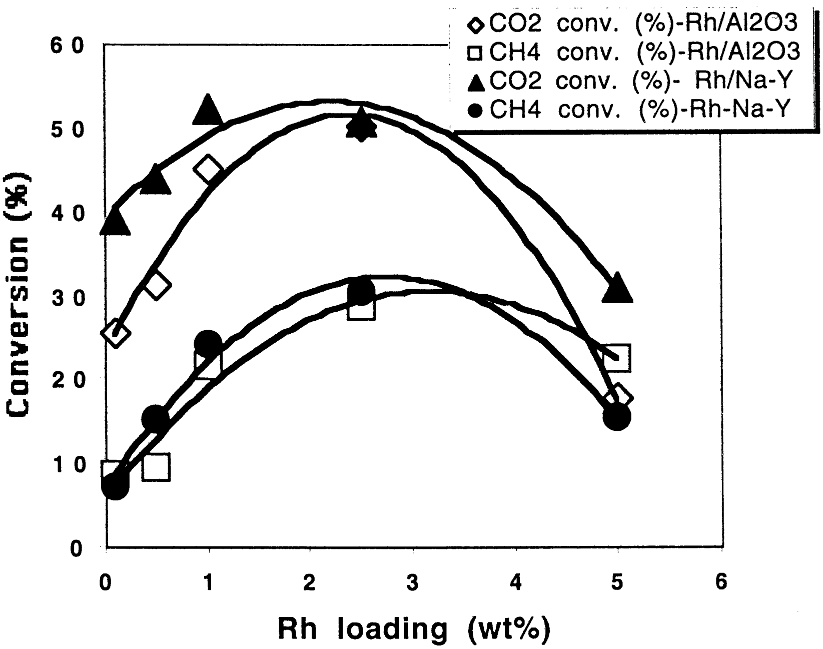

Figure 3. *Effect of Rh loading on CO_2 and CH_4 conversion over Rh/Na-Y (IWI) and Rh/Al_2O_3 (IWI) catalysts in CO_2 reforming of CH_4 at 27 atm and 750 °C (TOS: 90 min).*

catalysts begin to deactivate within 5 hours of TOS. The 1 wt% Rh/Na-Y (IWI) catalyst appears to be better than the 1 wt% Rh/Na-Y (IE) catalyst under high pressure CO_2 reforming conditions in terms of higher CO and H_2 yields and similar catalyst stability.

We have also studied the effect of Rh metal loading in Rh/Na-Y (IWI) and Rh/Al_2O_3 (IWI) prepared from Rh chloride precursor on conversion and product yield in CO_2 reforming of CH_4 at 27 atm and 750°C. CO_2 and CH_4 conversion as a function of Rh loading is shown in Figure 3. It can be seen in Figure 3 that CO_2 conversion is higher than CH_4 conversion for both Rh/Na-Y and Rh/Al_2O_3 catalysts. In the case of Rh/Na-Y catalyst, CO_2 and CH_4 conversions increase with increasing Rh loading up to 2.5 wt%, beyond that the conversions decreased with further increase in metal loading. Rh/Al_2O_3 catalyst also shows a

Downloaded by UNIV MASSACHUSETTS AMHERST on September 16, 2012 | http://pubs.acs.org
Publication Date: January 24, 2002 | doi: 10.1021/bk-2002-0809.ch019

similar trend, where CO_2 and CH_4 conversions increase with increasing Rh loading up to about 2.5 wt%, beyond which both conversions decreased. CO and H_2 yields increased with increasing Rh loading (CO yield: 23.4% at 0.1 wt% Rh to 34.9% at 5 wt% Rh; H_2 yield: 14.1% at 0.1 wt% Rh to 23% at 5 wt% Rh), where as H_2/CO ratio was below unity at all Rh loadings.

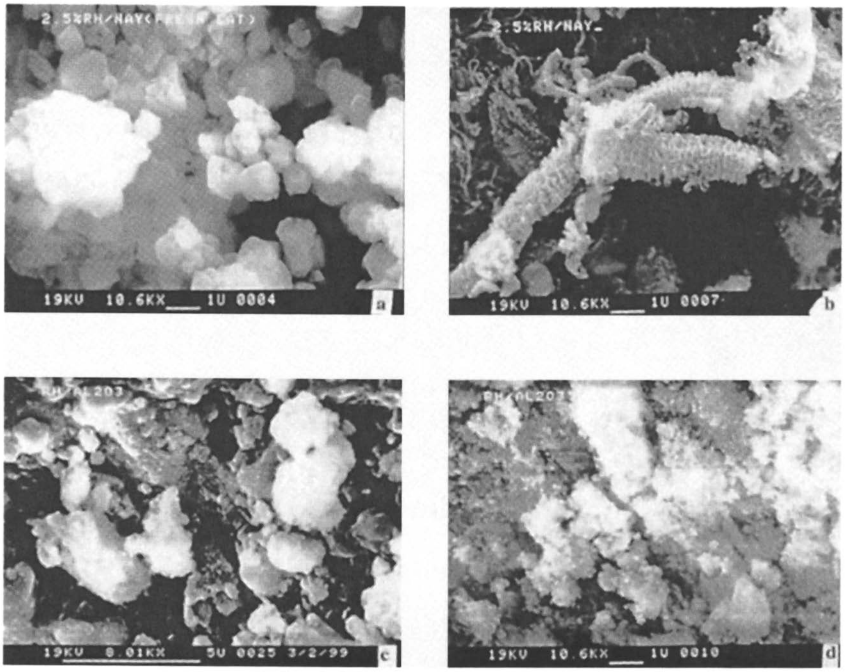
2.5%RH/NAY(FRESH CAT)
19KU 10.6KX 1U 0004
a
2.5%RH/NAY
19KU 10.6KX 1U 0007
b
RH/AL203
19KU 0.01KX 5U 0025 3/2/99
c
RH/AL203
19KU 10.6KX 1U 0010
d

Figure 4*. SEM photographs of fresh and used catalysts after CO_2 reforming of CH_4 at 27 atm and 750 °C (after TOS of 300 min): 2.5 wt% Rh/Na-Y (IWI) (a: fresh; b: used), 2.5 wt% Rh/Al_2O_3 (IWI) (c: fresh; d: used).*

Figure 4 shows SEM photographs of 2.5 wt% Rh/Na-Y (IWI) (fresh and used catalyst) and 2.5 wt% Rh/Al_2O_3 (IWI) (fresh and used catalyst) after CO_2 reforming of CH_4 at 27 atm and 750°C for 300 min TOS. It is very interesting to

Downloaded by UNIV MASSACHUSETTS AMHERST on September 16, 2012 | http://pubs.acs.org
Publication Date: January 24, 2002 | doi: 10.1021/bk-2002-0809.ch019

note that, on the used 1 wt% Rh/Na-Y (IWI) catalyst (prepared by IWI using rhodium chloride precursor), the texture of carbon deposit is entirely different when compared to those on used Ni catalysts. The carbon in the form of closely-knit coils dominate on the Rh/Na-Y catalyst, and there is also some amorphous carbon and filamentous carbon. The absence of filamentous or coiled carbon on Rh/Al_2O_3 is also interesting. It is worth to mention here that the TPO characterization of this catalyst showed very small amount of carbon deposits (1.4 %).

Temperature programmed oxidation (TPO) studies of used catalysts by TGA showed only a very small amount of carbon deposits on used Rh/Al_2O_3 catalyst in the form of amorphous carbon. For example, TPO profiles of 1 wt%

Downloaded by UNIV MASSACHUSETTS AMHERST on September 16, 2012 | http://pubs.acs.org
Publication Date: January 24, 2002 | doi: 10.1021/bk-2002-0809.ch019

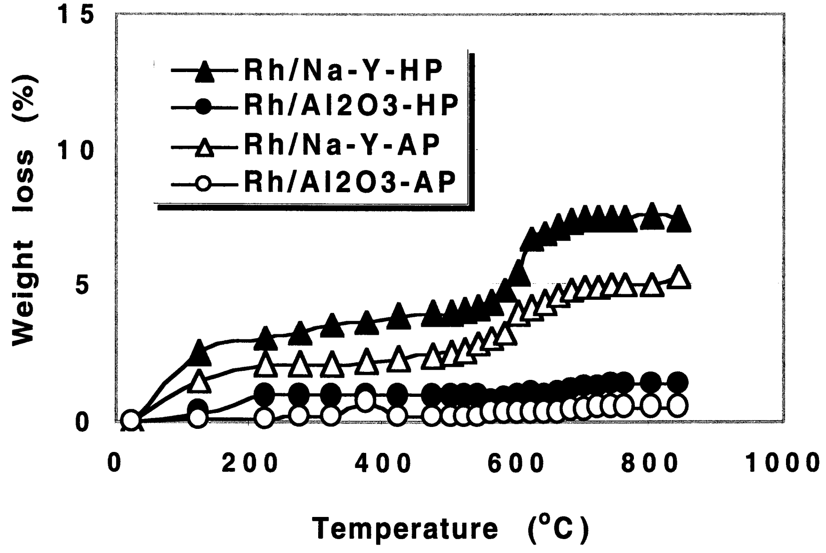

Figure 5. Temperature programmed oxidation profiles from TGA of used 1 wt% Rh/Na-Y (IWI) and 1 wt% Rh/Al_2O_3 (IWI) used catalysts after CO_2 reforming of CH_4 at 1 atm and 27 atm and 750 °C (after TOS of 300 min).

Rh/Na-Y (IWI) and 1 wt% Rh/Al_2O_3 (IWI) catalysts (prepared from rhodium chloride precursor) after CO_2 reforming of CH_4 at 1 atm and 27 atm and 750°C are shown in Figure 5. It can be seen from Figure 5 that, Rh/Na-Y catalysts results in more carbon formation (7.5% in terms of weight loss from TGA), where as Rh/Al_2O_3 results in less carbon formation at high pressure (1.4% in terms of weight loss from TGA). On the other hand at atmospheric pressure Rh/Na-Y catalysts results in more carbon formation (5.3% in terms of weight loss from TGA), where as Rh/Al_2O_3 results in very little carbon formation at high pressure (0.5% in terms of weight loss from TGA).

Various types of carbon have been observed on "coked" catalysts. They range from amorphous or microcrystalline species to highly aromatic/graphitic carbons and to carbides [15], and these usually arise from polymerization and/or cracking of hydrocarbons. In the presence of CH_4 in its CO_2 reforming, CH_4 disproportionation as well as CH_4-CH_4 coupling may give rise to filamentous carbon growth on Ni particles [16]. On the other hand, the reactant adsorption effects may also greatly influence the carbon formation on metal catalysts [17]. The movement of catalyst particles is a known phenomenon and surface diffusion, temperature driven dissolution-precipitation have also been found to be responsible for carbon formation [18]. In surface diffusion, surface migration of adsorbed species is an established mechanism, and it is suggested that carbon fibers may grow behind a nickel crystallite by a similar mechanism [19]. Thus adsorption of a hydrocarbon on a clean metal surface may lead to the diffusion of these species across the surface to the carbon-metal interface, where decomposition occurs to give growth of the filament. From studies of Boudouard reaction, it was observed that nucleation of carbon occurred on specific steps and kinks of the nickel surface [19]. Alternatively, adsorption of carbon may be followed by decomposition and by diffusion of carbon to the growing filament [20]. The carbon deposits on metal can be caused by the decomposition of CO and/or CH_4 or other gaseous reactions [20]:

$$2CO \rightarrow C + CO_2 \qquad (a)$$

$$CH_4 \rightarrow C + 2\,H_2 \qquad (b)$$

$$CO_2 + 2H_2 \rightarrow C + 2H_2O \qquad (c)$$

$$CO + H_2 \rightarrow C + H_2O \qquad (d)$$

These reactions will be favored by metals acting as oxygen receptors. The carbon species originally produced is believed to be atomic carbon and is highly active in nature. These carbon species are also important intermediates in reactions such as methanation or methane steam reforming [21,22]. In fact, steam is a more effective gasifying agent than CO_2. It is possible that carbon and

Downloaded by UNIV MASSACHUSETTS AMHERST on September 16, 2012 | http://pubs.acs.org
Publication Date: January 24, 2002 | doi: 10.1021/bk-2002-0809.ch019

surface oxygen recombine to form CO [23]. As a result, carbons may also be a major intermediate in CO_2 reforming of CH_4, and the produced water in this reaction is expected to react with reactive surface carbon to give H_2, CO and CO_2. Consequently, in CO_2 reforming of CH_4, hydrogenation of CO_2 proceeds through adsorbed species produced by dehydrogenation of CH_4 and the dissociation of C-H bond in CH_4 may be a rate limiting step [24]. Similarly, the dissociative adsorption of CO_2 on metal surface results from hydrogenation of CO_2. It is believed that the carbon species deposited on Ni surface are important intermediates in the reaction of CO_2 with CH_4. However, relative surface concentrations and the adsorption coverage for different reactant molecules could effect the catalytic properties of Ni and noble metal catalysts in CO_2 reforming of CH_4.

Downloaded by UNIV MASSACHUSETTS AMHERST on September 16, 2012 | http://pubs.acs.org
Publication Date: January 24, 2002 | doi: 10.1021/bk-2002-0809.ch019

Concluding remarks

The reaction system pressure significantly affect the CO_2 and CH_4 conversion over Rh catalysts and CO and H_2 yields as well as H_2/CO ratios during CO_2 reforming of CH_4. Both CO_2 and CH_4 conversion decrease significantly with increasing pressure from atmospheric pressure to 27 atm.

The reaction pressure has different impacts on H_2 formation and CO formation, and thus increasing pressure not only decreases CO_2 and CH_4 conversion, but also can change the H_2/CO ratio of the products.

Catalyst stability during CO_2 reforming of CH_4 can significantly decrease upon increasing pressure from 1 atm to 27 atm for Rh/Na-Y and Rh/Al_2O_3. Some Rh catalysts that showed superior performance at atmospheric pressure can begin to deactivate within hours at high pressure.

Significant effects of Rh loadings on catalyst activity were observed for Rh/Na-Y and Rh/Al_2O_3, and 2.5 wt% seems to be optimum Rh loading to get maximum activity.

TPO characterization of carbon deposits in used catalysts showed that, Rh supported on Na-Y and Al_2O_3 show much smaller amounts of carbon deposition after the reaction compared with Ni catalysts. SEM investigation of used catalysts show different effect of type of support (Na-Y or Al_2O_3) on the carbon structure. A very unusual form of carbon on used Rh/Na-Y catalyst was observed by SEM, where the carbon deposits in the form of closely-knit coils dominate.

Acknowledgment

We are pleased to acknowledge the start-up funding provided to CS for this work by the Energy Institute (for purchasing reactor parts) and the Department of Materials Science and Engineering (for purchasing mini-GC) of the

Pennsylvania State University. We thank Air Products & Chemicals Inc., Dr. John Armor of APCI and members of APCI/PSU SAMCOM for funding the work on high-pressure CO_2 reforming of CH_4. We are grateful to Prof. Alan W. Scaroni and Prof. Harold H. Schobert for their encouragement for this work, and to Mr. Ron M. Copenhaver and Dr. Jian-Ping Shen for assistance in setting up the flow reactor and on-line GC.

References

1. Rostrup-Nielsen, J. *Natural Gas Conversion II,* Curry-Hyde, H., Howe, R., Eds.; Elsevier, New York, 1994, p25.
2. Armor, J.N. *Appl. Catal A: Gen.* **1999,** *176*, 159.
3. Gunardson, H.H.; Abrardo, J.M., *Hydrocarbon Processing,* April 1999, p 87.
4. Choudhary, V.R.; Uphade, B.S.; Mamman, A.S.,*Appl. Catal. A: Gen.* **1998,** *168*, 33.
5. Wang, S.; Lu, G. Q. *CHEMTECH,* **1999,** *29*, 37.
6. Song, C.; Murata, S.; Srinivas, S.T.; Sun, L.; Scaroni, A.W. *Am. Chem. Soc. Div. Petrol. Chem. Prepr.,* **1999,** *44*, 160.
7. Bhat, R. N.; Sachtler, W. M. H. *Appl. Catal. A. Gen.* **1997,** *150*, 279.
8. Bradford, M.C.J.; Vannice, M.A. *J. Catal.* **1999,** *183*, 69.
9. Matsui, N.; Anzai, K.; Akamatsu, N.; Nakagawa, K.; Ikenaga, N.; Suzuki, T. *Appl. Catal. A: Gen.* **1999,** *179*, 247.
10. Chang, J. -S.; Park, S. -E.; Chon, H. *Appl. Catal. A: Gen.* **1996,** *145*,111.
11. Song, C.; Srinivas, S.T.; Sun, L.; Armor, J.N. *Am. Chem. Soc. Div. Petrol. Chem. Prepr.,* **2000,** *45*, 143.
12. Pan, W.; Srinivas, T.S.; Song, C. 16 th International Pittsburgh Coal Conference, Pittsburgh, USA, October 11-15, 1999, Paper No. 26-2. CD-ROM ISBN 1-890977-16-0 1999.
13. Ross, J.R.H.; van Keulen, A.N.J.; Hegarty, M.E.S.; Seshan, K. *Catal. Today.* **1996,** *30*, 193.
14. Xu, X.; Moulijn, J. A. *Energy & Fuels,* **1996,** *10*, 305.
15. Lobo, L.S.; Trimm, D.L. *J. Catal.,* **1973,** *29*, 15.
16. Bernardo, C.; Trimm, D.L. *Carbon,* **1976,** *14*, 225.
17. Nishiyama, Y.; Tamai, Y. *Carbon,* **1976,** *14*, 13.
18. Rostrup-Nielsen, J.; Trimm, D.L. *J. Catal.,* **1977,** *48*, 155.
19. Gadalla, A.M.; Bower, B. *Chem. Eng. Sci.,* **1988,** *35*, 3049.
20. Satterfield, C. Heterogeneous Catalysis in Practice, McGraw-Hill, New York, 1980, p.280.
21. McCarty, J.G.; Wise, H. *J. Catal.,* **1979,** *57*, 406.
22. Davis, S.M.; Zaera, F.; Somorjai, G. *J. Catal.,* **1982,** *77*, 439.
23. Bernardo, C.A.; Trimm, D.L. *Carbon,* **1979,** *17*, 115.
24. Kim, G.J.; Cho, D.S.; Kim, K.H.; Kim, J.H. *Catal. Lett.,* **1994,** *28*, 41.

Downloaded by UNIV MASSACHUSETTS AMHERST on September 16, 2012 | http://pubs.acs.org
Publication Date: January 24, 2002 | doi: 10.1021/bk-2002-0809.ch019

Downloaded by STANFORD UNIV GREEN LIBR on September 16, 2012 | http://pubs.acs.org
Publication Date: January 24, 2002 | doi: 10.1021/bk-2002-0809.ch020

Chapter 20

Methane Reforming with Carbon Dioxide and Oxygen under Atmospheric and Pressurized Conditions Using Fixed- and Fluidized-Bed Reactors

Keiichi Tomishige, Yuichi Matsuo, Mohammad Asadullah,
Yusuke Yoshinaga, Yasushi Sekine, and Kaoru Fujimoto

Department of Applied Chemistry, School of Engineering, The University of Tokyo, Hongo, Bunkyo-ku, Tokyo 113–8656, Japan

Effect of the reactor in methane reforming with carbon dioxide and oxygen over NiO-MgO catalysts under atmospheric and pressurized conditions was investigated. Under atmospheric pressure, the stable activity was observed using the fluidized bed reactor. However, in the fixed bed reactor, the activity decreased gradually with time on stream. On the other hand, at low temperature and high space velocity, methane conversion decreased rapidly to the level of methane combustion using fluidized bed reactor. Under pressurized condition, the stable production of syngas was possible even at high space velocity since the catalyst is in more reducing atmosphere at higher pressure. The fluidized bed reactor enhanced more effective conversion of methane to syngas than the fixed bed reactor.

Dry reforming of methane ($CH_4 + CO_2 \rightarrow 2CO + 2H_2$ ΔH=247 kJ/mol) is a suitable to the production of CO-rich syngas which can be utilized to Fischer-

In CO2 Conversion and Utilization; Song, C., et al.;
ACS Symposium Series; American Chemical Society: Washington, DC, 2002.

Tropsch, methanol and dimethyl ether syntheses (*1*). One of the problems in CO_2 reforming of methane is the heat supply because the reaction is highly endothermic. Internal heat supply by the combination of the reforming with the combustion ($CH_4 + 2O_2 \rightarrow CO_2 + 2H_2O$ ΔH=-861 kJ/mol) is one of the solutions (*2-6*). Some researches about this kind of methane reforming including the partial oxidation in the fixed bed reactor have been carried out (*2, 3*). It has been reported that methane combustion is followed by methane reforming and water-gas shift reaction. In that case, significant temperature gradient in the catalyst bed was generated. Groote et. al. simulated the temperature gradient of catalyst bed in partial oxidation of methane using the fixed bed reactor (*2*). They pointed out that the inlet temperature of the catalyst bed increased up to 1700 K though the reactor was controlled at about 1223 K. In addition, at the beginning of the catalyst bed, the catalyst was oxidized and exhibited low activity in the reforming reaction. Dissanayake et.al. have reported that the catalyst bed was divided into three parts in the partial oxidation of methane over Ni/Al_2O_3 using fixed bed reactor (*3*). The first part was composed of $NiAl_2O_4$, and the second part consisted of NiO/Al_2O_3. It is found that oxygen reached these two parts. Thus the catalyst in these two parts contributed to combustion of methane. However in the third part, surface nickel was in the metallic state and showed high activity in methane reforming.

Several researches on the reforming of methane with internal heat supply using the fluidized bed reactor have been reported (*4-6*). It has been insisted that the high rates of heat transfer and the stability of the operation were given by the fluidized bed reactor. Combustion proceeded in the front part of the catalyst bed and the reforming occurred in the rear part in both cases of fixed and fluidized bed. It is thought that both combustion and reforming proceed on one catalyst particle in fluidized bed reactor. Santos et al. have reported the partial oxidation of methane over Ni/MgO and Co/MgO using fluidized bed reactor (*4*). It has been discussed that Ni and Co change between oxidized and reduced states, and these continuous redox cycles can affect the stability and catalytic behaviors in the long run.

Pressurized syngas is more favorable because the synthesis reactions have been carried out under pressurized condition. The problem in CO_2 reforming of methane is the carbon deposition, which becomes more serious under higher pressure. Therefore, it is necessary to develop the catalyst with higher resistance to carbon deposition (*7*). Our research group has developed NiO-MgO solid solution catalysts with high resistance to carbon deposition in CO_2 reforming of methane (*8-16*). In this article, we investigated the effect of the internal heat supply in the CO_2 reforming of methane over NiO-MgO catalysts under atmospheric and pressurized conditions using the fixed and the fluidized bed reactors.

Downloaded by STANFORD UNIV GREEN LIBR on September 16, 2012 | http://pubs.acs.org
Publication Date: January 24, 2002 | doi: 10.1021/bk-2002-0809.ch020

Experimental

$Ni_xMg_{1-x}O$ (x=0.03, 0.10) catalysts were prepared by the coprecipitation method from aqueous solution of $Ni(CH_3COO)_2 \cdot 4H_2O$ (Kanto Chemical Co., inc. >98.0 %) and $Mg(NO_3)_2 \cdot 6H_2O$ (Kanto Chemical Co., inc. >99.0 %) using K_2CO_3 (Kanto Chemical Co., inc. >99.5 %) as the precipitant. After being filtered and washed with hot water, the precipitate was dried at 393 K for 12 h, and then pre-calcined in air at 773 K for 3 h. Furthermore, they were pressed into disks at 600 kg/m^2, and then calcined at 1423 K for 20 h. The catalysts were crushed and sieved to particles with 150-250 μm diameter.

Methane reforming was carried out in a fixed and a fluidized bed flow reaction systems under atmospheric and pressurized conditions. The illustration of the fluidized bed reactors is shown in Figure 1. The fluidized bed reactor under atmospheric pressure was the quartz tube (15 mmϕ i.d.) with a sintered quartz mesh as a distributor (Figure 1(a)). In the fixed bed reactor, quartz wool was put on the catalyst bed so as to prevent catalysts from moving. Pretreatment of catalysts was H_2 reduction at 1173 K for 0.5 h under atmospheric pressure. Oxygen was introduced to the reactor through the thin quartz tube, whose outlet was located just before the distributor. CO_2 and CH_4 were introduced outside the oxygen-feed tube. The partial pressure of the reactant gases was described in each result, and the total pressure was 0.1 MPa. Reaction temperature was monitored inside and outside the reactor. The reaction temperature was controlled by monitoring the thermocouple at the inside. The fluidized bed reactor under pressurized conditions was the quartz tube (6 mmϕ i.d.) which was placed inside the stainless steel tube (10 mmϕ i.d.) (Figure 1(b)). A sintered quartz mesh was used as a distributor in fluidized bed reactor. In the fixed bed reactor, quartz wool was put on catalyst bed so as to prevent catalysts from moving. Pretreatment of catalysts was H_2 reduction at 1173 K for 0.5 h at atmospheric pressure. CH_4 was introduced to the reactor through the thin quartz tube, whose outlet was located just before the distributor. CO_2 and O_2 were introduced into the reactor outside the CH_4 feed tube. The conversion of oxygen was 100% in all reaction results. GHSV is calculated on the basis of total gas flow rate of the reactants (CH_4+CO_2+O_2) at room temperature and under atmospheric pressure. The effluent gas was analyzed with FID gaschromatograph (Gaskuropack 54) equipped with a methanator for CH_4, CO, CO_2 and TCD gaschromatograph (Molecular Sieve 13X) for H_2. An ice bath was set between the reactor exit and a sampling port for GC analysis in order to remove water from the effluent gas. CH_4 (99.9%), O_2 (99 %), CO_2 (99.9 %), and H_2 (99 %) were purchased from Takachiho Co. Ltd., and were used without further purification.

Downloaded by STANFORD UNIV GREEN LIBR on September 16, 2012 | http://pubs.acs.org
Publication Date: January 24, 2002 | doi: 10.1021/bk-2002-0809.ch020

Downloaded by STANFORD UNIV GREEN LIBR on September 16, 2012 | http://pubs.acs.org
Publication Date: January 24, 2002 | doi: 10.1021/bk-2002-0809.ch020

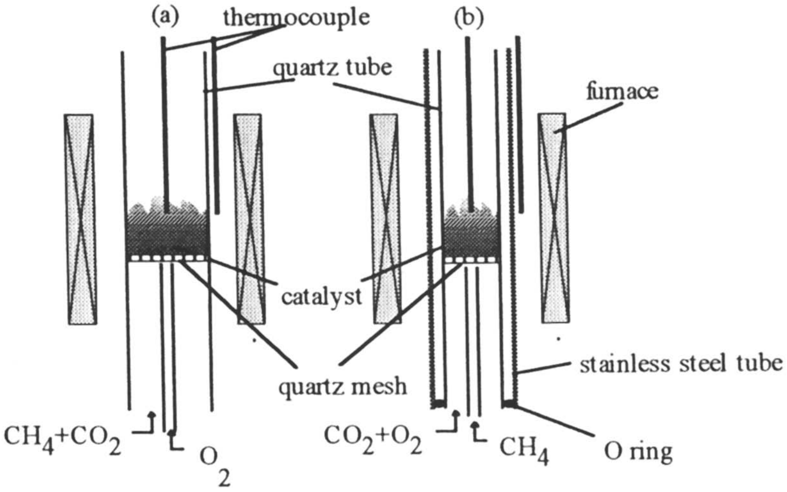

Figure 1. Illustration of the fluidized bed reactors. (a) atmospheric pressure condition, (b) pressurized condition.

Resutls and Discussion

Reforming under Atmospheric Pressure Condition

Figure 2 shows the dependence of conversion and H_2/CO ratio on the time on stream in the reforming of methane with CO_2 and O_2 over $Ni_{0.03}Mg_{0.97}O$ catalyst using fixed and fluidized bed reactors under atmospheric reaction condition. In fluidized bed reactor, high CH_4 and CO_2 conversions were maintained. On the other hand, the conversion decreased gradually with time on steam in the fixed bed reactor. The state of the catalyst in the reactors was observed after the reaction. In the fixed bed reactor, the catalyst near the inlet of the bed was green and the catalyst at the upper part was gray. The green catalyst is in the oxidized state and this indicates that oxygen can reach the green region. In contrast, the gray catalyst is in the reduced state. It has been reported that $Ni_{0.03}Mg_{0.97}O$ in oxidized state exhibited no reforming activity.

Downloaded by STANFORD UNIV GREEN LIBR on September 16, 2012 | http://pubs.acs.org
Publication Date: January 24, 2002 | doi: 10.1021/bk-2002-0809.ch020

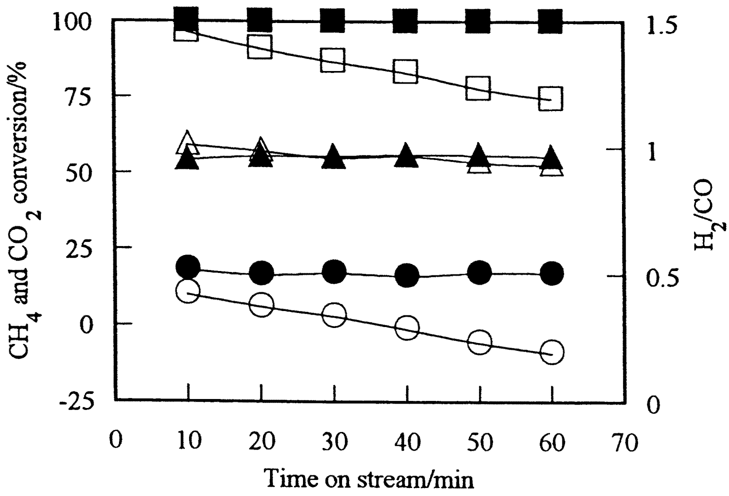

Figure 2. Comparison of CH_4 *(■,□) and* CO_2 *(●,○) conversion and* H_2/CO *(▲,△) between fluidized (■,●,▲) and fixed bed (□,○,△) reactors over* $Ni_{0.03}Mg_{0.97}O$*. Reaction conditions: reaction temperature 1123 K, total pressure 0.1 MPa,* $CH_4/CO_2/O_2=35/35/30$*, GHSV=19000* cm^3/gh*, 0.5 g-cat.*

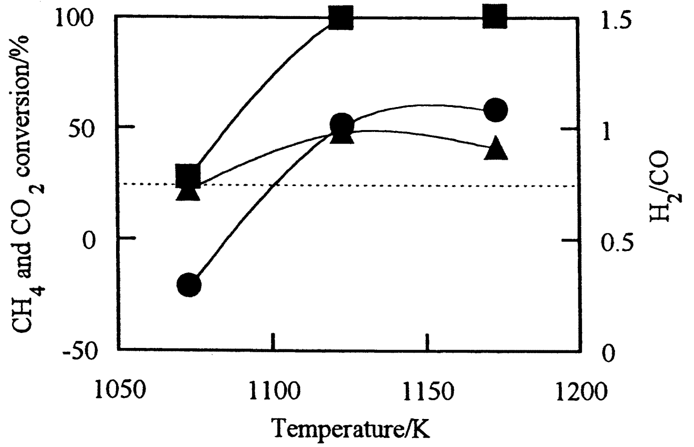

Figure 3. Effect of reaction temperature on CH_4 *(■),* CO_2 *(●) conversion and* H_2/CO *ratio (▲) over* $Ni_{0.03}Mg_{0.97}O$*. Reaction conditions: total pressure 0.1 MPa,* $CH_4/CO_2/O_2=40/40/20$*, GHSV=19000* cm^3/gh*, 0.5 g-cat, fluidized bed reactor. Dotted line represents methane conversion due to the combustion.*

It is suggested that the methane conversion decreased with the time on stream because the oxidized region became larger and larger. After the reaction the catalyst in the fluidized bed reactor was almost gray. This indicates that $Ni_{0.03}Mg_{0.97}O$ which is oxidized at the inlet of the catalyst bed can be reduced rapidly by produced syngas at the upper part of the catalyst bed.

Figure 3 shows the reaction temperature dependence of the conversion and H_2/CO ratio over $Ni_{0.03}Mg_{0.97}O$ using fluidized bed reactor. The reforming reaction proceeded at 1123 and 1173 K, where methane conversion reached about 100%. However, combustion was the main reaction at 1073 K. In this case, the rapid deactivation of the catalyst due to the catalyst oxidation was observed in the fluidized bed reactor. This is contrastive to the fact that the deactivation in the fixed bed is not so rapid as shown in Figure 2. Under the reaction conditions where the rate of the catalyst oxidation is faster than that of the catalyst reduction, the catalyst fluidization drastically enhances the deactivation rate.

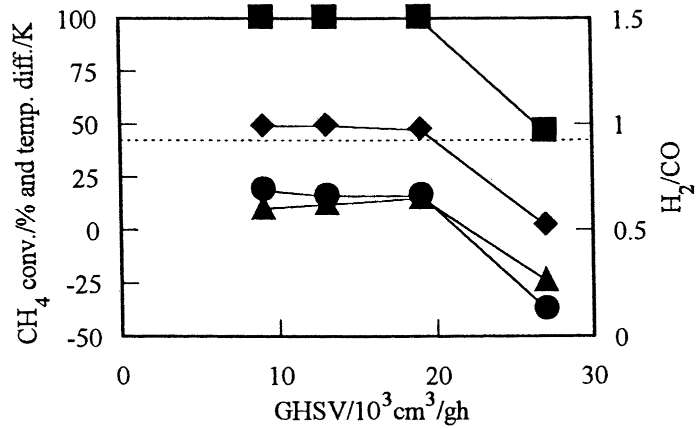

Figure 4. Dependence of CH_4 (■), CO_2 (●) conversion, H_2/CO ratio (◆), and temperature difference (▲) on space velocity over $Ni_{0.03}Mg_{0.97}O$. Reaction conditions: reaction temperature 1123 K, total pressure 0.1 MPa, $CH_4/CO_2/O_2$=35/35/30, 0.5 g-cat, fluidized bed reactor. Temperature difference = T(outside)-T(inside), and dotted line represents methane conversion due to the combustion.

The difference in methane conversion between experimental results and combustion can be assigned to methane reforming and CO production. Furthermore since H_2/CO ratio is close to one in the results, the reforming

Downloaded by STANFORD UNIV GREEN LIBR on September 16, 2012 | http://pubs.acs.org
Publication Date: January 24, 2002 | doi: 10.1021/bk-2002-0809.ch020

reaction is similar to dry reforming. At low temperature, methane conversion was close to that due to combustion, and the main product containing hydrogen is water. At high temperature, methane conversion reached 100%, the selectivity of hydrogen formation can be estimated to be 75%.

Figure 4 shows the dependence of the conversion, H_2/CO ratio, and temperature difference on space velocity over $Ni_{0.03}Mg_{0.97}O$. Methane conversion was high in the space velocity range of 9000-19000 cm^3/gh. Temperature difference between the reactor inside and outside was almost zero at these space velocities. However, at 27000 cm^3/gh, methane conversion decreased to the combustion level, and the large temperature difference was observed. At this condition, only methane combustion proceeded and thus the inside temperature was about 30 K higher than the outside temperature. This indicates that the catalyst amount in the oxidized state increased and exhibited no reforming activity at high space velocity. This is probably because the rate of oxidation is faster than that of the reduction of the catalyst.

Downloaded by STANFORD UNIV GREEN LIBR on September 16, 2012 | http://pubs.acs.org
Publication Date: January 24, 2002 | doi: 10.1021/bk-2002-0809.ch020

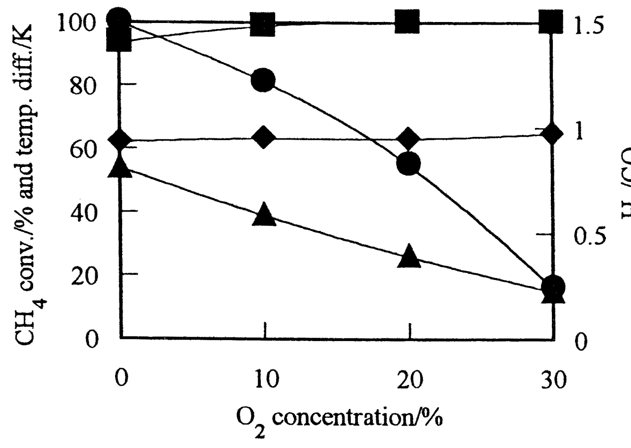

Figure 5. Effect of oxygen concentration on CH_4 *(■),* CO_2 *(●) conversion,* H_2/CO *ratio (◆), and temperature difference (▲) over* $Ni_{0.03}Mg_{0.97}O$*. Reaction conditions: reaction temperature 1123 K, total pressure 0.1 MPa,* $CH_4/CO_2/O_2=(50-x)/(50-x)/2x$ *(x=5, 10, and 15), GHSV=19000 cm*^{3}*/gh, 0.5 g-cat, fluidized bed reactor, temperature difference = T(outside)-T(inside).*

Figure 5 shows the effect of oxygen concentration in the reactant on conversion, H_2/CO ratio, and temperature difference. At 19000 cm^3/gh, the catalyst exhibited high methane conversion on all oxygen concentration. Temperature difference between the reactor inside and outside in methane reforming with only CO_2 was rather large (about 50 K). The addition of oxygen to the reactant gases made the temperature difference smaller. This is the effect of internal heat supply by the methane combustion. For the stable operation of methane reforming with CO_2 and O_2 over $Ni_{0.03}Mg_{0.97}O$ using the fluidized bed reactor, the space velocity of the reactant gases and the reaction temperature are key factors. This is the relation to the oxidizing and reducing atmosphere in the reactor.

Downloaded by STANFORD UNIV GREEN LIBR on September 16, 2012 | http://pubs.acs.org
Publication Date: January 24, 2002 | doi: 10.1021/bk-2002-0809.ch020

Reforming under Pressurized Condition

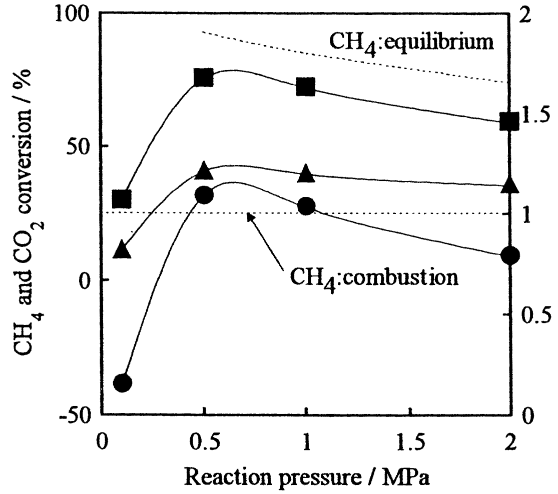

Figure 6. Dependence of CH_4 (■), CO_2 (●) conversion and H_2/CO ratio (▲) on the reaction pressure over $Ni_{0.03}Mg_{0.97}O$.
Reaction conditions: reaction temperature 1123 K, total pressure 0.1 MPa, $CH_4/CO_2/O_2$=50/25/25, GHSV=37000 cm^3/gh, 0.3 g-cat, fixed bed reactor. The reactant gas was introduced without using thin tube.

Figure 6 shows the dependence of conversion and H_2/CO ratio on the total pressure over $Ni_{0.03}Mg_{0.97}O$. At atmospheric pressure, methane combustion only proceeded because of the high space velocity. In contrast, under pressurized condition, methane reforming proceeded. Methane conversion decreased with the increase of the total pressure since the equilibrium conversion of methane is lower under higher reaction pressure. In each experiment, the methane conversion was very stable as a function of time on stream.

Downloaded by STANFORD UNIV GREEN LIBR on September 16, 2012 | http://pubs.acs.org
Publication Date: January 24, 2002 | doi: 10.1021/bk-2002-0809.ch020

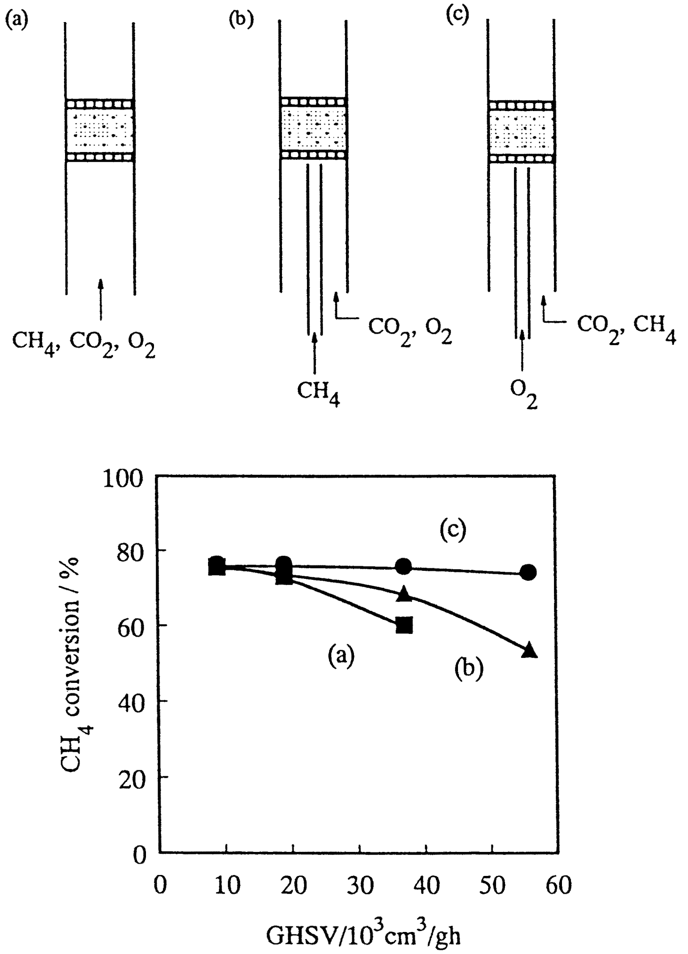

Figure 7. Effect of the introduction method on CH_4 conversion as a function of space velocity over $Ni_{0.03}Mg_{0.97}O$ using the fixed bed reactor. (a) CH_4+CO_2+O_2 without using the thin tube, (b) CH_4 (inside the thin tube), CO_2+O_2 (outside the thin tube), (c) O_2 (inside the thin tube), CH_4+CO_2 (outside the thin tube). Reaction conditions: reaction temperature 1123 K, total pressure 2.0 MPa, $CH_4/CO_2/O_2$=50/25/25, GHSV=37000 cm^3/gh, 0.3 g-cat, fixed bed reactor.

Figure 7 shows the effect of the introduction method on CH_4 conversion as a function of space velocity using the fixed bed reactor. It was found that the conversion was dependent on the gas introduction methods in methane reforming with CO_2 and O_2, and the order of methane conversion is as follows: (c)>(b)>(a). In contrast, the difference in methane conversion is so small in the reaction under atmospheric pressure. This suggested that homogeneous methane oxidation proceeds in the gas phase before the reactants reach the catalyst bed. This reaction proceeds more rapidly at higher pressure. Therefore, the amount of oxygen which reaches the catalyst bed in (a) must be smaller than that in (b) and (c). The stable operation was possible in (b). However, it was not in (c). The reaction temperature was not stable and often suddenly increased like the explosion. This is probably because the oxygen concentration was too high at the outlet of the introduction tube. Therefore, we used the reactor as shown in Figure 1(b).

Downloaded by STANFORD UNIV GREEN LIBR on September 16, 2012 | http://pubs.acs.org
Publication Date: January 24, 2002 | doi: 10.1021/bk-2002-0809.ch020

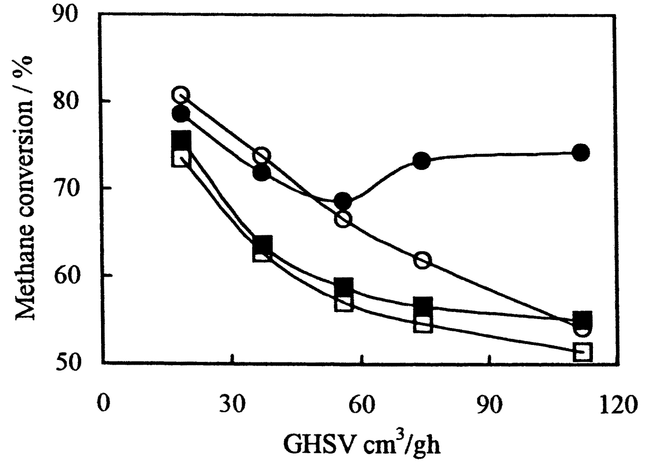

Figure 8. Dependence of CH_4 conversion on space velocity using fluidized bed (■,●) and fixed bed (□,○) reactor over $Ni_{0.03}Mg_{0.97}O$(■,□) and $Ni_{0.10}Mg_{0.90}O$ (●,○).Reaction conditions: reaction temperature 1073 K, total pressure 1.0 MPa, $CH_4/CO_2/O_2$=50/20/30, 0.2 g-cat.

Figure 8 shows the dependence of methane conversion on the space velocity over $Ni_{0.03}Mg_{0.97}O$ and $Ni_{0.10}Mg_{0.90}O$. Under pressurized condition, the conversion was stable at low reaction temperature (1073 K). Methane conversion decreased with the increase in the space velocity when the fixed bed

Downloaded by STANFORD UNIV GREEN LIBR on September 16, 2012 | http://pubs.acs.org
Publication Date: January 24, 2002 | doi: 10.1021/bk-2002-0809.ch020

reactor was used since the contact time became shorter. Methane conversion was almost the same at space velocity <56000 cm^3/gh in the fixed and fluidized bed reactors. However, methane conversion jumped at the space velocity of 70000 cm^3/gh, and the conversion in the fluidized bed reactor was higher than that in the fixed bed reactor. The fluidized bed reactor enhanced the conversion in methane reforming with CO_2 and O_2. This enhancement is more significant on $Ni_xMg_{1-x}O$ catalysts with higher Ni content. The methane conversion in CO_2 reforming of methane was not so different on these two catalysts under pressurized condition (*12*). This indicates that the enhancement effect of the fluidized bed is not caused by the catalytic activity in methane reforming. It has been reported that NiO-MgO solid solution with higher Ni content has higher reducibility (*11*).

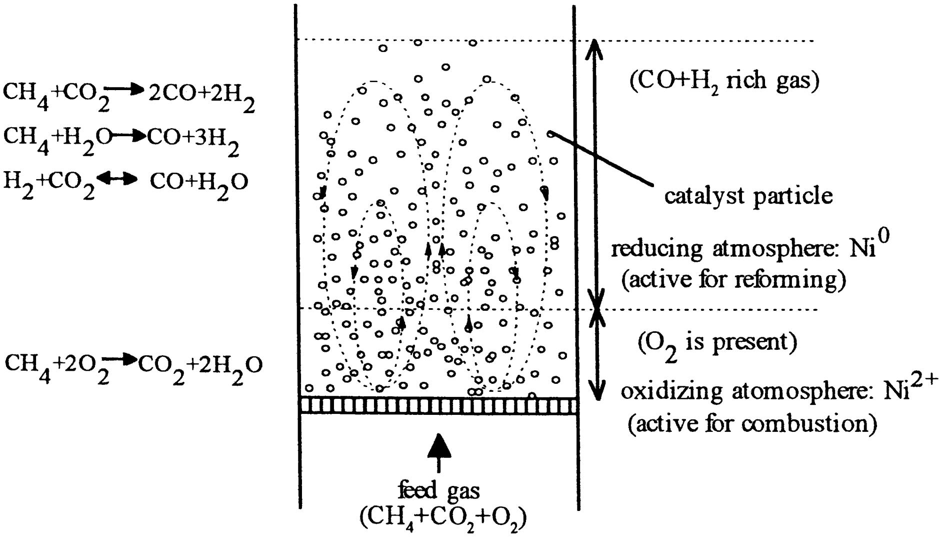
$CH_4+CO_2 \rightarrow 2CO+2H_2$
$CH_4+H_2O \rightarrow CO+3H_2$
$H_2+CO_2 \leftrightarrow CO+H_2O$
$CH_4+2O_2 \rightarrow CO_2+2H_2O$
($CO+H_2$ rich gas)
catalyst particle
reducing atmosphere: Ni^0
(active for reforming)
(O_2 is present)
oxidizing atomosphere: Ni^{2+}
(active for combustion)
feed gas
($CH_4+CO_2+O_2$)

Figure 9. A model of the fluidized bed reactor in methane reforming with CO_2 and O_2 over NiO-MgO catalysts.

From the results of methane reforming with CO_2 and O_2 under atmospheric pressure, the rapid deactivation was observed under the reaction conditions where the catalyst was easily oxidized. In the fluidized bed reactor, the oxidized catalyst can be re-reduced. On NiO-MgO with higher Ni content, the oxidized catalyst can be reduced more easily.

Figure 9 shows a model of the fluidized bed reactor in methane reforming with CO_2 and O_2. Since the combustion of methane proceeds more rapidly than methane reforming, oxygen is consumed near the inlet of the catalyst bed, where the catalyst is oxidized ($Ni^0 \rightarrow Ni^{2+}$). Oxidized NiO-MgO catalyzes the methane combustion, but it showed little reforming activity. In contrast, the upper part of the fluidized bed reactor is in the reducing atmosphere due to the presence of syngas. The catalyst which is oxidized in the bottom has a chance to be re-reduced at the upper part of the catalyst bed during the fluidization. On the other hand, the oxidized catalyst can't be re-reduced in the fixed bed reactor. Consequently, the amount of reduced catalysts in the fluidized bed reactor must be larger than that in the fixed bed reactor. This causes the enhancement of methane conversion.

Conclusions

Catalyst fluidization in methane reforming with CO_2 and O_2 over NiO-MgO catalysts under atmospheric pressure gave the stable activity. In the fixed bed reactor, the activity decreased gradually with time on stream. However, at low temperature (1073 K) and high space velocity, methane conversion rapidly decreased to the level of methane combustion using the fluidized bed reactor. This may be due to the higher rate of catalyst oxidation than that of the reduction. Under pressurized condition, the stable production of syngas was possible even at high space velocity and low reaction temprature since the catalyst is in more reducing atmosphere at higher total pressure. Methane conversion was higher in the fluidized bed reactor than in the fixed bed reactor. This enhancement of methane conversion using the fluidized bed reactor is related to the catalyst reducibility. This effect of the catalyst fluidization was more significant over NiO-MgO catalysts with higher Ni content.

Acknowledgement

This research has been supported by the Future Program of Japan Society for the Promotion of Science under the Project "Synthesis of Ecological High Quality of Transportation Fuels" (JSPS-RFTF98P01001).

References

1. Bradford, M. C. J.; Vannice, M. A. *Catal. Rev. -Sci. Eng.* **1999,** *41,* 1-42.
2. Groote, A. M. D.; Froment, G. F. *Appl. Catal. A: General* **1996,** *138,* 245-264.

Downloaded by STANFORD UNIV GREEN LIBR on September 16, 2012 | http://pubs.acs.org
Publication Date: January 24, 2002 | doi: 10.1021/bk-2002-0809.ch020

3. Dissanayake, D.; Rosynek, M. P.; Kharas, K. C. C.; Lunsford, J. H. *J. Catal.* **1991,** *132,* 117-127.
4. Santos, A.; Menendez, M.; Monzon, A.; Santamaria, J.; Miro, E. E.; Lombardo, E. A. *J. Catal.* **1996,** *158,* 83-91.
5. Bharadwaj, S. S.; Schmidt, L. D. *J. Catal.* **1994,** *146,* 11-21.
6. Opoku-Gyamfi, K.; Adesina, A. A. *Appl. Catal. A: General* **1999,** *180,* 113.
7. Armor, N. *Res. Chem. Intermed.* **1998,** *24,* 105-113.
8. Yamazaki, O.; Tomishige, K.; Fujimoto, K. *Appl. Catal. A: General* **1996,** *136,* 49-56.
9. Tomishige, K.; Fujimoto, K. *Catal. Survey from Japan* **1998,** *2,* 3-15.
10. Tomishige, K.; Chen, Y.; Fujimoto, K. *J. Catal.* **1999,** *181,* 91-103.
11. Chen, Y.; Tomishige, K.; Yokoyama, K.; Fujimoto, K. *J. Catal.* **1999,** *184,* 479-490.
12. Tomishige, K.; Himeno, Y.; Yamazaki, O.; Chen, Y.; Wakatsuki, T.; Fujimoto, K. *Kinet. Catal.* **1999,** *40,* 388-394.
13. Himeno, Y.; Tomishige, K.; Fujimoto, K. *Sekiyu Gakkaishi,* **1999,** *42,* 252-257.
14. Chen, Y.; Yamazaki, O.; Tomishige, K.; Fujimoto, K. *Catal. Lett.* **1996,** *39,* 91-95.
15. Chen, Y.; Tomishige, K.; Yokoyama, K.; Fujimoto, K. *Appl. Catal. A:General* **1997,** *165,* 335-347.
16. Yamazaki, O.; Nozaki, T.; Fujimoto, K., *Chem. Lett.* **1992,** 1953-1954.

Downloaded by STANFORD UNIV GREEN LIBR on September 16, 2012 | http://pubs.acs.org
Publication Date: January 24, 2002 | doi: 10.1021/bk-2002-0809.ch020

Downloaded by UNIV MASSACHUSETTS AMHERST on September 16, 2012 | http://pubs.acs.org
Publication Date: January 24, 2002 | doi: 10.1021/bk-2002-0809.ch021

Chapter 21

Computational Analysis of Energy Aspects of CO_2 Reforming and Oxy–CO_2 Reforming of Methane at Different Pressures

Wei Pan[1,2] and Chunshan Song[1,*]

[1]Clean Fuels & Catalysis Program, The Energy Institute, and Department of Energy and Geo-Environmental Engineering, Pennsylvania State University, 209 Academic Projects Building, University Park, PA 16802
[2]From State Key Laboratory of Cl Chemical Technology, Department of Chemistry, Tsinghua University, Beijing 100084, China
***Corresponding author: Fax: 814–865–3248; email: csong@psu.edu**

Calculation on energy requirement with different feedstock compositions, reaction temperatures, and reaction pressures in CO_2 reforming and oxy-CO_2 reforming was conducted in this paper. The thermo-neutral state in oxy-reforming system at different temperatures and pressures was also estimated by this calculation.

CO_2 reforming of methane is attracting attention worldwide in the past decade due to its specific features. First, this reaction could produce CO-rich synthesis gas from methane, which is an advantage for certain applications when compared to steam reforming of methane that has been widely commercialized for producing hydrogen or hydrogen-rich syngas (1).

In CO2 Conversion and Utilization; Song, C., et al.;
ACS Symposium Series; American Chemical Society: Washington, DC, 2002.

Secondly, this reaction could be used in some remote natural gas fields to convert CO_2-rich natural gas on site into CO-rich syngas and further to more valuable and/or easily transportable liquid products (2). Finally, this reaction could be potentially integrated into coal- or natural gas-fired power plants for CO_2 conversion by utilizing flue gas from these plants for tri-reforming without CO_2 separation (3). Compared to steam-reforming of methane which usually gives H_2-rich syngas with H_2/CO ratio of 3 or higher, more CO-rich synthesis gas with H_2/CO ratio of around 2 is required in methanol synthesis and Fischer-Tropsch synthesis, for which CO_2 reforming can also be used to adjust the H_2/CO ratio (4).

Most previous studies reported in literature on this reaction were conducted at atmospheric pressure. However, it is important to consider high-pressure reactions, and our on-going experimental study focuses on this reaction under high pressure (5-6, 11). High-pressure operation is preferred for syngas and H_2 production in industrial operations due to higher process efficiency. And since synthesis gas from CO_2 reforming of methane will be used for methanol synthesis or Fischer-Tropsch synthesis, high-pressure reforming would eliminate the need to decompress the feed gas streams and the need to re-compress the produced synthesis gas in order to meet the pressure requirement in the preceding processes.

In our recent computational study, we have examined the thermodynamic equilibrium conversions and carbon formation for the reaction systems of CO_2 and oxy-CO_2 reforming of methane under high pressures as well as atmospheric pressure (7). The effect of reaction pressures, reaction temperatures, and feedstock compositions on global carbon formation, methane conversion, CO_2 conversion, and product distribution was extensively discussed (7).

This paper presents the results of our computational study on another important aspect of these reaction systems - energy balance under various conditions. It is well known that CO_2 or steam reforming of methane is a highly endothermic reaction. How much energy is required for this reaction at different reaction conditions and how to provide that energy would be critical information needed for the design of a reactor or even the whole reaction configuration. Unfortunately this aspect is somehow ignored in literature, especially the energy balance under high pressures. Only few research groups paid some attention to this aspect for reactions under atmospheric pressure (2).

Computational Method

The software system, HSC Chemistry, which has already been used to carry out all the thermodynamic calculation in our recent study (7) was employed in this work. It was obtained from Outokumpu Research Oy in Finland. The

Downloaded by UNIV MASSACHUSETTS AMHERST on September 16, 2012 | http://pubs.acs.org
Publication Date: January 24, 2002 | doi: 10.1021/bk-2002-0809.ch021

thermodynamic properties (e.g. enthalpy or entropy) of each component in the reaction system were derived directly from the database of this software.

To calculate the energy balance, the first step is to calculate the equilibrium composition at different reaction conditions. Since all the results of these calculations have been presented in our previous paper, we have no intention to repeat those data here. We will directly use those data for the following energy balance calculation. By calculating and comparing the energy in reactants before reactions and products after reactions at a specific reaction condition, the reaction heat required or released in those reactions could be obtained. Subsequently, if all the reaction heat at different conditions is calculated, the effect of reaction conditions on reaction heat could be evaluated.

The advantage of this computational analysis is that it enables us to calculate the energy or mass balance of not only one single reaction, but also the global reaction incorporating all the reactions taking place in the system. Therefore, the calculation results from this software could give us a global and comprehensive picture of this reaction system.

Downloaded by UNIV MASSACHUSETTS AMHERST on September 16, 2012 | http://pubs.acs.org
Publication Date: January 24, 2002 | doi: 10.1021/bk-2002-0809.ch021

Results and Discussions

Effect of reaction temperature and pressure on reaction heat of CO_2+CH_4=2CO+2H_2

It is well known that CO_2 reforming of methane is a highly endothermic reaction. The enthalpy change of this reaction at STP condition is 247 kJ/mol. The data is obtained assuming that reactants are completely converted to products. And reactants and products are all at STP condition. However, this assumption does not apply in most practical reactions. Fig. 1 shows the trend of changes in reaction heat with temperatures and pressures. The data in this figure was obtained on the basis that reactants and products are at the same reaction temperature. Of course, calculation could also be done assuming reactants are at room temperature while products are at reaction temperature. The only difference between these two calculations is the energy required for heating up the reactants from ambient temperature to reaction temperatures. The more of this temperature difference, the more energy is required for pre-heating.

Curves in Fig. 1 indicate that the reaction heat of this reaction is very low, almost close to zero at temperatures less than 400°C. When reaction temperature goes above 400°C, the reaction heat starts to gradually increase. The explanation for these phenomena is that thermodynamically CO_2 reforming of methane have a very low conversion at temperatures lower than 400°C. Only when temperature goes above 400°C can its conversion become higher and higher. As

Downloaded by UNIV MASSACHUSETTS AMHERST on September 16, 2012 | http://pubs.acs.org
Publication Date: January 24, 2002 | doi: 10.1021/bk-2002-0809.ch021

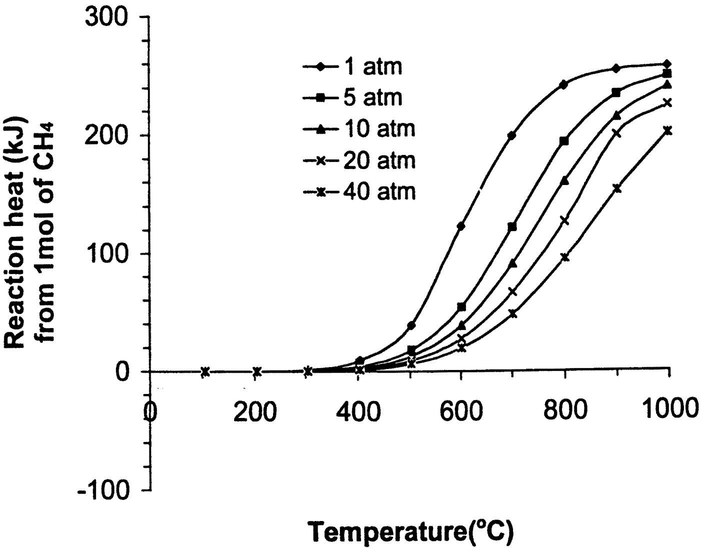

Fig. 1 Temperature and pressure effects on reaction heat in the reaction of CO_2 reforming of methane

discussed above, CO_2 reforming is an endothermic reaction. The higher the conversion, the more the reaction heat required. For example, at 1 atm, the maximum reaction heat is required around 850°C or higher due to complete conversion of methane and CO_2 into synthesis gas.

Almost in all the temperature range, the reaction heat decreases when reaction pressure changes from 1 atm to 40 atm. Our calculation results on equilibrium composition (7) show that the conversion of methane conversion decreases with the increase of reaction pressure. At the same time, the reaction heat in Fig. 1 is expressed on the base of one mole of reactant (e.g. CH_4). Low conversion of methane means less methane is converted which subsequently leads to lower reaction heat required for this reaction.

Downloaded by UNIV MASSACHUSETTS AMHERST on September 16, 2012 | http://pubs.acs.org
Publication Date: January 24, 2002 | doi: 10.1021/bk-2002-0809.ch021

Effect of O_2/CH_4 and CO_2/CH_4 ratios on reaction heat

For CO_2 reforming of methane, carbon deposition is one of the major problems. Besides that, energy supply for this reaction is another important issue due to its highly endothermic nature. Addition of O_2 into this reaction system was examined in several laboratory studies to make the system more energy efficient or to suppress carbon formation (8-10). We have reported the calculation results on the effect of O_2 addition on carbon formation and methane conversion (7). For O_2 addition, it can not only suppress carbon formation, but also relieve the energy requirement due to the exothermic properties of oxidation reaction. Here we will present our study on the effect of O_2 addition on the reaction heat and thus the energy supply and demand situations.

In the reaction system containing O_2 as one of reactants, the principle endothermic or exothermic reactions include:

Endothermic reactions:
$CO_2 + CH_4 = 2CO + 2H_2$ $\Delta H° = 247$ kJ/mol (1)
$CH_4 + H_2O = CO + 3H_2$ $\Delta H° = 206$ kJ/mol (2)
$CH_4 = C + 2H_2$ $\Delta H° = 75$ kJ/mol (3)
$C + H_2O = CO + H_2$ $\Delta H° = 131$ kJ/mol (4)

Exothermic reactions:
$CO_2 + H_2 = CO + H_2O$ $\Delta H° = -41$ kJ/mol (5)
$2CO = C + CO_2$ $\Delta H° = -172$ kJ/mol (6)
$CH_4 + 0.5\,O_2 = CO + 2H_2$ $\Delta H° = -35.5$ kJ/mol (7)
$2CO + O_2 = 2CO_2$ $\Delta H° = -440$ kJ/mol (8)
$CH_4 + 2O_2 = CO_2 + 2H_2O$ $\Delta H° = -880$ kJ/mol (9)

In our calculation, we have considered specific reactions individually and incorporated all those reactions as a whole globally. Therefore, the calculated reaction heat would represent the global reaction heat in the reaction system, not the reaction heat of a single reaction.

Fig. 2 and Fig. 3 show the effect of CO_2/CH_4 and O_2/CH_4 ratio in feedstock on reaction heat under 1 atm at 801°C. Fig. 2 was obtained assuming reactants are at room temperature and products at 801°C. And Fig. 3 was obtained assuming both reactants and products are all at the same reaction temperature (801°C). In general, Fig.2 shows that more reaction heat is required comparing with Fig. 3 at same conditions due to the required energy for heating reactants up to reaction temperature.

In Fig. 2 and Fig. 3, it is apparent that the reaction heat could change from positive (requiring heat input from outside) to negative (releasing heat to outside) with the change of O_2/CH_4 ratio in the feedstock. The more O_2/CH_4 ratio, the more heat is released. This is due to the exothermic property of oxidation reaction related to O_2. At certain O_2/CH_4 ratio, the reaction heat could be zero, which means the system does not require or release any energy to the outside. The system can maintain its temperature by itself through the balance between the exothermic and endothermic reactions in the system. This is the so-called thermo-neutral state. Comparing high CO_2/CH_4 in the feedstock with low CO_2/CH_4, the reaction heat required is high or the reaction released is less at high CO_2/CH_4. Especially in Fig. 2, the difference is even larger. This is due to two reasons. One is that addition of CO_2 will change the equilibrium composition in products. Another is that more heat is required to heat the additional CO_2 up to reaction temperature.

Comparison of effects of CO_2/CH_4 and O_2/CH_4 ratios on reaction heat at different temperatures

Fig. 4 compares the effects of CO_2/CH_4 and O_2/CH_4 ratio on reaction heat at the same pressure (1 atm) while at different temperatures. When reaction temperature goes from 642 °C to 702°C and 801°C. The sensitivity of reaction heat to CO_2/CH_4 ratio becomes less and less. At 642 °C, the O_2/CH_4 value for thermo-neutral operation could range from 0.24 to 0.5 when CO_2/CH_4 changes from 1 to 5. However, at 801°C, O_2/CH_4 value only ranges from 0.47 to 0.53. This phenomenon could be attributed to the less impact of CO_2/CH_4 on equilibrium composition at higher temperature (e.g. 801°C).

Downloaded by UNIV MASSACHUSETTS AMHERST on September 16, 2012 | http://pubs.acs.org
Publication Date: January 24, 2002 | doi: 10.1021/bk-2002-0809.ch021

Downloaded by UNIV MASSACHUSETTS AMHERST on September 16, 2012 | http://pubs.acs.org
Publication Date: January 24, 2002 | doi: 10.1021/bk-2002-0809.ch021

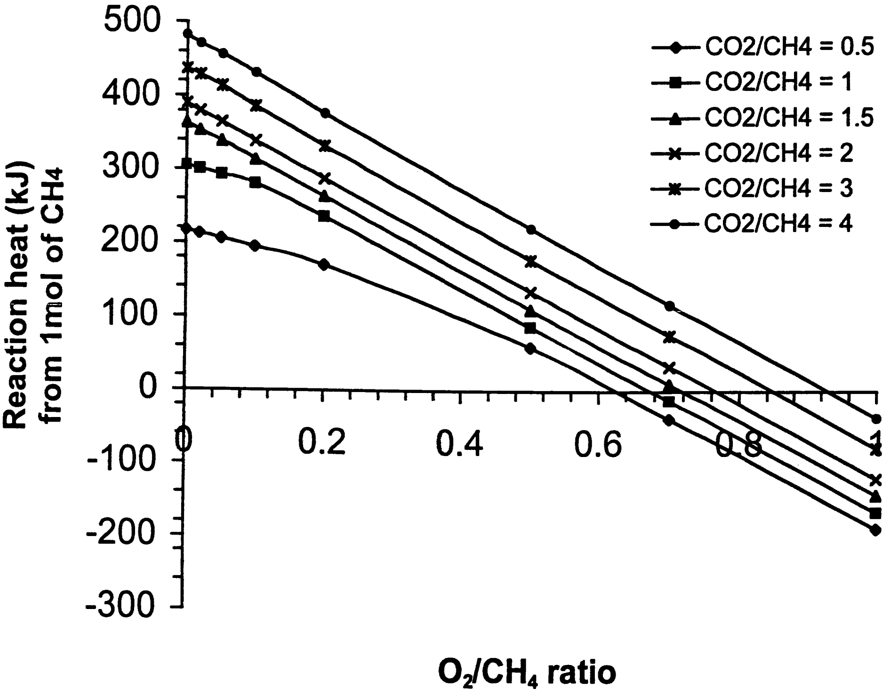

Fig. 2 Effect of CO_2/CH_4 and O_2/CH_4 ratio in feedstock on global reaction heat in the reaction systems of CO_2 or oxy-CO_2 reforming of methane (reaction pressure: 1 atm, only products are at reaction temperatures of 801°C)

Downloaded by UNIV MASSACHUSETTS AMHERST on September 16, 2012 | http://pubs.acs.org
Publication Date: January 24, 2002 | doi: 10.1021/bk-2002-0809.ch021

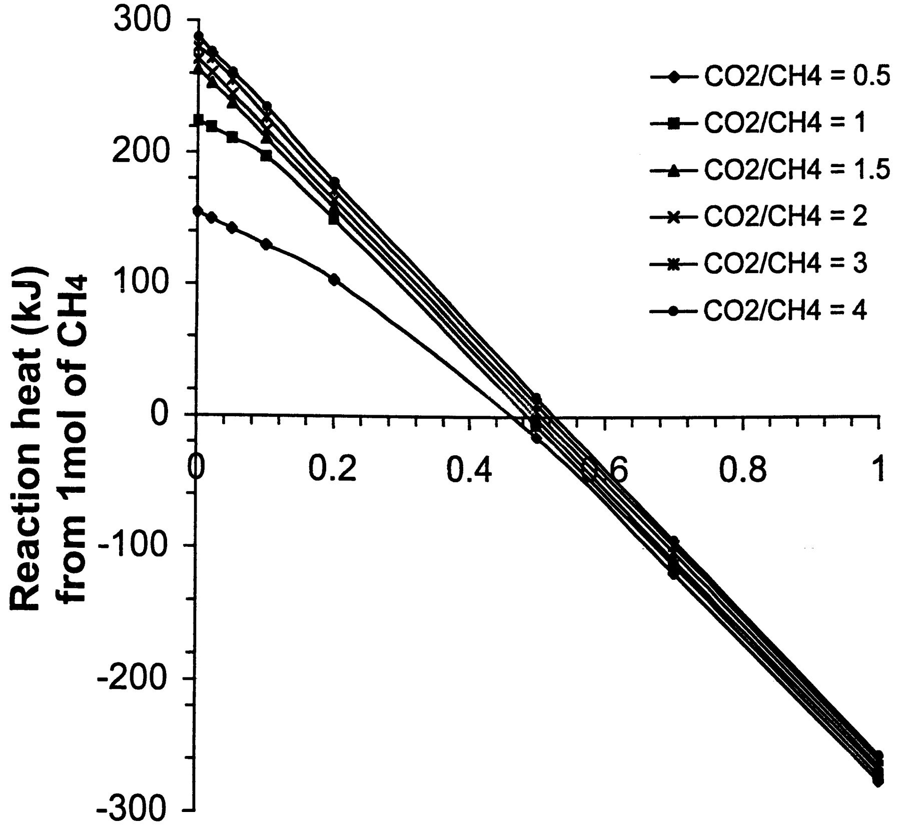

Fig. 3 Effect of CO_2/CH_4 and O_2/CH_4 ratio in feedstock on global reaction heat in the reaction systems of CO_2 or oxy-CO_2 reforming of methane (reaction pressure: 1 atm, both reactants and products are at reaction temperatures of 801°C)

Downloaded by UNIV MASSACHUSETTS AMHERST on September 16, 2012 | http://pubs.acs.org
Publication Date: January 24, 2002 | doi: 10.1021/bk-2002-0809.ch021

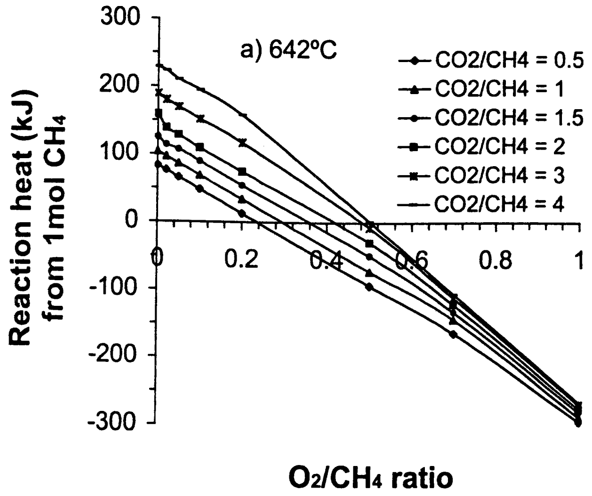

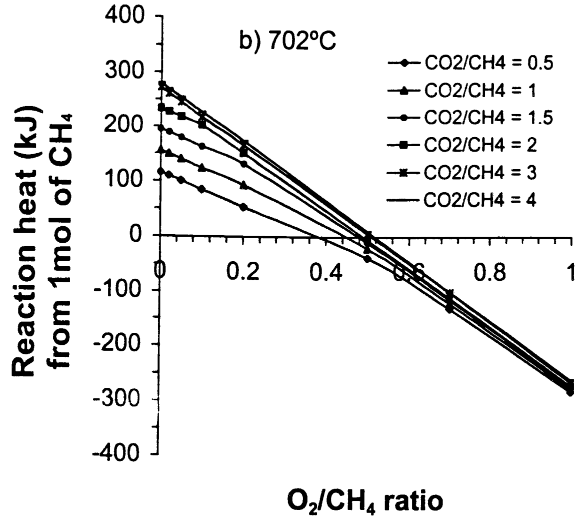

Fig. 4 Effect of CO_2/CH_4 and O_2/CH_4 ratio in feedstock on global reaction heat in the reaction systems of CO_2 or oxy-CO_2 reforming of methane at (a) 642°C; (b) 702°C; and (c) 801°C (reaction pressure: 1 atm, both reactants and products are at reaction temperatures)

Downloaded by UNIV MASSACHUSETTS AMHERST on September 16, 2012 | http://pubs.acs.org
Publication Date: January 24, 2002 | doi: 10.1021/bk-2002-0809.ch021

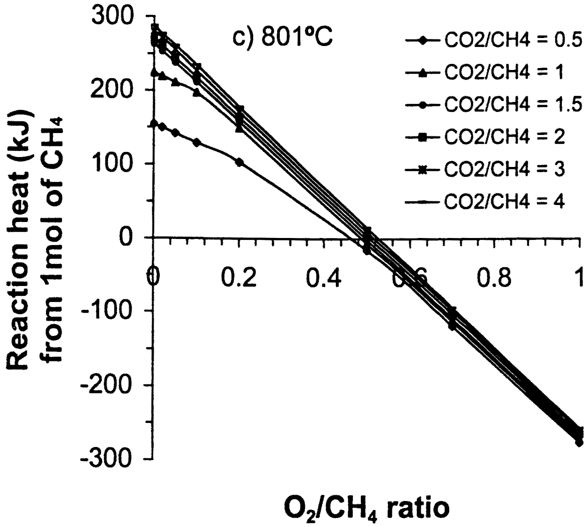

Fig. 4. *Continued.*

Comparison of the effects of CO_2/CH_4 and O_2/CH_4 ratio on reaction heat at different pressures.

Fig. 5 shows the effect of CO_2/CH_4 and O_2/CH_4 ratio on reaction heat at 702°C under 1 atm and 40 atm, respectively. In this case, both reactants and products are all at 702°C. Apparently, reaction at 1 atm needs more energy to reach equilibrium while reaction at 40 atm needs less on the base of 1 mol of CH_4 reactant. The O_2/CH_4 range of thermo-neutral state at 40 atm is 0.06 - 0.18 when CO_2/CH_4 changes from 1 to 5. However, at 1 atm, the O_2/CH_4 range of thermo-neutral state is 0.4 - 0.5 depending the CO_2/CH_4 ratio in feedstock. This difference is obviously related to the effect of high pressure on equilibrium composition.

Summary

By computational analysis of the reaction system of CO_2 and oxy-CO_2 reforming of methane, we have investigated the effects of reaction temperature, pressure, and feedstock composition on the energy balance, namely the reaction heat needed as energy input for the reaction or released as energy output. Effects of pressure and temperature on the overall energy balance of the reaction system are closely related to their effects on equilibrium composition. Addition of oxygen in the feedstock could turn the global reaction from an endothermic system to an exothermic one. The O_2 concentration in feedstock which could lead to the thermo-neutral state in the reaction system strongly depends on the pressure, and it could be calculated and compared under various conditions although only some examples are illustrated in this paper. These data could be very useful for future design of processing scheme and reactor design.

Acknowledgement

We are pleased to acknowledge the partial financial support of this work by the Pennsylvania State University (PSU) and the partial support on CO_2 reforming by the Air Products and Chemicals Inc. (APCI). We are grateful to Dr. John N. Armor of APCI, to Prof. Alan W. Scaroni and Prof. Harold H. Schobert of PSU for their encouragement and helpful discussions, to the members of the APCI/PSU SAMCOM for their support, and to Dr. Srinivas T. Srimat for technical assistance and helpful discussions.

Downloaded by UNIV MASSACHUSETTS AMHERST on September 16, 2012 | http://pubs.acs.org
Publication Date: January 24, 2002 | doi: 10.1021/bk-2002-0809.ch021

Downloaded by UNIV MASSACHUSETTS AMHERST on September 16, 2012 | http://pubs.acs.org
Publication Date: January 24, 2002 | doi: 10.1021/bk-2002-0809.ch021

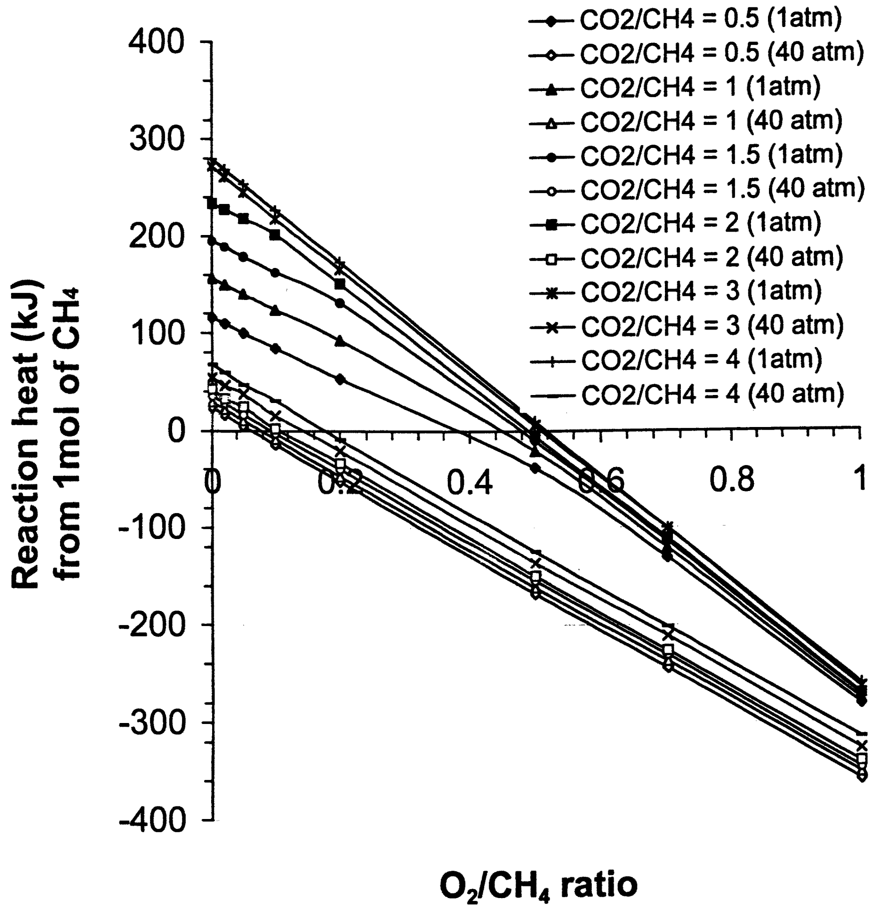

Fig. 5 Effect of CO_2/CH_4 and O_2/CH_4 ratio in feedstock on global reaction heat in the reaction systems of CO_2 or oxy-CO_2 reforming of methane at different pressures (upper group: 1 atm, lower group: 40 atm, both reactants and products are at 702°C)

Literature Cited

1. Armor J.N., Appl. Catal. A: General **1999**, 176, 159.
2. Choudhary V.R.; Rajput A.M.; and Prabhakar B. Angew. Chem. Int. Ed. Engl. **1994**, 33, 2104.
3. (a) Song, C. Chemical Innovation (formerly Chemtech, ACS), **2001**, 31, 21; (b) Song C. Proc. 16th International Pittsburgh Coal Conference: Pittsburgh, USA, October 11-15, **1999**, Paper No. 16-5, CD-ROM ISBN 1-890977-16-0.
4. Gunardson, H.H.; Abrardo, J.M. Hydrocarbon Processing **April 1999**, 87.
5. Song, C.; Srinivas, S.T.; Sun, L.; Armor, J.N. Am. Chem. Soc. Div. Petrol. Chem. Prepr., **2000**, 45, 143.
6. Srinivas, S.T.; Song, C. Am. Chem. Soc. Div. Petrol. Chem. Prepr., **2000**, 45, 153.
7. Pan, W.; Srinivas, T.S.; Song, C. 16th International Pittsburgh Coal Conference: Pittsburgh, USA, October 11-15, **1999**; Paper No. 26-2. CD-ROM ISBN 1-890977-16-0.
8. Choudhary, V.R.; Rajput, A.M.; Prabhakar, B., Catal. Lett. **1995**, 32, 391.
9. O'Connor, A.M.; Ross, J.R.H. Catal. Today, **1998**, 46, 203.
10. Ruckenstein, E. and Hu, Y.H. Ind. Eng. Chem. Res., **1998**, 37,1744.
11. Song, C.; Murata, S.; Srinivas, S.T.; Sun, L.; Scaroni, A.W. Am. Chem. Soc. Div. Petrol. Chem. Prepr., **1999**, 44, 160.

Downloaded by UNIV MASSACHUSETTS AMHERST on September 16, 2012 | http://pubs.acs.org
Publication Date: January 24, 2002 | doi: 10.1021/bk-2002-0809.ch021

Downloaded by UNIV OF GUELPH LIBRARY on September 16, 2012 | http://pubs.acs.org
Publication Date: January 24, 2002 | doi: 10.1021/bk-2002-0809.ch022

Chapter 22

Photocatalytic Reduction of CO_2 with H_2O on Various Titanium Oxide Catalysts

Hiromi Yamashita*, Keita Ikeue, and Masakazu Anpo*

Department of Applied Chemistry, Graduate School of Engineering, Osaka Prefecture University, Gakuen-cho 1-1, Sakai, Osaka 599–8531, Japan

The characteristic features of the photocatalytic reduction of CO_2 with H_2O on various types of active titanium oxide catalysts has been clarified. UV-irradiation of active titanium oxide catalysts in the presence of CO_2 and H_2O at 275 K led to the photocatalytic reduction of CO_2. The reactions on TiO_2 powders produced CH_4 as the major product while, on the highly dispersed titanium oxide anchored on porous glass and zeolites, the formations of CH_3OH as well as CH_4 were observed as the major products. The CH_3OH formation is linked to unique properties of the charge transfer excited state, i.e., $(Ti^{3+}—O^{-})^*$ of the tetrahedral coordinated titanium oxides species.

Introduction

The design of highly efficient and selective photocatalytic systems that work without any loss in the use of solar energy through chemical storage like the natural plant photosynthesis is of vital interest (1-8). Especially, the development of efficient photocatalytic systems which are able to reduce CO_2 with H_2O into chemically valuable compounds such as CH_4 or CH_3OH are among the most desirable and challenging goals (2,3).

The utilization of solar energy for the reduction and/or fixation of CO_2 can

In CO2 Conversion and Utilization; Song, C., et al.;
ACS Symposium Series; American Chemical Society: Washington, DC, 2002.

Downloaded by UNIV OF GUELPH LIBRARY on September 16, 2012 | http://pubs.acs.org
Publication Date: January 24, 2002 | doi: 10.1021/bk-2002-0809.ch022

be made possible by considering the photocatalytic reduction and/or fixation of CO_2 with H_2O into CO, HCOOH, CH_3OH, and CH_4, etc. using reactive photocatalysts such as small particle powdered TiO_2 semiconductors. Inoue and Fujishima, *et al.* (9) have first reported that HCOOH, HCHO, and CH_3OH are produced by the reduction of CO_2 with H_2O under irradiation of aqueous suspension systems involving a variety of semiconductor powders such as TiO_2 and $SrTiO_3$. Although the pioneering works on the photoreduction of CO_2 on semiconductors in aqueous suspension systems were summarized by Halmann (10), the efficiency of CO_2 reduction was low when water was used as the reductant. Recently, we have reported that these photocatalytic reactions successfully proceed in solid-gas systems on powdered TiO_2 and highly dispersed titanium oxide catalysts at room temperature (2,3,11-22).

With these objectives of research in mind, in this chapter, we will focus on the photocatalytic reduction and/or fixation of CO_2 with H_2O on various types of active titanium oxide catalysts using heterogeneous gas-solid photocatalytic reaction systems. Studies have been carried out on extremely small TiO_2 particles and on highly dispersed anchored titanium oxide catalysts under UV-irradiation (11-22).

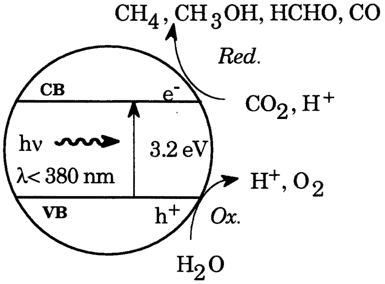

Fig. 1. Reaction scheme for the photocatalytic reduction of CO_2 with H_2O on bulk TiO_2.

Photocatalytic Reaction on Various Titanium Oxide Catalysts

The efficiency for the photosynthetic reduction of CO_2 with H_2O to produce CH_4 and CH_3OH depends strongly upon the types of the photocatalyst used (11-22). Among photocatalysts, the semiconducting TiO_2 is the most reactive and stable. Figure 1 shows the primary processes for the photocatalytic reduction and/or fixation of CO_2 with H_2O on semiconducting TiO_2 photocatalysts. When the particle size of the semiconducting TiO_2 is decreased, the band gap between the conduction band and the valence band becomes larger, making it suitable and applicable for the reduction of CO_2 (2,3). For extremely fine particle TiO_2 photocatalysts less than 100 Å of the particle, the size quantum effect and/or the effects of the surface modification in its coordination geometry plays a significant role in the reactivity of the photocatalyst (2,3). As a result, the electrons and holes which are produced by UV-irradiation within the ultrafine particles of TiO_2 and the highly dispersed titanium oxide species exhibit more unique and high reactivities than for those produced in large particle TiO_2 photocatalysts.

Small particle TiO_2 catalysts

UV-irradiation of the powdered TiO_2 catalysts in the presence of a gaseous mixture of CO_2 and H_2O led to the evolution of CH_4 into the gas phase at 275 K (13,14). Trace amounts of C_2H_4 and C_2H_6 were also produced. The yields of these products increased with the UV-irradiation time, while no products were detected under dark conditions. The CH_4 yield was almost zero in the reaction of CO_2 without H_2O and increased when the amount of H_2O was increased. These results suggest that for powdered TiO_2 catalysts, the photocatalytic reduction of CO_2 to produce CH_4 and C_2-compounds from CO_2 and H_2O takes place photocatalytically in the solid-gas phase systems. The formation of CH_4 as the main product has also been recently observed by Saladin et al., and the partially reduced $TiO_{2-\delta}$ species formed under UV-irradiation is considered to be the active species (23).

The yields of CH_4 formation in the photocatalytic reduction of CO_2 with H_2O on several different types of TiO_2 catalyst are shown in Table 1. The level of photocatalytic reactivity, based on the CH_4 yields, was found to depend on the type of TiO_2 catalyst, in the order of JRC-TIO-4 > -5 > -2 > -3 (14). As shown in Table 1, the tendency for catalytic activity for the reduction of CO_2 with H_2O is in a manner similar to those for the hydrogenation of olefins (24,25), proving that the reduction of CO_2 with H_2O occurs photocatalytically over the powdered TiO_2 catalyst. It is likely that the anatase-type TiO_2 which has a large band gap and numerous surface -OH groups is preferable for efficient photocatalytic reactions. The band gap increase is accompanied by a shift in the conduction band edge to higher energy levels. This shift causes the reductive potential to shift to more negative values which in turn causes a great enhancement in the photocatalytic reactivity. Concerning the role of the surface -OH groups, the surface -OH groups and/or physisorbed H_2O play a significant role in photocatalytic reactions *via* the formation of OH radicals and H radicals.

Figure 2 shows the ESR signals obtained under UV-irradiation of the anatase-type TiO_2 catalyst in the presence of CO_2 and H_2O at 77 K (14). The ESR signals are attributed to the characteristic photogenerated Ti^{3+} ions ($g_{\perp}=1.9723$ and $g_{//}=1.9628$) and H radicals (with 490 G splitting), as well as CH_3 radicals having a hyperfine splitting (Ha=19.2 G, g=2.002). The signal intensity of CH_3 radicals decreased with increasing the amount of H_2O, indicating that CH_3 radicals react easily to form CH_4 in the presence of H_2O.

Downloaded by UNIV OF GUELPH LIBRARY on September 16, 2012 | http://pubs.acs.org
Publication Date: January 24, 2002 | doi: 10.1021/bk-2002-0809.ch022

These results clearly suggest that CH_3 radicals are the intermediate species and react with H radicals that are formed by the reduction of protons (H^+) supplied from H_2O adsorbed on the catalyst.

Table 1. Physical properties and photocatalytic activity of TiO_2 catalysts. *(CO_2: 0.12 mmol, H_2O: 0.37 mmol, irradiation time:6 hr,).*

Catalyst (JRC-TIO-)	Surface area (m^2 g^{-1})	Relative - OH conc.	Band gap (eV)	Reduction[a] of CO_2 (μmol h^{-1} g^{-1})	Hydrogenation[b] of olefins (μmol h^{-1} g^{-1})
2 (anat.)	16	1	3.47	0.03	0.20
3 (ruti.)	51	1.6	3.32	0.02	0.12
4 (anat)	49	3.0	3.50	0.17	8.33
5 (ruti)	3	3.1	3.09	0.04	0.45

[a] CH_4 yield in reaction of CO_2 with H_2O.
[b] Conversion in reaction of methyl acetylene with H_2O.

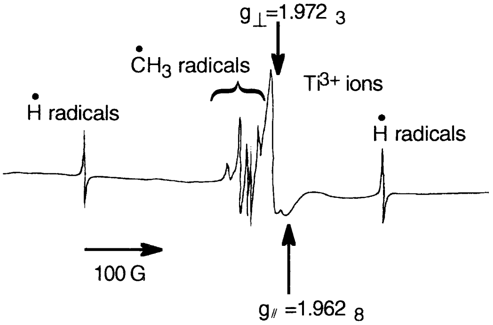

Fig. 2. ESR signals obtained with TiO_2 under UV-irradiation in the presence of CO_2 and H_2O at 77 K.

Cu-loaded and Pt-loaded TiO_2 powder

The effect of Cu-loading on the photocatalytic reduction of CO_2 with H_2O on TiO_2 catalysts was investigated (14). Although the loading of Cu (0.3~1.0 wt %) onto the small particle TiO_2, i.e., the Cu/TiO_2 photocatalyst, led to a suppression of the CH_4 yield, a new formation of CH_3OH could be observed. Characteristics of the XPS spectra observed with the Cu/TiO_2 suggest that the main species of copper in the catalyst is Cu^+. It has been also reported that Cu^+ catalysts play a significant role in the photoelectrochemical production of CH_3OH from CO_2 and H_2O system (26).

Downloaded by UNIV OF GUELPH LIBRARY on September 16, 2012 | http://pubs.acs.org
Publication Date: January 24, 2002 | doi: 10.1021/bk-2002-0809.ch022

The effect of Pt-loading on the TiO_2 catalyst was also investigated. The yield of CH_4 increased remarkably when the amount of Pt added was increased (0.1~1.0 wt%), but the addition of excess Pt was undesirable for an efficient reaction (13). Regarding the reaction intermediates, Solymosi et al. have observed the formation of CO_2^- species in bent form under UV-irradiation of the Rh/TiO_2 in the presence of CO_2 using FT-IR (27). The electron transfer from the irradiated catalyst to the adsorbed CO_2 takes place, resulting in the formation of a CO_2^- anion as the key step in the photochemical reduction of CO_2 using metal loaded TiO_2 semiconductor.

TiO_2 single crystals

With a well-defined catalyst surface such as a single crystal, detailed information on the reaction mechanism can be obtained at the molecular level (2,15). Therefore, the photocatalytic reduction of CO_2 with H_2O on rutile-type TiO_2(100) and TiO_2(110) single crystal surfaces have been carried out (15). As shown in Table 2, the efficiency and selectivity of the photocatalytic reactions strongly depend on the type of TiO_2 single crystal surface. UV-irradiation of the TiO_2(100) single crystal catalyst in the presence of a mixture of CO_2 and H_2O led to the evolution of CH_4 and CH_3OH in the gas phase at 275 K, whereas only CH_3OH yields was detected with the TiO_2(110) single crystal catalyst.

Table 2. Yields of the formation of CH_4 and CH_3OH in the photocatalytic reduction of CO_2 (124 μmol g^{-1}) with H_2O (372 μmol g^{-1}) at 275 K.

Single Crystal	Yields (nmol h^{-1} g-cat^{-1})	
	CH_4	CH_3OH
TiO_2 (100)	3.5	2.4
TiO_2 (110)	0	0.8

It is likely that the photo-formed electrons localize on the surface sites of the excited TiO_2 to play a significant role in the photoreduction of CO_2 molecules into intermediate carbon species (2,15). The surface Ti atoms may act as an electron moiety on the surfaces, i. e., a reductive site. According to the surface geometric models for TiO_2(100) and TiO_2(110), the atomic ratio (Ti/O) of the top-surface Ti and O atoms which have geometric spaces large enough to have direct contact with CO_2 and H_2O molecules, is higher on TiO_2(100) than on TiO_2(110) surface. In the excited state, the surface with a higher Ti/O surface ratio, i. e. TiO_2(100), exhibits a more reductive tendency than TiO_2(110). Such

Downloaded by UNIV OF GUELPH LIBRARY on September 16, 2012 | http://pubs.acs.org
Publication Date: January 24, 2002 | doi: 10.1021/bk-2002-0809.ch022

a reductive surface allows a more facile reduction of CO_2 molecules especially for the formation of CH_4.

Ti-oxide anchored on zeolite (ion-exchange)

The photocatalyst systems incorporated within the zeolite cavities and framework have been found to be effective for various reactions (28-31). The Ti-oxide anchored onto zeolite, Ti-oxide/Y-zeolite (1.1 wt% as TiO_2), was prepared by ion-exchange with an aqueous titanium ammonium oxalate solution using Y-zeolite (SiO_2/Al_2O_3 = 5.5) (ex-Ti-oxide/Y-zeolite) (16-18).

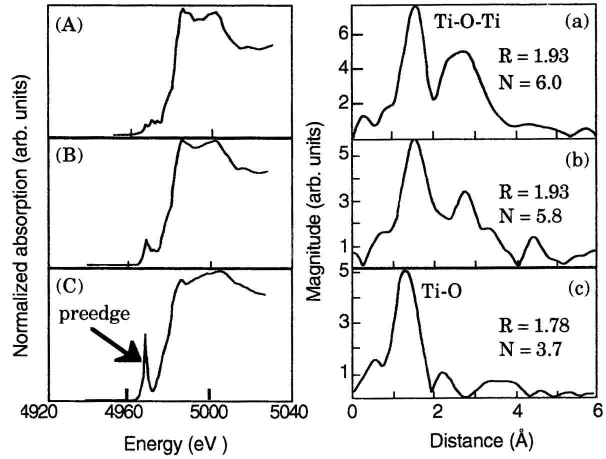

Fig. 3. Ti K-edge XANES (A-C) and FT-EXAFS (a-c) spectra of anatase TiO_2 powder (A, a), the imp-Ti-oxide/Y-zeolite (10.0 wt% as TiO_2) (B, b), and the ex-Ti-oxide/Y-zeolite (C, c), catalysts.
R: Ti-O bond distance (Å), N: coordination number

Figure 3 shows the XANES and the Fourier transformation of EXAFS (FT-EXAFS) spectra of the Ti-oxide/Y-zeolites. The XANES spectra of the Ti-oxide catalysts at the Ti K-edge show several well-defined preedge peaks which are related to the local structures surrounding the Ti atom (32). The ex-Ti-oxide/Y-zeolite exhibits an intense single preedge peak indicating that the Ti-oxide species have a tetrahedral coordination (1-3). On the other hand, the imp-Ti-oxide/Y-zeolite prepared by the impregnation exhibits three characteristic weak preedge peaks attributed to crystalline anatase TiO_2. The FT-EXAFS spectra of the ex-Ti-oxide/Y-zeolite exhibits only peak assigned to the neighboring oxygen atoms (Ti-O) indicating the presence of an isolated Ti-oxide species. These findings indicate that highly dispersed isolated tetrahedral Ti-oxide species are formed on the ex-Ti-oxide/Y-zeolite. On the other hand, the

Downloaded by UNIV OF GUELPH LIBRARY on September 16, 2012 | http://pubs.acs.org
Publication Date: January 24, 2002 | doi: 10.1021/bk-2002-0809.ch022

imp-Ti-oxide/Y-zeolite exhibits an intense peak assigned to the neighboring titanium atoms (Ti-O-Ti), indicating the aggregation of the Ti-oxide species.

Figure 4a shows a typical photoluminescence spectrum of the Ti-oxide anchored onto zeolite (ex-Ti-oxide/Y-zeolite) at 77 K. Excitation by light at around 250-280 nm brought about an electron transfer from the oxygen to titanium ion, resulting in the formation of pairs of the trapped hole center (O^-) and an electron center (Ti^{3+}) (1-3). The observed photoluminescence is attributed to the radiative decay process from the charge transfer excited state of the Ti-oxide moieties having a tetrahedral coordination, $(Ti^{3+}—O^-)^*$, to their ground state (33,34). As shown in Fig. 4b,c, the addition of H_2O or CO_2 molecules onto the anchored Ti-oxide species leads to the efficient quenching of the photoluminescence. Such an efficient quenching suggests not only that tetrahedrally coordinated Ti-oxide species locate at positions accessible to the added CO_2 or H_2O but also that added CO_2 or H_2O interacts and/or reacts with the Ti-oxide species in both its ground and excited states. Because the addition of CO_2 led to a less effective quenching than with the addition of H_2O, the interaction of the emitting sites with CO_2 was weaker than with H_2O.

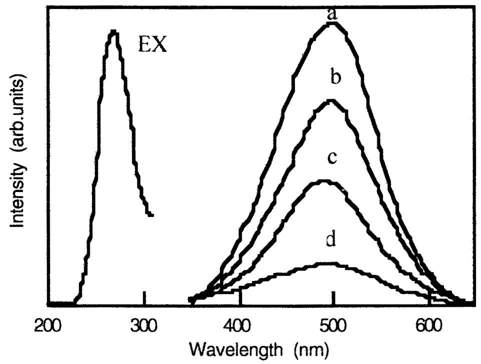

Fig. 4. Photoluminescence spectrum of the ex-Ti-oxide/Y-zeolite catalyst (a), its excitation spectrum (EX), and the effects of the addition of CO_2 and H_2O (b, c) and the loading of Pt (d) on the photoluminescence spectrum. Measured at 77 K, excitation at 290 nm, emission monitored at 490 nm, amounts of added CO_2: b) 8.5, and H_2O; c) 2.9 mmol g^{-1}.

UV-irradiation of powdered TiO_2 and Ti-oxide/Y-zeolite catalysts in the presence of a mixture of CO_2 and H_2O led to the evolution of CH_4 and CH_3OH in the gas phase at 328 K, as well as trace amounts of CO, C_2H_4 and C_2H_6 (16-18). The yields of these photoformed products increased linearly against the UV-irradiation time, indicating the photocatalytic reduction of CO_2 with H_2O on the catalysts. The specific photocatalytic reactivities for the formation of CH_4 and CH_3OH are shown in Fig. 5. The ex-Ti-oxide/Y-zeolite exhibits a

Downloaded by UNIV OF GUELPH LIBRARY on September 16, 2012 | http://pubs.acs.org
Publication Date: January 24, 2002 | doi: 10.1021/bk-2002-0809.ch022

high reactivity and a high selectivity for the formation of CH_3OH while the formation of CH_4 was found to be the major reaction on bulk TiO_2 as well as on the imp-Ti-oxide/Y-zeolite. These findings clearly suggest that the tetrahedrally coordinated Ti-oxide species act as active photocatalysts for the reduction of CO_2 with H_2O showing a high selectivity to produce CH_3OH.

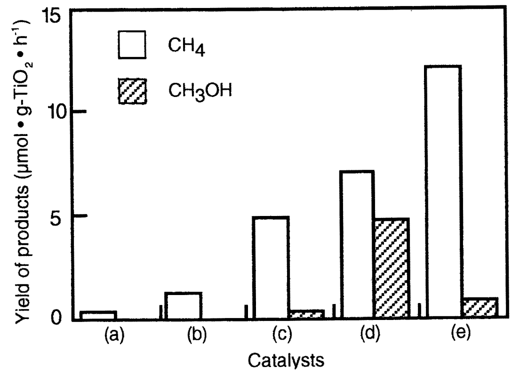

Fig. 5. The product distribution of the photocatalytic reduction of CO_2 with H_2O on anatase TiO_2 powder (a), the imp-Ti-oxide/Y-zeolite (10.0 wt% as TiO_2) (b), the imp-Ti-oxide/Y-zeolite (1.0 wt% as TiO_2) (c), the ex-Ti-oxide/Y-zeolite (1.1 wt% as TiO_2) (d), and the Pt-loaded ex-Ti-oxide/Y-zeolite (e) catalysts.

UV-irradiation of the anchored Ti-oxide catalyst in the presence of CO_2 and H_2O at 77 K led to the appearance of ESR signals due to the Ti^{3+} ions, H atoms, and carbon radicals (2,3). From these results, the reaction mechanism in the photocatalytic reduction of CO_2 with H_2O on the highly dispersed Ti-oxide catalyst can be proposed: CO_2 and H_2O molecules interact with the excited state of the photoinduced $(Ti^{3+}—O^{-})^{*}$ species and the reduction of CO_2 and the decomposition of H_2O proceed competitively. Furthermore, H atoms and OH• radicals are formed from H_2O and these radicals react with the carbon species formed from CO_2 to produce CH_4 and CH_3OH.

Ti-containing zeolite and mesoporous molecular sieves

The Ti-oxide species prepared within the zeolite framework have revealed a unique local structure as well as a high selectivity in the oxidation of organic substances with hydrogen peroxide (33-35). Ti-containing zeolites (TS-1, Ti-Beta) and mesoporous molecular sieves (Ti-MCM, Ti-HMS, Ti-FSM) have been hydrothermally synthesized (18-22, 35-37).

Downloaded by UNIV OF GUELPH LIBRARY on September 16, 2012 | http://pubs.acs.org
Publication Date: January 24, 2002 | doi: 10.1021/bk-2002-0809.ch022

Downloaded by UNIV OF GUELPH LIBRARY on September 16, 2012 | http://pubs.acs.org
Publication Date: January 24, 2002 | doi: 10.1021/bk-2002-0809.ch022

In situ photoluminescence, ESR, UV-VIS and XAFS investigations indicated that the Ti-oxide species in the Ti-mesoporous molecular sieves (Ti-MCM-41 and Ti-MCM-48) and in the TS-1 zeolite are highly dispersed within the zeolite framework and exist in a tetrahedral coordination. Upon excitation with UV light at around 250-280 nm, these catalysts exhibit photoluminescence spectra at around 480 nm. The addition of CO_2 or H_2O onto these catalysts results in a significant quenching of the photoluminescence, suggesting the excellent accessibility of the Ti-oxide species to CO_2 and H_2O (18-21).

UV-irradiation of the Ti-mesoporous molecular sieves and the TS-1 zeolite in the presence of CO_2 and H_2O also led to the formation of CH_3OH and CH_4 as the main products (18-21). The yields of CH_3OH and CH_4 per unit weight of the Ti-based catalysts are shown in Fig. 6. It can be seen that Ti-MCM-48 exhibits much higher reactivity than either TS-1 or Ti-MCM-41. Besides the higher dispersion state of the Ti-oxide species, other distinguishing features of these zeolite catalysts are: TS-1 has a smaller pore size (ca. 5.7 Å) and a three-dimensional channel structure; Ti-MCM-41 has a large pore size (>20 Å) but one-dimensional channel structure; and Ti-MCM-48 has both a large pore size (>20 Å) and three-dimensional channels. Thus, the higher reactivity and higher selectivity for the formation of CH_3OH observed with the Ti-MCM-48 than with the other catalysts may be due to the combined contribution of the high dispersion state of the Ti-oxide species and the large pore size with a three-dimensional channel structure. These results strongly indicate that mesoporous molecular sieves with highly dispersed Ti-oxide species are promising candidates as effective photocatalysts.

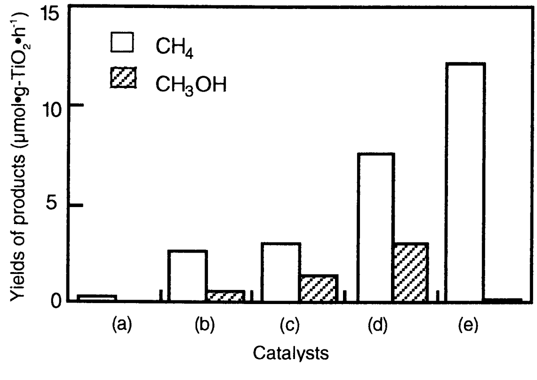

Fig. 6. The product distribution of the photocatalytic reduction of CO_2 with H_2O on TiO_2 powder (a), TS-1 (b), Ti-MCM-41 (c), Ti-MCM-48 (d), and the Pt-loaded Ti-MCM-48 (e) catalysts.

The effect of Pt-loading on the photocatalytic reactivity of Ti-containing zeolite has also been investigated and the changes in the yields of CH_4 and

Downloaded by UNIV OF GUELPH LIBRARY on September 16, 2012 | http://pubs.acs.org
Publication Date: January 24, 2002 | doi: 10.1021/bk-2002-0809.ch022

CH_3OH formation are shown in Figs. 5 and 6. Although the addition of Pt onto the Ti-containing zeolites is effective for an increase in the photocatalytic reactivity, only the formation of CH_4 is promoted (16,18).

Recently a large-pore Ti-containing zeolite, Ti-Beta, has been hydrothermally synthesized (35-37). The H_2O affinity of Ti-Beta zeolites changes significantly depending on the preparation methods and their hydrophobic-hydrophilic properties can modify the catalytic properties (35-37). As shown in Fig. 7, the photocatalytic reduction of CO_2 with H_2O to produce CH_4 and CH_3OH was found to proceed in the gas phase at 323 K with different reactivities and selectivities on hydrophilic Ti-Beta(OH) and hydrophobic Ti-Beta(F) zeolites prepared in the OH^- and F^- media, respectively. The higher reactivity for the formation of CH_4 observed with Ti-Beta(OH) and the higher selectivity for the formation of CH_3OH observed with the Ti-Beta(F) may be attributed to the different abilities of zeolite pores on the H_2O affinity. These results suggest that the affinity of the H_2O molecules to adsorb on the zeolite is one of important factors for the selectivity in the photocatalytic reduction of CO_2 and H_2O.

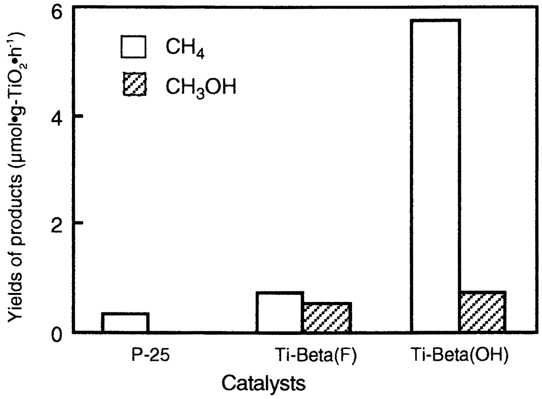

Fig. 7. The product distribution of the photocatalytic reduction of CO_2 with H_2O on Ti-Beta(F), Ti-Beta(OH), and TiO_2 powder (P-25) as the reference catalyst.

In summary, an efficient photocatalytic reactivity and selectivity for the formation of CH_3OH in the photocatalytic reduction of CO_2 with H_2O was achieved with the zeolite and mesoporous molecular sieves having highly dispersed tetrahedral Ti-oxide species in their cavities or frameworks, while the formation of CH_4 in the photocatalytic reduction of CO_2 with H_2O was found to proceed on the bulk TiO_2 catalysts and on the catalysts involving aggregated Ti-oxide species.

Ti-oxide anchored on porous silica glass (CVD)

The Ti-oxide anchored onto porous silica glass (PVG) plate was prepared using a facile reaction of $TiCl_4$ with the surface OH groups on the transparent porous Vycor glass (Corning code 7930) in the gas phase at 453-473 K, followed by treatment with H_2O vapor to hydrolyze the anchored compound (11-13). UV-irradiation of the anchored Ti-oxide catalysts in the presence of a mixture of CO_2 and H_2O led to the evolution of CH_4, CH_3OH and CO in the gas phase at 323 K. The total CH_4, CH_3OH and CO yields were larger under UV-irradiation at 323 K than at 275 K. The efficiency of the photocatalytic reaction strongly depends on the ratio of H_2O/CO_2 and its reactivity increases with an increase in the H_2O/CO_2 ratio; however, an excess amount of H_2O suppresses the reaction rates. Figure 8 shows the effect of the number of anchored Ti-O layers on the absorption edge of the catalysts and the efficiency of the photocatalytic reactions as well as the relative yields of the photoluminescence (11-13). It was found that only catalysts with highly dispersed monolayer Ti-oxide exhibit high photocatalytic reactivity and photoluminescence at around 480 nm. Only the tetrahedral Ti-oxide species exhibit photoluminescence when it is excited at around 250-280 nm. These findings also clearly suggest that the tetrahedrally coordinated Ti-oxide species act as active photocatalysts for the reduction of CO_2 with H_2O.

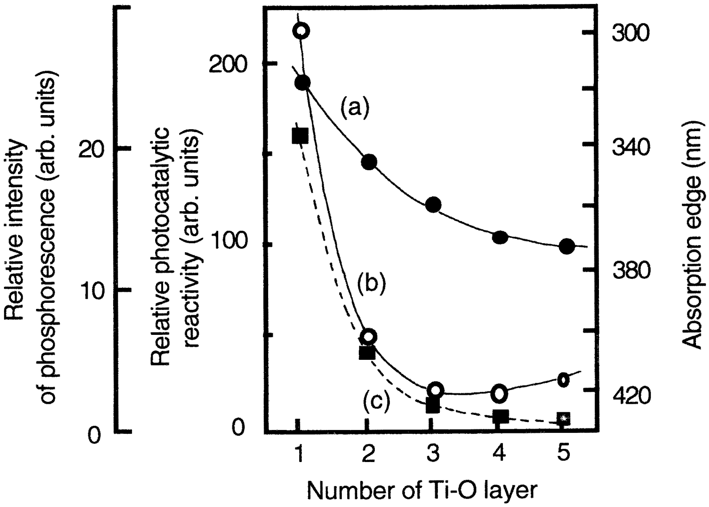

Fig. 8. The effects of the number of the Ti-O layers of the anchored titanium oxide catalysts on the absorption edge of the catalysts (a), the reaction yields (b), and the relative yields of the photoluminescence (c).

Downloaded by UNIV OF GUELPH LIBRARY on September 16, 2012 | http://pubs.acs.org
Publication Date: January 24, 2002 | doi: 10.1021/bk-2002-0809.ch022

Downloaded by UNIV OF GUELPH LIBRARY on September 16, 2012 | http://pubs.acs.org
Publication Date: January 24, 2002 | doi: 10.1021/bk-2002-0809.ch022

Ti/Si binary oxide (sol-gel)

Ti/Si binary oxides involving different Ti contents were prepared by the sol-gel method using mixtures of tetraethylorthosilicate and titanium-*iso*-propoxide. Ti/Si binary oxides with only a small Ti contents exhibited the photoluminescence at around 480 nm upon excitation at around 280 nm (22, 38). UV-irradiation of the Ti/Si binary oxide catalysts in the presence of a gaseous mixture of CO_2 and H_2O was found to lead to the formation of CH_4 and CH_3OH as the main product. As shown in Fig. 9, a parallel relationship between the specific photocatalytic activities of the titanium oxide species and the photoluminescence yields of the Ti/Si binary oxides clearly indicates that the appearance of high photocatalytic activity for the binary oxides is closely associated with the formation and reactivity of the charge transfer excited complex of the highly dispersed tetrahedral Ti-oxide species.

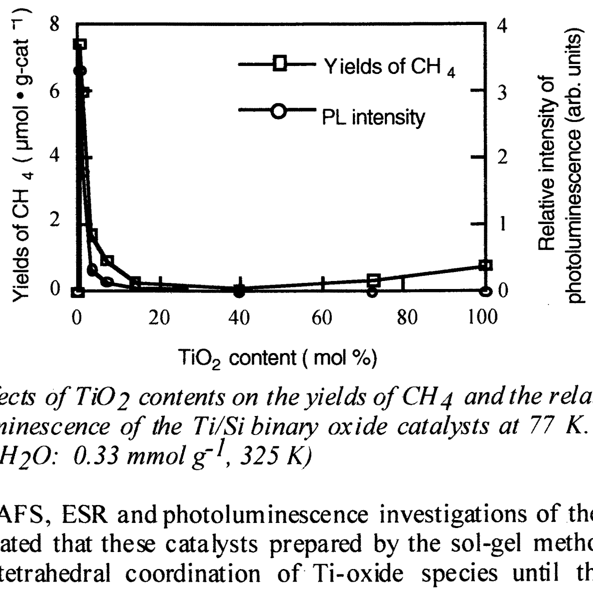

Fig. 9. Effects of TiO_2 contents on the yields of CH_4 and the relative intensity of photoluminescence of the Ti/Si binary oxide catalysts at 77 K. (CO_2: 0.07 mmol g^{-1}, H_2O: 0.33 mmol g^{-1}, 325 K)

The XAFS, ESR and photoluminescence investigations of the Ti/Si binary oxide indicated that these catalysts prepared by the sol-gel method are able to sustain a tetrahedral coordination of Ti-oxide species until the Ti content reaches approximately up to 20 wt% as TiO_2. Thus, we can see that the Ti/Si binary oxides having a high Ti content (up to 20 wt%) can be successfully utilized as active photocatalysts for the efficient reduction of CO_2 with H_2O in the gas-solid system.

Conclusions

The characteristic features of the photocatalytic reduction of CO_2 with H_2O on various types of active Ti-oxide catalysts has been clarified. UV-irradiation of active Ti-oxide catalysts in the presence of CO_2 and H_2O at 275 K led to the photocatalytic reduction of CO_2. The reactions on TiO_2 powders produced CH_4 as the major product, while on the highly dispersed titanium oxide anchored on porous glass and zeolites, the formations of CH_3OH as well as CH_4 were observed as the major products. The yields of the photocatalytic reactions strongly depended on the type of catalysts, the value of CO_2/H_2O, and the reaction temperature. In situ spectroscopic studies of the system indicated that the photocatalytic reduction of CO_2 with H_2O is linked to a much higher reactivity of the charge transfer excited state, i.e., $(Ti^{3+}—O^{-})^*$ of the tetrahedral coordinated Ti-oxide species formed on the surface.

Downloaded by UNIV OF GUELPH LIBRARY on September 16, 2012 | http://pubs.acs.org
Publication Date: January 24, 2002 | doi: 10.1021/bk-2002-0809.ch022

References

1. Anpo. M; Yamashita, H. In *Surface Photochemistry*; Anpo. M. Ed.; John Wiley & Sons; Chichester, **1996**, pp. 117-164.
2. Anpo. M; Yamashita, H. In *Heterogeneous Photocatalysts*; Schiavello. M. Ed; John Wiley & Sons; Chichester, **1997**, pp. 133-168.
3. Yamashita, H.; Zhang, J.; Matsuoka, M.; Anpo, M. In *Photofunctional Zeolites*; Anpo, M. Ed.; NOVA; New York; **2000**, pp. 129-168.
4. Anpo, M.; Yamashita, H.; Zhang, S. G. *Current Opinion in Solid State & Materials Science* **1996**, *1*, 219-224.
5. Anpo, M. *Res. Chem. Intermed.* **1989**, *9*, 67-112.
6. Anpo, M.; Ichihashi, Y.; Takeuchi, M.; Yamashita, H. *Res. Chem. Intermed.* **1998**, *24*, 143-149.
7. Yamashita, H.; Ichihashi, Y.; Takeuchi, M.; Kishiguchi, S.; Anpo, M. *J. Synchrotron Rad.* **1999**, *6*, 451-452.
8. Yamashita, H.; Honda, M.; Harada, M.; Ichihashi, Y.; Anpo, M. *J. Phys. Chem. B* **1998**, *102*, 10707-10711.
9. Inoue, T.; Fujishima, A.; Konishi S.; Honda, K. *Nature* **1979**, *277*, 637-640.
10. Halmann, M. In *Energy Resources through Photochemistry and Catalysis*; Grätzel M. Ed.; Academic Press, New York, **1983**, pp. 507-565.
11. Anpo, M.; Chiba, K. *J. Mol. Catal.* **1992**, *74*, 207-302.
12. Yamashita, H.; Shiga, A.; Kawasaki, S.; Ichihashi, Y.; Ehara, S.; Anpo, M. *Energy Conv. Manag.* **1995**, *36*, 617-620.
13. Anpo, M.; Yamashita H.; Ichihashi Y.; Ehara S. *J. Electroanal. Chem.* **1995**, *396*, 21-26.
14. Yamashita, H.; Nishiguchi, H.; Kamada, N.; Anpo, M.; Teraoka, Y.; Hatano, H.; Ehara, S.; Kikui, K.; Palmisano, L.; Sclafani, A.; Schiavello M.; Fox, M. A. *Res. Chem. Intermed.* **1994**, *20*, 815-823.
15. Yamashita, H.; Kamada, N.; He, H.; Tanaka, K.; Ehara, S.; Anpo, M. *Chem. Lett.* **1994**, 855-858.
16. Anpo, M.; Yamashita, H.; Ichihashi, Y.; Fujii, Y.; Honda, M. *J. Phys. Chem.B* **1997**, *101*, 2632-2636.

17. Anpo, M.; Yamashita, H.; Fujii, Y.; Ichihashi, Y.; Zhang, S. G.; Park, D. R.; Ehara, S.; Park, S. E.; Chang, J. S.; Yoo. J. W. *Stud. Surf. Sci. Catal.* **1998**, *114*, 177-182.
18. Yamashita, H.; Fuji, Y.; Ichihashi, Y.; Zhang, S. G.; Ikeue, K.; Park, D. R.; Koyano, K.; Tatsumi, T.; Anpo, M. *Catal.Today* **1998**, *45*, 221-227.
19. Anpo, M.; Zhang, S. G.; Fujii, Y.; Ichihashi, Y.; Yamashita, H.; Koyano, K.; Tatsumi. T. *Catal. Today* **1998**, *44*, 327-332.
20. Ikeue, K.; Yamashita, H.; Anpo, M. *Chem. Lett.* **1999**, 1135-1136.
21. Yamashita, H.; Ikeue, K.; Takewaki, T. *Topics in Catal.* in press.
22. Yamashita, H.; Kawasaki, S.; Fujii, Y.; Ichihashi, Y.; Ehara, S.; Park, S. E.; Chang, J. S.; Yoo. J. W.; Anpo, M. *Stud. Surf. Sci. Catal.* **1998**, *114*, 561-564.
23. Saladin, F.; Forss, L.; Kamber, I. *J. Chem. Soc., Chem. Commun.* **1995**, 533-534.
24. Anpo, M.; Tomonari, M.; Fox, M. A. *J. Phys. Chem.* **1989,** ***93***, 7300-7303.
25. Yamashita, H.; Ichihashi, Y.; Harada, M.; Stewart, G.; Fox M. A.; Anpo, M. *J. Catal.*, **1996**, *158*, 97-101.
26. Frese, K. W. *J. Electrochem. Soc.* **1991**, *138*, 3338-3343.
27. Raskö, J.; Solymosi, F. *J. Phys. Chem.* **1994**, *98*, 7147-7152.
28. Anpo, M.; Matsuoka, M.; Shioya, Y.; Yamashita, H.; Giamello, E.; Morterra, C.; Che, M.; Patterson, H. H.; Webber, S.; Ouellette, S.; Fox, M. A. *J. Phys. Chem.*, **1994**, *98*, 5744-5750.
29. Yamashita, H.; Matsuoka, M.; Tsuji, K.; Shioya, Y.; Anpo M.; Che, M. *J. Phys. Chem.* **1996**, *100*, 397-402.
30. Yamashita, H.; Ichihashi, Y; Anpo M.; Hashimoto, M.; Louis, C.; Che, M. *J. Phys. Chem.* **1996**, *100*, 16041-16044.
31. Yamashita, H.; Zhang, S. G.; Ichihashi, Y.; Matsumura, Y.; Souma, S.; Tatsumi, T.; Anpo, M. *Appl. Surf. Sci.* **1997**, *121*, 305-309.
32. Farges, F.; Brown G. E. Jr.; Rehr, J. H. *Geochim. Cosmochim. Acta* **1996**, *60*, 3023-3060.
33. Anpo, M; Aikawa, N.; Kubokawa, Y.; Che, M.; Louis, C.; Giamello, E. *J. Phys. Chem.* **1985**, *89*, 5017-5021.
34. Anpo, M.; Aikawa, N.; Kubokawa, Y.; Che, M.; Louis, C.; Giamello, E. *J. Phys. Chem.* **1985**, *89*, 5689-5694.
35. Takewaki, T.; Hwang, S. J.; Yamashita, H.; Davis, M. E. *Micropor. Mesopor. Mater.* **1999**, *32*, 265-273.
36. Camblor, M. A.; Corma, A.; Esteve, P.; Martines M.; Valencia, S. *Chem. Commun.* **1997**, 795-796.
37. Tatsumi, T.; Jappar, N. *J. Phys. Chem. B* **1998**, *102*, 7126-7131.
38. Yamashita, H.; Kawasaki, S.; Ichihashi, Y.; Harada, M.; Anpo, M.; Stewart, G.; Fox, M. A.; Louis, C.; Che, M. *J. Phys. Chem. B* **1998**, *102*, 5870-5875.

Downloaded by UNIV OF GUELPH LIBRARY on September 16, 2012 | http://pubs.acs.org
Publication Date: January 24, 2002 | doi: 10.1021/bk-2002-0809.ch022

Downloaded by COLUMBIA UNIV on September 16, 2012 | http://pubs.acs.org
Publication Date: January 24, 2002 | doi: 10.1021/bk-2002-0809.ch023

Chapter 23

Electrochemical Reduction of CO_2 with Gas-Diffusion Electrodes Fabricated Using Metal and Polymer-Confined Nets

K. Ogura, H. Yano, and M. Nakayama

Department of Applied Chemistry, Yamaguchi University, Tokiwadai 2–16–1,
Ube 755-8611, Japan

Electrochemical reduction of CO_2 has been performed with a Cu/gas-diffusion electrode, a Cu plate electrode, and a modified Pt/gas-diffusion electrode in KCl (pH 3) and $KHCO_3$ (pH 7.2) solutions. Among these electrolysis systems, the most efficient reduction of CO_2 was obtained in a KCl solution of pH 3 with a Cu/gas-diffusion electrode on which CO, C_2H_4 and CH_4 were mainly formed with some quantities of solution products such as lactic acid and ethanol. The hydrogen evolution was sufficiently retarded even at highly negative potential, and the total current efficiency was almost 100 %. On the other hand, the electrochemical reduction of CO_2 was carried out at a Cu plate electrode in a $KHCO_3$ solution of pH 7.2. This solution has been exclusively used as an electrolyte in the reduction of CO_2 at a Cu plate electrode. Major products were CH_4 and C_2H_4, and the total current efficiency was about 43 %. The cause for such a low current efficiency was attributed to the formation of graphitic carbon and/or

In CO2 Conversion and Utilization; Song, C., et al.;
ACS Symposium Series; American Chemical Society: Washington, DC, 2002.

copper oxide. At a Prussian blue (PB)/polyaniline (PAn)/metal complex-confined Pt/gas-diffusion electrode in a KCl solution of pH 3, lactic acid was mainly produced, and alcohols and acetic acid were minor products. In this electrolysis system, CO_2 is bifunctionally captured and activated by PAn and a metal complex: the electrophilic carbon atom of CO_2 is bound to the amino group of PAn, and the basic oxygen atom coordinates to the central metal of the complex.

Downloaded by COLUMBIA UNIV on September 16, 2012 | http://pubs.acs.org
Publication Date: January 24, 2002 | doi: 10.1021/bk-2002-0809.ch023

Chemical fixation of carbon dioxide is of importance in connection with the mitigation of the concentration of green-house gas in the atmosphere. Many processes have been proposed for the chemical conversion of CO_2 including the hydrogenation over heterogeneous and homogeneous catalysts at high temperature and electrochemical reduction (*1*). One of the most essential matters in CO_2 fixation is to achieve it under an input energy as low as possible to avoid a secondary generation of CO_2. Because of this, an electrochemical reduction process taking place at room temperature seems to be promising. In the application of this method, however, there are still difficult problems to be settled, e. g., the deactivation of electrode in a prolonged electrolysis.

There are many works on the electrochemical reduction of CO_2 with Cu electrode in a hydrogencarbonate solution (*2-9*). This electrolysis system is known to produce mainly methane and ethylene. In a prolonged electrolysis of CO_2, however, the rate of formation of hydrocarbons is found to go down to very small value. It is pointed that the high faradaic efficiencies of CH_4 and C_2H_4 reported in most of literatures are not the steady-state values but rather maximum efficiencies observed in a short period of electrolysis (*8*). This is attributed to the formation of a poisoning species. Therefore, it is very difficult to use the electrochemical process with Cu electrode for the reduction of CO_2 over long periods. The poisoning of this reaction has been attempted to be alleviated by applying a periodic anodic polarization, and the reactivation of the electrode been confirmed (*8*). Although a neutral hydrogencarbonate solution is the unique electrolyte in which hydrocarbons are produced on a Cu plate electrode in the reduction of CO_2, this solution becomes alkaline with the progress of the reduction, resulting in less efficiency of CO_2 conversion. On the other hand, a Cu plate electrode does not lead to the reduction of CO_2 in acidic solution but only to the hydrogen evolution.

In the present study, we have developed a gas-diffusion electrode consisting of a metal mesh electrode and a glass filter. As described later, the electrolysis of CO_2 at the gas-diffusion electrode with Cu mesh electrode led chiefly to the formation of CO and C_2H_4 with high yields in acidic solution, and the poisoning problem of the electrode was not involved. In the gas-diffusion electrode, CO_2 can be always supplied in large quantities to the electrode surface and the hydrogen evolution was effectively suppressed even in acidic solution. In addition to the experiments with Cu plate and mesh electrodes, a platinum mesh substrate on which an inorganic conductor and a conducting polymer were immobilized was also used as an electrode for the CO_2 reduction.

Downloaded by COLUMBIA UNIV on September 16, 2012 | http://pubs.acs.org
Publication Date: January 24, 2002 | doi: 10.1021/bk-2002-0809.ch023

Experimental

The electrolysis cell with a gas-diffusion electrode used (Figure 1) was essentially the same as that reported elsewhere (*10*). The working electrodes were a copper mesh, a copper plate and a platinum mesh, and their effective surface areas coming into contact with electrolyte were 10.2 cm^2, 10.2 cm^2 and 19.3 cm^2, respectively. Copper mesh and copper plate were made from pure copper (99.9 % purity, Nilaco Co.). The platinum mesh was modified with Prussian blue (PB, $KFe^{III}[Fe^{II}(CN)_6]$) (inner layer), conducting polymer (PAn) (outer layer), and a metal complex, following the procedure described previously (*11*). Anions incorporated in the prepared Pt mesh/PB/PAn electrode were released by immersing it in a phosphate buffer of pH 7, and bis(1,8-dihydroxynaphthalene-3,6-disulfonato) ferrate(II) ($Fe^{II}L^-$) complex was electrodeposited from its aqueous solution. As shown in Figure 1, these mesh electrodes were put on a glass filter through an O-ring, and both were bound to a Teflon cylinder tightened with a Teflon screw cup. This was connected to the cathode compartment through an O-ring which was separated from the anode compartment by a cation-exchange membrane. The average pore size of glass filter was 20 μ m. Purified CO_2 gas was forced up through the glass filter, and the liquid meniscuses spread out on the mesh electrode to form a thin layer electrolyte. The electrolysis with a Cu plate electrode was performed using a H-type cell. The electrolytes used were 0.5 M KCl solutions of various pH's and 0.5 M $KHCO_3$ solution of pH 7.2. These solutions were prepared from reagent grade KCl, $KHCO_3$, HCl and KOH with doubly distilled water. The counter electrode was a platinum plate, and the reference electrode was a Ag/AgCl/saturated KCl electrode. The quantitative analyses of the reaction products were done with a gas

Downloaded by COLUMBIA UNIV on September 16, 2012 | http://pubs.acs.org
Publication Date: January 24, 2002 | doi: 10.1021/bk-2002-0809.ch023

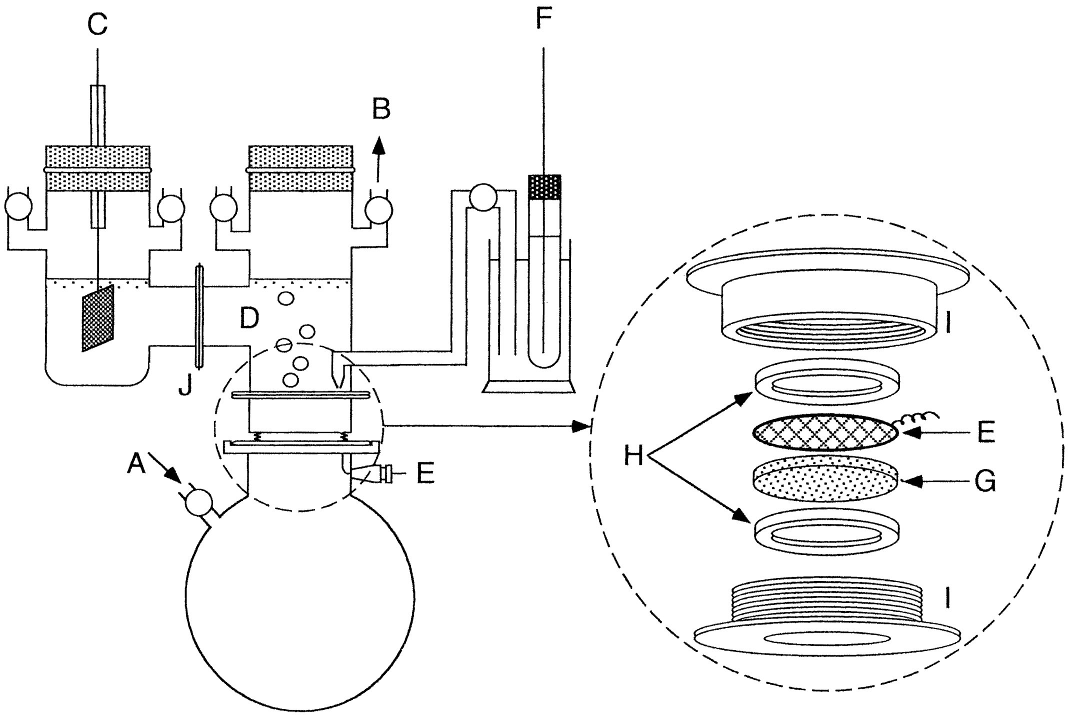

Figure 1. Schematic diagram of the electrolysis cell. A, gas inlet; B, gas outlet; C, counter electrode; D, electrolyte; E, working electrode; F, reference electrode; G, glass filter; H, O-ring; I, Teflon screw cap; J, cation-exchange membrane.

chromatograph (Shimadzu GC-8A), a steam chromatograph (Ohkura SSC-1) and an organic acid analyzer (Shimadzu LC-LoAD).

Results and Discussion

Reduction of CO_2 with Copper/Gas-Diffusion and Copper Plate Electrodes

The electrochemical reduction of CO_2 was performed with Cu/gas-diffusion and Cu plate electrodes in a 0.5 M KCl solution of pH 3 and a 0.5 M $KHCO_3$ of pH 7.2, respectively, and the results are shown versus potential in Figure 2. These solutions were selected because the yields of CO_2 reduction were maximum in each electrolysis system. As seen from this figure, the reduction of CO_2 occurs at more negative potential than -1.2 V vs Ag/AgCl on the Cu plate electrode, but on the Cu/gas-diffusion electrode the CO_2 reduction is observed even around -0.6 V although the full-scale reduction begins from -1.2 V. The total concentration of the products obtained with the gas-diffusion electrodes was about 3.5 times as large as that with the plate electrode at -2.4 V. Hence, the gas-diffusion electrode is found to be much more effective for the CO_2 reduction than the plate electrode.

Faradaic efficiencies for the products obtained in the electrochemical reduction of CO_2 with a Cu plate electrode and a Cu/gas-diffusion electrode are shown in Table I and II, respectively. The major products except hydrogen are CH_4 and C_2H_4 on the Cu plate electrode, and the total current efficiency averages about 43 % (Table I). This value is very low compared to that obtained with the Cu/gas-diffusion electrode as noted below. The cause for such a low current efficiency may be attributed to the formation of poisoning species on the Cu plate electrode. The identification of this species is under investigation, but graphitic carbon is one of candidates (*5*). On the other hand, the major products obtained with the Cu/gas-diffusion electrode are CO, C_2H_4 and CH_4 as shown in Table II. The total current efficiency was almost 100 %, which is a contrast to the value of about 43 % on the Cu plate electrode. It is therefore indicated that the electrolysis system with the Cu/gas-diffusion electrode is not subject to poisoning. This is probably because the poisoning process is considerably suppressed in acidic solution.

Major compounds generated in the two electrolysis systems are shown versus potential in Figures 3 and 4. The formation of CH_4 and C_2H_4 was observed on the Cu plate electrode at more negative potential than -1.4 V,

Downloaded by COLUMBIA UNIV on September 16, 2012 | http://pubs.acs.org
Publication Date: January 24, 2002 | doi: 10.1021/bk-2002-0809.ch023

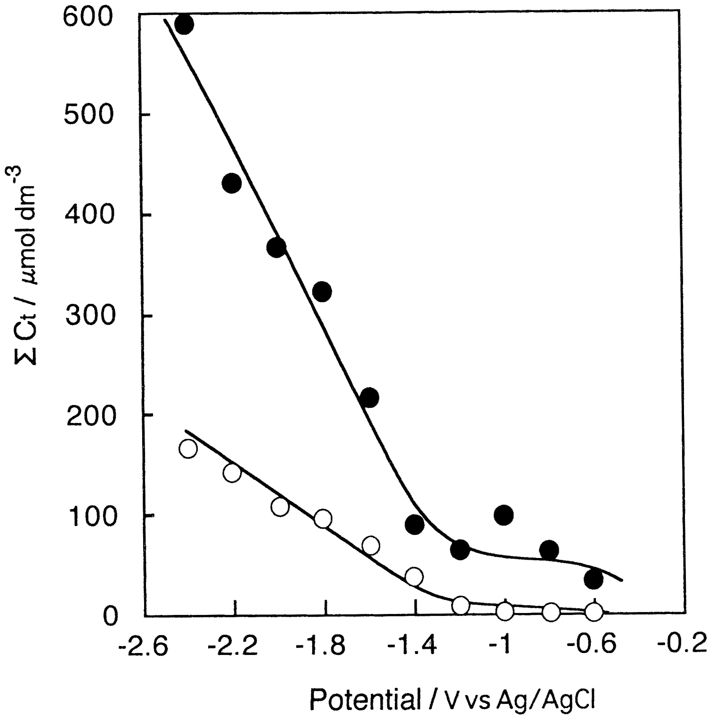

Figure 2. Relationship between the total concentration (ΣC_t) of the products based on the C content and the electrode potential on Cu plate (○) and Cu/gas-diffusion (●) electrodes in 0.5 M $KHCO_3$ and 0.5 M KCl solutions, respectively. $\Sigma C_t = [CH_3OH] + [HCOOH] + [CO] + [CH_4] + 2([CH_3CHO] + [C_2H_5OH] + [CH_3COOH] + [C_2H_4] + [C_2H_6]) + 3([CH_3COCH_3] + [CH_3CH(OH)COOH] + [CH_3CH_2CH_2OH])$. Electrolysis was performed for 30 min at each potential.

Downloaded by COLUMBIA UNIV on September 16, 2012 | http://pubs.acs.org
Publication Date: January 24, 2002 | doi: 10.1021/bk-2002-0809.ch023

Downloaded by COLUMBIA UNIV on September 16, 2012 | http://pubs.acs.org
Publication Date: January 24, 2002 | doi: 10.1021/bk-2002-0809.ch023

Table I. Faradaic efficiencies for the products obtained in the electrochemical reduction of CO_2 with a Cu plate electrode in a 0.5M $KHCO_3$ solution[a]

Potential	Faradaic efficiency (%)													Q[b]	ΣC_t[c]	η[d]
(V)	MeOH	EtOH	1-Pr	RCHO	Acetone	Formic	Acetic	Lactic	CO	CH_4	C_2H_4	C_2H_6	H_2	(C)	(μM)	(%)
-0.6	0.0	0.0	0.0	0.0	0.0	0.0	0.0	0.0	0.2	7.7	0.0	0.0	0.6	2.8	0.4	8.5
-0.8	0.1	0.0	0.0	0.0	0.5	0.0	0.0	0.0	0.1	4.3	0.0	0.0	7.2	4.3	0.8	12.3
-1.0	0.2	0.9	0.0	0.0	3.1	0.0	0.0	0.0	0.5	8.5	0.3	0.0	16.6	3.8	3.2	29.9
-1.2	0.1	2.3	0.0	0.0	1.4	0.0	0.0	0.0	1.9	3.8	0.4	0.0	39.7	10.2	7.7	49.7
-1.4	0.1	0.0	0.0	0.0	0.1	0.2	0.0	1.5	4.0	1.7	0.2	0.0	60.2	51.5	37.8	67.9
-1.6	0.0	0.0	0.0	0.0	0.1	0.0	0.0	0.9	5.2	4.6	0.3	0.0	59.1	105	68.5	70.2
-1.8	0.0	0.4	0.6	0.1	0.0	0.0	0.0	0.0	0.1	7.9	1.9	0.0	22.6	214	94.6	34.3
-2.0	0.0	0.1	0.0	0.0	0.0	0.0	0.0	0.0	0.3	8.3	0.8	0.0	50.4	521	107	59.9
-2.2	0.0	0.2	0.1	0.0	0.0	0.0	0.0	0.1	0.3	8.6	1.2	0.0	48.8	552	142	59.3
-2.4	0.0	0.1	0.0	0.0	0.0	0.0	0.0	0.5	0.0	2.3	0.1	0.0	36.8	1145	168	39.8

[a] Electrolysis Potential, V vs Ag/AgCl; initial pH, 7.2; electrolysis time, 30 min; net area of the Cu Plate electrode, 10.2 cm^2.

[b] Electric charge passed during the electrolysis.

[c] Total concentration of the products on the basis of C content, μ mol dm^{-3}.

$$\Sigma C_t = [CH_3OH] + [HCOOH] + [CO] + [CH_4] + 2([CH_3CHO] + [C_2H_5OH] + [CH_3COOH] + [C_2H_4] + [C_2H_6]) + 3([CH_3COCH_3] + [CH_3CH(OH)COOH] + [CH_3CH_2CH_2OH])$$

[d] Faradaic efficiency for the reduction of CO_2.

Downloaded by COLUMBIA UNIV on September 16, 2012 | http://pubs.acs.org
Publication Date: January 24, 2002 | doi: 10.1021/bk-2002-0809.ch023

Table II. Faradaic efficiencies for the products obtained in the electrochemical reduction of CO_2 with a Cu/gas-diffusion electrode in a 0.5M KCl solution[a]

Potential	*Faradaic efficiency (%)*													Q[b]	ΣC_t[c]	η[d]
(V)	*MeOH*	*EtOH*	*1-Pr*	*RCHO*	*Acetone*	*Formic*	*Acetic*	*Lactic*	*CO*	CH_4	C_2H_4	C_2H_6	H_2	*(C)*	*(μM)*	*(%)*
-0.6	1.1	1.9	0.0	0.0	4.4	4.4	0.0	46.4	0.2	12.9	0.0	0.0	30.3	2.7	35.8	101
-0.8	1.0	2.4	0.0	6.9	12.7	2.5	0.0	43.4	0.1	6.1	0.0	0.0	21.2	4.5	64.7	96.4
-1.0	2.2	1.5	0.0	2.1	1.5	0.1	0.0	44.9	0.1	4.6	0.0	0.0	30.8	8.4	101	93.5
-1.2	3.4	3.6	0.0	2.6	8.8	2.2	0.0	7.5	6.0	2.1	0.0	0.0	47.8	11.6	66.7	84.1
-1.4	0.1	0.3	0.0	0.0	2.2	1.1	0.0	5.8	31.9	1.2	0.2	0.2	51.3	26.0	92.4	95.1
-1.6	0.2	0.4	0.0	0.8	1.5	1.4	0.0	9.7	39.1	0.8	1.8	0.0	43.7	44.5	218	99.6
-1.8	0.1	0.7	0.5	0.3	0.6	1.8	1.0	6.5	38.6	2.9	9.2	0.2	37.4	70.2	324	99.8
-2.0	0.1	4.0	2.1	0.7	0.8	0.3	0.0	2.1	39.8	9.8	25.4	0.2	28.4	95.6	367	115
-2.2	0.1	3.6	1.8	0.6	0.1	0.3	0.4	2.9	30.7	8.1	25.6	0.1	37.0	138	431	111
-2.4	0.1	5.1	2.0	1.1	0.3	0.2	0.2	2.2	25.0	10.1	36.5	0.2	25.6	171	589	109

[a] Electrolysis Potential, V vs Ag/AgCl; initial pH, 3.0; electrolysis time, 30 min; net area of the Cu mesh electrode, 10.2 cm^2.

[b] Electric charge passed during the electrolysis.

[c] Total concentration of the products on the basis of C content, μ mol dm^{-3}.

$\Sigma C_t = [CH_3OH] + [HCOOH] + [CO] + [CH_4] + 2([CH_3CHO] + [C_2H_5OH] + [CH_3COOH] + [C_2H_4] + [C_2H_6]) + 3([CH_3COCH_3] + [CH_3CH(OH)COOH] + [CH_3CH_2CH_2OH])$

[d] Faradaic efficiency for the reduction of CO_2.

Downloaded by COLUMBIA UNIV on September 16, 2012 | http://pubs.acs.org
Publication Date: January 24, 2002 | doi: 10.1021/bk-2002-0809.ch023

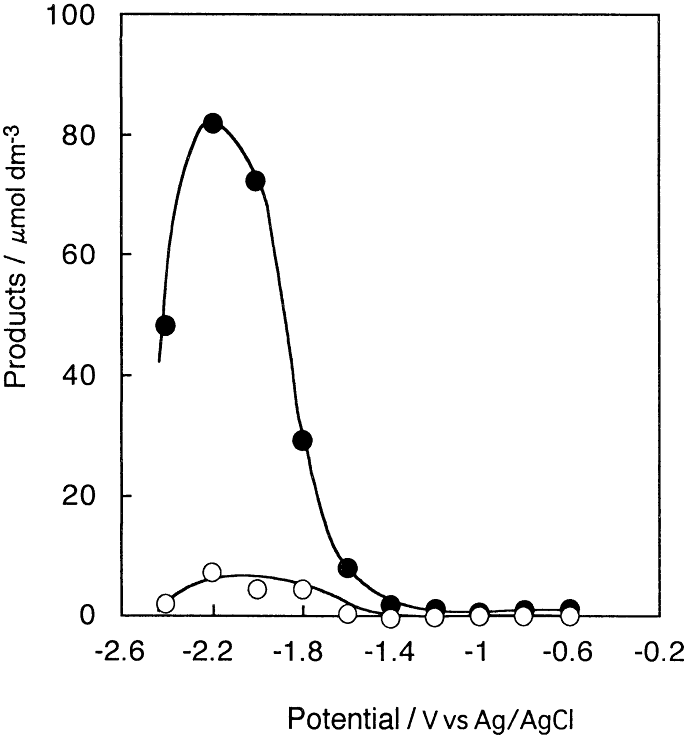

Figure 3. Relationship between the concentrations of CH_4 (●) and C_2H_4 (○) and the electrode potential. The electrolysis was performed with a Cu palte electrode for 30 min in a 0.5 M $KHCO_3$ solution of pH 7.2.

Downloaded by COLUMBIA UNIV on September 16, 2012 | http://pubs.acs.org
Publication Date: January 24, 2002 | doi: 10.1021/bk-2002-0809.ch023

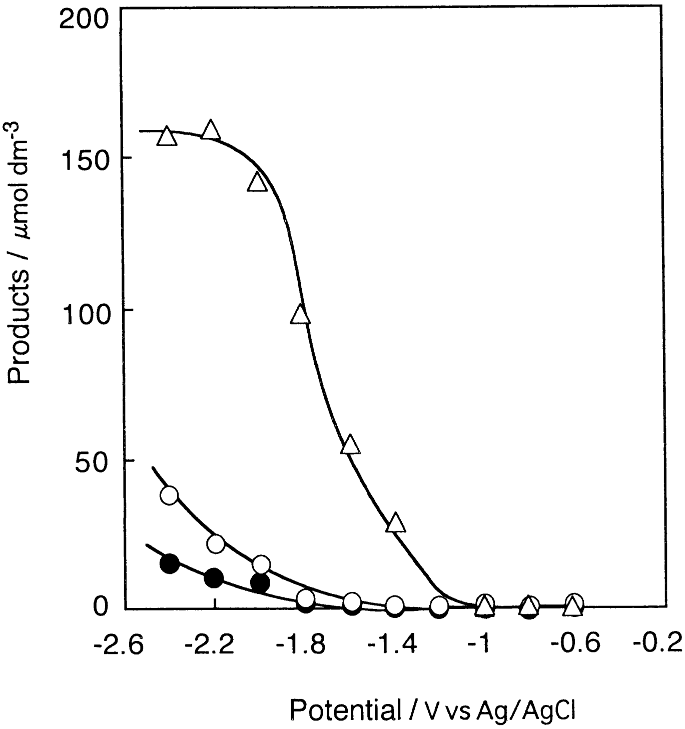

Figure 4. Relationship between the concentrations of CH_4 (●), C_2H_4 (○) and CO (△) and the electrode potential. The electrolysis was performed with a Cu/gas-diffusion electrode for 30 min in a 0.5 M KCl solution of pH 3.0.

and the yields were maximum around -2.2 V (Figure 3). On the other hand, the species such as CO, CH_4 and C_2H_4 were mainly formed on the Cu/gas-diffusion electrode. As compared to the results at the plate electrode, a great difference is that the most abundant product was CO of instead of CH_4, the yield of C_2H_4 was much larger than that of CH_4, and the solution products (lactic acid and alcohols) were not negligible. Hence, it is suggested that the reaction scheme for the electrochemical reduction of CO_2 is completely different on the plate and gas-diffusion electrodes.

In Figure 5, the total concentration of the products are plotted as a function of the electric charge on the plate electrode in a 0.5 M $KHCO_3$ solution, indicating that the products are generated via electrochemical processes. In a 0.5 M KCl solution of pH 6.0, however, there was no such a linear relationship, and the total concentration was very small independent of electric charge in the electrolysis beyond 100 C. It was only in neutral buffer solution that a good linear relationship between the total concentration and electric charge was valid on the Cu plate electrode. On the other hand, the total concentration is proportional to the electric charge on the Cu/gas-diffusion electrode in both KCl solutions of pH 3.0 and 6.0 as shown in Figure 6.

At the Cu/gas-diffusion electrode in acidic solution, the yield of CO was highest, and C_2H_4, CH_4 and solution products were generated irrespective of the buffer property of electrolyte. This suggests that CO is first produced in the reduction of CO_2, and the formation of C_2H_4 and CH_4 is followed by the reduction of CO.

$$CO_2 + 2H^+ + 2e^- \rightarrow CO + H_2O \qquad (1)$$

$$2CO + 8H^+ + 8e^- \rightarrow C_2H_4 + 2H_2O \qquad (2)$$

$$CO + 6H^+ + 6e^- \rightarrow CH_4 + H_2O \qquad (3)$$

CO_2 is always supplied to the electrode surface at the Cu/gas-diffusion electrode, and the hydrogen evolution is suppressed even at highly negative potential. Such a stepwise process may lead to the favorable occurrence of some side reactions involving the formation of lactic acid and alcohols.

Bard et. al have reported that a black film attributable to graphitic carbon deposits on the surface of Cu electrode during the reduction of CO_2 in a $KHCO_3$ solution (*5*). We also found a black film on Cu plate electrode in the electrolysis of CO_2 in hydrogencarbonate solution. The total current efficiency which was estimated from the yields of reduction products of CO_2 and the hydrogen evolution was considerably low (about 43 %), and

Downloaded by COLUMBIA UNIV on September 16, 2012 | http://pubs.acs.org
Publication Date: January 24, 2002 | doi: 10.1021/bk-2002-0809.ch023

Downloaded by COLUMBIA UNIV on September 16, 2012 | http://pubs.acs.org
Publication Date: January 24, 2002 | doi: 10.1021/bk-2002-0809.ch023

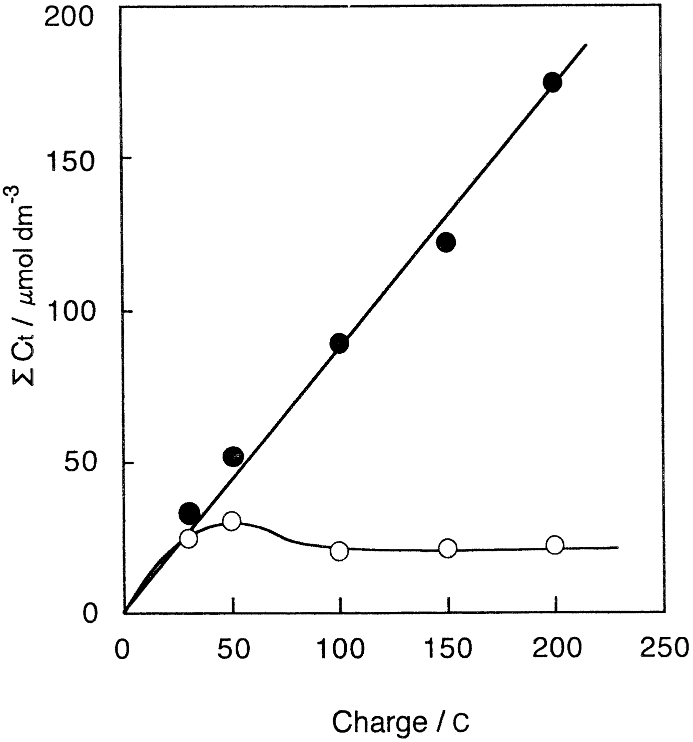

Figure 5. Relationship between the total concentration (ΣC_t) of the products and the electric charge passed during the reduction of CO_2 on a Cu plate electrode in a 0.5 M $KHCO_3$ solution of pH 7.2 (●) and a 0.5 M KCl of pH 6.0 (○).

Downloaded by COLUMBIA UNIV on September 16, 2012 | http://pubs.acs.org
Publication Date: January 24, 2002 | doi: 10.1021/bk-2002-0809.ch023

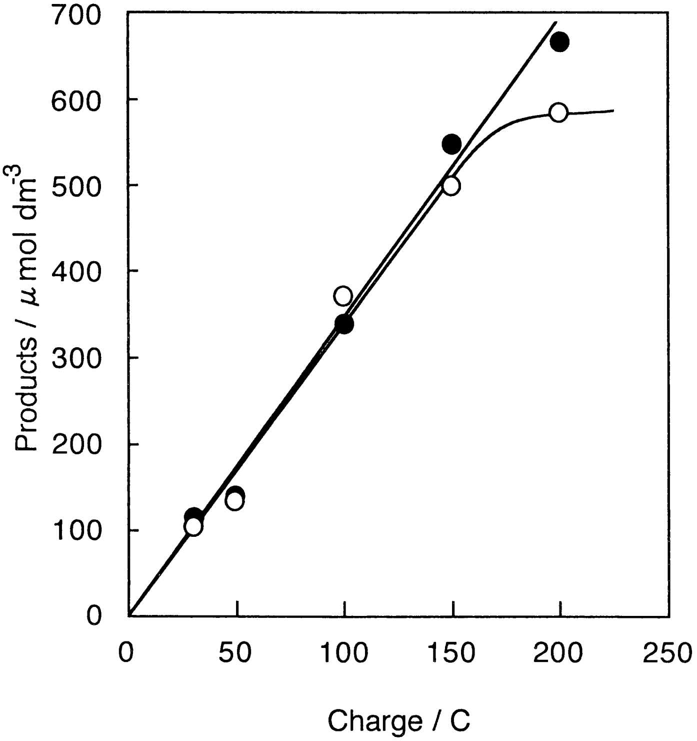

Figure 6. Relationship between the total concentration (Σ C_t) of the products and the electric charge passed during the reduction of CO_2 on a Cu/gas-diffusion electrode in 0.5 M KCl solutions of pH 3.0 (●) and 6.0 (○).

the yields of CO and solution products were negligibly small. From these facts, it is suggested that the reduction of CO_2 on Cu plate electrode does not proceed via a stepwise process like that described above but graphite is first produced and CH_4 and C_2H_4 are generated by the further reduction of graphite.

$$CO_2 + 2H_2O + 4e^- \rightarrow C + 4OH^- \qquad (4)$$

$$C + 4H_2O + 4e^- \rightarrow CH_4 + 4OH^- \qquad (5)$$

$$2C + 4H_2O + 4e^- \rightarrow C_2H_4 + 4OH^- \qquad (6)$$

The standard potentials for reaction (4) and (5) are known to be 0.206 V vs SHE and 0.132 V vs SHE, respectively. As another possible scheme for the formation of graphite instead of reaction (4), the involvement of copper oxide is considered as following.

$$CO_2 + Cu + H_2O + 2e^- \rightarrow C + CuO + 2OH^- \qquad (7)$$

In fact, copper oxide has been detected on the Cu plate electrode used for the CO_2 reduction in hydrogencarbonate solution (*9*). The formation of carbon on the catalyst surface has been often referred in the reduction of CO over a heterogeneous catalyst at high temperature, and hydrocarbons are produced by hydrogenation of surface carbon (*12*). The formation of surface carbon has been identified also in the methanation of CO_2 (*13*). However, a striking difference between electrochemical and high temperature reduction of CO_2 is that the former reduction on Cu plate electrode is not accompanied by the generation of CO. The cause for such a difference should be clarified by further investigation.

Reduction of CO_2 with a Modified Pt/Gas-Diffusion Electrode

The electrochemical reduction of CO_2 was performed with a modified Pt/gas-diffusion electrode. The modification of a Pt substrate was achieved with an inorganic conductor and a conducting polymer, and besides a metal complex was immobilized to the conducting polymer (*10*). The results obtained are shown in Table III, where the flow rate of CO_2 was changed from 2.0 to 99.0 ml min^{-1}. The major product was lactic acid, and methanol, ethanol, acetone, 2-propanol, and formic and acetic acids were formed as minor products. The current efficiency for the reduction of CO_2

Downloaded by COLUMBIA UNIV on September 16, 2012 | http://pubs.acs.org
Publication Date: January 24, 2002 | doi: 10.1021/bk-2002-0809.ch023

Downloaded by COLUMBIA UNIV on September 16, 2012 | http://pubs.acs.org
Publication Date: January 24, 2002 | doi: 10.1021/bk-2002-0809.ch023

Table III. Faradaic efficiencies for the products obtained in the electrochemical reduction of CO_2 with a polymer composite/gas-diffusion electrode as a function of gas flow rate in a solution of 0.5M KCl[a]

Flow rate	*Faradaic efficiency (%)*							*V* [b]	*Q* [c]	ΣC_t [d]	η [e]
(*ml min*$^{-1}$)	*MeOH*	*EtOH*	*2-Pr*	*Acetone*	*Formic*	*Acetic*	*Lactic*	(*cm*^{3})	(*C*)	(μ*M*)	(%)
2.0	0.6	1.0	0.0	2.8	4.1	0.0	28.3	141	2.3	16.9	36.8
9.8	0.0	5.1	2.7	7.8	2.0	4.9	32.0	137	3.3	32.8	54.5
16.0	0.7	1.0	0.0	3.3	3.0	20.6	57.0	134	2.2	36.6	85.5
27.0	2.8	1.1	0.0	5.6	5.0	26.7	63.7	135	2.2	44.3	105
99.0	21.4	17.0	4.3	11.7	2.5	12.7	15.1	142	1.9	25.6	87.6

[a] Electrolysis Potential, -0.8 V vs Ag/AgCl; initial pH, 3.0; electrolysis time, 3 h; net area of the substrate, 19.3 cm^2.

[b] Volume of the catholyte after electrolysis.

[c] Electric charge passed during the electrolysis.

[d] Total concentration of the products on the basis of C content, μmol dm^{-3}.

$\Sigma C_t = [CH_3OH] + [HCOOH] + 2([C_2H_5OH] + [CH_3COOH]) + 3([CH_3COCH_3] + [CH_3CH(OH)COOH] + [CH_3CH(OH)CH_3])$

[e] Faradaic efficiency for the reduction of CO_2.

increased with an increase of the flow rate of CO_2, but became lower at the flow rate of 99.0 ml min^{-1}. At this flow rate, the electric charge passed during the electrolysis was also smaller. These results are probably attributed to the limited area of the liquid meniscus which was found to be important for the CO_2 reduction on the mesh metal/gas-diffusion electrode, because a part of the mesh electrode could not keep contact with the electrolyte under such a high flow rate.

In the mediated reduction of CO_2, PB and PAn are in the reduced states as represented by reaction (8) and (9), respectively.

$$\underset{\text{(PB)}}{KFe^{III}[Fe^{II}(CN)_6]} + K^+ + e^- \rightarrow \underset{\text{(Everitt's salt, ES)}}{K_2Fe^{II}[Fe^{II}(CN)_6]} \qquad (8)$$

$$PAn^+/Fe^{II}L^- + K^+ + e^- \rightarrow PAn/Fe^{II}L^-/K^+ \qquad (9)$$

The reduction scheme of CO_2 on the polymer-modified electrode (*11*) is schematically shown in Figure 7. In this scheme, CO_2 is bifunctionally captured by PAn and the metal complex: the electrophilic carbon atom of CO_2 is bound to the amino group of PAn, and the basic oxygen atom coordinates to the central metal of the complex. Electrons from the Pt substrate reach the PAn/PB interface where H^+ is catalytically reduced to H_{ads} on the zeolitic lattice of ES. The bifunctionally activated CO_2 is hydrogenated by H_{ads}. The reaction intermediates are stabilized in the nonaqueous atmosphere of conducting polymer, and various products including lactic acid and methanol are generated by further advanced hydrogenation.

References

1. Halmann, M. *Chemical Fixation of Carbon Dioxide;* CRC Press: Boca Raton, FL, 1993.
2. Hori, Y.; Kikuchi, K.; Suzuki, S. *Chem. Lett.* **1985,** 1695-1698.
3. Hori, Y.; Kikuchi, K.; Murata, A.; Suzuki, S. *Chem. Lett.* **1986,** 897-898.
4. Cook, R. L.; MacDuff, R. C.; Sammells, A. F. *J. Electrochem. Soc.* **1987,** *134,* 1873-1874.
5. DeWulf, D. W.; Bard, A. J. *Catal. Lett..* **1988,** *1,* 73-79.
6. DeWulf, D. W.; Jin, T.; Bard, A. J. *J. Electrochem. Soc.* **1989,** *136,* 1689-1691.

Downloaded by COLUMBIA UNIV on September 16, 2012 | http://pubs.acs.org
Publication Date: January 24, 2002 | doi: 10.1021/bk-2002-0809.ch023

Downloaded by COLUMBIA UNIV on September 16, 2012 | http://pubs.acs.org
Publication Date: January 24, 2002 | doi: 10.1021/bk-2002-0809.ch023

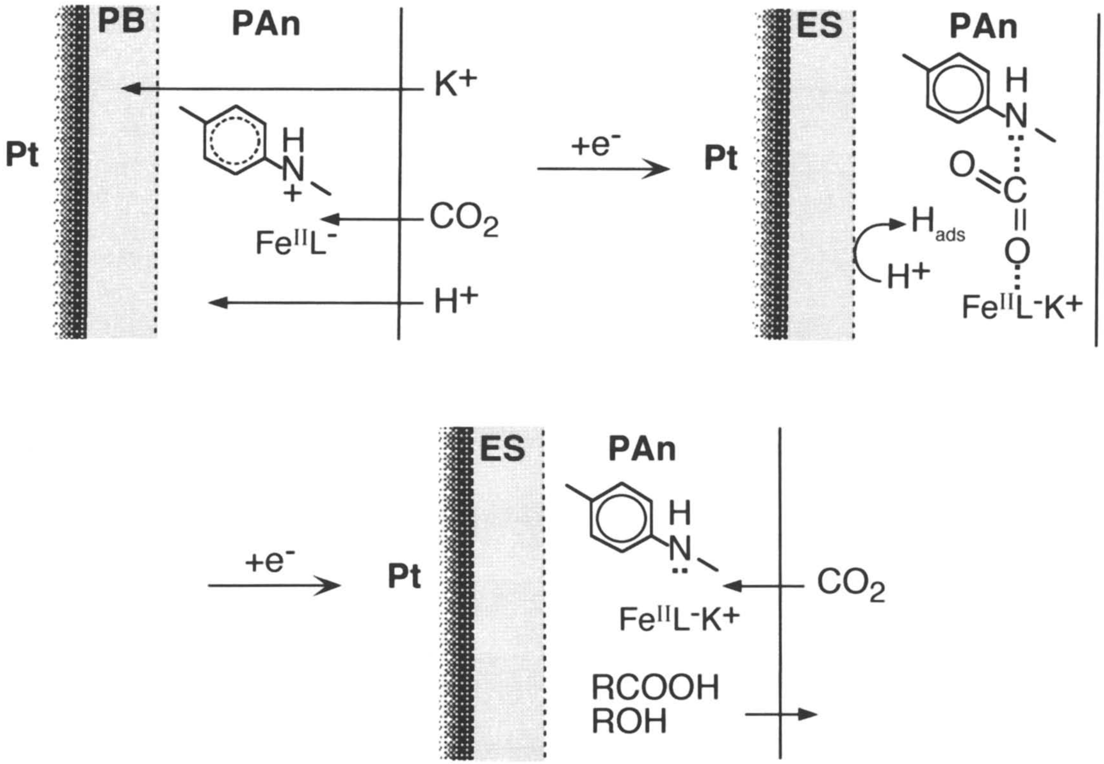
Pt
PB
PAn
H
N
+
K^+
CO_2
$Fe^{II}L^-$
H^+
$+e^-$
Pt
ES
PAn
H
N
O
C
O
H_{ads}
H^+
$Fe^{II}L^-K^+$
$+e^-$
Pt
ES
PAn
H
N
CO_2
$Fe^{II}L^-K^+$
RCOOH
ROH

Figure 7. Schematic representation of the electrochemical reduction of CO_2 on a Pt/PB/PAn-Fe^{II}L electrode.

7. Hori, Y; Wakebe, H.; Tsukamoto, T.; Koga, O. *Electrochim. Acta* **1994,** *39*, 1833-1839.
8. Jermann, B.; Augustynski, J. *Electrochim. Acta* **1994,** *39*, 1891-1896.
9. Smith, B. D.; Irish, D. E.; Kedzierzawski, P.; Augustynski, J. *J. Electrochem. Soc.* **1997**, *144*, 4288-4296.
10. Ogura, K.; Endo, N. *J. Electrochem. Soc.* **1999,** *146*, 3736-3740.
11. Ogura, K.; Endo, N.; Nakayama, M. *J. Electrochem. Soc.* **1998,** *145*, 3801-3809.
12. Reymond, J. P.; Mériaudeau, P.; Teichner, S. J. *J. Catal.* **1982,** *75*, 39-48.
13. Sulymosi, F.; Erdohelyi, A.; Kocsis, M. *J. Chem. Soc., Faraday Trans. 1* **1981,** *77*, 1003-1012.

Downloaded by COLUMBIA UNIV on September 16, 2012 | http://pubs.acs.org
Publication Date: January 24, 2002 | doi: 10.1021/bk-2002-0809.ch023

Downloaded by UNIV OF GUELPH LIBRARY on September 16, 2012 | http://pubs.acs.org
Publication Date: January 24, 2002 | doi: 10.1021/bk-2002-0809.ch024

Chapter 24

Use of Dense-Phase Carbon Dioxide in Catalysis

Bala Subramaniam[1] and Daryle H. Busch[2]

Departments of [1]Chemical and Petroleum Engineering and [2]Chemistry, University of Kansas, Lawrence, KS 66045

Starting in the early 90's, green chemistry research has been the focus of many investigations. This paper reviews heterogeneous and homogeneous catalysis in dense phase CO_2 including CO_2-expanded solvents. The advantages of using dense phase CO_2 include replacement of organic solvents with environmentally-benign CO_2, the enhanced miscibility of reactants such as O_2 and H_2, alleviating interphase transport limitations, and the chemical inertness of CO_2. In addition, the physicochemical properties of CO_2-based reaction media can be pressure-tuned to obtain unique fluid properties (e.g., gas-like transport properties, liquid-like solvent power and heat capacities). The advantages of CO_2-based reaction media for optimizing catalyst activity and product selectivity are highlighted for a variety of reactions such as these: alkylation on solid acid catalysts; hydrogenation on supported noble metal catalysts; and a broad range of homogeneous oxidations with transition metal catalysts and dioxygen or organic peroxides as oxidant. The overview concludes with an assessment of the potential and outlook of CO_2-based reaction media in industrial chemicals processing.

Concerns about solvents have propelled research efforts aimed at developing environmentally-benign chemical processing techniques that either eliminate or significantly mitigate pollution at the source *(1, 2, 3, 4, 5)*. A major research focus in chemical processing has been the replacement of traditional solvents with *sc*CO_2. Supercritical and near-critical dense carbon dioxide phases have been heralded as environmentally-benign solvents of great promise in many chemical applications, including the long used process for decaffeination of coffee beans, the chemical process industry, and, more recently, to replace the conventional organic solvents used in pharmaceutical processing and the cleaning of garments. The low toxicity and limited reactivity of CO_2 make it suitable for use around foods and other consumer goods, and its low cost supports its use in very broad ranges of applications. Detailed reviews of reactions in *sc* media *(6, 7, 8, 9, 10, 11)* are provided elsewhere.

This overview is focused on applications of dense CO_2 media in catalytic processing. Historically, emphasis has rested on *sc*CO_2, and the many advantages of that medium over traditional solvents are first discussed. Attention is then directed to the even greater advantages of CO_2 expanded organic solvents, new media that were first introduced for oxidation reactions in our laboratories. These extremely variable solvent systems retain solubility characteristics of the two combined solvents and still enjoy the environmental advantages of more familiar dense CO_2 media. Applications of dense phase CO_2 in heterogeneous and homogeneous catalytic systems are first briefly reviewed. In homogeneous catalysis, the emphasis will be on oxidation systems that have been the subject of several years of collaborative research at the University of Kansas among researchers from the Departments of Chemical & Petroleum Engineering and Chemistry. Thus, homogeneous polymerization, hydrogenation reactions and phase-transfer catalysis are not reviewed in detail here. These are reviewed elsewhere [*12*, 13].

Carbon dioxide is considered environmentally acceptable, non-toxic, relatively cheap (~5 cents/lb), non-flammable, inert toward oxidation and readily available. Supercritical reaction media, in general, have the potential to increase reaction rates, to enhance the selectivities of chemical reactions and to facilitate relatively easy separation of reactants, products, and catalysts after reaction. At ambient temperatures, the solubility of the much-favored terminal oxidant, atmospheric oxygen, in water and conventional organic solvents is limited. However, oxygen and carbon dioxide are miscible in all proportions under *sc* conditions. The increased concentration of reactants within an *sc* phase has the potential to accelerate reaction rates. In addition, the elimination of interphase (gas-liquid) mass transfer resistances may also increase reaction rates. The one-to-two-orders-of-magnitude higher intrinsic diffusivities of solutes in *sc* media compared to organic solvents could also accelerate reactions in the case of processes wherein the overall rate of reaction is limited by diffusion of reactants to form encounter pairs, which subsequently react to form products. The solubilities of solutes in *sc* fluids depend strongly on pressure and temperature in the vicinity of the critical point. Therefore, reactants, products and the catalyst can be separated by relatively simple pressure and/or temperature programming. Furthermore, if the phase behavior of the reaction mixture is such that the products fall out of the reaction mixture at the reaction P and T, *in situ* product separation is achieved. However, in the case of CO_2, the dielectric constant remains virtually unaffected over a wide range of pressure. Thus, pressure-tuning effects in the *sc* region on conversion and selectivity may be investigated with minimal change in solvent dielectric constant.

Downloaded by UNIV OF GUELPH LIBRARY on September 16, 2012 | http://pubs.acs.org
Publication Date: January 24, 2002 | doi: 10.1021/bk-2002-0809.ch024

Thermodynamic and Kinetic Aspects

The principles developed for gas or liquid phase reactions may be applied to supercritical phase reactions as well. When the reaction medium density is gas-like, the concepts developed for gas-phase reactions, such as kinetic theory of gases, may be applied. For liquid-like reaction mixtures, principles of liquid-phase kinetics have been applied. Parameters such as the solvent's solubility parameter, dielectric constant or solvatochromic shift, routinely used to interpret liquid-phase reactions, have been employed to understand the effect of a given *sc* solvent on chemical reaction (*6*). In the vicinity of the critical point, *sc* reaction media admit sensitive pressure effects on reaction rate and equilibrium constants.

Downloaded by UNIV OF GUELPH LIBRARY on September 16, 2012 | http://pubs.acs.org
Publication Date: January 24, 2002 | doi: 10.1021/bk-2002-0809.ch024

Pressure effects

Reactions in *sc* media typically involve elevated pressures that could have either an enhancing or inhibiting effect on rate and equilibrium constants. Based on transition-state theory, the pressure dependence on the rate constant is given by the following equation:

$$\left(\frac{\partial \ln k_x}{\partial P}\right)_{T,x} = -\frac{\Delta \upsilon^*}{RT} \tag{1}$$

where k_x is the mole-fraction based rate constant, $\Delta\upsilon^*$ is the activation volume (defined as the difference between the partial molar volume of the activated complex and sum of the partial molar volumes of the reactants), R is the universal gas constant, P is the pressure and T is the absolute temperature. If the rate constant is related to a pressure-dependent measure of concentration (such as partial pressure), then the following equation is used:

$$\left(\frac{\partial \ln k_c}{\partial P}\right)_{T,c} = \frac{\Delta \upsilon^*}{RT} + \left(\frac{1-n}{P}\right)\left[1 - \left(\frac{\partial \ln \kappa_T}{\partial \ln P}\right)_{T,c}\right] \tag{2}$$

where k_c is the pressure-dependent rate constant, n is the molecularity of the reaction and κ_T is the isothermal compressibility factor. Equations (1) and (2) assume that the transition-state transmission coefficient is independent of pressure. In a similar manner, the effect of pressure on equilibrium constant is given by:

$$\left(\frac{\partial \ln K_x}{\partial P}\right)_{T,x} = \frac{\Delta \upsilon_r}{RT} \tag{3}$$

$$\left(\frac{\partial \ln K_c}{\partial P}\right) = -\frac{\Delta \upsilon_r}{RT} + \kappa_T \sum \nu_i \tag{4}$$

where $\Delta \upsilon_r$ is the reaction volume (defined as the difference between the partial molar volumes of reactants and products), K_x is the mole-fraction based equilibrium constant, K_c is the concentration-based equilibrium constant and ν_i is the stoichiometric coefficient. The reported values of activation and reaction volumes in *sc* reaction media are up to two orders of magnitude greater those encountered in liquid phase reactions, implying that pressure effects on rate and equilibrium constants can be significant in *sc* phase reactions. The rather large $\Delta \nu$ values in *sc* media are due to the fact that the partial molar volumes can assume large negative values near the critical point.

Critical Phase Behavior of Fluid Mixtures

Reliable knowledge of the phase border curves of reaction mixtures in pressure-temperature-composition (*P-T-x*) space is essential for identifying the appropriate operating pressure and temperature required for supercritical operation, to properly interpret conversion data, and to rationally develop post-reaction product separation schemes. These phase border curves separate regions of different states of matter and can be two-phase liquid-liquid (LL) or liquid-vapor (LV) boundaries, three-phase liquid-liquid-vapor (LLV) or solid-liquid-vapor (SLV), or sometimes four-phase solid-solid-liquid-vapor (LLSV) boundaries. Any given system can admit one or more of these regions. Using three-dimensional *P-T-x* diagrams, lucid descriptions of the critical phase behavior exhibited by binary systems are available in the literature. For simple binary systems, where the critical LV locus of various binary mixtures is a continuous curve between the critical points of pure components, the LV phase border curve can usually be reliably predicted with an appropriate equation of state. In contrast, for binary systems that exhibit a region of liquid-liquid immiscibility (the so-called Type II system) or for ternary systems, predictive methods may not be reliable. The *sc* reaction mixtures surrounding a solid catalyst typically involve several components requiring experimental determination of the critical phase behavior. Detailed treatment of the classification of the types of phase behavior exhibited by fluid mixtures along with experimental and theoretical methods available for determining phase border curves may be found elsewhere (*14*).

Heterogeneous Catalytic Reactions

The pressure-tunable density and transport properties of $sc\mathrm{CO_2}$ have been exploited in heterogeneous chemical reaction systems in various ways such as these: enhanced desorption and transport of heavy molecules (such as coke

Downloaded by UNIV OF GUELPH LIBRARY on September 16, 2012 | http://pubs.acs.org
Publication Date: January 24, 2002 | doi: 10.1021/bk-2002-0809.ch024

precursors) in mesoporous catalysts alleviating pore-diffusion limitations and improving catalyst effectiveness; *in situ* removal of primary products stabilizing primary product selectivity; eliminating O_2 or H_2 solubility limitations in the liquid phase (and thereby eliminating interphase mass transfer resistances) in multiphase reaction systems; enhanced heat capacity ameliorating the problem of parametric sensitivity in exothermic fixed-bed reactors. Recent reviews (*7, 8, 15*) provide a comprehensive survey of the types of heterogeneous catalytic reactions investigated at supercritical conditions including alkylation, amination, cracking, disproportionation, esterification, hydrogenation, isomerization and oxidation. Some of these examples are described here to show how to systematically exploit sc media in heterogeneous catalysis.

Downloaded by UNIV OF GUELPH LIBRARY on September 16, 2012 | http://pubs.acs.org
Publication Date: January 24, 2002 | doi: 10.1021/bk-2002-0809.ch024

Alleviation of internal pore-diffusion resistances

Pore-diffusion limitations in porous catalysts affect catalyst and/or product selectivity. Two instances are considered here. The first involves a parallel reaction network in which the desired product is produced in one reaction and "coke" precursors form via the second reaction. Accumulation of the coke precursors in the catalyst leads to catalyst "fouling" and causes a continuous decline in catalyst activity. The second example is a series reaction network of the type A → B → C. Clearly, pore-diffusion limitations would hinder the removal of B (the desired product) from the catalyst, favoring further reaction to the ultimate product, C. Examples are presented below to show how pressure tuning with *sc* media may be exploited to either desorb the coke precursors *in situ* (thereby stabilizing catalyst activity) or to desorb products, thereby enhancing intermediate product selectivity.

Several applications of the *in situ* decoking concept have appeared in the literature. One such application involves stabilizing the activity of solid acid catalysts such as in alkylation reactions. As reviewed elsewhere (*16*), numerous efforts aimed at developing solid acid alkylation catalysts and solid acid-based isobutane-olefin alkylation processes have been reported for more than three decades. However, to-date, none of the solid alkylation catalysts has gained acceptance in industry for one or more of the following reasons: rapid catalyst deactivation due to coke formation, unacceptable product quality (i.e., low alkylate fraction) and thermal degradation of catalyst during the regeneration step. "Supercritical" alkylation, performed with excess isobutane (P_c = 36.5 bar; T_c = 135°C) above the critical temperature (T_c) and critical pressure (P_c) of isobutane, has been reported to slow down deactivation of solid acid catalysts (*17, 18, 19*). Fan et al. (18) carried out an investigation over Y-zeolite catalysts under liquid, gas, and near-critical phases. The use of sc reaction media provided extended alkylate activity compared to the liquid and gas phases, but the activity declined in all cases. However, at reaction temperatures exceeding 135°C, undesirable side reactions such as oligomerization and cracking dominate, resulting in unacceptable product quality. Clark and Subramaniam (*20*) employed CO_2 (P_c = 71.8 bar; T_c = 31.1°C) as a diluent in the hydrocarbon feed to realize *sc* reaction mixtures with pressure-tunable properties in the 50-100°C range. The lower reaction temperatures favored alkylation reactions over oligomerization. The alkylate production attains a nearly steady value after a few hours on stream with *sc*CO_2-based reaction media, indicating that *sc*CO_2-based reaction medium is capable of maintaining the activity of the strong acid sites. However, both the butene conversion (20%) and the alkylate selectivity (around 5%) are small suggesting the pore sizes and/or acidity in these catalysts are such that it is not possible to effectively balance the coke formation rate with the coke removal rate from the pores. Recent studies in our laboratory (*21*) show that enhanced alkylate selectivity can be obtained on a SiO_2-supported Nafion catalyst (Engelhard SAC-13), which has an acidity comparable to sulfuric acid (used in conventional alkylate processing) and has relatively large pores when compared to zeolitic catalysts. Steady C_8 alkylates production activity during experimental runs lasting up to two days was demonstrated during the alkylation of isobutene with 1-butene over silica-supported Nafion® catalyst particles suspended in a CO_2-based supercritical reaction mixture in a slurry reactor. At a butene space velocity of 0.05 h^{-1}, 95°C (1.1 T_c) , molar feed I/O ratio of 5 with 70 mole% CO_2 in feed, pressure-tuning studies revealed that while the butene conversion was relatively insensitive to pressure at 80% between 80 (~1.0 P_c) and 167 bar (~2.2 P_c), the C_8 alkylates selectivity decreased fourfold from approximately from 30% at 80 bar to 7% at 167 bar (see Figure 1). The overall C_8 selectivity decreased from approximately 74% to 30% in the same pressure range with heavier (C_{12} and higher) products being formed in denser supercritical reaction mixtures. Clearly, milder supercritical pressures provide the optimum combination of liquid-like densities and gas-like transport properties to desorb the C_8 products and transport them out of the catalyst pores before they are transformed to heavier products.

Gläser and Weitkamp (*22*) employed *sc*CO_2 as a reaction medium to significantly reduce the deactivation rates of LaNaY-73 and H-mordenite zeolites during the isopropylation of naphthalene on these zeolites. These examples further demonstrate the ability of sc media for enhancing the stability of porous catalysts against deactivation by coke formation. The foregoing studies provide compelling evidence that CO_2-based supercritical reaction mixtures in conjunction with properly designed solid acid catalysts (optimum pore structure, acidity and accessibility) offer an excellent opportunity for developing environmentally benign alternatives to conventional processes that employ mineral acids.

Eliminating inter-phase mass transfer resistances

Conventional solid-catalyzed hydrogenation reactions are typically carried out in multiphase reactors involving the sparging of hydrogen through a slurry of the reactant and finely powdered catalyst particles. Typically, these reactions are fast and hence their rates are limited by the low solubility of hydrogen in the solvent. The other drawbacks of the conventional process include large reactor

Downloaded by UNIV OF GUELPH LIBRARY on September 16, 2012 | http://pubs.acs.org
Publication Date: January 24, 2002 | doi: 10.1021/bk-2002-0809.ch024

Downloaded by UNIV OF GUELPH LIBRARY on September 16, 2012 | http://pubs.acs.org
Publication Date: January 24, 2002 | doi: 10.1021/bk-2002-0809.ch024

volumes and costs associated with separating the product and the catalyst from the product mixture. Supercritical reaction media have been investigated for alleviating transport limitations in solid-catalyzed multiphase reactions such as in catalytic hydrogenations (*23, 24, 25, 26*). In addition to eliminating interphase mass transfer resistances, the enhanced extraction of heavy hydrocarbons and their facile transport from the catalyst pores by the near-critical reaction mixture alleviate internal pore diffusion limitations -- as discussed in the preceding section. Consequently, increased catalyst effectiveness factors and enhanced primary product selectivities (in the case of a series reaction network) are observed when pressure-tuning in the near critical region. The ensuing enhanced reaction rates reduce holdup of hazardous reactants making the process inherently safer. Additionally, due to its liquid-like heat capacity, *sc*C O_2-based hydrogenation offers the possibility of performing the reactions in a fixed-bed reactor with controlled temperature rise in the bed. Further, product separation from CO_2 is achieved by depressurization of the reactor effluent stream. By solubilizing the reactants (organic substrate and hydrogen) in a single, environmentally benign *sc* solvent such as CO_2, or propane, it has been shown that selective hydrogenation of vegetable oils and fats (to *cis*- fatty acid in preference to *trans*- fatty acid) can be performed on supported Ni catalysts at significantly high rates (about 400 times faster) relative to conventional slurry phase operation (*23*). Employing *sc*CO_2 as a reaction medium, a wide variety of organic functional groups (alkene, cyclic alkenes and alkanes, aldehydes, ketones, etc) can be hydrogenated with good throughput on polysiloxane-supported noble metal catalysts such as Pd and Pt (*27*). Supercritical propane was preferred in the case of nitrogen-containing compounds to avoid the formation of carbamic acid salts by the reactions of amine groups with CO_2. Employing dense CO_2 as the solvent medium, Bertucco *et al.* (*30*) systematically investigated the hydrogenation of unsaturated ketones by a supported Pd catalyst in a stirred reactor to minimize transport gradients. Kröcher *et al.* (*28*) demonstrated the synthesis of *N, N*- dimethyl formamide and methyl formate from a homogenous mixture of CO_2 and H_2, using heterogeneous silica-based hybrid-type Ru catalysts. Thus, CO_2 functions as both a reactant and a solvent. The turnover frequencies with the heterogenized catalyst were twofold higher than the homogeneous counterpart.

During hydrogenation of cylcohexene on supported Pd catalysts using *sc*CO_2 as solvent, significant axial temperature gradients exceeding 100°C were reported by Hitzler *et al.* (*27*). Another important issue during hydrogenation in *sc*CO_2 is that of catalyst deactivation. Minder et al. (*29*) investigated the batch hydrogenation of ethyl pyruvate to (R)-ethyl lactate over a modified Pt/Al_2O_3 catalyst in *sc* reaction media. When using *sc* CO_2 as the reaction medium, they report catalyst deactivation, presumably as a result of Pt poisoning by CO formed from the reverse water-gas shift reaction between CO_2 and H_2. In contrast, none of the *continuous* catalytic hydrogenation studies in *sc*CO_2 (*23, 24, 30*) report catalyst deactivation. Recently, we revisited the hydrogenation of cyclohexene in *sc*CO_2 on a supported Pd catalyst to investigate temperature control and catalyst deactivation issues (*31*). At near-critical experimental conditions (136 bar and 70°C), the maximum temperature rise observed was 12°C, which is less than the adiabatic temperature rise at total conversion. In the presence of approximately 180 ppm peroxides in the feed, there is a gradual but steady deactivation of the catalyst (roughly 2%/h) during the 18 h run. The spent catalyst at the end of the run showed significant surface area and pore volume losses. In contrast, when the peroxide content in the feed is mitigated to <6 ppm, nearly constant activity is obtained over a period of 24 h (Figure 2) with minimal surface area and pore volume losses. The selectivity towards cyclohexane is nearly 100% in all cases. Organic peroxides (ROOH) are commonly formed when alkenes are exposed to atmospheric oxygen and sunlight. These feed peroxides are known to have a detrimental effect on catalytic activity. During Pt/γ-Al_2O_3 catalyzed isomerization of 1-hexene, reduction of these peroxides to <10ppm is essential to attain steady isomerization activity at *sc* conditions (*32*). The formation of other potential deactivating agents such as carbon monoxide and formates was also considered. No CO was detected in the reactor effluent during the extended runs characterized by either steady cyclohexene conversion or the conversion decreasing continuously with time. Furthermore, no hydrogen attributable to decomposition of formate complexes was observed upon depressurizing the reactor. These results clearly demonstrate the potential for performing solid catalyzed hydrogenations in *sc*CO_2 with excellent temperature control and steady activity.

Other heterogeneous catalytic systems in which dense-phase CO_2 has been exploited to eliminate interphase mass transfer resistances include selective oxidations *(33, 34, 35, 36, 37, 38, 39*), hydroformylation (*40*) and esterification (*41*). Dooley and Knopf (*33*) reported aerobic heterogeneous catalytic oxidation of toluene in *sc*CO_2 using a range of alumina-supported oxide (CoO and MoO_3) and mixed-metal oxide (W, Ni) catalysts as well as on SiO_2/Al_2O_3. Toluene was effectively oxidized to benzaldehyde, benzyl alcohol and cresol isomers in both the redox as well the acid catalysts. The CoO catalyst, partly oxidized to Co^{3+}, was found to be the most selective catalyst due to the Co^{3+}/Co^{2+} redox property. Zhou and Akgerman (*35*) reported on the catalytic oxidation of ethanol and acetaldehyde over a 4.45% Pt/TiO_2 catalyst in *sc*CO_2 at 200°C and 90 bar. The oxidation, at 5:1 oxygen/ethanol molar ratio, produced acetaldehyde, carbon dioxide and trace amounts (less than 2%) of carbon monoxide. But at an oxygen/ethanol molar ratio of 4.7:1, acetaldehyde is completely oxidized to carbon dioxide and only trace amounts of carbon monoxide. The authors suggested a combination of parallel and consecutive reaction mechanisms for

Downloaded by UNIV OF GUELPH LIBRARY on September 16, 2012 | http://pubs.acs.org
Publication Date: January 24, 2002 | doi: 10.1021/bk-2002-0809.ch024

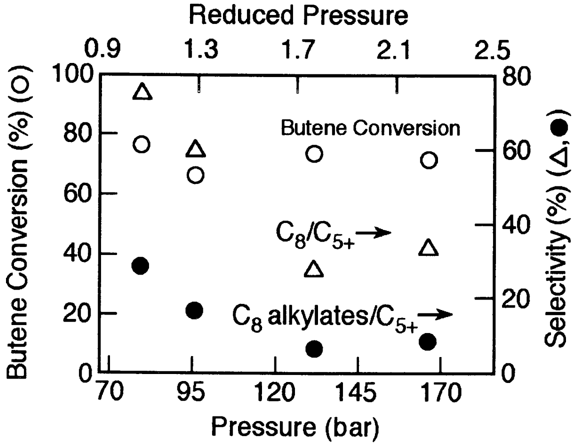

Figure 1. Pressure tuning effects on solid-acid catalyzed alkylation activity in sc media. (95°C, I/O=5, 0.05 h^{-1}).

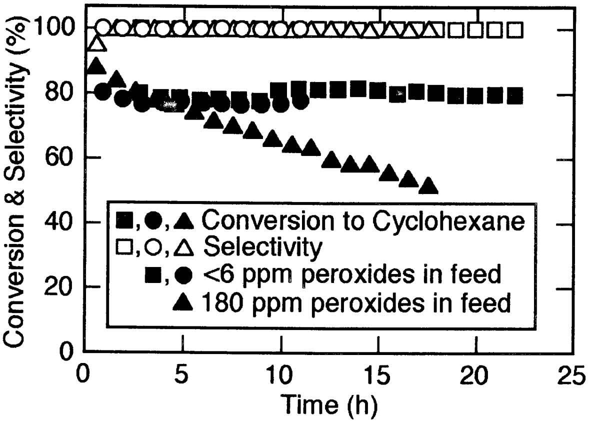

Figure 2. Conversion and selectivity histories during cyclohexene hydrogenation in sc CO_2. (70°C, 136 bar, OWHSV = 20 h^{-1}).

Downloaded by UNIV OF GUELPH LIBRARY on September 16, 2012 | http://pubs.acs.org
Publication Date: January 24, 2002 | doi: 10.1021/bk-2002-0809.ch024

Downloaded by UNIV OF GUELPH LIBRARY on September 16, 2012 | http://pubs.acs.org
Publication Date: January 24, 2002 | doi: 10.1021/bk-2002-0809.ch024

ethanol oxidation and a dissociative adsorption of acetaldehyde on the catalyst surface with surface reaction rate control for the acetaldehyde oxidation. Oakes *et al.* (*37*) reported on the diastereoselective oxidation of cysteine derivatives in *sc*CO_2 using *t*-BuOOH and Amberlyst 15 ion exchange resin catalyst. The method, even with excess oxidant, produced high yield and good selectivity for the sulfoxide formation, At constant temperature (40°C), the product selectivity was sensitively tuned with pressure. The major isomer selectivity for the oxidation of CysSMe-OMe was nearly 100% at 180 bar but falls off as the pressure is increased further. The fact that no diastereoselectivity is observed in conventional solvents reveals a clear advantage of *sc*CO_2 media in inducing setereoselectivity. Gaffney and Sofranko (*39*) examined the feasibility of heterogeneous propylene epoxidation to propylene glycol in a stream of propylene, water, and air in CO_2 at *sc* conditions (140°C and 140 bar). Of the several solid-supported catalysts evaluated, optimal results were reported with an α–Al_2O_3 supported $CuI/Cu_2O/MnO_2$ catalyst. However, the authors concluded that the production rate was about an order of magnitude too low for commercialization purposes. Recently, *sc*CO_2 has been demonstrated as a reaction medium for the continuous hydroformylation of oct-1-ene on silica-supported Rh catalysts at 80°C and 120 bar (*40*). The stated advantages include elimination of fluid phase mass transfer resistances and the extended (up to 30 h) production of nonanal. Vieville et al. (*41*) reported the esterification of oleic acid with methanol over a cation exchange catalyst (sulfonic acid resins) employing *sc*CO_2 as the reaction medium to solubilize the reactants and products. Ester yield of 50% was reported at 40°C and 160 bar. The hydrophobic nature of the resins is attributed with retarding the diffusion of the reactants in the macropores. Hence, the reaction is believed to occur mostly on the outer surface of the resin. The higher reaction rate in *sc*CO_2 (compared to *n*-hexane) is therefore attributed to enhanced desorption and transport of the methyl oleate from the catalyst surface.

Homogeneous Oxidations in *sc*CO_2

Homogenous catalytic oxidations in *sc*CO_2 and closely related media have been explored by a number of research groups in the past few years, and the majority of these studies can be grouped into alkene, alkane and alcohol oxidations. Whereas the first studies of homogeneous solutions of transition metal compounds in *sc*CO_2 may be attributed to Wai and coworkers (*42*), Leitner et al. (*43*) opened the subject of solubilizing catalysts for homogeneous catalysis in *sc*CO_2 showing that perfluoroalkyl side chains increase the solubility of their rhodium phosphine catalysts.

Early in their pioneering work on oxidation catalysis in *sc*CO_2, Tumas, Morgenstern et al. (*44*) reported the ruthenium catalyzed two-phase oxidation of cyclohexene to adipic acid. In this process, ruthenium *oxo*-complexes also act as phase transfer catalysts between the aqueous solution of the terminal oxidant, NaOCl, and the *sc*CO_2 phase that contains the organic substrate.

The Tumas group also studied the catalytic oxidation of alkenes in *sc*CO_2, using oxygen as the oxidant and halogenated porphyrins as catalysts. Cyclohexene was oxidized in the presence of Fe(PFTPP)Cl and Fe(Br_8PFTPP)Cl (Figure 3) under rather harsh conditions, 80°C and total pressure of 345 bar (*45*) yielding five products: cyclohexene oxide, 2-cyclohexene-1-ol, 2-cyclohexene-1-one, oxabicyclo[4.1.0]heptan-2-one and 4-hydroxy-2-cyclohexene-1-one. Organic solvents were totally replaced, but the turnover numbers were lower than those observed in common organic solvents; e.g., using Fe(PFTPP)Cl and the same reaction conditions: benzene 1520 h^{-1}, methylene chloride 2170 h^{-1} and *sc*CO_2 580 h^{-1}. Product distribution is influenced by changes of pressure and temperature, suggesting relatively easy tunability of reaction conditions.

Tumas and coworkers showed the efficacy of a very different kind of catalyst in the selective oxidation of activated alkenes, allylic and homoallyilic alcohols, in dense phase CO_2 using *t*-BuOOH as the terminal oxidant (*46*). The best yields and selectivity were found for $VO(OPr^i)_3$, but a variety of related complexes ($VO(acac)_2$, $Mo(CO)_6$ and $Ti(OPr^i)_4$) was also found to be catalytically active. Enantioselective epoxidation was observed in the presence of chiral tartrate ligands. At 0°C, 87% enantioselectivity and 99% conversion were achieved.

Haas and Kolis (*47*) oxidized a number of unactivated alkenes using the same catalyst. Product distribution depended on the alkene chosen as the substrate, and the epoxide product is accompanied by the corresponding 1,2-diol in the presence of water. For alkenes having phenyl substituents, C-C bond cleavage was observed, and the rates of diol and epoxide formation are considerably faster for *cis*-alkene than for *trans*-alkene oxidations. Hass and Kolis (*48*) also designed and synthesized a vanadium(IV) catalyst using a Schiff base ligand for epoxidation of allylic alcohols, using a 1:1 substrate to *t*-BuOOH mole ratio, 45-50°C and 213 bars. The authors reported that the yields and diastereoselectivities obtained in the *sc*CO_2 medium are comparable to those obtained in traditional organic solvents.

Jia *et al.*[49] find that, by using $PdCl_2$, $PdCl_2(CH_3CN)_2$, $CuCl_2$ and CuCl in the presence of methanol as co-solvent, acrylate esters can be oxidized aerobically to acetals (e.g., 3,3-dimethoxylpropanoate) with >96% selectivity.

Wu and coworkers (*50*) demonstrated the catalysis by Fe(PFTPP)Cl of the aerobic oxidation of cyclohexane in the presence of acetaldehyde to cyclohexanol and cyclohexanone. Typical reaction conditions were 1 h reaction time, 70°C, 1.0 mmol of cyclohexane, 0.25 mmol of acetaldehyde, 0.5 μmol of catalyst, 1.0 mmol of O_2 and 90 bar, giving a total yield of 5% of cyclohexanol and cyclohexanone.

We studied the homogeneous oxidation catalysis of CH_3ReO_3 (MTO*)* and olefin epoxidation in *sc*CO_2 (*10*). We chose *t*-butyl hydroperoxide and completely homogeneous reactions were run for 48 h in a 60 mL Jurgeson cell at

Downloaded by UNIV OF GUELPH LIBRARY on September 16, 2012 | http://pubs.acs.org
Publication Date: January 24, 2002 | doi: 10.1021/bk-2002-0809.ch024

Downloaded by UNIV OF GUELPH LIBRARY on September 16, 2012 | http://pubs.acs.org
Publication Date: January 24, 2002 | doi: 10.1021/bk-2002-0809.ch024

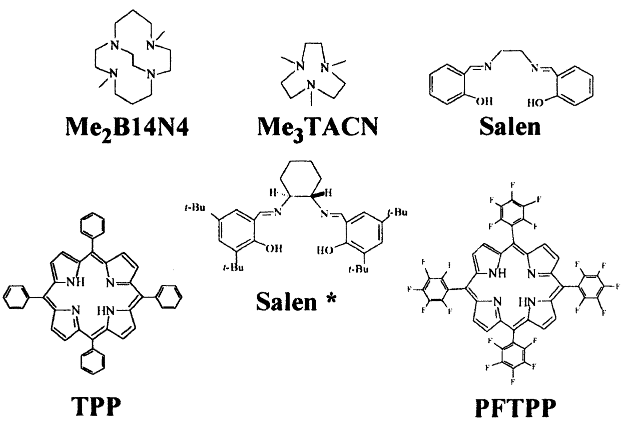
N
N
N
N
Me$_2$B14N4
N
N
N
Me$_3$TACN
N
N
OH
HO
Salen
H
H
t-Bu
N
N
t-Bu
OH
HO
t-Bu
t-Bu
Salen *
NH
N
N
HN
TPP
F
NH
N
N
HN
PFTPP

Figure 3. Catalyst/Ligand structures.

approximately 83 bar and 50°C. The terminal oxidant was delivered as a *t*-BuOOH/*t*-BuOH mixture that served as a co-solvent, substantially increasing the solubility of the catalyst. We identified the products and determined the yields from catalytic oxidation of cyclohexene, styrene, and *cis*- and *trans*-stilbene. Whereas the oxidation of cylohexene yielded the oxide and its hydrolysis product, the corresponding diol, the rest of the substrates also underwent C-C bond cleavage and yielded benzaldehyde, in addition to their epoxides. Conversion for cyclohexene was 64% and those for styrene and the stilbene isomers were similar. These preliminary results indicate that *sc*CO_2 is a viable solvent for this catalyst system.

Similar results were obtained with Jacobson's catalyst, Mn(salen*) (see Figure 3), which is sufficiently soluble in *sc*CO_2 to catalyze the epoxidation of a range of olefins using *t*-BuOOH in *t*-BuOH co-solvent as terminal oxidant. All reactions were run with 50 μM of catalyst and 83 bar total pressure at 50 °C and 70 % w/w in *t*-BuOOH/*t*-BuOH. As observed by Kolis (*47*) and in our work with CH_3ReO_3, epoxidation is accompanied by C=C cleavage in the case of olefins having phenyl groups as substituents. Our results are summarized as follows (substrate is followed by % yield of epoxide and then by % C=C cleavage: cyclohexene, 27% (epoxide 15% plus diol 12%, no cleavage); styrene, 17%, 23%; *cis*-stilbene, 12%, 19%; *trans*-stilbene, 16%, 20%. Kochi and coworkers have found similar results using the manganese complex of a different substituted salen, Mn{(*5,5'*-NO_2)$_2$salen}, and iodosobenzene as the terminal oxidant in CH_3CN as the solvent (*51*). Kochi's results are: cyclohexene, 56%, no cleavage; styrene, 37%, 10%; *cis*-stilbene, 35%, 7%; *trans*-stilbene, 40%, 6%.; showing considerable more selectivity toward epoxidation over C=C bond cleavage. While showing no conversion or selectivity advantage, the experiments with Mn(salen*) in *sc*CO_2 indicate the viability of dense CO_2 media for reactions involving this important catalyst, thereby retaining the possibility of an environmental sustainability advantage.

Oxygen is completely miscible with *sc*CO_2 media, but its solubility in most solvents is only a few millimoles per liter. This strongly suggests that *sc*CO_2 and other CO_2 derived media should enjoy advantages in reactions using O_2 as terminal oxidant. Proceeding on this basis, we have investigated well known oxidation reactions catalyzed by cobalt(II) dioxygen carriers, the oxidation of phenols to quinones. Further, the catalysts chosen were the inexpensive parent of the family, Co(salen) itself, and a second member of the family selected because its ligand (from Jacobson's catalyst) imparts high solubility to metal complexes in nonpolar solvents and because it too is readily available.

The catalytic oxidations of 2,6-di-*tert*-butylphenol, DTBP, and 3,5-di-*tert*-butylphenol, 35-DTBP, in *sc*CO_2 were studied in the presence of a large excess of O_2, 207 bar total pressure and a reaction temperature of 70°C (*52*). Under the experimental conditions, DTBP is converted to a mixture of just two products, 2,6-di-*tert*-butyl-1,4-benzoquinone, DTBQ, and the related product of radical

Downloaded by UNIV OF GUELPH LIBRARY on September 16, 2012 | http://pubs.acs.org
Publication Date: January 24, 2002 | doi: 10.1021/bk-2002-0809.ch024

coupling, 3,5,3',5'-tetra-*tert*-butyl-4,4'-diphenoquinone, TTDBQ. It should also be recognized that DTBQ and related materials are of interest in medicinal chemistry (*53*). Conversion and selectivity were studied as functions of temperature, pressure, and concentrations of catalyst, substrate, and terminal oxidant, O_2, and the results provide substantial mechanistic elucidation.

The contrasting temperature dependence of the conversion to products, versus that of selectivity between them, is most revealing. Conversion increased steadily with temperature as expected for an initial oxidation step involving a substantial activation energy; i.e., the formation of the phenoxy radical. In contrast, selectivity between the pathways producing the competing products is meaningfully temperature independent. This is consistent with the conclusion that the final product mixture is determined by competition between two parallel reactions, both of which are essentially radical-radical coupling reactions with vanishingly small activation energies. Thus, the very essence of the proposed mechanism for these long known reactions is strongly supported. The dependences of conversion and selectivity on oxygen concentration are equally revealing. Both parameters obey saturation models, a result that links both rate determining and product determining processes to the dioxygen complex of Co(salen). Since both conversion and selectivity become independent of oxygen concentration at high O_2 concentrations, it is clear that free O_2 is not involved in the initiation step that determines conversion or either of the parallel reactions that determine the relative yields of the products. Whereas there was no doubt that the initiation step involved the oxygen complex of Co(salen), this provided the first proof that the oxygen complex is responsible for capture of the phenoxy radical along the pathway that leads to DTBQ. It is also implicit in this result that no direct reaction occurs between the electrophilic phenoxy radical and O_2. The observed behavior provides strong support for the previously proposed mechanism for these reactions (*54*, 55).

Downloaded by UNIV OF GUELPH LIBRARY on September 16, 2012 | http://pubs.acs.org
Publication Date: January 24, 2002 | doi: 10.1021/bk-2002-0809.ch024

Oxidations in CO_2-Expanded Solvent Media

Significant limitations accompany the well-known advantages of *sc*-CO_2 for catalytic oxidations, including low reaction rates, high process pressures (on the order of hundreds of bars), and the limited number of transition metal catalysts that are sufficiently soluble in CO_2 without substantial structural modification. In processes demonstrated recently by us, conventional solvents are substantially, but not totally replaced by dense CO_2. The retained organic solvent preserves some of its desirable properties in the mixture, e.g., dielectric constant, solvation and coordination properties. The solution volume is multiplied by the CO_2 expansion without separation from the reaction mixture of the substrate, catalyst, or terminal oxidant from the reaction mixture, creating a completely homogeneous CO_2-expanded reaction mixture. The total pressure is ~ 50-90 bars (much lower than typical pressures for *sc*-CO_2) and the CO_2 mole fraction in the solvent is typically between 65 and 80%, a substantial reduction in organic solvent usage. Further, our measurements (*56*) have shown that the preferred terminal oxidant dioxygen is at least one or two orders of magnitude more soluble in these media than in the neat organic solvents. The examples that follow show striking advantages, including enhanced oxidation, improved selectivities, and increased operational safety.

Adding CO_2 to solvents having significant solubilities in CO_2 "expands" the solvent while decreasing the solubilities of the dissolved solutes in the mixture (*57, 58, 59*). This concept has also been used in separation schemes (*13*). We investigated the effect of isothermal CO_2 addition to a solution of CH_3CN containing dissolved catalyst [*N,N'*-Bis(3,5-di-*tert*-butylsalicylidene)1,2-cyclohexanediaminato(2-)] cobalt(II) {i.e., Co(Salen*)}. The volume of the homogeneous liquid phase expands rapidly as CO_2 is added. The catalyst solubility in the expanded solvent decreases continuously with the expansion and the catalyst precipitates out at a certain level of expansion, termed as the "maximum homogeneous expansion limit" $(V/V_0)_{max}$. The expansion factor is defined as the ratio of CO_2-expanded solvent volume (V) to the initial solvent volume (V_0 = 5 mL). For a given catalyst/solvent combination, the maximum homogeneous expansion limit decreases with increasing catalyst concentration and increases at higher temperatures. For the catalyst concentration employed in our reaction studies (0.4 mg/mL CH_3CN), the maximum homogeneous expansion limit is roughly 5 at 50°C. This implies the possibility of replacing up to 80 vol.% of the organic solvent by CO_2 while maintaining the catalyst in solution. It is noteworthy that the total pressures at the maximum homogenous expansion limit are tens of bars, as compared to hundreds of bars for *sc*CO_2.

Another advantage of CO_2-expanded reaction media is the enhanced solubility of O_2. The measured O_2 mole fraction in CO_2-expanded CH_3CN (V/V_0 = 2) is about two orders of magnitude higher than the O_2 solubility in neat CH_3CN (($5x10^{-4}$ mole fraction at 25°C and 1 bar [60]*)*, and is of the same order of magnitude as that observed in liquid CO_2 (*61*).

For comparison purposes, the homogeneous catalytic O_2-oxidation of 2,6-di-*tert*-butylphenol, DTBP, by Co(Salen*) was studied in *sc*-CO_2 (scheme given in Figure 4), in CO_2-expanded organic solvents (V/V_0 = 2), and in neat organic solvents. The common conditions are as follows: Catalyst amount = 0.41 mmol; catalyst:substrate:O_2 mole ratio = 1:40:80; volume of methyl imidizole = 2 μL. As seen from Figure 5, the turnover frequency (TOF), defined as the moles of DTBP converted per mole of catalyst per hour, in the CO_2-expanded CH_3CN (P = 60-90 bars) is between one and two orders of magnitude greater than in *sc*CO_2 (P = 207 bar). The observed selectivity toward DTBQ (80-88%) is comparable in *sc*CO_2 and CO_2-expanded CH_3CN and no CH_3CN oxidation was detected in either case. The TOF and DTBQ selectivity are lower in neat CH_3CN (O_2 bubbling, 28°C, 1 bar). Neat solvents can form explosive gaseous mixtures at higher temperatures and hence were avoided. The high TOFs observed in CO_2-

Downloaded by UNIV OF GUELPH LIBRARY on September 16, 2012 | http://pubs.acs.org
Publication Date: January 24, 2002 | doi: 10.1021/bk-2002-0809.ch024

Downloaded by UNIV OF GUELPH LIBRARY on September 16, 2012 | http://pubs.acs.org
Publication Date: January 24, 2002 | doi: 10.1021/bk-2002-0809.ch024

expanded CH_3CN are attributed to the ability of the polar solvent to stabilize the polar transition state, thereby lowering the activation energy and increasing the reaction rate. The rather sensitive temperature dependence of TOFs in the CO_2-expanded phase (more than 10-fold increase for the range 25-80°C) compared to *sc*CO_2 (2-fold increase over the 50-80°C range) supports this mechanistic hypothesis. The inexpensive and readily available Co(salen) catalyst is insoluble in *sc*CO_2. In sharp contrast, Co(salen) shows remarkable activity in CO_2-expanded CH_3CN. These results show that CO_2-expanded solvents complement scCO_2 as reaction media by broadening the range of conventional catalyst+solvent combinations with which homogeneous oxidations by O_2 can be performed.

Taking advantage of the solubility advantages, the oxidation of cyclohexene was investigated with a non-fluorinated iron porphyrin catalyst, (5,10,15,20-tetraphenyl-21*H*,23*H*-porphyrinato)iron(III) chloride, Fe(TPP)Cl, in addition to a fluorinated catalyst (5,10,15,20-tetrakis(pentafluorophenyl)-21*H*,23*H*-porphyrinato)iron(III) chloride, Fe(PFTPP)Cl (*56*). In both cases, molecular oxygen was used as the terminal oxidant. While Fe(TPP)Cl is insoluble and displays little activity in *sc*CO_2, it displays remarkably high activity in CO_2-expanded CH_3CN. GC/MS analysis revealed five products: cyclohexene oxide, 1,2-cyclohexane-diol, 2-cyclohexene-1-ol, 2-cyclohexene-1-one, and 4-hydroxy-2-cyclohexene-1-one. While the first two products are those of oxygen atom transfer, the rest are formed by a mechanism that involves allylic H-abstraction. The 1,2-cyclohexanediol is formed by hydration of cyclohexene oxide and, therefore, the epoxidation selectivity is based on the yields of both cyclohexene oxide and cyclohexanediol. Conversion histories of cyclohexene oxidation with Fe(TPP)Cl at 50°C in CO_2-expanded CH_3CN ($V/V_o = 2$) and in neat CH_3CN reveal an "induction" period, which presumably involves the buildup of radicals to a critical concentration. Remarkably, the induction period in CO_2-expanded CH_3CN is only 4 hours compared to nearly 16 hours in neat CH_3CN. We attribute this reduced induction period to the enhanced O_2 solubility in CO_2-expanded CH_3CN, assuming that the free radical initiation step involves molecular oxygen.

As shown in Table 1, the cyclohexene conversion obtained with the fluorinated catalyst Fe(PFTPP)Cl in the CO_2-expanded solvent at 90 bar and 80°C is 41% which is nearly 7-fold greater than that reported by Birnbaum *et al.* (*45*) in *sc*CO_2 with the identical catalyst at the same temperature, but 345 bar. Also, an approximately 1.5 fold higher epoxidation selectivity over *sc*CO_2 is obtained in CO_2-expanded CH_3CN. It is interesting to note that the non-fluorinated catalyst, Fe(TPP)Cl, which is insoluble in *sc*CO_2, displayed a higher TOF for cyclohexene oxidation, fully 10-fold greater than the result in *sc*CO_2, with comparable epoxidation selectivity.

Cyclohexene conversion and product distribution are sensitive to the CO_2-fraction in the reaction medium. Conversion increases from 24% in neat CH_3CN to a maximum of 31%, at 2-fold expansion, decreasing upon further CO_2-expansion. Epoxidation selectivity showed a similar trend. We attribute this behavior to the lower O_2 solubility in neat organic solvent and the progressively

Downloaded by UNIV OF GUELPH LIBRARY on September 16, 2012 | http://pubs.acs.org
Publication Date: January 24, 2002 | doi: 10.1021/bk-2002-0809.ch024

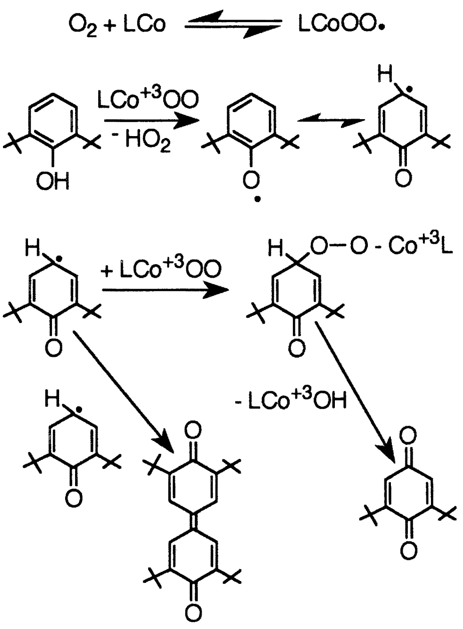

Figure 4. Scheme for the oxidation of 2,6-di-tert-butyl phenol by Schiff base cobalt catalysts.

Table 1. Cyclohexene oxidation by iron porphyrin complexes in different reaction media

p, bar	Reaction medium	X, %	S, %	Catalyst	Ref
90	CO_2-expanded CH_3CN	55	19.2	Fe(TPP)Cl	(*56*)
90	CO_2-expanded CH_3CN	40.9	28.3	Fe(PFTPP)Cl	(*56*)
345	*sc*CO_2	5.5	19	Fe(PFTPP)Cl	(*45*)

p: pressure; X: conversion; S: epoxidation selectivity. Conditions: 80°C; 4 h; 10 mL reactor; 2.8 μmol of catalyst; catalyst:O_2:cyclohexene mole ratio = 1:1500:2000; $(V/V_0) = 2$ (for CO_2-expanded CH_3CN).

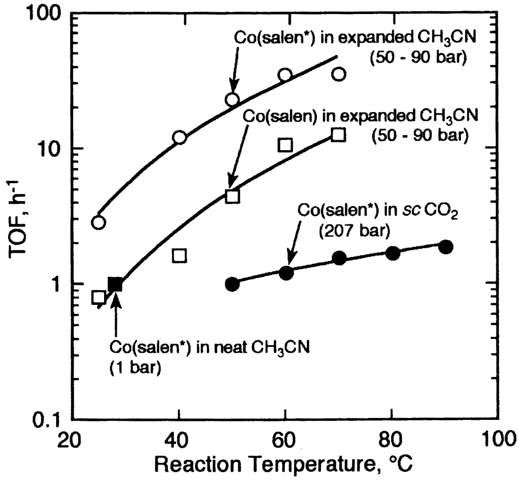

Figure 5. Turnover frequencies (TOFs) for 2,6-di-tert-butyl phenol oxidation with Co(Salen) and Co(salen).*

diminishing solvent polarity with increasing fraction of CO_2. This indicates that a continuum of reaction media with different properties may be realized by varying the CO_2/solvent ratio, and that the ratio may be optimized for a given process through a combination of solubility effects and solvent properties.

Concluding Remarks

The pressure-tunability of the density and transport properties of near-critical fluids can be exploited for achieving unique combinations of fluid properties (i.e., liquid-like densities yet significantly better transport properties compared to liquids). These properties are better suited than either gas phase or liquid phase reaction media to alleviate transport limitations in heterogeneous fluid-solid catalytic reactions. To attain pressure-tunable reaction mixtures, the reaction temperature must be in the vicinity of the critical temperature of the reaction mixture (1.05 – 1.2 T_c in general). To satisfy this criterion, the T_c of the reaction mixture may have to be suitably modified by adding an inert cosolvent such as carbon dioxide. For this purpose, reliable knowledge of the critical phase behavior of the reaction mixture including various cosolvent candidates is essential. The operating pressure that provides the optimum fluid properties for maximizing a given performance criterion (catalyst activity, effectiveness or selectivity) is determined by pressure-tuning studies. Higher-than-optimum pressure could introduce transport limitations that diminish catalyst effectiveness factor while lower-than-optimum pressure could limit the desorption of the heavy hydrocarbons, adversely affecting catalyst activity and product selectivity. The

Downloaded by UNIV OF GUELPH LIBRARY on September 16, 2012 | http://pubs.acs.org
Publication Date: January 24, 2002 | doi: 10.1021/bk-2002-0809.ch024

several examples provided in this chapter demonstrate how the pressure-tunable density and transport properties of supercritical reaction media have been exploited in heterogeneous catalysis such as: (a) enhanced desorption and transport of heavy molecules (such as coke precursors) in mesoporous catalysts alleviating pore-diffusion limitations and improving catalyst effectiveness; (b) *in situ* removal of primary products stabilizing primary product selectivity; and (c) eliminating O_2 or H_2 solubility limitations in the liquid phase (and thereby eliminating interphase mass transfer resistances) in multiphase reaction systems; and (d) enhanced heat capacity ameliorating the problem of parametric sensitivity in exothermic fixed-bed reactors. One or more of these advantages have been demonstrated for several classes of heterogeneous (i.e., solid-catalyzed) reactions such as alkylations, aminations, hydroformylations and hydrogenations, spanning a wide spectrum of chemical process industries including petrochemicals, fine chemicals, food, agricultural chemicals and pharmaceuticals. The use of *sc* media in these examples is more than merely as a replacement for organic solvents. In virtually every case, the *sc* reaction medium represents an enabling tool used to manipulate or control such factors such as catalyst stability, product selectivity and temperature rise in the reactor. Conventional reaction engineering theory provides us the approaches and tools for the modeling and rational analysis of *sc* phase reactors.

It follows from the many investigations reviewed herein that while the use of *sc*CO_2 in homogeneous catalytic oxidation has certain advantages over conventional solvents (such as total solvent replacement with an environmentally-benign solvent, complete O_2 miscibility in the reaction mixture, resistance to oxidation), a major drawback is the high pressures (on the order of hundreds of bars) required to ensure adequate solubility of many transition metal catalysts in CO_2. Fluorocarbon additives are known to enhance the solubility of transition metal complexes in *sc*CO_2 at moderate pressures; however, the fluorocarbon compounds are expensive. Recently, poly (ether-carbonate) copolymers that readily dissolve in CO_2 at lower pressures have been developed (*62*). Such research efforts aimed at developing low-cost, fluorine-free alternatives are expected to continue. Another limitation of *sc*CO_2 is the lack of tunability of the dielectric constant and other properties of the reaction medium. By adding a suitable solvent that is miscible with dense CO_2 (CO_2-expanded solvent), such properties as the dielectric constant may be readily varied with mixture composition while maintaining solubility of the substrate, oxidant and catalyst in the expanded phase. There are a number of traditional solvents, such as CH_2Cl_2, CH_3CN, DMF, acetone, methanol, ethanol, *tert*-butanol and isopropanol, that can be expanded with dense CO_2. The CO_2-expanded solvent mixtures represent a continuum of reaction media with different physicochemical properties that may be exploited for optimizing conversion and selectivity in well-known catalytic oxidation systems as discussed herein. Further, the low process pressures and the ability to separate and recycle the solvent make homogenous catalytic oxidation in CO_2-expanded solvents environmentally benign and more economical compared to *sc*CO_2-based oxidation.

Downloaded by UNIV OF GUELPH LIBRARY on September 16, 2012 | http://pubs.acs.org
Publication Date: January 24, 2002 | doi: 10.1021/bk-2002-0809.ch024

Downloaded by UNIV OF GUELPH LIBRARY on September 16, 2012 | http://pubs.acs.org
Publication Date: January 24, 2002 | doi: 10.1021/bk-2002-0809.ch024

Another kind of environmentally-benign solvent that is receiving increased attention is room temperature ionic liquids such as chloroaluminate(III) ionic liquids, specifically 1-butylpyridinium chloride-aluminum(III) chloride and 1-ethyl-3-methylimidazolium chloride-aluminum(III) chloride. Ionic liquids are extremely good solvents for a wide range of inorganic, organic and polymeric materials. Recently, it was shown that by sufficiently expanding ionic liquids with *sc*CO_2, hydrocarbon components can be selectively extracted from the reaction mixture (*63*). This suggests that controlled expansion of room temperature ionic liquids with CO_2 should be possible such that the hydrocarbon substrate and catalyst miscibilities in the reaction mixture are maintained while enhancing the solubilities of the such oxidants as dioxygen therein. Post reaction, the hydrocarbon components and the catalyst may be fractionated from the reaction mixture by stepwise addition of dense CO_2. Catalytic oxidations in CO_2-expanded ionic liquids thus offer the exciting possibility of developing novel integrated environmentally-benign reaction and separation schemes.

It should be clear that the advantages of CO_2-expanded phases can also be realized with heterogeneous catalytic systems in which the solid catalyst particles are exposed to the CO_2-expanded reaction mixture. Another area that shows much promise for exploitation in environmentally-benign oxidations is the use of biphasic CO_2/water emulsions (*64*). Water soluble catalysts are sequestered in highly dispersed water phase while the substrate and oxidant (such as dioxygen) are dissolved in the continuous *sc*CO_2 phase.

The outlook for industrial applications of supercritical reaction media in heterogeneous fluid-solid catalysis is promising. Economic factors that dictate the viability of supercritical processes include the capital costs associated with the high-pressure equipment and operating costs associated with the compression of the supercritical media for recycling purposes. Many examples discussed in this chapter show that the optimum pressure lies close to the critical pressure of the reaction mixture. Clearly, the critical pressure of the solvent medium and the extent of dilution of the reactants with the solvent medium are important parameters that would dictate the process economics. The announcements (*65*) of a development plant for producing fluoropolymers in supercritical carbon dioxide and of a supercritical phase hydrogenation plant are strong indicators that industries are seriously considering *sc* processes for chemical processes. The challenge will be in demonstrating processes that simultaneously display the following attributes: selective, environmentally-benign, stable and economical.

Acknowledgments

This work was supported in part by the National Science Foundation (CHE-9815321; CTS-9816969) and the Environmental Protection Agency (R827034-01-0).

References

1. Collins, T. J., *Green chemistry* in *Macmillan Encyclopaedia of Chemistry*, Macmillan, Inc., New York (1997).
2. Anastas, P. T. & Williamson, T. C., Green chemistry: an overview, in *Green Chemistry: Designing Chemistry for the Environment,* American Chemical Society Symposium Series No. 626 (ed. Anastas, P.T. & Williamson, T.C.), American Chemical Society, Washington, D.C., 1996, pp 1-17.
3. Anastas, P.T. & Warner, J.C., *Green chemistry: Theory and Practice,* Oxford University Press, Oxford (1998).
4. Clark, J. H., *Green Chemistry,* **1999**, *1*, 1-8.
5. Several articles in Anastas, P. T., Heine, L. G. and Williamson, T. C. (Eds.), in *Green Engineering*, American Chemical Society Symposium Series 766, 2000.
6. Savage, P.E. , Gopalan, G., Mizan, T. I., Martino, C.J. and Brock, E.E., *AIChE J.*, **1995**, *41*, 1723-1778.
7. Savage, P. E. in *Handbook of Heterogeneous Catalysis*, eds. Ertl, G., Knözinger, H. and Weitkamp, J. Vol. 3, Wiley-VCH, Weinheim, 1997, pp 1339-1344.
8. Baiker, A., *Chem. Rev.*, **1999**, *99*, 453-473.
9. Hutchenson, K. W., in *Supercritical Fluid Technology in Materials Science and Engineering, ed.* Y-P. Sun, (in press) Marcel Dekker, NY.
10. Musie, G., Wei, M., Subramaniam, B. and Busch, D. H. *Coord. Chem. Reviews*., in press.
11. Chemical Synthesis Using Supercritical Fluids, eds. Jessop, P. G., Leitner, W., Wiley-VCH, Weinheim, 1999.
12. Several chapters in *Chem. Rev*., **1999**, *99*.
13. Eckert, C. A., Bush, D., Brown, J. S. and Liotta, C. L. *Ind. Eng. Chem. Res.*, **2000**, *39*, 4615-4621.
14. McHugh, M. A. and Krukonis, V. J. *Supercritical Fluid Extraction*, 2nd Ed., Butterworth-Heinemann, Boston, 1994.
15. Subramaniam, B., Appl. Catal A Gen., **2001**, *212*, 199-213.
16. Weitkamp, J. and Traa, Y. *Catal. Today*, **1999**, *49*, 193-199.
17. Hussain, A., U.S. Pat. #5,304,698 (1994) to Mobil Oil Corporation.
18. Fan, L., Nakamura, I., Ishida, S. and Fujimoto, K.L. *Ind. Eng. Chem. Res.*, **1997**, *36*, 1458-1463.
19. Funamoto, G., Tamura, S., Segawa, K., Wan, K. and Davis, M.E., *Res. Chem. Intermed.*, **1998**, *24*, 449-459.
20. Clark, M. C. and Subramaniam, B. *Ind. Eng. Chem. Res.*, **1998**, *37*, 1243-1250.
21. Lyon, C. J., Subramaniam, B. and Pereira, C. J., **2001**, *Stud. Surf. Sci.* (in press).
22. Gläser, R. and Weitkamp, J., in *Proc. 12th Int. Zeolite Conf.*, Vol. 2, ed. M. Treacy, M. J., Mat. Res. Soc., Warendale, PA, 1999, pp 1447-1454.

Downloaded by UNIV OF GUELPH LIBRARY on September 16, 2012 | http://pubs.acs.org
Publication Date: January 24, 2002 | doi: 10.1021/bk-2002-0809.ch024

23. Härröd, M. and Møller, P. in *High Pressure Chem. Engng., Proc. Tech. Proc. 12*, eds., Ph. Rudolf von Rohr, Ch. Trepp, Elsevier, Amsterdam, 1996, pp 43-51.
24. Hitzler, M. G. and Poliakoff, M. *Chem. Commun.*, **1997**, 1667-1668.
25. Bertucco, A., Canu, P., Devetta, L. and Zwahlen, A., *Ind. Eng. Chem. Res.*, **1997**, *36*, 2626-2633.
26. Tacke, T., Wieland, S. and Panster, P. in *High Pressure Chem. Engng., Proc. Tech. Proc. 12*, eds., Ph. Rudolf von Rohr, Ch. Trepp, Elsevier, Amsterdam, 1996, pp 17.
27. Hitzler, M. G., Smail, F. R., Ross, S. K. and Poliakoff, M. *Org. Process Res. Dev.*, **1998**, *2*, 137-146.
28. Kröcher, O., Köppel, R. A., Fröba, M. and Baiker, A., *J. Catal.*, **1998**, *178*, 284-298.
29. Minder, B., Mallat, T., Pickel, K. H., Steiner, K. and Baiker, A. *Catal. Lett.*, **1995**, *34*, 1-9.
30. Devetta, L., Giovanzana, A., Canu, P., Bertucco, A. and Minder, B. J. *Catal. Today*, **1999**, *48*, 337-345.
31. Arunajatesan, V., Subramaniam, B., Hutchenson, K. W. and Herkes, F. E. *Chem. Eng. Sci.*, **2001**, *56/4*, 1363-1369.
32. Clark; M. C. and Subramaniam, B. *Chem. Eng. Sci.*, **1996**, *51*, 2369-2377.
33. Dooley, K.M. and Knopf, F.C., *Ind. Eng. Chem. Res.*, **1987**, *26*, 1910-1916.
34. Suppes, G.J., Occhiogrosso, R.N. and McHugh, M.A., *Ind. Eng. Chem. Res.*, **1989**, *28*, 1152-1156.
35. Zhou, L. and Akgerman, A., *Ind. Eng. Chem. Res.*, **1995**, *34*, 1588-1595.
36. Wang, C.-T. and Willey, R.J. *J. Non-Cryst. Solids*, **1998**, *225*, 173-177.
37. Oakes, R.S., Clifford, A.A., Bartle, K.D., Pett, M.T. and Rayner, C.M., *Chem. Commun.*, **1999**, 247-248.
38. Fan, L., Watanabe, T. and Fujimoto, K. *Appl. Catal. A: General*, **1997**, *158*, L41-L46.
39. Gaffney, M. and Sofranko, J. A. Preprints, American Chemical Society Division of Petroleum Chemistry, **1992**, *37*, 1273-1279.
40. Meehan, N. J., Sandee, A. J., Reek, J. N. H., Kamer, P. C. J., van Leeuwen, P. W. N. M. and Poliakoff, M. *Chem. Commun.*, **2000**, 1497-1498.
41. Vieville, C., Mouloungui, Z. and Gaset, A., *Ind. Eng. Chem. Res.*, **1993**, *32*, 1497-1498.
42. Lin, Y-H., Brauer, R. D., Laintz, K. E., and Wai, C. M. *Anal. Chem.*, **1992**, *65*, 2549-2551.
43. Kainz, S., Koch, D., Baumann and Leitner, W., *Angew. Chem. Int. Ed. Engl.*, **1997**, *36*, 1628-1630.
44. Morgenstern, D. A., LeLacheur, R. M., Morita, D. K., Borkowsky, S. L., Feng, S., Brown, G. H., Luan, L., Gross, M. F., Burk, M. J., and Tumas, W., in Anastas, P. T. and Williamson, T. C., Eds., *Green Chemistry: Designing Chemistry for the Environment*, ACS Symposium Series 626, Washington, D.C., 1996, pp. 132-151.
45. Birnbaum, E. R., Le Lacheur, R. M., Horton, A. C. & Tumas, W., *J. Mol. Catal.*, **1999**, *A 139*, 11-24.

Downloaded by UNIV OF GUELPH LIBRARY on September 16, 2012 | http://pubs.acs.org
Publication Date: January 24, 2002 | doi: 10.1021/bk-2002-0809.ch024

46. Pesiri, D. R., Morita, D. K., Glaze, W. and Tumas, W., , *Chem Commum,*, **1998**, 1015-1016.
47. Hass, G.R. and Kolis, J.W., *Tetrahedron Lett.* **1998**, *39*, 5923-5926.
48. Haas, G. R. and Kolis, J. W, Organometallics, **1998**, *17*, 4454-4460.
49. Jia, L., Jiang, H. and Li, J., *Chem. Commun.*, **1999,** 985-986.
50. Wu, X.-W., Oshima, Y. and Koda, S., *Chem. Lett.*, **1997,** 1045-.
51. Srinivasan, K., Michand, P. and Kochi, J. K., *J. Am. Chem. Soc.*, **1986,** *108* 2309-2320.
52. Musie, G. T., Wei, M., Subramaniam, B. and Busch, D. H., *Inorg. Chem.*, **2001**, *40(14)*, 3336-3341. .
53. Kolesnik, I. G., Zhizhina, E. G and Matveev, K. I., *J. Mol. Catal.* **2000**, *153*, 147-154.
54. Zombek, A., Drago, R. S., Corden, B. B. and Gaul, J. H., *J. Am. Chem. Soc.*, **1981**, *103*, 7580-758 .
55. Deng, Y. and Busch, D. H., *Inorg. Chem.*, **1995**, *34*, 6380-6386.
56. Wei, M., Musie, G. T., Busch, D. H. and B. Subramaniam (submitted for publication).
57. Gallagher, P. M., Coffey, M. P., Krukonis, V. J. and Klasutis, N, in *Amer. Chem. Sym. Ser.,* No. 406, American Chemical Society, Washington, D.C., (1989).
58. De la Fuente Badilla, J.C., Peters, C. J. and Arons, de Swaan, J., *J. Supercritical Fluids,* **2000**, *17*, 1-13.
59. Tai, C. Y and Cheng, C-S., *AIChE J,* **1998,** *44*, 989-992.
60. Hildebrand, J. H., Prausnitz, J. M. and Scott, R. L., *Regular and Related Solutions: the Solubility of Gases, Liquids, and Solids,* New York, Cincinnati, Toronto, London, Melbourne(1970).
61. Battino R. et al. (eds), *Solubility Data Series: Volume 7, Oxygen and Ozone*, Pergamon Press, Oxford, New York, Toronto, Sydney, Paris, Frankfurt (1981).
62. Sarbu, T., Styranec, T., Beckman, E. J. , *Nature*, **2000,** *405*, 165-168.
63. Blanchard, L. A., Hancu, D., Beckman, E. J., & Brennecke, J. F., *Nature*, **1999,** *399*, 28-29.
64. Jacobson, G.B., Lee, Jr., C.T., Johnston, K. P. and Tumas, W., *J. Am. Chem. Soc.* **1999**, *121*, 1902-1903.
65 . M. McCoy, *Chem. Eng. News*, 14 June 1999, 11.

Downloaded by UNIV OF GUELPH LIBRARY on September 16, 2012 | http://pubs.acs.org
Publication Date: January 24, 2002 | doi: 10.1021/bk-2002-0809.ch024

Downloaded by COLUMBIA UNIV on September 16, 2012 | http://pubs.acs.org
Publication Date: January 24, 2002 | doi: 10.1021/bk-2002-0809.ch025

Chapter 25

The Possibility of Coupling Supercritical Extractions in Petroleum Industry with CO_2 Conversion Plants to Lessen Investments

Marco Antonio G. Teixeira and Maria Luísa A. Gonçalves

**Petrobras Research and Development Center, Division of Chemistry,
Rio de Janeiro 21949–900, Brazil**

The investment and the operational costs are strong limiting factors for the CO_2 conversion processes, as they are for supercritical extraction implementation. A process solution to that is proposed, in which supercritical extraction with CO_2, that employs high temperature and pressure, is used to yield valuable products before admittance into a CO_2 conversion unit, thus sharing the energy costs with it. The extracted material is recovered by depressurization of the system, and the resulting CO_2 stream can be obtained in conditions for conversion. An application from petroleum industry is discussed, the extraction of valuable paraffins that also produces value-added paraffin-free asphalt. The temperature and pressure at which the CO_2 stream can be obtained after liberation of extracted paraffins are adequate as feedstock preparation for most of the conversion propositions in literature.

CO_2 mitigation has been the matter of several researches in the decade of the 90's, because of consequences of its liberation to the atmosphere to the global weather. Several scientific and technological meetings, like the

In CO2 Conversion and Utilization; Song, C., et al.;
ACS Symposium Series; American Chemical Society: Washington, DC, 2002.

1992, 1994 and 1996 International Conferences on Carbon Dioxide Removal (ICCDR) and the 1998 and 2000 International Conferences on Greenhouse Gas Control Technologies (GHGT), have discussed the mitigation possibilities, among which the conversion to products of commercial value, the main subject of the present publication, is a promising option. The technological development of process alternatives is a task that has been carried out in a very successful way by several researchers, many of them with contributions to this issue. However, large-scale applications require industrial plants, with all the cost involved first in the edification steps and in further operation, regarding energy to reach adequate temperature and pressure. These facts show that efforts should be developed to enhance the economical attractivity of the conversion projects.

The petroleum industry produces in its installations quantities of CO_2 infinitely smaller than the quantities generated by the use of its products as fuels. However, it is an industrial field very intense in capital and technology, and some contributions may be expected from this industry to the development of solutions. Streams with high CO_2 content can be found in refineries from the regeneration of FCC catalysts or from burning fuel oils in ovens, though pure CO_2 can be obtained in good purity in an easier way by pressurization of the stream generated after absorption of acid gases in ethanolamines and elimination of sulfur present in a Claus unit; though the CO_2 content is normally minor in these streams, the contaminants are basically only nitrogen and water, and CO_2 can be conveniently separated.

For the implementation of CO_2 conversion plants in refining facilities the need for financial attraction remains, and an industrial plant to the conversion of CO_2 to a given product would require a considerable price-to-market of that sole product.

In several fields, the use of CO_2 in supercritical conditions has opened excellent possibilities of applications. The 5th International Symposium on Supercritical Fluids, in 2000, brought together the experiences and developments in this field in the decade of the 90's, with a rich collection of papers that showed that CO_2 is by far the most studied fluid.

Possible applications of CO_2 in petroleum processing have directed the attention of the authors towards its use in supercritical conditions as a solvent for high value products. The conclusion of these studies, as it has been the conclusion of several researchers in the area, is that supercritical extraction with CO_2 is mainly attractive as an industrial process for the extraction of high value products, like drug precursors, in small plants, due to the investment necessary.

These studies have directed the authors to a different scenario for supercritical extraction and also for CO_2 conversion as a way of its mitigation, porposed here. The main idea is that the energy consumed to lead CO_2 to the conditions employed for the extraction of these economically attractive products could be shared with conversion plants. In supercritical extraction, the solvating capacity of CO_2 is dictated mainly by the use of high pressure and temperature. After extraction, the solute is

Downloaded by COLUMBIA UNIV on September 16, 2012 | http://pubs.acs.org
Publication Date: January 24, 2002 | doi: 10.1021/bk-2002-0809.ch025

normally recovered by depressurization of the extract. If suitable values for the thermodynamic parameters can be reached after depressurization, the stream of CO_2, after separation of the solute, can be directly lead to conversion plants without further energy cost. This approach has not been considered in a complete engineering project so far, but the indications available show that this is an approach able to lessen the operational cost of the units, and it can be a process solution to the attractivity of the conversion projects. In this chapter, this idea is shared with the reader as a possibility of improvement of developments in this area. After a brief discussion of the applications of extractions in petroleum industry and the advantages seen for the possible use of supercritical CO_2 in the generation of high value petroleum derivatives, an example is given of developments achieved by the authors with the extraction of a high value product for refineries, paraffin wax. It is taken as an evidence that works in this direction may bring profitable process solutions.

Downloaded by COLUMBIA UNIV on September 16, 2012 | http://pubs.acs.org
Publication Date: January 24, 2002 | doi: 10.1021/bk-2002-0809.ch025

Introduction

The applications of supercritical fluids in processing materials have been the subject of many researches, mainly from beginning of the decade of the 90's on. In the middle of that decade some developments were already real process options, and some other ones were promising alternatives *(1)*. By the end of the decade, though many other possibilities had been studied in addition to extraction *(2, 3)*, only two established industrial processes could be considered: decaffeination of coffee and the so-called residue oil supercritical extraction (ROSE). The former consists of an extraction process in which supercritical CO_2 is employed in substitution of liquid solvents, to avoid the residual contents present when organic solvents are employed for caffeine extraction.

ROSE is an improvement of the traditional deasphalting process employed in the petroleum industry to produce valuable products from vacuum distillation residua *(4)*. Distillation is unable to produce further fractionation of these residua for refining purposes, so extraction is employed. Both in classical deasphalting units or in ROSE plants the solvent employed (C_3 or a mixture of C_3 and C_4 hydrocarbons) is not in supercritical conditions in the extraction step. In the traditional scheme the solvent is recovered by distillation. In ROSE, the extracted material is separated from the effluent solution by leading the mixture to temperature and pressure conditions above the critical point of the solvent. Under these conditions its solvating capacity is dramatically lessened and the extracted components precipitate.

Deasphalting and some other extraction processes may gain more importance in petroleum industry from the end of the 90's on, because they bring possibilities for the generation of value-added products from distillation residua. One of the main difficulties in processing many high-density refinery feedstocks that are usual worldwide nowadays is the destination of their heavy fractions that can be very abundant after distillation and processing.

Good descriptions of the need to convert distillation residua to commercial products, the installed capacity of the ROSE process and the use of approaches to the work under supercritical conditions in the extraction step can be found in literature *(4)*. The applications of supercritical fluids in the development of new processes for petroleum refining can also be found reviewed *(5,6)*.

The applications in which potential commercial application can be seen also employ hydrocarbon solvents, as is the case in propane deasphalting, being pentane *(7)* or toluene *(8)* examples of that. The possible explanation is the obvious availability of these solvents in the petroleum and petrochemical industry and the chemical similarity with the materials to be extracted, which ensures good solvating power to these solvents. This is an important aspect because it ensures good yields of extracts, and the important product to be obtained is normally the soluble fraction. In these processes, the extracted components can be directed to applications like lubricant oils or feedstock to catalytical cracking units that produce gasoline and liquefied petroleum gas, very valuable products; the remaining fraction, consisting of very heavy hydrocarbons, can be employed as paving binders (asphalts), precursors for carbon materials or fuel oils, less valuable petroleum derivatives. That is the reason why the operation of extraction plants in petroleum industry tries to maximize extract yields.

Exactly because of the similarity with the families of petroleum constituents, the use of supercritical hydrocarbons in petroleum residua *(9)* is not a choice for selectivity in the extracts. However, the definition of the limiting properties of the extracts required for the subsequent applications is not a function of the presence of given chemical groups; they are mainly related to some physico-chemical properties. Therefore, the requirement of selective extractions is seldom the aim of the researches in the petroleum industry.

An exception is the production of paraffin waxes. These high-value products are employed for many uses, like candles, food, and impermeabilization. They are obtained by extraction with a ketone; normally the wax-free fraction undergoes deasphalting, and that integrates the extraction plants of a refinery. However, this scheme is very dependent on the kind of petroleum employed (a very paraffinic characteristic is required), exactly because of difficulties related to selectivity in these extraction approaches. Those difficulties have motivated even the search for alternative raw materials for the production of paraffin waxes *(10)*.

Extraction with supercritical CO_2 has been mentioned in literature as a good tool to achieve selectivity in extraction procedures, and since the beginning of the decade of the 90's several analytical applications based on

Downloaded by COLUMBIA UNIV on September 16, 2012 | http://pubs.acs.org
Publication Date: January 24, 2002 | doi: 10.1021/bk-2002-0809.ch025

this selectivity aspect were already developed. Supercritical CO_2 had been shown to be very selective for saturates among other petroleum components *(11)*, and by the end of that decade analytical approaches for the selective extraction of petroleum paraffins had already been proposed *(12)*. However, studies on industrial applications were not as stablished as analytical ones.

The present authors have considered that industrial applications could employ the same selectivity aspect that has brought successsful applications in analytical scale. As a first promising use of that solvent, work on the proposition of an extraction scheme for selective extraction of paraffinic materials from asphalts was developed. The interest to have asphalt as the substract of the extraction is due to the importance of the role of this product in the destination of heavy residua and also due to the fact that the extraction of paraffins matches the needs that some asphalt markets claim. In hot countries, direct action of the sun exposition may result in temperature levels in the asphaltic pavements high enough to reach the melting point of some of its components. The consequence is the fact that the rheological properties of the pavements become poorer, and deformations can be seen, mainly in curves, where a centrifuge action takes place with traffic.

This problem is very well-known for asphalts, as some other ones are; identically, specification and performance problems are known to happen with other heavy petroleum products. However, it is often quite difficult to reach process solutions, because of the limitations in characterization of the components of these heavy fractions. The determination of the group of constituents to be considered responsible for the problems in the behavior of those products and, as a consequence, the proposition of process solutions for them has been a task that has brought together many efforts from petroleum chemists and process engineers.

The main reason for that is the fact that heavy petroleum fractions are very difficult to be analyzed, *stricto sensu*, by chemical means. It is normally considered that these fractions, including asphalts, are constituted by four groups of constituents: asphaltenes (precipitated materials obtained by addition of n-heptane), paraffins, aromatics and resins (heteroatomic). These three later groups are normally obtained, based on the differences in their polarities, by preparative liquid chromatography of the whole material or of an asphaltene-free fraction. It could be said that further information has to be obtained by procedures specifically taylored to face a given problem under study.

Because of these limitations, some analytical approaches aim to be specific to the properties of given groups of constituents in the heavy fractions. An example is cited for paraffins. It has been reported in literature that paraffins in asphalt are the group of its constituents that show melting transition, by studies employing fractionation and analysis of the fractions by DSC, differential scanning calorimetry *(13)*. In these studies DSC is also employed for a quantitative estimation of paraffin contents in asphalt by the evaluation of the heat involved in the melting

Downloaded by COLUMBIA UNIV on September 16, 2012 | http://pubs.acs.org
Publication Date: January 24, 2002 | doi: 10.1021/bk-2002-0809.ch025

transition observed in asphalt samples of known weight, with the consideration of an average melting transition value of 200 J/g for paraffinic materials.

Even general analytical methods like the ones mentioned in the previous paragraph show several limitations. An example experienced by the authors can be cited. Asphaltenes are considered to be the main coke percursors in these heavy residua; however, no correlation could be found with the traditional methodology. Previous developments by the present authors had yielded quantitative and selective extraction conditions for the analytical extraction by pure supercritical CO_2 *(14)* of paraffinic materials which had been found to co-precipitate with asphaltenes *(15)*. A novel work was developed with paraffin-free asphaltenes, and the good performance of the methodology was validated by the improvement of correlations of asphaltene contents with carbon residue *(16)*, a very important parameter for studies on the technologies developed for catalytical cracking of residua *(17)*.

So, it can be seen that tayloring analytical methods are additional challenges in the development of applications of extraction fluids in petroleum industry; actually, that does not happen only for extraction monitoration, but for studies on heavy petroleum fractions in a general way, and it is a limiting aspect in the research related to those fractions. Since the attractivity of extraction processes is exactly related to the heavy fractions, that can explain the restricted implementation of extraction processes in petroleum industry so far; that has brought as a consequence very limited possibilities for CO_2 utilization as a solvent.

In the work presented here, where the efforts were directed to the development of conditions for selective extraction of paraffins from asphalts, a considerable fraction of the time was spent on the proposition of monitoration methods based on analytical means, and not only in specification criteria or physico-chemical properties, as it can be frequently seen in literature.

The use of pure supercritical CO_2 was considered a premise since the beginning of the work, since there are indications from our previous developments that the presence of co-solvents, even non-polar ones, enables extraction of non-saturates *(14)*. So, optimization of conditions aimed basically to reach selectivity and completeness in the extractions, and though differences in the materials can be observed with variations of extraction conditions, this point will not be discussed here.

In summary, extraction conditions and characteristics of both materials (soluble and insoluble ones) obtained by supercritical extraction with CO_2 of asphalt will be cited. The focus of the discussion will also comprise the analytical results obtained, since that is considered a relevant contribution to the developments in this area, due to the difficulty experienced for the proposition of characterization approaches to support such works.

Downloaded by COLUMBIA UNIV on September 16, 2012 | http://pubs.acs.org
Publication Date: January 24, 2002 | doi: 10.1021/bk-2002-0809.ch025

Downloaded by COLUMBIA UNIV on September 16, 2012 | http://pubs.acs.org
Publication Date: January 24, 2002 | doi: 10.1021/bk-2002-0809.ch025

Extraction conditions

Supercritical extraction for the present study was performed in a modified Suprex Prepmaster extraction system, specially adapted for needs of this particular development. The apparatus was initially employed for analytical purposes, and it has been modified for several process studies. This has been a general tendency in the use of hardware for supercritical extraction *(2)*.

CO_2 was passed through a tubular extraction cell (with ascendent CO_2 flow) at the desired pressure with the aid of a reciprocant pump. That pump controlled pressure, not flow. The extraction cell was placed in an oven, for temperature control. In the original conception of the apparatus, flow was obtained by opening a 6-port valve placed in the extract exit tubing, outside the oven. A system of restriction, an aperture of reduced size, controlled the flow rate. The size of the aperture was determined by a needle. Since flow variations happen during extraction process, this restrictor was controlled by an engine. So, it was built outside the body of the extractor. The collection of extracted material was done onto adsorbents, conditioned in a small metallic cylinder. Refrigeration gas could be admitted outside this cylinder wall to improve retention.

Paraffin depositions was a difficulty found in the operation of that original construction. So, some modifications were necessary to avoid that problem. All of the extract exit part of the apparatus was removed. Two slightly open needle valve were placed and they allowed the system to be under high pressure at the same time in which the extract was being collected; the use of two valves is explained by the fact that an only valve is unable to control the desired flow (measured by the displacement of the pump strokes) in the conditions at high pressure. After leaving the extraction cell, the CO_2 stream was lead to the bottom of a column of glass beads; there CO_2 was at room pressure again, going to the gas state, and the extracted material precipitated, being mechanically retained by the glass beads.

Analytical approaches were the next step considered in the development. The first aspect to be considered before characterization of the extracts, that is, the evaluation of extraction yields, was monitored by gravimetric means. Since the mass of asphalt placed in the extraction cell was always known, the extracted fraction collected in the glass beads and the remaining insoluble material were both weighed after each extraction, and the mass balance was checked.

Extraction temperature and CO_2 flow employed were obtained from previous experience *(14)*. Even high carbon-numbered standard paraffins are soluble enough at temperatures inferior to 120°C, so that was the minimum temperature considered. It will be seen that large variations in temperature were not possible, because of asphalt nature. The previous experience also showed that the CO_2 flow is the variable that dictates the time for extraction, since diffusion is not the aspect that controls the final amount in solution; the thermodynamic equilibrium is easily reached. So, only pressure was considered a variable to be explored in this study.

Analytical Monitoration of Paraffin Extraction of Asphalts

As it was mentioned before, the analysis of asphalts is a very difficult task, since the commonly employed analytical techniques in petroleum industry, like gas chromatography, show many limitations for application to the characterization of any of the heaviest fractions of petroleum *(18)*.

Characterization schemes of both the extracted fraction and the insoluble material were proposed mainly with use of thermal analysis. DSC was employed in a diverse manner of the previously cited application, in which an average heat of fusion was employed to a quantification of paraffin content *(13)*. In this work, two kinds of use were reserved for DSC graphs. The first one aimed to evaluate the result of continuously decreasing amounts of paraffins remaining in the asphaltic material by the increase of the extraction time. DSC curves, therefore, only brought a tendency of the softening point of the novel asphalts produced by paraffin removal, which is an interesting indication related to the properties of the extracted product. The second (and less frequent in this work) one was the monitoration of the few experiments in which quantitative removal of paraffins was desired, that aimed to yield an idea of the behavior of paraffin-freed asphalts. So, extraction was performed in these cases till a baseline was obtained in the DSC graphs.

Actually, in the beginning of the work, the heat flow used for melting remaining paraffins in the sample after extraction was compared to the value observed before extraction to be used as a quantification of remaining paraffins in asphalt. The results showed at once that neither this value nor the value of 200 J/g *(13)* employed for asphalt analysis can be trusted for quantification purposes, since the amounts of the fractions of paraffinic materials yielded by gravimetric evaluation of the preparative extraction never matched the one calculated with that average transition heat. This is probably due to the fact that the heat involved in that transitions is a function of the distribution of methyl and methylene groups in the aliphatic chains of the paraffins *(19)*. That distribution probably changes with the severity of the extraction, since the number of paraffinic components in asphalt is quite large, and different solubility behaviors can be expected. That makes it impossible to employ calorimetric measurements for these quantitative estimations, unless only semi-quantitative results are expected.

So, DSC measurements were only employed for the monitoration of the new transition onset temperatures obtained for the extracted asphalts. In some few cases where quantitative preparative extractions were desired,

Downloaded by COLUMBIA UNIV on September 16, 2012 | http://pubs.acs.org
Publication Date: January 24, 2002 | doi: 10.1021/bk-2002-0809.ch025

Downloaded by COLUMBIA UNIV on September 16, 2012 | http://pubs.acs.org
Publication Date: January 24, 2002 | doi: 10.1021/bk-2002-0809.ch025

the curves were also employed to the evaluation of the completeness of the extraction, which could be observed by the disappearance of the transition peak.

Another thermal analysis technique, thermogravimetry (TG), was used for rapid evaluation of the presence of co-extracted materials in the paraffinic fractions obtained, since selective extracts were sought. The application was based on the knowledge that paraffinic materials would not yield coke when heated under inert atmosphere *(20)*. So, a ready way to detect how selective a given extraction condition had been was to perform TG analysis up to 700°C under nitrogen. The presence of residue (coke) at that temperature indicated the presence of non-paraffinic material in the extract. Coke formed by the pyrolysis of those components could be burned by the introduction of air in the system at 700°C, and additional mass loss was observed.

Additionally, nuclear magnetic resonance (NMR) and elemental analysis (CHN) were also employed. These are typical analysis for heavy petroleum products, so they will not be longly discussed here. Briefly, it can be cited that ^{1}H NMR spectra show baseline elevation in the chemical shift range of 9 to 6 ppm when aromatic hydrogens are present in petroleum or its fractions *(21)*. The atomic ratio (C/H) of long-chained paraffins is 0.5, and the presence of meaningful amounts of aromatics may be detected with any deviation to a higher value.

It should be also mentioned that some other analytical approaches were tried in the beginning of the developments. The first technique considered to monitor the extraction performance was gas chromatography. However, elution could not be confirmed as quantitative, and resolution enough for such a heavy and complex system could not be achieved. Normal phase liquid chromatography was also considered, but separation of asphaltenes before injection would be necessary, to avoid irreversible adsorption onto stationary phase. Since that could bring doubt to the results expected, because of the possibilities of co-precipitation of the heavier paraffins *(15)*, and the whole procedure would become very tedious and time-consuming, further investigations on this technique were not performed.

Experimental Results for Extraction

The first criterium employed in the monitoration of the extractions was the heat flow employed for the melting transition of the remaining paraffins in the asphalt. This product was called modified asphalt. Figure 1 shows typical DSC curves of the original and modified asphalt; in this example, extraction was performed at 360 atm. The properties of the departing asphalt are cited in table 1.

Table 1. Main properties of the asphat studied

Parameter	Method	Found
Viscosity at 60°C, P	ASTM D-2171	2800
Penetration, 100g, 5 s, 25°C, tenths of mm	ASTM D-5	55
Flash point	ASTM D-92	238

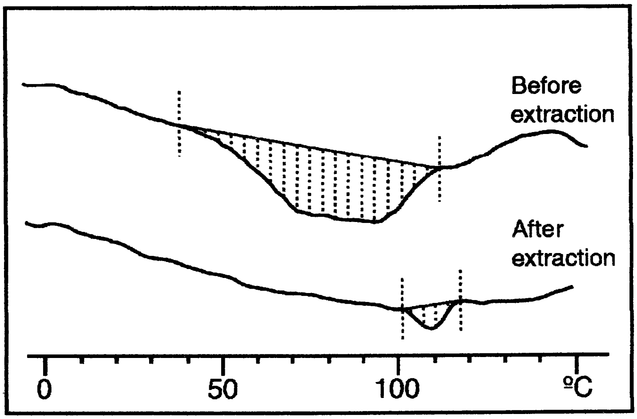

Figure 1. DSC graphs of asphaltic material before and after supercritical extration with CO_2 at 360 atm and 150ºC (CO_2 flow was 16mL/min)

From Figure 1, it can be seen that it was possible to achieve practically paraffin-free asphaltic material. Quantitative extraction is not adequate for paving purposes. Very high softening points make the application on the pavement quite difficult.

It can be also seen in Figure 1 that there is an elevation in the baseline after the paraffins melt. This means that the sample can be undergoing chemical modification. So, the maximum temperature to be reached could not be superior to about 120°C, and that was the adopted value for this parameter.

The data in Figure 1 bring some additional important aspects. Only the heaviest paraffinic components are not extracted, but their melting temperature range onset (related with softening) is about 100°C. This does not bring any mechanical problem for the utilization of the modified product obtained as asphalt binders; some problems would probably be verified in the use of the original material in many hot countries, since its onset is below 40°C, and that temperature level can be easily reached in summer in these places.

Though DSC measurements are very informative about characteristics of insoluble fraction, they could not inform about the selectivity of extraction. Characterization of nature of paraffinic fraction obtained was done by ^{1}H NMR and elemental analysis for C, H and N. Selectivity for saturates was clearly evaluated from results obtained by these two techniques. Nitrogen was absent in extracts. Atomic ratio C/H was almost exactly 0.5, while weight percent contents of C and H summed

Downloaded by COLUMBIA UNIV on September 16, 2012 | http://pubs.acs.org
Publication Date: January 24, 2002 | doi: 10.1021/bk-2002-0809.ch025

practically 100%. NMR spectra could not show presence of aromatic hydrogens in extract (Figure 2), while for the whole asphaltic material (Figure 3) the presence of aromaticity could be evaluated in 13% of the total hydrogen content. The single peaks at about 7.2 ppm in Figures 2 and 3 are due to the presence of $CHCl_3$ in the analysis solvent, $CDCl_3$.

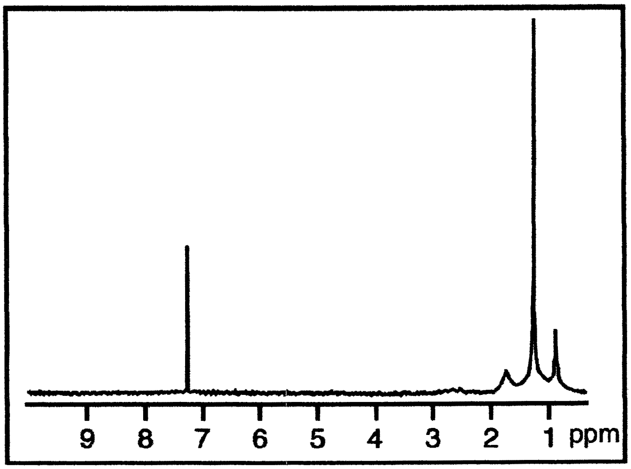

Figure 2. ^1H NMR spectrum of the extract obtained with supercritical CO_2

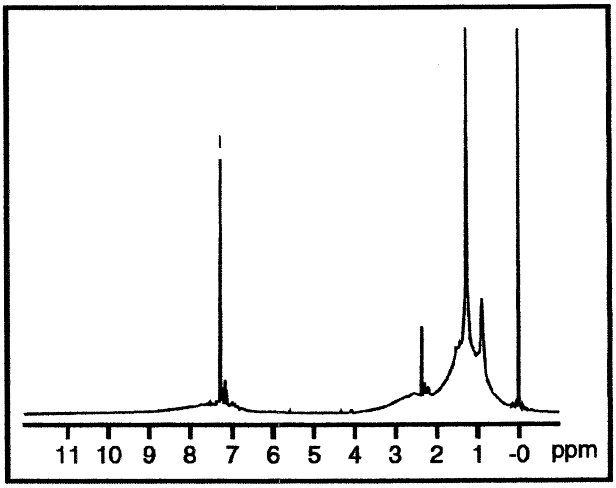

Figure 3. ^1H NMR spectrum of the whole asphaltic material before supercritical extraction

The ^1H NMR spectrum in Figure 3 also shows that are considerable amounts of aliphatic branches bonded to aromatic nuclei in the asphalts; that can be evaluated by the meaningful envelope from 4 to 2 ppm *(21)*. It was considered in the beginning of the work that these branched components could be a challenge for selectivity, because of the

Downloaded by COLUMBIA UNIV on September 16, 2012 | http://pubs.acs.org
Publication Date: January 24, 2002 | doi: 10.1021/bk-2002-0809.ch025

possibility of a hybrid behavior of the ones branched with long aliphatic chains. In Figure 2 it can be seen that CO_2 could be very selective.

Additional characterization of extracted material was achieved with thermogravimetry. Figures 4 and 5 show the difference between thermal behaviors of the asphaltic material and the extract.

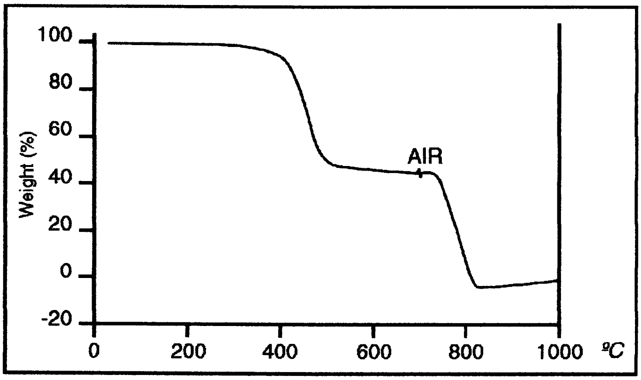

Figure 4. TG graph of the whole asphaltic material

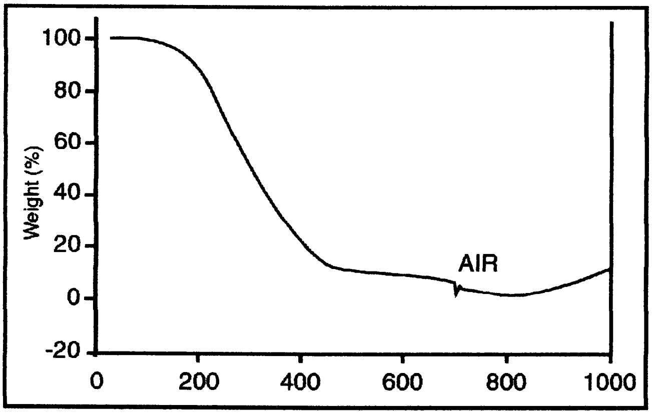

Figure 5. TG graph of paraffinic extract

Thermal behaviors show that structures in the original asphaltic material yield large amounts of coke (approximately 50%), while the extract does not; that is, after introduction of air, there is no considerable mass loss. This was taken as additional evidence of the selectivity of extraction for saturates.

Downloaded by COLUMBIA UNIV on September 16, 2012 | http://pubs.acs.org
Publication Date: January 24, 2002 | doi: 10.1021/bk-2002-0809.ch025

Extraction yields

Extraction yields vary with the conditions in which the extraction takes place. At 120°C, no extraction is achieved when the CO_2 pressure is 50 atm; a fraction of light paraffin is obtained when the pressure is about 200 atm; quantitative extraction is achieved when the pressure is 400 atm. Figure 6 shows the tendency observed with a CO_2 flow of 16 mL/min, after a 3 hour extraction time.

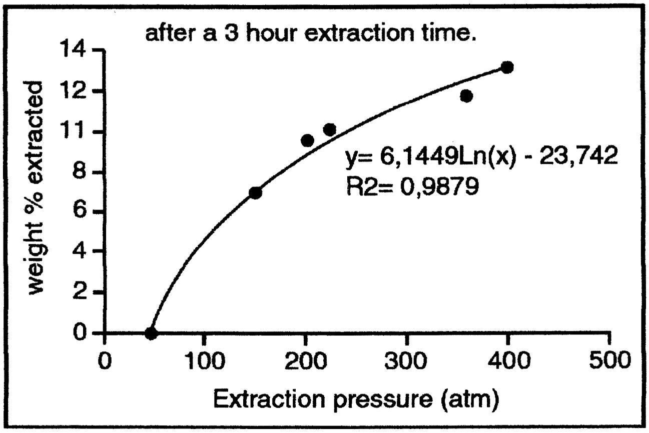

Figure 6. Extraction yield tendency with solvent variation

This means that the extraction conditions can be planned to reach different materials, depending on the need to produce micro or macrocrystalline paraffins; the characteristics of these fractions are mainly a function of the molecular weight range *(19)*, and since that range also defines the solubility, the extraction is an adequate way to obtain separately those products. This also means that if the CO_2 stream pressure after extraction is reduced to 50 atm, the paraffin wax precipitates, and CO_2, after generation of two value-added products, can be directly lead to conversion plants, without further energy costs on feedstock preparation to those plants. The pressure level mentioned here (50 atm) is adequate to most of the conversion developments seen in literature, many of them cited in this publication.

Conclusions

Supercritical extraction with pure CO_2 may yield valuable products, as it was seen here in the examples of paraffin wax and paraffin-free asphaltic material. This chapter reported the necessary steps employed for a successful development of conditions for selective and complete

Downloaded by COLUMBIA UNIV on September 16, 2012 | http://pubs.acs.org
Publication Date: January 24, 2002 | doi: 10.1021/bk-2002-0809.ch025

extraction of paraffins from asphalts. Since heavy petroleum fractions are the possible field of application of extractions, it was seen that characterization schemes play a vey important role in the development of extraction conditions, because of difficulties in chemical characterization of the components of these fractions. This is expected to be a contribution to novel developments and to a more popular use of CO_2 in petroleum industry.

The optimization revealed conditions where the solubility of the material is null. If the extract is lead to those conditions, the extracted material precipitates and the CO_2 stream generated can be obtained in adequate temperature and pressure to be used in some further applications without additional energy consumption; it is proposed here that this stream can be a ready feedstock for conversion plants. The applicability of supercritical CO_2 opens large possibilities for those coupled processes, since investments and operational costs can be shared by two industrial units. The conversion to methanol, for example *(22)*, can be performed with CO_2 at 50 atm. At that pressure, all of the extract content would be precipitated after depressurization, so that the resulting CO_2 stream could be lead directly to the conversion plant.

About the economics of the process, it is very difficult to state about that without a whole engineering project. However, it can be cited that the values mentioned in literature *(22)* indicate that the cost of CO_2 conversion to methanol can be calculated in about US$50,00 per ton CO_2. That is a meaningful value, so that a previous use of CO_2 for the obtention of a product in the range of at least US$750,00/ton, as paraffin wax is, is certainly an attractive option to be considered.

References

1. Lynch, T. *J. Chem. Tech. Biotech.* **1996**, 65 (3), 293.
2. Perrut, M. *Proceedings of The 5th International Symposium on Supercritical Fluids, Atlanta, Georgia, April 8th-12th*, **2000**, Plenary Lecture 2.
3. Chordia, L.; Robey, R. *Proceedings of The 5th International Symposium on Supercritical Fluids, Atlanta, Georgia, April 8th-12th*, **2000**, Plenary Lecture 3.
4. Kim, M. S.; Yang, K. S.; Hwang, J. S. *Pet. Sci. Tech.* **1997**, 15, (9/10), 921.
5. Rudzinski, W. E.; Aminabhavi, T. M. *Energy & Fuels* **2000**, 14, (2), 464.
6. Dadashev, M. N.; Stepanov, G. V. *Chem. Tech Fuels & Oils* **2000**, 36, (1), 8.
7. Stegeman, J. R. et al. *Fuel Sci. Tech. Int.*, **1992**, 10, (4-6), 767.
8. Zhuang, Mark S.; Thies, Mark C. *Energy & Fuels* **2000**, 14(1), 70.
9. Deo, M. D.; Hanson, F. H. *Fuel* **1994**, 73 (9), 1493.

Downloaded by COLUMBIA UNIV on September 16, 2012 | http://pubs.acs.org
Publication Date: January 24, 2002 | doi: 10.1021/bk-2002-0809.ch025

10. Badyshtova, K.M.; Shabalina, T.N. ; Kitova, M.V. *Chem. Tech Fuels & Oils* **1996**, 32(3), 119.
11. Singh, I. et al. *Fuel Sci. Tech. Int.* **1992**, 10(2), 267.
12. Oschmann, H.J.; Prahl, U.; Severin, D. *Pet. Sci. Tech.* **1998**, 16,(1/2), 133.
13. Burlé, B. et al. *Symposium on Chemistry and Characterization of Asphalts Proceedings*, **1990**, 330.
14. Teixeira, M. A. G.; Oliveira, L. B., *Proceedinds of the 3rd Brazilian Meeting on Supercritical Extraction of Natural Products*, Rio de Janeiro, **1999**, Paper#60.
15. Teixeira, M. A. G.; Gonçalves, M. L. A., *Petroleum Science and Technology* **2000,** 18(3-4), 273.
16. Teixeira, M. A. G.; *Proceedings of The Rio Oil and Gas Expo and Conference*, **2000**, Paper#250.
17. Baptista, C. M A.; Bonfadini, P. R.; Gilbert, W. R.; Teixeira, M. A. G. *Proceedings of the National Petrochemical & Refiners Association Annual Meeting , San Antonio*, **2000** , paper #AM -00-23.
18. Teixeira, M. A. G.; Faria, F. R. D.; Albuquerque, F. C. , *Proceedings of the Second International Symposium on Colloid Chemistry in Oil Production*, **1997**, Paper#44.
19. Gupta, A. K.; Brouwer, L.; Severin, D. *Pet. Sci. Tech.* **1998**, 16(1-2), 59.
20. Teixeira, M. A. G.; Gonçalves, M. L. A., *Petroleum Science and Technology*, **1999,** 17(1&2), 1.
21. 12. Hassam, M. H. et al. *Fuel* **1983**, 62.
22. Steinberg, M. *American Chemical Society, Division of Petroleum Chemistry, Inc. Preprints, International Symposium on CO_2 Conversion and Utilization in Refinery and Chemical Processing, 219th American Chemical Society Meeting, San Francisco*, **2000**, 45, (1), 74.

Downloaded by COLUMBIA UNIV on September 16, 2012 | http://pubs.acs.org
Publication Date: January 24, 2002 | doi: 10.1021/bk-2002-0809.ch025

Author Index

Akamatsu, Noriyasu, 205
Anpo, Masakazu, 330
Aresta, Michele, 54
Armor, John N., 258
Asadullah, Mohammad, 303
Babcock, R. E., 224
Busch, Daryle H., 364
Chang, Char-Fu, 102
Cheng, Zhen-Xing, 197
Choudhary, V. R., 224
Dibenedetto, Angela, 54
Effendi, A., 275
Fujimoto, Kaoru, 71, 303
Furusawa, Yutaka, 71
Gaffney, Anne M., ix
Gonçalves, Maria Luísa A., 387
Haraguchi, K., 241
Hideshima, Shigeo, 205
Hsu, Tsung-Ju, 102
Ikeda, Yoshiki, 71
Ikenaga, Na-oki, 205
Ikeue, Keita, 330
Inui, Tomoyuki, 130
Ishiguro, G., 153
Li, Jin-Lu, 197
Mahajan, D., 166
Mamman, A. S., 224
Manzer, Leo E., 39
Matsui, Na-oko, 205
Matsuo, Yuichi, 303
Murata, Satoru, 258
Nakagawa, Kiyoharu,205
Nakayama, M., 344
Ogura, K., 344
Ohtsuka, Yasuo, 85
Omata, K., 153
Pan, Wei, 258, 316
Scaroni, Alan W., 166, 258
Sekine, Yasushi, 303
Shamsi, Abolghasem, 182
Song, Chunshan, 2, 166, 258, 289, 316
Srimat, Srinivas T., 258, 289
Steinberg, M., 31
Subramaniam, Bala, 364
Sun, Lu, 258
Suzuki, Toshimitsu, 205
Tan, Chung-Sung, 102
Teixeira, Marco Antonio G., 387
Tomishige, Keiichi, 71, 303
Uphade, B. S., 224
Ushizaki, K., 153
Wang, Ye, 85
Wei, Jun-Mei, 197
Xu, Bo-Qing, 197
Yamada, M., 153
Yamashita, Hiromi, 330
Yano, H., 344
Yoo, Jin S., 112
Yoshida, T., 241, 275
Yoshinaga, Yusuke, 303
Zhang, Z.-G., 241, 275
Zhu, Qi-Ming, 197

Downloaded by 217.66.152.143 on September 14, 2012 | http://pubs.acs.org
Publication Date: January 24, 2002 | doi: 10.1021/bk-2002-0809.ix001

Subject Index

A

Acrolein, propylene oxidation, 42
Acrylic acid
  oxidation of propane, 44*t*
  propylene oxidation, 42
Acrylonitrile, ammoxidation of propane, 44*t*
Adsorption, separation of gas mixtures, 10
Aerobic oxidations
  vs. anaerobic, 40–43
  See also Catalytic oxidations
Alcohol, allylic and homoallylic, oxidation in dense phase CO_2, 374
Alcohol synthesis
  alcohol distribution for different catalysts, 143, 145*f*
  catalyst design, 140, 143, 147
  comparison of temperature-programmed-reduction (TPR) profiles for various catalysts, 143, 144*f*
  ethanol, 140
  ethanol synthesis from CO_2 on various catalysts, 142*f*
  Schulz–Flory plots for different catalysts, 143, 146*f*
  See also Catalytic conversion
Aldehydes. *See* Gas-phase O_2 oxidation of alkylaromatics
Alkenes, catalytic oxidation in *sc*CO_2, 374, 375*f*
Alkylaromatics. *See* Gas-phase O_2 oxidation of alkylaromatics
Alkylation reactions, dense phase CO_2, 368–369
Ammoxidation, propane to acrylonitrile, 44*t*
Anaerobic oxidations
  vs. aerobic, 40–43
  See also Catalytic oxidations
Aromatics. *See* Gas-phase O_2 oxidation of alkylaromatics
Asphalt
  analytical of paraffin extraction, 394–395
  asphaltenes, 392
  ^{13}C NMR spectrum of material before extraction, 397*f*
  constituents, 391
  differential scanning calorimetry (DSC) before and after supercritical extraction, 396*f*
  extraction results, 395–398
  extraction yields, 399
  ^{1}H NMR spectrum of extract, 397*f*
  main properties, 396*t*
  paraffins, 391–392
  thermogravimetry of asphaltic material, 398*f*
  thermogravimetry of paraffinic extract, 398*f*
Atmospheric pressure. *See* Pressure effects

B

Benzene, dinitrogen oxide oxidation, 47*f*
Binary catalysts. *See* Methane conversion
Binary oxide, Ti/Si, 341
Biotechnology

Downloaded by 217.66.152.143 on September 14, 2012 | http://pubs.acs.org
Publication Date: January 24, 2002 | doi: 10.1021/bk-2002-0809.ix002

Downloaded by 217.66.152.143 on September 14, 2012 | http://pubs.acs.org
Publication Date: January 24, 2002 | doi: 10.1021/bk-2002-0809.ix002

  coupling chemistry with, 66–68
  synthesis of 4-OH-benzoic acid, 68
Boudouard reaction
  carbon deposition, 208, 210
  pressure drop across catalyst bed, 237
Brookhaven National Laboratory, integrating CO_2 sequestration with conversion in geologic formations, 178–179
Building blocks. *See* Synthetic chemistry
Burial, sequestration option, 167
Butadiene, oxidative dehydrogenation of butane, 42
Butane, oxidative dehydrogenation to butadiene, 42
Butane oxidation
  maleic anhydride, 42–43
  selectivity, 40*t*
  See also Catalytic oxidations

C

Ca-based binary catalysts. *See* Methane conversion
Capture, CO_2, 9–10
Carbamates, synthesis, 65
Carbide catalysts
  methane dry reforming, 185*t*
  preparation, 185–186
  See also Methane dry reforming
Carbonates
  synthesis, 62, 64–65
  synthesis routes, 72–73
  See also Dimethyl carbonate (DMC)
Carbon dioxide, CO_2
  area for CO_2 control, 8*f*
  barriers for conversion and utilization, 20–21
  capture and sequestration, 9–10
  challenges and strategies for conversion and utilization, 16, 20–24
  chemical processes for conversion and utilization, 19*f*
  control of emissions, 6, 9
  conversion and utilization, 10–16
  current status and potential market for utilization, 14, 16
  estimates for utilization, 18*t*
  estimates for worldwide capacity of options for sequestration, 18*t*
  extraction by Carnol process, 32
  Gibbs free energy of formation, 13*f*
  green chemistry, 112
  greenhouse gases (GHG), 3, 8*t*
  key issues for control of greenhouse gas, 8*f*
  mild oxidant with chromium-based catalysts, 49, 50*t*
  occurrence, 2
  properties, 12t, 365
  reaction with hydrogen, 33
  sources of emissions, 3, 6
  stationary, mobile and natural sources, 4*t*
  strategy for research on utilization, 21–24
  technical options for emission control, 6
  thermodynamics of conversion, 11, 14
  U.S. emissions from different sectors, 7*t*
  U.S. emissions from electricity-generating units, 7*t*
  uses, 11
  U.S. production of liquid fuels in 1999, 17*t*
  U.S. production of synthetic plastics and related chemicals (1999), 15*t*

  utilization with and without chemical conversion processing, 22*f*
  world emissions from consumption of fossil fuels (1980–1997), 5*t*
  See also Catalytic reduction of CO_2; Dense phase carbon dioxide; Dimethyl carbonate (DMC); Simultaneous CO_2 and steam reforming of methane; Synthetic chemistry
Carbon dioxide mitigation. *See* Carnol process
Carbon supported cobalt catalysts. *See* Methane decomposition
Carboxylation
  mechanism, 58
  organic substrates, 60–62
Carnol process
  carbon dioxide extraction, 32
  CO_2 emission evaluation, 34, 36*t*, 38
  CO_2 from coal burning, 32–33
  economics, 34
  entire Carnol system, 37*f*
  hydrogen production, 32
  methanol and higher oxygenates as liquid automotive fuel, 33–34
  reacting hydrogen with CO_2, 33
  thermodynamics, 35*t*
Catalyst, Ni/SiO_2–MgO. *See* Methane reforming with CO_2 over Ni/SiO_2–MgO
Catalysts, Ca-based binary. *See* Methane conversion
Catalysts, Ni/Na-Y and Ni/Al_2O_3. *See* Methane reforming with CO_2 over Ni/Na-Y and Ni/Al_2O_3
Catalysts, supported Cu and Mn. *See* Methanol synthesis from CO_2 containing syngas
Catalytic conversions
  activity of CO_2 methanation for Ni–La_2O_3–Rh catalyst, 137*f*
  aimed reactions producing only syngas, 133
  alcohol distribution for different catalysts, 145*f*
  alcohol synthesis from CO_2–H_2 mixture, 140, 143, 147
  applying Ni–La_2O_3–Rh catalyst to higher space velocity of reaction gas, 137–138
  catalysts for alcohol synthesis, 143, 147
  CO_2-methanation and global warming, 136
  CO_2-methanation for Ni-based three-component composite catalyst, 136–137
  comparison of temperature-programmed reduction (TPR) profiles, 143, 144*f*
  CO- and CO_2-rich syngas, 147, 149
  Cu–Zn–Cr–Al mixed oxides catalyst by uniform gelation method, 138
  effect of catalytic oxidation of ethane and propane on CO_2-reforming of methane, 135*f*
  effect of Ga_2O_3 addition to four component catalyst, 140
  endothermic heat of reaction, 132
  ethane or propane addition in CO_2-reforming of methane, 135
  hydrocarbon synthesis from syngas, 148*f*
  methanol synthesis activity and combination of La_2O_3 and Pd or Ag, 138, 140
  methanol synthesis by CO_2 hydrogenation, 138–140
  methanol synthesis catalyst design considerations, 173, 175
  methanol synthesis for CO_2- and

Downloaded by 217.66.152.143 on September 14, 2012 | http://pubs.acs.org
Publication Date: January 24, 2002 | doi: 10.1021/bk-2002-0809.ix002

CO-rich syngas on four-component catalyst, 141*t*
methanol synthesis from CO_2 on various catalysts, 139*f*
Ni-based three-component catalyst, 132–133
Pd–Ga-modified catalyst and CO-rich syngas conversion, 140
rapid CO_2-methanation, 135–138
rapid CO_2-reforming of methane, 131–135
reviews, 132
reviews of CO_2-methanation, 136
Rh addition to Ni–Ce_2O_3–Pt catalyst, 133, 134*f*
Schulz–Flory plots for alcohol synthesis, 146*f*
selective synthesis of light olefins and gasoline from CO_2–H_2 mixture, 147–149
superior to other CO_2 conversion methods, 131
synergistic activity of composite catalyst, 133
synergistic effect of composite catalysts and combined reactions, 132–133
synthesis of ethanol from CO_2 on various catalysts, 142*f*

Catalytic oxidations
  alternative oxidants, 46–49
  ammoxidation of propane to acrylonitrile, 44*t*
  anaerobic vs. aerobic, 40–43
  carbon dioxide as mild oxidant with chromium-based catalysts, 49
  chemistry under unusual conditions, 45–46
  cost of oxygen sources, 47*t*
  coupling methane to ethylene, 41–42
  incentive for direct oxidation of paraffins, 43*f*
  Lummus process for ammoxidation of *o*-xylene to *o*-phalonitrile, 41
  Mars–van Krevelen oxidation of butane to maleic anhydride, 41*f*
  N_2O as selective oxidant for aromatics, 46–47
  new methyl methacrylate process, 45
  new process chemistry, 45–46
  nylon intermediates manufacturing, 47
  oxidation of butane to maleic anhydride, 42–43
  oxidation of propane to acrylic acid, 44*t*
  oxidation of propylene to acrolein and acrylic acid, 42
  oxidative dehydrogenation of butane to butadiene, 42
  oxidative dehydrogenation of ethane to ethylene, 46*t*
  oxidative dehydrogenation of ethane with CO_2, 49*f*, 50*t*
  oxidative dimerization of isobutylene to 2,5-dimethylhexadiene (DMH), 42
  oxidative dimerization of toluene to stilbene, 42
  paraffin oxidations, 43–44
  preparation of propylene oxide from hydrogen/oxygen mixtures, 49*f*
  proposed mechanism for N_2O oxidation of benzene, 47*f*
  schematic of two-stage oxidation of *o*-xylene, 41*f*
  selectivity, 39–40
  selectivity of chromium-based catalysts, 49*t*
  titanosilicate oxidations, 48*f*
  titanosilicates, 47–48
  typical selectivity, 40*t*

Catalytic reduction of CO_2

Downloaded by 217.66.152.143 on September 14, 2012 | http://pubs.acs.org
Publication Date: January 24, 2002 | doi: 10.1021/bk-2002-0809.ix002

basis for proposing geologic formations as slurry reactors, 176–178
batch unit, 168
carbon management, 167
catalyst evaluation studies, 168–169
catalytic hydrogenation screening runs, 175*t*
CO_2 solubility data in various solvents, 171*t*
CO_2 solubility studies, 169, 171–173
effort at Brookhaven National Laboratory (BNL) and Pennsylvania State University (PSU), 178–179
elements of catalytic system converting sequestered CO_2 to liquid fuels, 177
endothermic transformation to liquid fuels, 167
equilibrium pressure-gas mol fraction isotherm for CO_2 solubility in PEG–400 at room temperature, 172*f*
evidence for catalytic effects of certain metals, 177–178
experimental, 168–169
general scheme for aquifer/ocean sequestration of CO_2, 170*f*
geologic formations, ultimate slurry reactor, 175–179
integrated approach to catalytic CO_2 hydrogenation, 169–175
liquid phase catalytic hydrogenation of CO_2/CO, 174*t*
methanol synthesis catalyst design considerations, 173, 175
oil and gas reservoirs, 176
proposed integrated system for production of ultra clean fuels from CO_2, 170*f*
sequestration options, 167
solubility studies, 168
temperature and pressure gradients of earth, 176–177
See also Liquid fuels; Photocatalytic reduction of CO_2
Chemical conversion processing, utilization of CO_2, 21–24
Chemical processes, CO_2 conversion and utilization, 19*f*
Chemical vapor deposition (CVD) Fe/Mo/DBH catalysts
  Ag-doping, 121
  silica modification, 120–121
  See also Gas-phase O_2 oxidation of alkylaromatics
Chromium-based catalysts, carbon dioxide as mild oxidant with, 49, 50*t*
Coal, Carnol process, 32–33
Cobalt catalysts, carbon supported
  apparatus, 243
  catalytic activity, 250, 252
  catalytic activity method, 244
  characterization, 244–250
  characterization methods, 243–244
  Co dispersion, 245, 247, 250
  Co state and particle size, 245, 246*f*
  effect of reduction conditions on relative CO dispersion, 247, 250, 251*t*
  H_2 production or carbon supported catalyst at 300 or 350°C, 253*f*
  hydrogenation experiments, 252
  molar ratio of produced H_2 to decomposed CH_4 vs. reaction time, 254*f*
  physical characteristics, 244–245, 246*t*
  preparation, 242–243
  profiles of concentrations of produced H_2 and unreacted CH_4, 251*f*
  temperature programmed

Downloaded by 217.66.152.143 on September 14, 2012 | http://pubs.acs.org
Publication Date: January 24, 2002 | doi: 10.1021/bk-2002-0809.ix002

    reduction (TPR) profiles for methane decomposition, 248*f*
  TPR patterns of hydrogen obtained, 249*f*
  typical profile of CH_4, C_2H_4, and C_3H_8 production vs. hydrogenation time, 254*f*
  See also Methane decomposition
Cobalt–nickel oxide catalysts
  catalyst characterization, 227
  catalyst characterization methods, 226
  catalytic reactions for CO_2 reforming and simultaneous steam and CO_2 reforming of methane, 226
  CO_2 reforming of methane, 229
  curves for temperature programmed reduction (TPR) of catalyst with different Co/Ni ratios, 228*f*
  effect of cobalt addition to catalyst, 233, 237
  experimental, 225–226
  influence of Co/Ni ratio on catalyst performance in simultaneous CO_2 and steam reforming, 233, 234*f*
  influence of Co/Ni ratio on conversion, H_2 selectivity, and H_2/CO product ratio, 231*f*
  influence of Co/Ni ratio on pressure drop across catalyst bed, 230*f*
  influence of temperature, space velocity, and CH_4/CO_2 feed ratio, 232*f*
  optimum CO/Ni ratio, 237
  performance of catalyst with optimum Co/Ni ratio on simultaneous CO_2 and steam reforming, 235*f*, 236*f*
  practical importance of simultaneous CO_2 and steam reforming process, 237–238
  preparation of supported $Co_xNi_{1-x}O$, 225–226
  pressure drop across reactor, 237
  simultaneous CO_2 and steam reforming of methane, 233
  surface area and degree of reduction (in TPR) of supported catalysts, 227*t*
CO disproportionation
  carbon formation during CO_2 reforming of CH_4, 269–270
  equation, 276
Coking
  applications of in situ decoking concept, 368
  carbonaceous species along fixed-bed, 285, 287
  characterization of nature, 282, 285
  deposited, 282, 285, 287
  determination method, 278
  equations, 300
  evidence of rapid catalyst deactivation in fixed-bed, 282, 283*f*
  graphitic carbon deposits, 354, 357
  origin, 269–270
  resistance of noble metals, 290
  See also Methane reforming with CO_2 over Ni/SiO_2–MgO
Computational analysis of energy of methane reforming
  comparison of effects of CO_2/CH_4 and O_2/CH_4 ratio on reaction heat at different pressures, 326, 327*f*
  comparison of effects of CO_2/CH_4 and O_2/CH_4 ratios on reaction heat at different temperatures, 321, 324*f*, 325*f*
  computational method, 317–318
  effect of CO_2/CH_4 and O_2/CH_4 ratio in feedstock on reaction heat under 1 atm, 322*f*, 323*f*

Downloaded by 217.66.152.143 on September 14, 2012 | http://pubs.acs.org
Publication Date: January 24, 2002 | doi: 10.1021/bk-2002-0809.ix002

Downloaded by 217.66.152.143 on September 14, 2012 | http://pubs.acs.org
Publication Date: January 24, 2002 | doi: 10.1021/bk-2002-0809.ix002

- effect of reaction temperature and pressure on reaction heat of $CO_2 + CH_4 = 2CO + 2H_2$, 318–320
- effects of O_2/CH_4 and CO_2/CH_4 ratios on reaction heat, 320–321
- endothermic reactions, 320
- exothermic reactions, 320
- trend of changes in reaction heat with temperatures and pressures, 319*f*

Conversion
- barriers for CO_2, 20–21
- challenges and strategies for CO_2, 16, 20–24
- chemical processes, 19*f*
- CO_2, 10–11
- energy requirements, 20
- thermodynamics of CO_2, 11, 14
- *See also* Catalytic conversions; Methane conversion

Copolymerization of CO_2 with epoxides
- ^{13}C NMR spectrum, 107*f*
- CO_2 with propylene oxide (PO), 103
- component ratios in rare-earth-metal coordination catalyst system, 109
- copolymerization scheme, 105
- effect of monomer ratio on yield and molecular weight, 109*t*
- effect of pressure, 108*t*
- effect of solvent, 104, 105*t*
- effect of temperature, 108*t*
- epoxides PO and cyclohexene oxide (CHO), 103–104
- experimental, 103–104
- ^1H NMR spectrum, 107*f*
- infrared spectrum, 106*f*
- results for different yttrium coordination catalyst systems, 105, 106*t*
- screening of solvents, 104, 105*t*
- ternary rare-earth-metal coordination system, 103
- yttrium-metal coordination catalyst, 103

Copper catalysts
- Cu-loaded TiO_2 powder, 333–334
- *See also* Methanol synthesis from CO_2 containing syngas

Copper plate electrodes. *See* Electrochemical reduction of CO_2

CO reduction, pressure drop across catalyst bed, 237

Costs
- barrier for CO_2 conversion and utilization, 20
- oxygen sources, 47*t*
- *See also* Economics

Critical phase behavior, fluid mixtures, 367

Cycloalkanes, reactivity towards CO_2, 63

Cyclohexene
- homogeneous oxidation in *sc*CO_2, 373–374
- hydrogenation on supported Pd catalysts using *sc*CO_2, 370–371, 372*f*
- oxidation with fluorinated iron porphyrin catalyst, 379, 380*t*
- oxidation with non-fluorinated iron porphyrin catalyst, 379

Cyclohexene oxide. *See* Copolymerization of CO_2 with epoxides

D

Deasphalting process
- petroleum industry, 389–390
- propane, 390
- residue oil supercritical extraction (ROSE), 389

Decaffeination of coffee, supercritical CO_2, 389
Dense phase carbon dioxide
  advantages over conventional solvents in homogenous catalytic oxidation, 382
  alkylation reactions, 368–369, 372*f*
  alleviation of internal pore-diffusion resistances, 368–369
  applications, 365
  applications of in situ decoking concept, 368
  catalytic oxidation of alkenes in *sc*CO_2, 374, 375*f*
  common conditions for homogeneous catalytic O_2-oxidation of di-*tert*-butylphenol (DTBP), 378–379, 380*f*
  contrasting temperature dependence of conversion to products vs. selectivity, 377
  critical phase behavior of fluid mixtures, 367
  eliminating inter-phase mass transfer resistances, 369–373
  expanding ionic liquids with *sc*CO_2, 383
  expanding solvents by adding CO_2, 378
  heterogeneous catalytic reactions, 367–373
  homogeneous oxidation catalysis of CH_3ReO_3 and olefin epoxidation in *sc*CO_2, 374, 376
  homogeneous oxidations in *sc*CO_2, 373–377
  hydrogenation of cyclohexene on supported Pd catalysts, 370–371, 372*f*
  hydrogenation reactions, 369–370
  industrial applications in heterogeneous fluid-solid catalysis, 383
  Jacobson's catalyst for epoxidation of olefins, 376
  limitations of *sc*CO_2, 377–378
  miscibility of oxygen with *sc*CO_2, 376
  oxidation of cyclohexene with fluorinated iron porphyrin catalyst, 379, 380*t*
  oxidation of cyclohexene with non-fluorinated iron porphyrin catalyst, 379
  oxidations, hydroformylation, and esterification, 371, 373
  oxidations in CO_2-expanded solvent media, 377–381
  oxidations of di-*tert*-butylphenol, 376–377
  pressure effects, 366–367
  pressure-tunability of density and transport properties of near-critical fluids, 381–382
  selective oxidation of activated alkenes, allylic and homoallylic alcohols, 374
  thermodynamic and kinetic aspects, 366–367
Dialkoxydibutyltin, dimethyl carbonate (DMC) formation, 73
Dimethyl carbonate (DMC)
  alcohols with urea, 72–73
  dependence of DMC amount and surface area of H_3PO_4/ZrO_2 calcined at 673 K on H_3PO_4 loading, 75, 78*f*
  dependence of DMC amount and surface area on calcination temperature of H_3PO_4/ZrO_2, 79, 80*f*
  dependence of DMC amount on reaction temperature over ZrO_2 and H_3PO_4/ZrO_2, 75, 78*f*
  effect of H_3PO_4/ZrO_2 preparation method on DMC formation, 81, 83*t*

Downloaded by 217.66.152.143 on September 14, 2012 | http://pubs.acs.org
Publication Date: January 24, 2002 | doi: 10.1021/bk-2002-0809.ix002

- effect of modified ZrO_2 catalysts calcined at 673 K and 925 K on DMC formation, 75, 77*t*
- ethylene oxide route, 73
- experimental, 74
- large-scale production methods, 72–73
- LRS spectra of fresh H_3PO_4/ZrO_2 by different preparation methods, 81, 82*f*
- methanol and CO_2 with dialkoxybutyltin, 73
- methanol and CO_2 with zirconia catalysts, 73–74
- methanol and phosgene in sodium hydroxide, 72
- oxidative carbonylation of methanol, 72
- oxidative carbonylation using palladium and methyl nitrite, 72
- preparing H_3PO_4/ZrO_2 by different method, 79
- results of methanol and carbon dioxide over heterogeneous catalysts, 75, 76*t*
- supercritical CO_2 and trimethyl orthoacetate, 73
- XRD patterns of fresh H_3PO_4/ZrO_2 by different preparation methods, 79, 81*f*
- XRD patterns of fresh H_3PO_4/ZrO_2 calcined at various temperatures, 79, 80*f*
- XRD patterns of fresh H_3PO_4/ZrO_2 with various H_3PO_4 loadings, 75, 79*f*

2,5-Dimethylhexadiene, oxidative dimerization of isobutylene, 42

Dinitrogen oxide (N_2O)
- nylon intermediates manufacturing, 47
- proposed mechanism for N_2O oxidation of benzene, 47*f*
- selective oxidant for aromatics, 46–47
- *See also* Catalytic oxidations

Di-*tert*-butylphenol (DTBP)
- homogeneous catalytic O_2-oxidation, 378–379, 380*f*
- oxidations in *sc*CO_2, 376–377

E

Economics
- Carnol process, 34
- *See also* Costs

Electrochemical reduction of CO_2
- black film on surface of electrodes, 354, 357
- CH_4 and C_2H_4 generation by graphite reduction, 357
- chemical fixation of CO_2, 345
- copper/gas-diffusion and copper plate electrodes, 348, 354, 357
- Cu electrode in hydrogen carbonate solution, 345
- Cu/gas diffusion and Cu plate electrodes vs. potential, 349*f*
- electrolysis cell with gas-diffusion electrode, 347*f*
- equations for formation of C_2H_4 and CH_4, 354
- experimental, 346–348
- Faradaic efficiencies with Cu/gas-diffusion electrode, 351*f*
- Faradaic efficiencies with Cu plate electrode, 350*f*
- graphite formation with copper oxide involvement, 357
- major products in two electrolysis systems vs. potential, 352*f*, 353*f*
- modified Pt/gas-diffusion electrode, 357–359
- products of modified Pt/gas-diffusion electrode, 358*t*
- reduction scheme on polymer-modified electrode, 359, 360*f*
- total concentration of products vs.

Downloaded by 217.66.152.143 on September 14, 2012 | http://pubs.acs.org
Publication Date: January 24, 2002 | doi: 10.1021/bk-2002-0809.ix002

Downloaded by 217.66.152.143 on September 14, 2012 | http://pubs.acs.org
Publication Date: January 24, 2002 | doi: 10.1021/bk-2002-0809.ix002

    electric charge on Cu/gas-diffusion electrode, 356*f*
  total concentration of products vs. electric charge on plate electrode, 355*f*
Electrodes, gas-diffusion. *See* Electrochemical reduction of CO_2
Emissions
  control issues, 8*f*
  control of CO_2, 6, 9
  energy choice, 6
  energy efficiency, 9
  evaluation of Carnol process, 34, 36t, 38
  greenhouse gases, 8*t*
  renewable energy, 9
  sources of CO_2, 3, 6
  stationary, mobile, and natural sources of CO_2, 4*t*
  U.S., of CO_2 from different sectors, 7*t*
  U.S., of CO_2 from electricity-generating units, 7*t*
  worldwide from consumption of fossil fuels, 5*t*
  See also Catalytic oxidations
Energetics
  carbon dioxide utilizing reactions, 55–56
  CO_2 transformation to liquid fuels, 167
  See also Computational analysis of energy of methane reforming; Gibbs free energy
Energy choice, CO_2 emission control, 6
Energy efficiency, CO_2 emission control, 9
Energy recovery, 24
Energy requirements, barrier for CO_2 conversion and utilization, 20
Energy supply, CO_2 formation, 3
Environmentally benign solvents
  expanding room temperature ionic liquids, 383
  supercritical and near-critical dense carbon dioxide, 364–365
  See also Dense phase carbon dioxide
Epoxides. *See* Copolymerization of CO_2 with epoxides
Esterification, dense phase CO_2, 371, 373
Ethane
  addition to CO_2-reforming of methane, 135
  oxidative dehydrogenation to ethylene, 45–46
  oxidative dehydrogenation with CO_2, 49, 50*t*
  See also Methane conversion
Ethylbenzene
  oxidation of derivatives, 122–123
  See also Gas-phase O_2 oxidation of alkylaromatics
Ethylene
  coupling methane, 41–42
  oxidative dehydrogenation of ethane, 45–46
  See also Methane conversion
Ethylene oxidation
  selectivity, 40*t*
  See also Catalytic oxidations
Extraction. *See* Supercritical extraction

F

Fe/Mo/DBH catalyst. *See* Gas-phase O_2 oxidation of alkylaromatics
Fischer–Tropsch synthesis catalysts, hydrocarbons and oxygen-containing compounds, 147
Fixation

Downloaded by 217.66.152.143 on September 14, 2012 | http://pubs.acs.org
Publication Date: January 24, 2002 | doi: 10.1021/bk-2002-0809.ix002

- greenhouse gas concentration in atmosphere, 345
- role of metal in CO_2, 56, 60

Fluidized- and fixed-bed reactors
- illustration of fluidized, 306*f*
- *See also* Methane reforming with CO_2 and O_2; Methane reforming with CO_2 over Ni/SiO_2–MgO

Fluid mixtures, critical phase behavior, 367

Formation, routes for CO_2, 3

Fuel production. *See* Carnol process

Fuels, liquid, U.S. production in 1999, 17*t*

G

Gas-diffusion electrodes. *See* Electrochemical reduction of CO_2

Gasoline and olefins
- CO- and CO_2-rich syngas, 147, 149
- hydrocarbon synthesis from syngas, 148*f*
- selective synthesis from CO_2–H_2 mixture, 147–149
- *See also* Catalytic conversions

Gas-phase O_2 oxidation of alkylaromatics
- active catalytic sites form terephthaldehyde and *p*-tolualdehyde formation, 114, 115
- alkylaromatics over chemical vapor deposition (CVD) Fe/Mo/DBH (deboronated borosilicate molecular sieve HAMS-1B-3) catalyst, 113
- anaerobic condition in presence of CO_2 without O_2 in feed stream, 118*f*
- chemical modification of CVD Fe/Mo/DBH with Ag-doping, Ag/Fe/Mo/DBH, 121
- chemical modification of CVD Fe/Mo/DBH with silica deposition, Si/Fe/Mo/DBH, 120–121
- controlling molar ratio of terephthaldehyde to *p*-tolualdehyde, 114
- co-presence of CO_2 in O_2 feed stream, 113
- effect of CO_2 on *p*-xylene over CVD Fe/Mo/DBH vs. reaction temperature, 116*f*
- *p*-ethylbenzene and styrene in CO_2 plus O_2 over CVD Fe/Mo/DBH, 122*t*
- ethylbenzene derivatives, 122–123
- experimental results on *p*-xylene oxidation, 117*t*
- mechanism, 123–125
- peroxocarbonate intermediate, 124–125
- polymethylbenzenes, 117
- preparation of CVD Fe/Mo/DBH, 113
- selectivity of terephthaldehyde and *p*-tolualdehyde, 117, 119*f*
- synergistic interaction of catalytic species with DBH, 123–124
- *p*-xylene over Ag/Fe/Mo/DBH, 121*t*
- *p*-xylene over CVD Fe/Mo/DBH, 113–117
- *p*-xylene over DBH host matrix, 124*t*
- *p*-xylene over silica modified catalyst, CVD Si/Fe/Mo/DBH, 120*t*

Geologic formation
- basis for approach as slurry reactor, 176–178
- effort at Brookhaven National

Downloaded by 217.66.152.143 on September 14, 2012 | http://pubs.acs.org
Publication Date: January 24, 2002 | doi: 10.1021/bk-2002-0809.ix002

  Laboratory (BNL) and Pennsylvania State University (PSU), 178–179
  evidence for catalytic effects of certain metals in naturally occurring rocks, 177–178
  oil and gas reservoirs, 176
  temperature and pressure gradients of earth, 176–177
  See also Catalytic reduction of CO_2
Gibbs free energy
  elimination pathways from metallo-carboxylate system, 59
  formation, 13*f*
  thermodynamics of CO_2 conversion, 11, 14
Global warming, CO_2 methanation, 136
Green chemistry, CO_2 attracting attention, 112
Greenhouse gas (GHG)
  carbon dioxide, 3
  emissions, 8*t*
  methane reforming with CO_2, 197–198

H

Heterogeneous catalytic reactions, dense phase CO_2, 367–373
High pressure. *See* Pressure effects
Hydroformylation, dense phase CO_2, 371, 373
Hydrogen
  production by Carnol process, 32
  reaction with carbon dioxide, 33
Hydrogenation
  Cu–Zn–Cr–Al mixed oxide catalyst by uniform gelation method, 138
  cyclohexene on supported Pd catalysts using *sc*CO_2, 370–371, 372*f*
  dense phase CO_2, 369–370
  effect of Ga_2O_3 addition to four component catalyst, 140
  first pilot test plant, 138
  integrated approach to catalytic, 169–175
  methanol synthesis activity, 138, 140
  methanol synthesis by CO_2, 138–140
  methanol synthesis for CO_2- and CO-rich syngas on four-component catalyst, 141*t*
  methanol synthesis from CO_2 on various catalysts, 139*f*
  Pd–Ga-modified catalyst for CO-rich syngas conversion, 140
  See also Catalytic conversion; Methanol synthesis from CO_2 containing syngas

I

Insertion reaction, CO_2 into C–C bonds, 62, 63
Investment incentives, barrier for CO_2 conversion and utilization, 20
Iridium-loaded catalysts, methane reforming of CO_2, 207
Isobutylene, oxidative dimerization to 2,5-dimethylhexadiene (DMH), 42
Isocyanates, synthesis, 65–66

K

Kinetics, dense phase CO_2, 366–367
Kolbe–Schmitt reaction, carboxylation, 66–67

Downloaded by 217.66.152.143 on September 14, 2012 | http://pubs.acs.org
Publication Date: January 24, 2002 | doi: 10.1021/bk-2002-0809.ix002

L

La_2O_3 catalysts, Ru-loaded. *See* Methane reforming with CO_2
Liquid fuels
  Carnol process, 33–34
  liquid phase catalytic hydrogenation of CO_2/CO, 174*t*
  methanol and higher oxygenates as automotive, 33–34
  proposed integrated system for producing ultra clean, from CO_2, 169, 170*f*
  U.S. production in 1999, 17*t*
  See also Catalytic reduction of CO_2
Low temperature methane decomposition. *See* Methane decomposition
Lummus process
  ammoxidation of *o*-xylene to *o*-phalonitrile, 41
  See also Catalytic oxidations

M

Maleic anhydride, butane oxidation to, 42–43
Manganese catalysts. *See* Methanol synthesis from CO_2 containing syngas
Manufacturing industrial products, CO_2 formation, 3
Market, potential, CO_2 utilization, 14, 16
Market size, barrier for CO_2 conversion and utilization, 20
Mars–van Krevelen
  oxidation of butane to maleic anhydride, 41*f*
  See also Catalytic oxidations
Mass transfer resistances, eliminating inter-phase, 369–373
Mechanism
  CO_2 conversion, 56–60
  oxidation, 123–125
  See also Synthetic chemistry
Metal oxides. *See* Methane conversion
Metals
  catalysis in butadiene-CO_2 chemistry, 62
  elimination pathways from metallo-carboxylate system, 59
  exchange reaction between olefin and Ni–CO_2 complex, 58
  free energy change, 59
  modes of interaction of M–olefin system with CO_2, 58
  role in CO_2 fixation, 56, 60
  See also Synthetic chemistry
Methanation reactions
  activity for Ni–La_2O_3–Ru catalyst, 137*f*
  applying Ni–La_2O_3–Ru catalyst higher space velocity of reaction gas, 137–138
  global warming, 136
  Ni-based three-component catalyst, 136–137
  rapid CO_2-, 135–138
  review, 136
Methane conversion
  amounts of CO_2 chemisorbed on Ca binary catalysts after reaction, 99*f*
  C_2 yield over Ca–Cr and Ca–Mn catalysts, 91, 93*f*
  catalyst characterization, 88–89
  catalyst composition, 89, 91
  catalyst materials and preparation, 86, 88
  catalytic runs and product analysis, 88
  chemisorption of CO_2 and catalyst state, 96, 98
  CO_2 hydrogenation, 138–140
  coupling to ethylene, 41–42
  dependence of, and C_2 selectivity

    on partial pressure of CO_2 over Ca–Ce catalyst, 91, 95*f*, 96
  dependence of, and C_2 selectivity on partial pressure of CO_2 over Ca–Cr or Ca–Mn, 96, 97*f*
  dependence of yields of C_2H_6 and C_2H_4 at equilibrium on CO_2/CH_4 ratio and temperature, 87*f*
  effect of catalyst composition on, with binary Ca–Cr and Ca–Mn catalysts, 91, 92*f*
  effect of catalyst composition on performance of binary Ca–Ce catalysts, 89, 90*f*
  effect of time on stream of C_2 yield over Ca binary catalysts, 91, 95*f*
  equations for formation of C_2 hydrocarbons, 86
  formation rates of products in reaction of CH_4 alone with Ca–Ce and Ca–Cr oxides, 94*f*
  partial pressure of CO_2, 91, 96
  profiles for CO_2 desorption during temperature programmed desorption (TPD) measurements in different atmospheres of Ca–Ce catalyst, 97*f*
  proposed reaction mechanisms, 98, 100
  relationship between CH_4 conversion and C_2 selectivity in reaction with various metal oxides, 87*f*
  results of catalyst characterization, 98, 99*t*
  results of CeO_2 impregnated with nitrate solutions, 89, 92*t*
Methane decomposition
  catalyst characterization, 244–250
  catalyst characterization methods, 243–244
  catalyst preparation, 242–243
  catalytic activity, 250, 252
  catalytic activity method, 244
  characteristics and activities of catalysts, 246*t*
  Co dispersion, 245, 247, 250
  Co state and particle size of catalysts, 245, 246*f*
  effect of reduction conditions on relative Co dispersion of catalyst, 247, 250, 251*t*
  equation, 276
  experimental apparatus, 243
  H_2 production on carbon supported catalyst at 300 or 350°C, 253*f*
  high surface area supports, 242
  hydrogenation experiments using Co supported catalyst, 252
  main phases of Co in high loading catalysts, 245, 247
  molar ratio of produced H_2 to decomposed CH_4 vs. reaction time, 254*f*
  physical characteristics of catalysts, 244–245
  pressure drop across catalyst bed, 237
  profiles of concentrations of produced H_2 and unreacted CH_4 for all catalysts, 251*f*
  reaction, 208, 210
  supported Pt, Ru and Co metal catalysts, 242
  temperature programmed reduction (TPR) profiles using all catalysts, 248*f*
  TPR patterns of hydrogen using all catalysts, 249*f*
  typical profile of CH_4, C_2H_4, and C_3H_8 production vs. hydrogenation time, 254*f*
Methane dry reforming
  activity and stability of catalysts, 183–184

Downloaded by 217.66.152.143 on September 14, 2012 | http://pubs.acs.org
Publication Date: January 24, 2002 | doi: 10.1021/bk-2002-0809.ix002

Downloaded by 217.66.152.143 on September 14, 2012 | http://pubs.acs.org
Publication Date: January 24, 2002 | doi: 10.1021/bk-2002-0809.ix002

  carbide and Ni-based catalysts, 185*t*
  catalyst preparation, 185–186
  deactivating nickel catalyst, 183
  experimental, 184
  high surface area tungsten and molybdenum carbides, 184
  initial catalytic activity of carbide, Ni-based, and noble metal catalysts, 193
  molybdenum carbide at 850°C, 186, 187*f*
  molybdenum carbide with TiO_2, 186
  molybdenum carbide with TiO_2 at 900°C, 188*f*
  Ni-based catalyst at 750°C, 194*f*
  nickel-based catalysts, 190
  photoelectron spectra of tungsten carbide catalyst before and after reaction, 192*f*
  rhodium supported on alumina, 193
  1% Rh on alumina at 716°C, 194*f*
  role of operating conditions and catalyst support, 183
  SEM photographs of tungsten carbide catalyst before and after reaction, 191*f*
  thermodynamic calculations for molybdenum and tungsten carbides, 190*t*
  tungsten carbide at 850°C, 187*f*
  tungsten carbide characterization before and after reaction, 186, 190
  X-ray diffraction pattern of tungsten carbide catalyst before and after reaction, 189*f*
Methane reforming with CO_2
  activity and stability of Ni/u-ZrO_2 catalysts, 199, 203
  aimed reactions producing only syngas, 133
  alumina, titania, and silica-supported catalysts, 208
  Boudouard reaction, 208, 210
  carbon formation over metal catalysts, 206–207
  catalyst preparation, 198
  CO/Ni catalysts, 229
  conversions of methane and CO_2 and selectivity to CO and H_2, 201*t*
  effect of Ar and CO_2 pretreatments, 217
  effect of pretreatment conditions on activity over Ru/La_2O_3, 212*f*, 213*f*
  effect of pretreatment conditions on activity over Ru/Y_2O_3, 214*f*, 215*f*
  effect of pretreatment on activity of noble metal-loaded Y_2O_3 catalysts, 217, 221*t*
  effect of pretreatment on activity over metal oxide supported Ru catalysts, 210, 216*t*
  effect of time on stream (TOS) on methane conversion over Ru-loaded catalysts, 208, 209*f*
  endothermic heat of reaction, 132
  equation, 276
  ethane or propane addition, 135
  experimental, 198, 207–208
  influence of Co/Ni ratio in catalyst on conversion, H_2 selectivity, and H_2/CO product ratio, 231*f*
  influence of Co/Ni ratio in catalyst on pressure drop across catalyst bed, 230*f*
  influence of space velocity (GHSV) on methane conversion over 27%Ni/u-ZrO_2, 199, 201*t*
  influence of temperature, space velocity and CH_4/CO_2 feed ratio, 232*f*

methane and CO_2 conversions vs. TOS over u-ZrO_2, 202*f*
methane conversion vs. reaction TOS over Ni catalysts, 200*f*
methane conversion vs. TOS over Ni/u-ZrO_2 catalysts with different Ni loadings, 200*f*
methane decomposition, 208, 210
Ni-based three-component catalyst, 132–133
performance of iridium-loaded catalysts, 207
producing synthesis gas, 197–198
product distributions for methane conversion over Ru-loaded catalysts, 208, 209*t*
rapid, 131–135
reactions for production of synthesis gas, 206
reviews, 132
Rh addition to Ni-based three-component catalyst, 133, 134*f*
Ru-loaded Y_2O_3 and La_2O_3 catalysts, 210
synergistic effect of composite catalysts and combined reactions, 132–133
transition metals (group VIII) on metal oxides as catalysts, 206
XRD analyses of Ru/La_2O_3 catalyst after reaction, 211*f*
XRD analyses of Ru/Y_2O_3 and Ru/Al_2O_3 catalysts before and after Ar or CO_2 pretreatments, 218*f*, 219*f*, 220*f*
See also Catalytic conversion; Cobalt-nickel oxide catalysts; Computational analysis of energy of methane reforming; Simultaneous CO_2 and steam reforming of methane

Methane reforming with CO_2 and O_2
comparison of CH_4 and CO_2 conversion, and H_2/CO between fluidized and fixed bed, 307*f*
dependence of CH_4 and CO_2 conversion, H_2/CO ratio and temperature difference on space velocity, 308*f*, 309
dependence of CH_4 conversion on space velocity using fluidized bed and fixed bed reactor, 312–313
dependence of conversion and H_2/CO ratio on total pressure over $Ni_{0.03}Mg_{0.97}O$, 310
effect of introduction method on CH_4 conversion vs. space velocity using fixed bed reactor, 311*f*, 312
effect of oxygen concentration on conversion, H_2/CO ratio, and temperature difference, 309–310
effect of reaction temperature on CH_4 and CO_2 conversion and H_2/CO ratio, 307*f*, 308
experimental, 305
heat supply problem, 304
illustration of fluidized bed reactors, 306*f*
internal heat supply using fluidized bed reactor, 304
model of fluidized bed reactor, 313–314
$Ni_xMg_{1-x}O$ catalyst preparation by coprecipitation, 305
pressurized syngas, 304
reforming method, 305
reforming under atmospheric pressure condition, 306–310
reforming under pressurized condition, 310–314
temperature gradient in catalyst bed, 304
See also Computational analysis of energy of methane reforming

Downloaded by 217.66.152.143 on September 14, 2012 | http://pubs.acs.org
Publication Date: January 24, 2002 | doi: 10.1021/bk-2002-0809.ix002

Methane reforming with CO_2 over Ni/Na-Y and Ni/Al_2O_3
  activity and performance of commercial catalysts, 270, 271*t*, 272
  analysis of used Ni/Na-Y and Ni/Al_2O_3 after reaction, 266–267
  carbon monoxide disproportionation, 269–270
  catalyst Ni/Na-Y and Ni/Al_2O_3 preparation, 259
  CO_2 conversion as function of time on stream (TOS) for catalysts, 261, 262*f*
  computational analysis of thermodynamics, 270
  conversion and product yields, 263*t*
  effect of Ni loading in Ni/Na-Y catalyst on CH_4 and CO_2 conversion, 265–266
  effect of reaction pressure on CO_2 and CH_4 conversion on Ni/Na-Y, 264*f*
  effect of reaction temperature on CO_2 and CH_4 conversion on Ni/Na-Y, 263*f*
  experimental, 259–260
  filamentous and amorphous carbon on catalyst surface, 269
  monitoring catalyst bed temperature, 260
  Ni/Na-Y by incipient wetness impregnation (IWI), 266
  origin of carbon formation, 269
  physicochemical properties of Ni catalysts supported on Na-Y and γ-Al_2O_3, 260–261
  preferring high pressure conditions for industrial operation, 258–259
  reaction conditions, 259–260
  resistance of Ni/MgO or Ni/CaO to coke formation, 270
  SEM photographs of Ni catalysts before and after use, 267, 268*f*, 269
  surface area determinations, 259
  temperature programmed oxidation (TPO) for catalysts before and after reaction, 267
Methane reforming with CO_2 over Ni/SiO_2–MgO
  apparatus and conditions for reforming, 277–278
  carbonaceous species along fixed-bed, 285, 287
  catalyst preparation and characterization, 277
  catalytic activity using fluidized- and fixed-bed reactors, 278, 280–287
  characterization of nature of coke, 282, 285
  coke determination, 278
  conditions for fluidized- and fixed-bed experiments, 278
  conversions as function of space velocity using fixed-bed reactor, 279*f*
  deposited coke, 282, 285, 287
  effects of catalyst-bed temperature, 280, 281*f*, 282
  equations, 276
  evidence of rapid catalyst deactivation in fixed-bed, 282, 283*f*
  fluidized-bed reactor use, 276
  limitations of fixed-bed reactor, 276
  profiles of pressure-drop, 282
  reforming results, 280*t*, 281*f*
  XPS analysis of fresh and spent catalyst, 284*f*
  XPS relative intensities of crystallized to amorphous forms and surface elemental compositions of catalyst, 285*t*
  XPS spectra of top and bottom

Downloaded by 217.66.152.143 on September 14, 2012 | http://pubs.acs.org
Publication Date: January 24, 2002 | doi: 10.1021/bk-2002-0809.ix002

Downloaded by 217.66.152.143 on September 14, 2012 | http://pubs.acs.org
Publication Date: January 24, 2002 | doi: 10.1021/bk-2002-0809.ix002

recovered catalyst samples, 286*f*

Methane reforming with CO_2 over Rh/Na-Y and Rh/Al_2O_3
- carbon types on coked catalysts, 300
- catalyst preparation by incipient wetness impregnation (IWI), 290
- CO_2 conversion for atmospheric- and high-pressure, 293*f*
- CO and H_2 yields at atmospheric- and high-pressure, 294*f*
- coking equations, 300
- conversion and product yields, 293*t*
- conversion and product yields for atmospheric- and high-pressure, over Rh/Na-Y (ion exchange, IE) and Rh/Na-Y (IWI), 296–297
- decrease in activity between atmospheric- and high-pressure operations, 292, 294
- effect of Rh loading in catalysts by IWI, 297–298
- experimental, 290–291
- H_2 and CO pulse chemisorption of Rh catalysts before and after, 294–295
- metals favoring coking, 300–301
- performance of supported Ni catalysts for atmospheric- and high-pressure, 295
- physico-chemical properties of catalysts, 291, 292*t*
- reaction conditions, 290–291
- resistance of noble metals to coking, 290
- Rh catalysts and deactivation, 294
- Rh/Na-Y by IE preparation vs. Rh catalysts on amorphous supports, 296
- SEM photographs of fresh and used catalysts, 298–299
- surface area determination, 290
- temperature programmed oxidation (TPO) of used catalysts, 299–300

Methanol
- catalyst design considerations, 173, 175
- liquid automotive fuel, 33–34

Methanol synthesis from CO_2 containing syngas
- activity of Cu–Mn oxide on commercial support, 159*f*
- catalysis of bulk Cu–Mn oxide, 156–158
- catalysis of Cu–Mn-O/TiO_2, 162
- catalysis of Cu–Mn-O/ZrO_2, 160
- catalysis of supported Cu–Mn oxide, 158, 160, 162
- comparison of Cu–Mn-O loading effect, 164*f*
- Cu–Mn synergy on TiO_2, 162*f*
- Cu–Mn synergy on ZrO_2, 161*f*
- effect of CO_2 on activity of Cu–Mn oxide bulk catalyst, 157–158
- effect of Cu–Mn-O loading on TiO_2, 164*f*
- effect of Cu–Mn-O loading on ZrO_2, 160*f*
- effect of Cu/Mn ratio on activity and surface area, 156
- experimental, 154–156
- list of commercial support, 154*t*
- preparation of high surface area support, 155
- preparation of TiO_2 support, 159*f*
- preparation of ZrO_2 and TiO_2 with high surface area, 158, 160
- STY and surface area as function of Cu content of Cu–Mn oxide, 156*f*

STY from CO/H_2 as function of Cu content of Cu–Mn oxide, 157*f*
synergistic effect of Cu and Mn, 153–154
XRD of Cu–Mn-O on TiO_2, 163*f*
XRD of Cu–Mn-O on ZrO_2, 161*f*
See also Catalytic conversions; Hydrogenation; Olefins and gasoline
Methyl methacrylate, new process, 45
Methyl nitrite, dimethyl carbonate (DMC) synthesis, 72
Mitigation technology. *See* Carnol process; Catalytic conversions
Molybdenum carbide
dry reforming of methane at 850°C, 187*f*
preparation and methane dry reforming, 186
thermodynamic calculations, 190*t*
with TiO_2, dry reforming of methane at 900°C, 188*f*
See also Methane dry reforming
Multi-functional catalysts. *See* Catalytic conversions

N

Nickel catalysts
addition of cobalt for conversion of methane to syngas, 225
commercial catalyst testing, 190
deactivation, 183
dry reforming of methane at 750°C, 194*f*
methane dry reforming, 185
See also Cobalt-nickel oxide catalysts; Methane dry reforming; Methane reforming with CO_2; Methane reforming with CO_2 and O_2
Ni/Na-Y and Ni/Al_2O_3 catalysts. *See* Methane reforming with CO_2 over Ni/Na-Y and Ni/Al_2O_3
Nylon intermediate manufacturing, dinitrogen oxide, 47

O

Olefin epoxidation, oxidation in dense phase CO_2, 374, 376
Olefins, epoxidation using Jacobson's catalyst, 376
Olefins and gasoline
CO- and CO_2-rich syngas, 147, 149
hydrocarbon synthesis from syngas, 148*f*
selective synthesis from CO_2–H_2 mixture, 147–149
See also Catalytic conversions
Oxidants
cost of oxygen sources, 46, 47*t*
N_2O as selective for aromatics, 46–47
N_2O in nylon intermediates manufacturing, 47
proposed mechanism for N_2O oxidation of benzene, 47*f*
titanosilicates, 47–48
Oxidations
dense phase CO_2, 371, 373
homogeneous, in *sc*CO_2, 373–377
See also Catalytic oxidations; Gas-phase O_2 oxidation of alkylaromatics
Oxygen
miscibility with *sc*CO_2, 376
See also Methane reforming with CO_2 and O_2
Oxygenates, methanol and higher, liquid automotive fuel, 33–34

Downloaded by 217.66.152.143 on September 14, 2012 | http://pubs.acs.org
Publication Date: January 24, 2002 | doi: 10.1021/bk-2002-0809.ix002

P

Paffin
  analytical of extraction of asphalts, 394–395
  asphalt constituents, 391–392
  extraction from asphalt, 395–398
  extraction yields from asphalt, 399
  incentive for direct oxidation, 43*f*
  oxidations, 43–44
  production, 390
  See also Asphalt
Pennsylvania State University (PSU), integrating CO_2 sequestration with conversion in geologic formations, 178–179
Petroleum industry
  applications of supercritical extraction, 388
  CO_2 production, 388
  deasphalting, 389–390
  tailoring analytical methods, 392
  See also Asphalt; Deasphalting process; Paraffin
Phenol, enzymatic conversion to 4-OH-benzoate, 67
Phosgene, dimethyl carbonate (DMC) synthesis, 72
Photocatalytic reduction of CO_2
  Cu-loaded and Pt-loaded TiO_2 powder, 333–334
  design of systems, 330
  effect of Pt-loading on photocatalytic activity of Ti-containing zeolite, 338–339
  effects of number of Ti-O layers of anchored Ti-oxide catalysts, 340*f*
  effects of TiO_2 contents on yields of CH_4 and relative intensity of photoluminescence of Ti/Si binary oxide catalysts, 341*f*
  ESR signals with TiO_2 under UV-irradiation in presence of CO_2 and H_2O, 333*f*
  photoluminescence spectrum of Ti-oxide anchored on zeolite, 336*f*
  physical properties and photocatalytic activity of TiO_2 catalysts, 333*t*
  product distribution of large-pore Ti-containing zeolite, Ti-Beta, 339
  product distributions of powdered TiO_2 and Ti-oxide/Y-zeolite catalysts, 336–337
  reaction scheme, 331*f*
  small particle TiO_2 catalysts, 332–333
  Ti-containing zeolite and mesoporous molecular sieves, 337–339
  TiO_2 single crystals, 334–335
  Ti-oxide anchored in zeolite (ion exchange), 335–337
  Ti-oxide anchored on porous silica glass (CVD), 340
  Ti/Si binary oxide (sol-gel), 341
  titanium oxide catalysts, 331–332
  utilization of solar energy, 330–331
  XANES and Fourier transformation of EXAFS spectra of Ti-oxide/Y-zeolites, 335*f*
  yields of CH_3OH and CH_4 per unit weight Ti-based catalysts, 338*f*
  yields of formation of CH_4 and CH_3OH in, with water, 334*t*
  See also Catalytic reduction of CO_2
Physical adsorption, separation of gas mixtures, 10
Platinum catalysts, Pt-loaded TiO_2 powder, 333–334

Downloaded by 217.66.152.143 on September 14, 2012 | http://pubs.acs.org
Publication Date: January 24, 2002 | doi: 10.1021/bk-2002-0809.ix002

Platinum/gas-diffusion electrode. *See* Electrochemical reduction of CO_2
Polymethylbenzenes. *See* Gas-phase O_2 oxidation of alkylaromatics
Pore-diffusion resistances, alleviation of internal, 368–369
Pressure effects
  dense phase CO_2, 366–367
  See also Computational analysis of energy of methane reforming; Methane reforming with CO_2 and O_2; Methane reforming with CO_2 over Ni/Na-Y and Ni/Al_2O_3; Methane reforming with CO_2 over Rh/Na-Y and Rh/Al_2O_3
Pretreatments. *See* Methane reforming with CO_2
Propane
  addition to CO_2-reforming of methane, 135
  ammoxidation to acrylonitrile, 44*t*
  oxidation to acrylic acid, 44*t*
Propylene, epoxidation to propylene oxide, 48, 49*f*
Propylene ammoxidation
  selectivity, 40*t*
  See also Catalytic oxidations
Propylene oxidation
  acrolein and acrylic acid, 42
  selectivity, 40*t*
  See also Catalytic oxidations
Propylene oxide. *See* Copolymerization of CO_2 with epoxides

R

Reaction heat. *See* Computational analysis of energy of methane reforming
Recycling
  CO_2, 24
  sequestration option, 167
Reduction. *See* Catalytic reduction of CO_2; Electrochemical reduction of CO_2; Photocatalytic reduction of CO_2
Renewable energy, CO_2 emission control, 9
Research, utilization of CO_2, 21–24
Residue oil supercritical extraction (ROSE), industrial process, 389
Reverse water-gas-shift (RWGS) reaction, equation, 276
Rh catalysts. *See* Methane reforming with CO_2 over Rh/Na-Y and Rh/Al_2O_3
Rhodium on alumina
  dry reforming of methane at 716°C, 194*f*
  noble metal catalyst for dry reforming of methane, 193
  See also Methane dry reforming
Ruthenium-loaded catalysts. *See* Methane reforming with CO_2

S

Sequestration
  CO_2, 9–10
  effort at Brookhaven National Laboratory (BNL) and Pennsylvania State University (PSU), 178–179
  scheme for aquifer/ocean, of CO_2, 169, 170*f*
  subterranean CO_2 options, 167
  See also Catalytic reduction of CO_2
Silica glass, Ti-oxide anchored on porous, 340
Simultaneous CO_2 and steam reforming of methane

Downloaded by 217.66.152.143 on September 14, 2012 | http://pubs.acs.org
Publication Date: January 24, 2002 | doi: 10.1021/bk-2002-0809.ix002

Downloaded by 217.66.152.143 on September 14, 2012 | http://pubs.acs.org
Publication Date: January 24, 2002 | doi: 10.1021/bk-2002-0809.ix002

- catalyst performance at optimum Co/Ni ratio, 235*f*, 236*f*
- Co/Ni catalysts, 233
- influence of Co/Ni ratio on catalyst performance, 234*f*
- *See also* Cobalt–nickel oxide catalysts

Solar energy, utilization, 330–331
Solubility
- CO_2 studies, 169, 171–173
- *See also* Catalytic reduction of CO_2

Solvent expansion
- addition of CO_2, 378
- ionic liquids with *sc*CO_2, 383

Solvents, environmentally benign chemical processing, 364
Steam reforming of methane. *See* Simultaneous CO_2 and steam reforming of methane
Stilbene, oxidative dimerization of toluene, 42
Styrene. *See* Gas-phase O_2 oxidation of alkylaromatics
Supercritical alkylation, dense phase CO_2, 368–369
Supercritical CO_2
- limitations, 377–378
- solvent expansion, 378, 383
- *See also* Dense phase carbon dioxide

Supercritical extraction
- analytical of paraffin extraction of asphalts, 394–395
- CO_2, 23
- experimental results, 395–398
- extraction conditions, 393–394
- selectivity, 390–391
- solvating capacity of CO_2, 388–389
- *See also* Asphalt; Paraffin; Petroleum industry

Supercritical fluids, applications in processing materials, 389
Supported copper and manganese. *See* Methanol synthesis from CO_2 containing syngas
Syngas
- methane reforming with CO_2, 197–198
- methanol syntheses from CO_2- and CO-rich, on four-component catalyst, 140, 141*t*
- pressurized, 304
- selective synthesis of light olefins and gasoline from CO_2–H_2 mix, 147–149
- *See also* Catalytic conversions; Methanol synthesis from CO_2 containing syngas

Synthesis. *See* Dimethyl carbonate (DMC)
Synthetic chemistry
- biotechnological synthesis of 4-OH-benzoic acid, 68
- carboxylation of organic substrates, 60–62
- carboxylation reactions, 58
- coupling chemistry with biotechnology, 66–68
- coupling of two CO_2 molecules, 61
- development of carbon dioxide-based industry, 55
- elimination pathways form metallo-carboxylate system, 59
- energetics of carbon dioxide utilizing reactions, 55–56
- enzymatic conversion of phenol to 4-OH-benzoate, 67
- exchange reaction occurring when olefin reacts with Ni–CO_2 complex, 58
- free energy change of elimination step, 59
- insertion of CO_2 into C–C bonds, 62, 63
- Kolbe–Schmitt reaction, 67

- mechanism of CO_2 conversion, 56–60
- metal catalysis in butadiene-CO_2 chemistry, 61–62
- modes of interaction of M–olefin with CO_2, 58
- reactivity of coordinated CO_2 towards electrophile, 57
- reactivity of cycloalkanes towards CO_2, 63
- reduction reactions, 56
- role of metal in CO_2 fixation, 56, 60
- synthesis of carbamates and isocyanates, 65–66
- synthesis of carbonates, 62, 64–65
- transesterification reactions, 66
- utilization of carbon dioxide, 55

Synthetic plastics, U.S. production in 1999, 15*t*

T

Temperature effects. *See* Computational analysis of energy of methane reforming

Temperature programmed oxidation (TPO), used Rh catalysts, 299–300

Temperature programmed reduction (TPR)
- curves of catalyst with different Co/Ni ratios, 227, 228*f*
- dependence of trend of curves on Co/Ni catalyst ratio, 233, 237
- methane decomposition on supported Co catalysts, 247, 248*f*
- patterns of hydrogen production for supported Co catalysts, 247, 249*f*
- surface area and degree of reduction of Co/Ni supported catalyst, 227*t*

Thermodynamics
- calculations for molybdenum and tungsten carbides, 190*t*
- Carnol process, 35*t*
- CO_2 conversion, 11, 14
- CO_2 transformation to liquid fuels, 167
- dense phase CO_2, 366–367
- Gibbs free energy of formation, 13*f*
- *See also* Computational analysis of energy of methane reforming

Ti/Si binary oxide, 341

Titania catalysts
- catalysis of Cu–Mn-O/TiO_2 for methanol synthesis, 162
- comparing Cu–Mn-O loading effect on zirconia and, 164*f*
- Cu–Mn synergy, 162*f*
- effect of Cu–Mn-O loading, 164*f*
- preparation with high surface area, 158, 160
- XRD of Cu–Mn-O on, 163*f*
- *See also* Methanol synthesis from CO_2 containing syngas

Titanium oxide catalysts
- Cu-loaded and Pt-loaded TiO_2 powder, 333–334
- small particle TiO_2 catalysts, 332–333
- Ti-containing zeolite and mesoporous molecular sieves, 337–339
- TiO_2 single crystals, 334–335
- Ti-oxide anchored on porous silica glass, 340
- Ti-oxide anchored on zeolite, 335–337
- Ti/Si binary oxide (sol-gel), 341
- *See also* Photocatalytic reduction of CO_2

Titanosilicates

Downloaded by 217.66.152.143 on September 14, 2012 | http://pubs.acs.org
Publication Date: January 24, 2002 | doi: 10.1021/bk-2002-0809.ix002

  epoxidation of propylene to propylene oxide, 48, 49*f*
  oxidations, 47–48
Toluene, oxidative dimerization to stilbene, 42
Transesterification, isocyanate synthesis, 65–66
Tungsten carbide
  dry reforming of methane at 850°C, 187*f*
  photoelectron spectra before and after reaction, 192*f*
  preparation and methane dry reforming, 185–186
  SEM photographs of, before and after reaction, 191*f*
  thermodynamic calculations, 190*t*
  X-ray diffraction pattern before and after reaction, 189*f*
  See also Methane dry reforming

U

Utilization
  annual U.S. production of CO_2 and related chemicals (1999), 15*t*
  barriers for CO_2, 20–21
  challenges and strategies for CO_2, 16, 20–24
  chemical processes, 19*f*
  CO_2, 10–11
  CO_2 as co-reactant or co-feed, 21
  converting CO_2 under geologic-formation conditions, 24
  copolymerization of CO_2 with epoxides, 103
  current status and potential market of CO_2, 14, 16
  energy recovery, 24
  lack of socio-economical and political driving forces, 21
  recycling CO_2, 24
  replacing hazardous or less effective substances, 23–24
  solar energy, 330–331
  strategies for research on CO_2, 21–24
  supercritical extraction, 23
  with and without chemical conversion processing, 22*f*
  See also Copolymerization of CO_2 with epoxides

W

Water. *See* Photocatalytic reduction of CO_2

X

o-Xylene, ammoxidation to *o*-phalonitrile, 41
Xylenes. *See* Gas-phase O_2 oxidation of alkylaromatics

Y

Y_2O_3 catalysts, Ru-loaded. *See* Methane reforming with CO_2
Yttrium-metal coordination catalyst
  copolymerization results for different catalyst systems, 105, 106*t*
  preparation, 104
  See also Copolymerization of CO_2 with epoxides

Z

Zeolite
  Ti-containing and mesoporous molecular sieves, 337–339
  Ti-oxide anchored on, 335–337

Downloaded by 217.66.152.143 on September 14, 2012 | http://pubs.acs.org
Publication Date: January 24, 2002 | doi: 10.1021/bk-2002-0809.ix002

See also Titanium oxide catalysts
Zirconia catalysts
  catalysis of Cu–Mn-O/ZrO_2 for methanol synthesis, 160
  comparing Cu–Mn-O loading effect on titania and, 164*f*
  Cu–Mn synergy, 161*f*
  dimethyl carbonate (DMC) formation, 73–74
  effect of H_3PO_4/ZrO_2 preparation method on DMC formation, 81, 83*t*
  preparation, 74
  preparation with high surface area, 158, 160
  See also Dimethyl carbonate (DMC); Methane reforming with CO_2; Methanol synthesis from CO_2 containing syngas

Downloaded by 217.66.152.143 on September 14, 2012 | http://pubs.acs.org
Publication Date: January 24, 2002 | doi: 10.1021/bk-2002-0809.ix002